Faculty of Engineering Aswan University

# Real Time Economic Dispatch Considering Renewable Energy Resources Uncertainty Using Effective Optimization Techniques

By

**Mohamed Hosny Hassan Salamaa**

M.Sc., Electrical Engineering, Cairo University

**A Thesis Submitted to the Faculty of Engineering**

**Aswan University**

**In Partial Fulfillment of the Requirements for the Degree of**

**Doctor of Philosophy**

In

**Electrical Engineering**

**April 2022**

# Real Time Economic Dispatch Considering Renewable Energy Resources Uncertainty Using Effective Optimization Techniques

Submitted By


**Mohamed Hosny Hassan Salamaa**

M. Sc., Electrical Engineering, Cairo University


For the degree of

**Doctor of Philosophy**

In

**Electrical Engineering**

## Supervision Committee

| Title/Name | Affiliation | Signature |
|---|---|---|
| Prof. Loai Saad Eldeen Nasrat | Elec. Eng. Dept., ASWU, Aswan, Egypt | |
| Prof. Francisco Jurado Melguizo | Elec. Eng. Dept., Jaen University, Spain | |
| Assoc. Prof. Salah Mohamed Kamel | Elec. Eng. Dept., ASWU, Aswan, Egypt | |

## Examination Committee

| Title/Name | Affiliation | Signature |
|---|---|---|
| Prof. Abdelazeem Abdullah Abdelsalam Abdullah | Suez Canal University, Ismailia, Egypt | |
| Prof. Mohamed Mahmoud Ali | Aswan University, Aswan, Egypt | |
| Prof. Loai Saad Eldeen Nasrat | Aswan University, Aswan, Egypt | |
| Assoc. Prof. Salah Mohamed Kamel | Aswan University, Aswan, Egypt | |

# Declaration and Certificate of Originality

I certify that in the preparation of this thesis, I have observed the provisions of the scientific code of ethics. Further; I certify that this work is free of plagiarism and all materials appearing in this thesis have been properly quoted and attributed.

I certify that all copyrighted material incorporated into this thesis is in compliance with the international copyright law and that I have received written permission from the copyright owners for my use of their work, which is beyond the scope of the law.

I agree to indemnify and save harmless Faculty of Engineering, Aswan University from any and all claims that may be asserted or that may arise from any copyright violation.

I hereby certify that the research work in this thesis is my original work and it does not include any copied parts without the appropriate citation.

Mohamed Hosny Hassan,

April, 2022

# ABSTRACT

Economic dispatch (ED) is one of the essential concepts in electrical power system management and operation systems. On the other side, with the increasing concern for pollutant emissions considerations, finding a solution for the emission has become an essential issue for the power generation system besides the total fuel cost all over the world. Decreasing the emission of greenhouse gases and the fuel cost are the main principles of the economic emission dispatch (EED) optimization problem. As an extension of the EED, the dynamic economic emission dispatch (DEED) that is more in line with the real short-term dispatching conditions, has acquired more academic interest, but the DEED issue is a highly dimensional, deeply correlated, nonconvex and nonlinear multi-objective optimization problem (MOP) taking into consideration the incompatible objectives and the operational limitations. During the last years, the electricity networks worldwide have rapidly developed, especially with the integration of many types of renewable energy sources (RESs). The optimal operation is an opportunity to increase the penetration level of stochastic RESs into the power grid to maximize energy efficiency. Uncertainty of the output power generated by RESs is forecasted based on probabilistic models. To minimize the total operating cost, the direct, underestimation, and overestimation costs of RESs are considered.

In this thesis, the EED problem is solved based on single/multi-objective functions using well-known and enhanced optimization algorithms. The following optimization algorithms are used to achieve the optimal solution for the EED problem based on a single objective function; Artificial Ecosystem-based Optimization Algorithm (AEO), Chaotic AEO Algorithm (CAEO), Manta ray foraging optimization (MRFO), Gradient-Based Optimizer (GBO), Hybrid (MRFO–GBO), supply-demand optimization (SDO) algorithm, eagle-strategy SDO algorithm with chaotic (ESCSDO), Marine Predators Algorithm (MPA) and modified MPA (MMPA). Also, Slime Mould Algorithm (SMA), and improved SMA (ISMA) are proposed and applied to solve the EED problems considering the valve point effect. Concerning the bi-objective problem, the Pareto approach is combined with the MMPA, MPA, SMA, ISMA, AEO, and CAEO techniques to reach a group of non-dominated (ND) solutions, and then the fuzzy method is utilized to choose the best compromise solution (BCS). In addition, the higher dimensional, strongly coupled, nonconvex and nonlinear multi-objective DEED model is designated considering the fuel costs and emissions objectives simultaneously. A Multi-objective Salp Swarm Algorithm (MSSA) is proposed to obtain the optimal dispatching schemes for the

DEED problem. Furthermore, the fuzzy decision-making (FDM) approach is employed to supply the decision-maker with the BCS.

The results show that the proposed algorithms are more robust than other well-known algorithms. Feasible solutions using the proposed algorithms are also achieved, which adjust the schedule of generation without violation of the operating generation limits. The simulation results present proof of the efficacious performance of the proposed techniques in solving great diversity of EED and DEED problems all over study cases. Also, Three different objective functions are considered, minimizing total operating cost, emissions, and power losses. The proposed CBO technique is verified on the modified IEEE-30 and IEEE-57 bus test systems to confirm the superiority and effectiveness of the proposed CBO to achieve the optimal solution. The simulation results prove the efficiency and robustness of CBO for finding the best solution to the EED problem with stochastic RESs.

*To all who have been great support and encouragement for me,*

*I dedicate this work*

# ACKNOWLEDGEMENT

In the beginning and foremost, praises and thanks to "ALLAH" of giving me patience and ability to complete this thesis.

I would say thanks to my supervisors **Prof. Loai Saad Eldeen Nasrat** and **Prof. Francisco Jurado** to guide me well throughout the research work from the title's selection to finding the results. Their immense knowledge, motivation and patience have given me more power and spirit to excel in the research writing. They are my mentor and better advisors for my doctorate study beyond the imagination. It would not have been possible to conduct this research without their precious support. No words of thanks can express my feeling toward my supervisor **Assoc. Prof. Salah Kamel**, who supported me, encouraged me and advanced me always. Without his guidance and challenging, I would never have been able to achieve this work. Moreover, I want to point to his humanism and his higher level of manners. I feel honored to have been given the opportunity to work under his supervision.

My appreciation also goes to my colleagues in Advanced Power Systems Research Laboratory (APSR Lab), Faculty of Engineering, Aswan University, & "Sala de Investigadores", University of Jaen, Spain, for the friendly academic atmosphere, the useful discussions, and their encouragement.

In the end, All my prayer from deep heart to the spirit of my father. I am extremely grateful to my family and friends, especially my mother and my wife for always believing in me and encouraging me to follow my dreams. I consider myself nothing without them. They gave me enough moral support, encouragement and motivation to accomplish the personal goals.

*Eng. Mohamed Hosny Hassan*

*May 2022*

# Table of Contents

**Chapter 1** .................... **2**

**Introduction** .................... **2**

**1.1 Background and Overview** .................... 2

**1.2 Economic Emission Dispatch** .................... 3

**1.3 Methods for Economic Emission dispatch** .................... 5

**1.4 Main Objectives of the Thesis** .................... 6

**1.5 Thesis Outlines** .................... 7

**Chapter 2** .................... **10**

**Literature Review** .................... **10**

**2.1 Introduction** .................... 10

**2.2 Application of Optimization Techniques for Optimal solution of ELD** .................... 10

**2.3 Conventional Methods for Solving EED Problem** .................... 11

**2.4 Recent Optimization Techniques for Optimal Solution of EED Problem** .................... 12

**2.5 Recent Optimization Techniques for Optimal Solution of EED Problem** .................... 14

**Chapter 3** .................... **17**

**Mathematical Formulation of EED and DEED Problems** .................... **17**

**3.1 Introduction** .................... 17

**3.2 Mathematical Formulation of EED Problem as Single-Objective Function** .................... 17

**3.2.1 First Formulation of EED Problem:** .................... 17

**3.2.2 Second Formulation of EED Problem:** .................... 19

**3.3 Mathematical Formulation of EED Problem as Bi-Objective Function** .................... 20

**3.4 Operating Constraints for EED Problem** .................... 21

**3.4.1 Power Balance Constraint** .................... 21

**3.4.2 Generating Capacity Constraint** .................... 22

**3.4.3 Ramp Rate Constraint** .................... 22

**3.4.4 Prohibited Operating Zones (POZs)** .................... 22

**3.5 Mathematical Formulation of DEED Problem** .................... 23

**3.6 System Constraints for DEED Problem** .................... 24

**3.6.1 Power Balance Constraint** .................... 24

**3.6.2 Generating Capacity Constraint** ........ 24
**3.6.3 Ramp Rate Constraint** ........ 25
**3.7 Mathematical Formulation of EED Problem Considering Stochastic RESs** ........ 25
**3.7.1 Cost Model for Conventional Thermal Generators** ........ 25
**3.7.2 Direct Cost of WT and SPV Generators** ........ 26
**3.7.3 Cost Assessment of Uncertainties for WT Generators** ........ 26
**3.7.4 Cost Assessment of Uncertainties for SPV Generators** ........ 27
**3.7.5 Carbon Tax Model** ........ 28
**3.7.6 Objective Functions** ........ 29
**3.7.7 Stochastic Wind Power and Solar Power Uncertainty Models** ........ 32
**Chapter 4 ........ 36**
**Recent and Developed Optimization Techniques for Solving EED, DEED Problems ........ 36**
**4.1 Introduction** ........ 36
**4.2 Conventional MRFO and Hybrid MRFO-GBO Algorithms** ........ 37
**4.2.1 Manta Ray Foraging Optimization (MRFO) Algorithm** ........ 37
**4.2.2 Hybrid MRFO- GBO Algorithm** ........ 38
**4.2.2.1 Gradient-Based Optimizer** ........ 38
**4.2.2.2 Shortcomings of Original MRFO Algorithm** ........ 42
**4.3 Conventional AEO and Developing Chaotic AEO Algorithms** ........ 44
**4.3.1 Artificial Ecosystem-Based Optimization (AEO) Algorithm** ........ 44
**4.3.1.1 Production** ........ 46
**4.3.1.2 Consumption** ........ 46
**4.3.1.3 Decomposition** ........ 47
**4.3.2 Proposed CAEO Techniques** ........ 47
**4.3.3 Multi-objective 4th Chaotic Function Artificial Ecosystem-based Optimization (MOCAEO4) Algorithm** ........ 50
**4.4 Conventional SMA and Improving SMA Algorithms** ........ 52
**4.4.1 Conventional Slime Mould Algorithm (SMA)** ........ 52
**Algorithm 1 Pseudo-code of SMA ........ 54**
**4.4.2 Improved Slime Mould Algorithm (ISMA)** ........ 55
**Algorithm 2 Pseudo-code of ISMA ........ 55**
**4.4.3 Proposed MOSMA and MOISMA** ........ 57

**4.5 Original MPA and Modified MPA Algorithms** ........ 58
**4.5.1 Original Marine Predators Algorithm** ........ 59
**4.5.2 Modified Marine Predators Algorithm** ........ 62
**4.5.2.1 Comprehensive Learning Strategy** ........ 62
**4.6 Original Supply Demand Based Optimization** ........ 65
**4.7 Eagle Strategy Chaotic Supply Demand Based Optimization** ........ 71
**4.7.1 Eagle Strategy** ........ 71
**4.7.2 Chaotic Maps** ........ 72
**4.8 Multi-Objective Optimization Algorithm for DEED Problem** ........ 74
**Algorithm 1 Pseudo-code of MSSA ........ 76**
**4.9 The Bonobo Optimizer** ........ 77
**4.10 The Proposed Chaotic Bonobo Optimizer** ........ 78
**Chapter 5 ........ 81**
**Results and Discussion ........ 81**
**5.1 Introduction** ........ 81
**5.2 Description of Test Systems** ........ 81
**5.3 Formulation of EED Problem as Single Objective Function** ........ 82
**5.3.1 Solving EED Problem using MRFO-GBO Algorithm** ........ 82
**5.3.1.1 Case 1: Five Thermal Units and Load Demand 1800 MW.** ........ 82
**5.3.1.2 Case 2: Three Thermal Units and Load demand.** ........ 83
**5.3.1.3 Case 3: Six Thermal Units and Load Demand.** ........ 86
**5.3.2 Solving EED Problem using CAEO Technique** ........ 91
**5.3.2.1 6-Unit Power Generation System** ........ 91
**5.3.2.1.1 Case 1: Estimation of Total Cost ($/h) for Load =150 MW** ........ 92
**5.3.2.1.2 Case 2: Simulation Results for Different Load Demands.** ........ 94
**5.3.2.2 11-Unit Power Generation 69-Bus System:** ........ 99
**5.3.2.2.1 Case 1: The Optimum Values of Fuel Cost.** ........ 99
**5.3.2.2.2 Case 2: Optimum Values of Total Emission.** ........ 101
**5.3.2.2.3 Case 3: Optimum Values of CEED** ........ 103
**5.3.3 Solving EED Problem using ISMA Algorithm** ........ 104
**5.3.3.1 CEC2019 Benchmark Functions** ........ 104
**5.3.3.2 Solving CEED using the ISMA Technique** ........ 109

**5.3.3.2.1 Case 1: 6 Thermal Units and Load Demand 2.834 p.u.** ..... 111
**5.3.3.2.2 Case 2: 10 Thermal Units and Load Demand (2000 MW)** ..... 114
**5.3.3.2.3 Case 3: 11 Thermal Units and Load Demand (2500 MW).** ..... 118
**5.3.3.2.4 Case 4: 40 Thermal Units and Load Demand (10,500 MW)** ..... 121
**5.3.3.2.5 Case 5: 110 Thermal Units and Load Demand (15,000 MW)** ..... 125
**5.3.4 Solving EED Problem using SDO Technique** ..... 128
**5.3.4.1 Case 1: Five Thermal Units and Load Demand 1800MW** ..... 129
**5.3.4.2 Case 2: Three Thermal Units and Load Demand** ..... 130
**5.3.4.3 Case 3: Six Thermal Units and Load Demand** ..... 135
**5.3.5 Solving EED Problem using MMPA Algorithm** ..... 140
**5.3.5.1 Mathematical Validation** ..... 140
**5.3.5.2 Solving CEED using the Proposed Technique** ..... 147
**5.3.5.2.1 Case 1: Five Thermal Units (Load=1800 MW).** ..... 148
**5.3.5.2.2 Case 2: 3 Thermal Units Considering Different Levels of System Load.** ..... 151
**5.3.5.2.3 Case 3: 6 Thermal Units Considering Different Levels of System Demand.** ..... 154
**5.3.5.2.4 Case 4: 26 Thermal Units Considering Two Load Levels (2000, 2200MW)** ..... 161
**5.4 Solving ELD Problem with using ESCSDO Algorithm** ..... 165
**5.4.1 Benchmark Functions** ..... 165
**5.4.2 Economic Load Dispatch (ELD) Problems** ..... 178
**5.4.2.1 Case 1: 6 Thermal Units and Load Demand 1263 MW.** ..... 178
**5.4.2.2 Case 2: 13 Units and the Load Demand 1800 MW.** ..... 184
**5.4.2.3 Case 3: 15 Units and the Load Demand 2630 MW.** ..... 186
**5.4.2.4 Case 4: 40 Units and the Load Demand 10,500 MW.** ..... 190
**5.4.3 Formulation of EED Problem as a Multi-objective Function** ..... 193
**5.4.3.1 Solving EED Problem using MOIMRFO Algorithm** ..... 193
**5.4.3.2 Solving EED Problem using MOCAEO Algorithm** ..... 194
**5.4.3.3 Solving EED Problem using MOISMA Algorithm** ..... 196
**5.4.3.4 Solving EED Problem using MOMMPA Algorithm** ..... 202
**5.5 Solving DEED Problem using the MSSA Algorithm** ..... 205
**5.6 Solving EED Problem Considering Stochastic RES using CBO Algorithm.** ..... 223

**5.6.1 Test System 1**.......... 223

**5.6.2 Test System 2**.......... 242

**Chapter 6 .......... 253**

**Conclusions and Future Works .......... 253**

**6.1 Conclusions of the Thesis**.......... 253

**6.2 Future Works**.......... 254

Appendix A .......... ب

Appendix B .......... ج

Appendix C .......... ج

Appendix D .......... د

Appendix E .......... ه

Appendix F .......... و

Appendix G .......... ح

Appendix H .......... ح

Appendix I .......... ط

الملخص العربى .......... أ

# List of Figures

Figure 1.1: Types of metaheuristic optimization techniques. ....6
Figure 3.1: Valve point loading effect on a fuel cost function. ....19
Figure 3.2: Membership of objective functions. ....21
Figure 3.3: Cost function of a generator with prohibited operating zones. ....23
Figure 4.1: Foraging behavior in MRFO. ....37
Figure 4.2: Flowchart of proposed MRFO–GBO algorithm based on MFRO and GBO algorithms. ....43
Figure 4.3: The energy Flow in an ecosystem. ....44
Figure 4.4: An ecosystem representation in the AEO technique. ....45
Figure 4.5: Flowchart of proposed CAEO4 technique. ....49
Figure 4.6: MOCAEO technique for the CEED problem. ....51
Figure 4.7: Potential positions in 2-dimensional and 3-dimensional. ....53
Figure 4.8: Evaluation of the fitness function. ....54
Figure 4.9: Flowchart of ISMA. ....57
Figure 4.10: Flowchart of MOISMA. ....58
Figure 4.11: MPA flowchart. ....59
Figure 4.12: MMPA flowchart. ....65
Figure 4.13: Two modes of supply–demand mechanism: (a) stability mode and (b) instability mode. ....66
Figure 4.14: The flow chart of the SDO algorithm. ....70
Figure 4.15: Different chaotic maps number distribution. ....72
Figure 4.16: The proposed ESCSDO algorithm Flow Chart. ....73
Figure 4.17: Bonobos' fission–fusion social groups. ....77
Figure 4.18: Flowchart of the proposed CBO technique. ....79
Figure 5.1: Fuel cost convergence of MRFO, GBO and MRFO- GBO for case study 1. ....83
Figure 5.2: Total cost for different levels of demand in 3-unit system (a) 550 MW (b) 600MW (c)700 MW (d) 800 MW (e)850 MW. ....86
Figure 5.3: Convergence Characteristics of MRFO, GBO and Hybrid MRFO-GBO for load demand 150MW in 6-unit system. ....89
Figure 5.4: Convergence Characteristics of MRFO, GBO and Hybrid MRFO-GBO for load demand 175MW in 6-unit system. ....89
Figure 5.5: Convergence Characteristics of MRFO, GBO and Hybrid MRFO-GBO for load demand 200MW in 6-unit system. ....90
Figure 5.6: Convergence Characteristics of MRFO, GBO and Hybrid MRFO-GBO for load demand 225MW in 6-unit system. ....90
Figure 5.7: Convergence characteristics of proposed CAEO and AEO. ....93
Figure 5.8: Variations of methods for different levels of demand in 6-unit system (a) Fuel cost ($/h) (b) Total cost ($/h). ....97
Figure 5.9: Convergence curves of the CAEO4 method for different levels of demand. ....98

Figure 5.10: Convergence Characteristics of AEO and CAEO4 for 3 levels of demand in 6-unit power system (a) Load Demand=175 MW (b) Load Demand=200MW (c) Load Demand=225MW. ....99
Figure 5.11: Fuel cost convergence curves of AEO and CAEO4 techniques (Case study 2) (a) 1000MW (b) 1500MW (c)2000MW (d)2500MW. ....101
Figure 5.12: Total Emission convergence curves of AEO and CAEO4 techniques (Case study 2) (a) 1000MW (b) 1500MW (c)2000MW (d)2500MW. ....103
Figure 5.13: Total Cost convergence curves of AEO and CAEO4 techniques (Case study (2) - 2500MW). ....104
Figure 5.14: The convergence behavior of the comparative methods using ten CEC2019 problems. ....109
Figure 5.15: Fuel cost convergence of different techniques (Case study 1). ....112
Figure 5.16: Total emission convergence curves of different techniques (Case study 1). ....113
Figure 5.17: Fuel cost convergence curves of different techniques (Case study 2). ....115
Figure 5.18: Total emission convergence curves of different techniques (Case study 2). ....117
Figure 5.19: Fuel cost convergence curves of different techniques (Case study 3). ....119
Figure 5.20: Total emission convergence curves of different techniques (Case study 3). ....121
Figure 5.21: Fuel cost convergence curves of different techniques (Case study 4). ....123
Figure 5.22: Total emission convergence curves of different techniques (Case study 4). ....124
Figure 5.23: Fuel cost convergence curves of different techniques (Case study 5). ....128
Figure 5.24: Boxplot and convergence characteristics of competitive algorithms for case study 1. ....130
Figure 5.25: Convergence characteristics of competitive algorithms for different levels of demand in the 3-unit system (case study 2): (a) 550 MW; (b) 600 MW; (c) 700 MW; (d) 800 MW; and (e) 850 MW ....133
Figure 5.26: Boxplot of competitive algorithms for different levels of demand in the 3-unit system (case study 2): (a) 550 MW; (b) 600 MW; (c)700 MW; (d) 800 MW; and (e) 850 MW. ....134
Figure 5.27: Convergence characteristics of competitive algorithms for different levels of demand in 6-unit system (case study 3): (a) 150 MW; (b) 175 MW; (c) 200 MW; and (d) 225 MW. ....139
Figure 5.28: Boxplot of competitive algorithms for different levels of demand in the 6-unit system (case study 3): (a) 150 MW; (b) 175 MW; (c) 200 MW; and (d) 225 MW. ....140
Figure 5.29: The mean convergence curves of MMPA and counterparts ....146
Figure 5.30: Fuel cost convergence of MPA and MMPA for Case 1. ....150
Figure 5.31: Best fuel cost boxplot in 30 runs of different algorithms for Case 1. ....150
Figure 5.32: Total cost convergence characteristics for different load levels in 3-unit system (a) 550 MW (b) 600MW (c)700 MW (d) 800 MW (e)850 MW. ....154
Figure 5.33: Convergence characteristics of MPA and MMPA for 150MW load demand in six-unit system. ....158
Figure 5.34: Convergence characteristics of MPA and MMPA for 175MW load demand in six-unit system. ....159

Figure 5.35: Convergence characteristics of MPA and MMPA for 200MW load demand in six-unit system. ....159
Figure 5.36: Convergence characteristics of MPA and MMPA for 225MW load demand in six-unit system. ....160
Figure 5.37: Convergence characteristics of the MMPA at different load levels. ....161
Figure 5.38: Convergence characteristics of MPA and MMPA for 2000MW load demand in a 26-unit power system. ....164
Figure 5.39: Convergence characteristics of MPA and MMPA for 2200MW load demand in a 26-unit power system. ....164
Figure 5.40: Qualitative metrics of twelve benchmark functions: 2D views of the functions, search history, average fitness history, and convergence curve using ESCSDO10 technique. ....168
Figure 5.41: Boxplots using the proposed techniques and the original SDO algorithm for the first unimodal benchmark function (F1). ....169
Figure 5.42: The convergence curves of the proposed techniques and the original SDO algorithm for the first unimodal benchmark function (F1). ....169
Figure 5.43: The convergence curves of all algorithms for 22 benchmark functions. ....176
Figure 5.44: Boxplots for all algorithms for 22 benchmark functions. ....178
Figure 5.45: Fuel cost convergence curves of different techniques (Case study 1). ....182
Figure 5.46: the best boxplot of different techniques (Case study 1). ....182
Figure 5.47: The best boxplot of different techniques (Case study 2). ....186
Figure 5.48: the convergence curves and the best boxplot of different techniques (Case study 3). ....189
Figure 5.49: the convergence curves and the best boxplot of different algorithms (Case study 4). ....193
Figure 5.50: Pareto-optimal front for (a) Fuel cost and SO2 emission (b) Fuel cost and NOx emission (c) Fuel cost and CO2 emission. ....196
Figure 5.51: PFs of MOSMA and MOISMA for Case 1. ....197
Figure 5.52: PFs of MOSMA and MOISMA for Case 2. ....198
Figure 5.53: PFs of MOSMA and MOISMA for Case 3. ....200
Figure 5.54: PFs of MOSMA and MOISMA for Case 4. ....202
Figure 5.55: Pareto front of Case 1 for load demand=225MW obtained by (a) MOMPA (b) MOMMPA. ....204
Figure 5.56: Pareto front of Case 2 for load demand=225MW obtained by (a) MOMPA (b) MOMMPA. ....204
Figure 5.57: Pareto front of Case 3 for load demand=225MW obtained by (a) MOMPA (b) MOMMPA. ....204
Figure 5.58: Single-line diagram of the IEEE 30-bus 6-generator test system. ....206
Figure 5.59: Load forecast curve for the IEEE 30-bus 6-generator test system. ....207
Figure 5.60: Single-line diagram of the 10-unit test system. ....208
Figure 5.61: Load forecast curve for the 10-generator test system. ....209
Figure 5.62: Load forecast curve for the IEEE 118-bus 14-generator test system. ....211

Figure 5.63: PF of the first case with power loss obtained by (a) MSSA (b) MALO (c) MOGOA (d) MSSA and comparison of optimal solutions. ....................................................213
Figure 5.64: Constraints check for the BCS of the case 1 using MSSA................................215
Figure 5.65: PF of the case 2 with power loss obtained by (a) MSSA (b) MALO (c) MOGOA (d) MSSA and comparison of optimum solutions. ................................................................216
Figure 5.66: Constraints check for the BCS of the second case using MSSA.......................218
Figure 5.67: PF of the third case with power loss obtained by (a) MSSA (b) MALO (c) MOGOA (d) MSSA and comparison of optimum solutions. ................................................219
Figure 5.68: Constraints check for the BCS of the third case using MSSA. ..........................222
Figure 5.69: Modified IEEE 30-bus test system. ...................................................................224
Figure 5.70: Wind speed distribution for WT generators at bus 5 and 11. ............................225
Figure 5.71: Solar irradiance distribution for SPV generators at bus13. ...............................225
Figure 5.72: Active power distribution in (MW) from SPV generator at bus 13. .................226
Figure 5.73: Variation of wind power cost components vs scheduled wind power. .............227
Figure 5.74: Variation of solar power cost components vs. scheduled solar power. .............228
Figure 5.75: Variation of wind power cost components vs Weibull scale parameter. ..........229
Figure 5.76: Variation of solar power cost components vs lognormal mean. .......................229
Figure 5.77: Convergence characteristic of all compared methods for case1. ......................233
Figure 5.78: Voltage magnitude of all compared methods for case1. ...................................233
Figure 5.79: Convergence characteristic of CBO5 and BO for cases 2& 3. .........................235
Figure 5.80: Voltage profiles of compared methods for cases 2 & 3. ...................................236
Figure 5.81: Convergence characteristic of CBO5 and BO for cases 4, 5 and 6. ..................241
Figure 5.82: Voltage profiles of compared methods for cases 4, 5 and 6.............................242
Figure 5.83: Convergence characteristic of CBO5 and BO for cases 7, 8 and 9. ..................245
Figure 5.84: Voltage profiles of compared methods for cases 7,8 and 9..............................246
Figure 5.85: Convergence characteristic of CBO5 and BO for cases 10,11and 12. ..............250
Figure 5.86: Voltage profiles of compared methods for cases 10, 11 and 12.......................251

# List of Tables


Table 4.1: Different chaos maps. ....47
Table 5.1: Comparison of results for case study 1. ....83
Table 5.2: Comparison of the proposed algorithms results for case study 2. ....84
Table 5.3: the results of fuel cost considering 4 levels of demand in the 6-unit system. ....87
Table 5.4: the results of SO2 emission considering 4 levels of demand in the 6-unit system. 87
Table 5.5: the results of NOx emission considering 4 levels of demand in the 6-unit system. ....87
Table 5.6: the results of CO2 emission considering 4 levels of demand in the 6-unit system.87
Table 5.7: the results of total emission considering 4 levels of demand in the 6-unit system. 87
Table 5.8: the results of total cost considering 4 levels of demand in the 6-unit system. ....88
Table 5.9: Results of CEED for the 6-unit system using MRFO, GBO and Hybrid MRFO-GBO. ....91
Table 5.10: statistical results of proposed CAEO and conventional AEO for the total cost of the 6-unit system (150mw load). ....94
Table 5.11: Estimated parameters of Cost for 150MW using CAEO, AEO, and other well-known optimization techniques. ....94
Table 5.12: the results of fuel cost considering 4 levels of demand in the 6-unit power generation system. ....95
Table 5.13: the results of SO2 emission considering 4 levels of demand in the 6-unit power generation system. ....95
Table 5.14: the results of NOx emission considering 4 levels of demand in the 6-unit power generation system. ....95
Table 5.15: the results of CO2 emission considering 4 levels of demand in the 6-unit power generation system. ....95
Table 5.16: the results of total cost considering 4 levels of demand in a 6-unit power generation system. ....96
Table 5.17: Results of CEED for the 6-unit system using AEO and CAEO4. ....96
Table 5.18: Results of the fuel cost for the 11-unit system using AEO and CAEO4. ....100
Table 5.19: The best solution values for the fuel cost of the case study 2 (2500 MW). ....101
Table 5.20: Results of the Total Emission for the 11-unit system using AEO and CAEO4. 102
Table 5.21: The best solution values for the Total Emission of the case study 2. ....103
Table 5.22: The best solution values for the CEED of the case study 2 (2500MW). ....104
Table 5.23: Description of the CEC2019 benchmark problems. ....105
Table 5.24: The results of the comparative methods using advanced CEC2019 problems....106
Table 5.25: Parameter settings of algorithms. ....110
Table 5.26: The best solution values of fuel cost for the six-unit system. ....111
Table 5.27: The best solution values for the total emission of the six-unit system. ....112
Table 5.28: Statistical results for Case 1. ....113
Table 5.29: The best solution values for the fuel cost of the ten-unit system. ....114
Table 5.30: The best solution values for the total emission of the ten-unit system. ....116

Table 5.31: Statistical results for Case 2. 117
Table 5.32: The best solution values for the fuel cost of the eleven-unit system. 118
Table 5.33: The best solution values for the total emission of the eleven-unit system. 120
Table 5.34: Statistical results for Case 3. 121
Table 5.35: The best solution values for the fuel cost of the forty-unit system. 122
Table 5.36: The best solution values for the total emission of the forty-unit system. 123
Table 5.37: Statistical results for Case 4. 125
Table 5.38: The best solution values for the fuel cost of the 110-units system. 125
Table 5.39: Statistical results for Case 5. 128
Table 5.40: Parameter settings of the selected techniques. 128
Table 5.41: Comparison of results for case study 1. 129
Table 5.42: Statistical analysis of best optimal solution for 30 independent runs on case study 1 129
Table 5.43: Comparison of results for case study 2. 130
Table 5.44: Statistical analysis of best optimal solution for 30 independent runs on case study 2 131
Table 5.45: Comparison of results for case study 3 (150 MW and 175 MW). 136
Table 5.46: Fuel cost results considering the 4 levels of demand in the 6-unit power generation system. 137
Table 5.47: Statistical analysis of best optimal solution for 30 independent runs on case study 3 138
Table 5.48: Parameter setting of MPA and MMPA for mathematical validation and solving CEED problems. 140
Table 5.49: The average and standard deviation values obtained by different optimization algorithms for 50D CEC2017. 142
Table 5.50: Ranks of different optimization algorithms for 50D CEC2017. 144
Table 5.51: P-values based on Wilcoxon rank-sum for MMPA versus the other algorithms. 144
Table 5.52: mean execution time in second for MMPA versus the other algorithms. 147
Table 5.53: Comparison of results for Case 1. 149
Table 5.54: Statistical results obtained by different techniques after 30 trials (Case 1). 150
Table 5.55: Results obtained by MMPA for Case 2. 151
Table 5.56: Comparison of results for Case 2. 151
Table 5.57: Statistical results obtained by different techniques after 30 trials (Case 2). 154
Table 5.58: Results obtained by different optimization techniques for the demand of 150MW. 155
Table 5.59: Results of fuel cost considering different levels of load in the six-unit system. 156
Table 5.60: Results of SO2 emission considering different levels of load in the six-unit system. 156
Table 5.61: Results of NOx emission considering different levels of load in the six-unit system. 156

Table 5.62: Results of $CO_2$ emission considering different levels of load in the six-unit system. ....157
Table 5.63: Results of total emission considering different levels of load in the six-unit system. ....157
Table 5.64: Results of total cost considering different levels of load in the six-unit system.157
Table 5.65: Results of CEED for the six-unit IEEE 30-bus system using MPA and MMPA. ....160
Table 5.66: Results of the total fuel cost considering 2000MW load demand in a 26-unit power generation system....162
Table 5.67: Results of the total fuel cost considering 2200MW load demand in a 26-unit power generation system....162
Table 5.68: the statistical Results of first unimodal benchmark function (F1) using the proposed techniques, the original SDO algorithm and other recent algorithms. ....168
Table 5.69: the statistical Results of 22 benchmark functions using the proposed ESCSDO10 technique and other recent techniques. ....170
Table 5.70: Optimal generations schedule of various algorithms for case study 1. ....180
Table 5.71: Fuel costs for Case 1 by various algorithms. ....183
Table 5.72: The best solution values of fuel cost for the thirteen-unit system with VPLE without considering transmission losses (PD = 1800 MW). ....185
Table 5.73: The best solution values of fuel cost for the thirteen-unit system with valve point loading without considering transmission losses (PD = 1800 MW)....186
Table 5.74: The best solution values of fuel cost for the fifteen-unit system for a demand of 2630 MW. ....188
Table 5.75: The best solution values of fuel cost for the fifteen-unit system for a demand of 2630 MW. ....189
Table 5.76: The best solution values of the total fuel cost for the forty-unit system....191
Table 5.77: The best solution values of the total fuel cost for the forty-unit system....193
Table 5.78: BCS for Multi-objective functions using MOCAEO4 (load=225MW). ....195
Table 5.79: BCS obtained by the conventional and proposed algorithms for 6-unit system.197
Table 5.80: BCS obtained by the conventional and proposed algorithms for the 10-unit system. ....198
Table 5.81: BCS obtained by the conventional and proposed algorithms for the 11-unit system. ....199
Table 5.82: BCS obtained by the conventional and proposed algorithms for the 40-unit system. ....200
Table 5.83: BCS of obtained by the MOMPA and MOMMPA algorithms for 6-unit generation system (load=225MW). ....203
Table 5.84: List of three studied cases. ....205
Table 5.85: The load demands (MW) of the IEEE 30-bus 6-generator test system. ....205
Table 5.86: Generator and emission coefficients of the IEEE 30-bus 6-generator test system. ....207
Table 5.87: The load demands (MW) of the 10-unit test system....208

Table 5.88: Generator coefficients of the 10-unit test system. ............................................209
Table 5.89: Emission coefficients and ramp rate of the 10-unit test system. ........................210
Table 5.90: The B-coefficients of the 10-unit test system. ..................................................210
Table 5.91: The load demands (MW) of the IEEE 118-bus 14-generator test system. .........210
Table 5.92: Generator and emission coefficients of the IEEE 118-bus 14-generator test system. ..........................................................................................................................211
Table 5.93: Comparison of the optimum objective values of case 1. ...................................213
Table 5.94: The BCS of the first case acquired using MSSA with power loss (p.u.)............214
Table 5.95: Comparison of the optimum objective values of case 2. ...................................217
Table 5.96: The BCS of the second case acquired using MSSA with transmission lossse (p.u.). ..........................................................................................................................217
Table 5.97: Comparison of the optimum objective values of case 2. ...................................220
Table 5.98: The BCS of the third case attained using MSSA with transmission losses (p.u.). ..........................................................................................................................221
Table 5.99: HV indicator values of results obtained for the three cases..............................222
Table 5.100: Simulation results of the proposed method and the BO method for case1.......231
Table 5.101: Statistical analysis of the total cost results obtained with different methods for Case1. ..........................................................................................................................234
Table 5.102: The Results of the proposed CBO5 method and BO method for cases 2 & 3..235
Table 5.103: Statistical analysis for cases 2 & 3. .................................................................236
Table 5.104: Comparison of CBO5 algorithm with the original BO algorithm and previous studies for single objective cases of IEEE 30-bus system. ..................................................237
Table 5.105: Results of the proposed CBO5 method and BO method for cases 4, 5 and 6. .239
Table 5.106: Statistical analysis for cases 4, 5 and 6. ...........................................................240
Table 5.107: Comparison of CBO5 algorithm with the original BO algorithm and previous studies for single objective cases (4, 5, and 6) of IEEE 30-bus system. ...............................242
Table 5.108: Results of the proposed CBO5 method and BO method for cases 7, 8 and 9. .243
Table 5.109: The Statistical analysis for cases 7,8 and 9......................................................246
Table 5.110: Comparison of CBO5 algorithm with the original BO algorithm and previous studies for single objective cases of IEEE 57-bus system. ..................................................247
Table 5.111: Results of the proposed CBO5 method and BO method for cases 10, 11 and 12. ..........................................................................................................................248
Table 5.112: The Statistical analysis for cases 10, 11 and 12...............................................249

# Nomenclature

## Acronyms

| | |
|---|---|
| DEED | Dynamic Economic and Emission Dispatch |
| FDM | Fuzzy decision-making |
| MSSA | Multi-objective Salp Swarm Algorithm |
| PF | Pareto Front |
| MALO | Multi objective ant lion optimizer |
| MOGOA | Multi-objective grasshopper optimization algorithm |
| EED | Economic and Emission Dispatch |
| SSA | Salp Swarm Algorithm |
| ODEA | the opposition based differential evolution algorithm |
| PSO | Particle swarm optimizer |
| MODE | Multi-objective Differential Evolution |
| CRO | Chemical Reaction Optimization |
| ITSA | Improved tunicate swarm algorithm |
| SQP | sequential quadratic programming |
| ELD | Economic Load Dispatch |
| ND | Non-dominated |
| BCS | Best Compromise Solutions |
| VPE | valve point effect |
| NSGA-II | Non-dominated Sorting Genetic Algorithm-II |
| MOP | multi-objective optimization problem |
| DED | Dynamic Economic Dispatch |
| IBFA | improved bacterial foraging algorithm |
| PSOCS | particle swarm optimization algorithm with a clone selection |
| DE | differential evolution |
| MAMODE | Modified Adaptive Multi-objective Differential Evolution |
| GSOMP | Group Search Optimizer with Multiple Producers |
| PPF | price penalty factor |
| SOP | single-objective problem |
| CEED | Combined Economic and Emission Dispatch |
| CAEO | Chaotic Artificial ecosystem-based optimization |

| | |
|---|---|
| AEO | Artificial ecosystem-based optimization |
| GA | Genetic Algorithm |
| ACO-ABC-HS | Ant Colony Optimization-Artificial Bee Colony-Harmonic Search |
| RGA | Real coded GA |
| FFA-BA | firefly-bat algorithm |
| MBO | Modified Biogeography Based Optimization |
| SSE | Sum of squared errors |
| RE | Relative error |
| MAE | Mean absolute error |
| ISA | Interior search algorithm |
| CSAISA | Chaotic self-adaptive interior search algorithm |
| MOCAEO4 | Multi-objective 4th chaotic function Artificial ecosystem-based optimization |
| SA | Simulated Annealing |
| MHBA | multi-objective hybrid bat algorithm |
| PSOGSA | PSO-the gravitational search algorithm |
| CSA | crow search algorithm |
| PSO- NN | PSO and Neural Network algorithm |
| QBA | Quantum-Behaved Bat |
| SCA | Sine cosine algorithm |
| SD | Standard deviation |
| RMSE | Root mean square error |
| HSA | Harmony search algorithm |
| GSA | Gravitational search algorithm |
| ESCSDO | eagle-strategy supply-demand based optimization algorithm with chaotic |
| SDO | supply-demand based optimization |
| ES | eagle strategy |
| VPLE | valve-point loading effect |
| POZ | prohibited operating zone |
| TLBO | teaching learning based optimization |
| HGWO | hybrid grey wolf optimizer |
| ALO | ant lion optimizer |
| ORCSA | one rank cuckoo search algorithm |
| MSOS | modified symbiotic organisms search algorithm |

| | |
|---|---|
| ACSS | adaptive charged system search algorithm |
| EMFO | enhanced moth-flame optimization algorithm |
| DAOA | distributed auction optimization algorithm |
| ACS | artificial cooperative search algorithm |
| Jaya | Jaya algorithm |
| Jaya-M | Jaya algorithm with multi-population |
| Jaya-SM | Jaya algorithm with self-adaptive multi-population |
| Jaya-SML | Jaya algorithm with self-adaptive multi-population and Lévy flights |
| SSGA | string structure GA |
| CMFA | Chaos firefly algorithm with self-adaptation mutation mechanism |
| FA | Firefly algorithm |
| ABC | artificial bee colony |
| MPSO-GA | modified PSO and GA |
| PSOSIF | Particle swarm optimization with smart inertia factor |
| GABC | Gbest guided artificial bee colony |
| GWO | gray wolf optimizer |
| ESSDO | eagle-strategy supply-demand based optimization algorithm |
| MCSA | modified crow search algorithm |
| HAAA | hybrid artificial algae algorithm |
| HGS | hunger games search |
| STD | standard deviation |
| CBA | chaotic bat algorithm |
| NPSO-LRS | new PSO local random search |
| MABC | modified artificial bee colony algorithm |
| ST-IRDPSO | Improved random drift particle swarm optimization with self-adaptive mechanism |
| HHS | hybrid harmony search |
| GAAPI | Hybrid GA with apicalis |
| EO | Equilibrium optimizer |
| EO-SCA | Hybrid EO-sine cosine algorithm |
| APSO | Adaptive particle swarm optimization |
| CPSO2 | Chaotic particle swarm optimization |
| TS | tabu search algorithm |
| DSPSO-TS | distributed Sobol PSO and TSA |
| BF-NM | Hybrid Bacterial foraging Nelder–Mead |

| | |
|---|---|
| CSO | cuckoo search optimization |
| CCSO | Clustering cuckoo search optimization |
| EPSO | evolutionary particle swarm optimization |
| IAEDP | immune algorithm with power redistribution |
| EMA | Exchange market algorithm |
| HSSA | Hybrid Salp Swarm Algorithm |
| QOPO | Quasi-Oppositional-Based Political Optimizer |
| SMA | Slime mould algorithm |
| ACO | Ant Colony Optimization |
| MOISMA | Multi-objective ISMA |
| BSA- ES | Binary successive approximation based evolutionary search |
| NGPSO | New global PSO |
| TSA | Tunicate Swarm Algorithm |
| EP | Evolutionary Programming |
| MVO | Multi-Verse Optimizer |
| CFO | Central Force Optimization |
| MOSMA | Multi-objective SMA |
| EHO | Elephant herding optimization |
| AOA | Arithmetic optimization algorithm |
| HHO | Harris Hawk Optimizer |
| OGHS | Opposition-based greedy heuristic search |
| SAIWPSO | Stability-based adaptive inertia weight PSO |
| MSA | Moth Swarm Algorithm |
| MGAIPSO | Modified GA and Improved PSO |
| JS | Jellyfish search optimizer |
| KHA | Krill herd algorithm |
| MPA | Marine Predators Algorithm |
| MRFO | Manta ray foraging optimization |
| MPA | Marine predators algorithm |
| MOMPA | Multi-objective Marine predators algorithm |
| MOMMPA | Multi-objective Modified Marine predators algorithm |
| LR | Langrage method |
| PPSO | Proposed PSO |
| GBO | Gradient-based optimizer |
| GOA | Grasshopper optimization algorithm |

| | |
|---|---|
| QITFA | Quantum-inspired tidal FA |
| MMPA | Modified marine predators algorithm |
| SDSM | Simplified direct search method |
| CLPSO | Comprehensive learning particle swarm optimizer |
| MRFO-GBO | Hybrid MRFO with GBO algorithm |
| QPSO | Quantum-inspired PSO |
| CL | comprehensive learning |
| WOA | whale optimization algorithm |
| HS | harmony search |
| LR | Lagrange’s method |
| MFO | moth–flame optimization algorithm |
| TSO | transient search optimization algorithm |
| BSA | backtracking search algorithm |
| BBO | biogeography-based optimization |

# Chapter 1

## Introduction

- *Background and Overview*
- *Economic Emission Dispatch*
- *Methods for Economic Emission Dispatch*
- *Main Objectives of the Thesis*
- *Thesis Outlines*

# Chapter 1

# Introduction

## 1.1 Background and Overview

The electric power supply system faces its main issues, which are the efficiency of the generation, transmission, and distribution grid [1]. Electricity production has been working in a more competitive and challenging environment. Reducing the overall running expenses is a major and critical issue in the modern power system. Previous efforts have been tried to find the optimum solutions for these issues by decreasing the operating cost of fuel consumption, which became an objective function besides many other requirements [2]. This is achieved through the appropriate scheduling of output power between the thermal units.

Under several constraints, the task of reducing fuel costs is well established according to the economic load dispatch (ELD) [3]. In the administration of the power system, fuel cost control is a major but not the only problem. There is another issue related to the negative effect of burning fossil fuels on the environment [4]. These greenhouse gases, such as sulfur, nitrogen, and carbon dioxide, are released via burning fossil fuels in the atmosphere and are responsible for disrupting environmental equilibrium and the chronic influences on human health caused by acid rain, global warming, and other harmful phenomena [5]. Hence, the multi-objective problem of integrated economic emission dispatch (EED) needs to be tackled.

Nonetheless, this study specifically concentrates on the static model that does not consider the relationship between various time intervals for dispatching and cannot guarantee global optimization from the entire schedule horizon. As an extension of the EED, the dynamic economic emission dispatch (DEED) that is more in line with the real short-term dispatching conditions, has acquired more academic interest [6], but the DEED issue is a highly dimensional, deeply correlated, nonconvex and nonlinear multi-objective optimization problem (MOP) taking into consideration the incompatible objectives and the operational limitations. If the transmission loss, the changing of the power load and the prohibited operating zone (POZ) were also involved, the DEED problem will be more extremely complex.

## 1.2 Economic Emission Dispatch

Nowadays, a competitive electric power market requires a high concentration to solve the ELD problem [7] of electric power generation, especially with a shortage of energy resources [8] and increasing electric energy demand [9]. The fundamental objective of the ELD [10] is to allocate the output of the available generating units to cover the load demand at minimum total fuel costs while fulfilling the physical and operating constraints of the power system. This ELD problem considers a non-convex, non-linear, and non-smooth optimization problem due to the characteristics of the valve point loading effect (VPLE) as a result of the multivalve steam turbine, power losses, ramp rate limits, and prohibited operation zones (POZ), which greatly increases the problem complication [11] [12].

On the other side, with the increasing concern for pollutant emissions considerations [13], finding a solution for the emission has become an essential issue for the power generation system besides the total fuel cost all over the world [14], [15]. However, the pollutant emission and operating cost functions are incompatible, which means while decreasing the emission, the operating cost is increased, and vice versa [16]. For this reason, the generation units are assigned with the aim of decreasing the total operating costs and/or reducing pollution emissions [17].

The economic emission dispatch (EED) aims to minimize the environmental effects produced by the burning of fuels in thermal power plants and the operating costs of these generating units simultaneously to produce the required demand fulfilling all technical constraints [18][19]. One of the most common methods to represent the EED problem is using the $2^{nd}$-order polynomial function [20]. However, the non-linearity of the actual thermal power generation system makes the solution of this problem deviates from the idealist and therefore nullify the approximation of the $2^{nd}$-order polynomial function.

It had been noted that the functions with an order higher than $2^{nd}$-order might represent the actual response of the thermal power generation system, and accordingly, these polynomials can help to improve the solutions [20]. However, the shortcoming of applying these polynomials, which have order higher than the second order on the EED problem makes it more complicated, and subsequently, it is hard to solve it. Therefore, to reach the most accurate solution for these two incompatible issues, several researchers have utilized a third order cost function to represent the EED problem. The 3rd-order cost function successfully decreases the increasing nonlinearities of the modern thermal generation system when it is utilized to represent the EED problem [21].

The continuous growth in energy consumption, the deregulation of the electricity markets, the need to reduce gas emissions, and the recent privileged prices of RESs have become motivated the rapid expansion of utilizing RESs in recent decades. It is proven that RESs are the preferable alternatives to fossil fuels for generating power. Because of enhanced technologies for generating power from RESs, a rapid increase in utilizing RESs has occurred, leading to decreased system installation costs [22]. As concluded in [23], the output power from wind turbine (WT) generators and solar photovoltaic (SPV) generators will soon be lower-priced than obtained by fossil fuels. Formulation and solution for constrained EED problem with the integration of stochastic RESs such as WT and SPV generators in power systems need more research as a few pieces of literature could be traced related to the same problem.

The incorporation of RESs into the power systems will cause several issues related to the economic operation of the grid, active power losses of the transmission system, the emissions from thermal plants, and the voltage of all buses [24]. Usually, RESs are managed by private operators, where the grid system operator announcement an agreement to purchase scheduled power. The main challenge of incorporating RESs such as WT and SPV generators is their intermittent nature. Furthermore, the generated power from RESs is uncertain, and it might be less than the scheduled power resulting in an overestimation of the available quantity. Therefore, power system operators need to have a spinning reserve, which increases the total operating cost.

In contrast, the generated power of RESs might be larger than the scheduled power resulting in underestimation. Therefore, the operators will pay a penalty cost as additional power goes wasted if not consumed [25][26]. Accordingly, the event neglecting uncertainty related to RESs when solving the EED problem will lead to inaccurate results in the system's total operating cost. To model the stochastic nature of solar irradiance, most authors use beta probability distribution function (PDF) [27] or lognormal PDF [28], whereas the stochastic behavior of wind speed can be described by Weibull PDFs [29].

## 1.3 Methods for Economic Emission dispatch

Several works of literature in science and engineering have suggested mathematical programming-based conventional methods to solve the non-linear and complex ELD and EED problems (such as Lagrange relaxation [30], Newton–Raphson [31], and quadratic programming) [32]. These approaches are very important but these methods are very sensitive to initial estimates and they are trapped in local minima [33]. Then, several intelligence methods have been developed as an alternative to the obsolete classical ways of solving the various EED problems. They have more advantages than the classical approaches, which make the researchers, used them to solve the EED problem and reach the best solution between lots of global solutions. Most of these technologies are nature-inspired. A number of the most renowned methods are GA [34], SA [35], PSO [36], flower pollination algorithm [37], Spider Monkey Optimization [38], Kernel search optimization [39], differential evolution (DE) [40], and ant lion optimization [41].

Currently, metaheuristic optimization techniques have become prevalent to find the best solution for the EED problem. They can be categorized based on their sources, as shown in Fig. 1 [42]. Some of these techniques were used to solve the EED problem in the literature. In [43], an improved GA was used to solve the power economic dispatch problem with valve point effect and multiple fuels without considering the transmission losses. In [44], a multi-objective evolutionary algorithm (MOEA) based on Pareto optimal-front has been used to optimize the economic and emission dispatch problem. A multi-objective differential evolution (DE) has been adopted to solve the EED problem [45]. The authors of [46] used the SA-PSO algorithm to solve the EED problem. In [47], the PSO algorithm has been used to solve the EED problem considering the generator constraints such as ramp rate limits and prohibited operating zones. The authors of [48] used the ACO for solving the dispatch problem. Other researchers used TLBO [49], GSA [50], MSA [51], and GWO [52]. In [53], an artificial cooperative search algorithm is used to solve the non-convex ELD problem. A krill herd (KH) algorithm was used to solve the Dynamic load dispatch problem, while the modified KH algorithm is proposed to solve the ELD problem [54].

Many researchers used hybrid methods that combine two or more algorithms to achieve better solutions than the original algorithms. In [55], a combination of PSO with SQP has been proposed to solve the ELD problems. In [56], a hybrid method based on the DE technique and SQP algorithm has been presented for finding the solution of the ELD dispatch problem. In [57], a hybrid approach based on GA and PSO has been proposed for solving the EED problem. Also, the EED problem has been solved using several developed techniques such as An improved quantum PSO algorithm [58], a parallel hurricane optimization algorithm (PHOA) [59], [60], and different multi-objective evolutionary algorithms [61]. However, developing an effective single and/or multi-objective economic and/or emission dispatch framework is still a hot research topic requiring more effort.

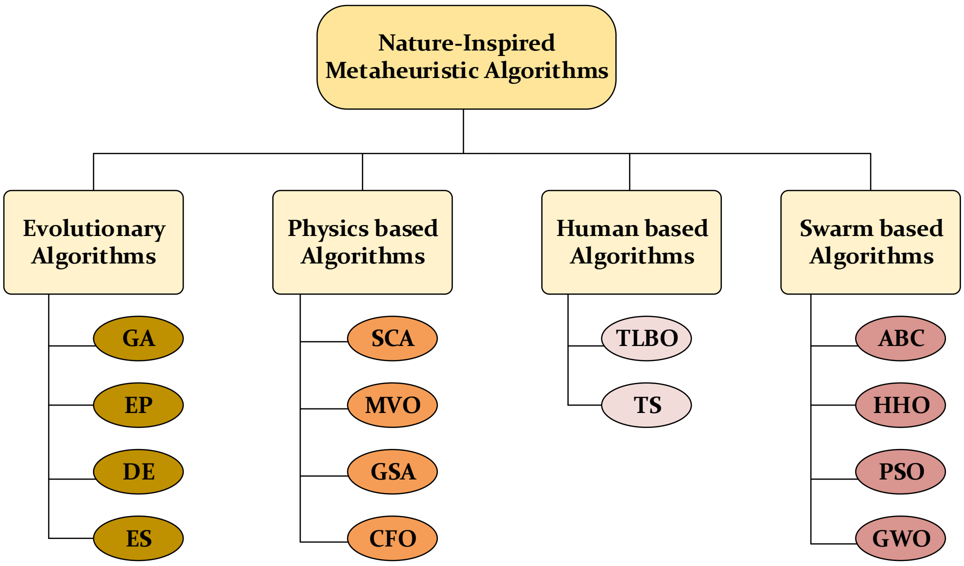


Figure 1.1: Types of metaheuristic optimization techniques.

## 1.4 Main Objectives of the Thesis

The main objectives of this thesis can be listed in these points:

- Developing and enhancing the convergence capabilities of the proposed techniques to achieve the optimum solutions and help them to avoid the local minima.
- Validating the performance of these proposed optimization algorithms using several benchmark functions.
- Analyzing and applying the proposed metaheuristic algorithms to solve the economic emission dispatch (EED) problem.

- Solving the Multi-objective EED problem using new multi-objective optimization techniques based on Pareto dominance concept and fuzzy decision-making.
- Solving the DEED problem using Multi-objective Salp Swarm Algorithm (MSSA).
- Solving several scenarios of EED problems for standard electrical power systems.
- Comparing and evaluating the results of the proposed algorithms to the recent and well-known optimization algorithms.
- Proposing an improved version of the classical BO based on chaos theory, called Chaotic Bonobo Optimizer (CBO), to improve the original BO's performance by avoiding being stuck in local optimums and solve EED considering the uncertainty modeling of WT and SPV generators.
- The superiority and reliability of the CBO-based methodology in solving the EED problem considering the uncertainty modeling of WT and SPV generators are proved.

## 1.5 Thesis Outlines

**Chapter 1: Introduction**

This chapter presents a general overview, the background and the motivation of the study.

**Chapter 2: Literature Review.**

This chapter gives a comprehensive survey of the previous solutions that have been suggested to solve the economic emission dispatch (EED) problem. In addition, this chapter discusses the methods, which have been proposed to find the best solution for the EED and DEED problems.

**Chapter 3: Formulation of Economic Emission Dispatch (EED) Problem**

In this chapter, the coordination problem is formulated as a single and multi-objective function. The main constraints for this problem are described in this chapter.

**Chapter 4: Recent and Developed Optimization Techniques for Solving EED Problem**

In this chapter, different optimization techniques are proposed to solve the EED problem. In addition, different enhancements and improvements are proposed to improve the performance of the conventional optimization algorithms, which theses algorithms can be summarized as follows; CAEO, ISMA, MMPA, ESCSDO, and SDO for the single EED problem and MOCAEO, MOISMA, MMMPA for the multi-objective EED problem. Furthermore, multi-objective optimization algorithm has been proposed for solving the DEED problem.

**Chapter 5: Results and Discussion**

This chapter presents the results and discussion of solving the EED problem using different algorithms. Different test systems are used to validate the performance of the proposed techniques. The results show the power of the proposed techniques to find the best optimal solutions for the fuel cost and emission. The obtained results prove the effectiveness of the proposed techniques compared with well-known and recent optimization algorithms.

**Chapter 6: Conclusions and Future Works**

This chapter gives a summary of the conclusions and highlights the achievement of this work. In addition, some topics for future work related to the subject of the thesis are also proposed.

# Chapter 2

## Literature Review

- *Application of Optimization Techniques for Optimal Solution of ELD.*
- *Conventional Methods for Solving the EED Problem.*
- *Recent Optimization Techniques for Optimal Solution of EED Problem.*
- *Recent Optimization Techniques for Optimal Solution of DEED Problem.*

# Chapter 2

# Literature Review

## 2.1 Introduction

In this chapter, a comprehensive survey and review of the previous research work including many types of EED methods, application of different optimization techniques to solve EED problems are presented.

## 2.2 Application of Optimization Techniques for Optimal solution of ELD

An optimal load dispatch maximizes the energy capability of thermal units, increases the reliability of the system and reduces the production cost. The research has been focused to achieve a global solution to the Economic load dispatch (ELD) optimization problem by applying exploration and exploitation procedures incorporating complex constraints. Several deterministic optimization techniques were proposed to solve the ELD problem, including gradient method [62], lambda iteration method [63], linear programming (LP) [64], quadratic programming (QP) [65], non-linear programming (NLP) method [66], Lagrangian relaxation algorithm [67] and dynamic programming (DP) [68]. The LP methods were used extensively to locate a solution for such a dynamic problem where the solution is limited to two variables due to the use of a graphical approach. The QP and LP methods were practiced to address many real dynamic problems due to their computational complexity and favorable results, but the major drawback of these methods is typically correlated with the approximate cost of the piecewise linear method. NLP methods suffer from a convergence issue in addition to high complexity.

Over the past decades, the electrical power market has become more competitive. In order to avail from this competition and heighten in this environment, companies today can no longer merely count on conventional means of power system planning. In ELD optimization, the search for optimum operating for the generator units of a power thermal plant system accordingly became very important in the design of superior power systems. Lessening the operational costs while meeting the power requirements of all customers are, however, a challenging task, particularly the units customarily have many nonlinear characteristics, which make precise mathematical methods impractical for ELD problems. On the other hand, metaheuristics have obtained considerable value in this area since they can offer sensible solutions that significantly reduce the consumption of generator fuel and offer these solutions at depressed computational costs.

Recently, to achieve a global solution while solving the ELD problem, meta-heuristic optimization techniques have been applied, such as Genetic algorithm (GA) [69], Differential Evolution (DE) [70], Particle Swarm Optimization (PSO) algorithm [71], Oppositional Real-Coded Chemical Reaction Optimization(ORCCRO) [72], Teaching Learning-Based Optimization (TLBO) [73], Biogeography-Based Optimization(BBO) [74], Gray Wolf Optimizer (GWO) [75], Ant Lion Optimizer (ALO) [76], Arithmetic optimization algorithm (AOA) based on elementary function disturbance [77], and An Enhanced Flower Pollination Algorithm [78].

## 2.3 Conventional Methods for Solving EED Problem

In the normal operation of power systems, it is inevitable that the generating units will produce a huge quantity of pollution emissions. It goes against the environmental conservation policies and regulations from the governments, which forces the electric utilities and power producers to pay close attention to the environmental effect of power generating plants [79]. For this purpose, the generation units are allocated according to the requirements of minimizing the total fuel costs and controlling the pollution emissions. The combined issue of fuel cost and emission is usually called the economic emission dispatch (EED) [80] or the combined economic environmental dispatch (CEED) [81]. It is essentially a type of multi-objective optimization problem and aims to minimize the fuel cost and pollution emission simultaneously on the premise that the requirements of the power balance constraint and generation limits are satisfied. All of these complicated factors make the EED very intractable to solve because of its highly nonlinear characteristic.

The conventional methods like lambda iteration technique, gradient technique, quadratic programming, LP, Lagrangian multiplier (LM) technique, and classical technique depending on coordination were employed for resolving issues on EED [82][83]. The basic concept of these methods is performed by linearization of the objective function, application of sensitivity analysis and optimization methods depending on gradient. However, these conventional approaches require the incremental cost curves to be raised monotonically. For the previous decades, many kinds of research and techniques had attempted to overcome the issues of EED [84].

## 2.4 Recent Optimization Techniques for Optimal Solution of EED Problem

Evolutionary algorithms (EAs) are characterized by their modelling capability and search power, which promote the implementation of EED in the power systems. Many researchers are focusing on solving EED problem using intelligent algorithms capable of finding better solutions of various problems.

Chatterjee, Ghoshal, and Mukherjee have implemented an improved approach to solve the issues in EED [85]. Evolutionary algorithms (EAs) were considered the well-identified optimization techniques to compact the non-linear and composite difficulties. On the other hand, various population-dependent approaches were considered computationally exclusive depending on the deliberated personality of the evolutionary method. Here, it includes the HS algorithm in which it attains motivation from the inventiveness approach of penetrating for a faultless circumstance of harmony. This approach was exploited to improve the convergence rate. The prospective of this approach was evaluated depending on a wide-ranging proportional revise of the clarification attained for four classical EED issues of power systems. From the simulation outcomes, it was clear that this approach attains better convergence speed when compared with the other standard approaches.

Liang and Juarez had presented a normalization approach for solving the problems in CEED [86]. The main intention of this approach was to attain the minimum probable outlay with the negligible quantity of contaminant, and this issue was considered CEED. Here, this design involves a normalization concept in which it includes two incompatible objective functions depending on the mean and standard deviation of the components in the population-dependent approaches. An improved population-based approach known as Virus Optimization Algorithm (VOA) was incorporated along with other metaheuristic algorithms. From the experimental outcome, it was obvious that this approach attains enhanced concert concerning the eminence and computational effectiveness.

Pandi et al. have proposed a novel multi-objective algorithm based on bacterial foraging for finding a better optimal Pareto front in the EED [87]. Performance metrics such as divergence and spacing were also calculated for the 30 trial run results of the proposed algorithm, which proved the suitability of the proposed algorithm for the EED problem.

Khan, Sidhu, and Gao have presented an enhanced optimization technique for solving the problems [88]. The transmission of power at a reduced outfitted outlay of thermal energy resources has been considered as an important component. In recent times concerning the growing awareness of renewable energy resources, the optimal CEED was considered to be a demanding problem. From the simulation outcomes, it was evident that this technique achieves better efficiency when compared with the other existing methods

Rizk-Allah, El-Sehiemy, and Wang have formulated an improved optimization approach to solve the problems in CEED [89]. Here, a parallel hurricane optimization algorithm (PHOA) was proposed for resolving the issues that occur in CEED. In PHOA, various sub-populations were stirring autonomously depending on the search space to optimize the objective issues concurrently with respect to the confined performance connecting subpopulations. Thus, it was proposed for searching the Pareto optimal solutions in contrast with the solitary optimal solution. Furthermore, the intrinsic distinctiveness of the corresponding scheme was deployed to improve the Pareto solutions. Thus, it was used to improve the convergence rate to attain the Pareto optimal solutions. From the experimental results, it was apparent that this technique attains enhanced power reservation when compared with the other standard techniques

Finally, several metaheuristic algorithms such as Particle swarm optimization (PSO) [90], Quantum-inspired PSO (QPSO) [91], Firefly algorithm (FA) [92], Modified Biogeography Based Optimization (MBO) [93], and Grasshopper optimization algorithm (GOA) [94] have been successfully used to solve the CEED problem. In [95], the Sine and cosine algorithm (SCA) has been used for solving the CEED problem. CEED problem has also been solved using Quantum-behaved bat algorithm (QBA) in [96], while it has been solved using the Quantum-inspired tidal FA (QITFA) in [97].

## 2.5 Recent Optimization Techniques for Optimal Solution of EED Problem

In opinion of the complicatedness and significance of the DEED issue, it is completely essential to select a suitable dispatch model and choose proficient algorithms to acquire the best dispatching scheduling for the power generation. Recently, meta-heuristic approaches have become extremely popular for achieving the optimum solutions for numerous electric engineering problems including the estimation of PV parameters [98], optimal power flow incorporating renewable energy [99], optimum reactive power dispatch with renewable energy uncertainty [100]. This popularity is because of many principal causes: gradient-free mechanism, flexibility, and local optima avoidance of these techniques [101].

Some studies have been published to handle the DEED problem. At first, the atmospheric pollutants were not taken into consideration as an objective in the dynamic economic dispatch (DED). In [102], a model was constructed without the ramp rate limits of the power generators, the emission, and the security constraints, to the DED problem. Over the recent years, with the development of high effectiveness and more precision solving techniques, the research direction of the DEED problem has changed to consider both fuel cost and atmospheric pollutants as multi-objectives. In [103], Basu employed an evolutionary programming-based fuzzy satisfying algorithm to solve the DEED as a single-objective problem (SOP). Benhamida [104], Pandit [105], and Thenmalar [106] transformed DEED to a SOP based on the price penalty factor (PPF) method and achieved the best solution for it using the neural network, the improved bacterial foraging algorithm (IBFA), and the opposition based differential evolution algorithm (ODEA). In [107], [108], and [109], the single-objective DEED models are solved using the PSO based goal-attainment method, fuzzy adaptive modified theta-PSO, and hybrid DE- sequential quadratic programming (SQP), respectively. All of these researches mentioned above has attained acceptable results. Nevertheless, because of the boundary of the single-objective DEED model, it is challenging to acquire more than one optimum solution in a single run, and the true Pareto front (PF) is surely difficult to achieve. In [110], [111], [112], [113], and [114], the Non-dominated Sorting Genetic Algorithm-II (NSGA-II), the Multi-objective DE (MODE), the Modified Adaptive Multi-objective DE (MAMODE), the improved NSGA-II and the Chemical Reaction Optimization (CRO) techniques are proposed to solve the DEED as a real MOP with competing and non-commensurable objectives. Also, Guo [115] proposed the Group Search Optimizer with Multiple Producers (GSOMP) technique and modeled DEED as a series of static EED based on the time intervals of dispatching that would have intricacies in the combination of global best solutions from various time intervals. Improved tunicate swarm algorithm (ITSA) [116] and an improved PSO algorithm with a clone selection (PSOCS) [117] were improved to reach the optimal solution for the DEED problem.

Recently, DEED has become the essential problem in the dynamic dispatch field of micro-grid and smart grid. For such complex MOPs, it would be permanently the effort of literatures to use a high-performance technique that achieve more accuracy solutions based on the particular characteristics of the problems. In recent decades, the optimization algorithm has received extensive attention and application.

Formulation and solution for constrained EED problem with the integration of stochastic RESs such as WT and SPV generators in power systems need more research as a few pieces of literature could be traced related to the same problem. This study proposes multi objectives of both economic and environmental problem formulation with WT and SPV generators. However, wind and solar power are modeled using Weibull and lognormal PDFs, respectively. Penalty and reserve costs of these intermittent sources to represent both underestimation and overestimation of these sources are suitably added to the generation cost.

# Chapter 3

## Mathematical Formulation of EED and DEED Problems

- *Introduction*
- *Mathematical Formulation of EED Problem as Single-Objective Function*
- *Mathematical Formulation of EED Problem as Bi-Objective Function*
- *Mathematical Formulation of DEED Problem*
- *Operating Constraints*

.

# Chapter 3

# Mathematical Formulation of EED and DEED Problems

## 3.1 Introduction

The economic emission dispatch (EED) problem requires that the fuel cost and the pollution emission are minimized simultaneously on the premise of satisfying the constraints. In this chapter, the mathematical model of the EED problem is first established. Then optimization objectives and objective functions of the EED problem are described. Finally, various constraints are taken into consideration.

## 3.2 Mathematical Formulation of EED Problem as Single-Objective Function

In this thesis, the EED problem is formulated and solved in two formulations as follows:

### 3.2.1 First Formulation of EED Problem:

Combined economic emission dispatch (CEED) is a multi-objective optimization problem that generally aims to reduce both fuel cost and risky gases emission while sustaining all technical constraints [18]. The reduction of $SO_2$, $NO_x$, and $CO_2$ as three independent objectives is studied in this thesis. Thus, The CEED becomes a four-objective optimization problem after adding the ELD with the three objective emissions functions [96]. The fuel cost $F(P)$ in (\$/h) can be firstly determined from the cubic equation as follows:

$$F(P) = \sum_{i=1}^{n} \{a_i P_i^3 + b_i P_i^2 + c_i P_i + d_i\} \tag{3.1}$$

where, $P_i$ is the actual output power of ith generating unit, $n$ indicates the total number of generating units; $a_i$, $b_i$, $c_i$, and $d_i$ are the fuel cost coefficients for *ith* generating unit.

Then, the total emission of dangerous gases is separated into three independent objectives and it is mathematically formulated as follows:

$$E_{SO_2}(P) = \sum_{i=1}^{n} \{e_{SO_2i}P_i^3 + f_{SO_2i}P_i^2 + g_{SO_2i}P_i + h_{SO_2i}\} \tag{3.2}$$

where, $E_{SO2}(P)$ in (kg/h) is the emission function of $SO_2$. $e_{SO_2i}$, $f_{SO_2i}$, $g_{SO_2i}$, and $h_{SO_2i}$ are the $SO_2$ emission coefficients of the ith generating unit.

$$E_{NO_x}(P) = \sum_{i=1}^{n} \{e_{NO_xi}P_i^3 + f_{NO_xi}P_i^2 + g_{NO_xi}P_i + h_{NO_xi}\} \tag{3.3}$$

where, $E_{NO_x}(P)$ in (kg/h) is the emission function of $NO_x$. $e_{NO_xi}$, $f_{NO_xi}$, $g_{NO_xi}$, and $h_{NO_xi}$are the $NO_x$ emission coefficients of the ith generating unit.

$$E_{CO_2}(P) = \sum_{i=1}^{n} \{e_{CO_2i}P_i^3 + f_{CO_2i}P_i^2 + g_{CO_2i}P_i + h_{CO_2i}\} \tag{3.4}$$

where, $E_{CO_2}(P)$ in (kg/h) is the emission function of $CO_2$. $e_{CO_2i}$, $f_{CO_2i}$, $g_{CO_2i}$, and $h_{CO_2i}$are $CO_2$ emission coefficients of the generating unit $i$.

In this thesis, a max/max PPF [96] is utilized to turn the 4 objectives functions (minimizing the economic dispatch and the total emissions of $CO_2$, $SO_2$, and $NO_x$) into a single-objective (total cost). The aim of the proposed MMPA technique is to achieve the optimum value of this single-objective. This objective function $F_T$ in (\$/h) can be stated as:

$$OF = \min(F_T)$$

$$F_T = \sum_{\mathrm{i}=1}^{\mathrm{n}} \{\mathrm{F}(\mathrm{P_i}) + \mathrm{h_{Si}}\mathrm{E_{SO_2i}}(\mathrm{P_i}) + \mathrm{h_{Ni}}\mathrm{E_{NO_xi}}(\mathrm{P_i}) + \mathrm{h_{Ci}}\mathrm{E_{CO_2i}}(\mathrm{P_i})\} \tag{3.5}$$

where, $\mathrm{F}(\mathrm{P_i})$ is the fuel cost (\$/h) of each generating unit i. $\mathrm{E_{SO_2i}}(\mathrm{P_i})$, $\mathrm{E_{NO_xi}}(\mathrm{P_i})$, and $\mathrm{E_{CO_2i}}(\mathrm{P_i})$ are the $SO_2$ emission (kg/h), $NO_x$ emission (kg/h), and$CO_2$ emission (kg/h) of each ith generating unit.

The PPF ($\mathrm{h_i}$) can be explained by dividing the maximum total fuel cost into the maximum emissions for each gases from the power plants $SO_2$, $NO_x$, and $CO_2$. It can be represented for each gas as below:

$$\mathrm{h_{Si}} = \sum_{i=1}^{n} \frac{F(P_{i.\max})}{E_{SO2}(P_{i.\max})} \tag{3.6}$$

$$\mathrm{h_{Ni}} = \sum_{i=1}^{n} \frac{F(P_{i.\max})}{E_{NOx}(P_{i.\max})} \tag{3.7}$$

$$\mathrm{h_{Ci}} = \sum_{i=1}^{n} \frac{F(P_{i.\max})}{E_{CO2}(P_{i.\max})} \tag{3.8}$$

### 3.2.2 Second Formulation of EED Problem:

Solving the EED problem aims to achieve two objectives. The first one is to minimize the fuel cost of power systems, while the second one is to minimize the pollutant emissions produced from the generating units. The fuel cost function comprises a quadratic and a sinusoidal function [118]. The sinusoidal function part is calculated when the valve-point effect is taken into consideration. Figure 3.1 shows a multi-valve loading effect on the fuel cost function. The total fuel costs  based on the output of thermal generating units along with its constraints, is given below [119]:

$$F_1 = \sum_{i=1}^{N_G} [a_i + b_i P_{Gi} + c_i P_{Gi}^2 + \left| d_i \sin\left(e_i\left(P_{Gi}^{min} - P_{Gi}\right)\right)\right|] \tag{3.9}$$

where, $a_i$; $b_i$; $c_i$; $d_i$ and $e_i$ represent the cost coefficients for the ith unit; $P_{Gi}$ represents the power output of ith (i = 1; 2; 3; . . ; $N_G$) unit, and $N_G$ represents the number of generating units.

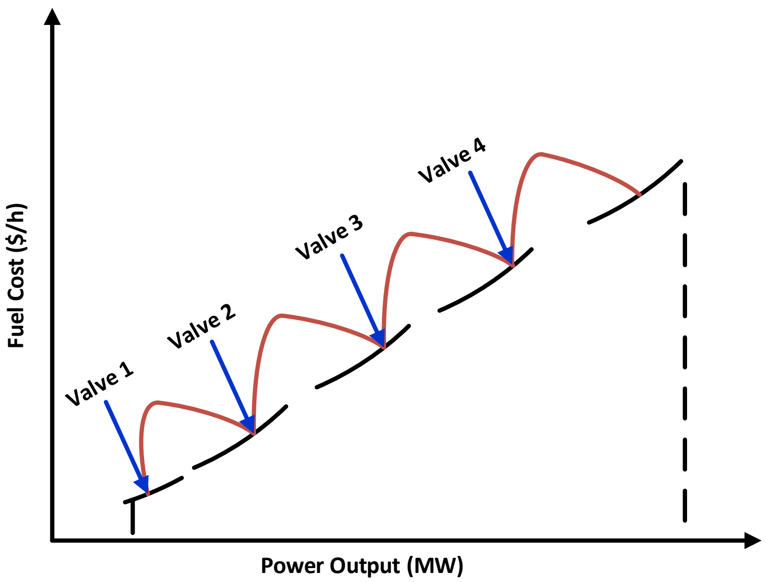


Figure 3.1: Valve point loading effect on a fuel cost function.

The second objective, the emission function, is that it takes into account two primary pollutant emissions ($SO_x$ and $NO_x$) caused by fossil-fueled thermal units. The total pollutant emission is expressed as:

$$F_2 = \sum_{i=1}^{N_G} [10^{-2}(\alpha_i + \beta_i P_{Gi} + \gamma_i P_{Gi}^2) + \eta_i \exp(\delta_i P_{Gi})] \tag{3.10}$$

where, $\alpha_i$; $\beta_i$; $\gamma_i$; $\eta_i$ and $\delta_i$ represent the emission coefficients for the ith unit.

## 3.3 Mathematical Formulation of EED Problem as Bi-Objective Function

A Bi-objective optimization technique is ordinarily employed to achieve the optimal solution for two objectives, simultaneously [32], [121]. The obtained solutions in each iteration using an optimization technique are categorized as dominated and ND solutions, according to the two objective functions. The Pareto dominance theory is employed to perform this sorting. Then, the ND solutions are stored in the archiving matrix and then the Best Compromise Solution (BCS) is chosen by the Fuzzy decision-making (FDM). However, various methods have been used to find the BCS [122]. The FDM is the most popular approach which is usually utilized to determine BCS for decision-making problems [123], [124]. Therefore, in this thesis, The FDM was applied to find the BCS from the achieved solutions using the final Pareto front as follows:

### 3.3.1 Pareto Approach

Firstly, Pareto approach achieve a set of feasible solutions. After that, a solution $x_1$ is considered dominates the solution $x_2$ according to the Pareto approach when [125]:

$$\forall_i \in \{1,2,\dots,M\}, f_i(x_1) \le f_i(x_2) \tag{3.11}$$

$$\exists_i \in \{1,2,\dots,M\}: f_i(x_1) < f_i(x_2) \tag{3.12}$$

### 3.3.2 Determination of the BCS

The fuzzy membership approach normalize the objective function value F of each ND solution (k) which is shown in Figure 3.2 as follows [122]:

$$\mu_i^k = \begin{cases} 1 & F_i \leq F_i^{min} \\ \dfrac{F_i^{max} - F_i}{F_i^{max} - F_i^{min}} & F_i^{min} < F_i < F_i^{max} \\ 0 & F_i \geq F_i^{max} \end{cases} \tag{3.13}$$

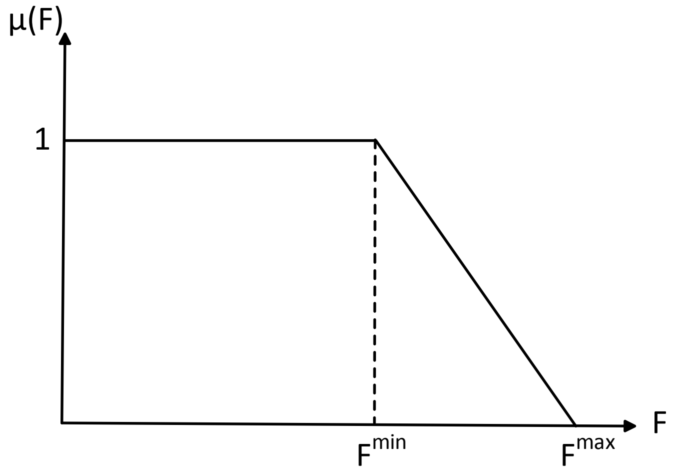


Figure 3.2: Membership of objective functions.

where, $F_i^{max}$ and $F_i^{min}$ are the maximum and minimum values of $F_i$ between all ND solutions, respectively.

The normalized membership function ($\mu_k$) is given by the following equation:

$$\mu^k = \frac{\sum_{i=1}^{Nobj} \mu_i^k}{\sum_{k=1}^{M} \sum_{i=1}^{Nobj} \mu_i^k} \tag{3.14}$$

where, $M$ is the number of ND solutions. The value of $\mu^k$ is used to determine the BCS from all ND solutions where it has the maximum value of $\mu^k$.

## 3.4 Operating Constraints for EED Problem

### 3.4.1 Power Balance Constraint

The equality constraint related to power balance in the system ensures that the total active output power generated by the generators $P_T$ (in MW) covers both the total power demand $P_D$ (in MW) and the total power losses of the grid $P_L$ (in MW). This equality constraint can be expressed as:

$$P_T = \sum_{i=1}^{n} P_i = P_D + P_L \tag{3.15}$$

where $P_L$ can be calculated by Kron's formula:

$$P_L = \sum_{i=1}^{n}\sum_{j=1}^{n} P_i B_{ij} P_j + \sum_{i=1}^{n} B_{i0} P_i + B_{00} \tag{3.16}$$

where $B_{ij}$, $B_{i0}$, $B_{00}$ are the B-matrix coefficients for $P_L$.

### 3.4.2 Generating Capacity Constraint

Further, an inequality constraint is included to ensure that each generating unit operates within its respective specified limits of production, which can be given by equation as:

$$P_{i,min} \leq P_i \leq P_{i,max} \tag{3.17}$$

where, $P_i$ should be within its minimum $P_{i,min}$, and maximum $P_{i,max}$ limits.

### 3.4.3 Ramp Rate Constraint

Under practical conditions, the operating limit of every generator is bounded by its ramp rate limit, therefore the output power Pi cannot be adjusted immediately. The up and down ramp limits are as follows:

$$P_i - P_i^0 \leq UR_i \; and \; P_i^0 - P_i \leq DR_i \tag{3.18}$$

where $P_i$ is the current power output, $P_i^0$ is the previous power output, $UR_i$ and $DR_i$ is the up and down limit of generator i respectively.

From Eqs. (2.17)–(2.18) the output power is expressed as:

$$\max(P_i^{min}, P_i^0 - DR_i) \leq P_i \leq \min(P_i^{max}, P_i^0 + UR_i) \tag{3.19}$$

### 3.4.4 Prohibited Operating Zones (POZs)

In practice, since there are physical constraints when operating the generator, the completely operating zones are not regularly available. POZs lead to discontinuous regions for the OF. POZs are due to the shaft bearing vibrations caused by a steam valve or because of associated ancillary equipment such as a boiler or feed pumps. In practice, the setting of the output power of a unit should be outside prohibited zones [126]. The Output power $P_i$ has POZs constraints as follows:

$$P_i^{min} \le P_i \le P_{i,1}^{l}$$
$$P_{i,k-1}^{u} \le P_i \le P_{i,k}^{l}, \qquad k=2,\ldots.., pzi \qquad (3.20)$$
$$P_{i,pz_i}^{u} \le P_i \le P_{i,1}^{max}$$

where $P_{i,k}^{l}$ and $P_{i,k}^{u}$ are the lower and upper limits of the kth prohibited zone of unit i, respectively, k is the index of POZs (pzi). In Figure 3.3, the discontinuous fuel-cost characteristic of generators by considering prohibited zones is shown.

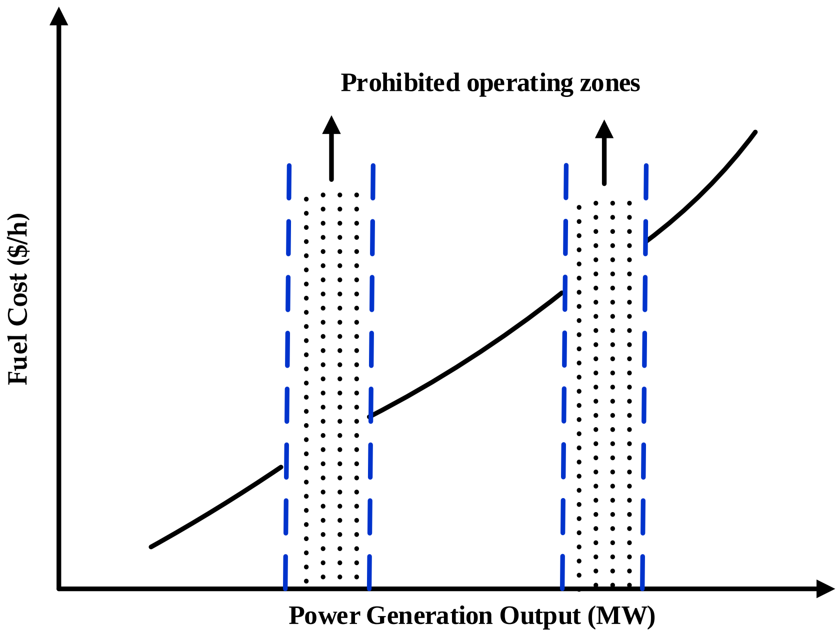


Figure 3.3: Cost function of a generator with prohibited operating zones.

## 3.5 Mathematical Formulation of DEED Problem

The fuel cost of each generator taken into consideration the valve point effect (VPE) is modeled as the summation of a quadratic and a sinusoidal function. Therefore, the total fuel cost of $N_G$ generating units through $T$ dispatching time intervals is given from the following equation [127]:

$$F_1 = \sum_{t=1}^{T}\sum_{i=1}^{N_G}[a_i + b_i P_{Gi,t} + c_i P_{Gi,t}^2 + \left|d_i \sin\left(e_i\left(P_{Gi}^{min} - P_{Gi,t}\right)\right)\right|] \tag{3.21}$$

where, $a_i$; $b_i$; $c_i$; $d_i$ and $e_i$ represent the cost coefficients for the ith unit; $P_{Gi,t}$ represents the power output of ith ($i$ = 1; 2; 3; . . ; $N_G$) unit at the dispatching time interval $t$, and $N_G$ represents the number of generating units.

Commonly, atmospheric pollutants such as Co2, SOx, and NOx caused by fossil-fueled thermal generators are mathematically represented as the totality of a quadratic and an exponential function. Accordingly, the emission of $N_G$ generators through the dispatching interval is expressed as [128]:

$$F_2 = \sum_{t=1}^{T}\sum_{i=1}^{N_G}[\alpha_i + \beta_i P_{Gi,t} + \gamma_i P_{Gi,t}^2 + \eta_i \exp(\delta_i P_{Gi,t})] \tag{3.22}$$

where, $\alpha_i$; $\beta_i$; $\gamma_i$; $\eta_i$ and $\delta_i$ represent the emission coefficients for the ith unit.

## 3.6 System Constraints for DEED Problem

### 3.6.1 Power Balance Constraint

The total power generated must equal the summation of the total power demand $P_{D,t}$ and the complete transmission losses $P_{L,t}$, which is formulated as:

$$\sum_{i=1}^{n} P_{i,t} - P_{D,t} - P_{L,t} = 0 \tag{3.23}$$

where $P_{L,t}$ is calculated by Kron's formula:

$$P_{L,t} = \sum_{i=1}^{n}\sum_{j=1}^{n} P_{i,t} B_{ij} P_{j,t} + \sum_{i=1}^{n} B_{i0} P_{i,t} + B_{00} \tag{3.24}$$

where $B_{ij}$, $B_{i0}$, $B_{00}$ are the B-matrix coefficients for $P_{L,t}$.

### 3.6.2 Generating Capacity Constraint

The power output $P_{i,t}$ must be within the minimum and maximum power generation limits, as represented by:

$$P_i^{min} \leq P_{i,t} \leq P_i^{max} \tag{3.25}$$

where $P_i^{max}$ is the maximum limit of the ith generator.

### 3.6.3 Ramp Rate Constraint

Under practical conditions, the operating limit of every generator is bounded by its ramp rate limit, therefore the output power Pi cannot be adjusted immediately. The up and down ramp limits are as follows [129]:

$$\begin{cases} P_{i,t} - P_{i,t-1} - UR_i \times \Delta T \leq 0 \\ P_{i,t-1} - P_{i,t} - DR_i \times \Delta T \leq 0 \end{cases} \tag{3.26}$$

where $UR_i$ and $DR_i$ is the up and down limit of generator i respectively. $\Delta T$ denotes the length of each dispatching time interval.

## 3.7 Mathematical Formulation of EED Problem Considering Stochastic RESs

It is worth noticing that the EED problem is a highly complex nonlinear problem. The solution of EED is determining the optimal control variables which minimize the objective function, considering different operational constraints. The main objective function in this study is reducing the total operating cost that includes the fuel cost of the conventional thermal generators, with or without the direct reserve and penalty costs resulting from the nature of intermittency in the outputs of WT and SPV generators. Further, the optimal control variables of the EED problem are generators active/reactive power and voltages, transformer tap ratio, and shunt VAR capacitors.

### 3.7.1 Cost Model for Conventional Thermal Generators

The conventional thermal generators are operated based on fossil fuel. The fuel cost can be expressed as [130]:

$$F(P_{cg}) = \sum_{i=1}^{N_g} \alpha_i P_{cg,i}^2 + \beta_i P_{cg,i} + \gamma_i \tag{3.27}$$

where $F$ is the fuel cost of generated power, $N_g$ is the total number of the conventional thermal generators, $P_{cg,i}$ represents the real power generated from unit i and $\alpha_i$ , $\beta_i$ , and $\gamma_i$ are the cost coefficients related to the ith conventional thermal generators. However, considering the valve point loading effect, the quadratic cost function becomes precise and more realistic [131]. The valve-point loading effect occurs because the valves of thermal generation units are opened in case of steam admission and these cause the losses to increase suddenly and lead to ripples in the cost function curve. Consequently, the cost function can be described as follows:

$$F(P_{cg}) = \sum_{i=1}^{N_g} \alpha_i P_{cg,i}^2 + \beta_i P_{cg,i} + \gamma_i + \left| e_i \times \sin(g_i (P_{cg,i}^{min} - P_{cg,i})) \right| \tag{3.28}$$

where $e_i$ and $g_i$ are valve point cost coefficients of unit i, while $P_{cg,i}^{min}$ represents the minimum real power that the ith conventional generators produces when it is in operation.

### 3.7.2 Direct Cost of WT and SPV Generators

WT and SPV generators need no fuel for operation. Only the initial maintenance or spending cost of the RESs is assigned [132]. The scheduled power produced from RES is charged according to the mutually agreed contract. A direct cost function of WT and SPV generators belongs to private parties and is given in [133]:

$$C_{W_j}\left(P_{W_{s,j}}\right) = g_{W_d} P_{W_{s,j}} \tag{3.29}$$

where $C_{W_j}$ is the direct cost of the jth WT generator, $g_{W_d}$ denotes the direct cost coefficient of the WT generator, and $P_{W_{s,j}}$ represents the scheduled power of the jth WT generator. In the same manner, the direct cost of the kth SPV generator in terms of scheduled power can be expressed as follows:

$$C_{S_k}\left(P_{S_{s,k}}\right) = g_{S_d} P_{S_{s,k}} \tag{3.30}$$

where $g_{S_d}$ denotes the direct cost coefficient of the SPV generator, and $P_{S_{s,k}}$ represents the scheduled power of the $k^{th}$ SPV generator.

### 3.7.3 Cost Assessment of Uncertainties for WT Generators

In terms of the output power of RES, two cases may occur. The first case arises when the output power of RES is greater than the expected value (underestimated output power). In this case, the surplus power can be potentially lost. System operators aim to reduce produced power from conventional thermal generators to avoid this. However, the associated cost is referred to as penalty cost. The penalty cost is paid by the system operators commensurate with the additional power from WT generators is expressed as follows:

$$C_{U_{w,j}}\left(P_{W_{a,j}} - P_{W_{s,j}}\right) = p_{W,j}\left(P_{W_{a,j}} - P_{W_{s,j}}\right) \tag{3.31}$$
$$= p_{W,j}\int_{P_{W_{s,j}}}^{P_{W_{r,j}}}\left(P_{W,j} - P_{W_{s,j}}\right) F_W\left(P_{W,j}\right)\, dP_{W,j}$$

where $P_{W_{a,j}}$ , $P_{W_{s,j}}$, and $P_{W_{r,j}}$are the available, schedule and rated output power from j$^{th}$ WT generator, respectively, $p_{W,j}$ denotes the penalty cost coefficient of the j$^{th}$ WT generator and $F_W\left(P_{W,j}\right)$ is the PDF for the generated power of the j$^{th}$ WT generator.

The second case is when the output power of RES is less than the estimated value (overestimated output power). To face this situation, system operators need to allocate spinning reserves on conventional generators to compensate for overestimated RES power and thus ensure uninterrupted power to consumers. The cost related to this power reserve is called reserve generation cost [134] and is described as follows:

$$C_{O_{w,j}}\left(P_{W_{s,j}} - P_{W_{a,j}}\right) = R_{W,j}\left(P_{W_{s,j}} - P_{W_{a,j}}\right) \tag{3.32}$$
$$= R_{W,j}\int_{0}^{P_{W_{s,j}}}\left(P_{W_{s,j}} - P_{W_{a,j}}\right) F_W\left(P_{W,j}\right)\, dP_{W,j}$$

where $R_{W,j}$ represents the reserve cost coefficient of the j$^{th}$ WT generator. Further, the generated power probability determination of various WT generators at different wind speeds is presented in the later section.

### 3.7.4 Cost Assessment of Uncertainties for SPV Generators

Also, The generated power from SPV system in the power network is uncertain in nature. The procedure to solve under and over estimation of SPV generators is similar to that used for WT generators except that the solar radiation is expressed by a lognormal PDF. In this study, the penalty and reserve costs models are introduced as in [135]. Anyway, the penalty cost for the k$^{th}$ SPV generators is written as follows:

$$C_{U_{S,K}}\left(P_{S_{a,K}} - P_{S_{s,K}}\right) = p_{S,K}\left(P_{S_{a,K}} - P_{S_{s,K}}\right) \tag{3.33}$$
$$= p_{S,K}\cdot F_S\left(P_{S_{a,K}} > P_{S_{s,K}}\right)\cdot\left[\, E\left(P_{S_{a,K}} > P_{S_{s,K}}\right) - P_{S_{s,K}}\right]$$

Where $P_{S_{a,K}}$ *and* $P_{S_{s,j}}$ are the available and schedule output power from the K^th SPV generator, respectively, $p_{S,K}$ *is* the penalty cost coefficient pertaining to the K^th SPV generators, $F_S(P_{S_{a,K}} > P_{S_{s,K}})$ denotes to the probability of excess power generated by the k^th SPV generator compared to $P_{S_{a,K}}$ , and $E(P_{S_{a,K}} > P_{S_{s,K}})$ is the predictable surplus output power. In case of overestimation, the reserve cost is evaluated as follows:

$$C_{O_{S,K}}(P_{S_{s,K}} - P_{S_{a,K}}) = R_{S,K}(P_{S_{s,K}} - P_{S_{a,K}}) \tag{3.34}$$
$$= R_{S,K} \cdot F_S(P_{S_{a,K}} < P_{S_{s,K}}) \cdot [\, P_{S_{s,K}} - E(P_{S_{a,K}} < P_{S_{s,K}})]$$

Where $R_{S,K}$ represents the reserve cost coefficient of the K^th SPV generator, $F_S(P_{S_{a,K}} < P_{S_{s,K}})$ defines the shortage probability of the SPV generators, and $E\left(P_{S_{a,K}} < P_{S_{s,K}}\right)$ is the expected power of the SPV generator less than $P_{S_{s,K}}$.

### 3.7.5 Carbon Tax Model

The conventional thermal generators release gasses to the environment. When the generation from thermal generators increases, the emission gasses such as $SO_x$ and $NO_x$ also increase. The harmful emissions are represented in tons per hour (ton/hr) as follows:

$$E = \sum_{i=1}^{N_G} (a_i P_{cg,i}^2 + b_i\, P_{cg,i} + c_i) \times 0.01 + \omega_i e^{(P_{cg,i}\, \mu_i)} \tag{3.35}$$

Where $a_i, b_i, c_i, \omega_i$ *and* $\mu_i$ denote the emission coefficients of the conventional thermal generators. These coefficients have values are like those in [136].

Recently, several countries are forcing a CT on harmful gas emissions to safeguard the environment, produce clean energy, and address global warming risks [137]. Moreover, the energy production companies are subjected to enormous pressure to generate clean energy from RES and/or to reduce their emissions. In this thesis, a CT is imposed on the gas emissions model. The carbon emission cost ($/hr) is formulated as follows:

$$C_{EC} = C_T \times E \tag{3.36}$$

Where $C_T$ carbon tax per unit value of gasses.

### 3.7.6 Objective Functions

In this thesis, the objective functions of the EED problem are expressed from different model components presented above in the previous subsections. In this thesis, there are two considered objective functions as follow:

**A. Minimization of Total Operating Costs**

The first objective function in this thesis is based on minimizing the sum of all costs without considering the emissions, while the second objective includes the emissions. So, the first objective will minimize:

$$\begin{aligned} F_1 = F(P_{cg}) &+ \sum_{j=1}^{N_W} \Big[ C_{W_j}\left(P_{W_{s,j}}\right) + C_{U_{w,j}}\left(P_{W_{a,j}} - P_{W_{s,j}}\right) \\ &+ C_{O_{w,j}}\left(P_{W_{s,j}} - P_{W_{a,j}}\right)\Big] \\ &+ \sum_{K=1}^{N_P} \left[ C_{S_k}\left(P_{S_{s,k}}\right) + C_{U_{S,K}}\left(P_{S_{a,K}} - P_{S_{s,K}}\right)\right. \\ &\left.+ C_{O_{S,K}}\left(P_{S_{s,K}} - P_{S_{a,K}}\right)\right] \end{aligned} \tag{3.37}$$

where $N_W$ $and$ $N_P$ are the number of WT and SPV generators, respectively.

Considering CT's modeling, the second objective function is formulated by adding the carbon emission cost as follows:

$$\begin{aligned} F_2 = F(P_{cg}) &+ \sum_{j=1}^{N_W} \Big[ C_{W_j}\left(P_{W_{s,j}}\right) + C_{U_{w,j}}\left(P_{W_{a,j}} - P_{W_{s,j}}\right) \\ &+ C_{O_{w,j}}\left(P_{W_{s,j}} - P_{W_{a,j}}\right)\Big] \\ &+ \sum_{K=1}^{N_P} \left[ C_{S_k}\left(P_{S_{s,k}}\right) + C_{U_{S,K}}\left(P_{S_{a,K}} - P_{S_{s,K}}\right)\right. \\ &\left.+ C_{O_{S,K}}\left(P_{S_{s,K}} - P_{S_{a,K}}\right)\right] + C_{EC} \end{aligned} \tag{3.38}$$

Further, the two above objective functions are subjected to equality and inequality constraints as described below.

### B. Minimization of Real Power Losses

The minimizing of real power losses is considered as one of the most major issue targets for system operators that can be described as follows [130]:

$$P_L = \sum_{k=1}^{n_l} G_k[V_i^2 + V_j^2 - 2V_iV_j cos(\theta_i - \theta_j)] \tag{3.39}$$

where $P_L$ is the real power loss, $G_k$ is the conductance of $k$'th line, $V_i$ ,$V_j$, $\theta_i$ and $\theta_j$ indicate to the voltage magnitudes and their angles at buses i and j, respectively.

### C. Minimization of Voltage Deviations at Load Buses

To guarantee the system's security, one of the most important indicators is decreasing the voltage deviations of load buses to get a sound voltage profile. The voltage deviations can be represented as follows [130]:

$$V_D = \sum_{j=1}^{N_L} |V_k - 1| \tag{3.40}$$

where a nominal value is 1 p.u. which is taken as a reference value. $N_L$ is the total number of load buses.

### D. Equality Constraints

The equality constraints illustrate the typical load flow equations that are used for power balancing as follows:

$$P_{Gi} - P_{Di} - V_i \sum_{j=1}^{N_L} V_j(G_{ij}\cos\theta_{ij} + B_{ij}\sin\theta_{ij}) = 0 \tag{3.41}$$

$$Q_{Gi} - Q_{Di} - V_i \sum_{j=1}^{N_L} V_j(G_{ij}\sin\theta_{ij} - B_{ij}\cos\theta_{ij}) = 0 \tag{3.42}$$

where $P_{Gi}$ and $Q_{Gi}$ are the real and reactive power generated, respectively. While $P_{Di}$ and $Q_{Di}$ are demand real and reactive power of bus j, respectively. $G_{ij}$ is the transfer conductance between two buses and $B_{ij}$ is the susceptance between two buses.

### E. Inequality Constraints

The inequality constraints are the operating limits for the components of the power system and the security constraints related to the lines and load buses.

- **Generator Constraints**

The voltages and active power at all generating buses should be limited within their upper and lower values:

$$V_{Gi}^{min} \leq V_{Gi} \leq V_{Gi}^{max} \quad , \qquad i = 1,2,3 \dots, N_T \tag{3.43}$$

$$P_{cg,i}^{min} \leq P_{cg,i} \leq \ P_{cg,i}^{max} \ , \qquad i = 1,2,3 \dots, N_g \tag{3.44}$$

$$P_{W_{s,j}}^{min} \leq P_{W_{s,j}} \leq P_{W_{s,j}}^{max} \ , \qquad j = 1,2,3 \dots, N_W \tag{3.45}$$

$$P_{S_{s,K}}^{min} \leq \ P_{S_{s,K}} \leq P_{S_{s,K}}^{max} \ , \qquad k = 1,2,3 \dots, N_P \tag{3.46}$$

$$Q_{cg,i}^{min} \leq Q_{cg,i} \leq \ Q_{cg,i}^{max} \ , \qquad i = 1,2,3 \dots, N_g \tag{3.47}$$

$$Q_{W_{s,j}}^{min} \leq Q_{W_{s,j}} \leq Q_{W_{s,j}}^{max}, \qquad j = 1,2,3 \dots, N_W \tag{3.48}$$

$$Q_{S_{s,K}}^{min} \leq \ Q_{S_{s,K}} \leq Q_{S_{s,K}}^{max} \ , \qquad k = 1,2,3 \dots, N_P \tag{3.49}$$

$$S_{li} \leq S_{li}^{max} \ , \quad i = 1,2,3 \dots, N_l \tag{3.50}$$

$$V_{Li}^{min} \leq V_{Li} \leq V_{Li}^{max} \ , \qquad i = 1,2,3 \dots, N_L \tag{3.51}$$

where $N_T$ the total number of generator buses. Eq. (3.43) represents the voltage limits on the generator buses. Eqs. (3.44)−(3.49) represent active power limits for the conventional thermal generators, WT, and SPV generators. Eqs. (3.50)−(3.51) denote reactive power capabilities for all generating buses.

- **Constraints of Line and Load Bus Voltages**

where $S_{li}$ is the apparent power of the line i'th. $S_{li}^{max}$ denotes the maximum limit of the apparent power of line i'th. $V_{Li}^{min}$ , $V_{Li}^{max}$ are the minimum and maximum voltage magnitude at load buses, respectively. $N_l$ denotes the total number of transmission lines.

### 3.7.7 Stochastic Wind Power and Solar Power Uncertainty Models

To determine the mean power of WT generators, Weibull PDFs are used [138] as follows:

$$f_v(v)=\frac{K}{C}\cdot\left(\frac{v}{C}\right)^{K-1}.e^{-\left(\frac{v}{C}\right)^{K}} \tag{3.52}$$

where $v$ is the wind speed m/s, while $K$ is the Weibull distribution shape parameter or the slope parameter, which is a kind of numerical parameter of a parametric family of probability distributions., and $C$ is the Weibull distribution scale parameter or characteristic life that is also a special kind of numerical parameter of probability distributions.

The mean of Weibull distribution is defined,

$$M_{wt}=C\,.\,\Gamma\left(1+{}^{1}/_{K}\right) \tag{3.53}$$

The gamma function is computed as:

$$\Gamma X=\int_{0}^{\infty} t^{X-1}e^{-t}\,dt \quad , X>0 \tag{3.54}$$

The output of WT generators essentially depends on the wind speed and the power curve of WT [41] and is expressed as follows:

$$P_w(v)=\begin{cases} 0 & v\le v_{ci}\ \ \&\ \ v>v_{co} \\ \dfrac{v^2-v_{ci}^2}{v_{nom}^2-v_{ci}^2}\,.\,P_{W_r} & v_{ci}< v\le v_{nom} \\ P_{W_r} & v_{nom}< v\le v_{co} \end{cases} \tag{3.55}$$

where $v_{ci}$ , $v_{co}$ , and $v_{nom}$ denote the cut-in, cut-out and rated wind speed of the WT, respectively. Whilst $P_{W_r}$ represent the rated power from the WT. With reference to Eq.29, one can observe that if $v$ is above $v_{co}$ and below $v_{ci}$ , there is no output power. Also, the WT produces power when wind speed between $v_{nom}$ and $v_{co}$. Probabilities are described for these discrete zones as follows [26]:

$$F_w(P_w)\{P_w=0\}=1-\exp\left(-\left(\frac{v_{ci}}{C}\right)^{k}\right)+\exp\left(-\left(\frac{v_{co}}{C}\right)^{k}\right) \tag{3.56}$$

$$F_w(P_w)\{P_w = P_{wr}\} = \exp\left(-\left(\frac{v_{nom}}{C}\right)^k\right) - \exp\left(-\left(\frac{v_{co}}{C}\right)^k\right) \tag{3.57}$$

In contrast to the mentioned discrete zones, the output power of WT is continuous between rated and cut-in speeds of wind. So, the probability for this zone can be described as follows [26]:

$$F_w(P_w)=\frac{K(v_{nom}-v_{ci})}{C^K * P_{wr}}\left(v_{ci}+\frac{P_w}{P_{wr}}(v_{nom}-v_{ci})\right)^{k-1} * \exp\left(-\left(\frac{v_{ci}+\frac{P_w}{P_{wr}}(v_{nom}-v_{ci})}{c}\right)^k\right) \tag{3.58}$$

Similarly, when the weather conditions are more dispersive, the lognormal function is used to describe the frequency distribution quite better. The mean and standard deviation (STD) of the global irradiation are utilized to compute the parameters for the lognormal distribution function. The output of SPV generators is directly proportional to the solar irradiance (I) that follows the lognormal PDF. The solar irradiance probability is described as follows:

$$f_I(I)=\frac{I}{I\boldsymbol{\mu}\sqrt{\boldsymbol{2\pi}}} \cdot e^{\left(\frac{-[\ln X-\sigma]^2}{2\mu}\right)}, \quad I>0 \tag{3.59}$$

where $\mu$ and $\sigma$ are the mean and STD, respectively. The lognormal distribution mean is expressed as follows:

$$M_{ld}=e^{\left(\boldsymbol{\sigma}+\frac{\boldsymbol{\mu}^2}{2}\right)} \tag{3.60}$$

The direct relationship between solar irradiance and energy for the SPV system is described as [139].

$$P_{sr}(I)=\begin{cases} P_{sr}\left(\frac{I^2}{I_{sr}I_c}\right) & ; \quad 0<I<I_c \\ P_{sr}\left(\frac{I}{I_{sr}}\right) & ; \quad I>I_c \end{cases} \tag{3.61}$$

where $P_{sr}$ is the rated output from SPV generator, $I_c$ define a specific irradiance point, and $I_{sr}$ is the solar irradiance at rated environment. It is significant to notice that scheduled power does not have a constant value rather there is a mutually known power between the system operators and the private side that sells solar power. The following equations are utilized to calculate the under and overestimation costs of the SPV generators [133].

$$C_{U_S}(P_{S_a} - P_{S_s}) = p_S(P_{S_a} - P_{S_s}) = p_S \sum_{N=1}^{N+} [P_{S_{S+}} - P_{S_S}] * f_{ps+} \tag{3.62}$$

$$C_{O_S}(P_{S_s} - P_{S_a}) = R_S(P_{S_s} - P_{S_a}) = R_S \sum_{N=1}^{N-} [P_{S_S} - P_{S_{S-}}] * f_{ps-} \tag{3.63}$$

Where $P_{S_{S+}}$ and $P_{S_{S-}}$ denote the surplus power and shortage power. $f_{ps+}$ and $f_{ps-}$ represent the relative frequencies for the occurrence of $P_{S_{S+}}$ and $P_{S_{S-}}$.

# Chapter 4

## Recent and Developed Optimization Techniques for Solving EED and DEED Problems

- *Introduction*
- *Conventional MRFO and Hybrid MRFO-GBO Algorithms*
- *Conventional AEO and Developing Chaotic AEO Algorithms*
- *Conventional SMA and Improving SMA Algorithms*
- *Original MPA and Modified MPA Algorithms*
- *Original Supply Demand Based Optimization*
- *Eagle Strategy Chaotic Supply Demand Based Optimization*
- *Multi-Objective Salp Swarm Algorithm (MSSA)*
- *Conventional Bonobo Optimizer (BO) and Chaotic BO Algorithms*

# Chapter 4

# Recent and Developed Optimization Techniques for Solving EED, DEED Problems

## 4.1 Introduction

In mathematics and computer science, the optimization process is called mathematical programming as it is related to computer programming. The optimization process is used in different fields especially engineering systems. It is applied to obtain the best solution of the single objective function or multi-objective function between numbers of variables under desired constraints. Many optimization algorithms are suggested in this thesis to solve the EED, EED Considering Stochastic Renewable Energy Resources, and DEED problems. In addition, different enhancements and improvements are proposed to improve the performance of the conventional algorithm. These algorithms are:

- MRFO, MRFO-GBO and MOMRFO-GBO.
- AEO, CAEO and MOCAEO.
- SMA, ISMA and MOISMA.
- MPA, MMPA and MOMMPA.
- SDO.
- ESCSDO.
- MSSA.
- BO and CBO.

## 4.2 Conventional MRFO and Hybrid MRFO-GBO Algorithms

### 4.2.1 Manta Ray Foraging Optimization (MRFO) Algorithm

Manta Ray Foraging Optimization (MRFO) proposed by Zhao et al. in 2020 [140]. It mimics the Manta ray behavior. MRFO is formulated by imitating the main foraging strategies such as chaining, cyclone, and somersault. Figure 4.1 shows the movement of the manta ray to find the foraging.

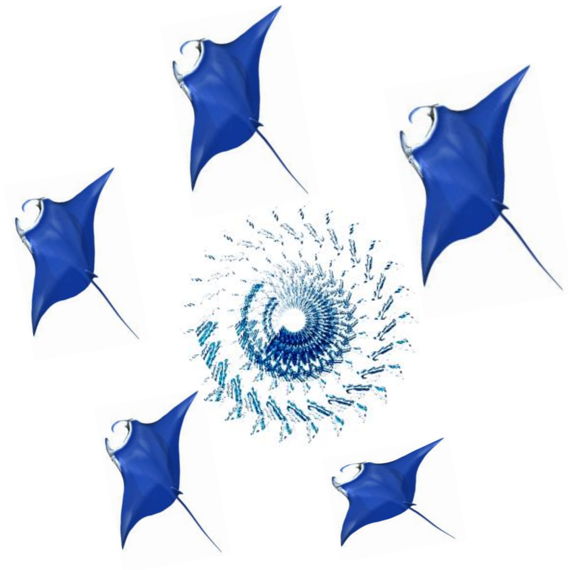

Figure 4.1: Foraging behavior in MRFO.

Even though MRFO is similar to several meta-heuristic algorithms, its initialization step is defined randomly by (4.1).

$$X_{ij}(:) = Lb_{ij} + r(:) \times \left(Hb_{ij} - Lb_{ij}\right)\forall_i \in N_{pop}, j \in N_{Var} \tag{4.1}$$

The Manta ray behavior is modified to the best foodstuffs in the chaining strategies using the mathematical formula given in (4.2) to change their positions ($X_{ij}$).

$$X_{i,j}(t+1) = \begin{cases} X_{i,j}(t) + \left(X_{best,j}(t) - X_{i,j}(t)\right) \times (r(:) - \lambda)\Delta\forall_i = 1, j \in N_{Var} \\ X_{i,j}(t) + \left(X_{i-1,j}(t) - X_{i,j}(t)\right) \times (r(:) - \lambda)\Delta\forall_i > 1 : N_{pop} \end{cases} \tag{4.2}$$

$$\varphi = 2 \times r(:) \times \sqrt{\left|\log\left(r(:)\right)\right|} \tag{4.3}$$

On the other hand, the swarm is swimming in a spiral similar to cyclones after noticing the foodstuff. At last, the latest Manta ray positions are adjusted around the best position in this operator scheme using the formula expressed in (4.4).

$$X_{i,j}(t+1) = X_{i,j}(t) + SF \times \left(r_2 X_{best,j} - r_3 X_{i,j}(t)\right) \Delta\forall_i \in N_{pop} \tag{4.4}$$

$X_{best,j}$ can be defined as depicted in (4.5) which defines the best location with high food concentration. If the low concentration is verified, the random position is set as shown in (4.8).

$$X_{i,j}(t+1) = \begin{cases} X_{best,j}(t) + \Delta X_{i,j} \times (r-\beta) \Delta\forall_i = 1, j \in N_{Var} \\ X_{best,j}(t) + r \times \left(x_{i-1,j}(t) - X_{i,j}(t)\right) + \beta \times \Delta X_{i,j} \Delta\forall_i > 1{:}\, N_{pop} \end{cases} \tag{4.5}$$

$$\beta = 2 \times exp\left(r_1 \times \frac{T_{max} - t + 1}{T_{max}}\right) \times \sin(2\pi r_1) \tag{4.6}$$

$$X_{i,j}(t+1) = \begin{cases} X_{rand}(t) + \Delta X_{i,j} \times (r-\beta) \Delta\forall_i = 1, j \in N_{Var} \\ X_{best,j}(t) + r \times \left(x_{i-1,j}(t) - X_{i,j}(t)\right) + \beta \times \Delta X_{i,j} \Delta\forall_i > 1{:}\, N_{pop} \end{cases} \tag{4.7}$$

$$X_{rand}(:) = Lb + r(:) \times (Hb - Lb) \tag{4.8}$$

In fact, metaheuristic algorithms share two specific behaviors, exploration and exploitation. Based on these two behaviors, metaheuristic algorithms have superiority over other algorithms [141]. In MRFO, if $t/T_{max}$ is less than rand, the cycle of exploitation will be performed, otherwise, search spaces will be performed. $N_{pop}$, $T_{max}$, and $SF$ describe the MRFO control system, which should be carefully followed to ensure its good performance.

### 4.2.2 Hybrid MRFO- GBO Algorithm

#### 4.2.2.1 Gradient-Based Optimizer

The original Gradient Based Optimizer (GBO) [142], combines gradient and population-based approaches, it utilizes the newton's method that specifies the search direction to examine the search domain with the use of a group of vectors and two main operators, namely gradient search rule (GSR) and local escaping operators (LEO).

*A. Initialization Process*

Like many algorithms, the original GBO comprises $N$ vector (members of populations) in the D-dimensional search space. The initial population is randomly produced by the following way:

$$X_n = X_{min} + rand(0,1) \times (X_{max} - X_{min}) \tag{4.9}$$

where $X_n$ refers to the nth vector, $X_{min}, X_{max}$ are the limits of the solution space in each problem and $rand(0,1)$ denotes a random number defined in the range of [0, 1].

*B. Gradient Search Rule (GSR) Process*

In the GBO algorithm, GSR is based on the gradient-based method where the aim of using the GSR is exploration tendency improvement and increasing the convergence rate. Therefore, the new position $X_{n+1}$ is defined as:

$$X_{n+1} = X_n - \frac{2\Delta x \times f(X_n)}{f(X_n + \Delta x) - f(X_n - \Delta x)} \tag{4.10}$$

The Eq. (4.10) will be adjusted to include the population-based search theory, which is presented by Eq. (4.11).

$$GSR = randn \times \frac{2\Delta x\, X_n}{(x_{worst} - x_{best} + \varepsilon)} \tag{4.11}$$

where $randn$ is a random number with a normal distribution, $x_{worst}, x_{best}$ denote the worst and best solutions obtained during the process of optimization, $\varepsilon$ denotes a small number within the interval [0, 0.1], and $\Delta x$ refers to the change in position at each iteration. From the previous equations, the GSR can be defined as:

$$GSR = randn \times \rho_1 \times \frac{2\Delta x\, X_n}{(x_{worst} - x_{best} + \varepsilon)} \tag{4.12}$$

where $\rho_1$ denotes the randomly generated parameter and it is calculated from the following equation:

$$\rho_1 = (2 \times\ rand \times \alpha) - \alpha \tag{4.13}$$

$$\alpha = \left|\beta\ \sin\left(\frac{3\pi}{2} + \sin\left(\beta\,\frac{3\pi}{2}\right)\right)\right| \tag{4.14}$$

$$\beta = \beta_{min} + (\beta_{min} - \beta_{min})\left(1 - \left(\frac{m}{M}\right)^3\right)^2 \tag{4.15}$$

where $\alpha$ represents a sine function for the transference from exploration to exploitation, $\beta_{min}$ and $\beta_{max}$ are constant values 0.2 and 1.2, respectively, $m$ is the current number of iteration, and $M$ represents the total number of iterations. The change $\Delta x$ between the best solution $x_{best}$ and a randomly chosen position $x_{r1}^{m}$ is given by:

$$\Delta x = rand(1{:}N) \times |step| \tag{4.16}$$

$$step = \frac{(x_{best} - x_{r1}^{m}) + \delta}{2} \tag{4.17}$$

$$\delta = 2 \times rand \times (\left|\frac{x_{r1}^{m} + x_{r2}^{m} + x_{r3}^{m} + x_{r4}^{m}}{4}\right| - x_{n}^{m}) \tag{4.18}$$

where $rand(1{:}N)$ denotes a random vector with N dimensions, $r1$, $r2$, $r3$, and $r4$ ($r1 \neq r2 \neq r3 \neq r4 \neq n$) are different integers randomly chosen from [1, N], $step$ denotes a step size. The new position $X_{n+1}$ represents updated based on the GSR as follows:

$$X_{n+1} = X_{n} - GSR \tag{4.19}$$

The direction of movement (DM) is added for better exploitation of the nearby area of $X_n$ which can be calculated as:

$$DM = rand \times \rho_2 \times (x_{best} - x_n) \tag{4.20}$$

$$\rho_2 = (2 \times\ rand \times \alpha) - \alpha \tag{4.21}$$

Therefore, the new position $X1_{n}^{m}$ is calculated from the following equation after taking the GSR and DM into consideration:

$$X1_{n}^{m} = x_{n}^{m} - \mathrm{GSR} + \mathrm{DM} \tag{4.22}$$

$$X1_{n}^{m} = x_{n}^{m} - randn \times \rho_1 \times \frac{2\Delta x \times x_{n}^{m}}{(x_{\mathrm{worst}} - x_{best} + \varepsilon)} + rand \times \rho_2 \times (x_{best} - x_{n}^{m}) \tag{4.23}$$

The GBO used another position to increase the local search by putting the best-so-far solution ($x_{\mathrm{best}}$) rather than the position $x_{n}^{m}$. The new positon ($X2_{n}^{m}$) is calculated as follows:

$$X2_{n}^{m} = x_{\mathrm{best}} - randn \times \rho_1 \times \frac{2\Delta x \times x_{n}^{m}}{(yp_{n}^{m} - yq_{n}^{m} + \varepsilon)} + rand \times \rho_2 \times (x_{r1}^{m} - x_{r2}^{m}) \tag{4.24}$$

where

$$yp_n = rand \times (\frac{[z_{n+1}+x_n]}{2} + rand \times \Delta x) \tag{4.25}$$

$$yq_n = rand \times (\frac{[z_{n+1}+x_n]}{2} - rand \times \Delta x) \tag{4.26}$$

According to the positions$X1_n^m$, $X2_n^m$, and the current position ($X_n^m$), the new position at the next iteration ($x_n^{m+1}$) is defined as:

$$x_n^{m+1} = r_a \times (r_b \times X1_n^m + (1 - r_b) \times X2_n^m) + (1 - r_a) \times X3_n^m \tag{4.27}$$

$$X3_n^m = X_n^m - \rho_1 \times (X2_n^m - X1_n^m) \tag{4.28}$$

*C. Local Escaping Operator (LEO)*

The LEO is applied to enhance the performance of the GBO algorithm and to escape the local solutions for solving the complicated problems. The LEO generates an appropriate solution ($X_{LEO}^m$) by using several solutions, which include $x_{\text{best}}$, the solutions $X1_n^m$, and $X2_n^m$, two random solutions $x_{r1}^m$ and$x_{r2}^m$, and a new randomly generated solution ($x_k^m$). The solution $X_{LEO}^m$ is formulated as:

$if\ rand < pr$

$if\ rand < 0.5$

$$X_{LEO}^m = X_n^{m+1} + f_1 \times (u_1 \times x_{\text{best}} - u_2 \times x_k^m) + f_2 \times \rho_1 \times (u_3 \times (X2_n^m - X1_n^m) + u_2 \times (x_{r1}^m - x_{r2}^m))/2$$

$X_n^{m+1} = X_{LEO}^m$

$Else$ (4.29)

$$X_{LEO}^m = x_{\text{best}} + f_1 \times (u_1 \times x_{\text{best}} - u_2 \times x_k^m) + f_2 \times \rho_1 \times (u_3 \times (X2_n^m - X1_n^m) + u_2 \times (x_{r1}^m - x_{r2}^m))/2$$

$X_n^{m+1} = X_{LEO}^m$

$End$

$End$

where $f_1$ denotes a uniform distributed random number in the range of [-1,1], $f_2$is a random number from a normal distribution with a mean of 0 and a standard deviation of 1, $pr$ is the probability, and $u_1$, $u_2$, and $u_3$ are random values generated as follows:

$$u_1 = \begin{cases} 2 \times rand & if\ \mu_1 < 0.5 \\ 1 & otherwise \end{cases} \tag{4.30}$$

$$u_2 = \begin{cases} rand & if\ \mu_1 < 0.5 \\ 1 & otherwise \end{cases} \tag{4.31}$$

$$u_3 = \begin{cases} rand & if\ \mu_1 < 0.5 \\ 1 & otherwise \end{cases} \tag{4.32}$$

where $rand$ represents a random number in the range of [0, 1], and $\mu_1$ refers to a number in the range of [0, 1]. The above equations are simply explained as follows:

$$u_1 = L_1 \times 2 \times rand + (1 - L_1) \tag{4.33}$$

$$u_2 = L_1 \times rand + (1 - L_1) \tag{4.34}$$

$$u_3 = L_1 \times rand + (1 - L_1) \tag{4.35}$$

where $L_1$ denotes a binary parameter with a value of 0 or 1. If parameter $\mu_1$<0.5, the value of $L_1$ = 1, otherwise, $L_1$= 0. The solution $x_k^m$ is generated as follows:

$$x_k^m = \begin{cases} x_{rand} & if\ \mu_2 < 0.5 \\ x_p^m & otherwise \end{cases} \tag{4.36}$$

$$x_{rand} = X_{min} + rand(0,1) \times (X_{max} - X_{min}) \tag{4.37}$$

where $x_{rand}$ is a random generated solution, $x_p^m$ is a randomly chosen solution of the population ($p \in [1, 2, \ldots, N]$), and $\mu_2$ represents a random number in the range of [0, 1]. Eq. (4.36) is simplified as:

$$x_k^m = L_2 \times x_p^m + (1 - L_2) \times x_{rand} \tag{4.38}$$

where $L_2$ denotes a binary parameter with a value of 0 or 1. If $\mu_2$<0.5, the value of $L_2$=1, otherwise, $L_2$=0.

#### 4.2.2.2 Shortcomings of Original MRFO Algorithm

The original MRFO algorithm simulates manta ray foraging behaviors Chain foraging, Cyclone foraging, and finally apply Somersault foraging. Applying these strategies randomly on solutions allow generated solutions to divers correctly sometimes, however in some optimization cases, the original MRFO algorithm get stuck in sub-regions, especially in complex and high dimensions problems. While each solution updates its position based on the previous one, reduces the algorithm convergence rate, and does not cover search space solutions effectively, leading to premature convergence in the MRFO algorithm [143]. Therefore, MRFO–GBO algorithm is proposed to solve these issues. The GBO algorithm operators like Local Escaping operator (LEO) is employed to avoid trapping into sub-regions, also solving premature convergence, since LEO strategy update solution following a robust strategy, with a randomly selected solution over search space to update solutions. Moreover, the intuitive and detailed process of MRFO-GBO is shown in Figure 4.2.

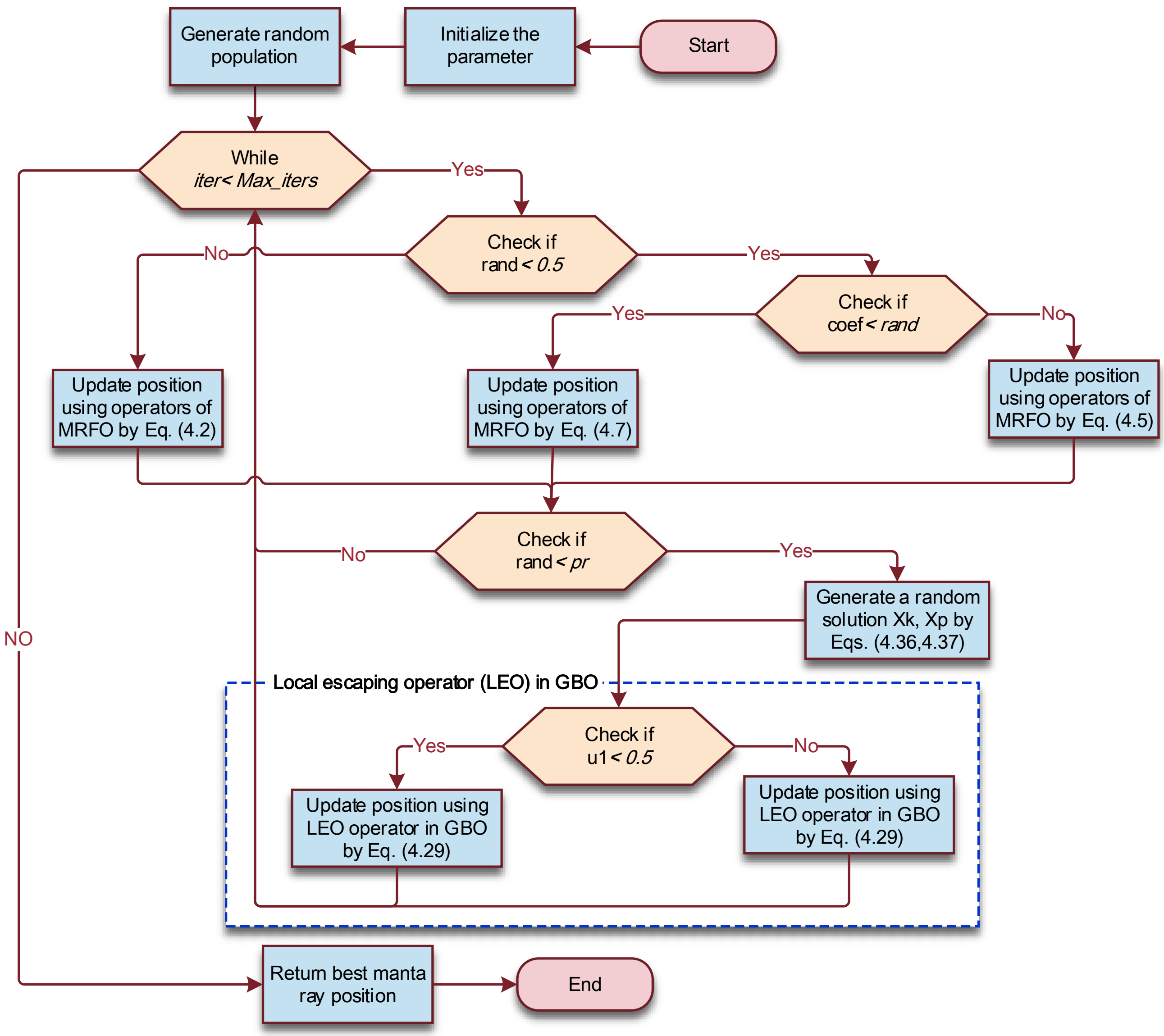


Figure 4.2: Flowchart of proposed MRFO–GBO algorithm based on MFRO and GBO algorithms.

## 4.3 Conventional AEO and Developing Chaotic AEO Algorithms

The conventional AEO method and Developing CAEO technique developed by using 10 chaotic maps are described in this section.

### 4.3.1 Artificial Ecosystem-Based Optimization (AEO) Algorithm

This subsection presents the conventional AEO algorithm was firstly developed by Zhao et al. This algorithm is based on the energy flow in a natural ecosystem [144]. An ecosystem is a group of living creatures, which exist in a specific area, and it demonstrates the ecological relations among these creatures. As any population-based optimization technique, AEO has included production, consumption, and decomposition behaviors of creatures on the earth and the sequence of those behaviors represent the energy flow in an ecosystem.

Figure 4.3 shows the energy flow in an ecosystem, wherever most producers (green plants) depend on the photosynthesis process to gets their food energy. After the green plants were growing, a number of the consumers (animals) feed only on a part of these plants, and these consumers are known as herbivores. Other animals are dividing into two types. One of them feeds on both plants and animals and they are called omnivores.

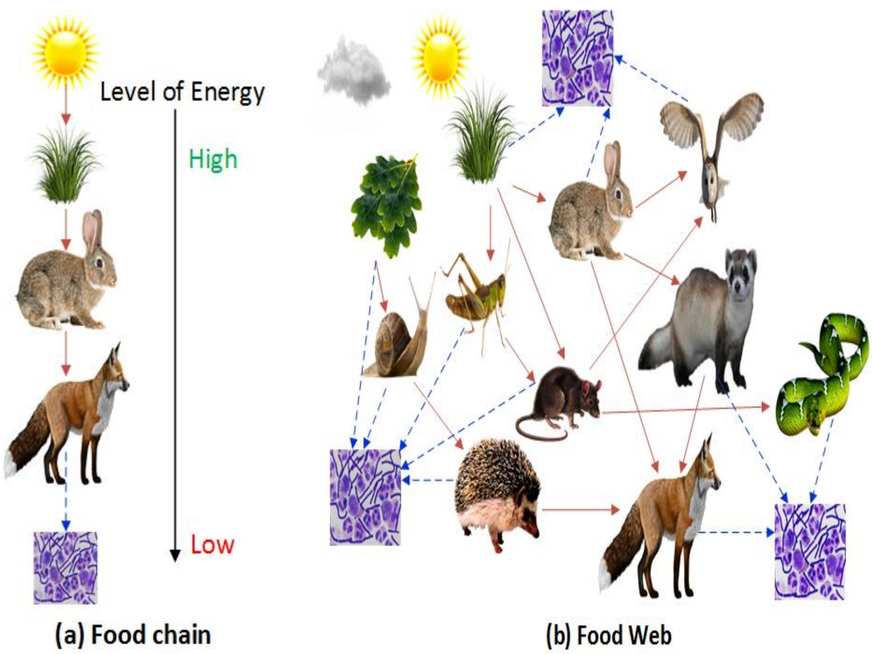


Figure 4.3: The energy Flow in an ecosystem.

The last type of animal is known as carnivores and this type eats only other animals. Decomposers are most bacteria and fungi. This phase starts once the producers and animals die when Decomposers convert them into small particles, like minerals, carbon dioxide, and water. The black arrow in Figure 3.a represents the various energy levels that reduce from plants (producers) to bacteria and fungi (decomposers), whereas the arrows within Figure 3.b refer to the energy transfer path.

Based on the previous discussion, the AEO consists of three operators;

i. The production is used to strengthen the balance between the exploration and exploitation phases,
ii. The role of consumption is an improvement of exploration,
iii. Decomposition is used to enhance the exploitation of the AEO.

The individuals in the population of the AEO algorithm are divided into three groups as follows, only one of them is a producer and only one is a decomposer, while all other individuals are consumers from the three predefined sorts and they have the same probability. The energy level of each individual is set by the fitness function of that individual.

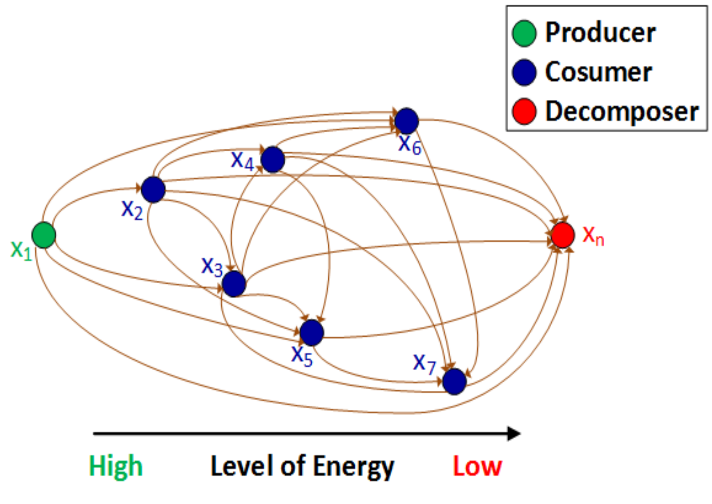


Figure 4.4: An ecosystem representation in the AEO technique.

The representation of the AEO technique is shown in Figure 4.4. The energy flow is represented by the brown arrows. $x_1$ (producer) is the worst individual and having the highest function fitness value and $x_n$ (decomposer) is the best individual having the lowest function fitness value. Consumers are the other individuals, and according to the previous classification of consumers, it is supposed that $x_2$ and $x_5$ are the types of herbivores, $x_3$ and $x_7$ are omnivores while $x_4$ and $x_6$ are carnivores.

#### 4.3.1.1 Production

The production operator can be modelled mathematically as follows:

$$x_1(t+1) = (1-a)x_n(t) + ax_{rand}(t) \tag{4.39}$$

$$a = (1 - \frac{t}{max\_iter})r_1 \tag{4.40}$$

$$x_{rand} = r(U_b - L_b) + L_b \tag{4.41}$$

where $a$ is a linear weight coefficient, $n$ is the population size, $x_{rand}$ is an individual position of randomly produced in the search space, $\max\_iter$ is the maximum number of iterations, $r_1$ is a random number within the range of [0, 1], $r$ is a random vector within the range of [0, 1], and $L_b$ and $U_b$ are the lower and upper limits, respectively.

#### 4.3.1.2 Consumption

A consumption parameter having the Levy flight feature is given as [144]:

$$C = \frac{1}{2}\frac{v_1}{|v_2|} \tag{4.42}$$

$$v_1 \sim N(0,1), \qquad v_2 \sim N(0,1), \tag{4.43}$$

where $N(0,1)$ is a normal distribution.

The following equations of three types of consumers depend on the randomly chosen and how each type of them deals with the producers and the other consumers where:

A. herbivore can be presented mathematically as follows:

$$x_i(t+1) = x_i(t) + C.\left(x_i(t) - x_1(t)\right), \quad i \in [2, \dots., n] \tag{4.44}$$

B. carnivore can be mathematically formulated as follows:

$$\begin{cases} x_i(t+1) = x_i(t) + C.\left(x_i(t) - x_j(t)\right), \\ i \in [2, \dots., n] \\ j = randi([2i-1]) \end{cases} \tag{4.45}$$

C. omnivore can be modeled mathematically as below:

$$\begin{cases} x_i(t+1) = x_i(t) + C.\left(x_i(t) - x_1(t)\right) + (1 - r_2) \\ \left(x_i(t) - x_j(t)\right), \quad i = 3, \dots, n \\ j = randi([2i - 1]) \end{cases} \tag{4.46}$$

#### 4.3.1.3 Decomposition

The i-th individual position $x_i$ in the population can be improved to the better position depending on the decomposer $x_n$ , the decomposition factor $D$, and the weight coefficients $e$ and $h$ as follow:

$$x_i(t+1) = x_n(t) + D.\left(e.x_n(t) - h.x_i(t)\right), \quad i = 1, \dots, n \tag{4.47}$$

$$D = 3u, \quad u \sim N(0,1) \tag{4.48}$$

$$e = r_3.randi([12]) - 1 \tag{4.49}$$

$$h = 2.r_3 - 1 \tag{4.50}$$

### 4.3.2 Proposed CAEO Techniques

The proposed CAEO technique is to improve early convergence of conventional AEO to local optimum or convergence to near-global optimum with an increase in the number of iterations and enhance the non-dominated solution of the algorithm to solve multi-objective functions to obtain the best value. This modification is based on chaotic maps. Instead of using random parameters, a set of chaotic equations [145] is used to improve the convergence properties of the conventional AEO. Table 4.1 presents the ten chaotic maps are applied for the conventional AEO to update the parameter of exploration q as below [146]:

$$q = y_{k+1} \tag{4.51}$$

where $y_{k+1}$ is the chaos map that is chosen to solve the problem and it is presented in Table 4.1. The description of CAEO is displayed in the flowchart of Figure 4.5.

Table 4.1: Different chaos maps.

| No. | Name | Chaotic map formula |
|---|---|---|
| CAEO1 | Chebyshev | $y_{k+1} = \cos(k \cos^{-1}(y_k))$ |
| CAEO2 | Circle | $y_{k+1} = \mathrm{mod}(y_k + b_1 - \left(\frac{b_2}{2\pi}\right)\sin(2\pi y_k), 1)$ <br> $b_1 = 0.5, b_2 = 0.2$ |

| | | |
|---|---|---|
| CAEO3 | Gauss/ mouse | $y_{k+1} = \begin{cases} 1 & y_k = 0 \\ \dfrac{1}{mod(y_k)} & otherwise \end{cases}$ |
| CAEO4 | Iterative | $y_{k+1} = \sin\left(\dfrac{b\pi}{y_k}\right), b = 0.7$ |
| CAEO5 | Logistic | $y_{k+1} = by_k(1\text{-}y_k), b = 4$ |
| CAEO6 | Piecewise | $y_{k+1} = \begin{cases} \dfrac{y_k}{H} & 0 \le y_k \le H \\ \dfrac{y_k - H}{0.5 - H} & H \le y_k \le 0.5 \\ \dfrac{1 - H - y_k}{0.5 - H} & 0.5 \le y_k \le 1 - H \\ \dfrac{1 - y_k}{H} & 1 - H \le y_k \le 1 \end{cases}, H = 0.4$ |
| CAEO7 | Sine | $y_{k+1} = \dfrac{b}{4}\sin(\pi\, y_k), b = 4$ |
| CAEO8 | Singer | $y_{k+1} = u\begin{pmatrix} 7.86{y_k}^1 - 23.31{y_k}^{12} \\ -28.75{y_k}^3 - 13.302875{y_k}^4 \end{pmatrix}, u = 1.07$ |
| CAEO9 | Sinusoidal | $y_{k+1} = by_k^1 \sin(\pi y_k), b = 2.3$ |
| CAEO10 | Tent | $y_{k+1} = \begin{cases} \dfrac{y_k}{0.7} & y_k < 0.7 \\ \dfrac{10}{3}(1 - y_k) & y_k \ge 0.7 \end{cases}$ |

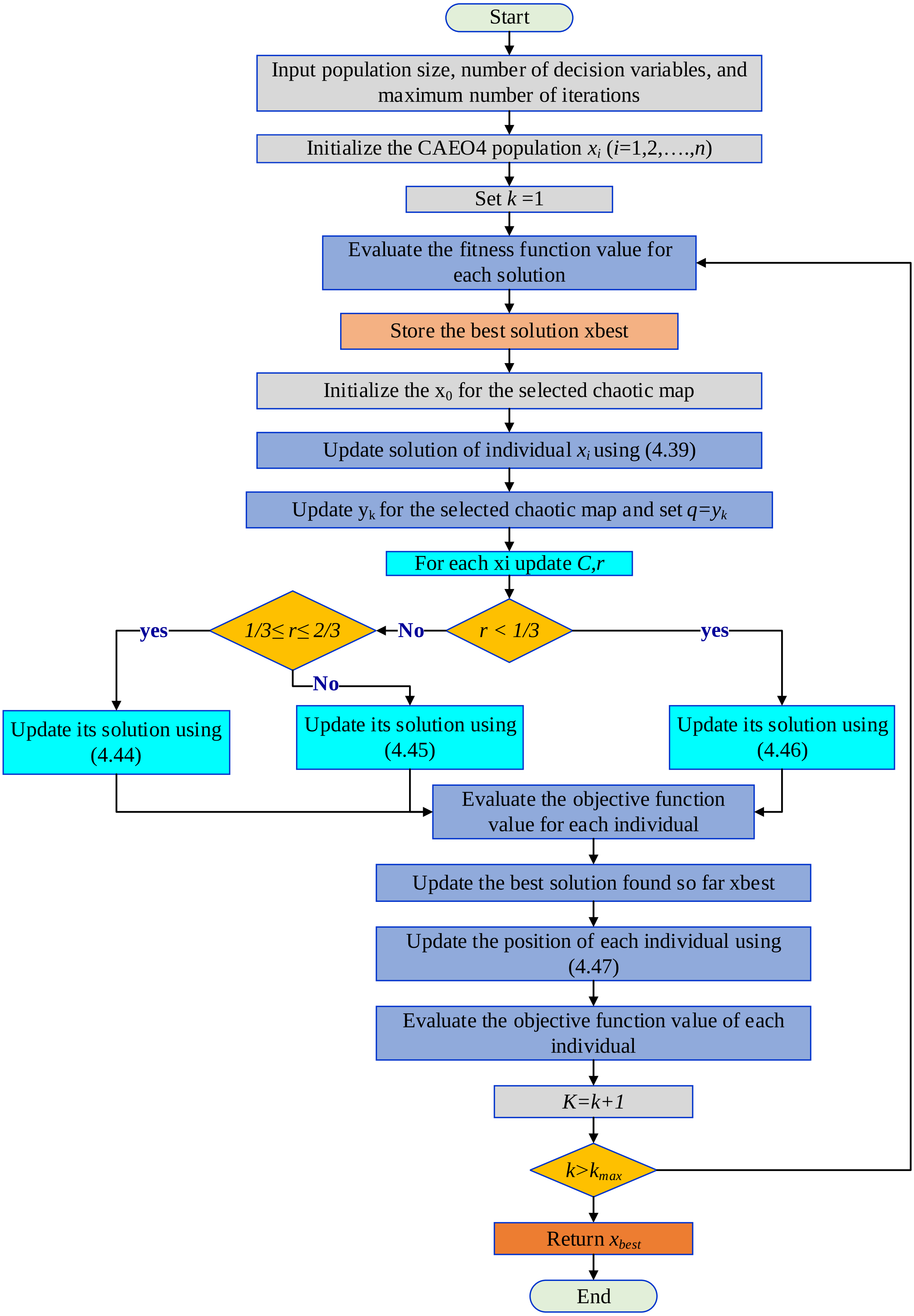


Figure 4.5: Flowchart of proposed CAEO4 technique.

### 4.3.3 Multi-objective 4th Chaotic Function Artificial Ecosystem-based Optimization (MOCAEO4) Algorithm

Two main structures called archive, and chaotic maps help to implement the Multi-objective $4^{th}$ chaotic function artificial ecosystem-based optimization (MOCAEO4) algorithm. The function of the archive is to organize the non-dominated solutions obtained so far while the chaotic maps are used to enhance the strength of AEO and to lead the individuals to update their position directly to the next best position. Finally, an appropriate decision-making approach is necessary to obtain the best compromise solution between the NDS [147]. The flow chart of the (MOCAEO4) algorithm is shown in Figure 4.6, which is used to solve the CEED problem.

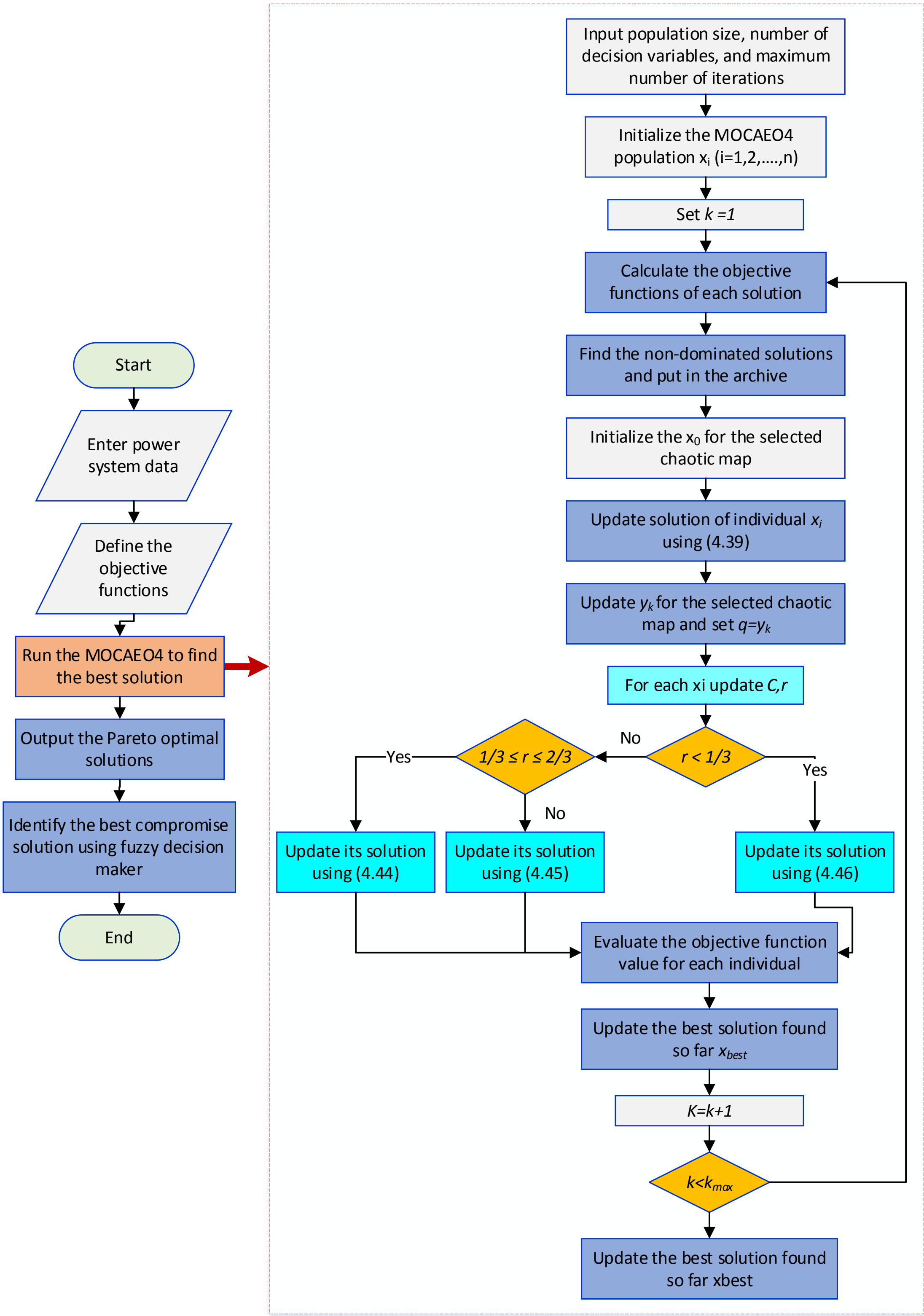


Figure 4.6: MOCAEO technique for the CEED problem.

## 4.4 Conventional SMA and Improving SMA Algorithms

### 4.4.1 Conventional Slime Mould Algorithm (SMA)

The slime mould mentioned often introduces the physarum polycephalum. It is named slime mould because it is listed as a fungus [148].

#### 4.4.1.1 Approach Food

SMA behavior is presented as the following mathematical model [149]. The following equations are presented to simulate the contraction method:

$$\overrightarrow{X(t+1)} = \begin{cases} \overrightarrow{X_b(t)} + \overrightarrow{vb} \cdot \left(\overrightarrow{W} \cdot \overrightarrow{X_A(t)} - \overrightarrow{X_B(t)}\right), r < p \\ \overrightarrow{vc} \cdot \overrightarrow{X(t)}, r \geq p \end{cases} \quad (4.52)$$

where, $\overrightarrow{vb}$ denotes to a parameter value with a range of $[-a, a]$, $\overrightarrow{vc}$ a value decreases linearly from 1 to 0. $t$ denotes to the tth iteration, $\overrightarrow{X_b}$ denotes to the individual position with the more odor focus currently found, $\vec{X}$ denotes to the position of slime mould (solution), $\overrightarrow{X_A}$ and $\overrightarrow{X_B}$ denote to two individuals randomly chosen from the population, $\overrightarrow{W}$ denotes the weight of slime mould (solution).

The $p$ value is calculated as:

$$p = \tanh|S(i) - DF| \quad (4.53)$$

where, $i \in 1, 2, 3, . \ldots, n$, $S(i)$ denotes to the fitness value of $\vec{X}$, $DF$ denotes to the best fitness taken over all iterations.

The $\overrightarrow{vb}$ value is calculated as follows:

$$\overrightarrow{vb} = [-a, a] \quad (4.54)$$

$$a = \operatorname{arctanh}(-\left(\frac{t}{\max\_iter}\right) + 1) \quad (4.55)$$

The $\overrightarrow{W}$ value is calculated as follows:

$$\overrightarrow{W(SmellIndex(i))} = \begin{cases} 1 + r \cdot log\left(\dfrac{bF - S(i)}{bF - wF} + 1\right), condition \\ 1 - r \cdot log\left(\dfrac{bF - S(i)}{bF - wF} + 1\right), \quad\quad others \end{cases} \quad (4.56)$$

$$SmellIndex = sort(S) \quad (4.57)$$

where, condition denotes that $S(i)$ ranks first half of the given solutions $r$ denotes to the random number in between $[0,1]$, $bF$ is the optimal fitness value found in the current iteration, $wF$ denotes the worst fitness found in the current iteration, $SmellIndex$ is the sequence of the sorted fitness function values. Figure 4.7 shows the impacts of (4.52).

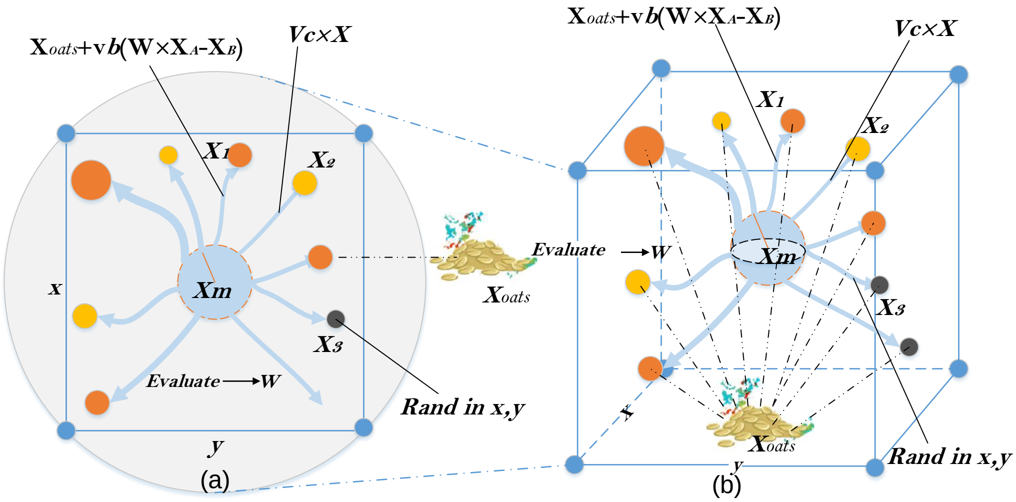


Figure 4.7: Potential positions in 2-dimensional and 3-dimensional.

#### 4.4.1.2 Wrap Food

When the food group is satisfied to extend to a region where the food concentration is low, the importance of that area will be decreased, thus turning to explore other areas of the food distribution, which are not as important as the food group. Figure 4.8 shows the rule of evaluating fitness functions for slime mould.

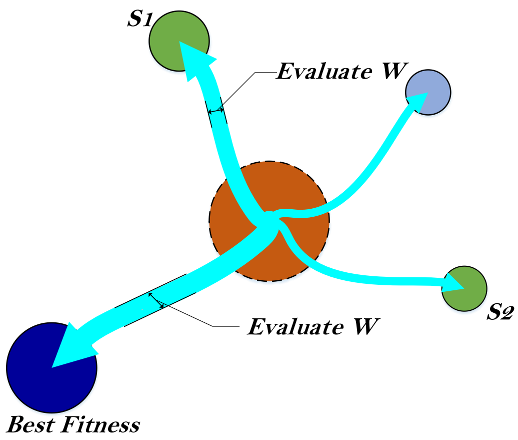


Figure 4.8: Evaluation of the fitness function.

The mathematical model for updating solution locations is as:

$$\overrightarrow{X^*} = \begin{cases} rand \cdot (UB - LB) + LB, rand < z \\ \overrightarrow{X_b(t)} + \overrightarrow{vb} \cdot \left(W \cdot \overrightarrow{X_A(t)} - \overrightarrow{X_B(t)}\right), r < p \\ \overrightarrow{vc} \cdot \overrightarrow{X(t)}, r \geq p \end{cases} \tag{4.58}$$

where, $LB$ and $UB$ are the lower bound and upper limits of the search space, $rand$ and $r$ are the random value in between [0,1], $z$ is a parameter within a range of [0, 0.1].

#### 4.4.1.3 Grabble Food

$\overrightarrow{vb}$ is a vector of random values between $[-a, a]$ and regularly approaches zero as the repetitions progress. The $\overrightarrow{vc}$ values are taken between [-1,1] and direct to zero ultimately. Synergistic cooperation between $\overrightarrow{vb}$ and $\overrightarrow{vc}$ simulates the particular behavior of slime mould. To find a more reliable source of food, even if slime mould got a better-feed source, it would yet distribute organic material for searching other regions to get a higher-class food source rather than spending all of it in one source. Algorithm 1 shows the general procedure of the SMA algorithm.

| Algorithm 1 Pseudo-code of SMA |
|---|
| Initialize the parameters *population size, dim, lb, ub, z,* $max\_iter$; |
| Initialize the set of random slime mould positions $X_i (i = 1,2, \dots, n)$; |
| **While** $(t \leq max\_iter)$ |

Calculate and sort the fitness of all slime mould;

$Update\ the\ bestFitness$ , *the worst fitness*

Calculate the *weight of slime mould (W)* by (4.56);

*update the best fitness,* $the\ best\ position(X_b)$

**For** $each\ search\ agent$

$Update\ p, vb, vc$;

$Update\ the\ Position\ of\ search\ agents\ by$ **Eq.** (4.58);

**End For**

$t = t + 1$;

**End While**

**Return** $bestFitness,\ the\ best\ position(X_b)$;

### 4.4.2 Improved Slime Mould Algorithm (ISMA)

The proposed ISMA is derived from the original SMA. In the proposed ISMA, two extra equations (4.59)-(4.60) are adopted from are [150] to enhance the search capabilities and to make a balance between the exploration and exploitation phases.

$$X_i^{t+1} = X_j^t + r_1 \times sin(r_2)\ |r_3\, p_i^t - X_j^t| \tag{4.59}$$

$$X_i^{t+1} = X_j^t + r_1 \times cos(r_2)\ |r_3\, p_i^t - X_j^t| \tag{4.60}$$

where $\mathrm{X}_\mathrm{j}^\mathrm{t}$ presents the current position of the ith solution, $\mathrm{r}_1, \mathrm{r}_2, \mathrm{r}_3$ are random number taken between zero and 1, and $\mathrm{p}_\mathrm{i}^\mathrm{t}$ presents the destination position in ith dimension. The mentioned two equations are used according to a random (rand) value, if the rand < 0.5, (4.59) will be executed; otherwise, (4.60) will be executed. These two equations are working after the SMA procedure in each iteration to keep the diversity of the solutions, which can help the SMA in avoiding getting stuck in local search and maintain an excellent coverage shape during the improvement process. The pseudo-code of ISMA is shown in Algorithm 2. Moreover, Figure 4.9 shows the procedure of ISMA in a flow chart.

Algorithm 2 Pseudo-code of ISMA

Initialize the parameters *population size, dim, lb, ub, z,* $max\_iter$;

Initialize the set of random slime mould positions $X_i (i = 1,2, \dots, n)$;

**While (**$t \leq max\_iter$)

Calculate and sort the fitness of all slime mould;

$Update\ the\ bestFitness$ , *the worst fitness*

Calculate the *weight of slime mould (W)* by **Eq.** (4.56);

*update the best fitness,* $the\ best\ position(X_b)$

**For** $each\ search\ agent$

Check **if** (rand<z)

Update slime mould positions $x_i$

**else**

**if** (rand<0.7)

$Update\ p, vb, vc$;

$Update\ the\ Position\ of\ search\ agents\ by$ **Eq.** (4.58);

**else**

$Update\ the\ Position\ of\ search\ agents\ by\ SCA$ by **Eqs.** (4.59), (4.60);

**End For**

$t = t + 1$;

**End While**

**Return** $bestFitness,\ the\ best\ position(X_b)$;

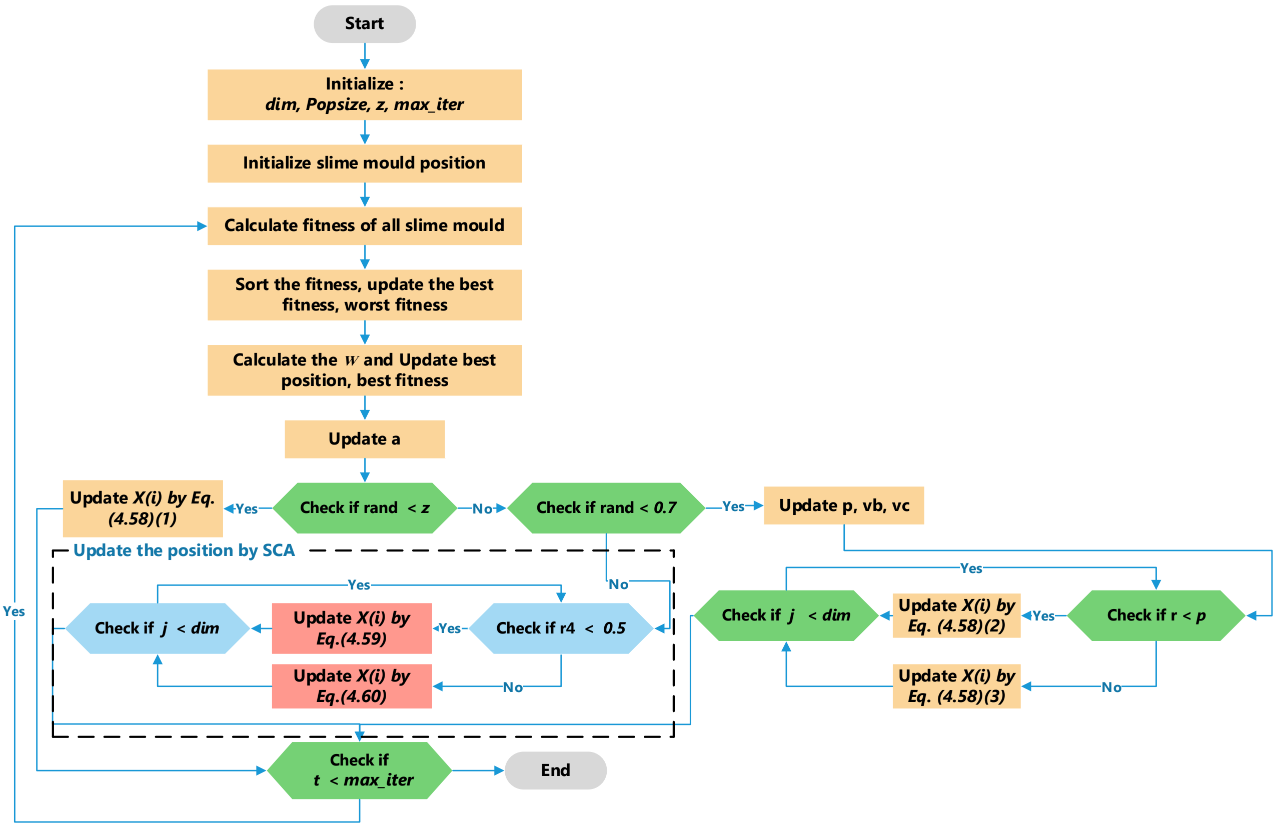


Figure 4.9: Flowchart of ISMA.

### 4.4.3 Proposed MOSMA and MOISMA

The multi-objective CEED problem, according to the Bi-objective function section, is defined as minimizing the total fuel cost and the emission simultaneously of thermal generating units of a power system while satisfying the constraints. Figure 4.10 displays the flow chart of the MOISMA technique, which is used to solve the multi-objective CEED problem. As the same approach, the MOSMA has been executed on the conventional SMA algorithm.

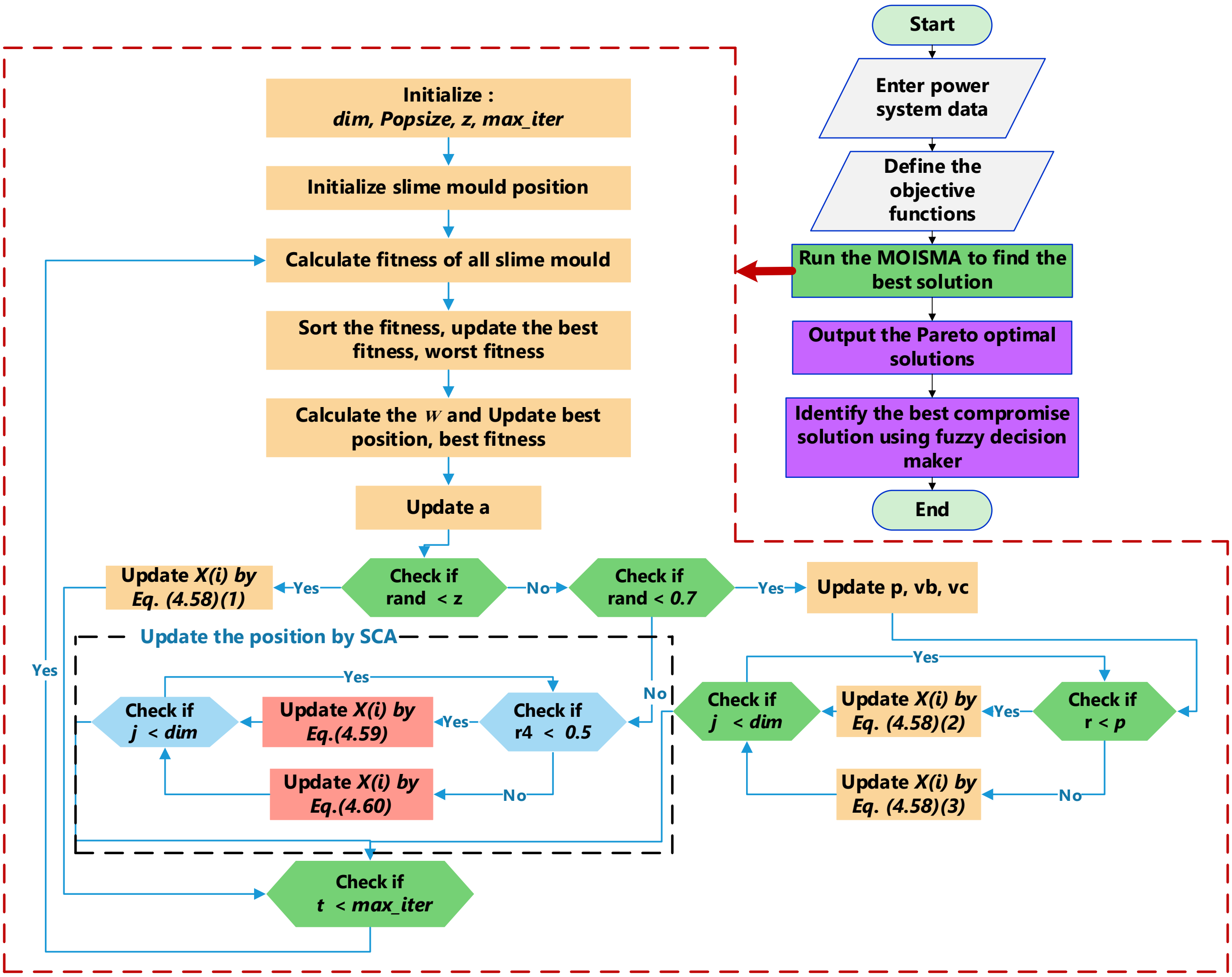


Figure 4.10: Flowchart of MOISMA.

Meta-heuristic optimization algorithms can be an attractive alternative to conventional optimization methods in several real applications. However, tuning exploration and exploitation phases are key to attain optimal solutions, especially in the case of multi-model optimization problems as in the case of CEED. From this perspective, in this section, we introduce a novel variant for Marine Predators to enhance its exploration and exploitation capabilities for global optimization problems and CEED real applications. The details of the proposed algorithm are explained below.

## 4.5 Original MPA and Modified MPA Algorithms

### 4.5.1 Original Marine Predators Algorithm

The MPA is a newly developed meta-heuristic algorithm that mimics the relation among the prey and predator in nature [151]. In nature, the main target of the creatures to survive is finding foods, not only the predators search for foods but also the prey. Utilizing the concept of this target, Faramarzi et al. [151] introduced the MPA by accounting for both a predator and a prey as solutions. MPA starts with a set of initial randomly drawn solutions for both, the predator and the prey, then these solutions are modified using the main structure of the MPA, as shown in Figure 4.11.

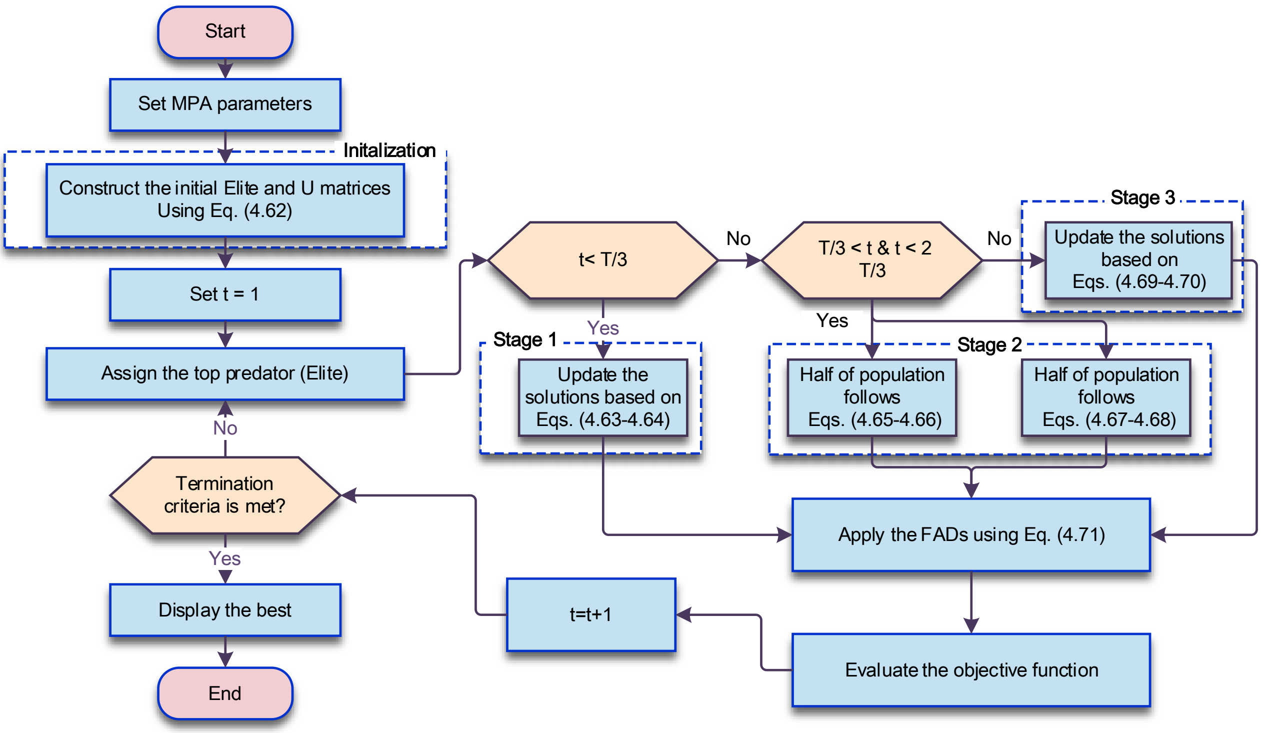


Figure 4.11: MPA flowchart.

The MPA starts with the initialization phase, where a random set of the solutions ($Inital_{solutions}$) can be generated for both the prey and predator based on the following formula:

$$Inital_{solutions} = lower + r_1 \times (upper - lower) \qquad (4.61)$$

where, $lower$ and $upper$ are the lower and upper limits in t-times search landscape, and $r_1$ refers to a random vector in the interval of (0,1). Using (15), the initial positions of the prey (U) and predator (Elite) can be determined as:

$$Elite = \begin{bmatrix} U_{11}^1 & U_{12}^1 & U_{13}^1 & \dots\dots\dots\dots\dots & \dots & U_{1d}^1 \\ U_{21}^1 & U_{22}^1 & U_{23}^1 & \dots\dots\dots\dots\dots & \dots & U_{2d}^1 \\ U_{31}^1 & U_{32}^1 & U_{33}^1 & \dots\dots\dots\dots\dots & \dots & U_{3d}^1 \\ \dots & \dots & \dots & \dots\dots\dots\dots\dots & \dots & \dots \\ U_{N1}^1 & U_{N2}^1 & U_{N3}^1 & \dots\dots\dots\dots\dots & \dots & U_{Nd}^1 \end{bmatrix},$$

$$U = \begin{bmatrix} U_{11} & U_{12} & U_{13} & \dots\dots\dots\dots\dots & \dots & U_{1d} \\ U_{21} & U_{21} & U_{23} & \dots\dots\dots\dots\dots & \dots & U_{2d} \\ U_{31} & U_{31} & U_{33} & \dots\dots\dots\dots\dots & \dots & U_{3d} \\ \dots & \dots & \dots & \dots\dots\dots\dots\dots & \dots & \dots \\ U_{N1} & U_{N2} & U_{N3} & \dots\dots\dots\dots\dots & \dots & U_{Nd} \end{bmatrix} \quad (4.62)$$

where, the $Elite$ matrix is the solution of the fittest predator, $d$ is the dimension of the considered optimization problem. The matrix of $U$ refers to the prey matrix.

After the initialization phase, three stages are implemented to mimics the behavior of the prey/predator in nature as depicted in Figure 4.11. The first stage states for the first third portion of the considered iteration numbers, then the second stage is executed for the second third of the iterations number, at the end the third stage is implemented for the last third in the iteration numbers. A high ratio in the velocity between the prey and predator is the main feature of the first stage, whereas unit- and low-velocity ratios are the features of the second and third stages, respectively. More details about each step are presented below.

Stage 1: The prey in this stage searches for its food in all places, thereby it moves very fast searching for its food while the predator stands and observes its motion (high ratio in the velocity between the prey and predator). Accordingly, the prey position $(U_i)$ is upgraded based on the following equations with step $(S_i)$.

$$S_i = R_B \otimes (\mathrm{Elite_i} - \mathrm{R_B} \otimes \mathrm{U_i}), \qquad \mathrm{i} = 1,2,3, \dots \mathrm{N} \quad (4.63)$$

$$U_i = U_i + P.R \otimes S_i \quad (4.64)$$

where, $R$ refers to a random vector drawn from a uniform distribution in the interval of [0 1] and p is a constant value, Feramarzi et al. [30] used P=0.5. The symbol $R_B$ is Brownian distribution. The ⊗ refers to the process of element-wise multiplications.

Stage 2: Both the prey and predator are moving to exploit the detected best locations. This is the intermediate stage in MPA; since it is the transition phase between exploration and exploitation phases. The predator uses a Brownian distribution to express its motion while the prey adopts the levy flight. Therefore, Faramarzi et al. [151], have divided the populations into two groups, the first group follows levy flight and the second group follows a Brownian distribution during their movement, as described below:

By using (19)-(20), the first group of the population (prey) can express its motion as:

$$S_i = R_L \otimes (\mathrm{Elite_i} - \mathrm{R_L} \otimes \mathrm{U_i}), \qquad \mathrm{i} = 1,2,3, \dots \mathrm{N}/2 \tag{4.65}$$

$$U_i = U_i + P.R \otimes S_i \tag{4.66}$$

where, $R_L$ is a vector that follows levy flight distribution. Equations (19)-(20) are implemented for the first group of the population which represents the exploitation stage.

The second group of the population (predator) follows the Brownian distribution while it updates its position as described in (21)-(22).

$$S_i = R_B \otimes (\mathrm{R_B} \otimes \mathrm{Elite_i} - \mathrm{U_i}), \qquad \mathrm{i} = \frac{\mathrm{N}}{2}, \dots\dots, \mathrm{N} \tag{4.67}$$

$$U_i = \mathrm{Elite_i} + P.CF \otimes S_i\,, \quad CF = \left(1 - \frac{t}{T}\right)^{\left(\frac{2\,t}{T}\right)} \tag{4.68}$$

where, $CF$ is a parameter that controls the step size of movement for the predator.

Stage 3: this is the last stage in the journey of searching the prey/predator for their food. The prey and predator are keeping moving with a low-velocity ratio to catch their food. The predator adopts a Levy flight in its step of motion ($S_i$) during updating its location to catch the prey.

$$S_i = R_L \otimes (\mathrm{R_L} \otimes \mathrm{Elite_i} - \mathrm{U_i}), \qquad \mathrm{i} = 1,2,3, \dots \mathrm{N} \tag{4.69}$$

$$U_i = \mathrm{Elite_i} + P.CF \otimes S_i\,, \quad CF = \left(1 - \frac{t}{T}\right)^{\left(\frac{2\,t}{T}\right)} \tag{4.70}$$

In MPA, Faramarzi et al. [151] realized the surrounded environmental conditions for the prey and predator therefore, the eddy formation and Fish Aggregating Devices' effect (FADS) have been considered as they have significant impacts on the prey/predator. Faramarzi et al. [151] modifies the position of the populations based on the FADS to avoid falling them into local optimum solutions. This stage can be calculated by the following equation:

$$\mathrm{U_i} = \begin{cases} U_i + CF\ [U_{min} + R \otimes (U_{max} - U_{min})] \otimes W & r_2 \leq FADs \\ U_i + [FADs\ (1-r) + r\ ]\ (U_{r1} - U_{r2}) & r_2 > FADs \end{cases} \tag{4.71}$$

In (25), Faramarzi et al. [151] assumed the FAD equals 0.2 and $W$ is a binary number (0 or 1). The $W$ number can be determined based on the value of the random solution, where if the random solution is less than or equal to 0.2, $W$ becomes 0, otherwise, it becomes 1. The symbol $r$ represents a random number while $r_1, r_2$ are the random indices of the prey.

In MPA, Faramarzi et al. [151] deemed the memory of the marine predator in nature as an essential feature to avoid falling into local solutions. The implementation is performed by saving the previous best solutions of a prior iteration and comparing them with the current ones. The solutions are modified based on the optimum solution during the comparison phase.

## 4.5.2 Modified Marine Predators Algorithm

### 4.5.2.1 Comprehensive Learning Strategy

The relations among the search agents in the population is the main stage in detecting the global solutions, therefore, exchanging the best experiences among the individual is an attractive strategy to ensure sharing the best experiences among all search agents and thereby avoiding premature convergence. The comprehensive learning strategy represents an indispensable part in balancing the structures of exploration and exploitation [152], [153], [154]. Each individual learns from other search agents' best experiences (exemplars) to preserve the diversity of the population to inhibit a premature convergence [152], [153], [154]. Here, the exemplar is selected based on learning probability values ($P_l$). The $P_l$ has different values for different agents and it can be calculated for each individual according to the following relation [152].

$$P_{l_i} = c + e * \frac{\left(\exp\left(\frac{10(i-1)}{N-1}\right) - 1\right)}{(\exp(10) - 1)} \tag{4.72}$$

where, $N$ is the number of population size, c and e are constants which have values of 0.05 and 0.25, respectively [152].

The selection strategy of the exemplars when using a CL approach is illustrated in Algorithm 1, where the learning probability value ($P_{l_i}$) of (26) is compared with a random number (r) and two agents are randomly drawn from the population with indexes ($F1_i^d, F2_i^d$) and their objective functions are compared. Then the following scenarios may be occurred:

- While the learning probability value ($P_{l_i}$) of (26) is greater than the random value (r), the exemplar may be selected based on the winner agent which has a less objective function (minimization process).
- While the learning probability value ($P_{l_i}$) of (26) is lower than the random value (r), the agent ($i$) will learn from its own therefore $F_i^d = i$.

Algorithm 1 Pseudo code of the CL strategy

**for** $i$ = 1 to $N$
Generate random number r
Calculate the learning probability value ($P_{l_i}$) of (26).
Select two random agents with indexes $F1_i^d, F2_i^d$ , d = 1,2,3,…..D.
**If** $P_{l_i} > r$
**If** $obj\left(U_{F1_i^d}\right) < obj(U_{F2_i^d})$
exemplar = $U_{F1_i^d}$
else
exemplar = $U_{F2_i^d}$
else
exemplar = $U_i$

The CL approach is used to boost the exploration ability of stage 1 using the best-experienced agents of the previous iteration. The CL is also used to enhance the transient stage between the exploration and intensification phases of stage 2 in the conventional MPA. Hence, stages 1 and 2 of the MPA are modified to gain from the best historical individuals while discovering the best solutions.

<u>CL applied in Stage 1</u>: In this stage, the prey moves very fast to search for its food. The searchability is improved by diverting the swarm and sharing beneficial information among the search agents. Based on this principle, Eq. (17) can be reformulated as:

$$S_i = R_B \otimes (\text{ Elite}_\text{i} - R_B \otimes + K * rand \otimes (U_{best_{F_i}} - U_i)), \qquad \text{i} = 1,2,3, \dots \text{N} \qquad (4.73)$$

$$U_i = U_i + P.R \otimes S_i \qquad (4.74)$$

where,

$$K = \left( a - b * \frac{t}{T} \right), \ \ t = 1,2,3, \ldots, T$$

where, rand is a drawn random number from [0 1] and K is a weighted coefficient. The value of K linearly decreases from a to b to enhance the exploration phase, which has values of 3 and 1.5, respectively. These values for a and b are defined based on numerous tries.

CL applied in Stage 2: In stage 2 of MPA, the velocity of the prey and predator becomes close. In this stage, the exploration phase transmits to the exploitation phase gradually. This is why Faramarzi et al. [151] divided the population into two halves, the exploration, and the exploitation groups, respectively. In the proposed MMPA, the CL approach is applied on both groups of (19)-(21) to enhance the transient stage between the exploration and exploitation and avoid premature convergence. Hence, the following equation can be obtained.

$$S_i = R_L \otimes \left( \mathrm{Elite_i} - \mathrm{R_L} \otimes \mathrm{U_i} + c1 * rand \otimes \left( U_{best_{F_i}} - U_i \right) \right), \quad \mathrm{i} = 1,2,3, \ldots \mathrm{N}/2 \tag{4.75}$$

$$U_i = U_i + P.R \otimes S_i \tag{4.76}$$

where,

$$c1 = \frac{1}{1 + \exp^{-\gamma * \frac{t}{T}}} + 2 * \left( \frac{t}{T} - 1 \right)^2, \qquad t = 1,2,3, \ldots, T$$

$$S_i = R_B \otimes \left( \mathrm{R_B} \otimes \mathrm{Elite_i} - \mathrm{U_i} + c2 \ * rand \otimes \left( U_{best_{f_i}} - U_i \right) \right), \quad \mathrm{i} = \frac{\mathrm{N}}{2}, \ldots, \mathrm{N} \tag{4.77}$$

$$U_i = \mathrm{Elite_i} + P.CF \otimes S_i \, , \quad CF = \left( 1 - \frac{t}{T} \right)^{\left( \frac{2\,t}{T} \right)} \tag{4.78}$$

where,

$$\mathrm{c2} = = \frac{1}{1 + \exp^{-\gamma * \frac{t}{T}}} + 2 * \left( \frac{t}{T} \right)^2, \qquad t = 1,2,3, \ldots, T$$

where, c1 and c2 refer to acceleration coefficients which defined by sigmond functions. The value of $\gamma = 0.0001$ allows to change c1 and c2 between [2.5- 0.5] and [0.5-2.5], respectively. These values are selected to maintain the smooth transition among the exploration and exploitation phases.

The main structure of the proposed MMPA is depicted in Figure 4.12.

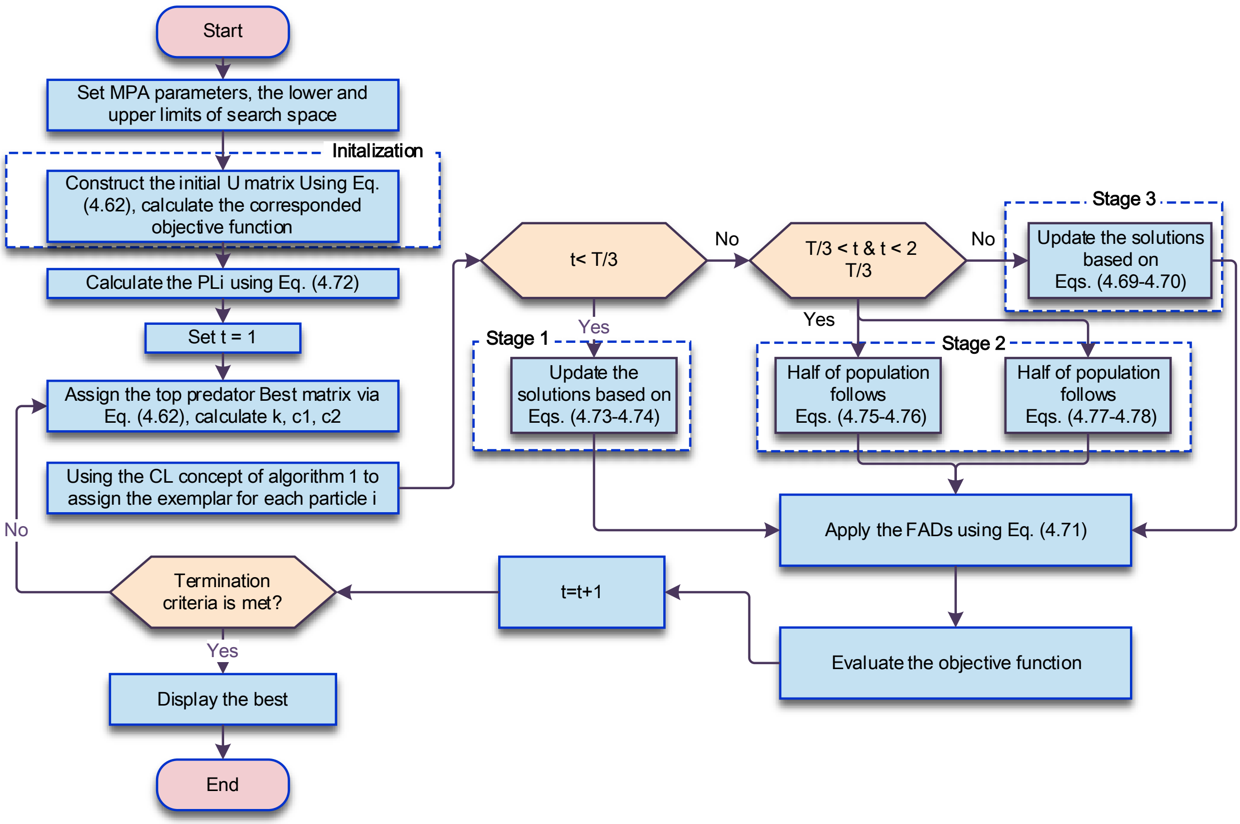


Figure 4.12: MMPA flowchart.

## 4.6 Original Supply Demand Based Optimization

The SDO technique assumes that there are several markets for commodities [155]. The quantity and cost of each product are standard. Overall, there are two modes of the supply–demand system, which are displayed in Figure 4.13. One is the stability mode, as illustrated in Figure 4.13a. If so, Ab < 1, the supply function f is steeper than g, and oscillations then decrease to a magnitude every time the price and sum of the product curve tend towards spiraling inward with regard to time. The cost and quantity converge to the balance after a certain amount of iteration (x0, y0). The other is the mode of instability, as displayed in Figure 4.13b. If the demand function g is higher than the supply function f, then each time the oscillations rise in magnitude, a price and quantity curve appear to spiral with regard to time. The price and quantity, thus, diverge more and more over time from the equilibrium point (x0, y0) [155][156].

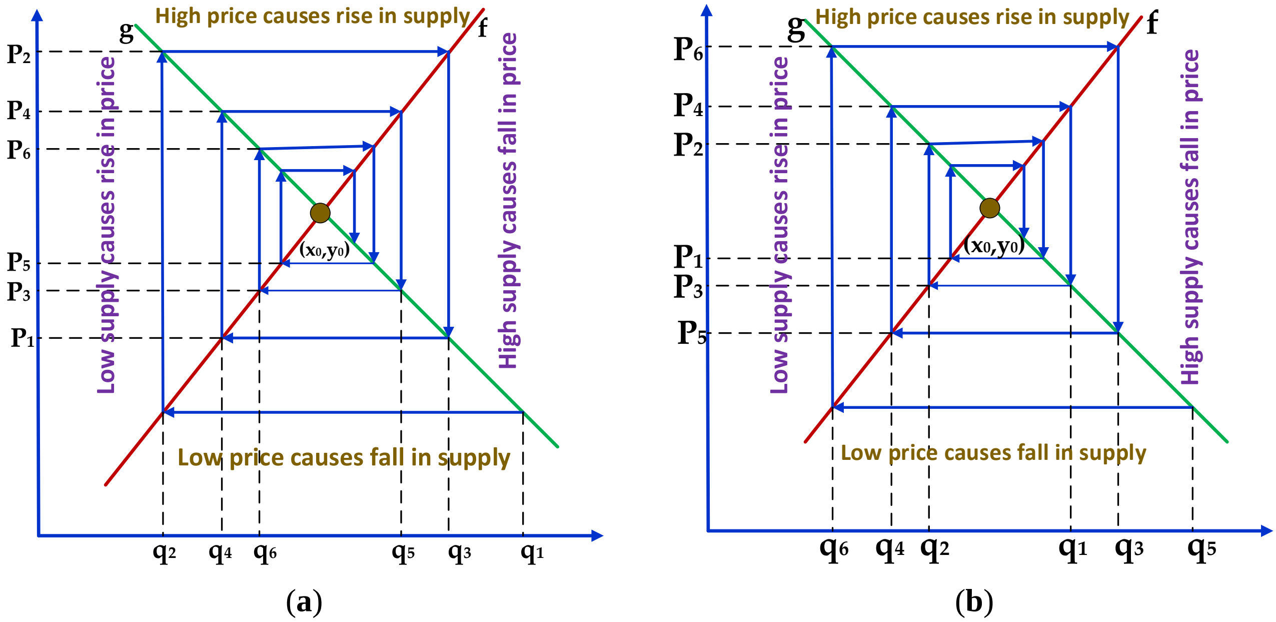


Figure 4.13: Two modes of supply–demand mechanism: (a) stability mode and (b) instability mode.

The cost of the commodity and the markets' volume is as follows:

$$X = \begin{bmatrix} x_1 \\ x_2 \\ . \\ . \\ . \\ x_n \end{bmatrix} = \begin{bmatrix} x_1^1 & x_1^2 & \cdots & \cdots & x_1^d \\ x_2^1 & x_2^2 & \cdots & \cdots & x_2^d \\ \vdots & \vdots & \vdots & \vdots & \vdots \\ \vdots & \vdots & \vdots & \vdots & \vdots \\ x_n^1 & x_n^2 & \cdots & \cdots & x_n^d \end{bmatrix} \tag{4.79}$$

where

- d is the number of commodity prices;
- n is the number of markets;
- $x_i^j$ (i = 1, …, n; j = 1, …, d) is the jth commodity price in the ith market;
- $x_i$ (i = 1, …, n) is the ith commodity price vector.

$$Y = \begin{bmatrix} y_1 \\ y_2 \\ . \\ . \\ . \\ y_n \end{bmatrix} = \begin{bmatrix} y_1^1 & y_1^2 & \cdots & \cdots & y_1^d \\ y_2^1 & y_2^2 & \cdots & \cdots & y_2^d \\ \vdots & \vdots & \vdots & \vdots & \vdots \\ \vdots & \vdots & \vdots & \vdots & \vdots \\ y_n^1 & y_n^2 & \cdots & \cdots & y_n^d \end{bmatrix} \tag{4.80}$$

where

- d is the number of commodity quantities;
- n is the number of markets;
- $y_i^j$ (i = 1, …, n; j = 1, …, d) is the jth commodity quantity in the ith market;
- $y_i$ (i = 1, …, n) is the ith commodity quantity vector.

The cost and quantity of commodities for each market evaluate the values of the decision variable in the function of fitness:

$$\begin{bmatrix} F_x \\ F_y \end{bmatrix} = \begin{bmatrix} F_{x1}\ F_{x2} \ldots\ F_{xn} \\ F_{y1}\ F_{y2} \ldots\ F_{yn} \end{bmatrix}^T \tag{4.81}$$

where

- T denotes the transpose of the matrix.

The updated cost and quantity are accessed by using the fitness function. If the value of the number of commodities' fitness function is more significant than its price, its cost will be replaced by its quantity of commodities as a candidate solution.

The balance costs y0 and balance volume vector x0 are randomly selected based on their probability of stopping the SDO algorithm from getting stuck in local optima.

$$N_i = \left| F_{yi} - \frac{1}{n}\sum_{i=1}^{n} F_{yi} \right| \tag{4.82}$$

$$Q = \frac{N_i}{\sum_{i=1}^{n} N_i} \tag{4.83}$$

where

- y0 = yk;
- k = roulette wheel section (Q).

$$M_i = \left| F_{xi} - \frac{1}{n}\sum_{i=1}^{n} F_{xi} \right| \tag{4.84}$$

$$P = \frac{M_i}{\sum_{i=1}^{n} M_i} \tag{4.85}$$

$$x_o = \begin{cases} r_1 . \sum_{1}^{n} \frac{x_i}{n} & \text{if rand } < o.5 \\ x_k, \quad k = \text{Roulette wheel selection (FP)} & \text{if rand} \geq 0.5 \end{cases} \tag{4.86}$$

where

- $r_1$ is a random number.

The following quantities and costs of the product are modified by correction of the supply–factor α and demand–factor β, based on equilibrium cost and balance quantity:

$$y_i(t+1) = y_o + \alpha.(x_i(t) - x_0), \tag{4.87}$$

$$x_i(t+1) = x_o + \beta.(y_i(t) - y_0), \tag{4.88}$$

At the ith iteration, $x_i(t)$ and $y_i(t)$ are the ith cost and sum of a product, respectively.

The commodity cost can be represented as

$$x_i(t+1) = x_o + L.(x_i(t) - x_0) \tag{4.89}$$

To balance exploration and exploitation, alpha and beta are represented as

$$\alpha = \frac{2(T - t + 1)}{T} sin(2\pi r), \tag{4.90}$$

$$\beta = 2\, cos(2\pi r), \tag{4.91}$$

where

- t is the present iteration;
- r is a random vector;
- T is the number of iteration.

A novel L variable is formulated as follows to help the SDO technique transition between exploration and exploitation efficiently:

$$L = \alpha\beta = \frac{2(T - t + 1)}{T} sin(2\pi r)\, cos(2\,\pi r) \tag{4.92}$$

The cost of each demand ranges from the cost of balance of $|L| > 1$ to converge to the cost of balance of $|L| < 1$. Figure 4.14 displays the flow chart of SDO algorithm.

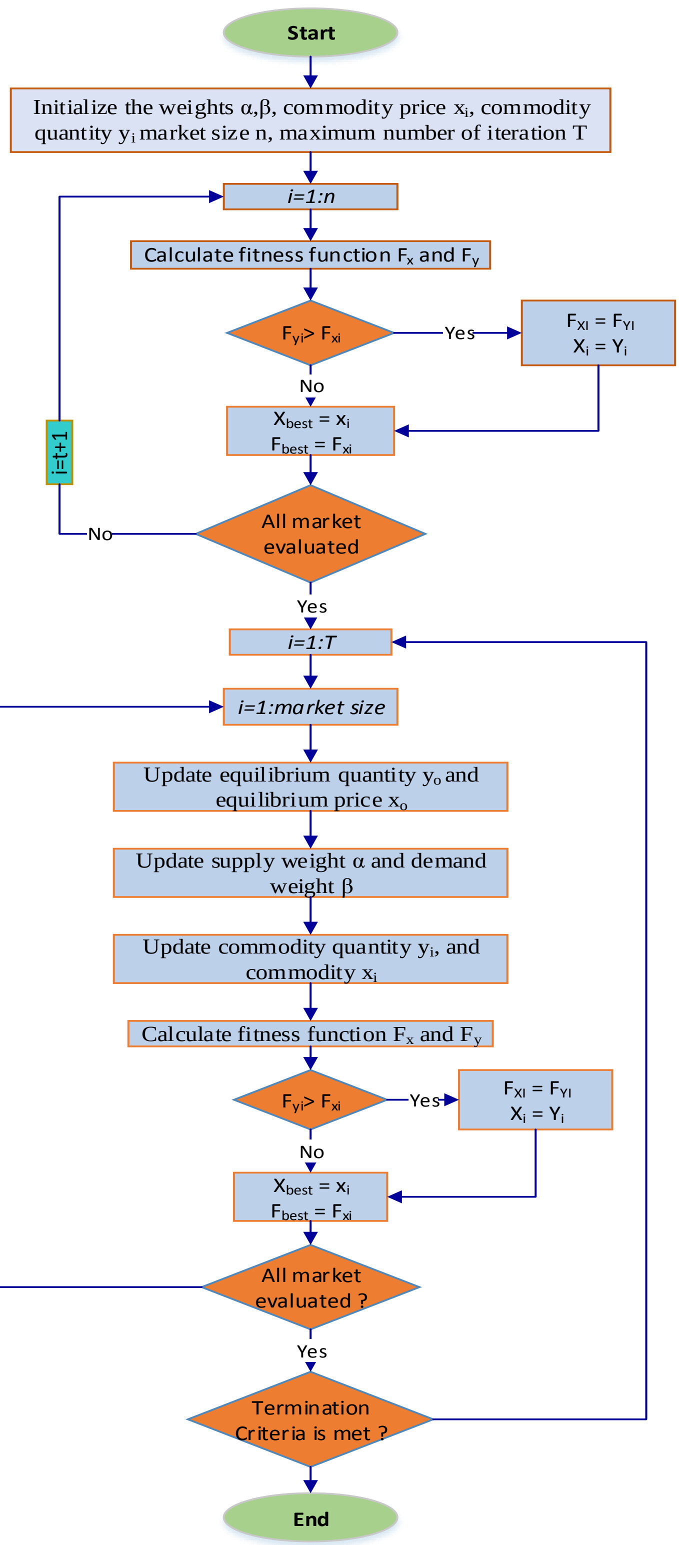


Figure 4.14: The flow chart of the SDO algorithm.

## 4.7 Eagle Strategy Chaotic Supply Demand Based Optimization

The proposed eagle strategy chaotic supply demand based optimization (ESCSDO) algorithm is the combination of the conventional SDO with eagle strategy and chaotic maps. In this subsection, the concepts of eagle strategy and chaotic maps are discussed to develop the proposed ESCSDO algorithm.

### 4.7.1 Eagle Strategy

The Eagle strategy (ES) is proposed for solving real-world optimization problems that is developed by Yang et al. [157]. It is inspired by the foraging the eagles behavior that fly randomly in analogy to the Levy flights. It is the two-stage method: global search randomization stage and an intensive local search [158]. The first stage aims mainly to investigate the search space globally and rapidly obtain a promising solution, while the target of the second stage is to get the optimal solution through making an intensive local search based on the achieved solution in the first stage. The benefit of this strategy is that there is no limit to the kinds of techniques or algorithms used in each stage. Any technique that is able to achieve better results in a flexible way could be used in any stage [158].

During the iteration of the proposed technique, the new candidate solution is generated by Levy flight as follows:

$$x_i(t+1) = x_i(t) - \gamma(x_i(t) - X_{best}) \oplus Levy(\lambda) = x_i(t) + \frac{0.01u}{|v|^{1/\lambda}}(x_i(t) - X_{best}) \qquad (4.93)$$

where γ is the step scaling size, the ⊕ refers to the process of element-wise multiplications, λ is the Levy flight exponent, while u and v can be expressed as:

$$u \sim N(0, \sigma_u^2) \quad , v \sim N(0, \sigma_v^2) \qquad (4.94)$$

The standard deviations $\sigma_u$ and $\sigma_v$ are explained as:

$$\sigma_u = \left[\frac{\sin\left(\frac{\lambda\pi}{2}\right) . \Gamma(1+\lambda)}{2^{(\lambda-1)}\lambda . \Gamma(\frac{1+\lambda}{2})}\right]^{1/\lambda} , \sigma_v = 1 \qquad (4.95)$$

where Γ is the Gamma function.

### 4.7.2 Chaotic Maps

Chaotic systems are deterministic systems that present unpredictable conduct, whose action is complex and similar to that of randomness [159]. In [159], it was proposed chaos-based exploration rate to enhance the performance of three well-known optimization algorithms. Based on this proposed, the real random number ($v$) in Eq. (4.94) is replaced by a chaotic number in the Eagle strategy. This modification makes the value of $v$ linearly decreased from 2 to 0 throughout the course of iterations. Table 4.1 shows the 10 chaotic maps are applied for the conventional SDO to update the parameter of exploration q as follows [160]:

$$q = y_{k+1} \tag{4.96}$$

where $y_{k+1}$ is the chaos map that is selected to find the solution of the problem and the chaos map distribution is shown in Figure 4.15 [161]. The steps of the proposed ESCSDO are presented in the flowchart illustrated in Figure 4.16.

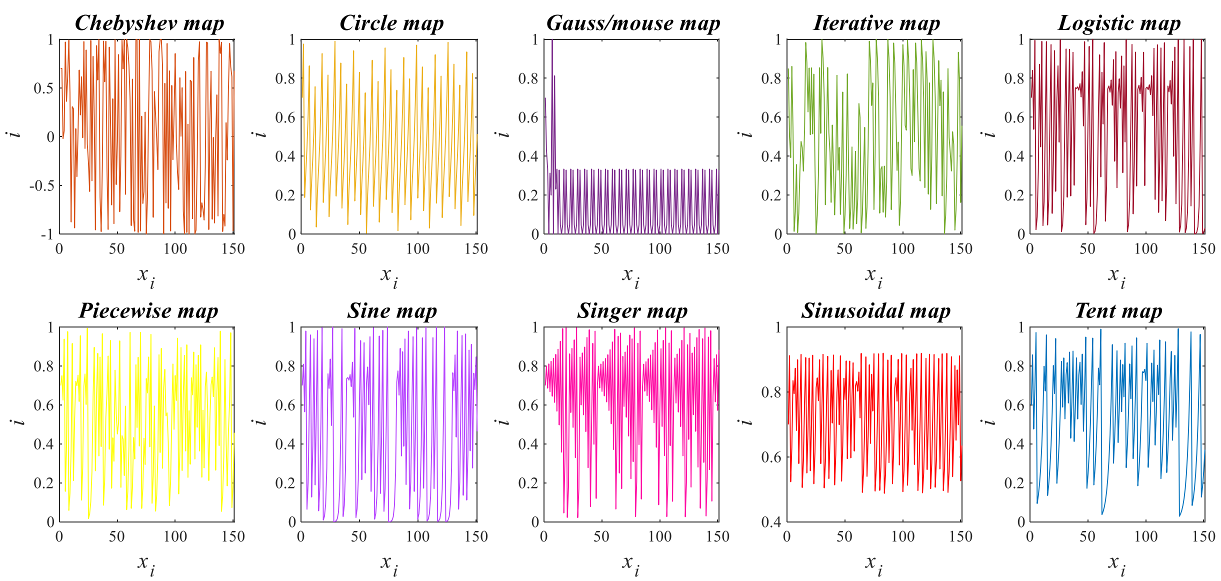


Figure 4.15: Different chaotic maps number distribution.

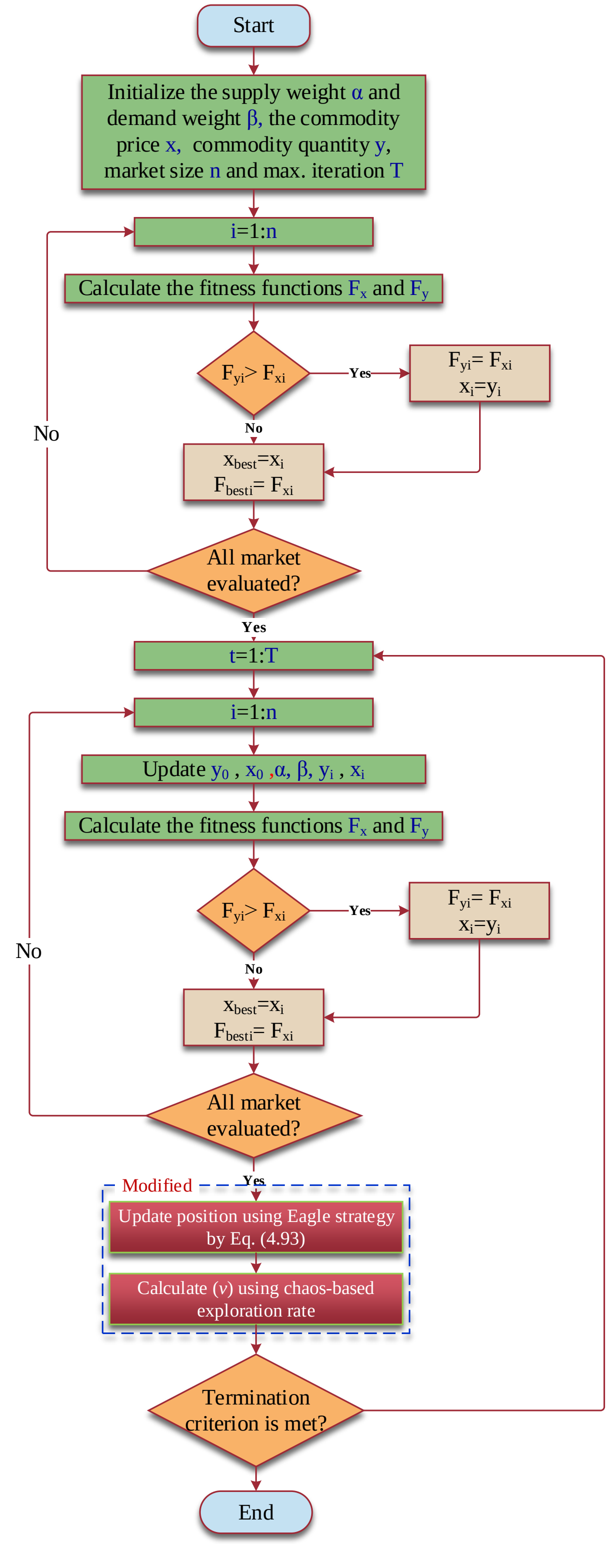


Figure 4.16: The proposed ESCSDO algorithm Flow Chart.

## 4.8 Multi-Objective Optimization Algorithm for DEED Problem

The multi-objective algorithm has been employed to solve several MOPs. In this thesis, a recent multi-objective algorithm that is called Multi-Objective Salp Swarm Algorithm (MSSA) is presented.

*A. Multi-Objective Optimization Problem*

The DEED model is represented as a MOP with nonlinear constraints based on the objective functions and system constraints as follows:

$$\begin{cases} \qquad \min \qquad [F_1(P), F_2(P)] \\ s.t. \qquad g_i(P) = 0, \qquad k = 1,2,\ldots.,u \\ \qquad h_i(P) \leq 0, \qquad i = 1,2,\ldots.,q \end{cases} \tag{4.97}$$

where $F_1(P)$ and $F_2(P)$ are the fuel cost and pollution emission objective functions, respectively. $g_i(P)$ and $h_i(P)$ are the equality and inequality constraints, and $u$ and $q$ are the corresponding formula numbers, respectively. $P$ is the active power decision control vector of the generating units.

With single objective, it can be confidently assessing that a solution is superior than another depending on comparing the single criterion, while in a MOP; there is more than single criterion to check and compare the obtained solutions. The principal approach to compare two solutions taken into consideration multiple objectives is named Pareto optimal dominance as described in [162]. There are two principal methods for solving MOPs: a priori and a posteriori. In the prior approach, the MOP is converted into a single-objective problem by summation the objectives with a set of weights specified by experts. The major shortcoming of this approach is that the Pareto optimal set and the front need to be constructed by re-running the technique and modifying the weights. Nevertheless, the posteriori approach maintains the multi-objective construction in the solving strategy, and the Pareto optimal set can be chosen in a single run. Without any weight to be explained by experts, this method can approximate any type of PF. Due to the posterior optimization benefits over the a priori method, the focus of our study is targeted at a posteriori multi-objective optimization.

*B. Multi-Objective Salp Swarm Algorithm*

Salps are a kind of marine organism from the family of Salpidae, with a comparable appearance to jellyfish. In the strategy of foraging food, these salps display a swarm behavior, establishing a salp-chain that stimulated the salp swarm algorithm (SSA) suggested by Mirjalili in [101]. The population in a salp-chain contains a leader and a set of followers, where the leader tries to find the source of the food while the followers vary their location according to the salp ahead of them, and accordingly to the leader. Regarding an optimization problem with n variables, and xi the location of salp i, denoted by a vector of n elements xi = [x1i, x2i, . . . , xni], the leader of the salp-chain updates its location through this equation:

$$x_j^1 = \begin{cases} F_j + c_1\left(\left(ub_j - lb_j\right)\right)c_2 + lb_j, c_3 > 0.5 \\ F_j - c_1\left(\left(ub_j - lb_j\right)\right)c_2 + lb_j, c_3 \leq 0.5 \end{cases} \tag{4.98}$$

where $F_j$ denotes the value in the jth dimension of the food source F (the best location), $ub_j$ and $lb_j$ are the upper and lower bounds, respectively, in the jth dimension and parameters $c_2$ and $c_3$ represent randomly produced numbers in the interval [0,1]. The parameter $c_1$ can be calculated from the equation below:

$$c_1 = 2e^{-\left(\frac{4t}{T}\right)^2} \tag{4.99}$$

where $t$ denotes the present iteration while T represents the total number of iterations.

When the leader updated its location, the followers are varying their location by the following equation:

$$x_j^i = \frac{1}{2}\left(x_j^i + x_j^{i-j}\right) \tag{4.100}$$

where $x_j^i$ is the location in jth dimension of salp i, with $2 \leq i \leq n$.

The swarm behavior of salp chains is simulated based on the mathematical equations explained above. When dealing with MOPs, two issues need to be modified for the SSA technique. Firstly, the multi-objective salp swarm algorithm (MSSA) needs to store many results as the best solutions for a MOP. Secondly, in each iteration, the SSA updates the food source with the optimal solution, but in the MOP, single best solutions do not exist.

In MSSA, the first problem is resolved by supplying the SSA technique with a repository of food sources. This repository can store a determinate number of non-dominated (ND) solutions. In the operation of optimization, the Pareto dominance operators are used to compare each salp with all the residents in the repository. If a salp dominates only a solution in the repository, it will be exchanged. If a salp dominates a group of solutions in the repository, they all should be eliminated from the repository and the salp should be added to the repository. If at minimum one of the repository residents dominates a salp in the new population, it should be rejected directly away. If a salp is non-dominated in comparison with all repository residents, it should be added to the archive. If the repository becomes full, it is needed to reject one of the similar ND solutions in the repository. For the second problem, a suitable method is to choose it from a group of ND solutions with the least crowded neighborhood. This is done by the same ranking process and roulette wheel selection. Algorithm 1 presents the pseudo code of MSSA:

**Algorithm 1** Pseudo-code of MSSA

Initialize the parameters *the number of salps, Obj_no, dim, lb, ub, Archive Maxsize,* $max\_iter$;

Initialize the salp population $x_i (i = 1,2, \dots, n)$;

Define the objective function (Dynamic Economic Emission Dispatch function)

**While (**$t \le max\_iter$)

    Calculate the fitness of all salp with Ob_func;

    Find the non-dominated salps

    Update the repository in regard to the obtained non-dominated salps

    ***If (***repository become full)

        Call the repository maintenance process to eliminate one repository neighborhood

        Add the non-dominated salp to the repository

    ***End If***

    Select a source of food from repository

    Update $c_1$ by **Equation** (9);

    **For** $each\ search\ agent$

        ***If*** (i==1)

            Update the location of the leading salp by **Equation** (8);

        ***Else***

            Update the location of the leading salp by **Equation** (10);

        ***End if***

    **End For**

    $t = t + 1$;

**End While**

**Return** repository

## 4.9 The Bonobo Optimizer

Bonobo optimizer (BO) is a well-known optimization technique that was developed by Amit Kumar Das et al. [163]. Bonobos show four different mating strategies: promiscuous, restrictive, consort ship, and extra-group mating. These mating strategies are artificially modeled in the original BO algorithm. The reproductive manner of Bonobos depends on the fission-fusion approach. The fission-fusion approach is the method that the Bonobo society follows to obtain its nourishment and others. The concept of the fission-fusion way is that the society is divided into small groups of various sizes for a few days to find the nourishment (fission process) then they are gathering another time at nighttime for sleep (fusion behavior), as shown in Fig. 4.17. According to the phase condition, the mating behavior of the bonobo community is chosen. There are two phases considered in the lifestyle of this society. The positive phase (PP) represents the availability of all living conditions such as food, security, and a successful mating procedure. On the other side, the negative phase (NP) shows the absence of such conditions. Promiscuous, restrictive mating strategies have higher probabilities in the PP case while consort ship mating and extra-group mating strategies are very familiar in the NP case.

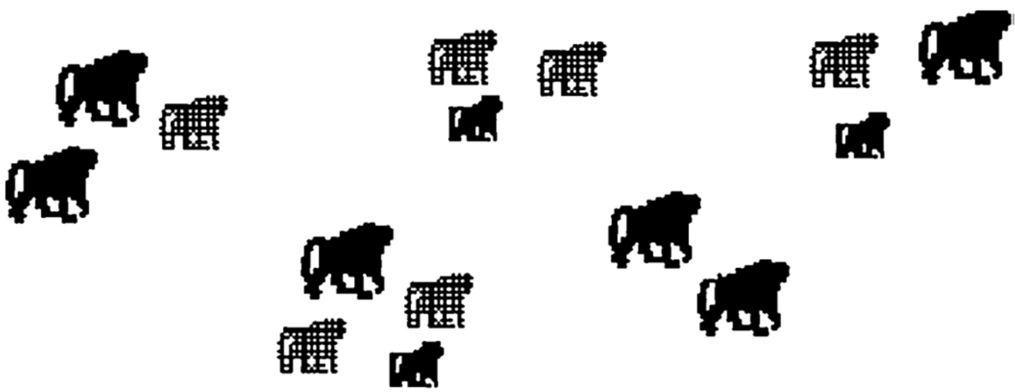

Figure 4.17: Bonobos' fission–fusion social groups.

*a) Promiscuous and Restrictive Mating Strategies:*

Either promiscuous or restrictive mating produces a new bonobo, and it is given as follows [164]:

$$new\_bonobo_j = bonobo_j^i + r_1 \times scab \times \left(\alpha_{bonobo}^j - bonobo_j^i\right) + (1 - r_1) \times scsb \times flag \times \left(bonobo_j^i - bonobo_j^P\right) \tag{4.101}$$

where $new\_bonobo_j$ and $\alpha_{bonobo}^j$ are the j[th] variables of the new offspring and the alpha bonobo, respectively, and j varies from 1 to *dim*, where *dim* is the total number of variables. $r_1$ is a random number in the range of [0,1]. $scab$ and $scsb$ are the sharing coefficients for the $\alpha_{bonobo}^{j}$ and chosen P[th]-bonobo, respectively. $flag$ gives either 1 or -1.

*b) Consortship and Extra-Group Mating Strategies*

The consortship and extra-group mating strategies are randomly created, based on phase probability (pp), and formed through the extra-group mating probability:

$$\beta_1 = e^{(r_4^2 + r_4 - \frac{2}{r_4})} \tag{4.101}$$

$$\beta_2 = e^{\left(-r_4^2 + 2r_4 - \frac{2}{r_4}\right)} \tag{4.102}$$

$$new\_bonobo_j = bonobo_j^i + \beta_1 \times (var\_max_j - bonobo_j^i) \tag{4.103}$$

$$new\_bonobo_j = bonobo_j^i - \beta_2 \times (bonobo_j^i - var\_min_j) \tag{4.104}$$

where $\beta_1$ and $\beta_2$ are the two intermediate measured values utilized to define the value of new _ bonobo. $r_4$ is a random number generated in between [0 1]. $var\_max_j$ and $var\_min_j$ are the lower and upper limits corresponding to the j[th]-variable, respectively.

## 4.10 The Proposed Chaotic Bonobo Optimizer

The proposed algorithm, named Chaotic Bonobo Optimizer (CBO) algorithm, is based on the BO algorithm plus the incorporation of chaotic maps. The proposed CBO technique improves the low convergence speed and the weak local optimum of the original BO algorithm thus enhancing the performance of the proposed algorithm to achieve the best value for the OF. This modification is based on chaotic theory, which is one of the most effective methods to overcome those issues. Instead of using random parameters, a set of chaotic equations [160] is used to enhance the convergence characteristics and strengthen the performance and robustness of the original BO.

The chaotic matrix is used instead of the random number $r_4$ in Eqs. (4.101) and (4.102) by using chaotic maps. Therefore, Eqs. (4.101) and (4.102) can be rewritten as follows:

$$\beta_1 = e^{(Chaotic_4^2 + Chaotic_4 - \frac{2}{Chaotic_4})} \tag{4.105}$$

$$\beta_2 = e^{\left(-Chaotic_4^2 + 2Chaotic_4 - \frac{2}{Chaotic_4}\right)} \tag{4.106}$$

The flowchart of the proposed CBO algorithm is displayed in Fig. 4.18.

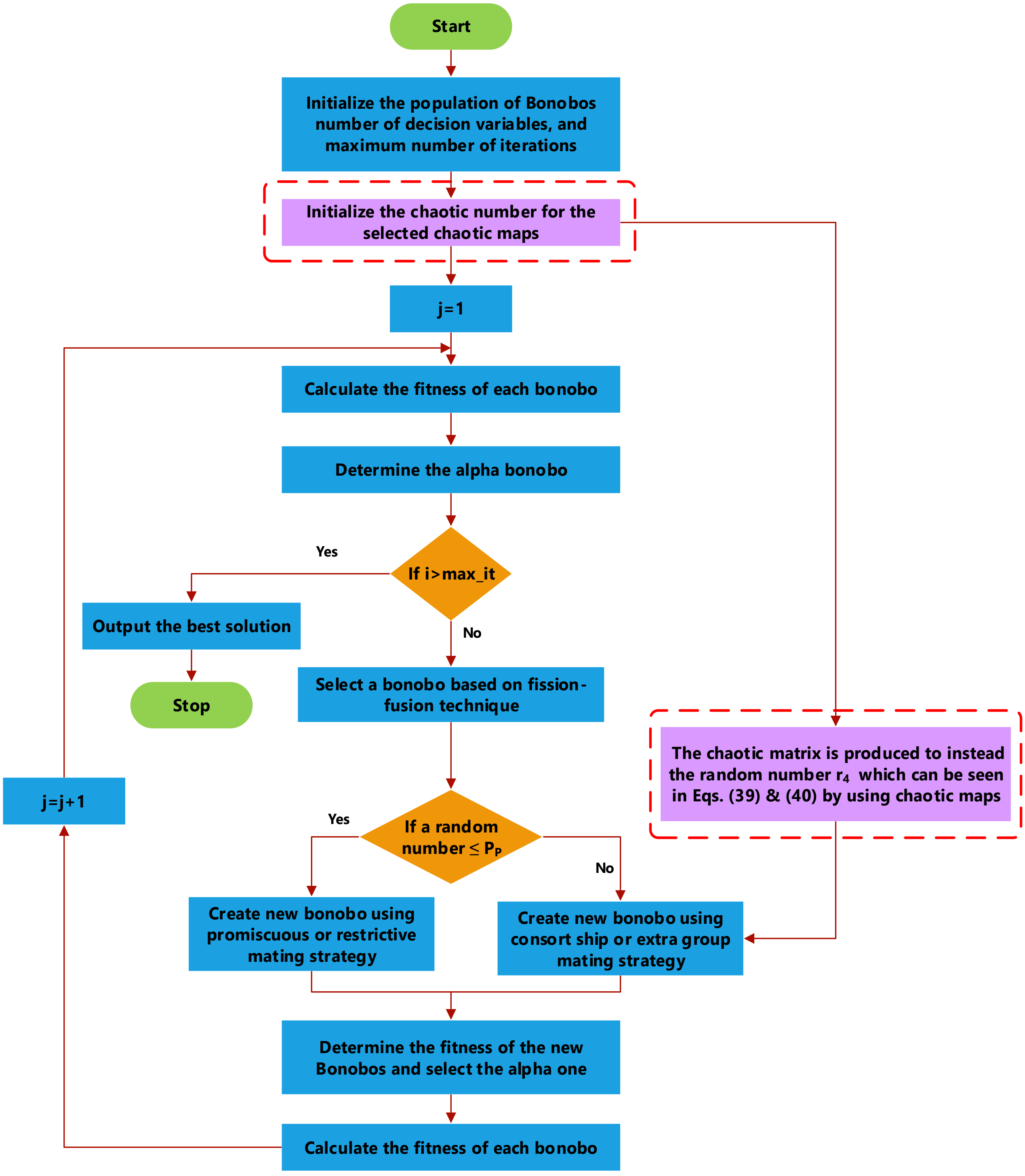


Figure 4.18: Flowchart of the proposed CBO technique.

# Chapter 5

## Results and Discussion

- *Introduction*
- *Description of Test Systems*
- *Formulation of the EED Problem as Single Objective Function*
- *Solving ELD Problem with using the ESCSDO Algorithm Considering Ramp Rate Limit, VPLE, and POZs.*
- *Formulation of the EED Problem as a Multi-Objective Function using the Proposed Four Multi-Objective Algorithms.*

# Chapter 5

## Results and Discussion

### 5.1 Introduction

This chapter refers to the results and discussions resulting from applying the proposed techniques in different systems. The EED problem has been solved using different methods, which can be summarized as below:

- Formulation EED problem as a single-objective function using the proposed MRFO-GBO, CAEO, ISMA, SDO, and MMPA algorithms.
- Solving ELD problem with using the ESCSDO algorithm considering equality constraints such as power balance constraint, and inequality constraints such as generating capacity limit, ramp rate limit, valve-point loading effect, and POZs.
- Formulation of EED problem as a multi-objective function using the proposed MOIMRFO, MOCAEO, MOISMA, and MOMMPA algorithms.
- Solving DEED problem with using the MSSA algorithm.
- Solving EED problem Considering Stochastic Renewable Energy Resources using CBO algorithm.

The proposed techniques are compared with recent and other well-known optimization algorithms to show their superiority in finding the best solution of the EED problem. The proposed techniques are simulated using the MATLAB environment and run on Windows 8.1 operative system. The description of the portable computer, which is used to solve this problem, are Intel Core i5-4210U CPU@2. 40GHz with a 4.00 MB RAM.

### 5.2 Description of Test Systems

In this chapter, different network systems have been used to verify the efficiency of the proposed methods. These systems are listed below:

- 3-unit test system with a different value of load demand ($P_D$ = 550, 600, 700, 800, and 850 MW);
- 5-unit test system (PD = 1800 MW);

- 6-unit power generation (IEEE 30-bus test system) with a various load demand (PD = 150, 175, 200, 225 MW);
- 10-unit test system (PD = 2000 MW);
- 11-unit power generation (69-bus test system) with a different value of load demand (PD = 1000, 1500, 2000, and 2500 MW);
- 13-unit test system(PD = 1800 MW);
- 15-unit test system (PD = 2630 MW);
- 26-unit test system (PD = 2000 and 2200 MW);
- 40-unit test system (PD = 10,500 MW);
- 110-unit test system (PD = 15,000 MW).

## 5.3 Formulation of EED Problem as Single Objective Function

In this subsection, the performance of proposed MRFO-GBO, CAEO, ISMA, SDO, and MMPA techniques are evaluated using different networks (3-unit, 5-unit, 6-unit, 10-unit, 11-unit, 26-unit, 40-unit and 110-unit). In each test network, the proposed techniques are compared with other well-known optimization algorithms to show their superiority in finding the optimal solution for the EED problem.

### 5.3.1 Solving EED Problem using MRFO-GBO Algorithm

The conventional MRFO, GBO and proposed MRFO–GBO techniques are adapted to solve the EED problem for 5 unit (1800 MW), 3 unit (550,600,700,800,850MW), and 6 unit systems with 4 levels of demand, where the first level of demand is 150 MW and it is increased by 25 MW in each time to reach 225 MW in the fourth level of demand. The following control variables have been assumed: the number of population is 30 and the maximum number of iterations is 1000 iterations. The number of 30 independent runs has been executed with the aim of overcoming the randomness of the studied optimization technique and checking the quality of the proposed MRFO–GBO algorithm.

#### 5.3.1.1 Case 1: Five Thermal Units and Load Demand 1800 MW.

The single-objective ELD problem is only solved in this case because the emission of pollutants are not taken into account. The system data are taken from [165]. The results of this case are presented in Table 5.1 and these results are compared to those obtained by GA [165], PPSO [165], QPSO [91], FA [92], and SCA [95]. It is clear from the table that the proposed MRFO-GBO gives a better solution than conventional MRFO, GBO and other methods. Figure 5.1 illustrates the convergence curves of MRFO-

GBO, MRFO and GBO for fuel cost where MRFO-GBO outperforms the conventional MRFO and GBO. The figure also demonstrates that MRFO-GBO, MRFO and GBO provide strong, fast convergence, and stability for solving the ELD problem.

Table 5.1: Comparison of results for case study 1.

| Output | GA | PPSO | QPSO | FA | SCA | MRFO | GBO | MRFO-GBO |
|---|---|---|---|---|---|---|---|---|
| P1 (MW) | 320 | 320 | 320.51 | 327.8 | 320 | 330.710 | 327.08 | 320 |
| P2 (MW) | 343.74 | 343.7 | 346.47 | 341.99 | 343.85 | 351.852 | 343.869 | 343.8698 |
| P3 (MW) | 472.6 | 472.6 | 482.95 | 460.42 | 472.3 | 464.269 | 472.075 | 472.2678 |
| P4 (MW) | 320 | 320 | 320 | 327.8 | 320 | 328.362 | 320 | 320 |
| P5 (MW) | 343.74 | 343.7 | 330.08 | 341.99 | 343.85 | 324.802 | 336.975 | 343.862 |
| Total power (MW) | 1800 | 1800 | 1800 | 1800 | 1800 | 1800 | 1800 | 1800 |
| Fuel cost ($/h) | 18611.07 | 18610.4 | 18610.03 | 18610 | 18609.694 | 18611.162 | 18609.984 | **18609.6904** |

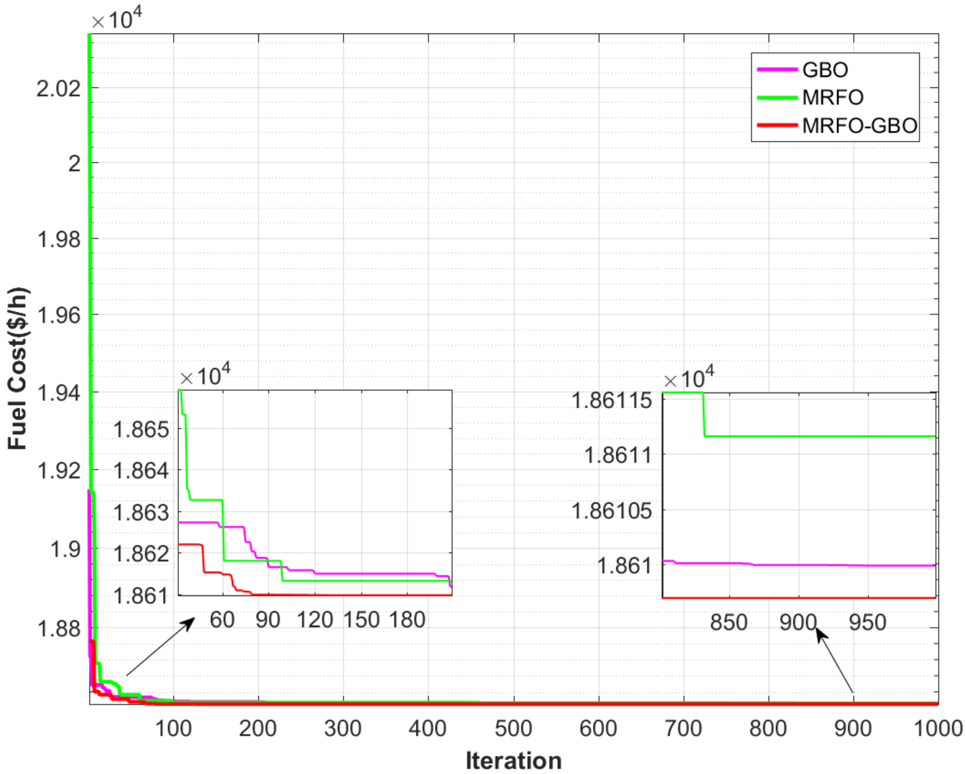


Figure 5.1: Fuel cost convergence of MRFO, GBO and MRFO- GBO for case study 1.

### 5.3.1.2 Case 2: Three Thermal Units and Load demand.

In this case, the proposed MRFO- GBO, conventional MRFO and GBO are implemented on test system having three thermal units to solve EED problem for different levels of demand: 550, 600, 700, 800 and 850 MW. The fuel cost, power loss, SO2 and NOx emissions are taken into account. The system data are taken from [166]. The comparison of the proposed MRFO- GBO results for this case with the conventional MRFO, GBO and other techniques is illustrated in Table 5.2. Table 5.2 shows the comparison of total cost for various levels of demand by using other techniques where the proposed MRFO- GBO has shown tremendous superiority and excellence, overall its counterparts like SA [167] , SCA [95], the conventional MRFO and GBO by providing the optimal solution which is the minimum total cost and the best value for fuel cost simultaneously for different levels of demand (550, 600, 700, 800 and 850 MW).

Table 5.2: Comparison of the proposed algorithms results for case study 2.

| **Output** | | **P1 (MW)** | **P2 (MW)** | **P3 (MW)** | **Total power (MW)** | **Power loss (MW)** | **Fuel cost ($/h)** | **$SO_2$ emission (ton/h)** | **$NO_x$ emission (ton/h)** | **Total cost ($/h)** |
|---|---|---|---|---|---|---|---|---|---|---|
| 550 | SA | 307.13 | 160.32 | 88.63 | 556.0859 | 6.0859 | 5581.479 | 6.0071 | 0.08805 | 18760.5958 |
| | SCA | 307.11 | 160.34 | 88.63 | 556.0861 | 6.0861 | 5581.474 | 6.0071 | 0.08805 | 18760.5954 |
| | MRFO | 308.12 | 158.65 | 89.293 | 556.0686 | 6.0686 | 5582.156 | 6.00172 | 0.088038 | 18756.1769 |
| | GBO | 308.80 | 159.61 | 87.669 | 556.0757 | 6.0757 | 5581.745 | 6.00084 | 0.08805 | 18755.9045 |
| | **MRFO - GBO** | 307.13 | 160.32 | 88.630 | 556.0858 | 6.0858 | 5581.480 | 6.00207 | 0.088047 | **18755.71385** |
| 600 | SA | 329.32 | 184.61 | 93.44 | 607.3685 | 7.3685 | 6028.708 | 6.4941 | 0.0882 | 19660.5278 |
| | SCA | 329.27 | 184.66 | 93.43 | 607.3692 | 7.3692 | 6028.695 | 6.4941 | 0.0882 | 19660.5274 |
| | MRFO | 329.14 | 183.99 | 94.225 | 607.3623 | 7.3623 | 6028.830 | 6.489377 | 0.088181 | 19655.7277 |
| | GBO | 328.88 | 184.69 | 93.790 | 607.3707 | 7.3707 | 6028.668 | 6.489438 | 0.088186 | 19655.6652 |
| | **MRFO - GBO** | 329.31 | 184.61 | 93.438 | 607.36858 | 7.36858 | 6028.707 | 6.489082 | 0.088182 | **19655.6457** |
| 700 | SA | 374.07 | 233.15 | 103.14 | 710.3669 | 10.3669 | 6939.248 | 7.4855 | 0.0902 | 21633.8869 |
| | SCA | 374.05 | 233.17 | 103.15 | 710.3673 | 10.3673 | 6939.244 | 7.4855 | 0.0902 | 21633.8863 |
| | MRFO | 374.98 | 233.71 | 101.68 | 710.374 | 10.374 | 6939.433 | 7.479722 | 0.090208 | 21629.49137 |
| | GBO | 378.36 | 227.16 | 104.73 | 710.255 | 10.255 | 6940.147 | 7.47742 | 0.090126 | 21630.60267 |
| | **MRFO-GBO** | 374.07 | 233.15 | 103.14 | 710.367 | 10.367 | 6939.247 | 7.480495 | 0.090232 | **21629.0045** |
| 800 | SA | 419.34 | 281.64 | 112.96 | 813.9456 | 13.9456 | 7871.446 | 8.5004 | 0.0947 | 23841.8787 |
| | SCA | 419.31 | 281.64 | 112.99 | 813.9458 | 13.9458 | 7871.443 | 8.5004 | 0.0947 | 23841.8780 |
| | MRFO | 418.53 | 283.25 | 112.20 | 813.988 | 13.988 | 7871.689 | 8.496199 | 0.094713 | 23837.5274 |
| | GBO | 420.19 | 280.45 | 113.27 | 813.915 | 13.915 | 7871.459 | 8.494525 | 0.094644 | 23837.0585 |
| | **MRFO-GBO** | 419.33 | 281.65 | 112.96 | 813.945 | 13.945 | 7871.446 | 8.495337 | 0.094681 | **23836.9960** |
| 850 | SA | 442.17 | 305.85 | 117.93 | 865.9536 | 15.9536 | 8345.746 | 9.0166 | 0.0978 | 25035.121 |
| | SCA | 442.17 | 305.84 | 117.94 | 865.9533 | 15.9533 | 8345.744 | 9.0166 | 0.0978 | 25035.120 |
| | MRFO | 442.04 | 305.49 | 118.42 | 865.9442 | 15.9442 | 8345.695 | 9.011641 | 0.097827 | 25030.34685 |
| | GBO | 441.96 | 306.49 | 117.52 | 865.9714 | 15.9714 | 8345.826 | 9.011908 | 0.097819 | 25030.26857 |
| | **MRFO-GBO** | 442.17 | 305.86 | 117.92 | 865.9536 | 15.9536 | 8345.747 | 9.011611 | 0.097813 | **25030.2386** |

Figure 5.2 represents total cost convergence characteristics of the MRFO- GBO comparing with original MRFO and GBO to solve EED problem for various load demands.

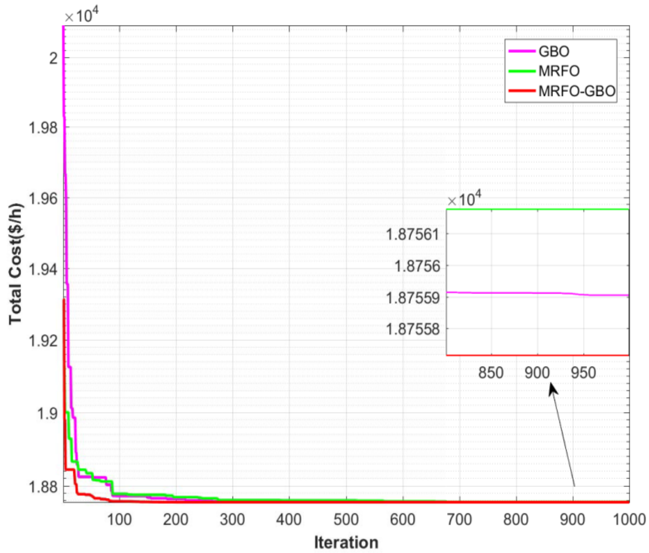


*(a)*

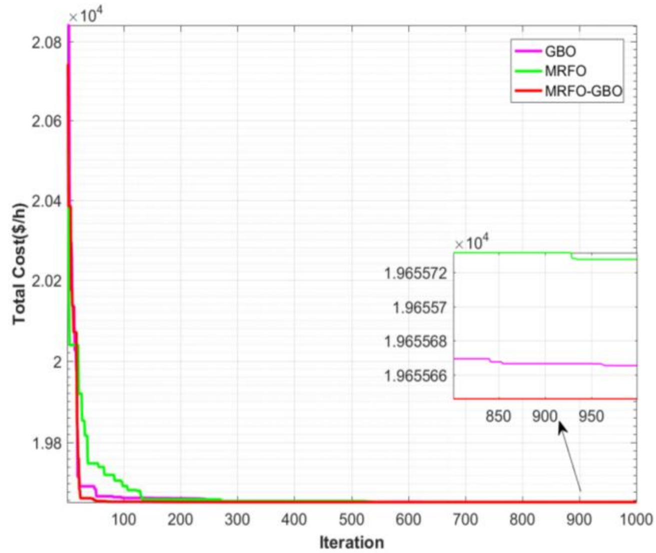


*(b)*

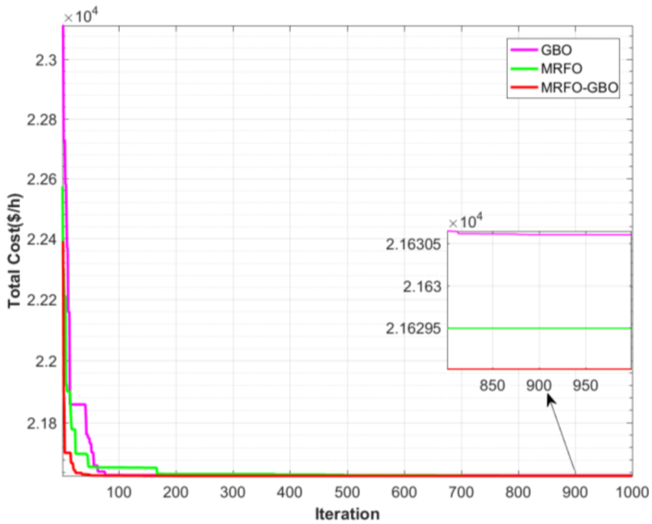


*(c)*

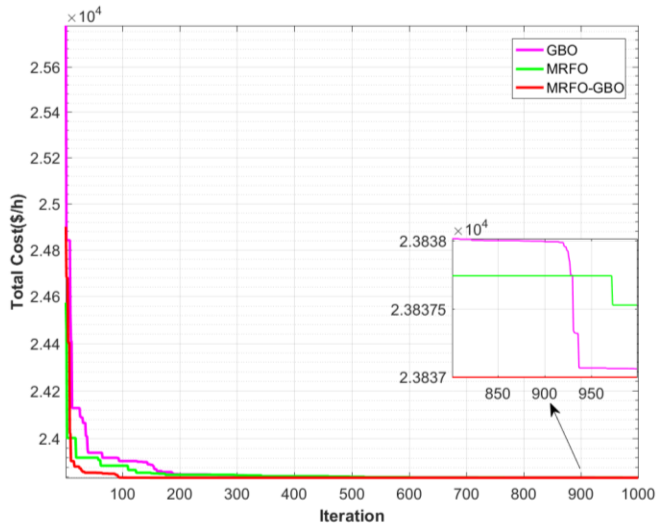


*(d)*

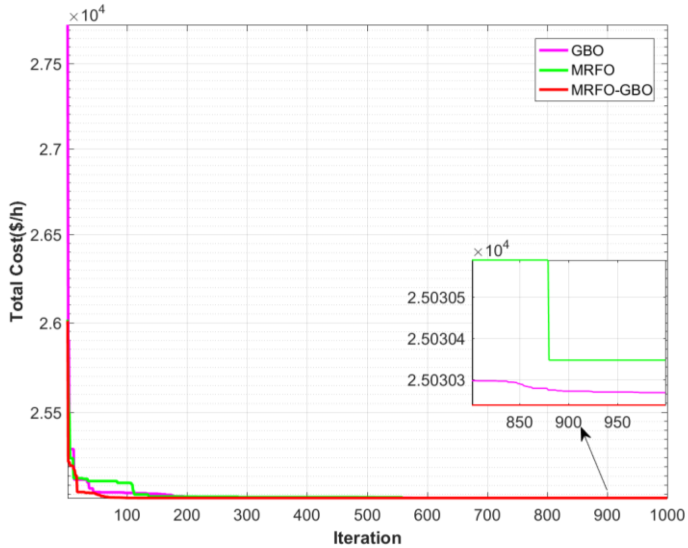


***(e)***

Figure 5.2: Total cost for different levels of demand in 3-unit system (a) 550 MW (b) 600MW (c)700 MW (d) 800 MW (e)850 MW.

#### 5.3.1.3 Case 3: Six Thermal Units and Load Demand.

In this case, the proposed MRFO-GBO technique is tested on the IEEE 30-bus test system having six thermal units with various levels of demand: 150, 175, 200, and 225 MW. The system data of this case are taken from Appendix (A) where the coefficients of Fuel cost and operational limits are given in the table A-1 , the coefficients of SO2 Emission and its max/max PPF are taken from the table A-2, the coefficients of NOx Emission and its max/max PPF are given in the table A-3, and the coefficients of CO2 Emission and its max/max PPF are taken from the table A-4.

The results for the 6-unit system considering the four levels of demand are provided in Table 5.3, 5.4, 5.5,5.6, 5.7, and 5.8. These results are including the value of fuel cost, the value of three types of emission (SO2, NOx, and CO2, respectively), the value of total emission and the value of total cost. These tables display the comparison between the results obtained from the proposed MRFO-GBO technique and the results of the conventional MRFO, GBO as well as the other recent optimization techniques that studied this problem previously. From these Tables, we conclude that MRFO-GBO method is better than the conventional MRFO, GBO as well as other recent optimization techniques such as PSO [90], SA [168], QBA [96], MBO [93], SCA [95], GOA [94], and QITFA [97] methods.

Table 5.3: the results of fuel cost considering 4 levels of demand in the 6-unit system.

| Load (MW) | Total fuel cost ($/h) | | | | | | | | | |
|---|---|---|---|---|---|---|---|---|---|---|
| | PSO | SA | QBA | MBO | SCA | GOA | QITFA | MRFO | GBO | MRFO-GBO |
| 150 | 2,734.20 | 2,705.21 | 2,704.97 | 2,704.92 | 2,704.92 | 2,704.87 | 2,711.71 | 2714.62 | 2706.42 | 2706.58 |
| 175 | 3,236.30 | 3,220.51 | 3,188.10 | 3,188.13 | 3,188.15 | 3,188.08 | 3,189.91 | 3212.77 | 3206.50 | 3206.15 |
| 200 | 3,784.90 | 3,735.73 | 3,726.08 | 3,727.43 | 3,727.44 | 3,727.40 | 3,729.26 | 3743.52 | 3737.05 | 3742.84 |
| 225 | 4,402.30 | 4,321.52 | 4,314.63 | 4,315.63 | 4,315.05 | 4,315.15 | 4,316.34 | 4319.78 | 4317.91 | 4319.33 |

Table 5.4: the results of SO2 emission considering 4 levels of demand in the 6-unit system.

| Load (MW) | Emission of $SO_2$ (kg/h) | | | | | | | | | |
|---|---|---|---|---|---|---|---|---|---|---|
| | PSO | SA | QBA | MBO | SCA | GOA | QITFA | MRFO | GBO | MRFO-GBO |
| 150 | 3,193.60 | 3,138.45 | 3,147.38 | 3,146.83 | 3,146.83 | 3,146.74 | 3,087.92 | 3129.89 | 3148.80 | 3145.54 |
| 175 | 3,904.90 | 3,763.48 | 3,858.96 | 3,859.49 | 3,859.36 | 3,859.37 | 3,807.49 | 3795.02 | 3808.03 | 3804.23 |
| 200 | 4,670.60 | 4,553.97 | 4,598.20 | 4,592.64 | 4,592.49 | 4,592.46 | 4,528.28 | 4530.21 | 4552.96 | 4533.03 |
| 225 | 5,426.10 | 5,287.31 | 5,344.75 | 5,335.81 | 5,339.96 | 5,338.42 | 5,289.45 | 5316.61 | 5334.40 | 5318.66 |

Table 5.5: the results of NOx emission considering 4 levels of demand in the 6-unit system.

| Load (MW) | Emission of $NO_x$ (kg/h) | | | | | | | | | |
|---|---|---|---|---|---|---|---|---|---|---|
| | PSO | SA | QBA | MBO | SCA | GOA | QITFA | MRFO | GBO | MRFO-GBO |
| 150 | 2,424.60 | 2,379.35 | 2,408.10 | 2,406.24 | 2,406.237 | 2,406.18 | 2,406.79 | 2402.81 | 2412.23 | 2410.25 |
| 175 | 2,879.70 | 2,789.92 | 2,853.40 | 2,854.13 | 2,854.007 | 2,854.08 | 2,856.22 | 2842.71 | 2849.60 | 2838.31 |
| 200 | 3,373.20 | 3,285.65 | 3,327.78 | 3,325.35 | 3,325.339 | 3,325.31 | 3,313.29 | 3305.02 | 3315.82 | 3309.15 |
| 225 | 3,877.60 | 3,781.19 | 3,822.53 | 3,811.18 | 3,820.289 | 3,819.56 | 3,815.71 | 3806.30 | 3810.95 | 3810.87 |

Table 5.6: the results of CO2 emission considering 4 levels of demand in the 6-unit system.

| Load (MW) | Emission of $CO_2$ (kg/h) | | | | | | | | | |
|---|---|---|---|---|---|---|---|---|---|---|
| | PSO | SA | QBA | MBO | SCA | GOA | QITFA | MRFO | GBO | MRFO-GBO |
| 150 | 2,607.10 | 2,568.95 | 2,565.14 | 2,564.57 | 2,564.567 | 2,564.50 | 2,561.85 | 2548.02 | 2558.11 | 2562.82 |
| 175 | 3,178.00 | 3,094.69 | 3,129.78 | 3,129.20 | 3,129.187 | 3,129.07 | 3,133.60 | 3081.95 | 3097.19 | 3097.60 |
| 200 | 3,771.50 | 3,714.33 | 3,719.64 | 3,715.69 | 3,715.637 | 3,715.56 | 3,721.30 | 3681.01 | 3691.95 | 3681.42 |
| 225 | 4,403.00 | 4,324.30 | 4,323.47 | 4,328.07 | 4,322.521 | 4,322.26 | 4,322.39 | 4317.89 | 4324.63 | 4315.41 |

Table 5.7: the results of total emission considering 4 levels of demand in the 6-unit system.

| Load (MW) | Total Emission (kg/h) | | | | | | | | | |
|---|---|---|---|---|---|---|---|---|---|---|
| | PSO | SA | QBA | MBO | SCA | GOA | QITFA | MRFO | GBO | MRFO-GBO |

| | | | | | | | | | | |
|---|---|---|---|---|---|---|---|---|---|---|
| 150 | 8,225.3 | 8,086.74 | 8,120.62 | 8117.64 | 8117.63 | 8117.49 | 8,056.56 | 8080.72 | 8119.16 | 8118.62 |
| 175 | 9,962.6 | 9,648.09 | 9,842.14 | 9842.82 | 9842.55 | 9842.52 | 9,797.31 | 9719.68 | 9754.83 | 9740.14 |
| 200 | 11,815.3 | 11,553.9 | 11,645.62 | 11633.68 | 11633.47 | 11633.33 | 11,562.87 | 11516.23 | 11560.73 | 11523.59 |
| 225 | 13,706.7 | 13,392.8 | 13,490.75 | 13475.06 | 13482.77 | 13480.24 | 13,427.55 | 13440.81 | 13469.99 | 13444.95 |

Table 5.8 illustrate the results for total cost, which represents the main objective function in this studying. From this table, it can be seen that the MRFO-GBO method provides the best overall results for all levels of demand in the 6-unit power generation system.

Table 5.8: the results of total cost considering 4 levels of demand in the 6-unit system.

| Load (MW) | Total cost ($/h) | | | | | | | | | |
|---|---|---|---|---|---|---|---|---|---|---|
| | PSO | SA | QBA | MBO | SCA | GOA | QITFA | MRFO | GBO | MRFO-GBO |
| 150 | 10,385 | 10,261.49 | 10,255.28 | 10,255.21 | 10,255.208 | 10,254.98 | 10,254.91 | 10178.64 | 10177.19 | **10177.05** |
| 175 | 12,425 | 12,280.04 | 12,241.74 | 12,241.67 | 12,241.668 | 12,241.41 | 12,241.61 | 12136.42 | 12135.38 | **12134.42** |
| 200 | 14,642 | 14,421.30 | 14,413.88 | 14,413.71 | 14,413.709 | 14,413.52 | 14,413.56 | 14268.53 | 14268.48 | **14268.09** |
| 225 | 17,125 | 16,790.69 | 16,783.91 | 16,784.34 | 16,783.781 | 16,783.68 | 16,783.33 | 16599.99 | 16600.16 | **16599.71** |

The optimal scheduling results of the MRFO, GBO and Hybrid MRFO-GBO for four levels of demand in 6-unit system are tabulated in Table 5.9. While the convergence Characteristics of them for four levels of demand are illustrated in Figures 5.3, 5.4, 5.5, and 5.6 respectively. These figures show that using of hybrid MRFO-GBO improved their characteristics and make them reach to the optimum solution in all levels of demand.

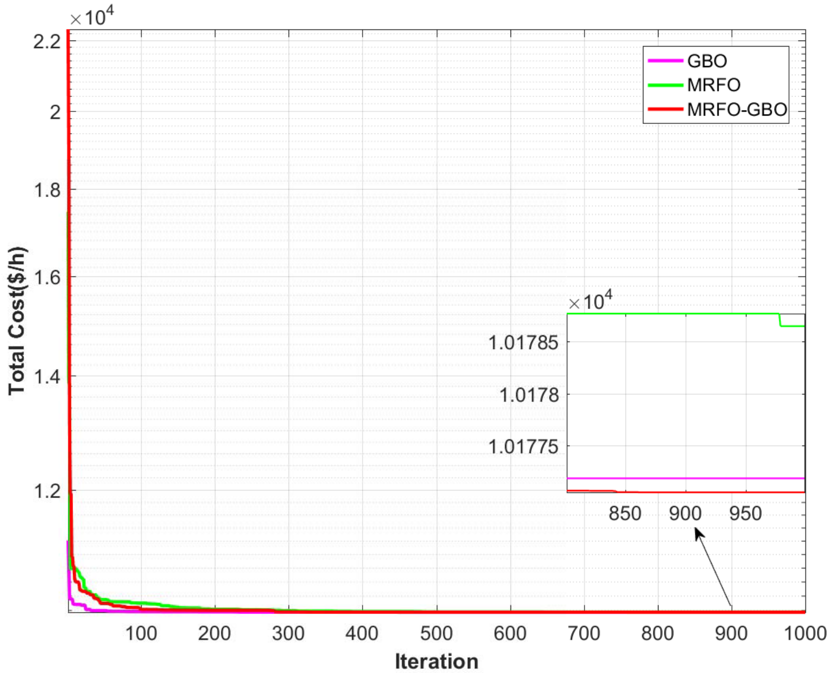


Figure 5.3: Convergence Characteristics of MRFO, GBO and Hybrid MRFO-GBO for load demand 150MW in 6-unit system.

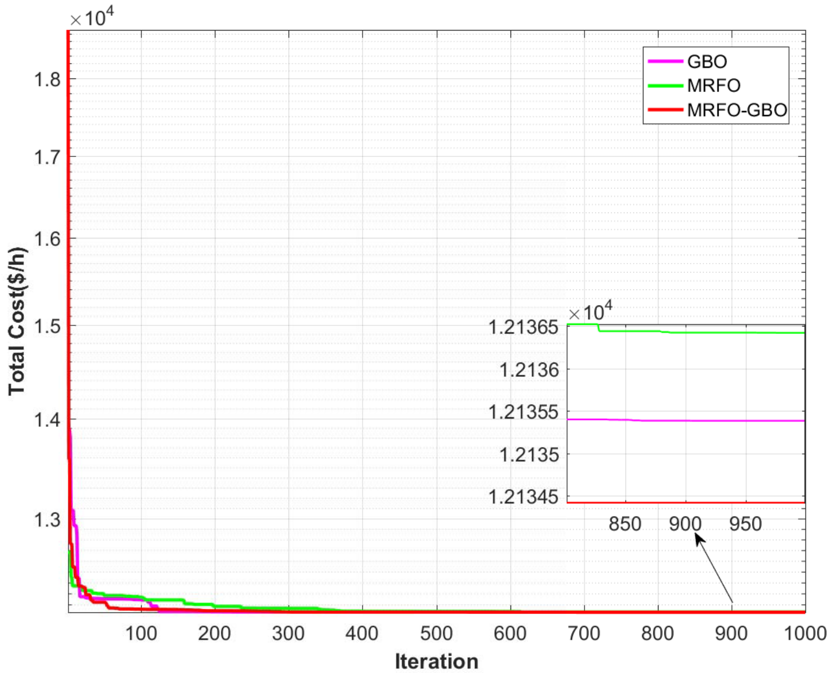


Figure 5.4: Convergence Characteristics of MRFO, GBO and Hybrid MRFO-GBO for load demand 175MW in 6-unit system.

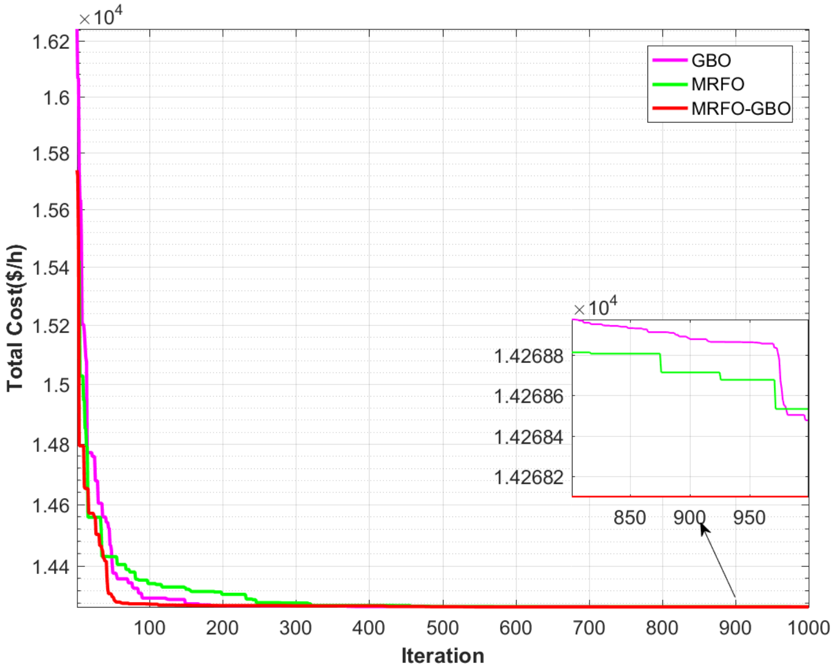


Figure 5.5: Convergence Characteristics of MRFO, GBO and Hybrid MRFO-GBO for load demand 200MW in 6-unit system.

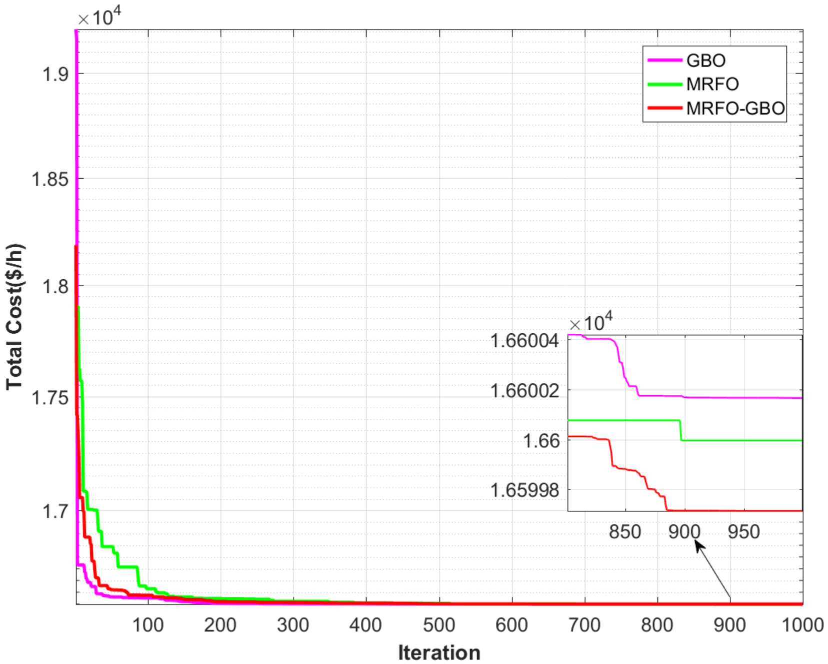


Figure 5.6: Convergence Characteristics of MRFO, GBO and Hybrid MRFO-GBO for load demand 225MW in 6-unit system.

Table 5.9: Results of CEED for the 6-unit system using MRFO, GBO and Hybrid MRFO-GBO.

| Method | MRFO | GBO | MRFO-GBO | MRFO | GBO | MRFO-GBO | MRFO | GBO | MRFO-GBO | MRFO | GBO | MRFO-GBO |
|---|---|---|---|---|---|---|---|---|---|---|---|---|
| Load (MW) | | 150 MW | | | 175 MW | | | 200 MW | | | 225 MW | |
| P1 (MW) | 50.01 | 50.00 | 50.00 | 50.02 | 50.00 | 50.00 | 50.00 | 50.00 | 50.00 | 50.00 | 50.00 | 50.00 |
| P2 (MW) | 21.36 | 20.00 | 20.21 | 28.50 | 27.62 | 27.60 | 35.14 | 33.71 | 35.10 | 41.33 | 41.17 | 41.18 |
| P3 (MW) | 15.00 | 15.00 | 15.00 | 15.00 | 15.00 | 15.00 | 15.04 | 15.00 | 15.00 | 16.46 | 15.87 | 16.52 |
| P4 (MW) | 25.33 | 25.93 | 25.35 | 31.86 | 31.65 | 31.32 | 37.39 | 38.03 | 37.52 | 43.29 | 43.68 | 43.58 |
| P5 (MW) | 17.09 | 16.97 | 16.77 | 22.13 | 21.71 | 22.72 | 28.29 | 28.39 | 28.01 | 33.97 | 34.28 | 33.77 |
| P6 (MW) | 21.20 | 22.09 | 22.67 | 27.48 | 29.02 | 28.36 | 34.14 | 34.87 | 34.37 | 39.94 | 39.99 | 39.94 |
| Fuel cost ($/h) | 2714.62 | 2706.42 | 2706.58 | 3212.77 | 3206.50 | 3206.15 | 3743.52 | 3737.05 | 3742.84 | 4319.78 | 4317.91 | 4319.33 |
| Emission of $SO_2$ (kg/h) | 3129.89 | 3148.80 | 3145.54 | 3795.02 | 3808.03 | 3804.23 | 4530.21 | 4552.96 | 4533.03 | 5316.61 | 5334.40 | 5318.66 |
| Emission of $No_x$ (kg/h) | 2402.81 | 2412.23 | 2410.25 | 2842.71 | 2849.60 | 2838.31 | 3305.02 | 3315.82 | 3309.15 | 3806.30 | 3810.95 | 3810.87 |
| Emission of $CO_2$ (kg/h) | 2548.02 | 2558.11 | 2562.82 | 3081.95 | 3097.19 | 3097.60 | 3681.01 | 3691.95 | 3681.42 | 4317.89 | 4324.63 | 4315.41 |
| Total Cost ($/h) | 10178.64 | 10177.19 | **10177.05** | 12136.42 | 12135.38 | **12134.42** | 14268.53 | 14268.48 | **14268.09** | 16599.99 | 16600.16 | **16599.71** |

### 5.3.2 Solving EED Problem using CAEO Technique

MATLAB (R2019a) is used to simulate conventional AEO and proposed CAEO techniques to solve the CEED problem for two power generation systems (6-unit and 11-units). The description of the portable computer, which is used to solve this problem, are Intel Core i5-4210U CPU@2. 40GHz with a 4.00 MB RAM.

#### 5.3.2.1 6-Unit Power Generation System

In this system, the CEED problem is solved for four levels of demand, where the first level of demand is 150 MW and it is increased by 25MW each time to reach 225 MW in the fourth level of demand. The best-estimated parameters achieved by the proposed CAEO have been confirmed using measured data of a CEED problem for the first level of demand (150 MW) provided in the research. Several operating scenarios have confirmed the proposed CAEO with 10 chaotic functions according to the previous section. In this research, the following control variables have been assumed: the number of population is 100 and the maximum number of iterations is 200. The number of 50 independent runs has been executed under each chaotic function in addition to the conventional AEO to overcome the randomness of the proposed optimization technique and to check the quality of these chaotic functions. According to the results of these independent runs, the best solution is taken as the lowest value of the fitness function. The system data of this case are taken from Appendix (A) where the coefficients of Fuel cost and operational limits are given in the table A-1 , the coefficients of SO2 Emission and its max/max PPF are taken from the table A-2, the coefficients of NOx Emission and its max/max PPF are given in the table A-3, and the coefficients of CO2 Emission and its max/max PPF are taken from the table A-4.

#### 5.3.2.1.1 Case 1: Estimation of Total Cost ($/h) for Load =150 MW

To validate the strength of proposed CAEO for the parameters identification of Total cost ($/h) to solve a CEED problem for load demand equals 150 MW, a statistical analysis is presented for the lowest values of fitness function (SSE) which obtained from 50 individual runs This analysis is presented to provide a clear estimation of 10 chaotic functions and choose the most precise one for completing the study of the suggested system with other levels of demand in the rest of this thesis.

The comparisons between the proposed CAEO according to 10 chaotic functions and the conventional AEO are executed regarding nine metrics. The first four of these metrics are the best and worst values of $SSE$, the mean value of $SSE$, and Median. The other metrics are $SD$, $RE$, $RMSE$, MAE, and $efficiency$ and these metrics can be calculated from the following equations [145]:

$$SD = \sqrt{\frac{\sum_{i=1}^{50}(SSE_i - \overline{SSE})}{50-1}} \tag{5.1}$$

$$RE = \frac{\sum_{i=1}^{50}(SSE_i - SSE_{min})}{SSE_{min}} \tag{5.2}$$

$$\mathrm{MAE} = \frac{\sum_{i=1}^{50}(\mathrm{SSE_i} - \mathrm{SSE_{min}})}{50} \tag{5.3}$$

$$RMSE = \sqrt{\frac{\sum_{i=1}^{50}(SSE_i - SSE_{min})^2}{50}} \tag{5.4}$$

$$efficiency = \frac{SSE_{min}}{SSE_i} \times 100\% \tag{5.5}$$

where $SSE_i$ is the lowest value of the objective function in each run. $\overline{SSE}$ is the mean value of $SSE$ overall. $SSE_{min}$ is the lowest best value of $SSE$ over the 50 runs. Table 5.10 presents the statistical results of ten proposed CAEO as well as the conventional AEO. From this table, it can be noticed that the lowest value of $SSE$ obtained by the 4th chaotic function is the best within all functions and the conventional AEO algorithm and gives the best value of Total cost (10179.349 \$/h). Therefore, the fourth chaotic function is selected to complete study of the suggested system with other levels of demand. Figure 5.7 illustrates the convergence characteristics of ten proposed CAEO and conventional AEO.

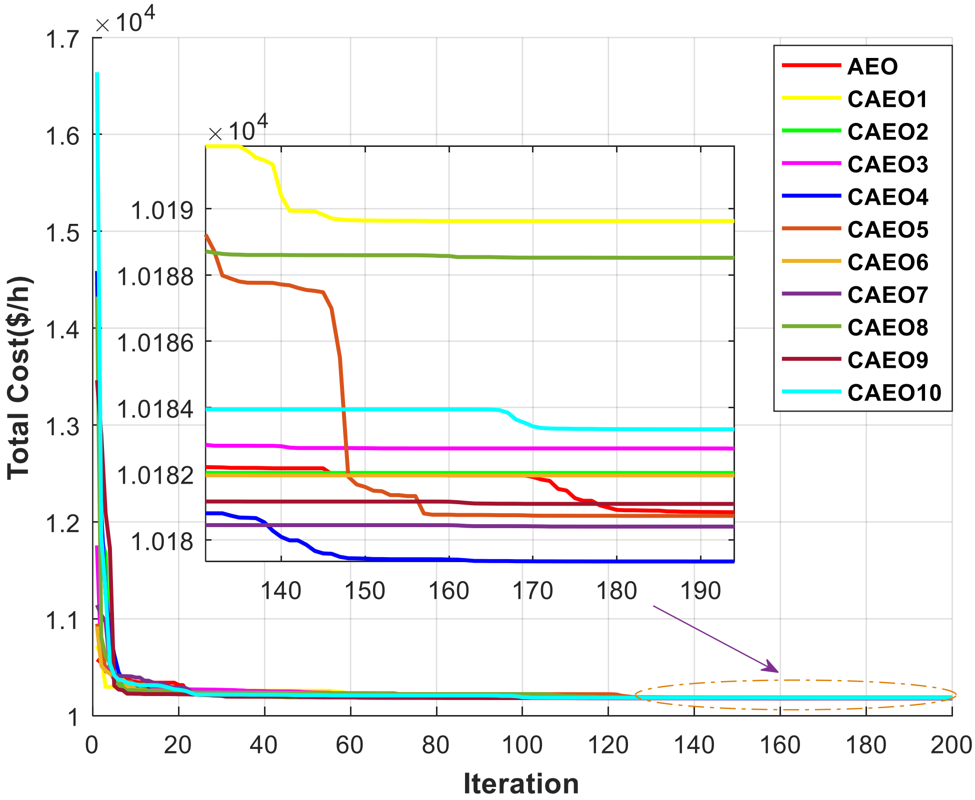


Figure 5.7: Convergence characteristics of proposed CAEO and AEO.

The results for the 6-unit system considering the first level of demand equals 150MW are provided in Table 5.11. These results include the value of fuel cost, the value of three types of emission ($SO_2$, $NO_x$, and $CO_2$, respectively), and the value of total cost. Table 5.11 displays the comparison between the results obtained by the proposed CAEO techniques and the results of the conventional AEO as well as the other recent optimization techniques, which studied this problem previously. From Table 5.11, we can see that the fuel cost, the value of three types of emission, and total cost, for the 150MW load demand obtained by CAEO4 are 2702.94 \$/h,2885.21 kg/h, 2249.1 kg/h, 2448.86 kg/h, 10179.349 \$/h, respectively.

It is concluded that CAEO4 technique is better than the others proposed CAEO and the conventional AEO as well as other recent optimization techniques such as LR [21], PSO [169], SA [170], QBA [85], MBO [171] and SCA [172] methods. Because CAEO4 has the best values for 150MW load demand, we will continue the next simulation results for other loads as single and multi-objective functions using CAEO4.

#### 5.3.2.1.2 Case 2: Simulation Results for Different Load Demands.

Table 5.12 and Figure 5.8.a show a comparison of fuel cost ($/h) considering four levels of demand in the 6-unit power generation system. It can be noticed from Table 5.11 that CAEO4 gives the best value of fuel cost for all levels of demand. The differences between the proposed CAEO4 method and the nearest method (conventional AEO) to it are 0.75 $/h for the first level of demand, 7.97 $/h for the second level of demand, 2.26 $/h for the third level of demand, and 0.59 $/h for the fourth level of demand.

Figure 5.8.a displays the comparison graph of different methods for levels of demand. According to Table 5.12 and Figure 5.8.a, we can conclude that CAEO4 provides the best value of fuel costs; conventional AEO closely follows the proposed CAEO, whereas MBO, QBA, SA, PSO, and LR methods provide the highest value of fuel cost.

Table 5.10: statistical results of proposed CAEO and conventional AEO for the total cost of the 6-unit system (150mw load).

| optimization techniques | Min | Max | MEAN | Median | SD | RE | MAE | RMSE | Eff. |
|---|---|---|---|---|---|---|---|---|---|
| AEO | 10180.834 | 10201.468 | 10187.4646 | 10187.499 | 601.491 | 0.0242 | 4.917 | 7.7220 | 99.95 |
| CAEO1 | 10189.257 | 10206.534 | 10193.4787 | 10191.777 | 637.238 | 0.0277 | 5.645 | 8.4655 | 99.94 |
| CAEO2 | 10182.023 | 10197.209 | 10187.0025 | 10185.448 | 504.950 | 0.0255 | 5.199 | 7.2122 | 99.95 |
| CAEO3 | 10180.948 | 10206.169 | 10187.8050 | 10185.155 | 677.080 | 0.0282 | 5.741 | 8.8252 | 99.94 |
| CAEO4 | 10179.349 | 10219.630 | 10186.6464 | 10183.197 | 778.508 | 0.0250 | 5.084 | 9.2329 | 99.95 |
| CAEO5 | 10180.724 | 10217.198 | 10188.0959 | 10184.764 | 766.531 | 0.0275 | 5.599 | 9.4304 | 99.95 |
| CAEO6 | 10181.969 | 10204.980 | 10188.2257 | 10184.733 | 576.669 | 0.0187 | 3.814 | 6.8655 | 99.96 |
| CAEO7 | 10180.402 | 10202.343 | 10186.7732 | 10186.442 | 548.832 | 0.0219 | 4.465 | 7.0324 | 99.96 |
| CAEO8 | 10188.519 | 10212.684 | 10196.0928 | 10193.216 | 811.825 | 0.0308 | 6.262 | 10.188 | 99.94 |
| CAEO9 | 10181.087 | 10205.830 | 10189.4777 | 10188.000 | 654.437 | 0.0261 | 5.318 | 8.3818 | 99.95 |
| CAEO10 | 10183.274 | 10192.094 | 10185.9889 | 10184.137 | 372.765 | 0.0152 | 3.095 | 4.8162 | 99.97 |

Table 5.11: Estimated parameters of Cost for 150MW using CAEO, AEO, and other well-known optimization techniques.

| Optimization techniques | Fuel cost ($/h) | $SO_2$ Emission (kg/h) | $NO_x$ Emission (kg/h) | $CO_2$ Emission (kg/h) | Total cost ($/h) |
|---|---|---|---|---|---|
| **CAEO1** | 2703.540 | 3037.750 | 2335.920 | 2502.55 | 10189.260 |
| **CAEO2** | 2702.217 | 3028.343 | 2339.656 | 2605.428 | 10182.023 |
| **CAEO3** | 2704.835 | 2931.922 | 2362.363 | 2528.619 | 10180.948 |
| **CAEO4** | 2702.944 | 2885.210 | 2249.105 | 2448.860 | 10179.349 |

| | | | | | |
|---|---|---|---|---|---|
| **CAEO5** | 2702.914 | 3071.733 | 2409.679 | 2649.255 | 10180.724 |
| **CAEO6** | 2704.007 | 2936.314 | 2305.776 | 2462.078 | 10181.969 |
| **CAEO7** | 2702.738 | 3129.145 | 2410.572 | 2571.062 | 10180.402 |
| **CAEO8** | 2701.003 | 3370.514 | 2589.438 | 2932.466 | 10188.519 |
| **CAEO9** | 2703.582 | 3051.836 | 2335.906 | 2551.257 | 10181.087 |
| **CAEO10** | 2701.254 | 2927.012 | 2282.086 | 2480.293 | 10183.274 |
| **AEO** | 2703.686 | 2978.035 | 2349.853 | 2480.418 | 10180.834 |
| **SCA** [172] | 2704.923 | 3146.831 | 2406.237 | 2564.567 | 10255.208 |
| **MBO** [171] | 2704.922 | 3146.831 | 2406.236 | 2564.572 | 10255.210 |
| **QBA** [85] | 2704.970 | 3147.380 | 2408.100 | 2565.140 | 10255.280 |
| **SA** [170] | 2705.210 | 3138.446 | 2379.350 | 2568.946 | 10261.490 |
| **PSO** [169] | 2734.200 | 3193.600 | 2424.600 | 2607.100 | 10385.000 |
| **LR** [21] | 2729.350 | 3091.648 | 2448.218 | 2537.122 | 10264.570 |

Table 5.12: the results of fuel cost considering 4 levels of demand in the 6-unit power generation system.

| Load (MW) | Total fuel cost ($/h) | | | | | | | |
|---|---|---|---|---|---|---|---|---|
| | LR [21] | PSO [169] | SA [170] | QBA [85] | MBO [171] | SCA [172] | AEO | CAEO4 |
| 150 | 2,729.35 | 2,734.2 | 2,705.2 | 2,704.97 | 2,704.92 | 2704.92 | 2,703.69 | **2,702.94** |
| 175 | 3,475.41 | 3,236.3 | 3,220.5 | 3,188.10 | 3,188.13 | 3188.15 | 3,187.31 | **3,179.34** |
| 200 | 4,210.30 | 3,784.9 | 3,735.7 | 3,726.08 | 3,727.43 | 3727.45 | 3,724.71 | **3,722.45** |
| 225 | 5,130.53 | 4,402.3 | 4,321.5 | 4,314.63 | 4,315.63 | 4315.05 | 4,314.97 | **4,314.38** |

Table 5.13: the results of SO2 emission considering 4 levels of demand in the 6-unit power generation system.

| Load (MW) | Emission of $SO_2$(kg/h) | | | | | | | |
|---|---|---|---|---|---|---|---|---|
| | LR [21] | PSO [169] | SA [170] | QBA [85] | MBO [171] | SCA [172] | AEO | CAEO4 |
| 150 | 3,091.65 | 3,193.60 | 3,138.45 | 3,147.38 | 3,146.83 | 3146.8310 | 2,978.03 | 2,885.21 |
| 175 | 4,142.18 | 3,904.90 | 3,763.48 | 3,858.96 | 3,859.49 | 3859.3593 | 3,829.72 | 3,891.64 |
| 200 | 5,053.58 | 4,670.60 | 4,553.97 | 4,598.20 | 4,592.64 | 4592.4934 | 4,618.24 | 4,589.87 |
| 225 | 6,106.50 | 5,426.10 | 5,287.31 | 5,344.75 | 5,335.81 | 5339.9612 | 5,235.67 | 5,360.57 |

Table 5.14: the results of NOx emission considering 4 levels of demand in the 6-unit power generation system.

| Load (MW) | Emission of $NO_x$ (kg/h) | | | | | | | |
|---|---|---|---|---|---|---|---|---|
| | LR [21] | PSO [169] | SA [170] | QBA [85] | MBO [171] | SCA [172] | AEO | CAEO4 |
| 150 | 2,448.22 | 2,424.60 | 2,379.35 | 2,408.10 | 2,406.24 | 2406.2374 | 2,349.85 | **2,249.11** |
| 175 | **2,604.89** | 2,879.70 | 2,789.92 | 2,853.40 | 2,854.13 | 2854.0066 | 2,883.36 | 2,847.56 |
| 200 | **3,102.08** | 3,373.20 | 3,285.65 | 3,327.78 | 3,325.35 | 3325.3389 | 3,362.90 | 3,301.53 |
| 225 | 3,798.38 | 3,877.60 | 3,781.19 | 3,822.53 | 3,811.18 | 3820.2894 | **3,758.10** | 3,832.07 |

Table 5.15: the results of CO2 emission considering 4 levels of demand in the 6-unit power generation system.

| Load (MW) | Emission of $CO_2$(kg/h) | | | | | | | |
|---|---|---|---|---|---|---|---|---|
| | LR [21] | PSO [169] | SA [170] | QBA [85] | MBO [171] | SCA [172] | AEO | CAEO4 |
| 150 | 2,537.12 | 2,607.10 | 2,568.95 | 2,565.14 | 2,564.57 | 2564.5670 | 2,480.42 | **2,448.86** |
| 175 | 3,613.53 | 3,178.00 | **3,094.69** | 3,129.78 | 3,129.20 | 3129.1869 | 3,136.06 | 3,154.93 |
| 200 | 4,473.37 | 3,771.50 | **3,714.33** | 3,719.64 | 3,715.69 | 3715.6370 | 3,719.48 | 3,725.20 |
| 225 | 5,502.52 | 4,403.00 | 4,324.30 | 4,323.47 | 4,328.07 | 4322.5213 | **4,255.72** | 4,322.68 |

Table 5.16: the results of total cost considering 4 levels of demand in a 6-unit power generation system.

| Load (MW) | Total cost ($/h) | | | | | | | |
|---|---|---|---|---|---|---|---|---|
| | LR [21] | PSO [169] | SA [170] | QBA [85] | MBO [171] | SCA [172] | AEO | CAEO4 |
| 150 | 10,264.57 | 10,385 | 10,261.49 | 10,255.28 | 10,255.21 | 10255.208 | 10,180.83 | **10,179.35** |
| 175 | 13,251.52 | 12,425 | 12,280.04 | 12,241.74 | 12,241.67 | 12241.668 | 12,172.06 | **12,164.36** |
| 200 | 16,077.41 | 14,642 | 14,421.30 | 14,413.88 | 14,413.71 | 14413.709 | 14,293.19 | **14,287.65** |
| 225 | 19,661.33 | 17,125 | 16,790.69 | 16,783.91 | 16,784.34 | 16783.781 | 16,617.10 | **16,603.90** |

Table 5.17: Results of CEED for the 6-unit system using AEO and CAEO4.

| Load (MW) | AEO | CAEO4 | AEO | CAEO4 | AEO | CAEO4 | AEO | CAEO4 |
|---|---|---|---|---|---|---|---|---|
| | 150 MW | | 175 MW | | 200 MW | | 225 MW | |
| P1 (MW) | 50.000 | 50.000 | 50.074 | 50.00823 | 50.010 | 50.002 | 50.0 | 50.004 |
| P2 (MW) | 20.024 | 20.007 | 22.683 | 21.24516 | 29.909 | 29.602 | 37.2 | 39.421 |
| P3 (MW) | 15.000 | 15.000 | 15.999 | 15.01373 | 15.213 | 15.002 | 16.8 | 16.079 |
| P4 (MW) | 24.096 | 23.968 | 30.159 | 32.97348 | 40.223 | 38.672 | 44.8 | 45.271 |
| P5 (MW) | 16.179 | 18.988 | 24.745 | 26.27831 | 27.354 | 30.327 | 36.4 | 34.260 |
| P6 (MW) | 24.701 | 22.038 | 31.339 | 29.48110 | 37.297 | 36.396 | 39.7 | 39.965 |
| Fuel cost ($/h) | 2703.686 | 2702.944 | 3187.307 | 3179.337 | 3724.708 | 3722.450 | 4315.0 | 4314.380 |
| Emission of $SO_2$ (kg/h) | 2978.035 | 2885.210 | 3829.720 | 3891.639 | 4618.244 | 4589.868 | 5235.7 | 5360.573 |
| Emission of $No_x$ (kg/h) | 2349.853 | 2249.105 | 2883.358 | 2847.565 | 3362.898 | 3301.527 | 3758.102 | 3832.066 |
| Emission of $CO_2$ (kg/h) | 2480.418 | 2448.860 | 3136.058 | 3154.931 | 3719.476 | 3725.202 | 4255.7 | 4322.681 |
| Total Cost ($/h) | 10,180.8 | 10,179.35 | 12,172.1 | 12,164.4 | 14,293.19 | 14,287.65 | 16,617.1 | 16,603.9 |

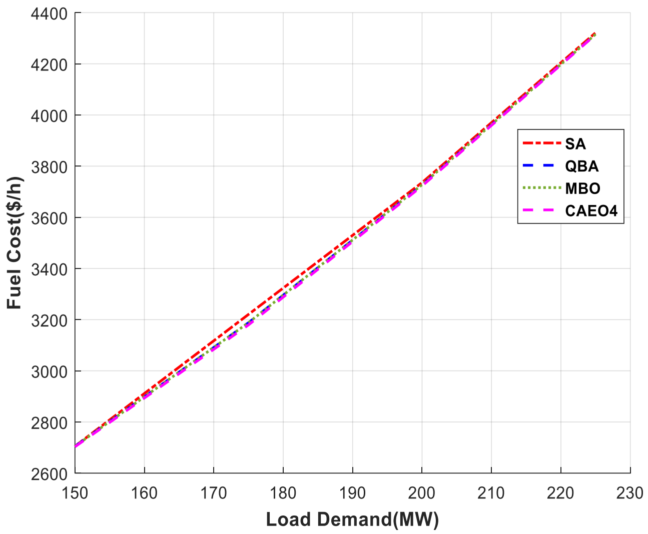


(a)

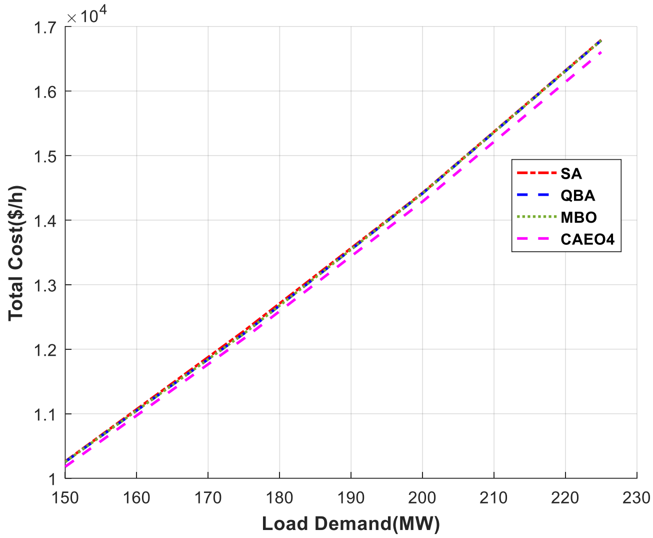


(b)

Figure 5.8: Variations of methods for different levels of demand in 6-unit system (a) Fuel cost ($/h) (b) Total cost ($/h).

From Table 5.13, we can see that the comparison of emission for SO2 considering 4 levels of demand in a 6-unit power generation system. CAEO4 provides the best value (2885.21 kg/h) for the first level, whereas SA provides the best results (3,763.48; 4,553.97 kg/h) for the second and third levels. Finally, AEO has the best value (5,235.67 kg/h) for the fourth level. From Table 5.14, we can see that the comparison of emission for NOx. CAEO4 provides the best value (2,249.11 kg/h) for the first level, whereas LR provides the best results (2,604.89; 3,102.08 kg/h) for the second and third levels. Finally, AEO has the best value (3,758.10 kg/h) for the fourth level. From Table 5.15, we can see that the comparison of emission for CO2. CAEO4 provides the best value (2,448.86 kg/h) for the first level, whereas SA provides the best results (3,094.69; 3,714.33 kg/h) for the second and third level. Finally, AEO has the best value (4,255.72 kg/h) for the fourth level.

Finally, Table 5.16 and Figure 5.8.b present a comparison of the lowest value of the total cost ($/h), which is considered the main objective in this studying as a single objective function. From this table, the CAEO4 method provides the best overall results for all levels of demand in the 6-unit power generation system. Figure 5.9 illustrates the convergence curves of the proposed CAEO4 technique for obtaining the optimum convergence to single-objective CEED problems using different levels of demand. From this Figure, it can be noticed that the curves tend to converge very fast and they are converging to achieve the optimal value through 200 iterations. It also displays that the CAEO4 technique has the highest computational prowess. The simulation results obtained from the four cases also show that they are robust and reliable. Finally, it can be confirmed that the proposed CAEO4 technique provides accurate and reliable solutions with strong computational competence after it is compared with the conventional AEO, MBO, QBA, SA, PSO, and LR.

Figure 5.10 shows the comparison between the convergence curves of proposed CAEO4 and the conventional AEO for the total cost at three levels of demand in a 6-unit power system. In addition, it can be seen from Table 5.17 that the results of CAEO4 are more reliable and robust than the conventional AEO for different levels of demand.

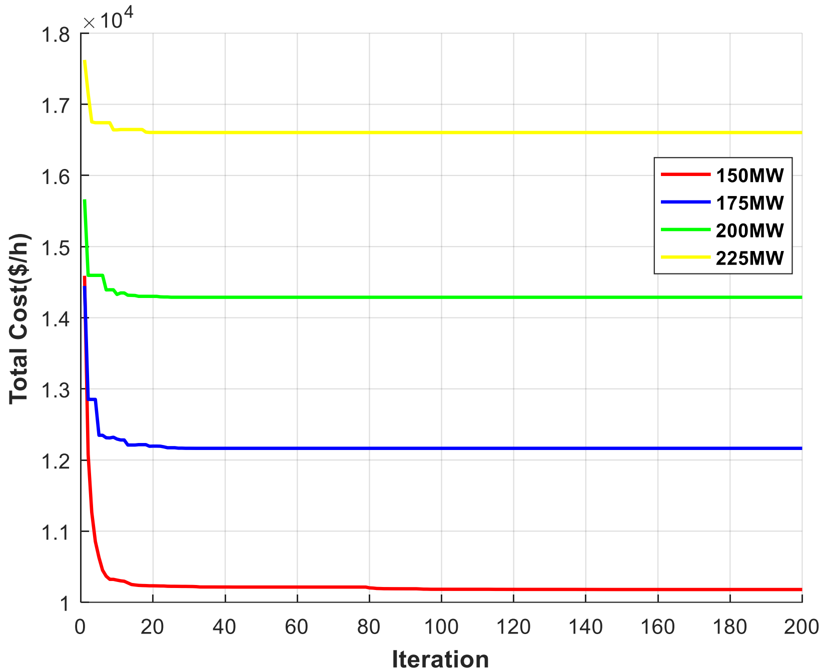


Figure 5.9: Convergence curves of the CAEO4 method for different levels of demand.

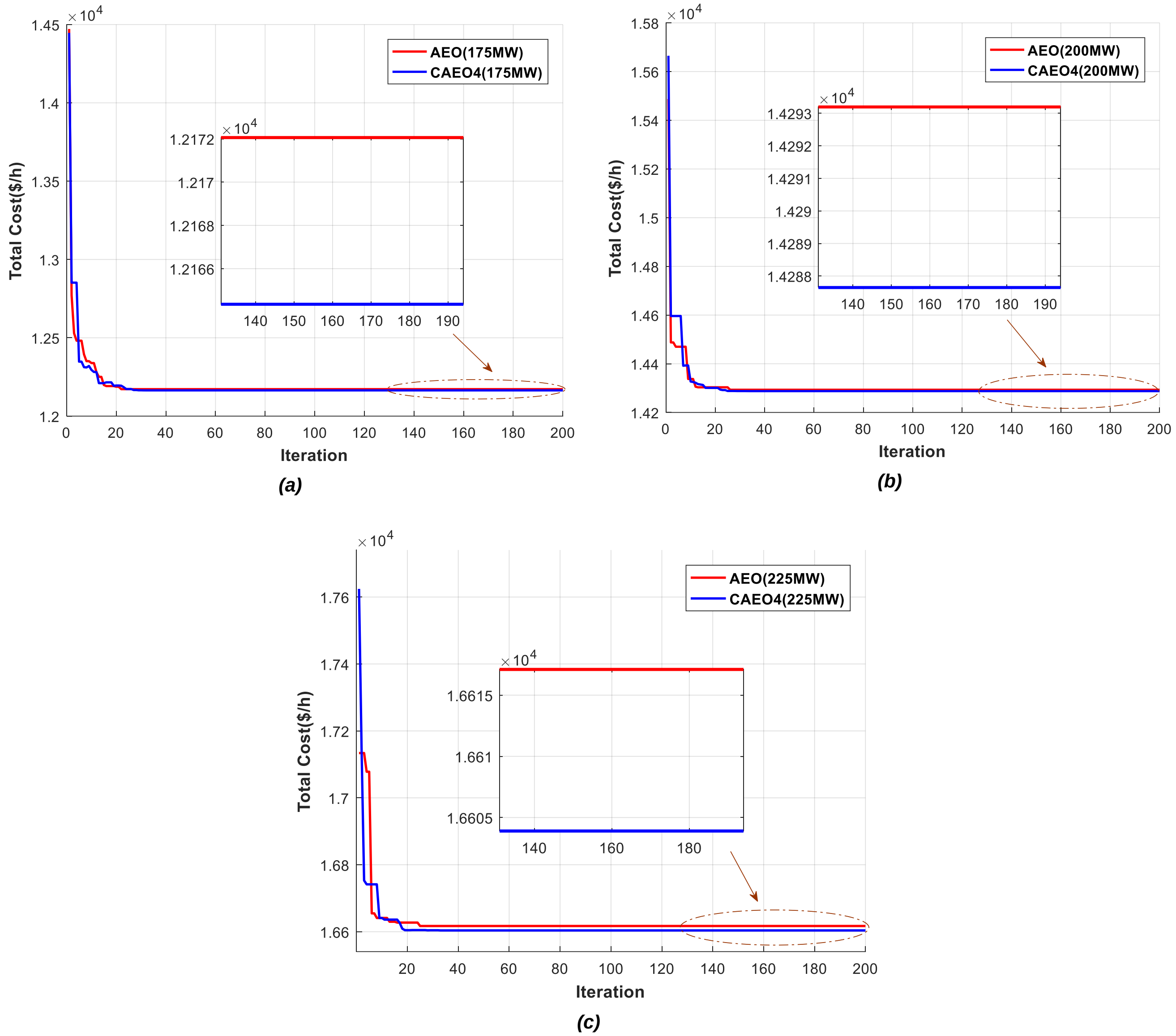


Figure 5.10: Convergence Characteristics of AEO and CAEO4 for 3 levels of demand in 6-unit power system (a) Load Demand=175 MW (b) Load Demand=200MW (c) Load Demand=225MW.

### 5.3.2.2 11-Unit Power Generation 69-Bus System:

#### 5.3.2.2.1 Case 1: The Optimum Values of Fuel Cost.

This test system consists of 11-generating units (69-bus, 11-generator, coal-fired power system) with different load demand values (1000, 1500, 2000, and 2500MW) and the optimal results obtained by the CAEO-4 are compared with the conventional AEO algorithm. At the load demand = 2500 MW, the results of the proposed algorithm are compared with six-recent methods beside the original AEO algorithm to check the effectiveness of the proposed technique. The number of populations is 20, and the maximum number of iterations is 2000. The Generation limits, Fuel cost coefficients, and emission coefficients of the system are given in Appendix B.1.

In Table 5.18, the best values of fuel cost attained using the proposed CAEO-4 were 8408.4307, 9623.5203, 10912.3379, and 12274.4028 $/h for the load demand of 1000, 1500, 2000, and 2500 MW, respectively. These results confirm the superiority of the proposed CAEO-4 method compared with the conventional AEO. The comparative convergence curves between the proposed CAEO4 and AEO are shown in Figure 5.11.

Table 5.18: Results of the fuel cost for the 11-unit system using AEO and CAEO4.

| Generating Unit, MW | 1000MW | | 1500MW | | 2000MW | | 2500MW | |
|---|---|---|---|---|---|---|---|---|
| | **AEO** | **CAEO4** | **AEO** | **CAEO4** | **AEO** | **CAEO4** | **AEO** | **CAEO4** |
| P1 | 28.1109 | 26.9032 | 38.2802 | 37.9728 | 47.6185 | 47.6678 | 57.0104 | 57.0440 |
| P2 | 20.1227 | 20.0474 | 23.1434 | 23.1548 | 31.7279 | 31.2992 | 40.4182 | 40.5110 |
| P3 | 20.0881 | 20.0000 | 29.7579 | 30.1502 | 43.4838 | 43.6162 | 57.6054 | 58.0006 |
| P4 | 119.0846 | 119.5868 | 174.2851 | 171.9100 | 226.1858 | 225.2687 | 277.8938 | 278.1442 |
| P5 | 44.0101 | 44.1590 | 91.7651 | 92.2375 | 138.7365 | 138.5868 | 187.2295 | 186.5444 |
| P6 | 126.3340 | 120.3953 | 166.6362 | 166.4011 | 208.0531 | 207.9147 | 249.7332 | 249.6237 |
| P7 | 60.2112 | 63.4011 | 101.0234 | 102.3885 | 139.8906 | 139.7655 | 177.4899 | 177.3503 |
| P8 | 166.2222 | 172.0383 | 242.3194 | 242.4297 | 309.2088 | 312.7202 | 380.3062 | 380.7580 |
| P9 | 154.6643 | 153.7968 | 215.9341 | 216.3218 | 278.0736 | 279.7097 | 341.2216 | 341.4758 |
| P10 | 132.8594 | 135.7267 | 213.5000 | 214.2392 | 297.6213 | 296.3373 | 378.5940 | 377.8372 |
| P11 | 128.2927 | 123.9454 | 203.3553 | 202.7944 | 279.3999 | 277.1138 | 352.4965 | 352.7109 |
| $P_T$ | 1000 | 1000 | 1500 | 1500 | 2000 | 2000 | 2500 | 2500 |
| Fuel cost, $/h | 8408.4353 | **8408.4307** | 9623.5218 | **9623.5203** | 10912.3394 | **10912.3379** | 12274.4032 | **12274.4028** |
| Emission, ton/h | 369.9576 | 368.8915 | 821.0156 | 819.0274 | 1541.7568 | 1541.4073 | 2541.9545 | 2540.7367 |
| Computation time (s) | 4.6609 | 4.6550 | 4.6613 | 4.6579 | 4.8261 | 4.7930 | 4.8812 | 4.8626 |

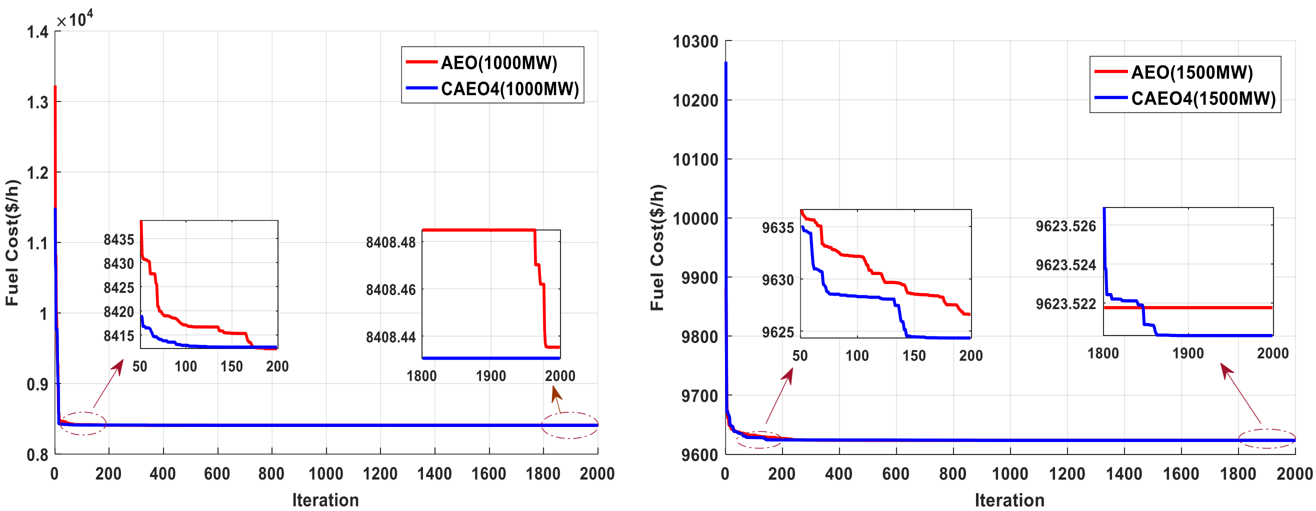


(a) (b)

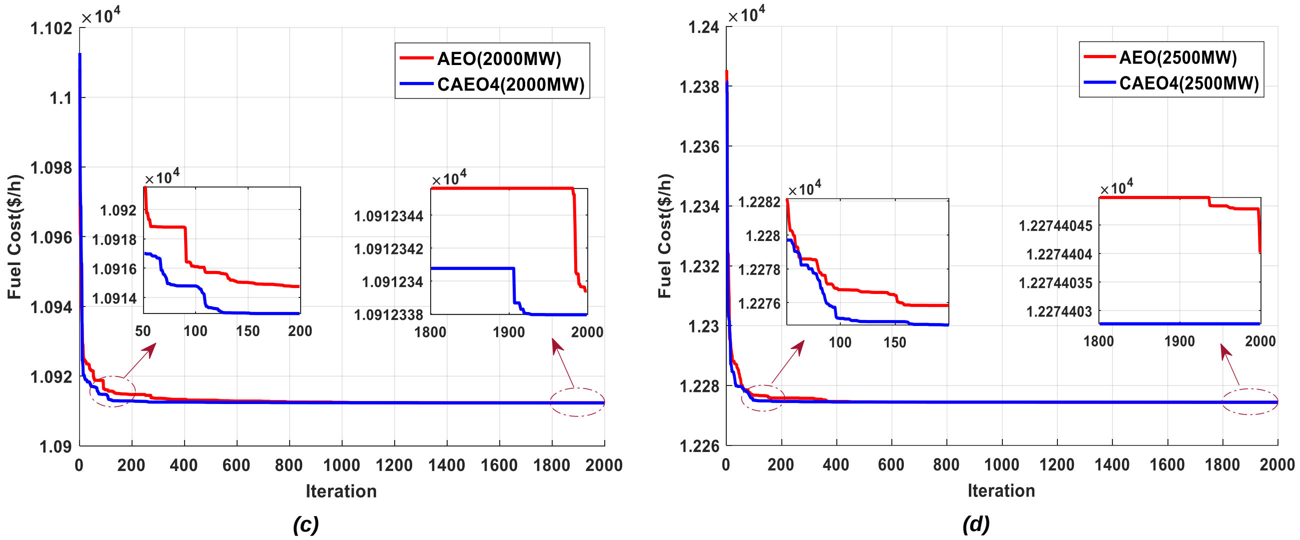


Figure 5.11: Fuel cost convergence curves of AEO and CAEO4 techniques (Case study 2) (a) 1000MW (b) 1500MW (c)2000MW (d)2500MW.

The best fuel cost results obtained by the proposed CAEO4, original AEO, and other metaheuristic (CSAISA [173], ISA [173], GA [173], PSO [173], DE [173], HAS [173]) techniques are compared in Table 5.19.

Table 5.19: The best solution values for the fuel cost of the case study 2 (2500 MW).

| Generating Unit, MW | HSA | DE | PSO | GA | ISA | CSAISA | AEO | CAEO4 |
|---|---|---|---|---|---|---|---|---|
| P1 | 56.5750 | 57.5683 | 57.6582 | 57.4565 | 57.3520 | 56.9465 | 57.0104 | 57.0440 |
| P2 | 41.7558 | 39.8234 | 41.7560 | 40.7339 | 40.3501 | 40.5882 | 40.4182 | 40.5110 |
| P3 | 58.8239 | 57.3622 | 57.0840 | 60.6382 | 58.5628 | 57.9381 | 57.6054 | 58.0006 |
| P4 | 277.6793 | 277.6343 | 279.6482 | 279.8546 | 278.7029 | 277.9182 | 277.8938 | 278.1442 |
| P5 | 189.5183 | 189.2732 | 189.7429 | 191.7492 | 189.2024 | 186.7996 | 187.2295 | 186.5444 |
| P6 | 250.1128 | 249.9246 | 249.7420 | 249.2131 | 249.5435 | 249.2460 | 249.7332 | 249.6237 |
| P7 | 176.9563 | 175.6345 | 176.6402 | 178.2341 | 176.0364 | 177.6527 | 177.4899 | 177.3503 |
| P8 | 379.8753 | 378.7465 | 377.7493 | 379.3367 | 379.9651 | 380.7402 | 380.3062 | 380.7580 |
| P9 | 341.0440 | 340.8126 | 341.8462 | 344.1547 | 340.7782 | 341.7721 | 341.2216 | 341.4758 |
| P10 | 379.8564 | 378.1122 | 378.7465 | 378.6473 | 378.8541 | 377.8633 | 378.5940 | 377.8372 |
| P11 | 351.6593 | 352.8493 | 350.8284 | 353.6394 | 350.6525 | 352.5351 | 352.4965 | 352.7109 |
| Fuel cost, $/h | 12275.46 | 12277.92 | 12276.42 | 12278.42 | 12274.42 | **12274.40** | **12274.40** | **12274.40** |
| Emission, ton/h | 2538.76 | 2538.74 | 2534.69 | 2531.32 | 2539.69 | 2540.41 | 2541.9545 | 2540.7367 |
| Time (s) | 12.65 | 12.68 | 12.69 | 12.71 | 12.65 | 12.64 | 4.8812 | 4.8626 |

#### 5.3.2.2.2 Case 2: Optimum Values of Total Emission.

The optimal power generation achieved by proposed CAEO4 and AEO algorithms with system demands rising from 1000 MW to 2500 MW for the best total emission are tabulated in Table 5.20. When the results are compared, the proposed CAEO4 gives the better values of total emission with different load demand than the AEO algorithm.

Figure 5.12 shows the convergence characteristics of the CAEO4 and AEO. From this Figure, it can be seen that the convergence characteristic curves of the CAEO4 is fast, smooth and smoothly reach to the optimal value of objective function, compared with the original AEO.

Table 5.20: Results of the Total Emission for the 11-unit system using AEO and CAEO4.

| Generating Unit, MW | 1000MW | | 1500MW | | 2000MW | | 2500MW | |
|---|---|---|---|---|---|---|---|---|
| | AEO | CAEO4 | AEO | CAEO4 | AEO | CAEO4 | AEO | CAEO4 |
| P1 | 114.9310 | 115.6166 | 170.3952 | 169.9899 | 222.3402 | 222.5858 | 250.0000 | 250.0000 |
| P2 | 110.4444 | 106.6322 | 157.8394 | 157.9584 | 203.2599 | 203.9822 | 210.0000 | 210.0000 |
| P3 | 108.5783 | 117.1041 | 168.7295 | 171.1396 | 222.5538 | 223.4453 | 249.9905 | 250.0000 |
| P4 | 63.5394 | 62.9325 | 95.1658 | 94.9936 | 127.2490 | 127.3814 | 170.6799 | 166.5864 |
| P5 | 50.0853 | 48.1375 | 77.0199 | 76.7260 | 105.7898 | 105.9247 | 145.3686 | 142.1694 |
| P6 | 61.4376 | 60.9420 | 95.2664 | 94.0723 | 126.8799 | 126.9826 | 166.7993 | 166.7366 |
| P7 | 47.0821 | 47.2607 | 76.9046 | 76.9785 | 105.3808 | 105.8052 | 142.5525 | 142.0880 |
| P8 | 116.3723 | 117.6070 | 178.7900 | 177.4586 | 239.7585 | 238.9238 | 313.1171 | 316.3717 |
| P9 | 105.8973 | 103.2849 | 158.6913 | 157.6715 | 210.4395 | 209.8031 | 274.0111 | 276.1787 |
| P10 | 110.0000 | 110.0001 | 164.2761 | 164.2563 | 226.9829 | 225.8490 | 305.3927 | 302.5881 |
| P11 | 111.6323 | 110.4824 | 156.9217 | 158.7554 | 209.3656 | 209.3168 | 272.0884 | 277.2812 |
| $P_T$ | 1000 | 1000 | 1500 | 1500 | 2000 | 2000 | 2500 | 2500.0000 |
| Fuel cost, $/h | 8606.9017 | 8610.7957 | 10042.1191 | 10045.6046 | 11607.8374 | 11612.4854 | 13046.2434 | 13046.8016 |
| Emission, ton/h | 184.9225 | **184.4483** | 452.0682 | **452.0588** | 937.8131 | **937.8040** | 1659.6402 | **1659.3528** |
| Computation time (s) | 4.92856 | 4.82575 | 5.04369 | 4.84046 | 4.89423 | 4.80766 | 7.88432 | 7.81721 |

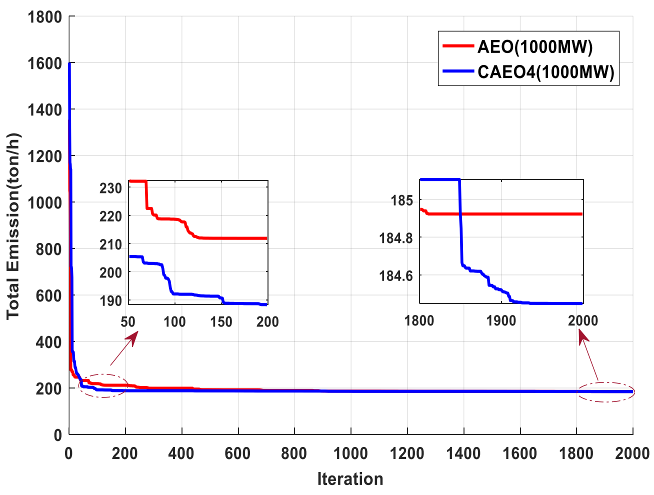


(a)

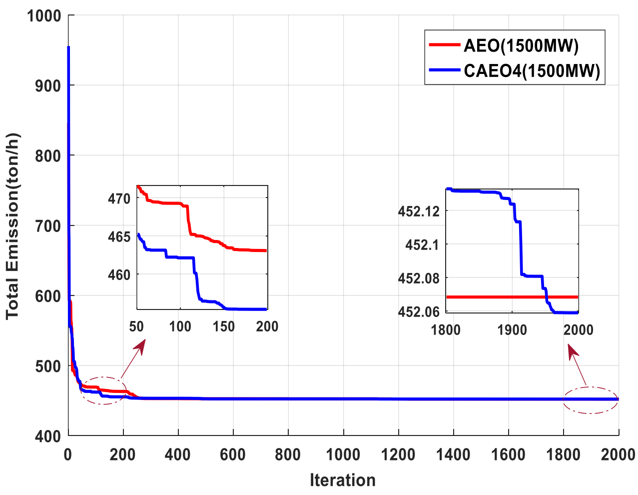


(b)

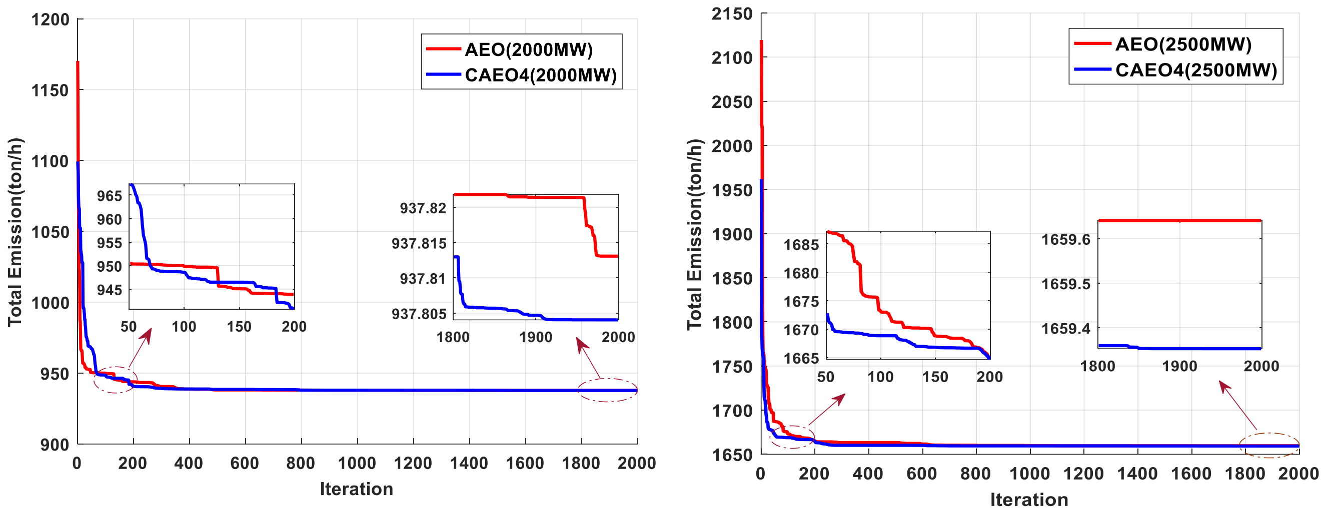


(c) (d)

Figure 5.12: Total Emission convergence curves of AEO and CAEO4 techniques (Case study 2) (a) 1000MW (b) 1500MW (c)2000MW (d)2500MW.

Table 5.21 presents the best solution values for the total emission of the case study 2 using the proposed CAEO4, original AEO and other algorithms. From Table 5.21, it can be observed that the optimal emission obtained using CAEO4 and CSAISA [173] was 1659.35 ton/h.

Table 5.21: The best solution values for the Total Emission of the case study 2.

| Generating Unit, MW | HAS | DE | PSO | GA | ISA | CSAISA | AEO | CAEO4 |
|---|---|---|---|---|---|---|---|---|
| P1 | 249.5765 | 249.2256 | 249.3756 | 249.2323 | 249.5639 | 250.0000 | 250.0000 | 250.0000 |
| P2 | 209.2341 | 209.0785 | 209.5345 | 209.1423 | 209.5641 | 209.9829 | 210.0000 | 210.0000 |
| P3 | 248.7676 | 248.6894 | 248.0876 | 248.4236 | 248.9627 | 250.0000 | 249.9905 | 250.0000 |
| P4 | 169.0712 | 169.0586 | 169.8945 | 169.6453 | 169.6364 | 169.9912 | 170.6799 | 166.5864 |
| P5 | 145.5326 | 145.2794 | 145.0675 | 145.9786 | 145.8813 | 142.9608 | 145.3686 | 142.1694 |
| P6 | 171.6924 | 171.5923 | 171.5547 | 171.3854 | 171.0137 | 166.0797 | 166.7993 | 166.7366 |
| P7 | 145.3356 | 145.4902 | 145.2246 | 145.3782 | 145.8453 | 142.2710 | 142.5525 | 142.0880 |
| P8 | 300.5643 | 300.4168 | 300.1156 | 300.2742 | 300.8375 | 316.6614 | 313.1171 | 316.3717 |
| P9 | 275.5923 | 275.4901 | 275.3345 | 275.1153 | 275.8335 | 275.4746 | 274.0111 | 276.1787 |
| P10 | 300.2686 | 300.4233 | 300.6754 | 300.7655 | 300.7452 | 300.8140 | 305.3927 | 302.5881 |
| P11 | 282.2216 | 282.5901 | 282.5646 | 282.3766 | 282.1124 | 275.7644 | 272.0884 | 277.2812 |
| Fuel cost, $/h | 13040.46 | 13040.83 | 13039.39 | 13036.95 | 13041.04 | 13046.31 | 13046.2434 | 13046.8016 |
| Emission, ton/h | 1661.96 | 1661.58 | 1663.74 | 1662.96 | 1661.36 | **1659.35** | 1659.64 | **1659.35** |
| Time (s) | 12.70 | 12.69 | 12.73 | 12.72 | 12.69 | 12.66 | 7.88432 | **7.81721** |

### 5.3.2.2.3 Case 3: Optimum Values of CEED

Table 5.22 gives the best optimal power output of generators for CEED problem using proposed CAEO4 technique, AEO, GA [174], and GSA [175] with 2500MW system demands for 11-generator system. From this table, it is clear that the proposed approach gives the best total cost (18953.49162 $/h). The convergence characteristic curve for the best total cost is shown in Figure 5.13. It can be observed that the proposed CAEO4 has a steady and faster convergence characteristic than the conventional AEO algorithm.

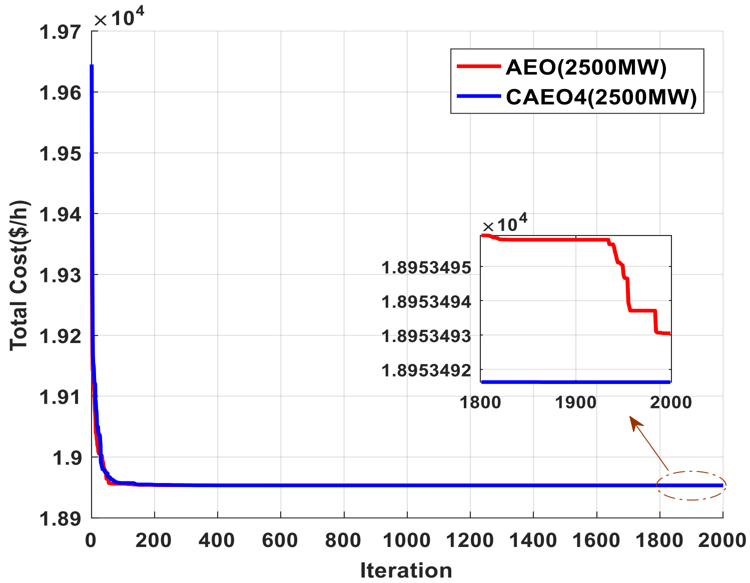


Figure 5.13: Total Cost convergence curves of AEO and CAEO4 techniques (Case study (2) - 2500MW).

Table 5.22: The best solution values for the CEED of the case study 2 (2500MW).

| Generating Unit, MW | GA similarity | GSA | AEO | CAEO4 |
|---|---|---|---|---|
| P1 | 138.8618 | 138.9382 | 139.7138708 | 139.5510382 |
| P2 | 112.1312 | 110.2728 | 112.7197442 | 112.7841557 |
| P3 | 146.7169 | 147.9728 | 145.8199968 | 145.8042388 |
| P4 | 222.1041 | 221.1072 | 221.7609406 | 221.6021175 |
| P5 | 137.1962 | 137.7986 | 136.8983313 | 136.739107 |
| P6 | 217.3208 | 217.9015 | 218.4680741 | 218.6680504 |
| P7 | 140.4711 | 141.3801 | 140.3670688 | 140.2660913 |
| P8 | 348.9008 | 349.6497 | 344.7404472 | 344.9562373 |
| P9 | 326.5188 | 327.3178 | 329.3798993 | 329.6177547 |
| P10 | 363.5275 | 363.4766 | 363.5154487 | 363.8805598 |
| P11 | 346.2508 | 344.1847 | 346.6159412 | 346.1306494 |
| Fuel cost, $/h | 12423.7667 | 12422.66 | 12424.90013 | 12424.77517 |
| Emission, ton/h | 2003.10456 | 2003.024 | 2003.420114 | 2003.613181 |
| Total Cost, $/h | 18953.9567 | 18954.73 | 18953.49305 | **18953.49162** |
| Time (s) | - | - | 10.8593 | **10.4268** |

## 5.3.3 Solving EED Problem using ISMA Algorithm

### 5.3.3.1 CEC2019 Benchmark Functions

In this subsection, the proposed ISMA is compared with other well-known methods using ten advanced CEC2019 benchmark problems. The description of the ten CEC2019 problems is given in Table 5.23.

Table 5.23: Description of the CEC2019 benchmark problems.

| F | Function name | F*i= Fi(x*) | Dim | Search range |
|---|---|---|---|---|
| 1 | Storn's Chebyshev Polynomial Fitting Problem | 1 | 9 | [-8192, 8192] |
| 2 | Inverse Hilbert Matrix Problem | 1 | 16 | [-16384, 16384] |
| 3 | Lennard-Jones Minimum Energy Cluster | 1 | 18 | [-4,4] |
| 4 | Rastrigin’s Function | 1 | 10 | [-100,100] |
| 5 | Griewangk’s Function | 1 | 10 | [-100,100] |
| 6 | Weierstrass Function | 1 | 10 | [-100,100] |
| 7 | Modified Schwefel’s Function | 1 | 10 | [-100,100] |
| 8 | Expanded Schaffer’s F6 Function | 1 | 10 | [-100,100] |
| 9 | Happy Cat Function | 1 | 10 | [-100,100] |
| 10 | Ackley Function | 1 | 10 | [-100,100] |

In Table 5.24, the results of the comparative methods using CEC2019 are given in terms of Worst, Average, Best, and standard deviation (STD) of the fitness function values. The comparative methods include PSO [176], SMA [149], EHO [177], KHA [178], SSA [101], MPA [179], AOA [180], and the proposed ISMA. The proposed ISMA got the best results in almost all the given test problems. As seen in Table 5.24, It is ranked the first method, followed by MPA, EHO, SSA, AOA, SMA, KHA, and PSO according to the Friedman ranking test. According to the STD values, it is evident that the proposed ISMA got close results by low distributions over multi runs, which proved its search ability and capabilities in finding the global best solutions. These results demonstrated the proposed ISMA's ability to solve versions complex problems compared to other methods, and this is its main advantage. Figure 5.14 shows the comparative methods' convergence behavior using the tested problems (ten CEC2019 functions). It is clear that the proposed ISMA has promising carves compared to other well-known methods. ISMA reaches almost all the best solutions in the given functions, and its convergence is stable more than the other methods. Consequently, the results shown confirmed that the proposed ISMA is a powerful and effective method for solving various problems. This demonstrated its ability based on comparisons with other similar and well-known methods and is considered one of its most important advantages and strengths by comparing it with the rest of the methods used in this research.

Table 5.24: The results of the comparative methods using advanced CEC2019 problems

| F | Measure | PSO | SMA | EHO | KHA | SSA | MPA | AOA | ISMA |
|---|---|---|---|---|---|---|---|---|---|
| cec01 | Worst | 1.10254E+13 | 8.81113E+04 | 3.16828E+11 | 6.40297E+09 | 3.56594E+10 | 3.37420E+08 | 1.16479E+11 | 5.52464E+04 |
| | Average | 3.67878E+12 | 6.16734E+04 | 1.32312E+11 | 3.57313E+09 | 2.05233E+10 | 9.22163E+07 | 6.18870E+10 | 4.70368E+04 |
| | Best | 1.19339E+12 | 4.25237E+04 | 1.48385E+10 | 2.23804E+09 | 8.81981E+09 | 4.42856E+06 | 1.47697E+08 | 4.10637E+04 |
| | STD | 4.89790E+12 | 2.15638E+04 | 1.30018E+11 | 1.94351E+09 | 1.23327E+10 | 1.63643E+08 | 5.85787E+10 | 6.41621E+03 |
| | Rank | 8 | 2 | 7 | 4 | 5 | 3 | 6 | 1 |
| cec02 | Worst | 2.89483E+04 | 1.73479E+01 | 1.73861E+01 | 1.75448E+01 | 1.73449E+01 | 1.73429E+01 | 1.99398E+01 | 1.73429E+01 |
| | Average | 2.29630E+04 | 1.73460E+01 | 1.73644E+01 | 1.74340E+01 | 1.73439E+01 | 1.73429E+01 | 1.95577E+01 | 1.73429E+01 |
| | Best | 1.32737E+04 | 1.73436E+01 | 1.73497E+01 | 1.73735E+01 | 1.73431E+01 | 1.73429E+01 | 1.88425E+01 | 1.73429E+01 |
| | STD | 7.42283E+03 | 2.19378E-03 | 1.53721E-02 | 7.99139E-02 | 7.83758E-04 | 7.98373E-07 | 4.88740E-01 | 1.57859E-06 |
| | Rank | 8 | 4 | 5 | 6 | 3 | 2 | 7 | 1 |
| cec03 | Worst | 1.27024E+01 | 1.27053E+01 | 1.27024E+01 | 1.27081E+01 | 1.27049E+01 | 1.27024E+01 | 1.27080E+01 | 1.27024E+01 |
| | Average | 1.27024E+01 | 1.27040E+01 | 1.27024E+01 | 1.27046E+01 | 1.27030E+01 | 1.27024E+01 | 1.27051E+01 | 1.27024E+01 |
| | Best | 1.27024E+01 | 1.27025E+01 | 1.27024E+01 | 1.27024E+01 | 1.27024E+01 | 1.27024E+01 | 1.27024E+01 | 1.27024E+01 |
| | STD | 8.62214E-11 | 1.15087E-03 | 3.07674E-15 | 2.54632E-03 | 1.24754E-03 | 5.81423E-10 | 2.27755E-03 | 1.46894E-12 |
| | Rank | 3 | 6 | 1 | 7 | 5 | 4 | 8 | 2 |
| cec04 | Worst | 5.31080E+03 | 1.44697E+02 | 5.61474E+01 | 2.52712E+02 | 8.45713E+01 | 1.58315E+02 | 3.60764E+04 | 5.12724E+01 |
| | Average | 2.11297E+03 | 8.61876E+01 | 4.04064E+01 | 1.89792E+02 | 6.46722E+01 | 8.28467E+01 | 1.89218E+04 | 2.63047E+01 |
| | Best | 2.58655E+02 | 3.47705E+01 | 2.98612E+01 | 1.26089E+02 | 4.57680E+01 | 3.51032E+01 | 8.01991E+03 | 9.46126E+00 |
| | STD | 2.28799E+03 | 4.78653E+01 | 1.16069E+01 | 7.01318E+01 | 2.12930E+01 | 5.41709E+01 | 1.33561E+04 | 1.83968E+01 |
| | Rank | 7 | 5 | 2 | 6 | 3 | 4 | 8 | 1 |
| cec05 | Worst | 2.36738E+00 | 1.75408E+00 | 1.40830E+00 | 4.87832E+00 | 1.41130E+00 | 1.37311E+00 | 1.57782E+00 | 1.04415E+00 |
| | Average | 1.71685E+00 | 1.40972E+00 | 1.21584E+00 | 2.78871E+00 | 1.26711E+00 | 1.25073E+00 | 1.44434E+00 | 1.03807E+00 |
| | Best | 1.28257E+00 | 1.16301E+00 | 1.04427E+00 | 1.87896E+00 | 1.13523E+00 | 1.10058E+00 | 1.29937E+00 | 1.02312E+00 |
| | STD | 4.60290E-01 | 2.55413E-01 | 1.77005E-01 | 1.40938E+00 | 1.39796E-01 | 1.25117E-01 | 1.24199E-01 | 1.00495E-02 |
| | Rank | 7 | 5 | 2 | 8 | 4 | 3 | 6 | 1 |
| cec06 | Worst | 1.21042E+01 | 8.46647E+00 | 8.37937E+00 | 1.10742E+01 | 9.01165E+00 | 4.79176E+00 | 6.01948E+00 | 9.25299E+00 |

| | | | | | | | | | |
|---|---|---|---|---|---|---|---|---|---|
| | Average | 1.12396E+01 | 7.05927E+00 | 5.90376E+00 | 9.58288E+00 | 7.06496E+00 | 3.41689E+00 | 4.79977E+00 | 7.44010E+00 |
| | Best | 1.03930E+01 | 6.16894E+00 | 4.32168E+00 | 8.27084E+00 | 5.46543E+00 | 2.16198E+00 | 1.67638E+00 | 6.54717E+00 |
| | STD | 9.04262E-01 | 1.03659E+00 | 1.85367E+00 | 1.15723E+00 | 1.52115E+00 | 1.12876E+00 | 2.09731E+00 | 1.23266E+00 |
| | Rank | 8 | 4 | 3 | 7 | 5 | 1 | 2 | 6 |
| cec07 | Worst | 6.40110E+02 | 6.76991E+02 | 8.75226E+02 | 7.11705E+02 | 8.12530E+02 | 3.70052E+02 | 3.09599E+02 | 2.16670E+02 |
| | Average | 4.79427E+02 | 3.12113E+02 | 4.33086E+02 | 4.47461E+02 | 3.89576E+02 | 2.98002E+02 | 2.10258E+02 | 6.44319E+01 |
| | Best | 2.41363E+02 | 6.24891E+01 | 1.37052E+02 | 2.35659E+02 | 3.88021E+02 | 1.84279E+02 | 1.28698E+02 | -6.47563E+00 |
| | STD | 1.81021E+02 | 2.63674E+02 | 3.18547E+02 | 2.29534E+02 | 3.87011E+02 | 7.97601E+01 | 9.36366E+01 | 1.02664E+02 |
| | Rank | 8 | 4 | 6 | 7 | 5 | 3 | 2 | 1 |
| cec08 | Worst | 7.38983E+00 | 6.47056E+00 | 6.45865E+00 | 6.08258E+00 | 6.22062E+00 | 5.74637E+00 | 6.01529E+00 | 3.08637E+00 |
| | Average | 6.60612E+00 | 6.16720E+00 | 5.07476E+00 | 5.92533E+00 | 6.02179E+00 | 4.93032E+00 | 5.17575E+00 | 2.82039E+00 |
| | Best | 6.04424E+00 | 5.93331E+00 | 3.34073E+00 | 5.75125E+00 | 5.87305E+00 | 4.56366E+00 | 4.01964E+00 | 2.39457E+00 |
| | STD | 5.68478E-01 | 2.35406E-01 | 1.29228E+00 | 1.53035E-01 | 1.55977E-01 | 5.48443E-01 | 8.48431E-01 | 3.07130E-01 |
| | Rank | 8 | 7 | 2 | 6 | 3 | 4 | 5 | 1 |
| cec09 | Worst | 2.01041E+03 | 5.46257E+00 | 3.48061E+00 | 5.42050E+00 | 4.13106E+00 | 4.76864E+00 | 4.92401E+00 | 2.68555E+00 |
| | Average | 5.05395E+02 | 4.61019E+00 | 3.09754E+00 | 4.12474E+00 | 3.26082E+00 | 3.69441E+00 | 3.94676E+00 | 2.60797E+00 |
| | Best | 3.42336E+00 | 3.57228E+00 | 2.70471E+00 | 3.37034E+00 | 2.79556E+00 | 2.65569E+00 | 2.93627E+00 | 2.46643E+00 |
| | STD | 1.00334E+03 | 7.82521E-01 | 4.28298E-01 | 9.42842E-01 | 6.01107E-01 | 9.31184E-01 | 8.56626E-01 | 1.00096E-01 |
| | Rank | 8 | 7 | 2 | 6 | 3 | 4 | 5 | 1 |
| ce10 | Worst | 2.15333E+01 | 2.12526E+01 | 2.12457E+01 | 2.12368E+01 | 2.11589E+01 | 2.10362E+01 | 2.10265E+01 | 2.12063E+01 |
| | Average | 2.14415E+01 | 2.11346E+01 | 2.10789E+01 | 2.09902E+01 | 2.09029E+01 | 2.07839E+01 | 2.08622E+01 | 2.10112E+01 |
| | Best | 2.13736E+01 | 2.10558E+01 | 2.09005E+01 | 2.05801E+01 | 2.07534E+01 | 2.06501E+01 | 2.06798E+01 | 2.08286E+01 |
| | STD | 7.40970E-02 | 8.73430E-02 | 1.52180E-01 | 2.94938E-01 | 1.76725E-01 | 1.76165E-01 | 1.44792E-01 | 1.54747E-01 |
| | Rank | 8 | 7 | 6 | 4 | 3 | 1 | 2 | 5 |
| | Summation | 73 | 51 | 36 | 61 | 39 | 29 | 51 | 20 |
| | Mean Ranking | 7.30 | 5.10 | 3.60 | 6.10 | 3.90 | 2.90 | 5.10 | 2.00 |
| | Final Ranking | 8 | 5 | 3 | 7 | 4 | 2 | 5 | 1 |

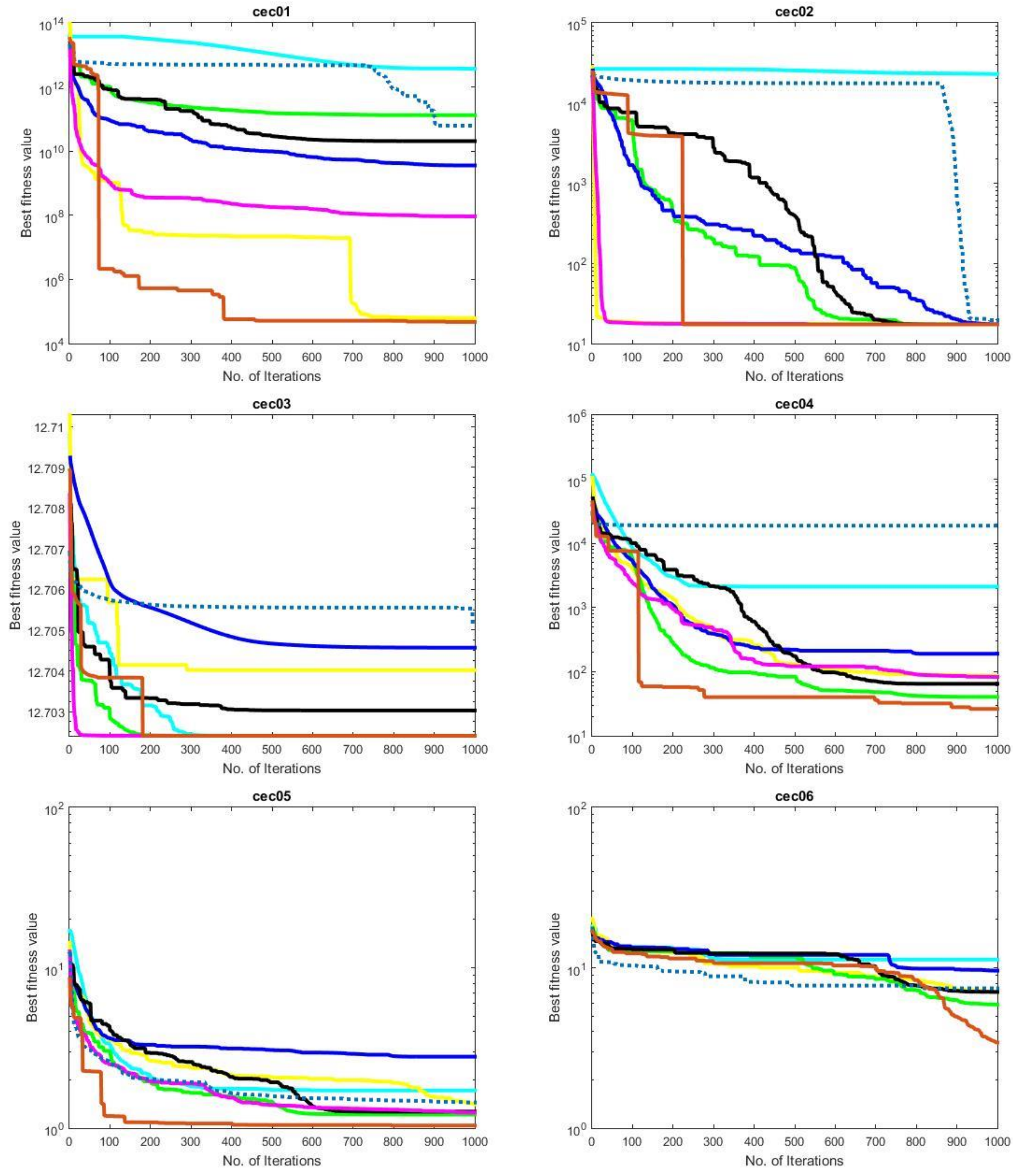
cec01
cec02
cec03
cec04
cec05
cec06
Best fitness value
No. of Iterations

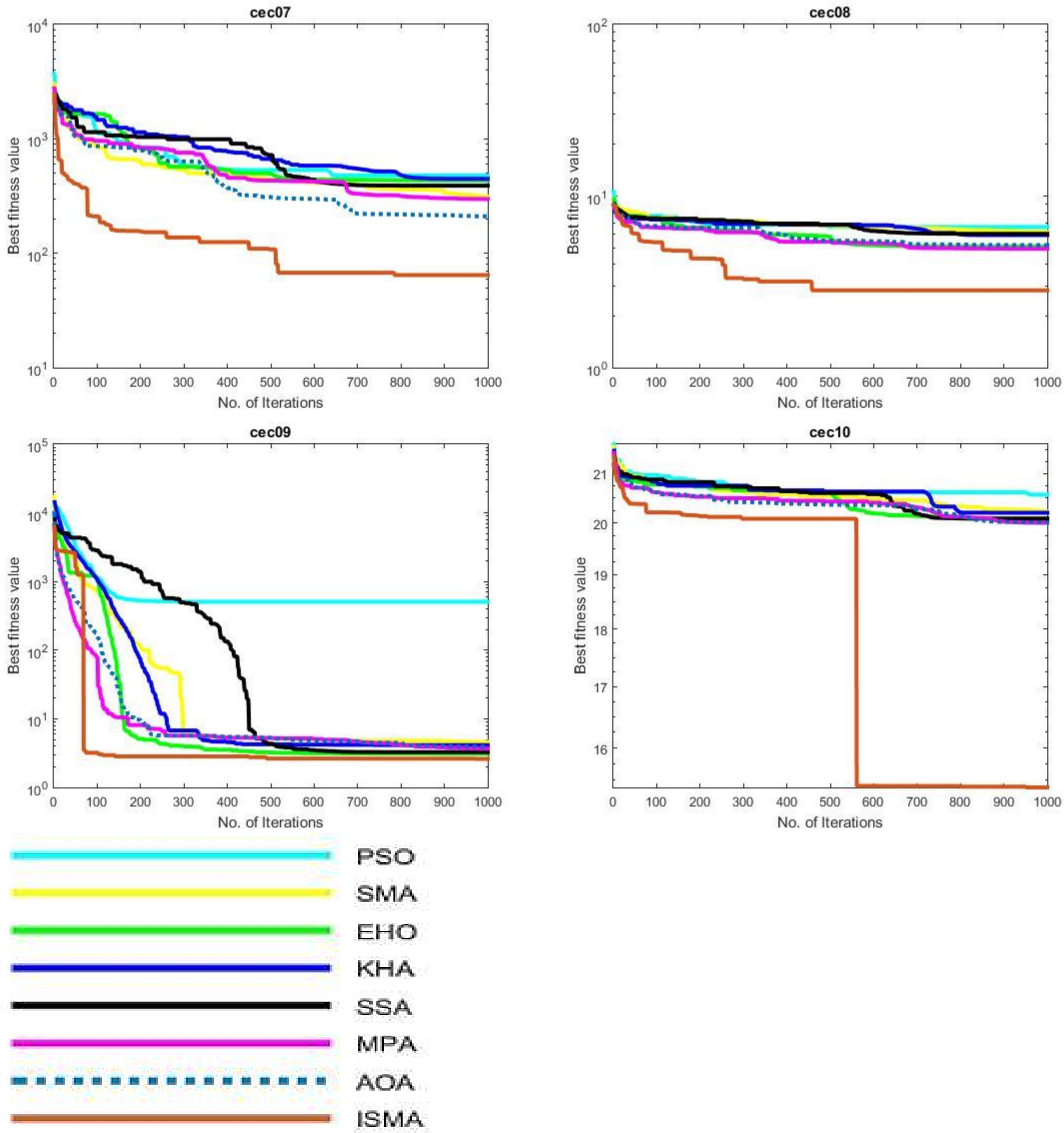


Figure 5.14: The convergence behavior of the comparative methods using ten CEC2019 problems.

#### 5.3.3.2 Solving CEED using the ISMA Technique

In this subsection, the performance of the proposed ISMA compared with conventional SMA and other well-known optimization techniques are evaluated via single and multi-objective functions. MATLAB (R2016a) is used to simulate the optimization techniques. The descriptions of the used portable computer are Intel Core i5-4210U CPU@2. 40GHz with a 4.00 MB RAM. In this thesis, 30 independent runs are executed for ISMA, SMA, and other optimization algorithms to overcome the randomness of the proposed algorithm and validate its quality. The parameter settings of all algorithms are presented in Table 5.25.

Table 5.25: Parameter settings of algorithms.

| Algorithm | Parameter settings |
|---|---|
| PSO | $C_1 = 2; C_2 = 2; V_{max} = 6;$ |
| TSA | $P_{min} = 1; P_{max} = 4;$ |
| SMA | $z = 0.03;$ |
| ISMA | $z = 0.03;$ |
| HHO | $beta = 1.5;$ |

The single-objective EED problem is solved using ISMA and its obtained results has been compared with those obtained using 4 well-known optimization algorithms (HHO, JS, TSA, and PSO) as well as the original Slime Mould Algorithm (SMA) and other recent published methods for solving the EED problem. However, the codes of these algorithms implemented in this study have been provided in Appendix H. Several thermal units with different load levels are considered as follows:

- Case 1: 6-unit system (PD = 2.834 p.u) and the system base is 100 MVA;
- Case 2: 10-unit system (PD = 2000 MW);
- Case 3: 11-unit system (PD = 2500 MW);
- Case 4: 40-unit system (PD = 10,500 MW).
- Case 5: 110-unit system (PD = 15,000 MW) and only ELD has been solved.

The total transmission line losses are considered in the first two cases only. The methodology for solving the EED problem in this thesis is to minimize the total fuel costs and the total emissions separately. Compared with fuel cost, total emission, and constraint violation is a more significant criterion in evaluating the proposed algorithm. It is usually accepted that a solution with a small objective function value will not be considered as an acceptable solution if it is not able better to meet the requirements of the constraint [119].

#### 5.3.3.2.1 Case 1: 6 Thermal Units and Load Demand 2.834 p.u.

In the first case, the test system is a six-unit system with a load demand of 2.834 p.u. The number of populations is 2000, and the maximum number of iterations is 500. The Generation limits, Fuel cost coefficients, and emission coefficients of the system are given in Appendix (C) [119]. The best solutions for the test system are presented in Table 5.26 and Table 5.27. The results for minimizing fuel costs are illustrated in Table 5.26. This table shows that the proposed ISMA reaches the optimal solution as 605.998 $/h with too little constraint violation (8.59E-11 MW). The convergence curves of the studied techniques for cost minimization are shown in Fig. 5.15. From this figure, although the three conventional algorithms converge to the best value faster than the proposed algorithm, they did not reach to the smallest value like the proposed ISMA.

Table 5.26: The best solution values of fuel cost for the six-unit system.

| Algorithm | ISMA | SMA | HHO | JS | TSA | PSO | GSA [50] | MSA [51] | NGPSO [119] |
|---|---|---|---|---|---|---|---|---|---|
| P1 | 0.121053 | 0.124766 | 0.071416 | 0.114364 | 0.130284 | 0.123197 | 0.120969 | 0.120951 | 0.120900 |
| P2 | 0.286634 | 0.284570 | 0.271884 | 0.269406 | 0.284005 | 0.289958 | 0.286312 | 0.286285 | 0.286300 |
| P3 | 0.583882 | 0.580216 | 0.645057 | 0.616772 | 0.580462 | 0.583320 | 0.583557 | 0.583571 | 0.583600 |
| P4 | 0.992567 | 0.993485 | 0.986364 | 0.979992 | 0.979929 | 0.984098 | 0.992854 | 0.992823 | 0.992800 |
| P5 | 0.523288 | 0.522768 | 0.542835 | 0.542771 | 0.530988 | 0.527391 | 0.523970 | 0.524007 | 0.523970 |
| P6 | 0.352132 | 0.353788 | 0.341194 | 0.335162 | 0.353698 | 0.351523 | 0.351899 | 0.351922 | 0.351900 |
| V(MW) | 8.59E-11 | 5.06E-09 | 1.7E-16 | 1.824E-05 | 7.82E-07 | 1.3E-08 | 1.37E-04 | 3.96E-05 | 1.37E-04 |
| PL | 0.025557 | 0.025593 | 0.024749 | 0.024449 | 0.025366 | 0.025486 | 0.255620 | 0.025561 | 0.025470 |
| C($/h) | 605.998 | 606.002 | 606.5292 | 606.3315 | 606.025 | 606.006 | 605.998 | 605.998 | 605.998 |
| E(ton/h) | 0.220699 | 0.220619 | 0.223369 | 0.221108 | 0.219594 | 0.220028 | 0.220729 | 0.220728 | 0.220700 |
| Time (s) | 63.2630 | 78.96508 | 178.7656 | 67.72068 | 66.67238 | 114.324 | - | - | - |

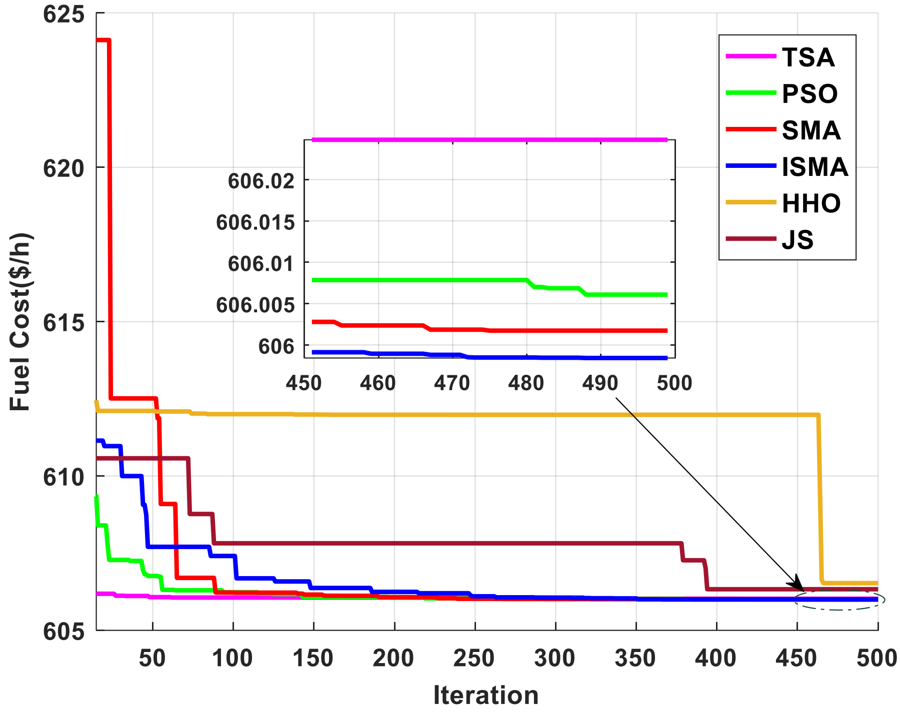


Figure 5.15: Fuel cost convergence of different techniques (Case study 1).

The results for the total emission obtained by the studied optimization techniques are presented in Table 5.27. From this table, it is clear that the ISMA outperforms the conventional SMA and recent algorithms because it has the least value of emission (0.194180 ton/h) with the lowest violation (2.74E-10), which indicates that the ISMA achieved the most accurate level for satisfying the equality constraints. Emission minimization convergence characteristics of studied techniques for the 6-unit system are shown in Figure 5.16. From this figure, it can be observed that the proposed ISMA converges to the optimal value faster than the other studied algorithms.

Table 5.27: The best solution values for the total emission of the six-unit system.

| Algorithm | ISMA | SMA | HHO | JS | TSA | PSO | GSA [50] | MSA [51] | NGPSO [119] |
|---|---|---|---|---|---|---|---|---|---|
| P1 | 0.409093 | 0.396517 | 0.329536 | 0.452183 | 0.421035 | 0.418509 | 0.410925 | 0.410929 | 0.410925 |
| P2 | 0.467882 | 0.469811 | 0.400795 | 0.471107 | 0.451248 | 0.433240 | 0.463668 | 0.463638 | 0.463667 |
| P3 | 0.536325 | 0.546135 | 0.617605 | 0.556268 | 0.581326 | 0.527962 | 0.544419 | 0.544388 | 0.544400 |
| P4 | 0.385894 | 0.431801 | 0.480737 | 0.446912 | 0.390196 | 0.436215 | 0.390374 | 0.390400 | 0.390370 |
| P5 | 0.553559 | 0.506014 | 0.573482 | 0.474448 | 0.522489 | 0.536796 | 0.544459 | 0.544466 | 0.544460 |
| P6 | 0.516638 | 0.518365 | 0.459909 | 0.470837 | 0.502958 | 0.516855 | 0.515485 | 0.515506 | 0.515490 |
| V(MW) | 2.74E-10 | 3.08E-08 | 1.59E-16 | 1.93E-07 | 1.87E-07 | 8.96E-12 | 6.98E-05 | 2.71E-05 | 6.98E-05 |

| | | | | | | | | | |
|---|---|---|---|---|---|---|---|---|---|
| PL | 0.035390 | 0.034644 | 0.028064 | 0.037754 | 0.035252 | 0.035576 | 0.353300 | 0.035330 | 0.035300 |
| C($/h) | 646.6609 | 642.5360 | 631.0487 | 644.562 | 646.0755 | 642.3391 | 646.2070 | 646.2048 | 646.2100 |
| E(ton/h) | 0.19418 | 0.19434 | 0.195728 | 0.194811 | 0.194304 | 0.194352 | 0.19418 | 0.19418 | 0.19418 |
| Time (s) | 63.5109 | 80.45378 | 133.2916 | 60.6306 | 57.3632 | 115.9881 | - | - | - |

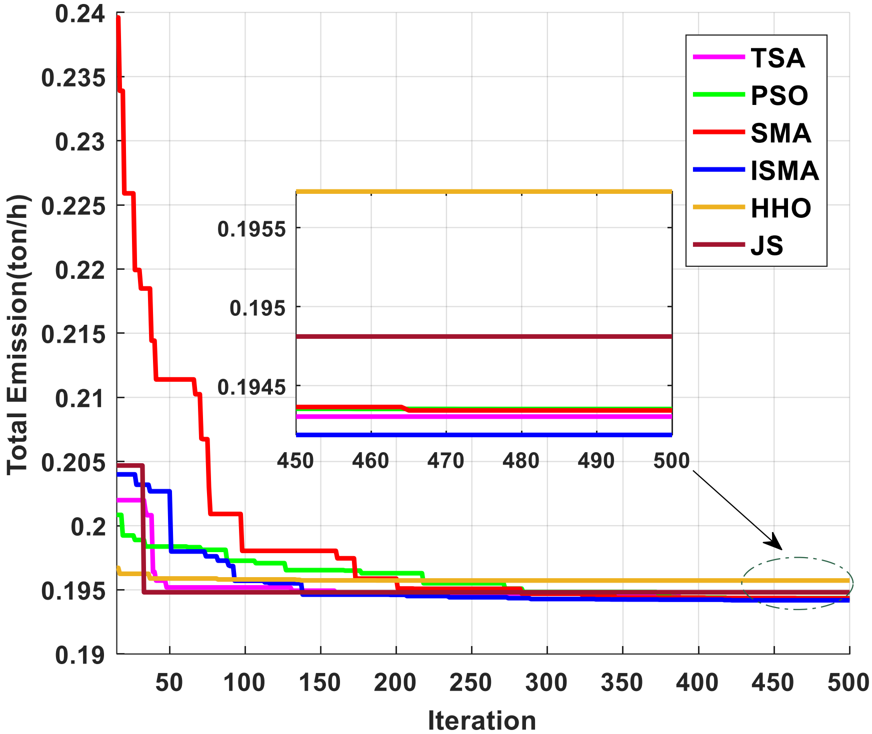


Figure 5.16: Total emission convergence curves of different techniques (Case study 1).

In addition, the comparison of best, worst, median, average, and standard deviation of the results obtained by TSA, PSO, HHO, JS, SMA, and ISMA over 30 runs are presented in Table 5.28. It is clear that the proposed ISMA approach provides better and more stable solutions compared to the original HHO, JS, TSA, PSO, and SMA.

Table 5.28: Statistical results for Case 1.

| Objective function | Algorithm | Best | Worst | Median | Average | Std. |
|---|---|---|---|---|---|---|
| Fuel cost ($/h) | ISMA | 605.9984 | 606.0374 | 606.0126 | 606.0130 | 0.0142 |
| | SMA | 606.0017 | 606.1084 | 606.0159 | 606.0227 | 0.0260 |
| | HHO | 606.5292 | 626.7676 | 611.3046 | 611.5524 | 3.826237 |
| | JS | 606.3315 | 607.6245 | 606.9829 | 606.9632 | 0.323814 |
| | TSA | 606.0248 | 606.4199 | 606.0501 | 606.1181 | 0.1508 |
| | PSO | 606.0060 | 606.0501 | 606.0225 | 606.0253 | 0.0171 |
| Emission (ton/h) | ISMA | 0.19418 | 0.19492 | 0.1943 | 0.19433 | 1.871E-04 |

| | | | | | |
|---|---|---|---|---|---|
| SMA | 0.194340 | 0.195966 | 0.1951 | 0.195107 | 5.215E-04 |
| HHO | 0.195728 | 0.233378 | 0.207657 | 0.209318 | 0.008736 |
| JS | 0.194811 | 0.198911 | 0.196775 | 0.196651 | 0.000962 |
| TSA | 0.1943040 | 0.194971 | 0.1945 | 0.194632 | 2.658E-04 |
| PSO | 0.194352 | 0.196861 | 0.1952 | 0.195386 | 9.957E-04 |

##### 5.3.3.2.2 Case 2: 10 Thermal Units and Load Demand (2000 MW)

In this case, the proposed ISMA and the other studied algorithms are tested on the 10-unit system with a load demand of 2000 MW. The considered populations are 2000, and the maximum number of iterations is 500. The Generation limits and Fuel cost coefficients of this system are given in Appendix D.1, while the Emission coefficients of this system are presented in Appendix D.2 [119]. Table 5.29 presents the optimum values of fuel costs obtained by all algorithms. From this table, it is clear that the proposed ISMA achieves the optimum value of fuel cost (111497.63 $/h) with the lowest violation (1.2E-06 MW) compared with the OGHS, which reaches the best solution (111497.61 $/h). However, the OGHS has a violation (3.08E-04 MW) higher than the violation of ISMA. The convergence characteristics of fuel cost minimization are depicted in Figure 5.17.

Table 5.29: The best solution values for the fuel cost of the ten-unit system.

| Algorithm | ISMA | SMA | HHO | JS | TSA | PSO | TLBO[49] | DE[45] | OGHS[181] | NGPSO[119] |
|---|---|---|---|---|---|---|---|---|---|---|
| P1 | 55.000 | 55.000 | 55.000 | 54.82972 | 55.000 | 55.000 | 55.000 | 55.000 | 55.000 | 55.000 |
| P2 | 80.000 | 80.000 | 80.000 | 79.95193 | 80.000 | 80.000 | 80.000 | 79.806 | 80.000 | 80.000 |
| P3 | 106.867 | 106.843 | 108.9857 | 106.6789 | 106.921 | 106.844 | 105.962 | 106.825 | 106.992 | 106.940 |
| P4 | 100.544 | 100.880 | 95.69826 | 99.48448 | 99.845 | 100.757 | 99.932 | 102.831 | 100.535 | 100.576 |
| P5 | 81.606 | 81.500 | 85.75969 | 81.66658 | 82.759 | 81.522 | 80.642 | 82.242 | 81.445 | 81.502 |
| P6 | 83.022 | 82.816 | 81.62431 | 85.20439 | 82.503 | 82.917 | 85.788 | 80.435 | 83.067 | 83.021 |
| P7 | 300.000 | 300.000 | 300.000 | 299.8178 | 300.000 | 300.000 | 300.000 | 300.000 | 300.000 | 300.000 |
| P8 | 340.000 | 340.000 | 340.000 | 339.8725 | 340.000 | 340.000 | 340.000 | 340.000 | 340.000 | 340.000 |
| P9 | 470.000 | 470.000 | 470.000 | 469.9709 | 470.000 | 470.000 | 469.698 | 470.000 | 470.000 | 470.000 |
| P10 | 470.000 | 470.000 | 470.000 | 469.4676 | 470.000 | 469.999 | 469.994 | 469.898 | 470.000 | 470.000 |
| V(MW) | 1.2E-06 | 6.7E-07 | 0 | 0.05439 | 1.43E-02 | 7.263E-05 | 3.86E-05 | 3.05E-06 | 3.08E-04 | 2.29E-05 |
| PL | 87.0387 | 87.0384 | 87.06791 | 86.99932 | 87.0422 | 87.0383 | 87.0161 | 87.0368 | 87.0389 | 87.0388 |
| C($/h) | 111497.63 | 111497.65 | 111503.9 | 111505.9 | 111498.42 | 111497.64 | 111500.42 | 111500.79 | 111497.61 | 111497.63 |
| E(ton/h) | 4571.68 | 4573.06 | 4562.218 | 4562.846 | 4568.87 | 4572.51 | 4563.34 | 4581.00 | 4572.27 | 4572.20 |
| Time (s) | 75.35445 | 109.30831 | 181.7545 | 72.60952 | 65.32695 | 123.0066 | - | - | - | - |

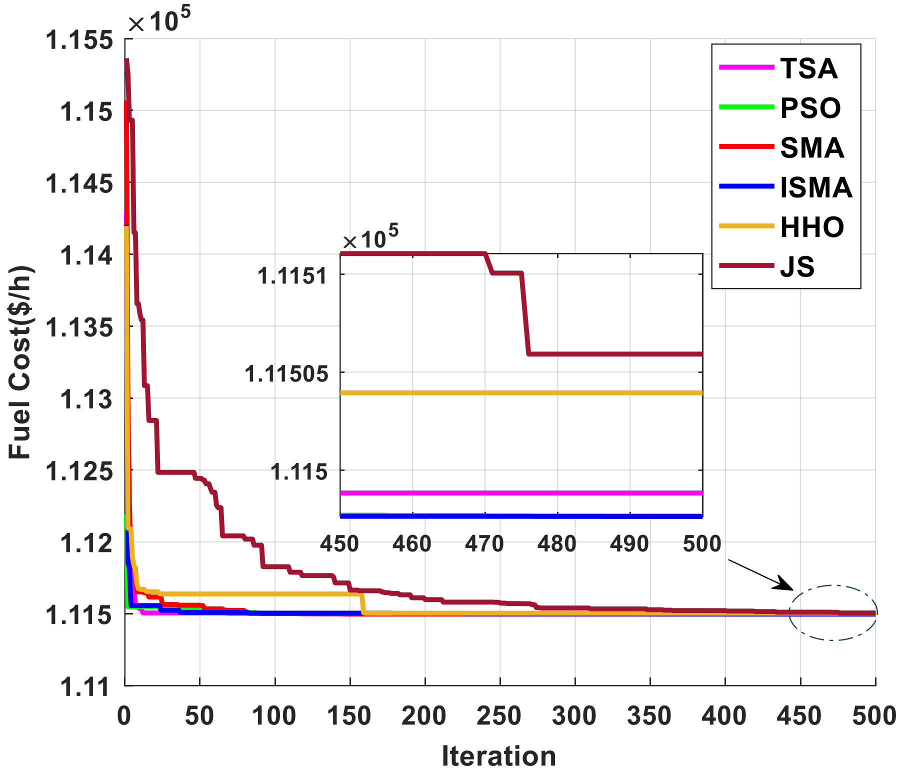


Figure 5.17: Fuel cost convergence curves of different techniques (Case study 2).

The comparative results for total emission minimization are presented in Table 5.30. When total emission is the objective function, ISMA reaches the best value of (3932.24 ton/h) with the least violation (3.16E-07 MW). From Table 5.30, it is clear that three methods reach the best value of the total emission, but their violations are higher than that of the ISMA. The convergence curves of emission minimization obtained by the studied techniques are shown in Figure 5.18. It can be seen from Figs. 5.17 and 5.18 that the proposed ISMA outperforms other algorithms in the final values and speed.

Table 5.30: The best solution values for the total emission of the ten-unit system.

| Algorithm | ISMA | SMA | HHO | JS | TSA | PSO | TLBO[49] | DE[45] | OGHS[181] | NGPSO[119] |
|---|---|---|---|---|---|---|---|---|---|---|
| P1 | 55.000 | 55.000 | 53.93999 | 54.24106 | 55.000 | 54.998 | 55.000 | 55.000 | 55.000 | 55.000 |
| P2 | 79.992 | 80.000 | 75.44689 | 71.83619 | 80.000 | 80.000 | 80.000 | 80.000 | 80.000 | 80.000 |
| P3 | 81.251 | 80.798 | 70.26107 | 82.06303 | 84.462 | 80.839 | 81.126 | 80.592 | 81.106 | 81.134 |
| P4 | 81.415 | 81.216 | 95.10304 | 78.99879 | 81.922 | 80.966 | 81.364 | 81.023 | 81.413 | 81.364 |
| P5 | 160.000 | 160.000 | 159.2534 | 158.3206 | 160.000 | 160.000 | 160.000 | 160.000 | 160.000 | 160.000 |
| P6 | 240.000 | 240.000 | 239.2819 | 234.7912 | 240.000 | 240.000 | 240.000 | 240.000 | 240.000 | 240.000 |
| P7 | 294.485 | 295.339 | 279.4015 | 289.182 | 300.000 | 297.569 | 294.479 | 292.743 | 294.507 | 294.485 |
| P8 | 296.943 | 297.778 | 306.5521 | 304.5176 | 302.164 | 298.464 | 297.244 | 299.121 | 297.262 | 297.270 |
| P9 | 397.044 | 395.070 | 402.6322 | 407.8186 | 390.390 | 396.267 | 396.804 | 394.515 | 396.735 | 396.766 |
| P10 | 395.465 | 396.395 | 399.827 | 400.2362 | 387.383 | 392.448 | 395.579 | 398.638 | 395.572 | 395.576 |
| V(MW) | 3.16E-07 | 1.4 E-07 | 0.034493 | 0.0418 | 4.1E-03 | 6.73E-04 | 1.12E-04 | 9.04E-05 | 2.02E-04 | 4.96 E-05 |
| PL | 81.5941 | 81.5963 | 81.66446 | 81.96348 | 81.3244 | 81.5494 | 81.5958 | 81.6334 | 81.5941 | 81.5951 |
| C($/h) | 116412.21 | 116416.26 | 116374.1 | 116119.3 | 116468.79 | 116430.59 | 116412.35 | 116404.29 | 116412.65 | 116412.44 |
| E(ton/h) | 3932.24 | 3932.28 | 3959.43 | 3954.422 | 3934.36 | 3932.48 | 3932.42 | 3932.42 | 3932.24 | 3932.24 |
| Time (s) | 81.49861 | 108.1124 | 163.05989 | 64.4501 | 60.601 | 115.0288 | - | - | - | - |

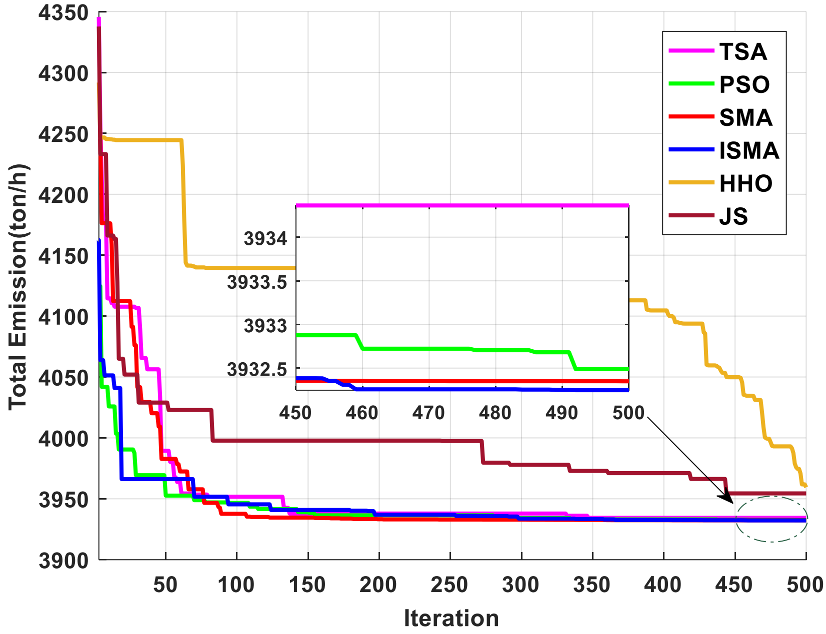


Figure 5.18: Total emission convergence curves of different techniques (Case study 2).

The statistical analysis of the ISMA and other algorithms is listed in Table 5.31. The ISMA is the most efficient algorithm in terms of all measured statistical parameters for both the fuel cost and emission values.

Table 5.31: Statistical results for Case 2.

| Objective function | Algorithm | Best | Worst | Median | Average | Std. |
|---|---|---|---|---|---|---|
| Fuel cost ($/h) | ISMA | 111497.63 | 111497.72 | 111497.65 | 111497.66 | 0.02839 |
| | SMA | 111497.65 | 111509.36 | 111497.78 | 111499.72 | 3.43854 |
| | HHO | 111503.9 | 111664.6 | 111565.6 | 111566.9 | 35.06826 |
| | JS | 111505.9 | 111513.3 | 111508.8 | 111508.9 | 1.578434 |
| | TSA | 111498.42 | 111503.88 | 111499.93 | 111500.55 | 1.876489 |
| | PSO | 111497.64 | 111497.83 | 111497.70 | 111497.71 | 0.06644 |
| Emission (ton/h) | ISMA | 3932.24 | 3932.64 | 3932.31 | 3932.35 | 0.12194 |
| | SMA | 3932.28 | 3932.99 | 3932.42 | 3932.45 | 0.16437 |
| | HHO | 3959.43 | 4048.06 | 3979.515 | 3984.25 | 18.78132 |
| | JS | 3954.422 | 3972.146 | 3964.747 | 3964.595 | 4.219434 |
| | TSA | 3934.36 | 3938.38 | 3935.98 | 3936.34 | 1.33555 |
| | PSO | 3932.48 | 3934.38 | 3932.87 | 3933.01 | 0.54464 |

### 5.3.3.2.3 Case 3: 11 Thermal Units and Load Demand (2500 MW).

In the third case, ISMA and other optimization algorithms are applied to solve the 11-unit system with load demand 2500 MW. The data on fuel cost and total emission is given in Appendix (C)[119]. The number of populations is 2000, and the maximum number of iterations is 1000. Table 5.32 presents the best results obtained by the studied optimization techniques for the 11-unit system. From this table, we can see that the minimum value of fuel cost obtained by ISMA is 12274.4005 $/h. We conclude that ISMA is better than the conventional SMA and other considered optimization techniques. Fuel cost convergence curves of different techniques are shown in Fig. 5.19.

Table 5.32: The best solution values for the fuel cost of the eleven-unit system.

| Algorithm | ISMA | SMA | HHO | JS | TSA | PSO | SAIWPSO | NGPSO | GWO |
|---|---|---|---|---|---|---|---|---|---|
| P1 | 57.133 | 57.270 | 56.86117 | 57.09685 | 59.564 | 57.121 | 57.061 | 57.113 | 57.113 |
| P2 | 40.455 | 40.303 | 40.42048 | 40.4501 | 36.075 | 40.417 | 40.298 | 40.435 | 40.440 |
| P3 | 57.823 | 58.030 | 58.11197 | 58.19468 | 62.638 | 57.676 | 57.922 | 57.880 | 57.882 |
| P4 | 277.706 | 277.228 | 276.9673 | 277.6863 | 294.765 | 277.231 | 278.149 | 277.704 | 277.706 |
| P5 | 186.889 | 186.476 | 186.7454 | 186.7212 | 189.438 | 187.179 | 188.110 | 186.877 | 186.882 |
| P6 | 249.077 | 249.612 | 248.7977 | 249.0306 | 228.438 | 249.035 | 249.384 | 249.187 | 249.182 |
| P7 | 177.084 | 176.450 | 177.8949 | 177.0301 | 177.963 | 176.884 | 177.867 | 177.073 | 177.079 |
| P8 | 380.048 | 380.023 | 380.585 | 380.5109 | 390.101 | 380.299 | 380.021 | 380.199 | 380.193 |
| P9 | 341.720 | 341.989 | 342.2482 | 341.4985 | 336.888 | 341.893 | 341.002 | 341.612 | 341.611 |
| P10 | 378.659 | 378.851 | 378.2707 | 378.5824 | 368.174 | 378.642 | 378.650 | 378.587 | 378.583 |
| P11 | 353.405 | 353.766 | 353.0972 | 353.1949 | 355.957 | 353.623 | 351.536 | 353.333 | 353.331 |
| V(MW) | 8.39E-06 | 3.52E-06 | 0 | 0.00346 | 2.71E-04 | 6.19E-05 | - | - | - |
| C($/h) | 12274.4005 | 12274.4030 | 12274.4043 | 12274.4019 | 12276.1918 | 12274.4015 | 12274.4080 | 12274.4005 | 12274.4005 |
| E(ton/h) | 2540.5381 | 2539.9353 | 2539.611 | 2539.582 | 2544.2528 | 2540.5886 | 2541.4590 | 2540.5366 | 2540.4167 |
| Time (s) | 155.8883 | 212.08926 | 313.06892 | 105.4101 | 97.12254 | 234.06696 | - | - | - |

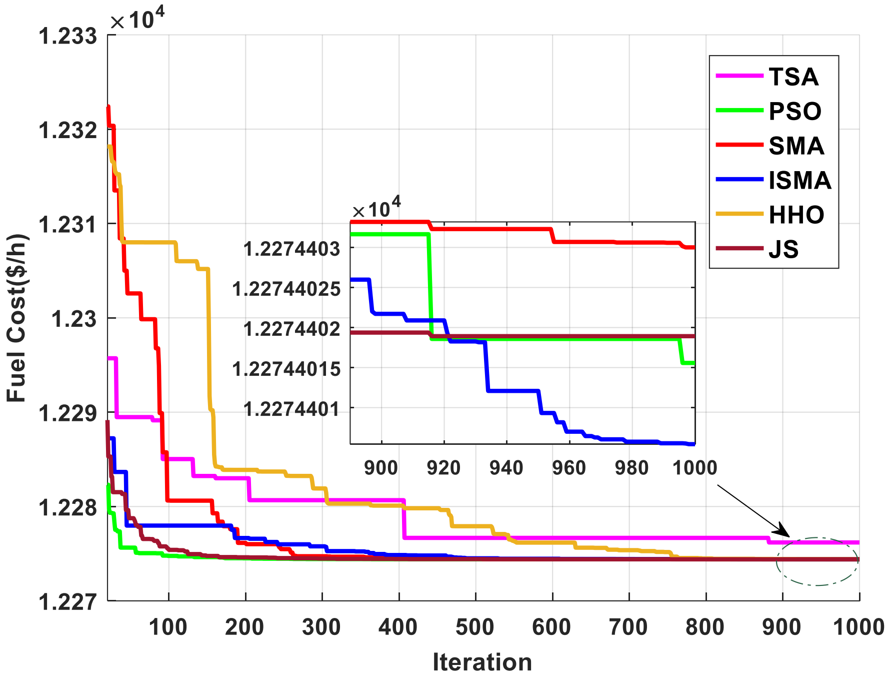


Figure 5.19: Fuel cost convergence curves of different techniques (Case study 3).

Table 5.33 presents the best results obtained by the studied optimization techniques in case of considering the total emission minimization is the primary objective function. As can be deduced from Table 5.33, ISMA gives competitive results compared with the other algorithms. The convergence characteristics of ISMA, SMA, PSO, and TSA algorithms for the EED problem of the 11-unit system for the total emission minimization are shown in Fig. 5.20. It can be seen that although the ISMA is not the fastest algorithm, in this case, it has the least optimization value. It can improve the chance of escaping from the local minimum and obtain excellent optimization performance.

Table 5.33: The best solution values for the total emission of the eleven-unit system.

| Algorithm | ISMA | SMA | HHO | JS | TSA | PSO | SAIWPSO[119] | NGPSO[119] | GWO[52] |
|---|---|---|---|---|---|---|---|---|---|
| P1 | 250.000 | 250.000 | 250 | 249.996 | 250.000 | 250.000 | 250.000 | 250.000 | 250.000 |
| P2 | 210.000 | 210.000 | 209.9166 | 209.9904 | 210.000 | 210.000 | 210.000 | 210.000 | 210.000 |
| P3 | 250.000 | 250.000 | 250 | 249.9912 | 250.000 | 250.000 | 250.000 | 250.000 | 250.000 |
| P4 | 167.221 | 167.232 | 166.21 | 166.8947 | 167.197 | 166.955 | 167.326 | 167.155 | 167.176 |
| P5 | 142.306 | 142.233 | 141.6201 | 142.8266 | 140.071 | 142.387 | 142.604 | 142.336 | 142.352 |
| P6 | 167.169 | 167.432 | 169.3593 | 166.8987 | 177.148 | 167.217 | 167.374 | 167.155 | 167.165 |
| P7 | 142.401 | 142.554 | 139.0052 | 142.5984 | 143.018 | 142.414 | 142.612 | 142.336 | 142.427 |
| P8 | 316.613 | 316.848 | 314.4685 | 316.5734 | 303.453 | 317.126 | 316.899 | 316.758 | 316.595 |
| P9 | 275.781 | 275.675 | 281.0086 | 276.1066 | 278.062 | 275.782 | 275.748 | 275.792 | 275.827 |
| P10 | 302.788 | 302.340 | 300.237 | 302.763 | 306.536 | 302.670 | 301.774 | 302.674 | 302.647 |
| P11 | 275.722 | 275.685 | 278.1747 | 275.3564 | 274.511 | 275.449 | 275.662 | 275.792 | 275.811 |
| V(MW) | 1.50E-06 | 7.73E-08 | 0 | 0.00461 | 5.30E-03 | 1.08E-05 | - | - | - |
| C($/h) | 13046.654 | 13046.675 | 13046.18 | 13046.68 | 13045.462 | 13046.697 | 13046.606 | 13046.666 | 13046.659 |
| E(ton/h) | 1659.3384 | 1659.3398 | 1659.683 | 1659.358 | 1660.7894 | 1659.3397 | 1659.3429 | 1659.3383 | 1659.3385 |
| Time (s) | 151.3722 | 209.14171 | 327.66158 | 117.9042 | 118.34604 | 209.17565 | - | - | - |

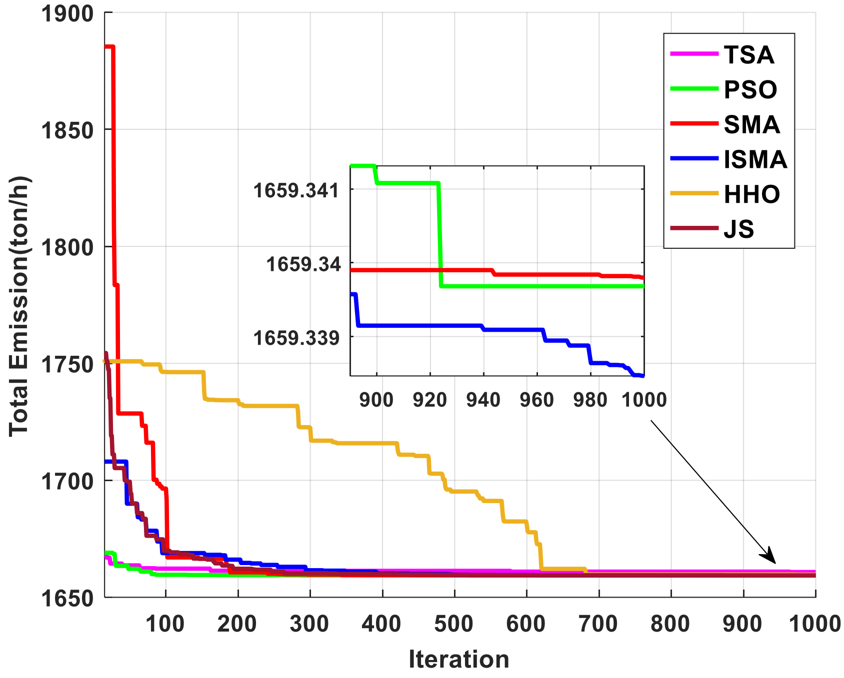


Figure 5.20: Total emission convergence curves of different techniques (Case study 3).

The statistical results for case 3 are presented and compared in Table 5.34. The results demonstrate the superiority of ISMA over the other algorithms in terms of most parameters for both fuel cost and emission.

Table 5.34: Statistical results for Case 3.

| Objective function | Algorithm | Best | Worst | Median | Average | Std. |
|---|---|---|---|---|---|---|
| Fuel cost ($/h) | ISMA | 12274.4005 | 12274.405 | 12274.401 | 12274.402 | 0.0014234 |
| | SMA | 12274.403 | 12274.406 | 12274.405 | 12274.406 | 0.0011628 |
| | HHO | 12274.4044 | 12274.446 | 12274.414 | 12274.417 | 0.0096 |
| | JS | 12274.4019 | 12274.404 | 12274.403 | 12274.403 | 0.000652 |
| | TSA | 12276.191 | 12285.525 | 12277.434 | 12278.435 | 2.732958 |
| | PSO | 12274.401 | 12274.557 | 12274.423 | 12274.441 | 0.0480398 |
| Emission (ton/h) | ISMA | 1659.3384 | 1659.3414 | 1659.3404 | 1659.3403 | 9.066E-04 |
| | SMA | 1659.3398 | 1659.3398 | 1659.3408 | 1659.3409 | 0.0013916 |
| | HHO | 1659.683 | 1662.414 | 1660.714 | 1660.821 | 0.644924 |
| | JS | 1659.358 | 1659.389 | 1659.373 | 1659.373 | 0.008014 |
| | TSA | 1660.7894 | 1663.0582 | 1661.1519 | 1661.3332 | 0.879082 |
| | PSO | 1659.3397 | 1659.3434 | 1659.3401 | 1659.3407 | 0.001554 |

#### 5.3.3.2.4 Case 4: 40 Thermal Units and Load Demand (10,500 MW)

In this case, tests are performed on the 40-unit extensive power generation system used in [119] under two different scenarios. The system data are taken from [119] where the generation limits and Fuel cost coefficients are given in Appendix E.1 while the Emission coefficients are given in Appendix E.2. The maximum number of iteration of the ISMA, SMA, HHO, JS, PSO, and TSA algorithms has been increased to 1500 to improve the overall performance of them for a large system. The generation schedules obtained by performing minimum economic are given in Table 5.35 as the first scenario. In contrast, the values of output power for minimum emission are shown in Table 5.36 as the second scenario. As seen from Table 5.35, the results of proposed ISMA are less than SMA, HHO, JS, PSO, TSA algorithms and other techniques for the fuel cost minimization problems. The convergence behaviors of the first scenario of the 40-unit system for minimizing fuel cost using the ISMA, SMA, HHO, JS, PSO, and TSA algorithms are presented in Fig. 5.21. It is clear that the performance of the ISMA algorithm to solve the ELD problem confirms the validity of the proposed technique.

Table 5.35: The best solution values for the fuel cost of the forty-unit system.

| Algorithm | ISMA | SMA | HHO | JS | TSA | PSO | DE[45] | TLBO[49] |
|---|---|---|---|---|---|---|---|---|
| P1 | 111.9975 | 114.000 | 111.2448 | 110.7989 | 111.237 | 110.928 | 110.952 | 110.868 |
| P2 | 112.0938 | 114.000 | 112.3608 | 110.8002 | 105.786 | 110.980 | 113.300 | 111.068 |
| P3 | 99.51333 | 120.000 | 119.6959 | 97.39703 | 104.757 | 97.401 | 98.616 | 97.633 |
| P4 | 180.2497 | 179.738 | 180.2359 | 129.8637 | 180.160 | 179.733 | 184.149 | 179.774 |
| P5 | 90.32857 | 97.000 | 90.53863 | 87.79977 | 54.282 | 87.948 | 86.401 | 88.272 |
| P6 | 139.9995 | 140.000 | 139.7996 | 105.3988 | 140.000 | 140.000 | 140.000 | 140.000 |
| P7 | 300 | 262.343 | 299.4461 | 259.5968 | 266.415 | 259.602 | 300.000 | 259.630 |
| P8 | 288.6401 | 300.000 | 293.8726 | 284.597 | 300.000 | 284.600 | 285.456 | 284.591 |
| P9 | 286.2 | 290.528 | 284.1988 | 284.5991 | 300.000 | 284.600 | 297.511 | 284.671 |
| P10 | 130.0052 | 130.000 | 279.5679 | 193.4505 | 211.529 | 130.000 | 130.000 | 130.096 |
| P11 | 168.7977 | 94.000 | 168.9173 | 168.7724 | 98.513 | 168.800 | 168.748 | 168.801 |
| P12 | 94.12146 | 94.000 | 94.29752 | 168.7947 | 94.000 | 243.600 | 95.695 | 168.352 |
| P13 | 125.0001 | 125.000 | 125.318 | 394.2679 | 324.487 | 214.760 | 125.000 | 304.425 |
| P14 | 394.2768 | 394.278 | 483.7442 | 394.2759 | 394.784 | 394.280 | 394.355 | 214.786 |
| P15 | 394.2952 | 394.279 | 307.2809 | 394.2685 | 311.344 | 394.279 | 305.523 | 484.177 |
| P16 | 304.5673 | 394.284 | 125.027 | 394.2759 | 305.081 | 304.520 | 394.715 | 304.844 |
| P17 | 489.3472 | 489.280 | 490.4497 | 399.5183 | 500.000 | 489.280 | 489.797 | 489.198 |
| P18 | 489.2759 | 489.297 | 491.9419 | 489.2774 | 496.197 | 489.280 | 489.362 | 489.467 |
| P19 | 511.3609 | 511.285 | 511.4378 | 511.2781 | 549.436 | 511.280 | 520.902 | 511.451 |
| P20 | 511.323 | 511.299 | 511.239 | 511.2799 | 550.000 | 511.280 | 510.641 | 511.289 |
| P21 | 523.3271 | 523.344 | 525.1631 | 523.278 | 550.000 | 523.280 | 524.534 | 523.244 |
| P22 | 523.3546 | 523.294 | 526.1478 | 523.2784 | 522.739 | 523.280 | 526.698 | 523.275 |
| P23 | 523.4576 | 523.295 | 523.3488 | 523.2783 | 550.000 | 523.280 | 530.747 | 523.400 |
| P24 | 523.2893 | 523.415 | 523.8503 | 523.2791 | 540.658 | 523.279 | 526.327 | 523.329 |
| P25 | 523.5651 | 523.279 | 528.8981 | 523.2784 | 527.313 | 523.279 | 525.654 | 523.382 |
| P26 | 523.3518 | 523.345 | 523.223 | 523.2792 | 538.587 | 523.280 | 522.950 | 523.275 |
| P27 | 10.00055 | 10.000 | 10.75621 | 10.00013 | 20.270 | 10.000 | 10.000 | 10.068 |
| P28 | 10.00008 | 10.002 | 10.93395 | 10.00121 | 10.438 | 10.000 | 11.552 | 10.018 |
| P29 | 10 | 10.000 | 10 | 10.00136 | 29.295 | 10.001 | 10.000 | 10.103 |
| P30 | 96.99946 | 96.999 | 97 | 87.79867 | 84.483 | 88.008 | 89.908 | 90.550 |
| P31 | 189.999 | 190.000 | 189.9145 | 159.7333 | 190.000 | 190.000 | 190.000 | 190.000 |
| P32 | 189.9998 | 189.999 | 190 | 159.733 | 186.309 | 159.758 | 190.000 | 190.000 |
| P33 | 190 | 190.000 | 189.9787 | 159.7329 | 188.063 | 190.000 | 190.000 | 190.000 |
| P34 | 199.9969 | 177.139 | 189.6983 | 164.7993 | 93.315 | 164.806 | 198.840 | 164.902 |
| P35 | 199.9987 | 200.000 | 199.2543 | 164.7976 | 190.181 | 165.044 | 174.178 | 164.861 |
| P36 | 199.9997 | 199.999 | 199.9485 | 164.7983 | 194.161 | 165.069 | 197.160 | 164.921 |
| P37 | 110 | 110.000 | 110 | 89.11441 | 26.745 | 110.000 | 110.000 | 110.000 |
| P38 | 109.9985 | 110.000 | 109.1275 | 89.11422 | 110.000 | 89.317 | 109.357 | 110.000 |
| P39 | 110 | 110.000 | 110 | 89.11435 | 28.030 | 89.892 | 110.000 | 110.000 |
| P40 | 511.2778 | 511.280 | 512.1426 | 511.2796 | 521.353 | 511.280 | 510.975 | 511.279 |
| V(MW) | 9.25E-03 | 6.34E-04 | 0 | 0.00041 | 5.35E-02 | 3.93E-05 | 1.00E-04 | - |
| C($/h) | 121546.89 | 121621.68 | 122439.2 | 122577.7 | 125385.34 | 121627.99 | 121840 | 121685.00 |
| E(ton/h) | 359501.02 | 362707.27 | 362707.3 | 362707.3 | 486165.74 | 349474.72 | 374790 | - |
| Time (s) | 377.7896 | 418.5727 | 222.22497 | 53.54932 | 252.66836 | 143.5182 | - | - |

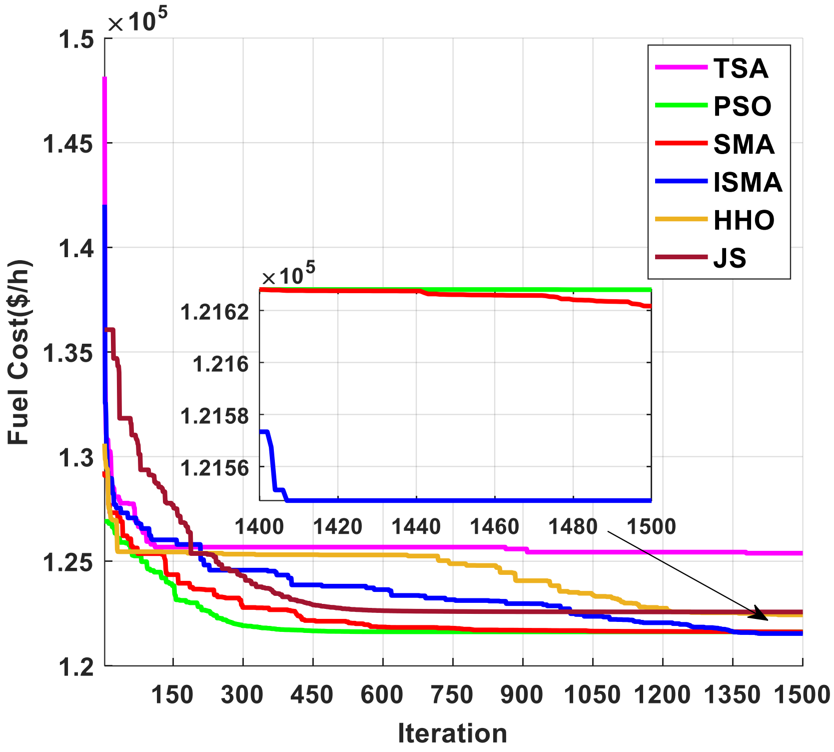


Figure 5.21: Fuel cost convergence curves of different techniques (Case study 4).

The best scheduling of generating units offered by the proposed ISMA, SMA, HHO, JS, PSO, TSA, and other recent methods for emission minimization are given in Table 5.36. It is cleared from Table 5.36 that the ISMA algorithm has the lowest value of the total emission (176682.67 ton/h), and its violation is also the lowest value (1.85E-05 MW). Therefore, the proposed ISMA has the best solution in this case. Convergence curves of the total emission minimization using SMA, HHO, JS, PSO, TSA, and ISMA for the test system are shown in Fig. 5.22. It is clear that the total emission obtained from the ISMA is the lowest and thus verify that the ISMA yields a better solution than others.

Table 5.36: The best solution values for the total emission of the forty-unit system.

| Algorithm | ISMA | SMA | HHO | JS | TSA | PSO | DE[45] | TLBO[49] |
|---|---|---|---|---|---|---|---|---|
| P1 | 114.000 | 114.000 | 114 | 113.9925 | 106.676 | 114.000 | 114.000 | 110.868 |
| P2 | 114.000 | 114.000 | 113.6966 | 113.9332 | 102.729 | 114.000 | 114.000 | 114.000 |
| P3 | 120.000 | 120.000 | 119.312 | 119.8388 | 110.513 | 120.000 | 120.000 | 120.000 |
| P4 | 169.336 | 169.750 | 166.9004 | 168.6255 | 169.305 | 169.053 | 169.293 | 169.276 |
| P5 | 97.000 | 97.000 | 96.93551 | 96.9967 | 69.963 | 96.986 | 97.000 | 97.000 |
| P6 | 124.377 | 123.979 | 124.8287 | 124.0389 | 120.298 | 124.282 | 124.283 | 124.291 |
| P7 | 299.777 | 299.685 | 297.6412 | 299.3626 | 251.540 | 299.974 | 299.456 | 299.718 |
| P8 | 298.041 | 298.404 | 295.5349 | 297.3101 | 294.467 | 299.143 | 297.855 | 297.922 |
| P9 | 297.188 | 297.709 | 297.4895 | 296.5745 | 280.702 | 297.100 | 297.133 | 297.257 |
| P10 | 130.000 | 130.047 | 132.6129 | 130.9473 | 169.974 | 130.328 | 130.000 | 130.201 |
| P11 | 298.440 | 298.572 | 298.3876 | 299.1056 | 322.187 | 297.945 | 298.598 | 298.388 |
| P12 | 297.925 | 298.087 | 296.5288 | 298.3445 | 260.958 | 298.377 | 297.723 | 298.268 |
| P13 | 433.391 | 433.690 | 433.2705 | 434.2811 | 422.063 | 432.512 | 433.747 | 433.566 |
| P14 | 421.759 | 420.844 | 422.1438 | 420.857 | 449.929 | 422.957 | 421.953 | 421.311 |
| P15 | 422.889 | 422.859 | 423.2788 | 423.2089 | 410.511 | 422.568 | 422.628 | 422.576 |
| P16 | 422.615 | 422.810 | 416.2584 | 423.3693 | 439.527 | 421.844 | 422.951 | 422.458 |

| | | | | | | | | |
|---|---|---|---|---|---|---|---|---|
| P17 | 439.462 | 439.153 | 444.4933 | 439.152 | 455.657 | 440.433 | 439.258 | 439.516 |
| P18 | 439.423 | 439.590 | 433.3867 | 438.4264 | 440.330 | 441.019 | 439.441 | 439.410 |
| P19 | 439.450 | 438.971 | 445.652 | 440.1189 | 430.238 | 439.777 | 439.491 | 439.295 |
| P20 | 439.396 | 440.285 | 436.6661 | 438.7007 | 436.612 | 439.324 | 439.619 | 439.738 |
| P21 | 439.632 | 438.573 | 437.7792 | 439.6865 | 420.027 | 440.824 | 439.225 | 439.543 |
| P22 | 439.268 | 439.490 | 438.9944 | 439.6078 | 476.445 | 438.398 | 439.682 | 439.536 |
| P23 | 439.607 | 439.239 | 438.1947 | 440.296 | 459.131 | 439.397 | 439.876 | 439.218 |
| P24 | 439.916 | 439.888 | 439.6987 | 440.6563 | 436.146 | 440.782 | 439.894 | 439.924 |
| P25 | 440.099 | 440.085 | 440.1826 | 439.3762 | 438.966 | 439.729 | 440.440 | 440.380 |
| P26 | 440.204 | 439.911 | 440.5794 | 440.3388 | 444.352 | 438.262 | 439.841 | 439.994 |
| P27 | 29.026 | 29.268 | 31.33714 | 29.72426 | 38.686 | 29.192 | 28.776 | 28.993 |
| P28 | 28.816 | 28.645 | 30.74377 | 29.31038 | 46.076 | 28.060 | 29.075 | 29.012 |
| P29 | 28.993 | 29.129 | 29.60857 | 29.65005 | 49.378 | 29.153 | 28.905 | 29.060 |
| P30 | 97.000 | 97.000 | 96.99997 | 96.99596 | 92.972 | 96.998 | 97.000 | 97.000 |
| P31 | 172.244 | 172.474 | 171.8262 | 171.6794 | 180.747 | 172.006 | 172.404 | 172.306 |
| P32 | 172.327 | 172.378 | 175.9959 | 171.6725 | 172.152 | 171.379 | 172.396 | 172.346 |
| P33 | 172.358 | 172.340 | 173.2208 | 171.735 | 166.430 | 172.551 | 172.314 | 172.464 |
| P34 | 200.000 | 200.000 | 199.8815 | 199.995 | 200.000 | 200.000 | 200.000 | 200.000 |
| P35 | 200.000 | 200.000 | 199.9912 | 199.9789 | 200.000 | 199.997 | 200.000 | 200.000 |
| P36 | 200.000 | 200.000 | 199.9999 | 199.9799 | 200.000 | 199.994 | 200.000 | 200.000 |
| P37 | 100.950 | 100.597 | 97.68673 | 100.7992 | 100.640 | 100.552 | 100.877 | 100.947 |
| P38 | 100.868 | 100.941 | 101.9846 | 100.9581 | 110.000 | 101.000 | 100.900 | 100.825 |
| P39 | 100.884 | 101.103 | 99.27437 | 100.4338 | 100.152 | 100.316 | 100.778 | 100.890 |
| P40 | 439.337 | 439.506 | 447.0027 | 439.9454 | 423.286 | 439.787 | 439.189 | 439.375 |
| V(MW) | 1.85E-05 | 7.53E-04 | 2.54295E-09 | 0.003616 | 2.63E-01 | 7.46E-04 | 1.00E-04 | 3.13 |
| C($/h) | 129948.69 | 129942.80 | 130075.9 | 130014.8 | 131551.85 | 129937.64 | 129960.00 | - |
| E(ton/h) | 176682.67 | 176687.25 | 177066.6 | 176711.3 | 193047.27 | 176708.03 | 176683.62 | 176683.50 |
| Time (s) | 379.8074 | 631.0481 | 774.33212 | 299.99302 | 147.44367 | 427.92706 | - | - |

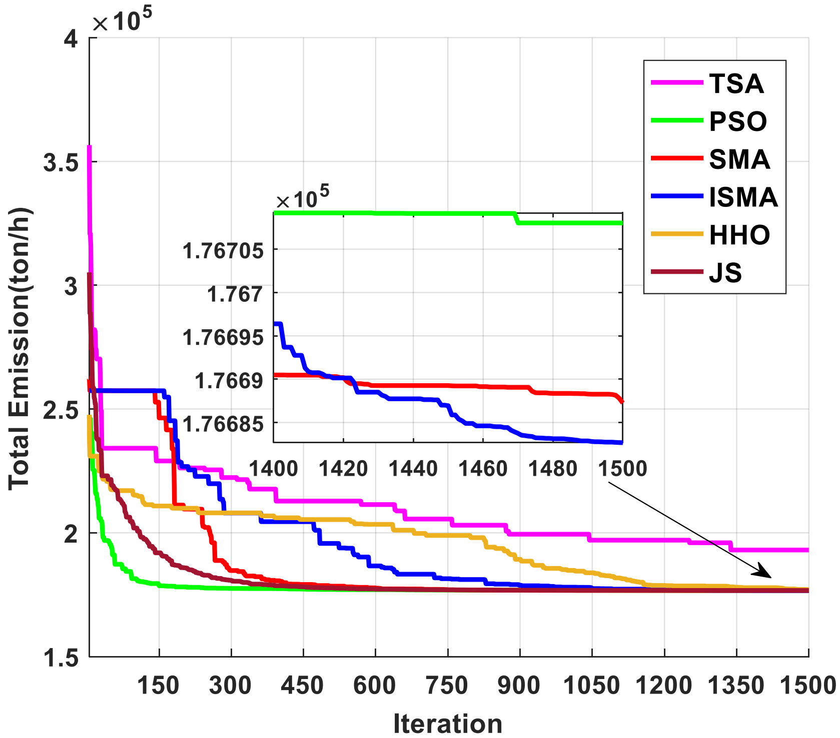


Figure 5.22: Total emission convergence curves of different techniques (Case study 4).

The performance of ISMA is compared with these algorithms in Table 5.37. From Table 5.37, it can be seen that the proposed ISMA achieved the smallest values of fuel cost and emission (121503.67 $/h, 176682.67 ton/h, respectively). In addition, it can be observed that ISMA obtained the best Min, Max, Median, and Std. values.

Table 5.37: Statistical results for Case 4.

| Objective function | Algorithm | Best | Worst | Median | Average | Std. |
|---|---|---|---|---|---|---|
| Fuel cost ($/h) | ISMA | 121546.89 | 121859.73 | 121726.95 | 121702.82 | 164.1745 |
| | SMA | 121621.68 | 121994.65 | 121781.88 | 121770.54 | 153.4794 |
| | HHO | 122439.237 | 123801.25 | 122974.36 | 122966.90 | 364.4271 |
| | JS | 122577.7 | 123413 | 123331 | 123181.8 | 246.9075 |
| | TSA | 125385.34 | 126380.35 | 125368.53 | 125628.15 | 661.7595 |
| | PSO | 121627.99 | 122077.55 | 121892.71 | 121893.32 | 151.4660 |
| Emission (ton/h) | ISMA | 176682.67 | 176686.74 | 176683.95 | 176684.41 | 1.5132 |
| | SMA | 176687.25 | 176726.13 | 176687.47 | 176694.99 | 17.4277 |
| | HHO | 177066.6 | 177754.9 | 177445 | 177463.8 | 164.4549 |
| | JS | 176711.3 | 176720.9 | 176716 | 176716.3 | 2.502253 |
| | TSA | 193047.27 | 199825.87 | 194145.19 | 195418.19 | 2.92E+03 |
| | PSO | 176708.03 | 176899.63 | 176708.03 | 176740.73 | 78.4224 |

#### 5.3.3.2.5 Case 5: 110 Thermal Units and Load Demand (15,000 MW)

This system comprising of 110 units and the load demand is equal to 15,000 MW with quadratic fuel cost characteristics and without considering transmission losses. The input system data of this case are given in Appendix F and also available in [182]. The number of populations are 2000, and the maximum number of iterations is 2500. The best generation schedule obtained using the ISMA, SMA, HHO, JS, TSA, and PSO algorithms tabulated in Table 5.38. It is seen from this table that the obtained results of ISMA is 198565.939 $/h which is the best value of Fuel cost for the 110 units system compared to the results of the original SMA and other recent techniques.

Table 5.38: The best solution values for the fuel cost of the 110-units system.

| Algorithm | ISMA | SMA | HHO | JS | TSA | PSO |
|---|---|---|---|---|---|---|
| P1 | 2.400507 | 2.622554 | 3.251242 | 7.754749 | 4.208569 | 5.429169 |
| P2 | 2.402228 | 2.400014 | 2.446104 | 7.063212 | 2.4 | 5.984534 |
| P3 | 5.055625 | 2.434698 | 2.673819 | 9.313971 | 6.254875 | 5.265683 |
| P4 | 2.629029 | 2.992649 | 2.4 | 7.880994 | 3.652992 | 5.215054 |
| P5 | 5.148627 | 2.4 | 6.930281 | 6.780552 | 6.845159 | 4.983332 |
| P6 | 4.015587 | 4.000001 | 17.8534 | 9.711549 | 4 | 8.783175 |
| P7 | 4 | 4.000016 | 15.81666 | 9.146754 | 4 | 15.71236 |
| P8 | 4.000003 | 4 | 4.208634 | 9.315038 | 6.652928 | 12.24616 |
| P9 | 4 | 4 | 14.57092 | 8.257969 | 4.25961 | 12.66345 |
| P10 | 31.08023 | 31.20057 | 70.62261 | 58.54666 | 17.16921 | 46.45249 |
| P11 | 37.18731 | 74.79637 | 73.38665 | 55.93619 | 71.98092 | 63.91511 |
| P12 | 68.82187 | 62.75893 | 15.34868 | 45.86718 | 49.87798 | 54.17195 |
| P13 | 36.44211 | 54.1428 | 46.67185 | 47.91778 | 56.4164 | 23.13882 |
| P14 | 25 | 25.07135 | 25 | 59.99423 | 40.80094 | 69.90858 |
| P15 | 25.13272 | 25.00599 | 99.95094 | 91.18138 | 25 | 63.16994 |
| P16 | 25.10509 | 25.00472 | 100 | 70.01365 | 26.76086 | 72.72672 |
| P17 | 154.9465 | 155 | 150.9899 | 122.5399 | 154.0009 | 103.6746 |
| P18 | 154.9773 | 154.9952 | 139.9565 | 121.9564 | 154.5085 | 147.5522 |

| | | | | | | |
|---|---|---|---|---|---|---|
| P19 | 155 | 154.9864 | 153.8162 | 110.0698 | 60.14006 | 134.0495 |
| P20 | 154.9998 | 102.5721 | 148.7462 | 111.4949 | 155 | 135.3134 |
| P21 | 68.90075 | 68.90202 | 191.3704 | 128.4118 | 68.9 | 84.59898 |
| P22 | 68.92731 | 68.90125 | 71.0292 | 101.3538 | 69.60551 | 73.9599 |
| P23 | 68.90613 | 68.90002 | 193.5053 | 134.7432 | 74.17907 | 68.9 |
| P24 | 349.9944 | 349.9845 | 141.1083 | 297.5706 | 349.4898 | 332.0594 |
| P25 | 399.9994 | 399.9994 | 399.2377 | 320.9977 | 394.8134 | 372.7378 |
| P26 | 399.9996 | 400 | 399.2539 | 340.024 | 400 | 380.5251 |
| P27 | 499.9994 | 499.9935 | 500 | 440.3133 | 460.2447 | 377.1125 |
| P28 | 500 | 499.7582 | 500 | 413.9115 | 500 | 465.3444 |
| P29 | 200 | 200 | 199.7186 | 157.803 | 200 | 141.5889 |
| P30 | 65.24203 | 99.99979 | 99.42779 | 72.18002 | 25.33283 | 76.40754 |
| P31 | 10 | 10.00203 | 47.54806 | 23.46039 | 13.70667 | 21.35197 |
| P32 | 9.845297 | 12.3444 | 17.82367 | 16.71267 | 5 | 16.30016 |
| P33 | 43.53132 | 65.56203 | 79.74497 | 67.75236 | 20.83792 | 32.81403 |
| P34 | 247.1876 | 249.9988 | 249.5816 | 203.9364 | 240.3992 | 224.3301 |
| P35 | 359.9998 | 359.9986 | 110 | 302.4475 | 360 | 313.3566 |
| P36 | 399.9987 | 400 | 399.7814 | 295.874 | 400 | 336.1917 |
| P37 | 29.29664 | 37.67582 | 37.67328 | 19.62342 | 10 | 30.30126 |
| P38 | 22.78959 | 56.83642 | 70 | 52.36611 | 67.79393 | 46.7252 |
| P39 | 56.98885 | 69.80126 | 100 | 72.73896 | 49.31385 | 70.77265 |
| P40 | 73.8338 | 120 | 20.48655 | 80.56785 | 35.22386 | 91.51613 |
| P41 | 152.8516 | 136.656 | 180 | 149.0712 | 142.8969 | 127.1847 |
| P42 | 216.2521 | 199.763 | 219.2555 | 171.7992 | 206.5694 | 171.7525 |
| P43 | 440 | 440 | 439.027 | 386.3775 | 440 | 439.5246 |
| P44 | 559.8904 | 560 | 560 | 496.5256 | 560 | 539.2588 |
| P45 | 659.9003 | 659.98 | 660 | 613.26 | 650.7611 | 659.6707 |
| P46 | 665.0369 | 627.7291 | 201.5122 | 584.1358 | 643.2216 | 699.1032 |
| P47 | 5.400547 | 5.4 | 5.413171 | 19.90796 | 6.386926 | 8.896871 |
| P48 | 5.40135 | 5.4 | 5.4 | 15.95955 | 11.53855 | 15.22545 |
| P49 | 8.40242 | 8.4 | 8.456699 | 20.85914 | 9.259809 | 16.476 |
| P50 | 8.4 | 8.40365 | 18.27208 | 18.80375 | 15.43206 | 17.37283 |
| P51 | 9.143902 | 29.36811 | 12.09866 | 31.13674 | 9.14778 | 20.70166 |
| P52 | 12 | 12.00028 | 55.31545 | 12.27959 | 17.01713 | 16.10337 |
| P53 | 12.00159 | 12 | 56.17757 | 31.29933 | 12 | 18.08727 |
| P54 | 12 | 12.00004 | 55.05448 | 27.44085 | 15.73463 | 12 |
| P55 | 12.02588 | 12 | 28.52544 | 32.13277 | 13.76349 | 12 |
| P56 | 57.86518 | 50.61099 | 95.8732 | 61.26164 | 67.83256 | 66.13336 |
| P57 | 31.45777 | 48.52262 | 94.78591 | 67.8837 | 38.50862 | 90.1559 |
| P58 | 35.73096 | 78.03548 | 35.19943 | 64.09942 | 47.12305 | 66.27956 |
| P59 | 68.23574 | 43.81391 | 94.98686 | 78.5817 | 54.9464 | 55.14429 |
| P60 | 45.00001 | 45.00002 | 46.0579 | 82.54965 | 49.96038 | 69.97685 |
| P61 | 45.68124 | 45.00181 | 45.09229 | 89.57682 | 48.05353 | 46.7225 |
| P62 | 45 | 45 | 45.70599 | 92.47066 | 52.58556 | 80.2357 |
| P63 | 171.6163 | 172.4597 | 178.2503 | 148.7598 | 175.9284 | 124.094 |
| P64 | 184.9205 | 183.893 | 185 | 141.8741 | 139.5947 | 131.7357 |
| P65 | 140.2055 | 169.6174 | 185 | 146.563 | 167.5547 | 102.7506 |
| P66 | 178.9734 | 183.8618 | 184.6745 | 146.7559 | 172.3518 | 95.38751 |
| P67 | 70 | 70 | 70 | 92.402 | 75.25628 | 91.54675 |
| P68 | 70.00026 | 70 | 141.384 | 82.05823 | 70 | 71.14942 |
| P69 | 70 | 70.03861 | 157.5767 | 126.1827 | 72.27206 | 70.00137 |
| P70 | 360 | 341.4428 | 150.7414 | 278.5144 | 360 | 357.01 |

| | | | | | | |
|---|---|---|---|---|---|---|
| P71 | 399.9998 | 400 | 183.9705 | 305.8564 | 356.0329 | 399.7669 |
| P72 | 399.9935 | 400 | 163.5678 | 362.3622 | 400 | 400 |
| P73 | 123.9319 | 68.58418 | 113.9575 | 240.8123 | 189.8934 | 205.3575 |
| P74 | 218.2584 | 152.5601 | 50.68172 | 173.5763 | 154.8527 | 207.1537 |
| P75 | 88.59486 | 89.99996 | 90 | 63.87866 | 88.59561 | 66.39232 |
| P76 | 49.92458 | 50 | 39.37313 | 36.65875 | 18.23135 | 18.65592 |
| P77 | 213.4715 | 217.3226 | 358.6811 | 328.8608 | 444.2485 | 398.096 |
| P78 | 409.1935 | 475.6029 | 596.0993 | 480.7542 | 521.2429 | 470.3499 |
| P79 | 118.107 | 164.0484 | 198.4682 | 135.729 | 148.8751 | 131.3772 |
| P80 | 59.67335 | 45.08554 | 41.10952 | 101.6286 | 93.48571 | 120 |
| P81 | 10.00007 | 10 | 10 | 15.2412 | 10.79623 | 27.02052 |
| P82 | 14.18621 | 24.34238 | 39.84965 | 23.28488 | 18.95082 | 28.82764 |
| P83 | 20.08657 | 35.59525 | 78.61837 | 74.96339 | 20.27248 | 65.47084 |
| P84 | 190.3161 | 93.71174 | 200 | 154.7158 | 193.7249 | 108.9955 |
| P85 | 303.3981 | 317.0912 | 324.6975 | 306.0136 | 325 | 252.2418 |
| P86 | 439.2509 | 439.8854 | 440 | 388.8152 | 440 | 322.0197 |
| P87 | 15.60837 | 34.79542 | 29.43413 | 28.32297 | 18.56994 | 24.29372 |
| P88 | 38.74103 | 21.69031 | 26.89821 | 42.10349 | 37.10903 | 41.20792 |
| P89 | 87.13813 | 95.82531 | 91.64617 | 69.15613 | 59.77801 | 85.42212 |
| P90 | 185.9027 | 98.83151 | 157.7866 | 172.1439 | 74.55329 | 155.852 |
| P91 | 91.40372 | 61.09157 | 130.961 | 101.2324 | 52.27296 | 92.10157 |
| P92 | 58.79787 | 73.36332 | 44.95655 | 69.15928 | 42.71309 | 80.56614 |
| P93 | 440 | 439.9993 | 440 | 388.1692 | 440 | 408.8525 |
| P94 | 499.9633 | 500 | 444.485 | 423.0998 | 490.0781 | 484.6226 |
| P95 | 599.7575 | 599.9999 | 266.2714 | 519.0924 | 600 | 599.8339 |
| P96 | 485.6981 | 510.9935 | 699.7426 | 557.2984 | 496.6494 | 565.447 |
| P97 | 3.6022 | 3.628945 | 14.1746 | 9.490354 | 6.899172 | 10.67644 |
| P98 | 3.604613 | 3.600182 | 13.22001 | 11.75729 | 5.627175 | 10.96358 |
| P99 | 4.684607 | 4.4 | 7.855119 | 8.937548 | 4.4 | 10.55868 |
| P100 | 4.451691 | 4.400179 | 4.4 | 10.6464 | 4.4 | 12.45633 |
| P101 | 10.79574 | 11.38262 | 10.43088 | 44.0155 | 13.16958 | 26.33527 |
| P102 | 20.26343 | 12.72674 | 10.35424 | 39.32774 | 10.30378 | 32.50203 |
| P103 | 20.00022 | 20.00019 | 81.95108 | 66.07252 | 30.17598 | 20 |
| P104 | 20.01489 | 20 | 20 | 46.10923 | 21.04744 | 20 |
| P105 | 40.00477 | 40 | 149.1945 | 64.03769 | 41.30849 | 42.48025 |
| P106 | 40 | 40 | 41.06758 | 56.98341 | 40 | 40.00812 |
| P107 | 50.00052 | 50.00015 | 50 | 56.62189 | 50 | 50 |
| P108 | 30 | 30 | 139.3279 | 78.03485 | 30 | 43.59824 |
| P109 | 40 | 40.00035 | 40 | 53.79532 | 40 | 58.57065 |
| P110 | 20.00106 | 20 | 20 | 67.19511 | 22.32584 | 23.1355 |
| V(MW) | **2.32567E-06** | 1.24816E-05 | 0 | 0.00828 | 0.052163 | 0.141891 |
| C($/h) | **198565.939** | 198618.5052 | 219950.7861 | 213126.3 | 200832.1 | 204974.8 |
| Time (S) | 899.7583 | 1159.0918 | 1106.04479 | 479.1843 | 551.6497 | 724.55812 |

The convergence characteristics obtained by these techniques are displayed in Fig. 5.23. The proposed ISMA technique exhibited a faster convergence to the optimum solution than the conventional SMA and other algorithms. The best, average, worst, median, Std., and fuel costs obtained by the different techniques over 30 independent trials are presented in Table 5.39. This table shows the supremacy and effectiveness of the proposed technique.

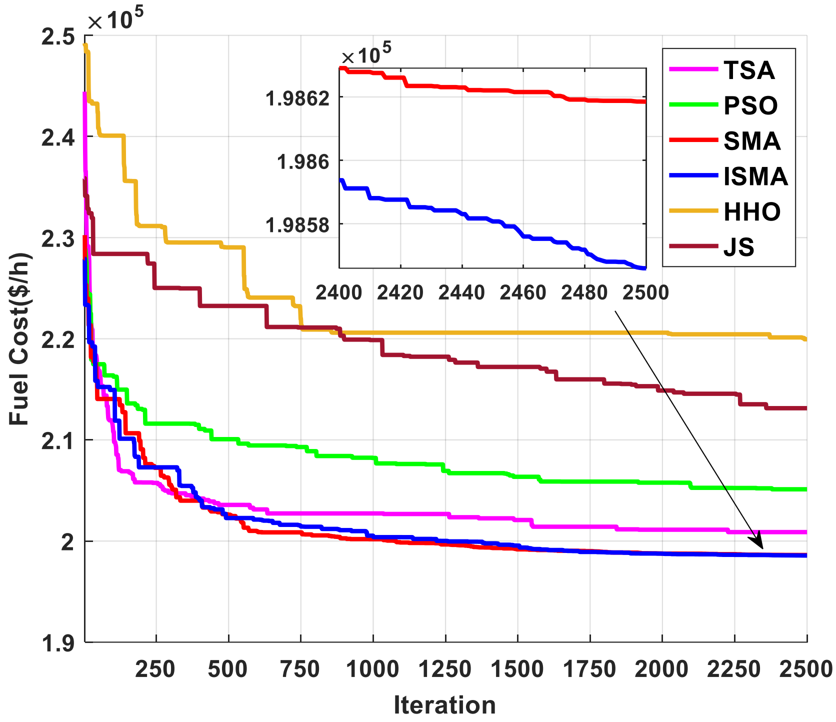


Figure 5.23: Fuel cost convergence curves of different techniques (Case study 5).

Table 5.39: Statistical results for Case 5.

| Objective function | Algorithm | Best | Worst | Median | Average | Std. |
|---|---|---|---|---|---|---|
| Fuel cost ($/h) | ISMA | 198565.9 | 198949.1 | 198826.5 | 198782.1 | 153.465 |
| | SMA | 198618.5 | 198924.3 | 198835.8 | 198790.5 | 144.4451 |
| | HHO | 219950.8 | 225741.9 | 221519.3 | 222320.1 | 2593.779 |
| | JS | 213120.4 | 213982.6 | 213274.1 | 213389.5 | 356.9868 |
| | TSA | 200832.1 | 203923.7 | 202357.4 | 202375.1 | 927.5175 |
| | PSO | 204974.8 | 206643.1 | 205634 | 205630.8 | 426.9417 |

### 5.3.4 Solving EED Problem using SDO Technique

MATLAB (R2016a) is employed to simulate the SDO algorithm to solve the EED problem for five units (1800 MW), three units (550,600,700,800,850 MW), and six unit systems with four levels of demand. The optimization algorithms are performed in 30 individual executions, and the parameters of SDO, GWO, MFO, TSO, and WOA are chosen as follows; the maximum iterations are considered as 500 while the population size equals 50. The setting of parameters for each algorithm is presented in Table 5.40.

Table 5.40: Parameter settings of the selected techniques.

| Algorithms | Parameters Setting |
|---|---|
| GWO | a variable decreases linearly from 2 to 0 |
| MFO | b = 1 and a decreases linearly from −1 to −2 |
| TSO | K = 1 (Default) |
| WOA | $a_1$ variable decreases linearly from 2 to 0 |

$a_2$ linearly decreases from −1 to −2

#### 5.3.4.1 Case 1: Five Thermal Units and Load Demand 1800MW

In this case the single-objective economic dispatch problem is firstly considered, while the emission dispatch is not taken into consideration. It is a five-unit system with a load of PD equals 1800 MW which is described in [183]. Table 5.41 presents the results of the first test system using the proposed SDO, GWO, MFO, TSO, and WOA, as well as those obtained by recently published methods such as GA [183], PSO [183], QPSO [20], FA [184], and SCA [95]. From the obtained results, it is obvious that the SDO optimizes the generating units more efficiently as the fuel cost obtained is the lowest (18,609.69046 USD/h) in comparison to other well-known methods. This demonstrates that the proposed SDO algorithm is more efficient to solve this problem.

Table 5.41: Comparison of results for case study 1.

| Output | GA | PSO | QPSO | FA | SCA | GWO | MFO | TSO | WOA | SDO |
|---|---|---|---|---|---|---|---|---|---|---|
| P1 (MW) | 320.00 | 320.00 | 320.51 | 327.800 | 320.000 | 324.7512 | 333.465 | 320.972 | 320.00 | 320.0000 |
| P2 (MW) | 343.74 | 343.70 | 346.47 | 341.989 | 343.850 | 347.8232 | 312.449 | 391.3358 | 361.30 | 343.9724 |
| P3 (MW) | 472.60 | 472.60 | 482.95 | 460.422 | 472.302 | 461.78 | 451.984 | 465.7936 | 498.70 | 472.3341 |
| P4 (MW) | 320.00 | 320.00 | 320 | 327.800 | 320.000 | 320.4659 | 320.000 | 320.972 | 320.00 | 320.0001 |
| P5 (MW) | 343.74 | 343.70 | 330.08 | 341.989 | 343.848 | 345.1789 | 382.102 | 300.9113 | 300.00 | 343.6934 |
| Total power (MW) | 1800.00 | 1800.00 | 1800 | 1800.00 | 1800.000 | 1799.999 | 1800.000 | 1799.985 | 1800.00 | 1800.000 |
| Fuel cost ($/h) | 18,611.07 | 18,610.40 | 18,610.03 | 18,610 | 18,609.694 | 18,610.08 | 18,612.727 | 18,614.51 | 18,612.30 | **18,609.69046** |

The best values obtained are in bold.

The results obtained from the 30 individual runs are used to provide the statistical analysis, including the mean value, the best value, the worst value, and standard deviation (STD). These results are presented in Table 5.42. From Table 5.42, it is clear that the proposed SDO has the lowest standard deviation (STD) value, showing that its stability is strong. Moreover, this table shows that the SDO algorithm's performance for this case is better than that of GWO, MFO, TSO, GWO, and WOA algorithms.

Table 5.42: Statistical analysis of best optimal solution for 30 independent runs on case study 1.

| Method | Best | Mean | Worst | STD |
|---|---|---|---|---|
| GWO | 18,611.1 | 18,613.22 | 18,618.14 | 1.975646 |
| MFO | 18,612.73 | 18,640.24 | 18,682.94 | 21.35502 |
| TSO | 18,614.51 | 18,649.61 | 18,725.11 | 27.70438 |
| WOA | 18,612.3 | 18,678.34 | 18,757.56 | 43.77738 |
| SDO | **18,609.69** | **18,609.7** | **18,609.75** | **0.012081** |

The best values obtained are in bold.

Figure 5.23a presents the boxplots for case 1. The minimum and maximum are the lowest and the largest data points acquired by the algorithm, i.e., the edges of the whiskers. A narrow boxplot denotes a strong agreement between the achieved data. In addition, the outlier was represented as the red plus sign. The outlier is a value that lies in a data series on its extremes, which is either very small or large. The outliers may be plotted as individual points. It can be observed that the boxplot of the SDO technique is very narrow with the lowest values compared with those of other methods. The convergence behavior of SDO, GWO, MFO, TSO, and WOA for case 1 is displayed in Figure 5.23b. It is shown that SDO achieves the best convergence characteristics compared to the other techniques as it converges to the optimum solution quickly.

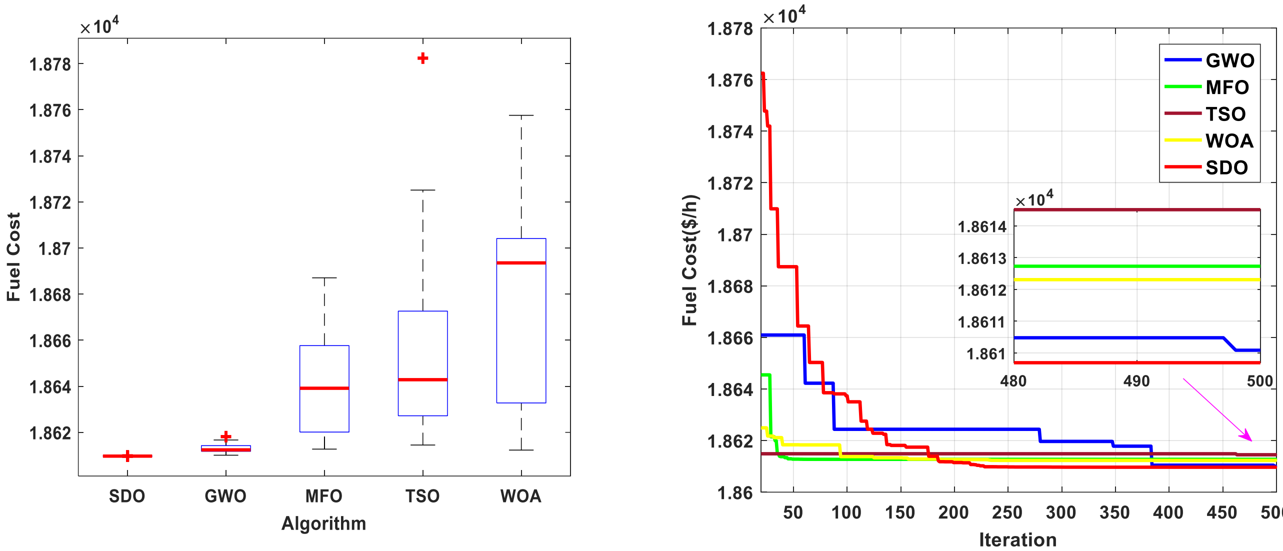


(a) Boxplot (1800 MW) (b) Fuel cost convergence (1800 MW)

Figure 5.24: Boxplot and convergence characteristics of competitive algorithms for case study 1.

#### 5.3.4.2 Case 2: Three Thermal Units and Load Demand

This test system comprises three units and the power load demand has five different values: 550, 600, 700, 800, and 850 MW. The objective function of this case is the total cost, which is the combination between the fuel and emission cost. In addition, the power loss is taken into account. The system data are taken from [185]. The best results obtained using the different methods are tabulated in Table 5.43 at each value of load demand. As displayed in this table, the proposed SDO algorithm outperforms the four comparative algorithms (GWO, MFO, TSO, and WOA) as well as the other earlier published techniques such as SA [167] and SCA [95] for all levels of demand values.

Table 5.43: Comparison of results for case study 2.

| Output | Method | P1 (MW) | P2 (MW) | P3 (MW) | Total Power (MW) | Power Loss (MW) | Fuel Cost (USD/h) | $SO_2$ Emission (t/h) | NOx Emission (t/h) | Total Cost (USD/h) |
|---|---|---|---|---|---|---|---|---|---|---|
| 550 | SA | 307.13 | 160.32 | 88.63 | 556.0859 | 6.0859 | 5581.479 | 6.0071 | 0.08805 | 18,760.5958 |
| | SCA | 307.11 | 160.34 | 88.63 | 556.0861 | 6.0861 | 5581.474 | 6.0071 | 0.08805 | 18,760.5954 |
| | GWO | 309.0085 | 157.3799 | 89.66934 | 556.0577 | 6.0577 | 5583.315 | 6.001373 | 0.088034 | 18,757.11817 |
| | MFO | 305.2371 | 162.8724 | 88.00239 | 556.1119 | 6.1119 | 5580.728 | 6.002984 | 0.088065 | 18,755.99933 |
| | TSO | 317.7065 | 145.6984 | 92.56283 | 555.9678 | 6.9678 | 5587.81 | 5.99831 | 0.088074 | 18,766.33266 |
| | WOA | 306.3277 | 172.6761 | 77.21019 | 556.214 | 6.214 | 5579.141 | 6.000284 | 0.08847 | 18,774.44 |
| | SDO | 307.1315 | 160.3242 | 88.63012 | 556.0859 | 6.0859 | 5581.48 | 6.002078 | 0.088048 | **18,755.7139** |
| 600 | SA | 329.32 | 184.61 | 93.44 | 607.3685 | 7.3685 | 6028.708 | 6.4941 | 0.0882 | 19,660.5278 |

| | | | | | | | | | | |
|---|---|---|---|---|---|---|---|---|---|---|
| | SCA | 329.27 | 184.66 | 93.43 | 607.3692 | 7.3692 | 6028.695 | 6.4941 | 0.0882 | 19,660.5274 |
| | GWO | 306.3277 | 172.6761 | 77.21019 | 556.214 | 6.214 | 5579.141 | 6.000284 | 0.08847 | 18,774.44 |
| | MFO | 330.0837 | 189.0994 | 88.23823 | 607.4212 | 7.4212 | 6028.039 | 6.487661 | 0.088267 | 19,659.28309 |
| | TSO | 339.1655 | 180.2745 | 87.86784 | 607.3078 | 7.3078 | 6036.004 | 6.482078 | 0.088178 | 19,668.21974 |
| | WOA | 347.4846 | 163.7357 | 95.91894 | 607.1393 | 7.1393 | 6035.845 | 6.480146 | 0.088133 | 19,674.76854 |
| | SDO | 329.3154 | 184.6149 | 93.43822 | 607.3686 | 7.3686 | 6028.707 | 6.489082 | 0.088182 | **19,655.64571** |
| 700 | SA | 374.07 | 233.15 | 103.14 | 710.3669 | 10.3669 | 6939.248 | 7.4855 | 0.0902 | 21,633.8869 |
| | SCA | 374.05 | 233.17 | 103.15 | 710.3673 | 10.3673 | 6939.244 | 7.4855 | 0.0902 | 21,633.8863 |
| | GWO | 371.2705 | 233.7384 | 105.3757 | 710.3846 | 10.3846 | 6939.123 | 7.48281 | 0.090327 | 21,629.95825 |
| | MFO | 383.021 | 229.847 | 97.42688 | 710.2949 | 10.2949 | 6940.712 | 7.473722 | 0.090045 | 21,635.12855 |
| | TSO | 370.1402 | 229.798 | 110.3914 | 710.3296 | 10.3296 | 6943.914 | 7.484344 | 0.090461 | 21,640.84311 |
| | WOA | 363.1866 | 242.9636 | 104.4283 | 710.5786 | 10.5786 | 6938.115 | 7.489486 | 0.090602 | 21,634.4439 |
| | SDO | 374.0686 | 233.1553 | 103.1431 | 710.367 | 10.367 | 6939.248 | 7.480495 | 0.090232 | **21,629.00454** |
| 800 | SA | 419.34 | 281.64 | 112.96 | 813.9456 | 13.9456 | 7871.446 | 8.5004 | 0.0947 | 23,841.8787 |
| | SCA | 419.31 | 281.64 | 112.99 | 813.9458 | 13.9458 | 7871.443 | 8.5004 | 0.0947 | 23,841.8780 |
| | GWO | 416.9318 | 282.8186 | 114.2291 | 813.9795 | 13.9795 | 7871.227 | 8.49738 | 0.094807 | 23,837.36654 |
| | MFO | 430.4856 | 268.0573 | 115.0725 | 813.6155 | 13.6155 | 7872.514 | 8.48578 | 0.094267 | 23,845.00244 |
| | TSO | 400.7381 | 289.57 | 123.9024 | 814.2105 | 13.2105 | 7874.926 | 8.512525 | 0.095937 | 23,865.78267 |
| | WOA | 423.7624 | 264.7467 | 125.0633 | 813.5723 | 13.5723 | 7872.082 | 8.491662 | 0.094954 | 23,861.35998 |
| | SDO | 419.3401 | 281.638 | 112.9675 | 813.9456 | 13.9456 | 7871.446 | 8.49533 | 0.09468 | **23,836.99605** |
| 850 | SA | 442.17 | 305.85 | 117.93 | 865.9536 | 15.9536 | 8345.746 | 9.0166 | 0.0978 | 25,035.121 |
| | SCA | 442.17 | 305.84 | 117.94 | 865.9533 | 15.9533 | 8345.744 | 9.0166 | 0.0978 | 25,035.120 |
| | GWO | 442.1641 | 302.2764 | 121.4178 | 865.8583 | 15.8583 | 8345.789 | 9.010977 | 0.097884 | 25,032.62337 |
| | MFO | 438.6103 | 309.106 | 118.3346 | 866.0509 | 16.0509 | 8345.754 | 9.015064 | 0.098019 | 25,030.83091 |
| | TSO | 436.3464 | 312.2227 | 117.5694 | 866.1385 | 16.1385 | 8351.57 | 9.017524 | 0.098145 | 25,038.08193 |
| | WOA | 462.8209 | 296.3094 | 106.5603 | 865.6906 | 15.6906 | 8349.505 | 8.995909 | 0.096883 | 25,058.47724 |
| | SDO | 442.172 | 305.8567 | 117.9249 | 865.9536 | 15.9536 | 8345.747 | 9.011611 | 0.097813 | **25,030.23861** |

The best values obtained are in bold.

The statistical analysis of total cost values, including the best, mean, worst, and STD for all the five algorithms over 30 independent runs, is tabulated in Table 5.44. The optimal total cost values reflect the accuracy, while the mean total cost values indicate the average accuracy, and STD reflects the reliability of the optimum output power of each generator. As shown in Table 5.44, it is seen that the best total cost value is achieved using the proposed SDO. Additionally, the SDO gives the best values for the other terms mean, worst and STD compared with the other algorithms at the different values of demand for case 2.

Table 5.44: Statistical analysis of best optimal solution for 30 independent runs on case study 2.

| Output | Method | Best | Mean | Worst | STD |
|---|---|---|---|---|---|
| 550 MW | GWO | 18,757.12 | 18,768.81 | 18,793.19 | 9.53064333 |
| | MFO | 18,756 | 18,974.4 | 19,399.97 | 199.893713 |
| | TSO | 18,766.33 | 18,914.69 | 19,409.59 | 164.505227 |
| | WOA | 18,774.44 | 19,115.64 | 20,206.58 | 357.224908 |
| | SDO | **18,755.71** | **18,755.71** | **18,755.71** | **$2.3334 \times 10^{-11}$** |
| 600 MW | GWO | 19,657.3 | 19,671.75 | 19,720.86 | 17.60894 |
| | MFO | 19,659.28 | 19,890.19 | 20,236.25 | 171.6149 |
| | TSO | 19,668.22 | 19,818.87 | 20,324.07 | 190.8788 |
| | WOA | 19,674.77 | 20,054 | 20,759.48 | 326.6113 |

| | | | | | |
|---|---|---|---|---|---|
| | SDO | **19,655.65** | **19,655.65** | **19,655.65** | **$1.57 \times 10^{-11}$** |
| 700 MW | GWO | 21,629.96 | 21,645.53 | 21,676.32 | 13.06491 |
| | MFO | 21,635.13 | 21,864.17 | 22,815.74 | 246.2461 |
| | TSO | 21,640.84 | 21,760.12 | 22,184.57 | 134.6336 |
| | WOA | 21,634.44 | 22,202.5 | 23,931.3 | 585.3308 |
| | SDO | **21,629** | **21,629** | **21,629** | **$7.49 \times 10^{-12}$** |
| 800 MW | GWO | 23,837.37 | 23,849.57 | 23,875.93 | 10.19397 |
| | MFO | 23,845 | 24,089.28 | 24,757.33 | 255.6961 |
| | TSO | 23,865.78 | 23,968.74 | 24,231.66 | 96.34443 |
| | WOA | 23,861.36 | 24,390.13 | 25,416.55 | 486.0704 |
| | SDO | **23,837** | **23,837** | **23,837** | **$1.49 \times 10^{-9}$** |
| 850 MW | GWO | 25,032.62 | 25,048.45 | 25,080.96 | 13.67632 |
| | MFO | 25,030.83 | 25,218.25 | 25,965.61 | 226.3887 |
| | TSO | 25,038.08 | 25,157.41 | 25,787.74 | 142.4899 |
| | WOA | 25,058.48 | 25,477.28 | 26,306.55 | 313.3439 |
| | SDO | **25,030.24** | **25,030.24** | **25,030.24** | **$3.12 \times 10^{-11}$** |

The best values obtained are in bold.

The variation between iterations of the total cost for various levels of demand in the 3-unit system is displayed in Figure 5.25. The graphical illustration explains that the proposed SDO technique achieves a perfect convergence rate compared with the other algorithms at the five levels of demand. Furthermore, the proposed approach requires only about 50 to 90 iterations to achieve the optimal solution in case 2.

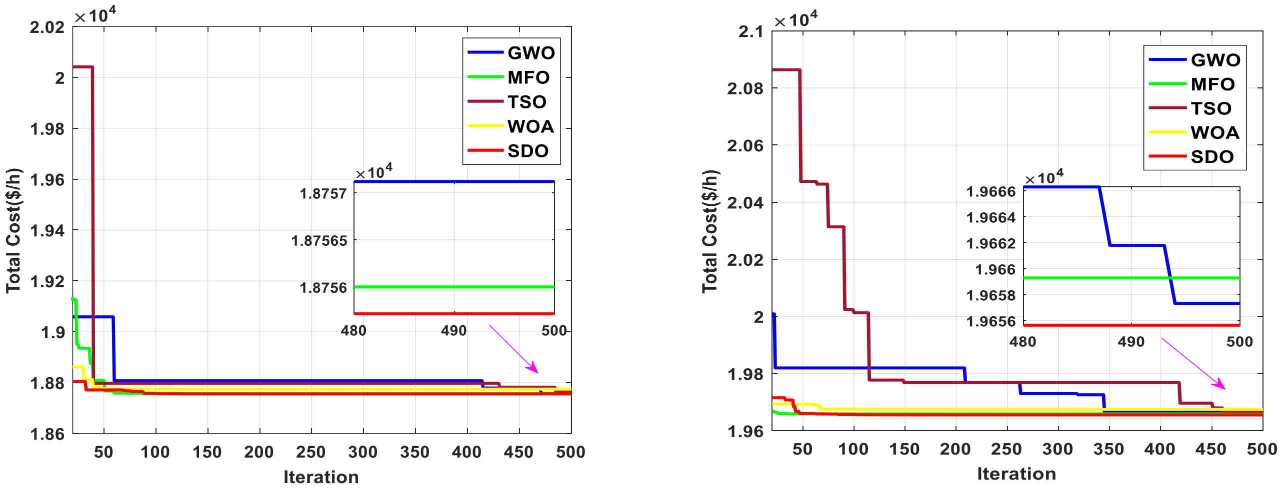


(**a**) 550 MW (**b**) 600 MW

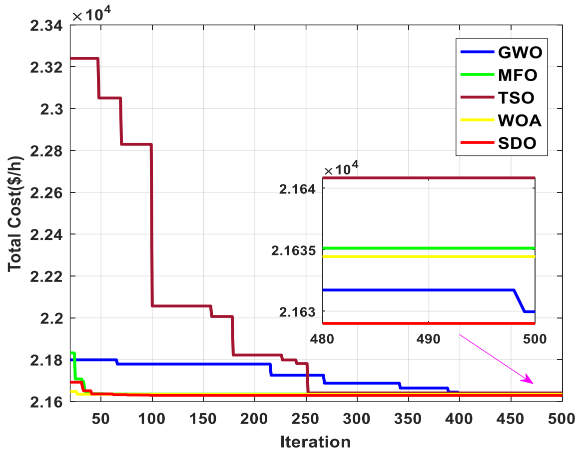


(**c**) 700 MW

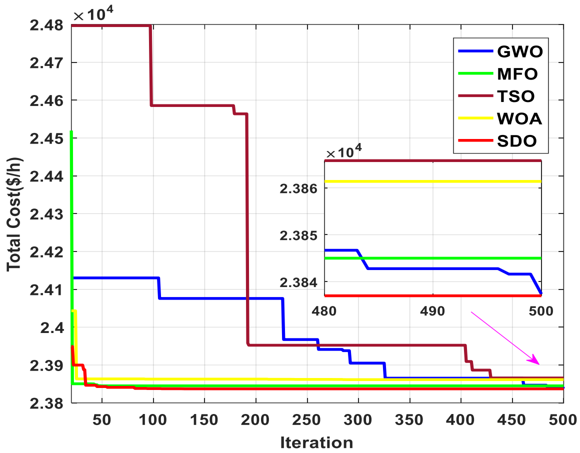


(**d**) 800 MW

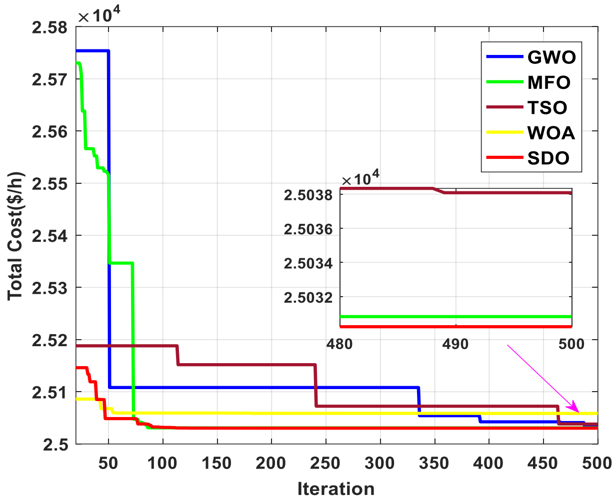


(**e**) 850 MW

Figure 5.25: Convergence characteristics of competitive algorithms for different levels of demand in the 3-unit system (case study 2): (a) 550 MW; (b) 600 MW; (c) 700 MW; (d) 800 MW; and (e) 850 MW.

Further, the box plot analysis for the total cost at different values of load using the proposed SDO, GWO, MFO, TSO, and WOA algorithms are presented in Figure 5.26. It is seen from Figure 5.26 that, in terms of stability of solutions, SDO outperformed the other algorithms, affirming the stability of these techniques.

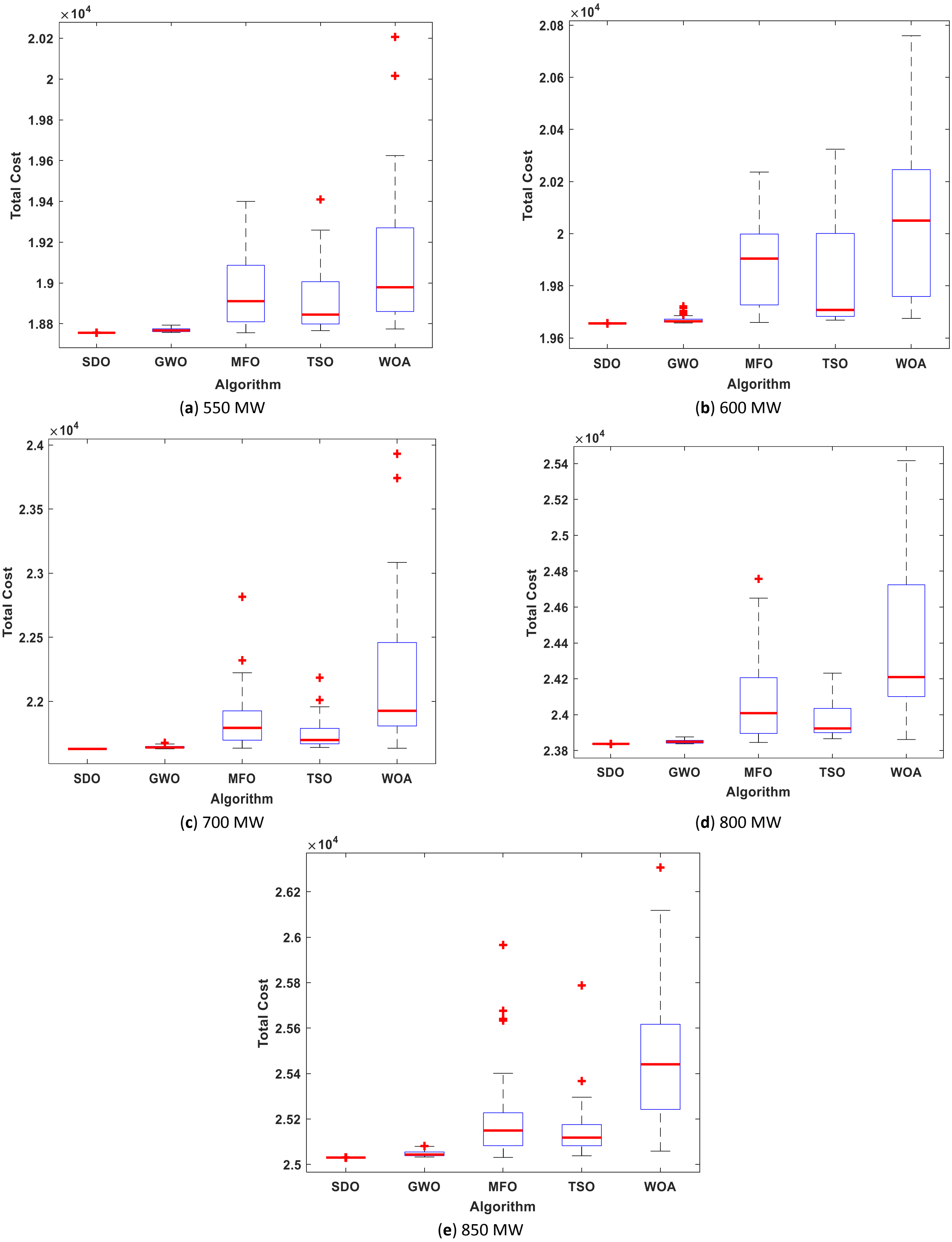


Figure 5.26: Boxplot of competitive algorithms for different levels of demand in the 3-unit system (case study 2): (a) 550 MW; (b) 600 MW; (c)700 MW; (d) 800 MW; and (e) 850 MW.

#### 5.3.4.3 Case 3: Six Thermal Units and Load Demand

In this case, six generators are considered with four values of the power demand and three kinds of emission were taken into account. The system data are taken from [185]. Table 5.45 shows the best optimal power output of generators for CEED problem of the proposed SDO versus the four-optimization algorithms with system demands rising from 150 to 225 MW. It can be clearly seen from those tables that SDO achieves better results than the other methods.

Table 5.46 presents the obtained results of fuel cost, SO2 emissions, NOx emission, CO2 emission, and total cost, respectively. It is clear from Table 5.46 that the proposed technique gives the best total cost solution compared with the recently published methods, i.e., LR [21], PSO [186], SA [168], QBA [20], MBO [171], SCA [95], GOA [187], and QITFA [97], and CAEO4 [188], as well as the four comparative algorithms, i.e., GWO, MFO, TSO, and WOA.

Table 5.45: Comparison of results for case study 3 (150 MW and 175 MW).

| Output | 150 MW | | | | | 175 MW | | | | |
|---|---|---|---|---|---|---|---|---|---|---|
| | GWO | MFO | TSO | WOA | SDO | GWO | MFO | TSO | WOA | SDO |
| P1 (MW) | 50 | 50 | 50 | 50 | 50 | 50 | 50 | 50 | 50 | 50 |
| P2 (MW) | 20.75886 | 20 | 20 | 20.33136 | 20.35391 | 27.50185 | 28.72184 | 30.08752 | 33.18849 | 27.58749 |
| P3 (MW) | 15 | 15 | 15 | 15 | 15.00001 | 15 | 15 | 15 | 15.12393 | 15.00001 |
| P4 (MW) | 25.29881 | 24.91282 | 26.98215 | 28.95298 | 25.1725 | 31.13365 | 31.34679 | 29.40553 | 26.82591 | 31.28936 |
| P5 (MW) | 17.01369 | 17.60108 | 16.14984 | 13.8491 | 17.17103 | 22.97238 | 21.92136 | 27.94373 | 21.9921 | 22.7153 |
| P6 (MW) | 21.92874 | 22.4861 | 21.86934 | 21.86655 | 22.30255 | 28.39188 | 28.01001 | 22.55015 | 27.86957 | 28.40784 |
| Total power (MW) | 150.0001 | 150 | 150.0013 | 150 | 150 | 174.9998 | 175 | 174.9869 | 175 | 175 |
| Fuel cost (USD/h) | 2710.098 | 2704.204 | 2709.296 | 2718.695 | 2707.082 | 3205.35 | 3212.61 | 3232.637 | 3235.258 | 3205.973 |
| Emission of $SO_2$ (kg/h) | 2555.781 | 2567.677 | 2549.385 | 2532.956 | 3142.284 | 3100.353 | 3086.113 | 3083.842 | 3089.089 | 3804.415 |
| Emission of $NO_x$ (kg/h) | 3137.583 | 3145.572 | 3153.413 | 3162.123 | 2405.352 | 3804.552 | 3791.651 | 3765.98 | 3729.825 | 2838.222 |
| Emission of $CO_2$ (kg/h) | 2405.56 | 2402.048 | 2424.639 | 2454.301 | 2561.676 | 2835.405 | 2840.691 | 2774.055 | 2800.421 | 3098.243 |
| Total cost (USD/h) | 10,176.95 | 10,176.96 | 10,179.57 | 10,190.23 | **10,176.76** | 12,134.5 | 12,135.54 | 12,177.65 | 12,163.91 | **12,134.42** |
| Output | 200 MW | | | | | 225 MW | | | | |
| | GWO | MFO | TSO | WOA | SDO | GWO | MFO | TSO | WOA | SDO |
| *P*1 (MW) | 50 | 50 | 50 | 50.06341 | 50 | 50 | 50 | 50 | 52.05189 | 50.00002 |
| *P*2 (MW) | 34.78159 | 35.61352 | 32.80429 | 43.40812 | 34.51204 | 40.87784 | 40.65315 | 45.91897 | 47.47468 | 41.06731 |
| *P*3 (MW) | 15 | 15.01478 | 15 | 19.88421 | 15.00001 | 16.52138 | 17.20828 | 15 | 16.41255 | 16.54637 |
| *P*4 (MW) | 37.24191 | 38.12485 | 39.89293 | 32.97922 | 37.65465 | 43.47432 | 43.58366 | 40.73255 | 37.4387 | 43.58443 |
| *P*5 (MW) | 28.05565 | 28.086 | 32.13791 | 24.53685 | 28.37898 | 34.12524 | 33.65396 | 40.7522 | 31.62218 | 33.80187 |
| *P*6 (MW) | 34.92126 | 33.16086 | 30.15185 | 29.12819 | 34.45431 | 40 | 39.90095 | 32.59872 | 40 | 40 |
| Total power (MW) | 200.0004 | 200 | 199.987 | 200 | 200 | 224.9988 | 225 | 225.0025 | 225 | 225 |
| Fuel cost (USD/h) | 3740.643 | 3747.437 | 3750.076 | 3819.378 | 3740.508 | 4318.736 | 4319.748 | 4372.503 | 4360.671 | 4318.963 |
| Emission of $SO_2$ (kg/h) | 3689.209 | 3666.724 | 3673.811 | 3594.432 | 4540.304 | 4319.761 | 4310.343 | 4328.178 | 4341.377 | 5319.707 |
| Emission of $NO_x$ (kg/h) | 4537.08 | 4526.615 | 4564.491 | 4337.238 | 3309.197 | 5321.476 | 5309.014 | 5285.344 | 5240.347 | 3811.103 |
| Emission of $CO_2$ (kg/h) | 3308.854 | 3309.179 | 3296.554 | 3262.163 | 3686.051 | 3807.963 | 3810.186 | 3709.759 | 3789.447 | 4316.36 |
| Total cost (USD/h) | 14,268.25 | 14,269.92 | 14,296.62 | 14,405.08 | **14,267.83** | 16,599.91 | 16,600.12 | 16,704.13 | 16,723.97 | **16,599.66** |

The best values obtained are in bold.

Table 5.46: Fuel cost results considering the 4 levels of demand in the 6-unit power generation system.

| Load (MW) | Total fuel cost (USD/h) | | | | | | | | | | | | | |
|---|---|---|---|---|---|---|---|---|---|---|---|---|---|---|
| | LR | PSO | SA | QBA | MBO | SCA | GOA | QITFA | CAEO4 | GWO | MFO | TSO | WOA | SDO |
| 150 | 2729.35 | 2734.20 | 2705.21 | 2704.97 | 2704.92 | 2704.92 | 2704.87 | 2711.71 | 2702.94 | 2710.098 | 2704.204 | 2709.296 | 2718.695 | 2707.082 |
| 175 | 3475.41 | 3236.30 | 3220.51 | 3188.10 | 3188.13 | 3188.15 | 3188.08 | 3189.91 | 3179.34 | 3205.35 | 3212.61 | 3232.637 | 3235.258 | 3205.973 |
| 200 | 4210.30 | 3784.90 | 3735.73 | 3726.08 | 3727.43 | 3727.44 | 3727.40 | 3729.26 | 3722.45 | 3740.643 | 3747.437 | 3750.076 | 3819.378 | 3740.508 |
| 225 | 5130.53 | 4402.30 | 4321.52 | 4314.63 | 4315.63 | 4315.05 | 4315.15 | 4316.34 | 4314.38 | 4318.736 | 4319.748 | 4372.503 | 4360.671 | 4318.963 |
| Load (MW) | Emission of $SO_2$ (kg/h) | | | | | | | | | | | | | |
| 150 | 3091.65 | 3193.60 | 3138.45 | 3147.38 | 3146.83 | 3146.83 | 3146.74 | 3087.92 | 2885.21 | 2555.781 | 2567.677 | 2549.385 | 2532.956 | 3142.284 |
| 175 | 4142.18 | 3904.90 | 3763.48 | 3858.96 | 3859.49 | 3859.36 | 3859.37 | 3807.49 | 3891.64 | 3100.353 | 3086.113 | 3083.842 | 3089.089 | 3804.415 |
| 200 | 5053.58 | 4670.60 | 4553.97 | 4598.20 | 4592.64 | 4592.49 | 4592.46 | 4528.28 | 4589.87 | 3689.209 | 3666.724 | 3673.811 | 3594.432 | 4540.304 |
| 225 | 6106.50 | 5426.10 | 5287.31 | 5344.75 | 5335.81 | 5339.96 | 5338.42 | 5289.45 | 5360.57 | 4319.761 | 4310.343 | 4328.178 | 4341.377 | 5319.707 |
| Load (MW) | Emission of $NO_x$(kg/h) | | | | | | | | | | | | | |
| 150 | 2448.22 | 2424.60 | 2379.35 | 2408.10 | 2406.24 | 2406.24 | 2406.18 | 2406.79 | 2249.11 | 3137.583 | 3145.572 | 3153.413 | 3162.123 | 2405.352 |
| 175 | 2604.89 | 2879.70 | 2789.92 | 2853.40 | 2854.13 | 2854.01 | 2854.08 | 2856.22 | 2847.56 | 3804.552 | 3791.651 | 3765.98 | 3729.825 | 2838.222 |
| 200 | 3102.08 | 3373.20 | 3285.65 | 3327.78 | 3325.35 | 3325.34 | 3325.31 | 3313.29 | 3301.53 | 4537.08 | 4526.615 | 4564.491 | 4337.238 | 3309.197 |
| 225 | 3798.38 | 3877.60 | 3781.19 | 3822.53 | 3811.18 | 3820.29 | 3819.56 | 3815.71 | 3832.07 | 5321.476 | 5309.014 | 5285.344 | 5240.347 | 3811.103 |
| Load (MW) | Emission of $CO_2$ (kg/h) | | | | | | | | | | | | | |
| 150 | 2537.12 | 2607.10 | 2568.95 | 2565.14 | 2564.57 | 2564.57 | 2564.50 | 2561.85 | 2448.86 | 2405.56 | 2402.048 | 2424.639 | 2454.301 | 2561.676 |
| 175 | 3613.53 | 3178.00 | 3094.69 | 3129.78 | 3129.20 | 3129.19 | 3129.07 | 3133.60 | 3154.93 | 2835.405 | 2840.691 | 2774.055 | 2800.421 | 3098.243 |
| 200 | 4473.37 | 3771.50 | 3714.33 | 3719.64 | 3715.69 | 3715.64 | 3715.56 | 3721.30 | 3725.20 | 3308.854 | 3309.179 | 3296.554 | 3262.163 | 3686.051 |
| 225 | 5502.52 | 4403.00 | 4324.30 | 4323.47 | 4328.07 | 4322.52 | 4322.26 | 4322.39 | 4322.68 | 3807.963 | 3810.186 | 3709.759 | 3789.447 | 4316.36 |
| Load (MW) | Total cost (USD/h) | | | | | | | | | | | | | |
| 150 | 10,264.57 | 10,385 | 10,261.49 | 10,255.28 | 10,255.21 | 10,255.208 | 10,254.98 | 10,254.91 | 10,179.35 | 10,176.95 | 10,176.96 | 10,179.57 | 10,190.23 | **10,176.76** |
| 175 | 13,251.52 | 12,425 | 12,280.04 | 12,241.74 | 12,241.67 | 12,241.668 | 12,241.41 | 12,241.61 | 12,164.36 | 12,134.5 | 12,135.54 | 12,177.65 | 12,163.91 | **12,134.42** |
| 200 | 16,077.41 | 14,642 | 14,421.30 | 14,413.88 | 14,413.71 | 14,413.709 | 14,413.52 | 14,413.56 | 14,287.65 | 14,268.25 | 14,269.92 | 14,296.62 | 14,405.08 | **14,267.83** |
| 225 | 19,661.33 | 17,125 | 16,790.69 | 16,783.91 | 16,784.34 | 16,783.781 | 16,783.68 | 16,783.33 | 16,603.90 | 16,599.91 | 16,600.12 | 16,704.13 | 16,723.97 | **16,599.66** |

The best values obtained are in bold.

The best, average, and worst results, as well as STD, for this case are presented in Table 5.47. It is visible from the table that the performance and reliability of SDO are far better than the other techniques.

Table 5.47: Statistical analysis of best optimal solution for 30 independent runs on case study 3.

| Output | Method | Best | Mean | Worst | STD |
|---|---|---|---|---|---|
| | GWO | 10,176.95 | 10,177.53 | 10,180.32 | 0.630143 |
| | MFO | 10,176.96 | 10,194.22 | 10,315.41 | 26.51734 |
| 150 MW | TSO | 10,179.57 | 10,317.84 | 10,597.16 | 100.5936 |
| | WOA | 10,190.23 | 10,341.22 | 10,771.87 | 144.4793 |
| | SDO | **10,176.76** | **10,177.02** | **10,178.45** | **0.412301** |
| | GWO | 12,134.5 | 12,135.67 | 12,137.17 | 0.693041 |
| | MFO | 12,135.54 | 12,156.94 | 12,193.62 | 16.72976 |
| 175 MW | TSO | 12,177.65 | 12,391.58 | 13,060.41 | 186.2542 |
| | WOA | 12,163.91 | 12,488.2 | 12,968.14 | 191.5428 |
| | SDO | **12,134.42** | **12,134.59** | **12,135.95** | **0.361005** |
| | GWO | 14,268.25 | 14,269.56 | 14,272.8 | 1.08758 |
| | MFO | 14,269.92 | 14,296.66 | 14,407.34 | 34.60848 |
| 200 MW | TSO | 14,296.62 | 14,701.93 | 15,323.14 | 255.9892 |
| | WOA | 14,405.08 | 14,822.59 | 15,611.04 | 364.6892 |
| | SDO | **14,267.83** | **14,268.02** | **14,269.38** | **0.327536** |
| | GWO | 16,599.91 | 16,601.19 | 16,604.3 | 1.170242 |
| | MFO | 16,600.12 | 16,619.1 | 16,717.74 | 22.83156 |
| 225 MW | TSO | 16,704.13 | 17,128.52 | 18,307.85 | 333.7764 |
| | WOA | 16,723.97 | 17,339.25 | 18,278.04 | 442.2791 |
| | SDO | **16,599.66** | **16,599.76** | **16,600.19** | **0.123662** |

The best values obtained are in bold.

Figure 5.27 shows a comparison between the techniques in terms of the convergence characteristics. In the plot, the SDO converges faster than the rest of the methods and the SDO is able to achieve the optimum value in around 250 iterations. The worst algorithm, in this case, is the WOA that converges in sub-optimal value in early iterations.

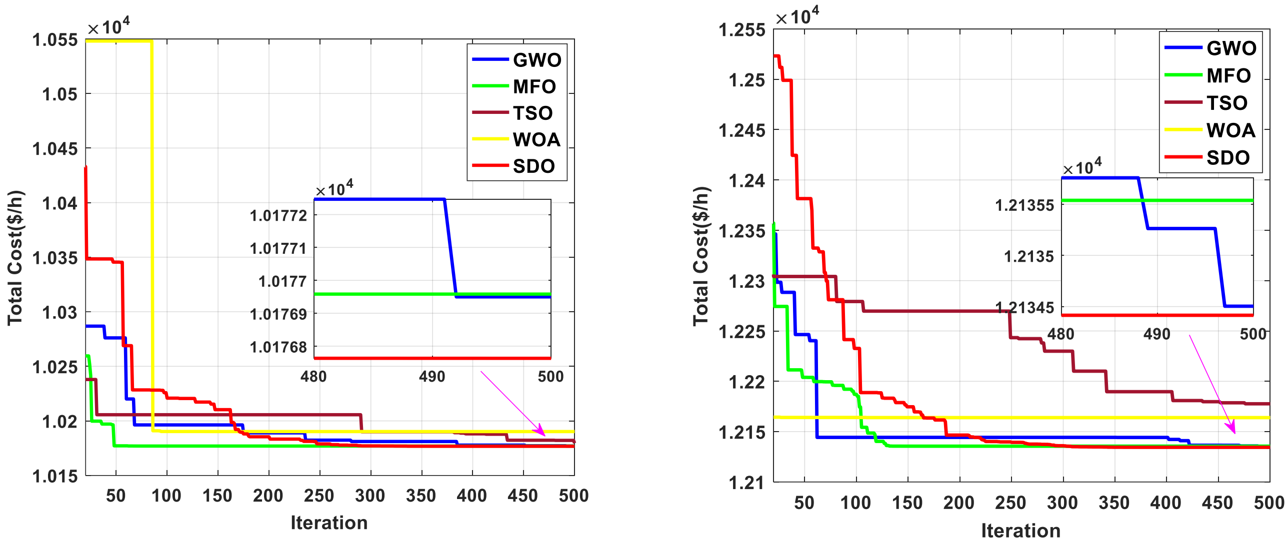


(**a**) 150 MW (**b**) 175 MW

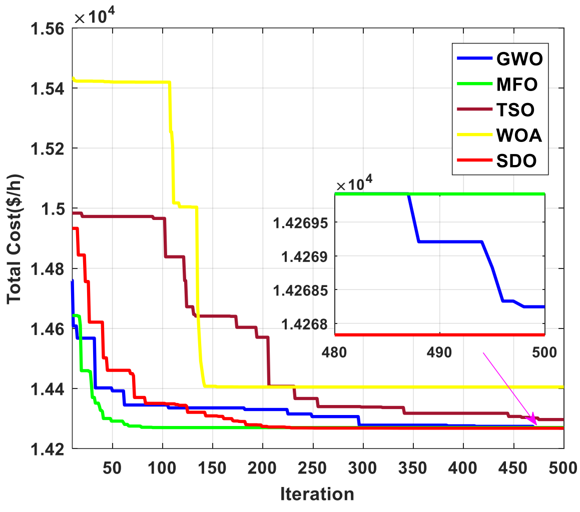


(c) 200 MW

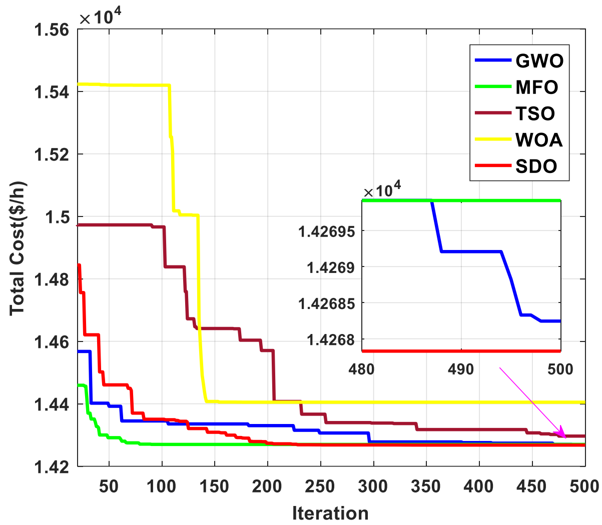


(d) 225 MW

Figure 5.27: Convergence characteristics of competitive algorithms for different levels of demand in 6-unit system (case study 3): (a) 150 MW; (b) 175 MW; (c) 200 MW; and (d) 225 MW.

Figure 5.28 is the box plot of the total cost for all the algorithms. From such plots, it is remarked that the performance of the SDO is superior.

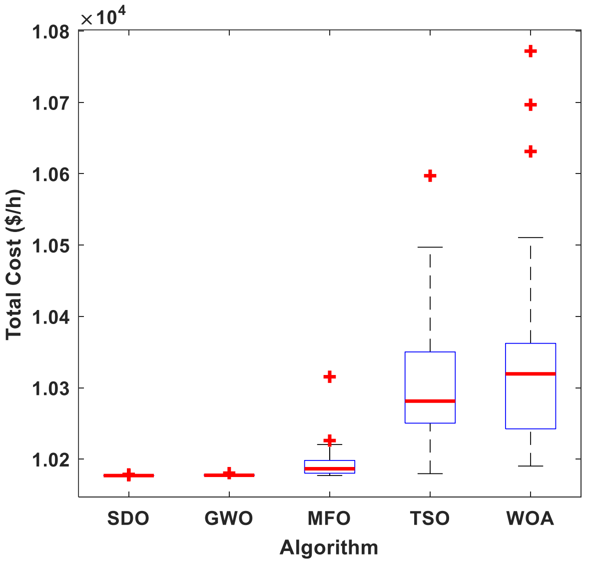


(a) 150 MW

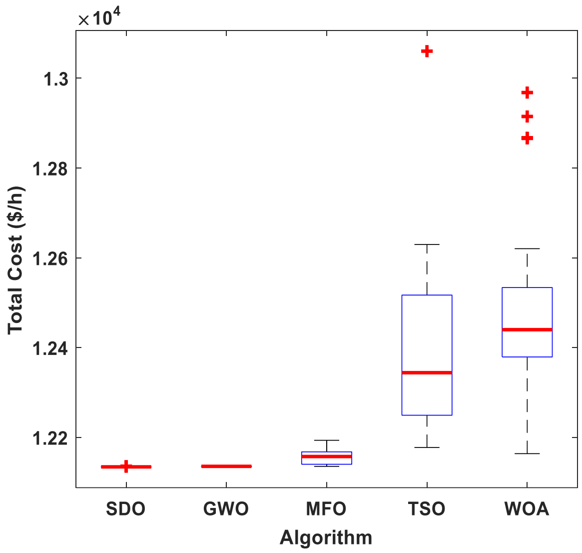


(b) 175 MW

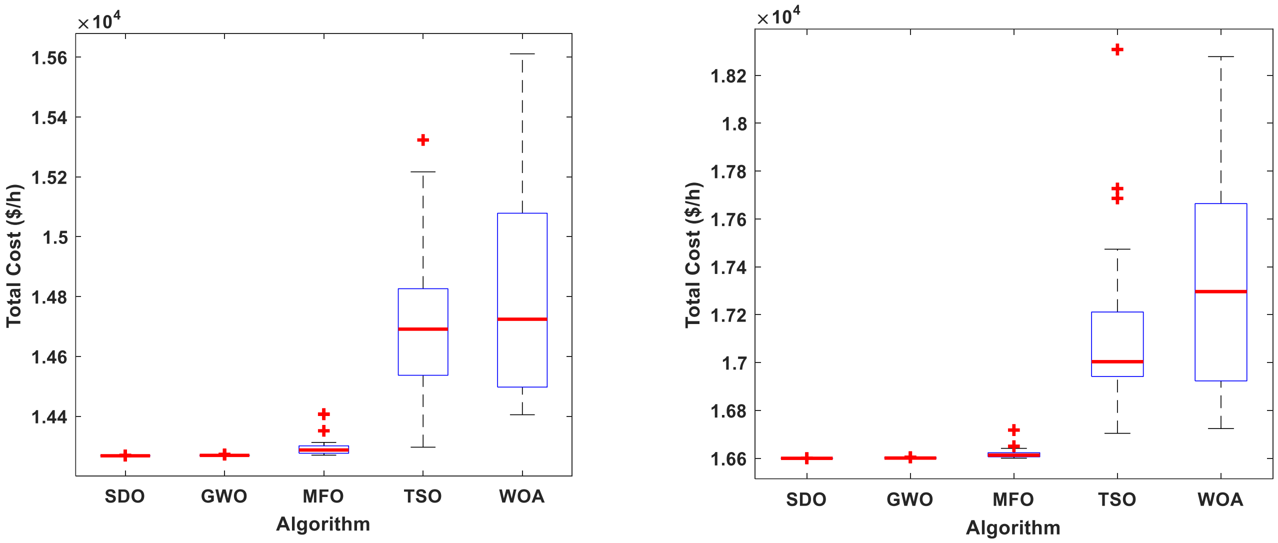


(c) 200 MW (d) 225 MW

Figure 5.28: Boxplot of competitive algorithms for different levels of demand in the 6-unit system (case study 3): (a) 150 MW; (b) 175 MW; (c) 200 MW; and (d) 225 MW.

### 5.3.5 Solving EED Problem using MMPA Algorithm

#### 5.3.5.1 Mathematical Validation

The quality of the proposed modified marine predators algorithm (MMPA) has been validated against the conventional MPA and several well-known algorithms with twenty-eight 50-dimensional benchmarks of CEC2017. The studied functions include four classes which are unimodal, simple multimodal, hybrid, and composition functions. Manta ray foraging optimization (MRFO) [189], Slime mould algorithm (SMA) [190], Sine-cosine algorithm (SCA) [191], and Comprehensive learning particle swarm optimizer (CLPSO) [192], are used in the comparison. All mentioned algorithms have been implemented for the maximum number of the evaluation function of 10000D (where D is the dimension of the considered functions, 50) and population size is 30. Each algorithm has been executed for 30 independent runs using Matlab R2018b'working on Windows10 64bit. All computations have been performed on a Core i7-6500U CPU, 2.5 GHz of speed, and 16 GB of RAM. The parameter setting of MPA and MMPA for mathematical validation and solving the CEED problems are presented in Table 5.48.

Table 5.48: Parameter setting of MPA and MMPA for mathematical validation and solving CEED problems.

| Parameters | Values |
|---|---|
| Maximum iterations (M) | M=2*$10^4$ for mathematical validation.<br>M=300 for Cases 1, 2, and 3;<br>M=1500 for Case 4. |

| | |
|---|---|
| Number of trials (T) | T=30 for mathematical validation and all Cases. |
| Population size (N) | N=30 for mathematical validation.<br>N=300 for Cases 1, 2, and 3;<br>N=1000 for Case 4. |
| Fish Aggregating Devices (FADs) | 0.2 |
| The constant of the prey position (P) | 0.5 |
| The first constant of learning probability values (c) | 0.05 |
| The second constant of learning probability values (e) | 0.25 |

The Average (Avg), standard deviation (Std) of the optimization problems, the ranks of the proposed algorithm, and the other peers based on the minimum Avg have been computed for the validation of MMPA as shown in Tables 5.49 and 5.50. A pairwise comparison has been performed based on Wilcoxon rank-sum test with a significant difference 0.05 among MMPA and the other counterparts as reported in Table 5.51.

From Table 5.49, it can be seen, that when considering the Avg values obtained by the different optimization algorithms, the MMPA has the least values for sixteen functions with high consistency in comparison with MPA, MRFO, SMA, and SCA. The CLPSO gives the optimal value of F6 and acts as the best variant for F7, F9, F11, F13, and F27 meanwhile MPA and MRFO show the best performance for F3 and F2, respectively. Based on the rank values of the different optimization algorithms shown in Table 5.50, the MMPA has the least average rank, which is why it occupies the first position followed by the MPA and CLPSO, which are in the second and third positions, respectively. To test the differences among the MMPA and the other counterparts, the non-parametric statistical of Wilcoxon rank-sum test with significant difference 0.05 has been performed. The pairwise comparison between MMPA and MPA based on p-values in Table 5.51 reveals that MMPA presents a better performance in 19 functions whereas MPA behaves better only in nine. This confirms the efficiency of the proposed changes for improving the performance of the MPA algorithm. The MMPA proves its superiority in solving F24, F25, and F22 versus MRFO, SMA, SCA, and CLPSO, respectively. Accordingly, it can be concluded that the MMPA shows a better performance than MPA and other algorithms in case of unimodal function (F3), multi-modal functions (F5, F8), hybrid functions (F14, F15, F16, F17, F18, F19), and composition functions (F21, F23, F24, F25, F28, F29, F30).

Based on the previous discussion, it is proved that sharing the best individual experiences among the agents (CL approach) is a good strategy for enhancing the exploitation and exploration abilities of the MPA.

Table 5.49: The average and standard deviation values obtained by different optimization algorithms for 50D CEC2017.

| | MMPA | | MPA | | MRFO | | SMA | | SCA | | CLPSO | |
|---|---|---|---|---|---|---|---|---|---|---|---|---|
| F(global) | Avg | | Avg | Std | Avg | Std | Avg | Std | Avg | Std | Avg | Std |
| F3(300) | 300.0975 | 0.044008 | 300.4364 | 0.390423 | 300.6137 | 1.424181 | 300.5154 | 0.333057 | 99393.53 | 11904.28 | 72893.98 | 11351.24 |
| F4(400) | 468.0495 | 41.14851 | 508.6117 | 40.75236 | 461.5246 | 45.20451 | 549.4002 | 53.51665 | 6127.009 | 1065.405 | 468.0773 | 24.19077 |
| F5(500) | 604.2451 | 16.02055 | 698.0269 | 31.29329 | 824.2549 | 39.91122 | 709.9173 | 43.07014 | 1050.435 | 36.46812 | 611.3479 | 12.48935 |
| F6(600) | 603.189 | 0.758184 | 603.13 | 1.179187 | 647.6513 | 11.22655 | 605.746 | 2.268862 | 667.3127 | 4.6816 | 600 | 2.20E-13 |
| F7(700) | 965.3987 | 24.88613 | 1032.768 | 59.93786 | 1497.711 | 135.8111 | 985.7757 | 46.81919 | 1616.757 | 67.7556 | 868.1671 | 14.19523 |
| F8(800) | 903.847 | 13.65722 | 996.7517 | 39.43965 | 1138.151 | 44.93314 | 988.2694 | 45.82579 | 1355.091 | 29.86346 | 917.3933 | 13.94149 |
| F9(900) | 2331.569 | 219.538 | 2533.258 | 424.1542 | 10261.6 | 2179.777 | 8804.487 | 4161.934 | 21617.19 | 3627.223 | 2096.495 | 460.9165 |
| F10(1000) | 5763.015 | 398.1289 | 5826.046 | 764.16 | 7478.069 | 864.2496 | 7333.519 | 817.5357 | 14244.23 | 459.8188 | 5143.969 | 399.416 |
| F11(1100) | 1273.742 | 29.44499 | 1286.913 | 43.04035 | 1250.377 | 28.3635 | 1390.553 | 72.41716 | 5788.484 | 1234.75 | 1207.474 | 32.68447 |
| F12(1200) | 1615676 | 630470 | 3039622 | 1979456 | 119855.1 | 54176.14 | 5610542 | 3363932 | 1.16E+10 | 2.21E+09 | 3075863 | 1635223 |
| F13(1300) | 3814.379 | 2781.284 | 6025.889 | 4848.089 | 5412.133 | 4802.605 | 35580.91 | 9061.873 | 2.6E+09 | 9.69E+08 | 1794.075 | 158.5738 |
| F14(1400) | 1490.842 | 15.41988 | 1503.65 | 21.11328 | 6270.26 | 5019.072 | 123286.7 | 81385.71 | 2097455 | 997053.9 | 431510.8 | 274394.2 |
| F15(1500) | 1703.795 | 48.22884 | 1773.17 | 113.6363 | 10393.76 | 6366.534 | 26559.91 | 7028.067 | 2.93E+08 | 1.04E+08 | 1851.537 | 466.0063 |
| F16(1600) | 2491.893 | 170.9159 | 2643.053 | 291.6628 | 3360.287 | 431.6334 | 3251.676 | 307.6245 | 5305.204 | 305.2795 | 2754.833 | 184.2877 |
| F17(1700) | 2280.327 | 145.5998 | 2430.245 | 138.7057 | 3217.094 | 356.3169 | 3100.664 | 388.3431 | 4187.586 | 261.1889 | 2489.239 | 142.3474 |
| F18(1800) | 3777.78 | 1153.383 | 5409.225 | 1867.121 | 62116.82 | 31234.82 | 652003.8 | 374362.6 | 12693517 | 5812094 | 732088.2 | 416771 |
| F19(1900) | 1985.185 | 27.2411 | 2010.932 | 61.31834 | 16593.93 | 8651.555 | 11179.57 | 14291.14 | 2.24E+08 | 91236860 | 2175.135 | 514.0696 |
| F20(2000) | 2408.492 | 105.7135 | 2373.697 | 147.2107 | 3255.452 | 282.3209 | 2984.724 | 266.5006 | 3806.405 | 163.6881 | 2623.191 | 186.8274 |
| F21(2100) | 2384.486 | 12.06941 | 2424.422 | 25.09515 | 2592.441 | 59.98147 | 2500.371 | 48.12996 | 2859.47 | 32.54401 | 2409.558 | 23.30995 |
| F22(2200) | 4937.303 | 2534.986 | 3249.09 | 2176.708 | 9720.216 | 1694.156 | 8590.648 | 882.3424 | 15890.74 | 471.3202 | 7160.765 | 968.5849 |
| F23(2300) | 2824.863 | 13.61225 | 2852.294 | 32.47222 | 3153.014 | 120.2482 | 2937.365 | 37.22863 | 3484.214 | 48.70893 | 2859.994 | 18.62149 |

| | | | | | | | | | | | | |
|---|---|---|---|---|---|---|---|---|---|---|---|---|
| F24(2400) | 3008.397 | 14.68335 | 3026.649 | 30.25332 | 3358.775 | 127.1381 | 3083.665 | 33.31345 | 3666.199 | 54.66627 | 3148.964 | 30.98615 |
| F25(2500) | 3016.644 | 33.49631 | 3042.723 | 37.88353 | 3062.441 | 40.91908 | 3027.163 | 39.17641 | 5904.852 | 504.0287 | 3028.419 | 14.68771 |
| F26(2600) | 5013.851 | 425.7338 | 3728.189 | 1216.719 | 7114.657 | 3932.788 | 5609.366 | 846.0763 | 11454.1 | 470.8038 | 4605.713 | 769.3189 |
| F27(2700) | 3358.747 | 37.37391 | 3381.478 | 85.92089 | 3728.405 | 202.8842 | 3363.789 | 66.76139 | 4340.531 | 166.7858 | 3319.885 | 24.7884 |
| F28(2800) | 3285.523 | 17.75591 | 3299.576 | 32.79625 | 3298.447 | 34.64038 | 3309.253 | 22.19632 | 6294.269 | 460.2388 | 3308.677 | 11.00459 |
| F29(2900) | 3523.214 | 138.8285 | 3623.599 | 165.1543 | 4624.109 | 315.0416 | 4345.228 | 232.1967 | 7144.307 | 592.7413 | 3654.762 | 142.3647 |
| F30(3000) | 645211.5 | 38291.02 | 682474.8 | 100671.3 | 900974.1 | 120161.7 | 1658556 | 306216.8 | 5.68E+08 | 1.86E+08 | 728370.4 | 55434.1 |

Table 5.50: Ranks of different optimization algorithms for 50D CEC2017.

| | MMPA | MPA | MRFO | SMA | SCA | CLPSO |
|---|---|---|---|---|---|---|
| **F3** | 1 | 2 | 4 | 3 | 6 | 5 |
| **F4** | 2 | 4 | 1 | 5 | 6 | 3 |
| **F5** | 1 | 3 | 5 | 4 | 6 | 2 |
| **F6** | 3 | 2 | 5 | 4 | 6 | 1 |
| **F7** | 2 | 4 | 5 | 3 | 6 | 1 |
| **F8** | 1 | 4 | 5 | 3 | 6 | 2 |
| **F9** | 2 | 3 | 5 | 4 | 6 | 1 |
| **F10** | 2 | 3 | 5 | 4 | 6 | 1 |
| **F11** | 3 | 4 | 2 | 5 | 6 | 1 |
| **F12** | 2 | 3 | 1 | 5 | 6 | 4 |
| **F13** | 2 | 4 | 3 | 5 | 6 | 1 |
| **F14** | 1 | 2 | 3 | 4 | 6 | 5 |
| **F15** | 1 | 2 | 4 | 5 | 6 | 3 |
| **F16** | 1 | 2 | 5 | 4 | 6 | 3 |
| **F17** | 1 | 2 | 5 | 4 | 6 | 3 |
| **F18** | 1 | 2 | 3 | 4 | 6 | 5 |
| **F19** | 1 | 2 | 5 | 4 | 6 | 3 |
| **F20** | 2 | 1 | 5 | 4 | 6 | 3 |
| **F21** | 1 | 3 | 5 | 4 | 6 | 2 |
| **F22** | 2 | 1 | 5 | 4 | 6 | 3 |
| **F23** | 1 | 2 | 5 | 4 | 6 | 3 |
| **F24** | 1 | 2 | 5 | 3 | 6 | 4 |
| **F25** | 1 | 4 | 5 | 2 | 6 | 3 |
| **F26** | 3 | 1 | 5 | 4 | 6 | 2 |
| **F27** | 2 | 4 | 5 | 3 | 6 | 1 |
| **F28** | 1 | 3 | 2 | 5 | 6 | 4 |
| **F29** | 1 | 2 | 5 | 4 | 6 | 3 |
| **F30** | 1 | 2 | 4 | 5 | 6 | 3 |
| **Average** | 1.433333 | 2.433333 | 3.9 | 3.733333 | 5.6 | 2.5 |
| **Final** | 1 | 2 | 5 | 4 | 6 | 3 |

Table 5.51: P-values based on Wilcoxon rank-sum for MMPA versus the other algorithms.

| | MPA | MRFO | SMA | SCA | CLPSO |
|---|---|---|---|---|---|
| **F3** | 3.08E-08 | 0.016285 | 1.07E-09 | 3.02E-11 | 3.02E-11 |
| **F4** | 0.00073 | 0.283778 | 3.81E-07 | 3.02E-11 | 0.630872 |
| **F5** | 3.02E-11 | 3.02E-11 | 3.34E-11 | 3.02E-11 | 0.185767 |
| **F6** | 0.982307 | 3.02E-11 | 2.83E-08 | 3.02E-11 | 6.43E-12 |
| **F7** | 5.09E-06 | 3.02E-11 | 0.149449 | 3.02E-11 | 5.49E-11 |
| **F8** | 6.70E-11 | 3.02E-11 | 2.15E-10 | 3.02E-11 | 0.000729 |
| **F9** | 0.019112 | 3.02E-11 | 3.02E-11 | 3.02E-11 | 0.067869 |
| **F10** | 0.888303 | 2.61E-10 | 8.48E-09 | 3.02E-11 | 1.11E-06 |
| **F11** | 0.258051 | 0.001767 | 5.97E-09 | 3.02E-11 | 2.60E-08 |
| **F12** | 0.000587 | 3.02E-11 | 3.01E-07 | 3.02E-11 | 0.000268 |
| **F13** | 0.082357 | 0.589451 | 3.02E-11 | 3.02E-11 | 5.09E-08 |
| **F14** | 0.016955 | 3.02E-11 | 3.02E-11 | 3.02E-11 | 3.02E-11 |

| | | | | | |
|---|---|---|---|---|---|
| **F15** | 0.007959 | 2.61E-10 | 3.02E-11 | 3.02E-11 | 0.42038 |
| **F16** | 0.05746 | 8.99E-11 | 3.02E-11 | 3.02E-11 | 1.03E-06 |
| **F17** | 0.000556 | 3.02E-11 | 3.69E-11 | 3.02E-11 | 3.32E-06 |
| **F18** | 0.000284 | 3.02E-11 | 3.02E-11 | 3.02E-11 | 3.02E-11 |
| **F19** | 0.099258 | 3.02E-11 | 3.02E-11 | 3.02E-11 | 2.43E-05 |
| **F20** | 0.332855 | 3.02E-11 | 5.07E-10 | 3.02E-11 | 4.12E-06 |
| **F21** | 5.53E-08 | 3.02E-11 | 3.69E-11 | 3.02E-11 | 5.97E-09 |
| **F22** | 0.007617 | 5.57E-10 | 1.29E-09 | 3.02E-11 | 0.002891 |
| **F23** | 0.001442 | 3.02E-11 | 3.02E-11 | 3.02E-11 | 3.82E-09 |
| **F24** | 0.025101 | 3.02E-11 | 8.99E-11 | 3.02E-11 | 3.02E-11 |
| **F25** | 0.011228 | 6.74E-06 | 0.12597 | 3.02E-11 | 0.118817 |
| **F26** | 0.001058 | 0.378997 | 7.69E-08 | 3.02E-11 | 0.079773 |
| **F27** | 0.3871 | 6.07E-11 | 0.841801 | 3.02E-11 | 2.00E-05 |
| **F28** | 0.018368 | 0.32552 | 8.84E-07 | 3.02E-11 | 9.53E-07 |
| **F29** | 0.015638 | 3.02E-11 | 3.02E-11 | 3.02E-11 | 0.000903 |
| **F30** | 0.363222 | 2.15E-10 | 3.02E-11 | 3.02E-11 | 2.19E-07 |
| +/=/- | 19/0/9 | 24/0/4 | 25/0/3 | 28/0/0 | 22/0/6 |

The convergence curve of each algorithm is another key aspect that should be studied for comparison purposes. Fig. 5.29 shows the mean convergence curve of the MMPA and the other algorithms. It can be seen that the MMPA converges to a high-qualified solution with a faster rate than the MPA and the other algorithms. This proves the superiority of the MMPA not only in getting accurate results but also in terms of the convergence rate to the best solutions.

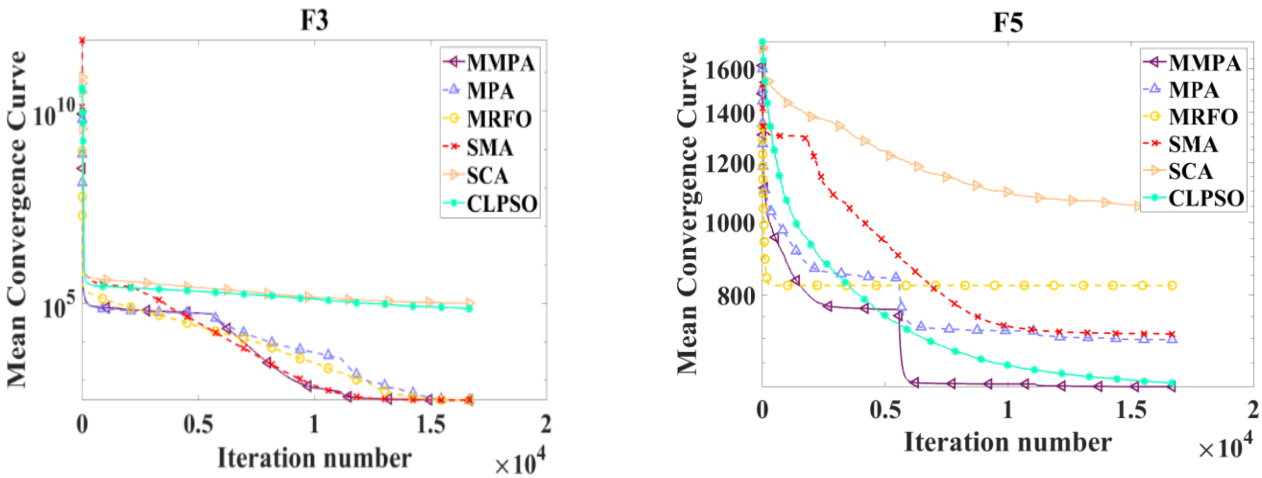

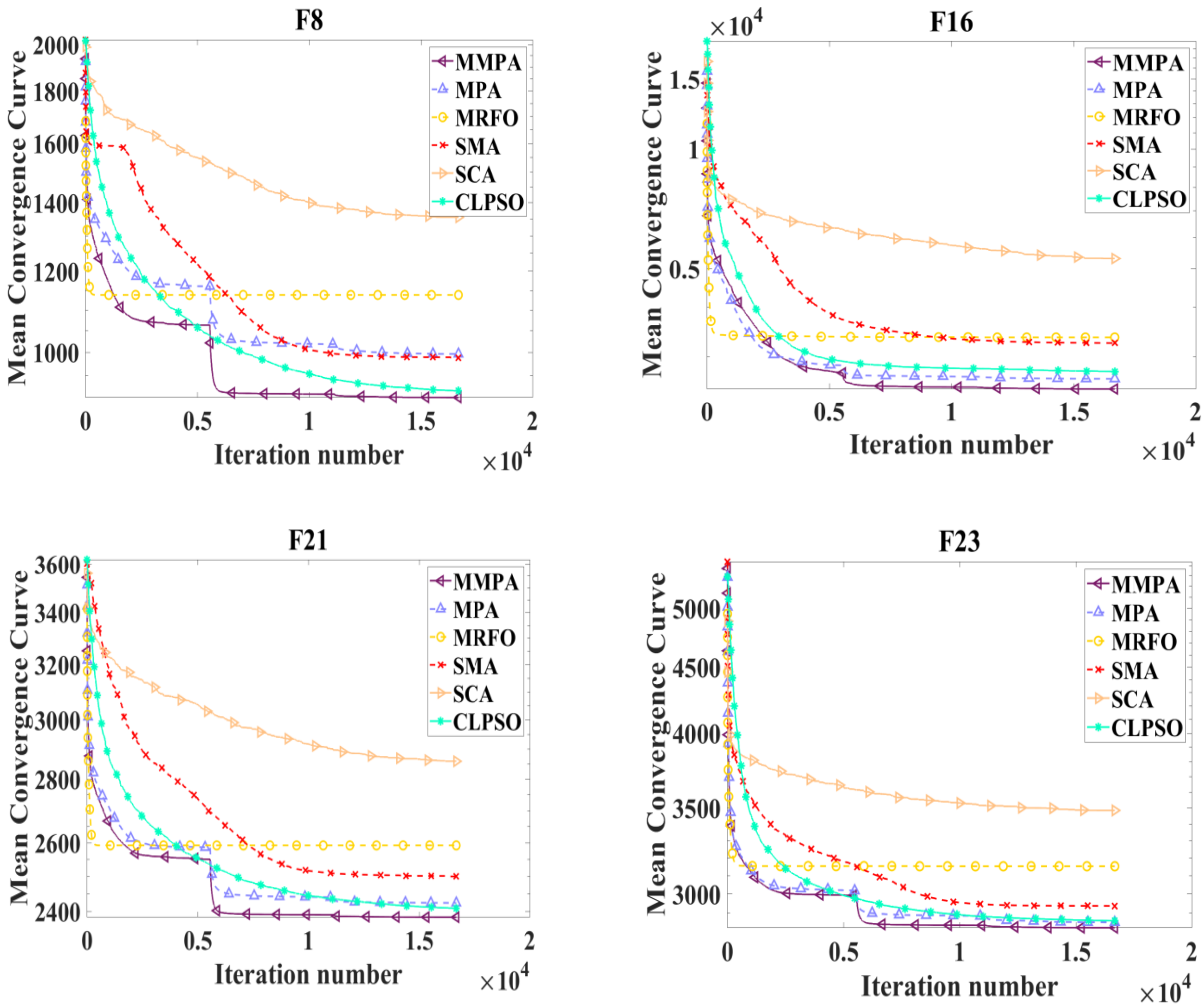


Figure 5.29: The mean convergence curves of MMPA and counterparts

The mean execution time by the proposed MMPA and the other optimizers is the last factor that should be highlighted for providing insight comparison between the optimizers. The mean execution time throughout the independent runs by the implemented algorithms for each function is computed and reported in Table 5.52. The reported results show the limitation of the proposed MMPA, where its mean execution time is longer than the basic MPA optimizer. This limitation is considered as the fee of achieving high-quality solutions. The MMPA has the fifth rank in the shorter execution time after the CLPSO, SCA, MRFO, and the basic MPA; meanwhile, it is former to the SMA. The fast convergence property of MMPA for the optimal solution compared to the basic MPA as depicted in Fig. 5.29 may solve the limitation of the proposed MMPA as it consumes a smaller number of iterations to discover the search space and converge to the high-quality solutions efficiently than the MPA.

Table 5.52: mean execution time in second for MMPA versus the other algorithms.

| | MMPA | MPA | MRFO | SMA | SCA | CLPSO |
|---|---|---|---|---|---|---|
| **F3** | 23.0247 | 20.9145 | 17.6637 | 99.5351 | 12.3194 | 12.5282 |
| **F4** | 20.7994 | 20.6569 | 17.3914 | 99.1476 | 11.8175 | 11.7053 |
| **F5** | 25.4977 | 22.8011 | 19.5110 | 99.7070 | 13.8183 | 14.2674 |
| **F6** | 44.7553 | 31.1938 | 27.8909 | 102.5317 | 15.6800 | 18.5772 |
| **F7** | 29.3055 | 23.2044 | 19.9506 | 99.8264 | 10.9305 | 16.0550 |
| **F8** | 27.9444 | 23.2199 | 19.9114 | 99.5468 | 10.8790 | 14.8416 |
| **F9** | 29.3343 | 23.2025 | 19.9127 | 99.7478 | 10.7418 | 14.7453 |
| **F10** | 32.3672 | 25.2361 | 21.8721 | 100.7914 | 11.8730 | 14.0607 |
| **F11** | 25.1066 | 21.9021 | 18.7098 | 99.1221 | 10.1773 | 13.6725 |
| **F12** | 29.0770 | 23.6470 | 20.4200 | 99.8567 | 11.4381 | 14.3005 |
| **F13** | 25.5976 | 22.2281 | 19.0022 | 99.7310 | 9.9592 | 13.5939 |
| **F14** | 28.3203 | 25.1794 | 22.0009 | 100.3393 | 11.5170 | 14.0164 |
| **F15** | 25.5270 | 21.5222 | 18.5648 | 99.1173 | 9.7727 | 13.3792 |
| **F16** | 27.6277 | 22.9073 | 19.7634 | 99.9039 | 10.5485 | 13.2635 |
| **F17** | 40.4040 | 30.1942 | 26.8064 | 102.8264 | 14.6737 | 17.6069 |
| **F18** | 28.0393 | 22.9467 | 19.6038 | 99.4772 | 10.2078 | 11.2316 |
| **F19** | 100.2314 | 66.6307 | 63.2414 | 116.0389 | 33.5994 | 35.0358 |
| **F20** | 38.2326 | 31.2902 | 28.4684 | 102.7884 | 15.0906 | 16.9192 |
| **F21** | 52.6379 | 41.2199 | 37.8724 | 106.2850 | 19.4864 | 20.7800 |
| **F22** | 57.4908 | 43.5756 | 40.1795 | 107.3774 | 21.3498 | 20.3568 |
| **F23** | 66.3308 | 50.2142 | 46.7561 | 109.9658 | 24.1375 | 24.3420 |
| **F24** | 70.8231 | 52.6492 | 49.0476 | 110.8656 | 26.0814 | 24.1214 |
| **F25** | 68.9882 | 52.3037 | 48.7383 | 111.1910 | 24.8875 | 26.7294 |
| **F26** | 80.9487 | 59.4871 | 56.0215 | 113.5902 | 28.8054 | 30.0394 |
| **F27** | 92.6305 | 68.6818 | 65.0075 | 117.3400 | 32.9701 | 28.0550 |
| **F28** | 82.6737 | 61.8437 | 58.2469 | 114.5881 | 29.4616 | 29.1462 |
| **F29** | 60.9591 | 47.1455 | 43.7012 | 109.2493 | 22.5825 | 19.1149 |
| **F30** | 117.7605 | 83.9420 | 80.2022 | 123.4611 | 41.5894 | 34.5959 |

#### 5.3.5.2 Solving CEED using the Proposed Technique

In this section, the proposed MMPA and conventional MPA are applied to find the optimum solution for the studied cases of single- and bi-objective CEED problem. Four power generation systems (3 units, 5 units, 6 units, and 26 units) with different load levels have been used to validate the proposed algorithm. These four power generation systems are considered standard well-known test systems used for validating the proposed optimization algorithms in solving Combined Economic Emission Dispatch Problems. They are used in several relevant published papers. Hence, the results of these test systems obtained by previous published algorithms are compared with those obtained by the developed algorithm with the aim of proving its effectiveness and superiority. Moreover, these systems are a combination of small, medium and large-scale power systems, which prove the effectiveness of the developed algorithm. The population size is 300 and the maximum iteration number is 300 for cases 1, 2, and 3 while the population size is 1000 and the maximum iteration number is 1500 for case 4. 30 independent runs have been executed for all studied optimization algorithms. The single-objective CEED problem is solved using MPA and MMPA. In total, four case studies are investigated.

#### 5.3.5.2.1 Case 1: Five Thermal Units (Load=1800 MW).

In this case, 5-unit and 1800 MW of total system load are considered. The system data can be adopted from [165]. The results of this case obtained by MPA and MMPA are presented in Table 5.53. These results are compared with those obtained by GA [165], PPSO [165], QPSO [91], FA [92], SCA [95], MRFO [193], Gradient-based optimizer (GBO) [193], and MRFO-GBO [193]. From this table, it is clear that the MMPA technique provides a more reliable solution than conventional MPA and other algorithms. Figure 5.30 presents the fuel cost convergence characteristics of MMPA and MPA. It can be seen that the MMPA outperforms conventional MPA. The figure also demonstrates that MMPA and MPA are able to provide fast convergence and stability for solving the ELD problem. In addition, the statistical results in Table 5.54 stress these superiorities over the conventional algorithm furthermore the provided boxplot in Figure 5.31.

Table 5.53: Comparison of results for Case 1.

| Output | GA | PPSO | QPSO | FA | SCA | MRFO | GBO | MRFO-GBO | MPA | MMPA |
|---|---|---|---|---|---|---|---|---|---|---|
| $P_1$ (MW) | 320 | 320 | 320.51 | 327.8 | 320 | 330.710 | 327.08 | 320 | 320.02 | 320.0134 |
| $P_2$ (MW) | 343.74 | 343.7 | 346.47 | 341.99 | 343.85 | 351.852 | 343.869 | 343.8698 | 343.99 | 345.24 |
| $P_3$ (MW) | 472.6 | 472.6 | 482.95 | 460.42 | 472.3 | 464.269 | 472.075 | 472.2678 | 471.96 | 471.23 |
| $P_4$ (MW) | 320 | 320 | 320 | 327.8 | 320 | 328.362 | 320 | 320 | 320.06 | 320.03 |
| $P_5$ (MW) | 343.74 | 343.7 | 330.08 | 341.99 | 343.85 | 324.802 | 336.975 | 343.862 | 343.96 | 343.52 |
| Total power (MW) | 1800 | 1800 | 1800 | 1800 | 1800 | 1800 | 1800 | 1800 | 1800 | 1800 |
| Fuel cost ($/h) | 18611.07 | 18610.40 | 18610.03 | 18610 | 18609.694 | 18611.162 | 18609.984 | 18609.6904 | 18609.693 | 18609.618 |

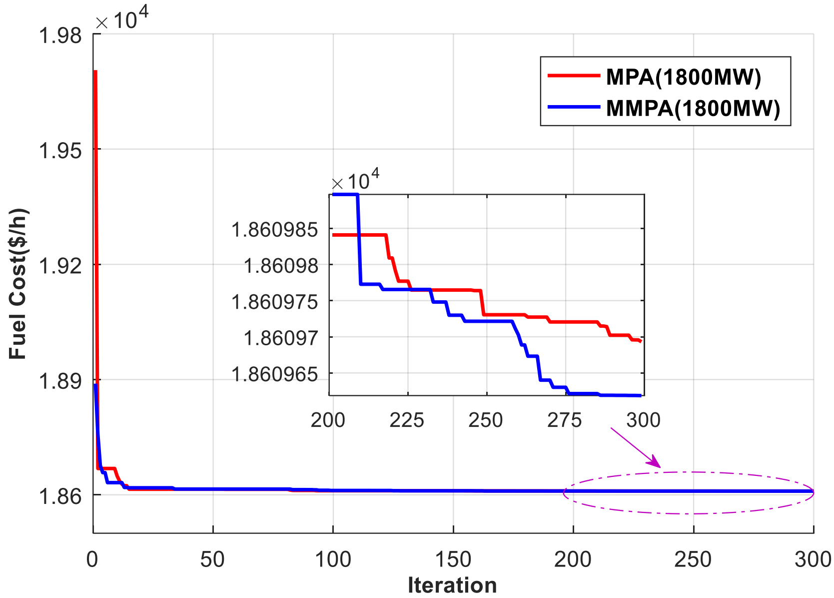


Figure 5.30: Fuel cost convergence of MPA and MMPA for Case 1.

Table 5.54: Statistical results obtained by different techniques after 30 trials (Case 1).

| Methods | Fuel cost ($/h) | | | | Std |
|---|---|---|---|---|---|
| | Min/best | Mean | Median | Max/worst | |
| MMPA | 18609.6182 | 18609.6233 | 18609.62278 | 18609.63332 | 0.004259486 |
| MPA | 18609.6931 | 18609.69818 | 18609.69844 | 18609.70575 | 0.003189959 |

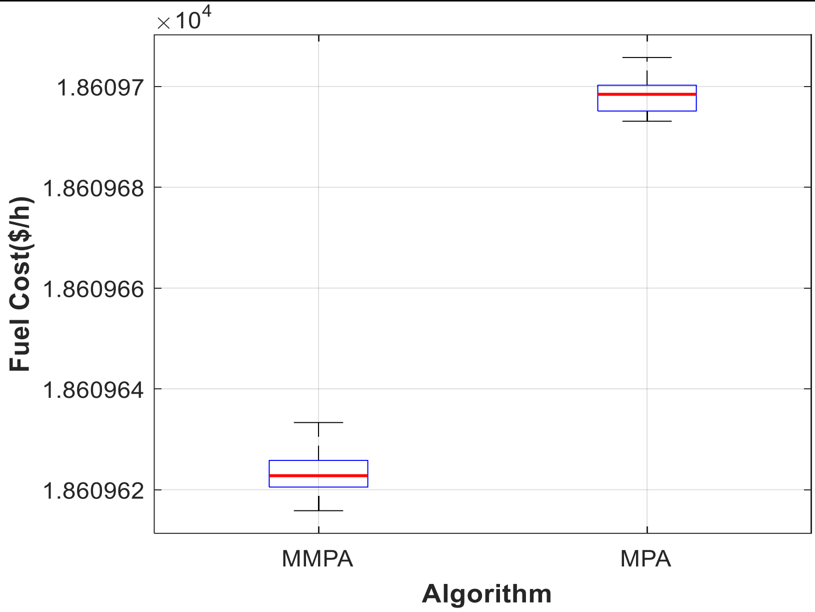


Figure 5.31: Best fuel cost boxplot in 30 runs of different algorithms for Case 1.

#### 5.3.5.2.2 Case 2: 3 Thermal Units Considering Different Levels of System Load.

In case 2, the proposed MMPA and original MPA algorithms are applied to achieve the best solution for the CEED problem of three thermal units considering different values of demand: 550, 600, 700, 800, and 850 MW. In this case, minimization of fuel cost, SO2, and NOx emissions are considered. The input data for the three unit system are taken from [45]. The results of the proposed MMPA are presented in Table 5.55. The results obtained using the proposed MMPA are compared with those obtained with the conventional MPA and other techniques. Table 5.56 summarizes these results, showing the total cost values for various levels of demand using other techniques. It can be observed that the MMPA allows for obtaining significantly better results than those obtained by their counterparts SA [167], SCA [95], MRFO [193], GBO [193], and MRFO-GBO [193]. Although the improvement over the MPA is not so significant, the solution found by the MMPA is still more economical than that obtained by the conventional MPA for five levels of system demand.

Table 5.55: Results obtained by MMPA for Case 2.

| Output | 550MW | 600MW | 700MW | 800MW | 850MW |
|---|---|---|---|---|---|
| $P_1$ (MW) | 307.129 | 329.315 | 374.073 | 419.3387 | 442.1718 |
| $P_2$ (MW) | 160.32 | 184.6148 | 233.1524 | 281.6404 | 305.8553 |
| $P_3$ (MW) | 88.627 | 93.438 | 103.1406 | 112.966 | 117.9254 |
| Total power (MW) | 556.076 | 607.368 | 710.366 | 813.9446 | 865.953 |
| Power loss (MW) | 6.076 | 7.368 | 10.366 | 13.9446 | 15.953 |
| Fuel cost ($/h) | 5581.3911 | 6028.6981 | 6939.239 | 7871.4369 | 8345.7371 |
| $SO_2$ emission (ton/h) | 6.00197 | 6.48907 | 7.48048 | 8.49532 | 9.0116 |
| $NO_x$ emission (ton/h) | 0.088047 | 0.088182 | 0.0902 | 0.09468 | 0.097813 |
| Total cost ($/h) | 18755.539 | 19655.6271 | 21628.9836 | 23836.9728 | 25030.2141 |

Table 5.56: Comparison of results for Case 2.

| Load (MW) | | 550 | 600 | 700 | 800 | 850 |
|---|---|---|---|---|---|---|
| Fuel cost ($/h) | SA | 5581.4797 | 6028.7083 | 6939.2481 | 7871.4467 | 8345.7465 |
| | SCA | 5581.4742 | 6028.6959 | 6939.2448 | 7871.4430 | 8345.7441 |
| | MRFO | 5582.156 | 6028.830 | 6939.433 | 7871.689 | 8345.695 |
| | GBO | 5581.745 | 6028.668 | 6940.147 | 7871.459 | 8345.826 |
| | MRFO-GBO | 5581.480 | 6028.707 | 6939.247 | 7871.446 | 8345.747 |

| | | | | | | |
|---|---|---|---|---|---|---|
| | MPA | 5581.48 | 6028.7069 | 6939.2485 | 7871.4456 | 8345.7475 |
| | MMPA | 5581.3911 | 6028.6981 | 6939.239 | 7871.4369 | 8345.7371 |
| $SO_2$ emission (ton/h) | SA | 6.0071 | 6.4941 | 7.4855 | 8.5004 | 9.0166 |
| | SCA | 6.0071 | 6.4941 | 7.4855 | 8.5004 | 9.0166 |
| | MRFO | 6.00172 | 6.489377 | 7.479722 | 8.496199 | 9.011641 |
| | GBO | 6.00084 | 6.489438 | 7.47742 | 8.494525 | 9.011908 |
| | MRFO-GBO | 6.00207 | 6.489082 | 7.480495 | 8.495337 | 9.011611 |
| | MPA | 6.0021 | 6.4891 | 7.48049 | 8.4953 | 9.0116 |
| | MMPA | 6.00197 | 6.48907 | 7.48048 | 8.49532 | 9.0116 |
| $NO_x$ emission (ton/h) | SA | 0.0880 | 0.0882 | 0.0902 | 0.0947 | 0.0978 |
| | SCA | 0.0880 | 0.0882 | 0.0902 | 0.0947 | 0.0978 |
| | MRFO | 0.088038 | 0.088181 | 0.090208 | 0.094713 | 0.097827 |
| | GBO | 0.08805 | 0.088186 | 0.090126 | 0.094644 | 0.097819 |
| | MRFO-GBO | 0.088047 | 0.088182 | 0.090232 | 0.094681 | 0.097813 |
| | MPA | 0.088047 | 0.08818 | 0.0902 | 0.09468 | 0.097813 |
| | MMPA | 0.0880 | 0.088182 | 0.0902 | 0.09468 | 0.097813 |
| Total cost ($/h) | SA | 18760.5958 | 19660.5278 | 21633.8869 | 23841.8787 | 25035.1214 |
| | SCA | 18760.5954 | 19660.5274 | 21633.8863 | 23841.8780 | 25035.1206 |
| | MRFO | 18756.1769 | 19655.7277 | 21629.49137 | 23837.5274 | 25030.34685 |
| | GBO | 18755.9045 | 19655.6652 | 21630.60267 | 23837.0585 | 25030.26857 |
| | MRFO-GBO | 18755.7138 | 19655.6457 | 21629.0045 | 23836.9960 | 25030.2386 |
| | MPA | 18755.7139 | 19655.6457 | 21629.005 | 23836.996 | 25030.2386 |
| | MMPA | 18755.5396 | 19655.6271 | 21628.9836 | 23836.9728 | 25030.2141 |

Figure 5.32 shows the total cost convergence behaviors of the MMPA comparing with conventional MPA in solving the CEED problem for various load levels. The MMPA succeeded to achieve the lowest cost in a comparatively short time with a comparison with the conventional MPA algorithm which can be concluded from figure 5.32 and Table 5.57.

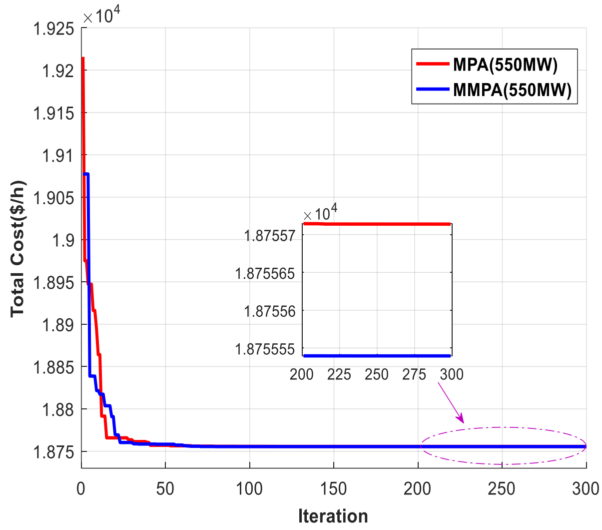
×10^4
MPA(550MW)
MMPA(550MW)
Total Cost($/h)
Iteration
1.925
1.92
1.915
1.91
1.905
1.9
1.895
1.89
1.885
1.88
1.875
0
50
100
150
200
250
300
×10^4
1.87557
1.875565
1.87556
1.875555
200
225
250
275
300

(a)

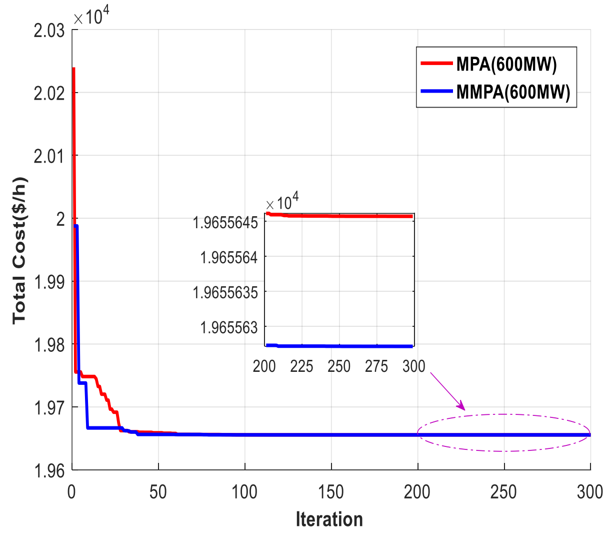
×10^4
MPA(600MW)
MMPA(600MW)
Total Cost($/h)
Iteration
2.03
2.02
2.01
2
1.99
1.98
1.97
1.96
0
50
100
150
200
250
300
×10^4
1.9655645
1.965564
1.9655635
1.965563
200
225
250
275
300

(b)

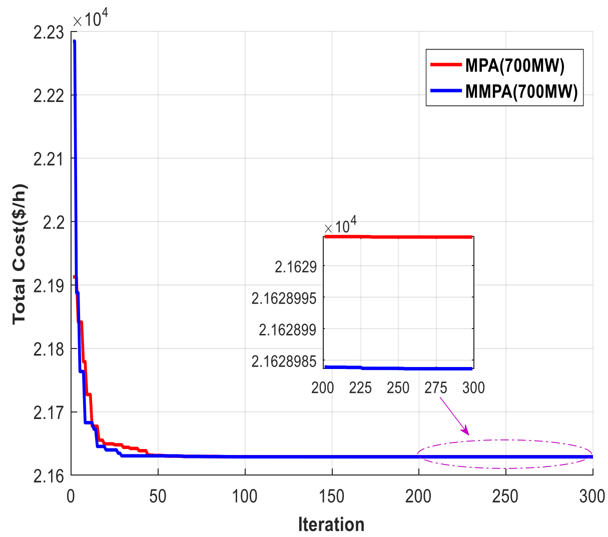
×10^4
MPA(700MW)
MMPA(700MW)
Total Cost($/h)
Iteration
2.23
2.22
2.21
2.2
2.19
2.18
2.17
2.16
0
50
100
150
200
250
300
×10^4
2.1629
2.1628995
2.162899
2.1628985
200
225
250
275
300

(c)

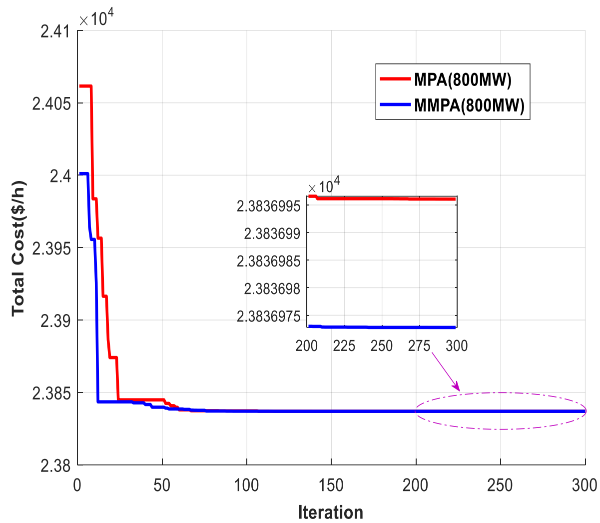
×10^4
MPA(800MW)
MMPA(800MW)
Total Cost($/h)
Iteration
2.41
2.405
2.4
2.395
2.39
2.385
2.38
0
50
100
150
200
250
300
×10^4
2.3836995
2.383699
2.3836985
2.383698
2.3836975
200
225
250
275
300

(d)

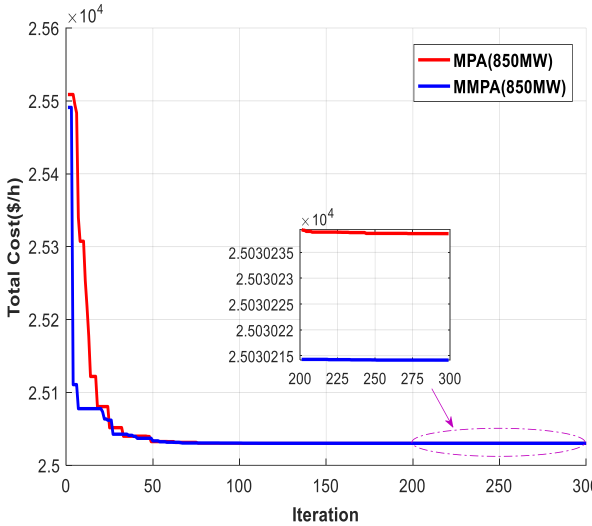


(e)

Figure 5.32: Total cost convergence characteristics for different load levels in 3-unit system (a) 550 MW (b) 600MW (c)700 MW (d) 800 MW (e)850 MW.

Table 5.57: Statistical results obtained by different techniques after 30 trials (Case 2).

| Load (MW) | Methods | Total cost ($/h) | | | | Std |
|---|---|---|---|---|---|---|
| | | Min/best | Mean | Median | Max/worst | |
| 550 MW | MMPA | 18755.53959 | 18755.53960 | 18755.53960 | 18755.53961 | 1.7719E-06 |
| | MPA | 18755.71385 | 18755.71385 | 18755.71385 | 18755.71386 | 9.6677E-07 |
| 600 MW | MMPA | 19655.627134 | 19655.627136 | 19655.627135 | 19655.62714 | 1.3619E-06 |
| | MPA | 19655.645707 | 19655.645709 | 19655.645709 | 19655.645711 | 9.729E-07 |
| 700 MW | MMPA | 21628.983640 | 21628.983643 | 21628.983642 | 21628.98365 | 1.861E-06 |
| | MPA | 21629.004540 | 21629.004543 | 21629.004542 | 21629.00455 | 1.4482E-06 |
| 800 MW | MMPA | 23836.972786 | 23836.972788 | 23836.972787 | 23836.972794 | 2.2664E-06 |
| | MPA | 23836.996052 | 23836.996055 | 23836.996054 | 23836.996063 | 2.7156E-06 |
| 850 MW | MMPA | 25030.214148 | 25030.214151 | 25030.214151 | 25030.214163 | 2.6159E-06 |
| | MPA | 25030.238613 | 25030.23862 | 25030.238614 | 25030.23862 | 1.9137E-06 |

#### 5.3.5.2.3 Case 3: 6 Thermal Units Considering Different Levels of System Demand.

The MMPA technique is tested on the six thermal units (IEEE 30-bus test system) with different load levels (150, 175, 200, and 225 MW). The input data for this system are taken from [96].

The results considering the first value of demand, which equal to 150MW, are provided in Table 5.58. The table includes the value of fuel cost, the value SO2, NOx, and CO2 emissions as well as, and the total cost value (objective function). From Table 5.58, it can be seen that in the case of 150 MW of demand, the total cost obtained by MMPA (10176.016 $/h) is lower than the cost obtained with conventional MPA and other novel optimization algorithms such as Langrage method (LR) [194], QBA [96], MBO [93], SCA [95], PSO [90], SA [168], GOA [94], QITFA [97], 4th Chaotic artificial ecosystem-based optimization algorithm (CAEO4) [188], and MRFO-GBO [193]. The comparison between the results of the MMPA and the other optimization techniques for the fuel cost, SO2, NOx, CO2 emissions, and total emission considering 4 values of demand in the test system are presented in Tables 5.59, 5.60, 5.61, 5.62, and 5.63, respectively.

Table 5.58: Results obtained by different optimization techniques for the demand of 150MW.

| Optimization techniques | Fuel cost ($/h) | Emission of $SO_2$ (kg/h) | Emission of $NO_x$ (kg/h) | Emission of $CO_2$ (kg/h) | Total cost ($/h) |
|---|---|---|---|---|---|
| MPA | 2706.588 | 3142.707 | 2404.887 | 2563.109 | 10176.7698 |
| MMPA | 2706.3903 | 3142.4913 | 2404.6192 | 2562.7216 | 10176.016 |
| MRFO-GBO | 2706.58 | 3145.54 | 2410.25 | 2562.82 | 10,177.05 |
| CAEO4 | 2702.944 | 2885.210 | 2249.105 | 2448.860 | 10179.349 |
| QITFA | 2711.71 | 3087.92 | 2406.79 | 2561.85 | 10,254.91 |
| GOA | 2704.87 | 3146.74 | 2406.18 | 2564.5 | 10254.98 |
| SCA | 2704.9226 | 3146.831 | 2406.2374 | 2564.567 | 10255.2078 |
| MBO | 2704.922 | 3146.831 | 2406.236 | 2564.572 | 10255.21 |
| QBA | 2704.97 | 3147.38 | 2408.1 | 2565.14 | 10255.28 |
| SA | 2705.21 | 3138.446 | 2379.35 | 2568.946 | 10261.49 |
| PSO | 2734.2 | 3193.6 | 2424.6 | 2607.1 | 10385 |

Table 5.59: Results of fuel cost considering different levels of load in the six-unit system.

| Load (MW) | Total fuel cost ($/h) | | | | | | | | | | |
|---|---|---|---|---|---|---|---|---|---|---|---|
| | PSO | SA | QBA | MBO | SCA | GOA | QITFA | CAEO4 | MRFO-GBO | MPA | MMPA |
| 150 | 2,734.20 | 2,705.21 | 2,704.97 | 2,704.92 | 2,704.92 | 2,704.87 | 2,711.71 | 2,702.94 | 2,706.58 | 2,706.588 | 2,706.3903 |
| 175 | 3,236.30 | 3,220.51 | 3,188.10 | 3,188.13 | 3,188.15 | 3,188.08 | 3,189.91 | 3,179.34 | 3,206.15 | 3,205.523 | 3,205.4868 |
| 200 | 3,784.90 | 3,735.73 | 3,726.08 | 3,727.43 | 3,727.44 | 3,727.40 | 3,729.26 | 3,722.45 | 3,742.84 | 3,740.5987 | 3,740.172 |
| 225 | 4,402.30 | 4,321.52 | 4,314.63 | 4,315.63 | 4,315.05 | 4,315.15 | 4,316.34 | 4,314.38 | 4,319.33 | 4,318.8852 | 4,318.059 |

Table 5.60: Results of SO2 emission considering different levels of load in the six-unit system.

| Load (MW) | Emission of $SO_2$(kg/h) | | | | | | | | | | |
|---|---|---|---|---|---|---|---|---|---|---|---|
| | PSO | SA | QBA | MBO | SCA | GOA | QITFA | CAEO4 | MRFO-GBO | MPA | MMPA |
| 150 | 3,193.60 | 3,138.45 | 3,147.38 | 3,146.83 | 3,146.83 | 3,146.74 | 3,087.92 | 2,885.21 | 3,145.54 | 3,142.707 | 3,142.4913 |
| 175 | 3,904.90 | 3,763.48 | 3,858.96 | 3,859.49 | 3,859.36 | 3,859.37 | 3,807.49 | 3,891.64 | 3,804.23 | 3,806.039 | 3,804.486 |
| 200 | 4,670.60 | 4,553.97 | 4,598.20 | 4,592.64 | 4,592.49 | 4,592.46 | 4,528.28 | 4,589.87 | 4,533.03 | 4,539.454 | 4,539.8767 |
| 225 | 5,426.10 | 5,287.31 | 5,344.75 | 5,335.81 | 5,339.96 | 5,338.42 | 5,289.45 | 5,360.57 | 5,318.66 | 5,320.155 | 5,319.859 |

Table 5.61: Results of NOx emission considering different levels of load in the six-unit system.

| Load (MW) | Emission of $NO_x$ (kg/h) | | | | | | | | | | |
|---|---|---|---|---|---|---|---|---|---|---|---|
| | PSO | SA | QBA | MBO | SCA | GOA | QITFA | CAEO4 | MRFO-GBO | MPA | MMPA |
| 150 | 2,424.60 | 2,379.35 | 2,408.10 | 2,406.24 | 2,406.23 | 2,406.18 | 2,406.79 | 2,249.11 | 2,410.25 | 2,404.89 | 2,404.62 |
| 175 | 2,879.70 | 2,789.92 | 2,853.40 | 2,854.13 | 2,854.01 | 2,854.08 | 2,856.22 | 2,847.56 | 2,838.31 | 2,839.19 | 2,837.15 |
| 200 | 3,373.20 | 3,285.65 | 3,327.78 | 3,325.35 | 3,325.34 | 3,325.31 | 3,313.29 | 3,301.53 | 3,309.15 | 3,308.58 | 3,308.34 |
| 225 | 3,877.60 | 3,781.19 | 3,822.53 | 3,811.18 | 3,820.29 | 3,819.56 | 3,815.71 | 3,832.07 | 3,810.87 | 3,811.36 | 3,810.97 |

Table 5.62: Results of $CO_2$ emission considering different levels of load in the six-unit system.

| Load (MW) | Emission of $CO_2$ (kg/h) | | | | | | | | | | |
|---|---|---|---|---|---|---|---|---|---|---|---|
| | PSO | SA | QBA | MBO | SCA | GOA | QITFA | CAEO4 | MRFO-GBO | MPA | MMPA |
| 150 | 2,607.10 | 2,568.95 | 2,565.14 | 2,564.57 | 2,564.57 | 2,564.50 | 2,561.85 | 2,448.86 | 2,562.82 | 2,563.11 | 2,562.72 |
| 175 | 3,178.00 | 3,094.69 | 3,129.78 | 3,129.20 | 3,129.18 | 3,129.07 | 3,133.60 | 3,154.93 | 3,097.60 | 3,098.49 | 3,098.57 |
| 200 | 3,771.50 | 3,714.33 | 3,719.64 | 3,715.69 | 3,715.64 | 3,715.56 | 3,721.30 | 3,725.20 | 3,681.42 | 3,686.44 | 3,686.56 |
| 225 | 4,403.00 | 4,324.30 | 4,323.47 | 4,328.07 | 4,322.52 | 4,322.26 | 4,322.39 | 4,322.68 | 4,315.41 | 4,316.40 | 4,315.86 |

Table 5.63: Results of total emission considering different levels of load in the six-unit system.

| Load (MW) | Total Emission (kg/h) | | | | | | | | | | |
|---|---|---|---|---|---|---|---|---|---|---|---|
| | PSO | SA | QBA | MBO | SCA | GOA | QITFA | CAEO4 | MRFO-GBO | MPA | MMPA |
| 150 | 8,225.3 | 8,086.7 | 8,120.62 | 8,117.64 | 8,117.63 | 8,117.48 | 8,056.56 | 7,583.18 | 8,118.62 | 8,110.70 | 8,109.83 |
| 175 | 9,962.6 | 9,648.1 | 9,842.14 | 9,842.82 | 9,842.55 | 9,842.52 | 9,797.31 | 9,894.13 | 9,740.14 | 9,743.718 | 9,740.21 |
| 200 | 11,815 | 11,553 | 11,645.6 | 11,633.68 | 11633.4659 | 11,633.33 | 11,562.87 | 11,616.60 | 11,523.59 | 11,534.48 | 11,534.78 |
| 225 | 13,706.7 | 13,392.8 | 13,490.8 | 13,475.06 | 13482.77 | 13,480.24 | 13,427.55 | 13,515.32 | 13,444.95 | 13,447.92 | 13,446.69 |

Table 5.64: Results of total cost considering different levels of load in the six-unit system.

| Load (MW) | Total cost ($/h) | | | | | | | | | | |
|---|---|---|---|---|---|---|---|---|---|---|---|
| | PSO | SA | QBA | MBO | SCA | GOA | QITFA | CAEO4 | MRFO-GBO | MPA | MMPA |
| 150 | 10,385 | 10,261.49 | 10,255.28 | 10,255.21 | 10,255.20 | 10,254.98 | 10,254.91 | 10,179.35 | 10,177.05 | 10,176.77 | 10,176.01 |
| 175 | 12,425 | 12,280.04 | 12,241.74 | 12,241.67 | 12,241.66 | 12,241.41 | 12,241.61 | 12,164.36 | 12,134.42 | 12,134.42 | 12,133.60 |
| 200 | 14,642 | 14,421.30 | 14,413.88 | 14,413.71 | 14,413.70 | 14,413.52 | 14,413.56 | 14,287.65 | 14,268.09 | 14,267.83 | 14,266.93 |
| 225 | 17,125 | 16,790.69 | 16,783.91 | 16,784.34 | 16,783.78 | 16,783.68 | 16,783.33 | 16,603.90 | 16,599.71 | 16,599.66 | 16,596.74 |

Table 5.64 presents the results of total cost considering 4 values of load in the six-unit IEEE 30-bus system. From this table, it can be seen that the MMPA gives the best solutions for all different values of demand in the 6-unit IEEE 30-bus system.

The optimal scheduling results of the MMPA and MPA for 4 load levels in a six-unit system are presented in Table 5.65. Further, the convergence curves for each load level are shown in Figures 5.33, 5.34, 5.35, and 5.36. Based on these figures it can be concluded that the MMPA provides better convergence characteristics in all levels of demand compared with the conventional MPA.

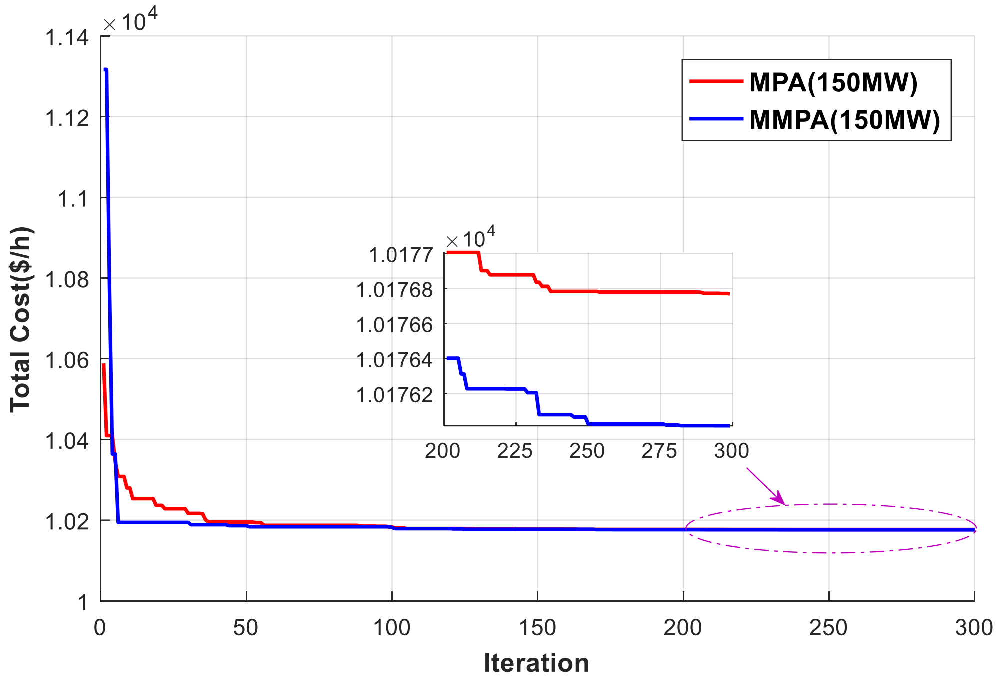


Figure 5.33: Convergence characteristics of MPA and MMPA for 150MW load demand in six-unit system.

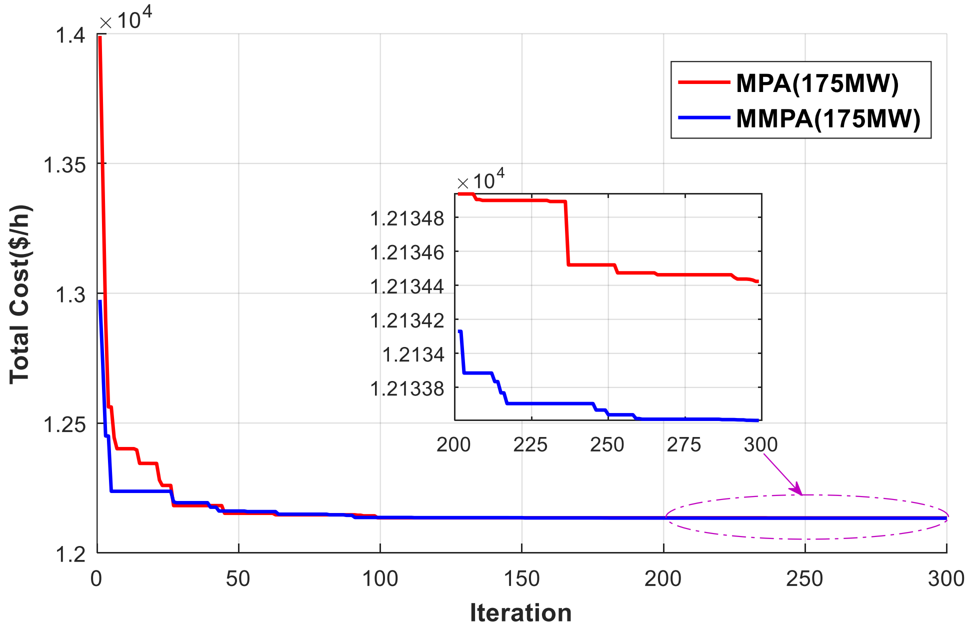


Figure 5.34: Convergence characteristics of MPA and MMPA for 175MW load demand in six-unit system.

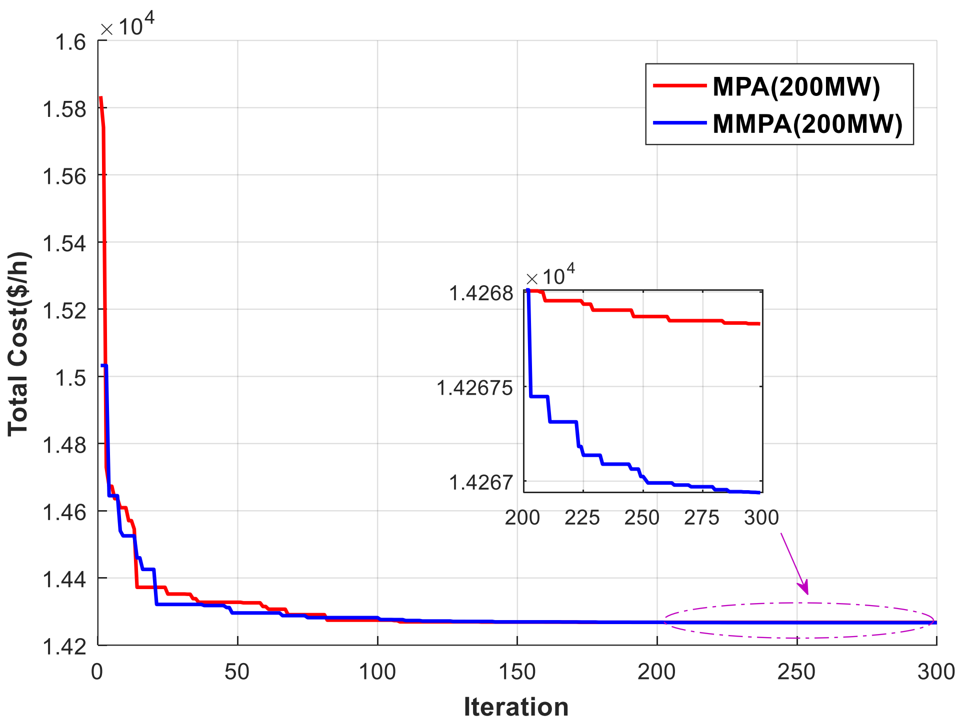


Figure 5.35: Convergence characteristics of MPA and MMPA for 200MW load demand in six-unit system.

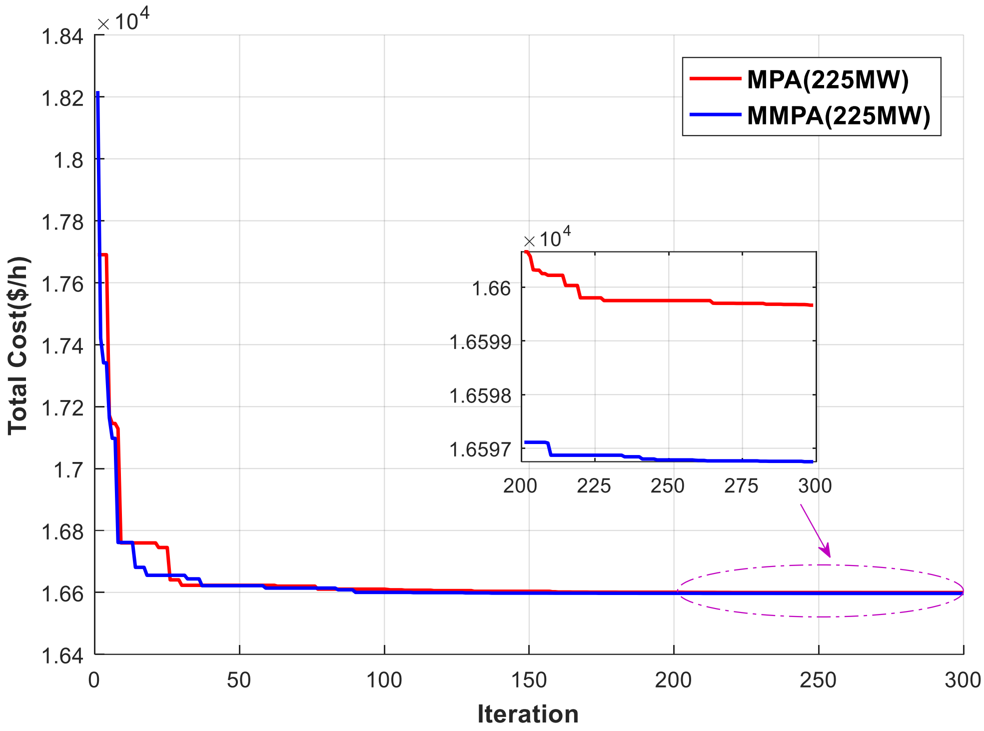


Figure 5.36: Convergence characteristics of MPA and MMPA for 225MW load demand in six-unit system.

Table 5.65: Results of CEED for the six-unit IEEE 30-bus system using MPA and MMPA.

| Method | MPA | MMPA | MPA | MMPA | MPA | MMPA | MPA | MMPA |
|---|---|---|---|---|---|---|---|---|
| Load (MW) | 150 MW | | 175 MW | | 200 MW | | 225 MW | |
| P1 (MW) | 50 | 50 | 50 | 50 | 50 | 50 | 50 | 50 |
| P2 (MW) | 20.306 | 20.298 | 27.481 | 27.532 | 34.564 | 34.5 | 41.035 | 40.998 |
| P3 (MW) | 15 | 15 | 15 | 15 | 15 | 15 | 16.549 | 16.537 |
| P4 (MW) | 25.089 | 25.102 | 31.38 | 31.265 | 37.576 | 37.593 | 43.6079 | 43.62 |
| P5 (MW) | 17.205 | 17.226 | 22.718 | 22.822 | 28.368 | 28.411 | 33.809 | 33.815 |
| P6 (MW) | 22.399 | 22.365 | 28.42 | 28.37 | 34.493 | 34.484 | 39.9999 | 39.999 |
| Fuel cost ($/h) | 2,706.588 | 2,706.3903 | 3,205.523 | 3,205.4868 | 3,740.598 | 3,740.172 | 4,318.885 | 4,318.059 |
| Emission of $SO_2$ (kg/h) | 3,142.707 | 3,142.4913 | 3,806.039 | 3,804.486 | 4,539.454 | 4,539.876 | 5,320.155 | 5,319.859 |
| Emission of $No_x$ (kg/h) | 2,404.887 | 2,404.6192 | 2,839.188 | 2,837.1526 | 3,308.579 | 3,308.344 | 3,811.360 | 3,810.971 |
| Emission of $CO_2$ (kg/h) | 2,563.109 | 2,562.7216 | 3,098.491 | 3,098.569 | 3,686.446 | 3,686.5629 | 4,316.403 | 4,315.867 |
| Total Cost ($/h) | 10,176.77 | 10,176.016 | 12,134.42 | 12,133.606 | 14,267.83 | 14,266.939 | 16,599.66 | 16,596.749 |

Figure 5.37 shows the convergence characteristics of the proposed MMPA for solving single-objective CEED problems at various load levels.

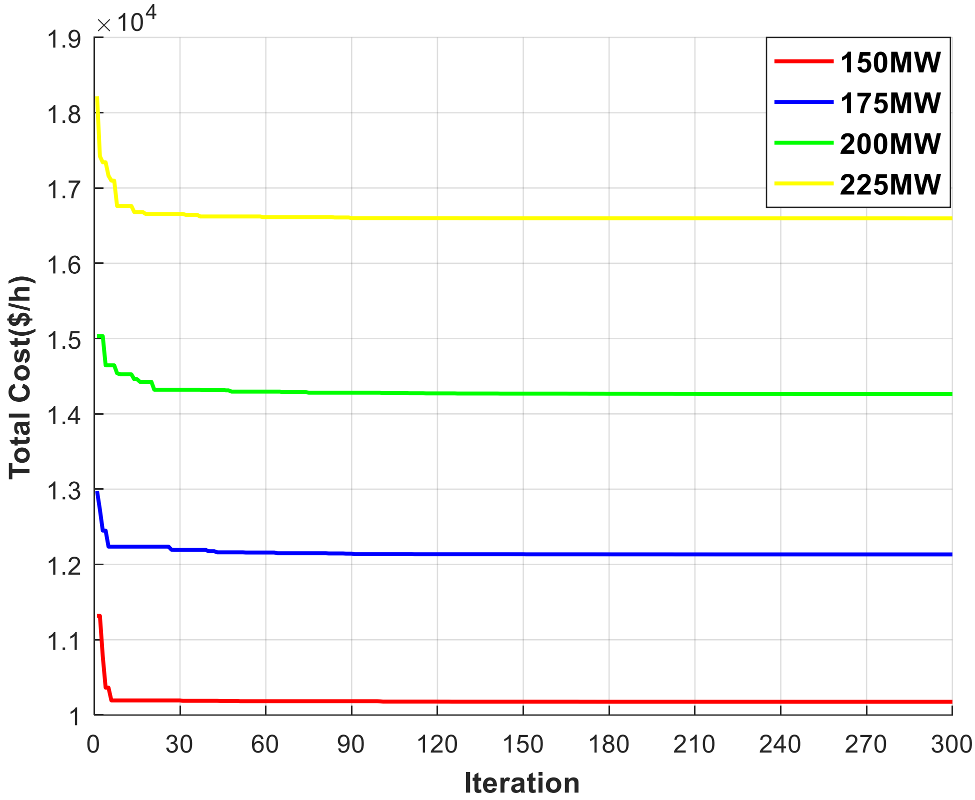


Figure 5.37: Convergence characteristics of the MMPA at different load levels.

#### 5.3.5.2.4 Case 4: 26 Thermal Units Considering Two Load Levels (2000, 2200MW)

In the fourth case, MPA and MMPA are applied for solving the 26-unit generation system in two cases of system demand. This case is executed to test the feasibility of MMPA in large power generation systems. The obtained results from MPA and MMPA are compared with other recent optimization techniques; non-iterative GA [165], PPSO [165], λ-logic-based algorithm [195], Simplified direct search method (SDSM) [196], and QPSO [91]. The results obtained in both cases are presented in Tables 5.66 and 5.67. The results allow concluding that MPA and MMPA outperform GA, PPSO, λ-logic-based algorithm, SDSM, and QPSO in both demand levels (2000 MW and 2200 MW). Still, MMPA gives a slightly better solution than MPA in both levels of demand.

Table 5.66: Results of the total fuel cost considering 2000MW load demand in a 26-unit power generation system.

| | $P_D$ = 2000 (MW) | | | | | | |
|---|---|---|---|---|---|---|---|
| Pi (MW) | GA | PPSO | λ-logic | SDSM | QPSO | MPA | MMPA |
| P1 | 2.4 | 2.4 | 2.4 | 2.4 | 2.4 | 2.4 | 2.4 |
| P2 | 2.4 | 2.4 | 2.4 | 2.4 | 2.4 | 2.4 | 2.4 |
| P3 | 2.4 | 2.4 | 2.4 | 2.4 | 2.4 | 2.4 | 2.401 |
| P4 | 2.4 | 2.4 | 2.4 | 2.4 | 2.4 | 2.4 | 2.4 |
| P5 | 2.4 | 2.4 | 2.4 | 2.4 | 2.4 | 2.413 | 2.4 |
| P6 | 4 | 4 | 4 | 4 | 4 | 4 | 4 |
| P7 | 4 | 4 | 4 | 4 | 4 | 4 | 4 |
| P8 | 4 | 4 | 4 | 4 | 4 | 4 | 4 |
| P9 | 4 | 4 | 4 | 4 | 4 | 4 | 4 |
| P10 | 15.2 | 15.2 | 15.2 | 15.2 | 15.2 | 15.2 | 15.201 |
| P11 | 15.2 | 15.2 | 15.2 | 15.2 | 15.2 | 15.212 | 15.221 |
| P12 | 15.2 | 15.2 | 15.2 | 15.2 | 15.2 | 15.201 | 15.2 |
| P13 | 15.2 | 15.2 | 15.2 | 15.2 | 15.21 | 15.2 | 15.2 |
| P14 | 25 | 25 | 25 | 25 | 25 | 25 | 25 |
| P15 | 25 | 25 | 25 | 25 | 25 | 25 | 25 |
| P16 | 25 | 25 | 25 | 25 | 25 | 25 | 25 |
| P17 | 129.71 | 129.69 | 129.71 | 123.60 | 123.45 | 121.833 | 119.643 |
| P18 | 124.71 | 124.69 | 124.70 | 121.25 | 128.06 | 121.637 | 120.562 |
| P19 | 120.42 | 120.40 | 124.41 | 118.25 | 111.52 | 116.122 | 118.629 |
| P20 | 116.72 | 116.70 | 116.71 | 116.25 | 116.62 | 119.83 | 120.614 |
| P21 | 68.95 | 68.95 | 68.95 | 68.95 | 68.95 | 68.95 | 68.95 |
| P22 | 68.95 | 68.95 | 68.95 | 68.95 | 68.95 | 68.95 | 68.95 |
| P23 | 68.95 | 68.95 | 68.95 | 68.95 | 68.95 | 68.95 | 68.95 |
| P24 | 337.76 | 337.85 | 337.69 | 350 | 349.69 | 349.9 | 349.866 |
| P25 | 400 | 400 | 400 | 400 | 400 | 400 | 400 |
| P26 | 400 | 400 | 400 | 400 | 400 | 400 | 400 |
| FT ($/h) | 27,671.2441 | 27,671.2276 | 27,246.75 | 27,246.42 | 27,245.05 | 27,244.8976 | 27,244.663 |

Table 5.67: Results of the total fuel cost considering 2200MW load demand in a 26-unit power generation system.

| | $P_D$ = 2200 (MW) | | | | |
|---|---|---|---|---|---|
| Pi (MW) | λ-logic [43] | SDSM [44] | QPSO [45] | MPA | MMPA |
| P1 | 2.4 | 2.4 | 2.4 | 2.4 | 2.4 |
| P2 | 2.4 | 2.4 | 2.4 | 2.423 | 2.4 |

| | | | | | |
|---|---|---|---|---|---|
| P3 | 2.4 | 2.4 | 2.4 | 2.4 | 2.401 |
| P4 | 2.4 | 2.4 | 2.4 | 2.4 | 2.4 |
| P5 | 2.4 | 2.4 | 2.4 | 2.4 | 2.402 |
| P6 | 4 | 4 | 4 | 4 | 4 |
| P7 | 4 | 4 | 4 | 4 | 4 |
| P8 | 4 | 4 | 4 | 4 | 4 |
| P9 | 4 | 4 | 4 | 4 | 4 |
| P10 | 33.20 | 35.2 | 33.21 | 38.01 | 31.066 |
| P11 | 31.01 | 33.2 | 21.78 | 36.01 | 41.65 |
| P12 | 29.03 | 28.2 | 34.6 | 19.162 | 24.956 |
| P13 | 26.91 | 26.2 | 30.72 | 26.945 | 22.477 |
| P14 | 25 | 25 | 25 | 25 | 25 |
| P15 | 25 | 25 | 25 | 25 | 25 |
| P16 | 25 | 25 | 25 | 25 | 25 |
| P17 | 155 | 154.25 | 154.98 | 154.998 | 155 |
| P18 | 155 | 154.25 | 154.96 | 154.9999 | 155 |
| P19 | 155 | 154.25 | 154.97 | 154.998 | 154.9996 |
| P20 | 155 | 154.25 | 154.97 | 155 | 154.9998 |
| P21 | 68.95 | 68.95 | 68.95 | 68.95 | 68.95 |
| P22 | 68.95 | 68.95 | 68.95 | 68.95 | 68.95 |
| P23 | 68.95 | 68.95 | 68.95 | 68.95 | 68.95 |
| P24 | 350 | 350 | 350 | 349.9999 | 349.999 |
| P25 | 400 | 400 | 399.99 | 400 | 400 |
| P26 | 400 | 400 | 399.97 | 400 | 400 |
| FT ($/h) | 29,725.48 | 29,725.32 | 29,724.64 | 29,723.664 | 29,723.519 |

The convergence characteristics of the MPA and MMPA for both levels of demand (2000 MW and 2200 MW) in a 26-unit power system are shown in figures 5.38 and 5.39, respectively. These figures present the ability of the proposed MMPA technique in obtaining the smallest total cost.

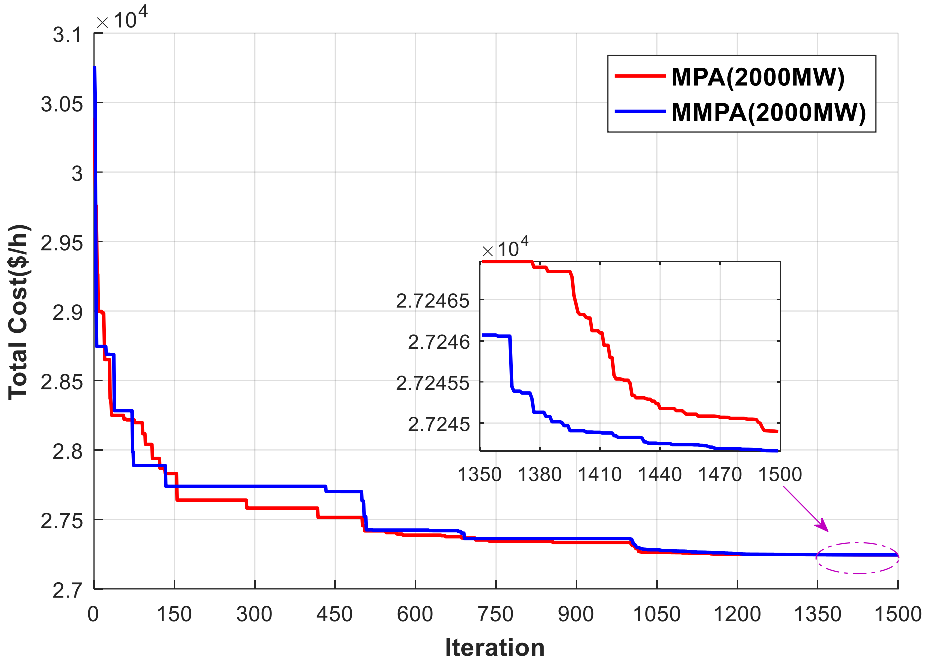


Figure 5.38: Convergence characteristics of MPA and MMPA for 2000MW load demand in a 26-unit power system.

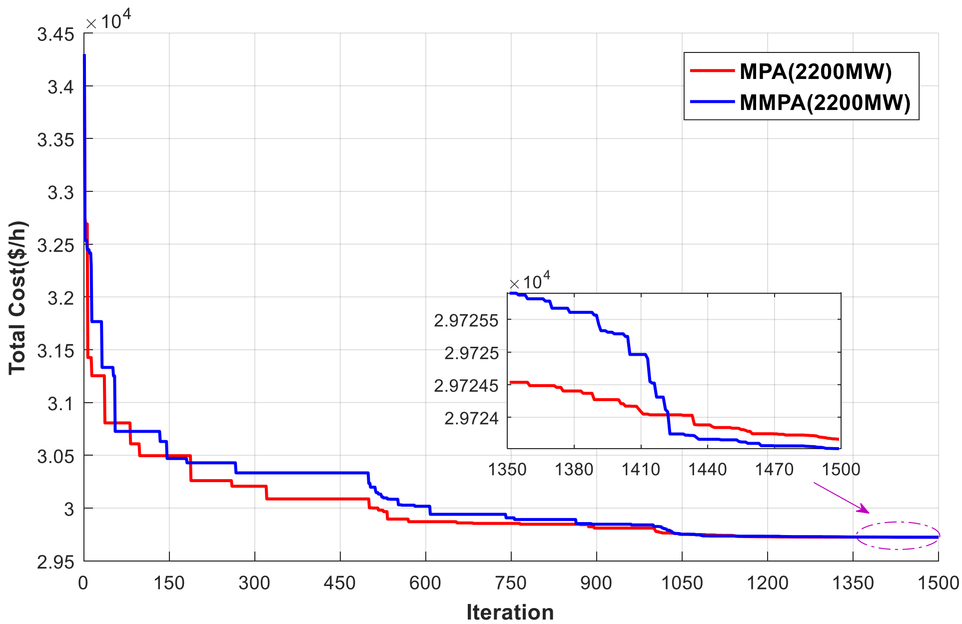


Figure 5.39: Convergence characteristics of MPA and MMPA for 2200MW load demand in a 26-unit power system.

## 5.4 Solving ELD Problem with using ESCSDO Algorithm

In this section, the superiority of the proposed ESCSDO10 technique is illustrated by six typical benchmark functions and four ELD cases. All the experiments are developed using MATLAB (R2020a) and executed on a computer with windows 10 Pro on Intel(R) Core(TM) i5- 9400F CPU 2.90 GHz with 8GB RAM environment.

### 5.4.1 Benchmark Functions

In this subsection, The efficacy and the precision of the proposed ESCSDO10 algorithm are evaluated on many benchmark functions including the best, mean, median, worst values, and standard deviation (STD) for the solutions achieved by the conventional SDO algorithm and the two recent optimization algorithms, including the gray wolf optimizer (GWO) [197], the tunicate Swarm Algorithm (TSA) [198], and ESSDO as well as the other tenth versions of the proposed ESCSDO algorithms that are only used in the comparison of the first benchmark function to choose the best one as shown in table 5.68. The obtained results of the proposed ESCSDO10 technique are compared with these recent algorithms in table 5.69. These algorithms have been performed for the maximum number of iterations is 200 and the population size is 50 for 20 independent runs. Figure 5.40 illustrates the Qualitative metrics using the proposed ESCSDO10 technique for twelve benchmark functions including 2D views of the functions, search history, average fitness history, and convergence curve. The Boxplot using the proposed techniques and the original SDO algorithm for the first unimodal benchmark function (F1) is presented in Fig. 5.41 while the convergence curves of these algorithms for this function is shown in Fig. 5.42.

F1

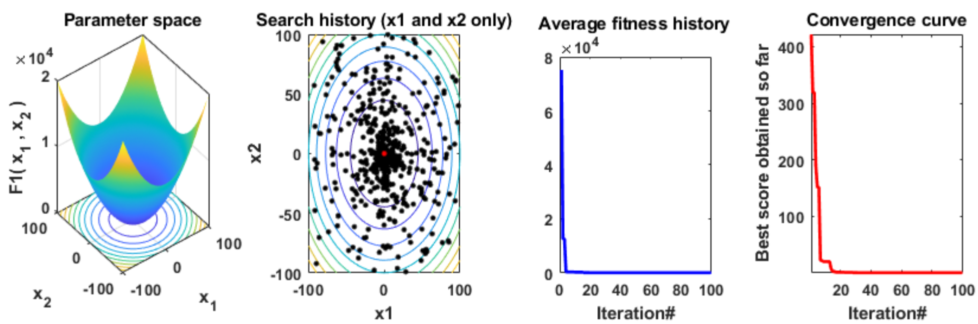

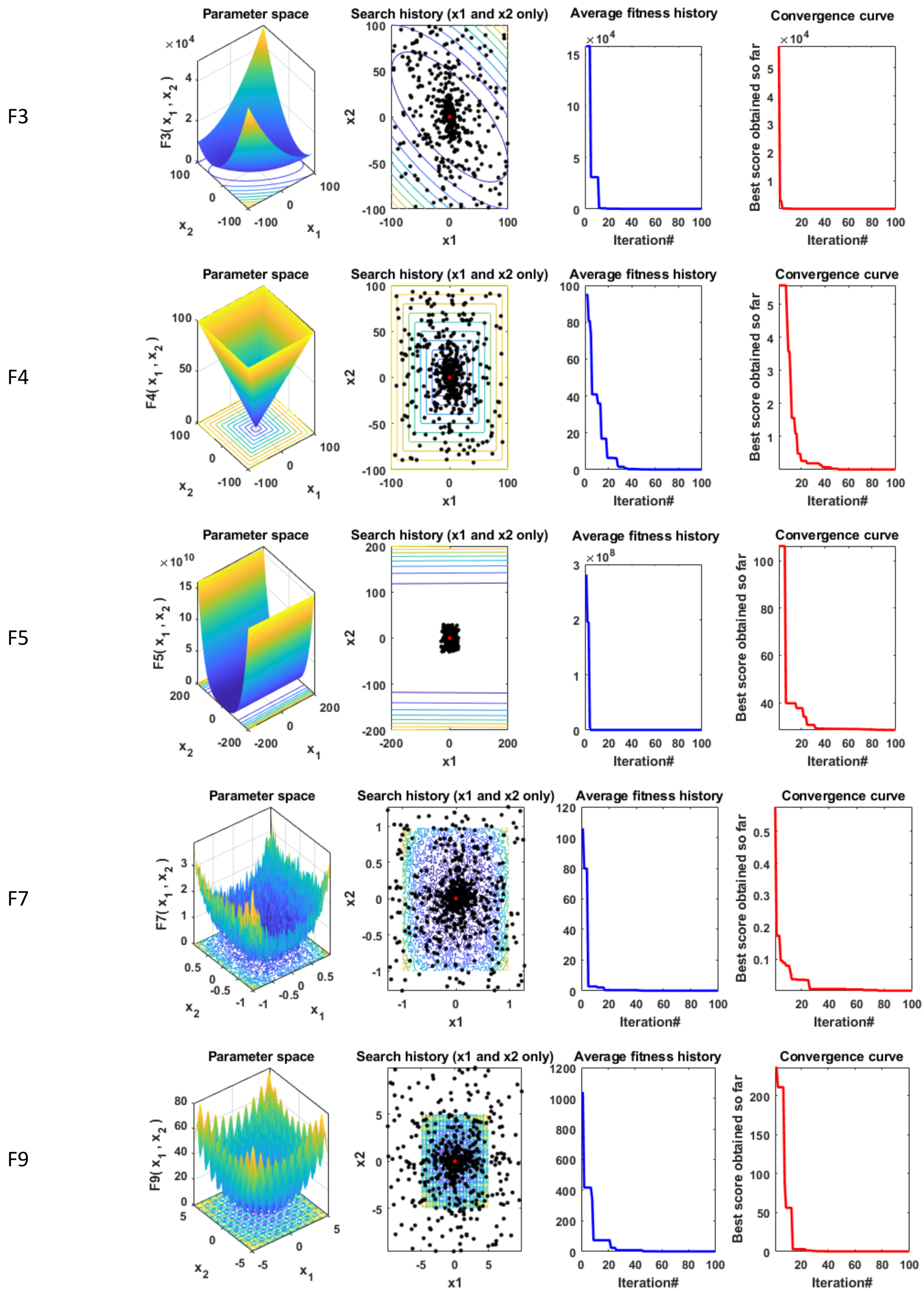
F3
F4
F5
F7
F9
Parameter space
Search history (x1 and x2 only)
Average fitness history
Convergence curve
Iteration#
Best score obtained so far
x1
x2

F12

F15

F16

F18

F20

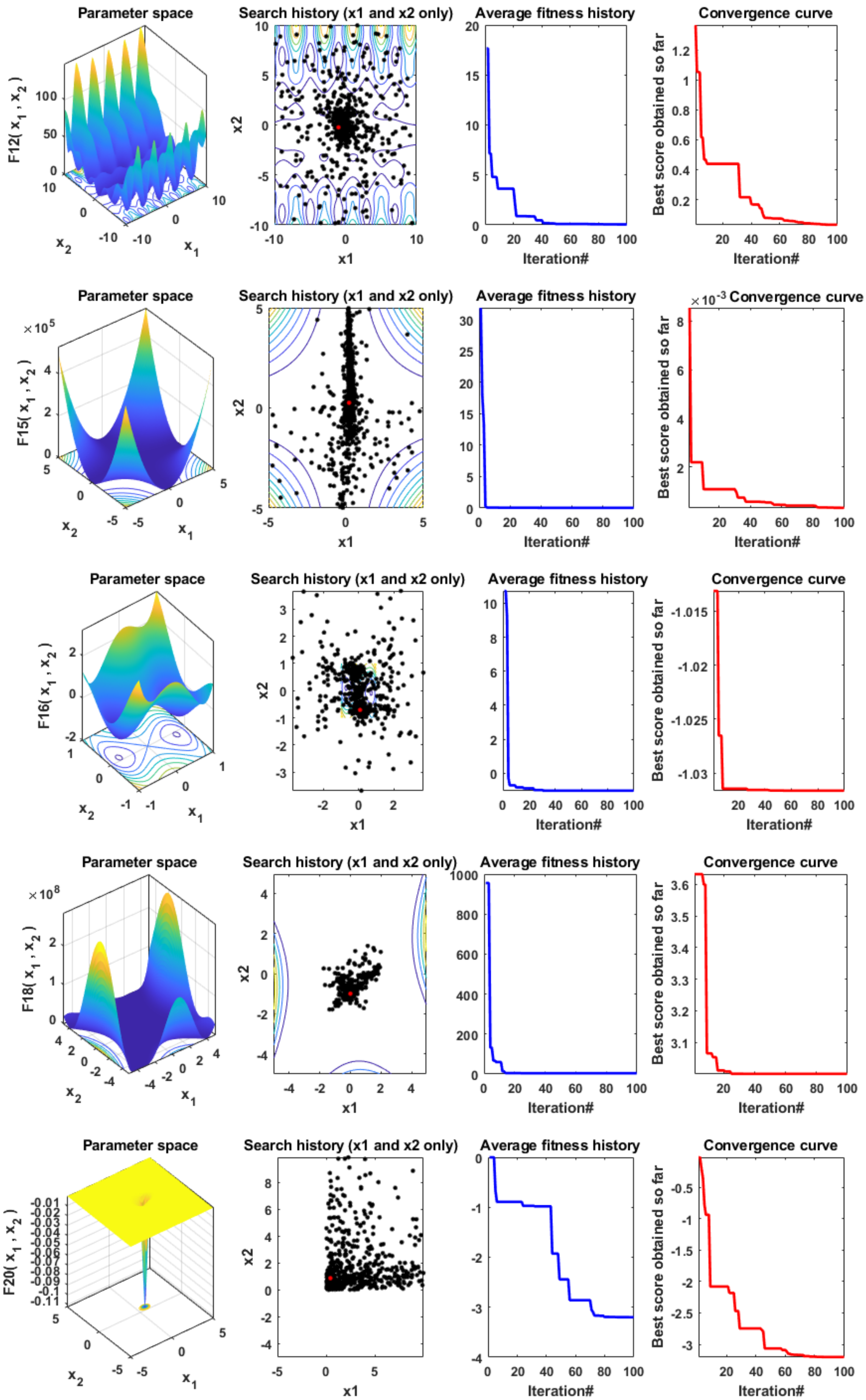

F22

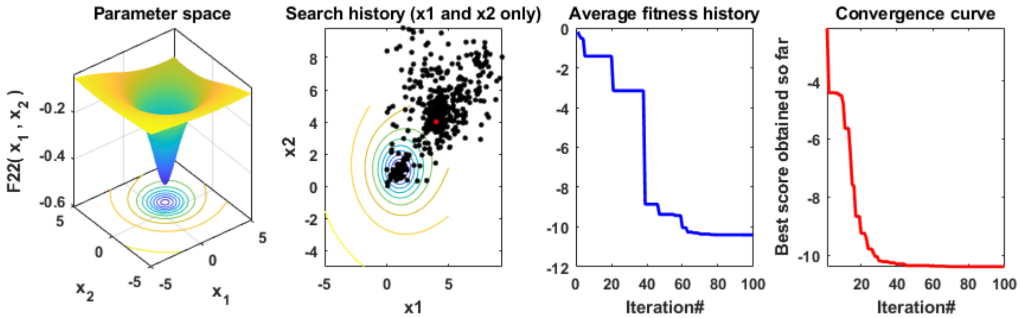


Figure 5.40: Qualitative metrics of twelve benchmark functions: 2D views of the functions, search history, average fitness history, and convergence curve using ESCSDO10 technique.

Table 5.68: the statistical Results of first unimodal benchmark function (F1) using the proposed techniques, the original SDO algorithm and other recent algorithms.

| Algorithm | Best | Mean | Median | Worst | STD |
|---|---|---|---|---|---|
| **SDO** | 1.39074E-55 | 1.49251E-51 | 3.73868E-54 | 8.43436E-51 | 2.99739E-51 |
| **ESSDO** | 3.02373E-56 | 3.5837E-52 | 6.35022E-54 | 2.16262E-51 | 7.24548E-52 |
| **ESCSDO1** | 6.74221E-57 | 1.78663E-53 | 3.97613E-54 | 7.85779E-53 | 2.73127E-53 |
| **ESCSDO2** | 1.03475E-56 | 1.48693E-52 | 1.50318E-54 | 1.19436E-51 | 3.53756E-52 |
| **ESCSDO3** | 1.63475E-56 | 1.35188E-51 | 2.67388E-54 | 7.93841E-51 | 3.07712E-51 |
| **ESCSDO4** | 1.99977E-57 | 9.02398E-53 | 3.29863E-54 | 5.89367E-52 | 1.6966E-52 |
| **ESCSDO5** | 2.90548E-56 | 8.47824E-52 | 2.92166E-54 | 6.99918E-51 | 2.12116E-51 |
| **ESCSDO6** | 1.58847E-57 | 2.49792E-52 | 2.47738E-54 | 2.81673E-51 | 8.09219E-52 |
| **ESCSDO7** | 1.27836E-57 | 4.64444E-52 | 9.23534E-54 | 3.92623E-51 | 1.14869E-51 |
| **ESCSDO8** | 1.90317E-57 | **3.37681E-54** | 4.37471E-55 | **1.6232E-53** | **5.21723E-54** |
| **ESCSDO9** | 1.41579E-57 | 6.15867E-53 | 1.75888E-53 | 3.55287E-52 | 1.0855E-52 |
| **ESCSDO10** | **2.1815E-58** | 1.42757E-53 | **1.98635E-55** | 6.40121E-53 | 2.48092E-53 |
| **TSA** | 3.78858E-08 | 4.63559E-07 | 1.17308E-07 | 4.08841E-06 | 1.14601E-06 |
| **GWO** | 6.34376E-12 | 3.13157E-11 | 2.42821E-11 | 7.40291E-11 | 2.25825E-11 |

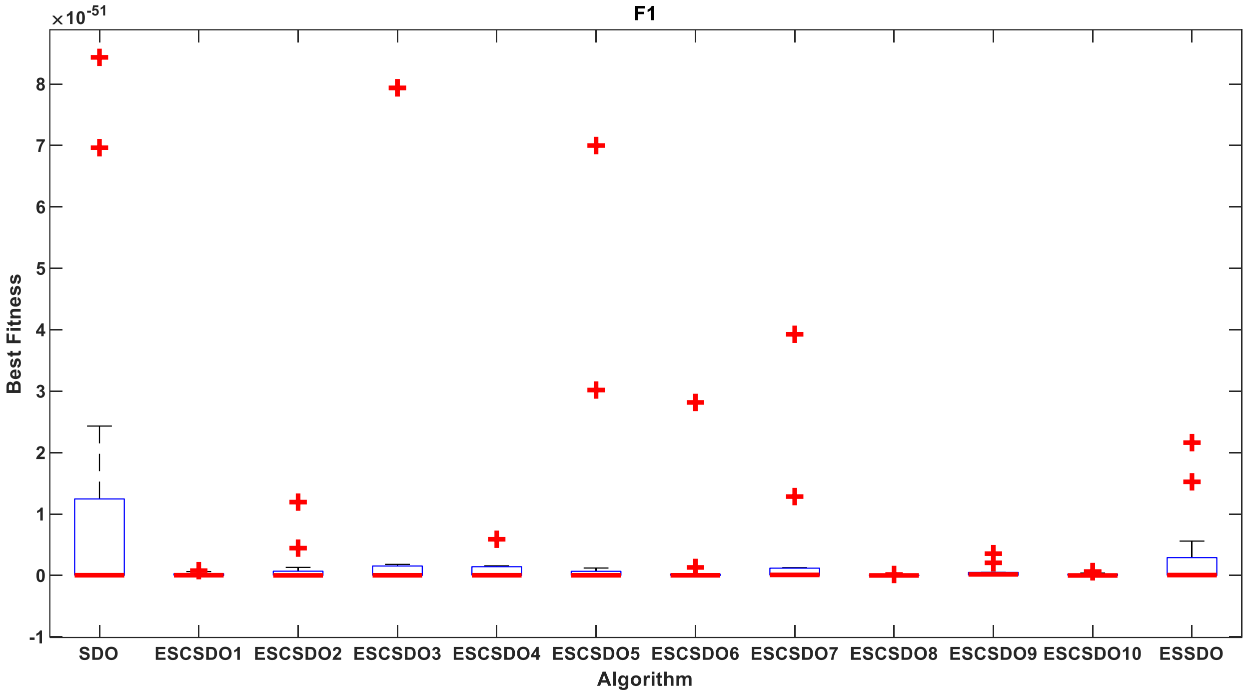


Figure 5.41: Boxplots using the proposed techniques and the original SDO algorithm for the first unimodal benchmark function (F1).

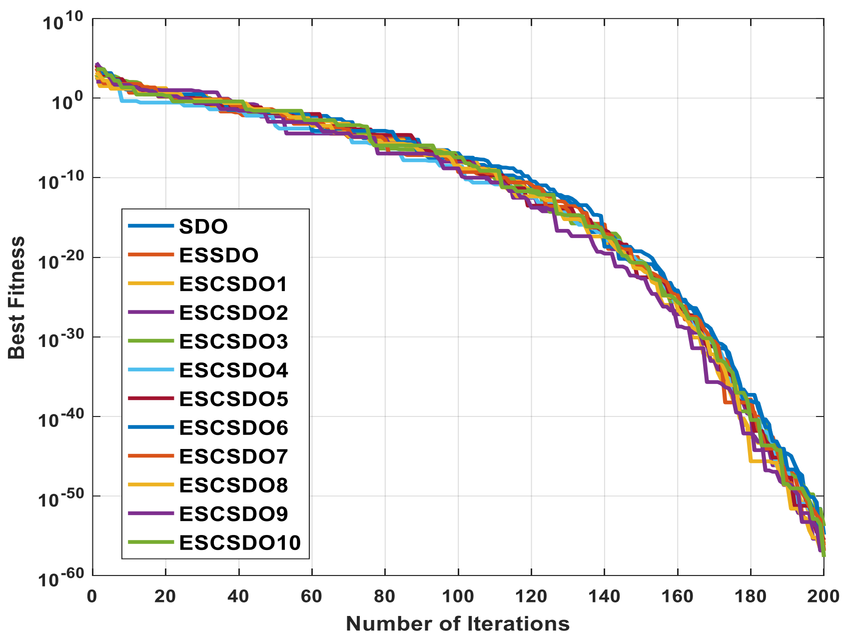


Figure 5.42: The convergence curves of the proposed techniques and the original SDO algorithm for the first unimodal benchmark function (F1).

Tables 5.69 shows the statistical results of the proposed ESCSDO10 algorithm and other resent techniques when used for unimodal benchmark functions, multimodal benchmark functions, and composite benchmark functions. The optimal values were obtained with the proposed ESCSDO10, ESSDO, SDO, TSA and GWO techniques shown in bold. It is obviously seen that the ESCSDO10 algorithm gives the optimum result for most of these benchmark functions. The convergence curves of these techniques for all benchmark functions are displayed in Fig. 5.43 and the Boxplots for each algorithm for these functions are presented in Fig. 5.44. From those figures, it is clear that the proposed technique reached a stable point for all functions and the boxplots of the ESCSDO10 technique are very narrow for many functions compared to the other algorithms.

Table 5.69: the statistical Results of 22 benchmark functions using the proposed ESCSDO10 technique and other recent techniques.

| **Function** | | **ESCSDO10** | **ESSDO** | **SDO** | **TSA** | **GWO** |
|---|---|---|---|---|---|---|
| | Best | **3.75E-32** | 5.77E-29 | 1.83E-29 | 2.44E-06 | 1.42E-07 |
| | Mean | **2.53E-25** | 1.83E-24 | 3.76E-25 | 1.9E-05 | 2.77E-07 |
| F2 | Median | **4.56E-27** | 1.72E-26 | 1.13E-26 | 1.86E-05 | 2.66E-07 |
| | Worst | **3.98E-24** | 3.32E-23 | 3.98E-24 | 3.68E-05 | 4.78E-07 |
| | std | **8.98E-25** | 7.38E-24 | 9.1E-25 | 9.44E-06 | 9.9E-08 |
| | Best | 1.77E-52 | **1.15E-52** | 6.27E-46 | 0.027608 | 0.008462 |
| | Mean | **3.2E-39** | 3.72E-38 | 6.91E-34 | 1.122677 | 0.610441 |
| F3 | Median | **6.1E-42** | 4.94E-41 | 1.4E-39 | 0.772195 | 0.185412 |
| | Worst | **3.12E-38** | 3.91E-37 | 1.38E-32 | 3.914695 | 3.567009 |
| | std | **8.03E-39** | 1.08E-37 | 3.09E-33 | 1.096313 | 0.827115 |
| | Best | 2E-28 | **4.09E-29** | 1.11E-26 | 0.67531 | 0.002608 |
| | Mean | 7.34E-18 | 4.98E-23 | **4.52E-23** | 3.616654 | 0.008 |
| F4 | Median | 8.37E-25 | **4.36E-25** | 1.14E-23 | 3.022253 | 0.007092 |
| | Worst | 1.4E-16 | 5.64E-22 | **1.94E-22** | 9.361516 | 0.016667 |
| | std | 3.13E-17 | 1.34E-22 | **6.34E-23** | 2.343658 | 0.003845 |

| | | | | | | |
|---|---|---|---|---|---|---|
| | Best | 27.80709 | 28.22188 | 27.90967 | 27.18973 | **25.92515** |
| | Mean | 28.56384 | 28.64064 | 28.65096 | 39.01094 | **27.18903** |
| F5 | Median | 28.76999 | 28.62557 | 28.74726 | 28.66203 | **27.09814** |
| | Worst | 28.98212 | 28.99968 | 28.98699 | 239.7785 | **28.79035** |
| | std | 0.388719 | **0.224746** | 0.295026 | 47.26339 | 0.72182 |
| | Best | **0.034921** | 0.101901 | 0.039957 | 2.886997 | 0.252254 |
| | Mean | 2.974648 | 2.571093 | 2.568541 | 3.800719 | **0.647554** |
| F6 | Median | 2.892489 | 1.796754 | 2.038779 | 3.736935 | **0.611378** |
| | Worst | 6.929499 | 7.022734 | 7.250251 | 4.850371 | **1.172757** |
| | std | 1.791856 | 2.038024 | 1.852701 | 0.527851 | **0.280888** |
| | Best | **3.76E-05** | 0.000171 | 8.66E-05 | 0.007604 | 0.001477 |
| | Mean | **0.001905** | 0.002752 | 0.002356 | 0.019206 | 0.004433 |
| F7 | Median | 0.001345 | 0.002072 | **0.001136** | 0.018479 | 0.003685 |
| | Worst | **0.006742** | 0.01296 | 0.013813 | 0.04436 | 0.01033 |
| | std | **0.001744** | 0.003485 | 0.003331 | 0.007628 | 0.002554 |
| | Best | -1683.41 | **-1696.97** | -1655 | -1394.45 | -1495.31 |
| | Mean | -1262.59 | -1249.19 | **-1312.83** | -1212.82 | -1245.57 |
| F8 | Median | -1367.32 | -1297.77 | **-1385.86** | -1232.52 | -1224.18 |
| | Worst | -504.28 | -501.104 | -598.802 | -976.635 | **-1123.85** |
| | std | 326.0333 | 280.296 | 294.008 | 122.0762 | **104.0153** |
| | Best | **3.26E-30** | 5.02E-29 | 4.33E-30 | 156.667 | 1.062467 |
| | Mean | **1.23E-24** | 1.16E-23 | 1.75E-22 | 228.0177 | 9.801018 |
| F9 | Median | **1.22E-26** | 2.33E-26 | 4.17E-25 | 228.634 | 9.824713 |
| | Worst | **1.96E-23** | 2.11E-22 | 3.02E-21 | 331.7581 | 24.96968 |
| | std | **4.37E-24** | 4.69E-23 | 6.75E-22 | 46.40919 | 5.565812 |
| F10 | Best | **8.88E-16** | **8.88E-16** | **8.88E-16** | 20.81133 | 20.76487 |
| | Mean | **8.88E-16** | **8.88E-16** | **8.88E-16** | 20.9608 | 20.92344 |

| | | | | | | |
|---|---|---|---|---|---|---|
| | Median | **8.88E-16** | **8.88E-16** | **8.88E-16** | 20.99356 | 20.94465 |
| | Worst | **8.88E-16** | **8.88E-16** | **8.88E-16** | 21.0961 | 21.06309 |
| | std | **0.00** | **0.00** | **0.00** | 0.091505 | 0.083433 |
| | Best | **0.00** | **0.00** | **0.00** | 1.3E-09 | 6.56E-13 |
| | Mean | **0.00** | **0.00** | **0.00** | 0.007018 | 0.009891 |
| F11 | Median | **0.00** | **0.00** | **0.00** | 1.44E-08 | 4.55E-12 |
| | Worst | **0.00** | **0.00** | **0.00** | 0.029126 | 0.055407 |
| | std | **0.00** | **0.00** | **0.00** | 0.010243 | 0.015766 |
| | Best | 0.003144 | 0.001941 | **0.001152** | 0.374956 | 0.006066 |
| | Mean | 0.21864 | 0.204276 | 0.23467 | 2.805889 | **0.026151** |
| F12 | Median | 0.111663 | 0.095715 | 0.067805 | 2.009833 | **0.023474** |
| | Worst | 1.458692 | 1.126465 | 1.492821 | 7.656863 | **0.047176** |
| | std | 0.335046 | 0.288399 | 0.352063 | 2.128936 | **0.013414** |
| | Best | 0.197555 | 0.067718 | **0.046216** | 2.372295 | 0.09955 |
| | Mean | 1.959641 | 1.667848 | 1.867552 | 3.298085 | **0.613832** |
| F13 | Median | 2.069862 | 1.389309 | 1.934246 | 3.22876 | **0.609981** |
| | Worst | 2.998356 | 2.998654 | 2.999924 | 4.16073 | **1.044** |
| | std | 0.899235 | 0.948713 | 0.961284 | 0.565835 | **0.280029** |
| | Best | **0.998004** | **0.998004** | **0.998004** | **0.998004** | **0.998004** |
| | Mean | **2.619458** | 3.050461 | 3.494696 | 8.298683 | 3.892106 |
| F14 | Median | **0.998004** | **0.998004** | 1.495017 | 10.76318 | 2.982105 |
| | Worst | **12.67051** | **12.67051** | **12.67051** | 18.30431 | **12.67051** |
| | std | **2.925827** | 3.965746 | 3.953203 | 5.533952 | 3.727681 |
| | Best | **0.000307** | **0.000307** | **0.000307** | 0.000308 | 0.00031 |
| | Mean | 0.003957 | **0.003019** | 0.00067 | 0.007136 | 0.003547 |
| F15 | Median | **0.000348** | 0.000536 | 0.000527 | 0.000505 | 0.000546 |
| | Worst | 0.059015 | 0.0291 | **0.002121** | 0.031699 | 0.020363 |

| | | | | | | |
|---|---|---|---|---|---|---|
| | std | 0.013212 | 0.007672 | **0.000473** | 0.010606 | 0.007255 |
| | Best | **-1.03163** | **-1.03163** | **-1.03163** | **-1.03163** | **-1.03163** |
| | Mean | -1.02983 | -1.03146 | -1.03005 | -1.0253 | **-1.03158** |
| F16 | Median | **-1.03163** | **-1.03163** | **-1.03163** | **-1.03163** | **-1.03163** |
| | Worst | -0.99643 | -1.0284 | -1.00046 | -0.99999 | **-1.03063** |
| | std | 0.007862 | 0.000722 | 0.006966 | 0.012981 | **0.000223** |
| | Best | **0.397887** | **0.397887** | **0.397887** | 0.39789 | 0.397888 |
| | Mean | 0.558321 | 0.401484 | **0.397987** | 0.397927 | 0.397891 |
| F17 | Median | **0.397887** | **0.397887** | **0.397887** | 0.397907 | 0.397891 |
| | Worst | 3.605753 | 0.435351 | 0.399795 | 0.398082 | **0.397897** |
| | std | 0.717291 | 0.01108 | 0.000426 | 4.53E-05 | **3.01E-06** |
| | Best | **3.00** | **3.00** | **3.00** | 3.000009 | **3.00** |
| | Mean | **3.00** | **3.00** | **3.00** | 8.400078 | 3.000068 |
| F18 | Median | **3.00** | **3.00** | **3.00** | 3.000084 | 3.000036 |
| | Worst | **3.00** | **3.00** | **3.00** | 84.00001 | 3.000238 |
| | std | 3.72E-09 | **1.43E-10** | 5.21E-08 | 18.78799 | 6.53E-05 |
| | Best | **-0.30048** | **-0.30048** | **-0.30048** | **-0.30048** | **-0.30048** |
| | Mean | -0.28754 | -0.28671 | -0.2893 | **-0.30048** | **-0.30048** |
| F19 | Median | -0.30038 | -0.30039 | -0.30038 | **-0.30048** | **-0.30048** |
| | Worst | -0.2104 | -0.18684 | -0.19165 | **-0.30048** | **-0.30048** |
| | std | 0.027383 | 0.030384 | 0.026531 | **1.14E-16** | **1.14E-16** |
| | Best | **-3.322** | -3.32198 | **-3.322** | -3.32148 | -3.32198 |
| | Mean | -3.06282 | -2.96633 | -3.09697 | -3.07223 | **-3.22876** |
| F20 | Median | -3.2031 | -3.20305 | -3.2031 | -3.20118 | **-3.26239** |
| | Worst | -0.36603 | -0.04417 | -0.89904 | -0.20816 | **-2.84039** |
| | std | 0.675966 | 0.770122 | 0.550986 | 0.679321 | **0.125558** |
| F21 | Best | **-10.1532** | **-10.1532** | **-10.1532** | -10.0895 | -10.1502 |

| | | | | | | |
|---|---|---|---|---|---|---|
| | Mean | -8.54286 | -8.43923 | **-8.703** | -5.89545 | -8.51218 |
| | Median | **-10.1532** | **-10.1532** | **-10.1532** | -4.90994 | -10.1413 |
| | Worst | -2.4537 | -2.34519 | **-4.99677** | -2.58642 | -2.62918 |
| | std | 2.599364 | 2.647115 | **2.23952** | 2.775111 | 2.963153 |
| | Best | **-10.4029** | **-10.4029** | **-10.4029** | -10.3637 | -10.4024 |
| | Mean | -7.89432 | -9.83094 | -8.45822 | -7.02119 | **-10.0134** |
| F22 | Median | -10.3509 | **-10.4029** | **-10.4029** | -9.8942 | -10.3959 |
| | Worst | **-2.97529** | -2.66539 | -1.0677 | -1.82478 | -2.76526 |
| | std | 2.870862 | 1.836785 | 3.128689 | 3.57071 | **1.706042** |
| | Best | **-10.5364** | **-10.5364** | **-10.5364** | -10.4599 | -10.5348 |
| | Mean | -9.10193 | -8.96843 | -7.90449 | -5.50502 | **-9.74305** |
| F23 | Median | **-10.5364** | -10.5363 | -10.5357 | -2.83596 | -10.5274 |
| | Worst | **-5.08423** | -2.13823 | -3.79083 | -1.66783 | -2.42135 |
| | std | **2.368897** | 2.914367 | 3.015319 | 3.728197 | 2.418464 |

The best values obtained are in bold.

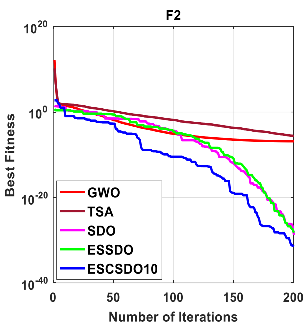


F2

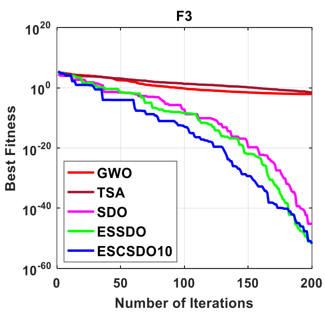


F3

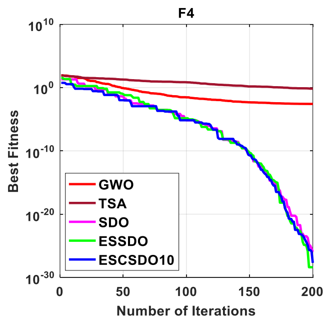


F4

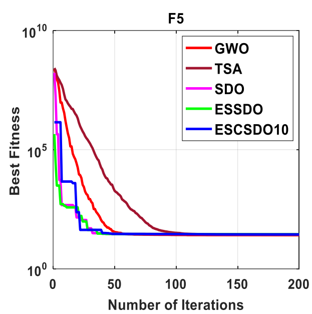


F5

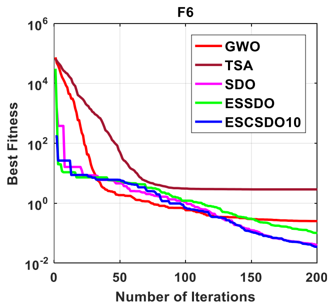


F6

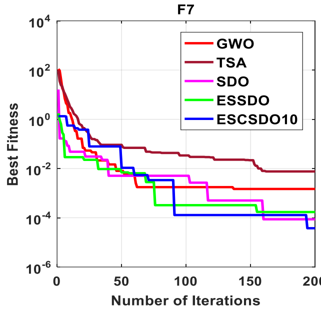


F7

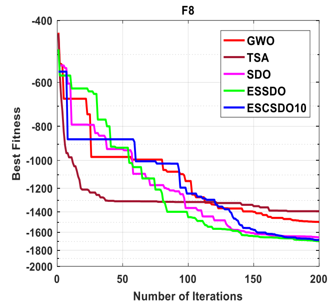


F8

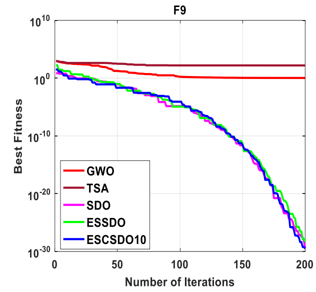


F9

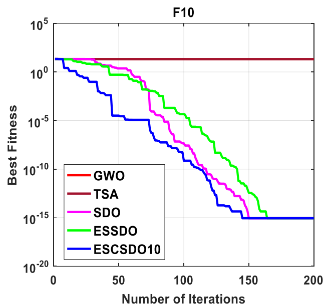


F10

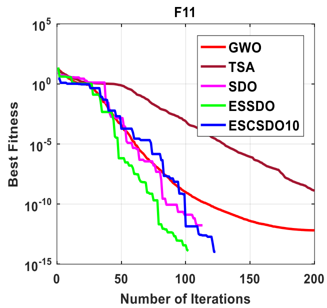


F11

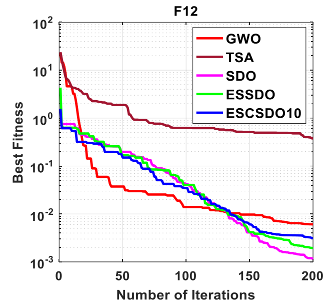


F12

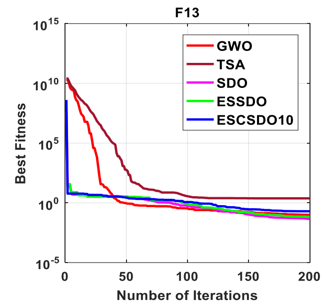


F13

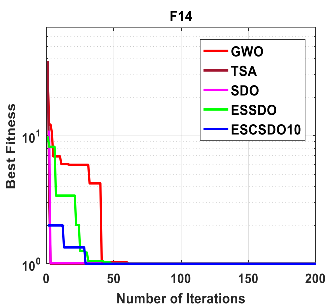


F14

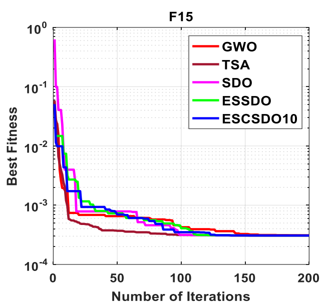


F15

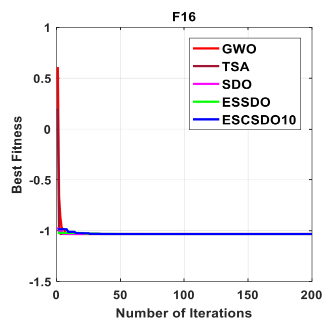


F16

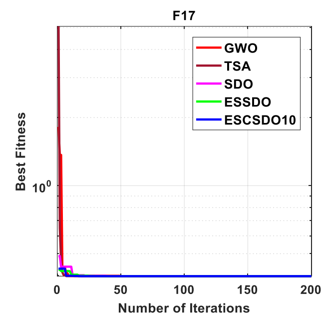


F17

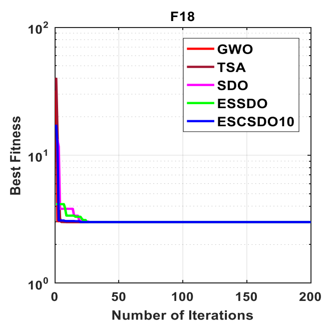


F18

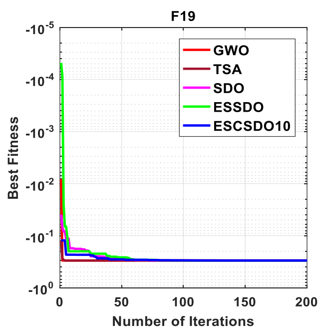


F19

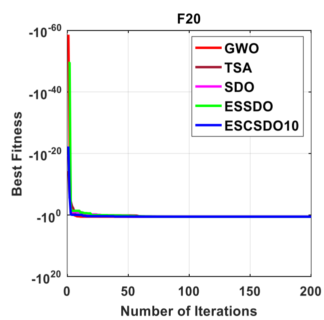


F20

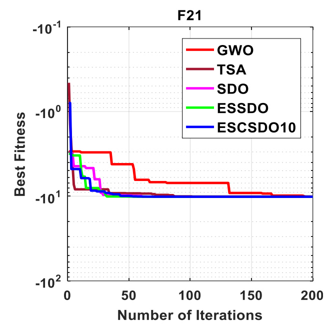


F21

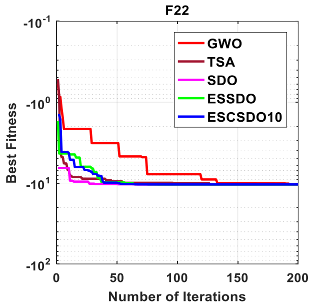


F22

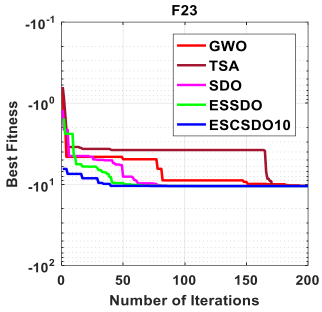


F23

Figure 5.43: The convergence curves of all algorithms for 22 benchmark functions.

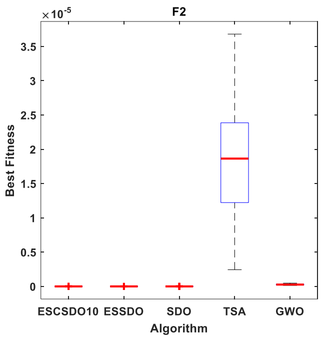


F2

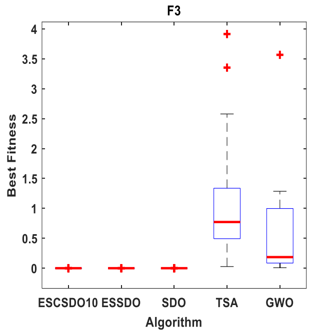


F3

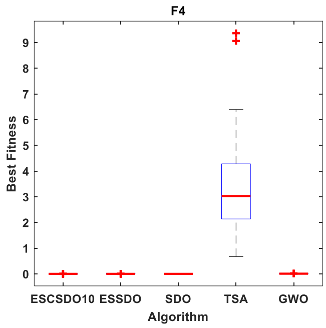


F4

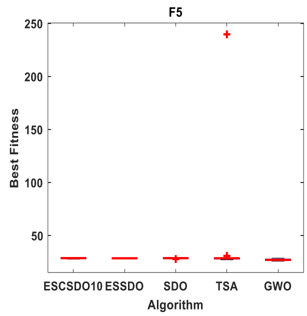


F5

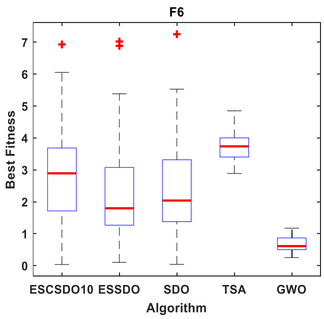


F6

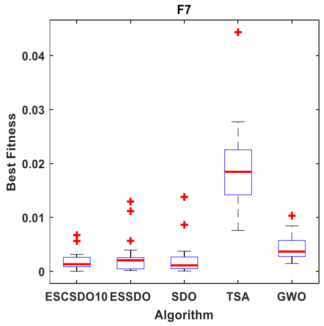


F7

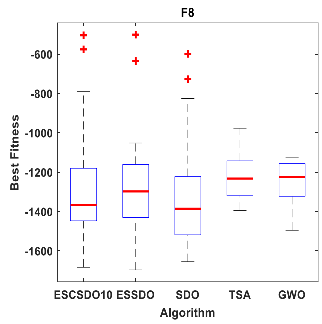


F8

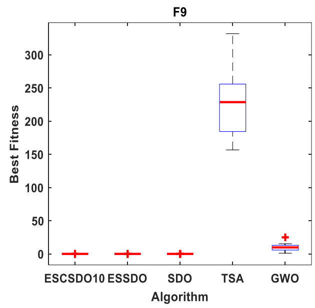


F9

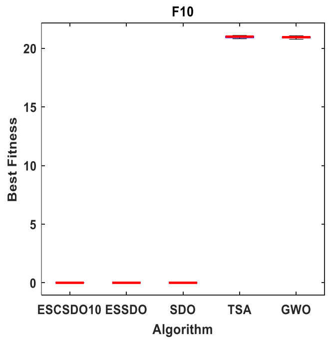


F10

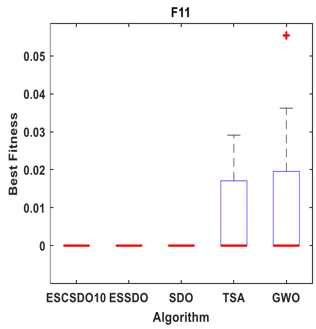


F11

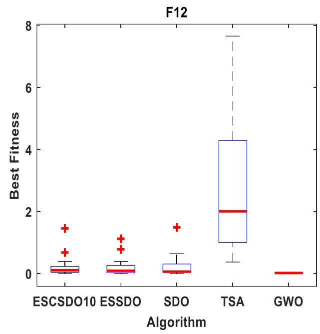


F12

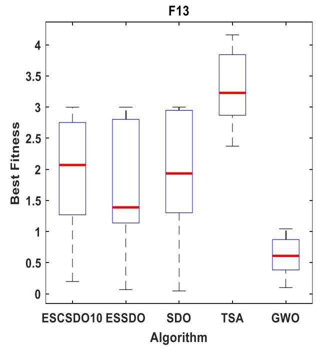


F13

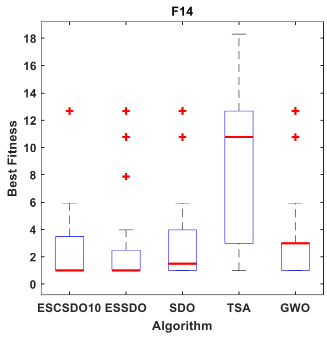


F14

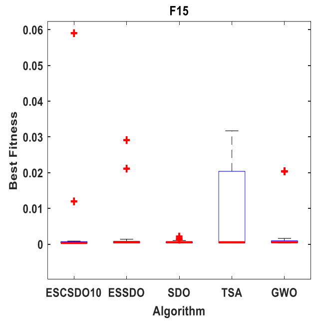


F15

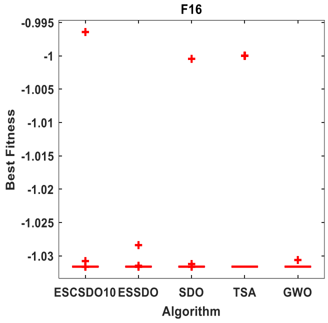


F16

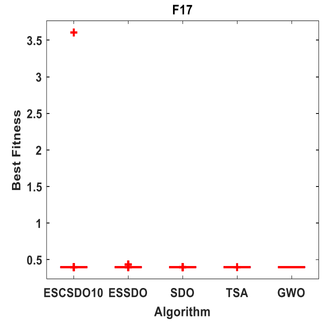


F17

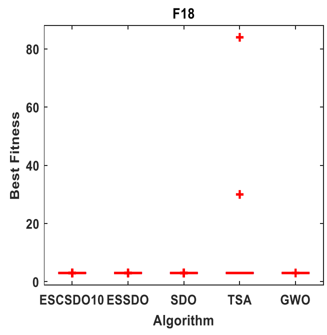


F18

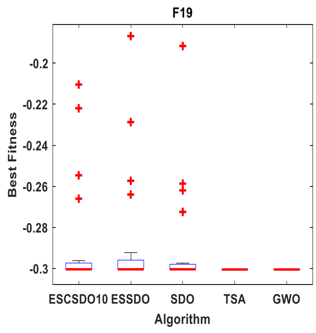


F19

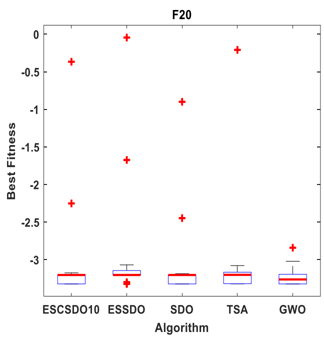


F20

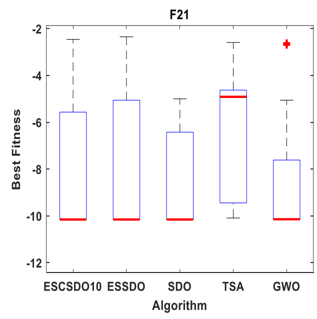


F21

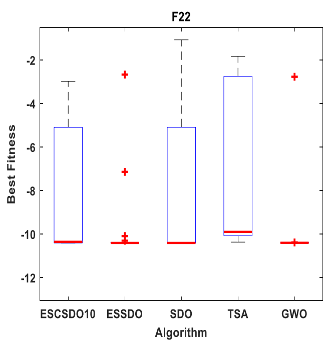


F22

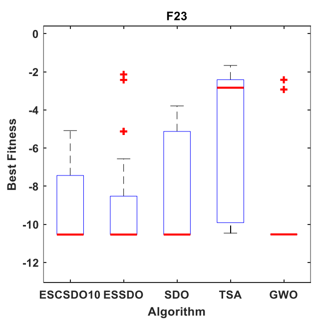


F23

F22 F23

Figure 5.44: Boxplots for all algorithms for 22 benchmark functions.

### 5.4.2 Economic Load Dispatch (ELD) Problems

In this subsection, the ELD problems with 6, 13, 15 and 40 generators subjected to various OF and constrained functions are experimented. The obtained results are compared with three recent algorithms as well as those of other published literature and the optimal results are highlighted in bold. The population size and the maximum iteration are set to 1000, 1500, respectively (for case one), 2000, 2000, respectively (for case two, three and four).

a) Case 1: 6-unit system (PD = 1263 MW);

b) Case 2: 13-unit system (PD = 1800 MW);

c) Case 3: 15-unit system (PD = 2630 MW);

d) Case 4: 40-unit system (PD = 10,500 MW);

#### 5.4.2.1 Case 1: 6 Thermal Units and Load Demand 1263 MW.

In this case, the system consists of six thermal units, 26 buses, and 46 transmission lines. The load demand is 1263 MW. Also, ramp-rate limit and power losses are considered and all thermal units have POZs. The characteristics of the system include the cost coefficients, the loss coefficients B and the upper and lower ramp limits, the POZs and the initial output of the units are given in the Appendix G.1 where the maximum and minimum power limit cost coefficients, ramp rates, initial power output, and POZs are given in Appendix A while the B loss coefficients are taken from Appendix G.2.

Table 5.70 presents The optimal scheduling results of the proposed ESCSDO10 with other techniques. The results display that the proposed approach provides better solution quality than other techniques in the operating cost. The cost is 15444.186310 \$/h and it is less than the optimal cost that had reported in the previous papers while satisfying all the constraints like ramp rate limits and POZs as well as the load demand and power generation boundary constraints. In addition, they can clearly handle the generation and demand equality constraint. To understand this, if the power inequality error is defined as error (V)= $P_i - P_D - P_L$ , using the pertinent data from Table 5.70. Fig. 5.45 shows the convergence characteristic curves of SDO, HGS, ESSDO, and ten chaotic maps enhanced for ESCSDO in the ELD problem for best performance in the test system, indicating that the tenth modified of ESCSDO has better convergence than the others. Therefore, it is used in the rest of thesis. Fig. 5.46 shows the boxplots for the first case study. It can be seen that the boxplots of the most of the proposed ESCSDO algorithms are very narrow with the lowest values compared with those of the conventional SDO algorithm. The statistical result consists of the best, the worst, the median, the standard deviation (STD), and the mean cost of generation during 20 independent executions shown in Table 5.71, which shows that the ten proposed ESCSDO algorithms have optimum results compared to others. Furthermore, it is obviously seen that the results of these ten proposed ESCSDO algorithms under each of the proposed modification processes have a better cost than the original SDO algorithm.

Table 5.70: Optimal generations schedule of various algorithms for case study 1.

| Algorithms | P1 | P2 | P3 | P4 | P5 | P6 | V(MW) | PL | C($/h) |
|---|---|---|---|---|---|---|---|---|---|
| **SDO** | 446.7266 | 173.1453 | 262.7876 | 143.4916 | 163.9212 | 85.34966 | 5.00E-08 | 12.422 | 15444.186312 |
| **ESSDO** | 446.7121 | 173.152 | 262.7918 | 143.4897 | 163.9107 | 85.36562 | 1.30E-07 | 12.4219 | 15444.186311 |
| **ESCSDO1** | 446.7148 | 173.1375 | 262.7985 | 143.4928 | 163.9214 | 85.35696 | 4.00E-08 | 12.422 | 15444.186311 |
| **ESCSDO2** | 446.7232 | 173.1516 | 262.7923 | 143.491 | 163.911 | 85.35285 | 2.27E-13 | 12.4219 | **15444.186310** |
| **ESCSDO3** | 446.7032 | 173.1557 | 262.8017 | 143.4953 | 163.9115 | 85.35442 | 6.00E-08 | 12.4218 | 15444.186312 |
| **ESCSDO4** | 446.7181 | 173.1414 | 262.8012 | 143.4898 | 163.923 | 85.34862 | 3.00E-08 | 12.4221 | 15444.186312 |
| **ESCSDO5** | 446.7195 | 173.1549 | 262.8009 | 143.4779 | 163.9094 | 85.35958 | 2.00E-08 | 12.4222 | 15444.186312 |
| **ESCSDO6** | 446.705 | 173.1506 | 262.8023 | 143.491 | 163.9192 | 85.35385 | 2.00E-08 | 12.422 | 15444.186311 |
| **ESCSDO7** | 446.7179 | 173.1517 | 262.7982 | 143.4863 | 163.9178 | 85.35023 | 1.00E-08 | 12.4221 | **15444.186310** |
| **ESCSDO8** | 446.7171 | 173.1498 | 262.7981 | 143.4809 | 163.916 | 85.36022 | 1.00E-07 | 12.4222 | **15444.186310** |
| **ESCSDO9** | 446.7188 | 173.1495 | 262.7911 | 143.4967 | 163.9145 | 85.35121 | 1.30E-07 | 12.4218 | 15444.186311 |
| **ESCSDO10** | 446.7116 | 173.1449 | 262.8022 | 143.4911 | 163.918 | 85.35426 | 5.00E-08 | 12.422 | **15444.186310** |
| **HGS** | 446.7435 | 174.2509 | 261.7852 | 143.8329 | 162.0692 | 86.70681 | 4.00E-08 | 12.3885 | 15444.25963 |
| **GA** [71] | 474.8066 | 178.6363 | 262.2089 | 134.2826 | 151.9039 | 74.1812 | NR[c] | 13.0217 | 15459 |
| **CBA** [199] | 447.4187 | 172.8255 | 264.0759 | 139.2469 | 165.6526 | 86.7652 | NR | 12.984 | 15450.2381 |
| **PSO** [71] | 447.497 | 173.3221 | 263.4745 | 139.0594 | 165.4761 | 87.128 | NR | 12.9584 | 15450 |

| | | | | | | | | | |
|---|---|---|---|---|---|---|---|---|---|
| **NPSO-LRS** [200] | 446.96 | 173.3944 | 262.3436 | 139.512 | 164.7089 | 89.0162 | NR | 12.9361 | 15450 |
| **MABC** [201] | 447.5039 | 173.3187 | 263.4622 | 139.065 | 165.4731 | 87.135 | NR | 12.9582 | 15449.8995 |
| **MSSA** [202] | 447.5029 | 173.3186 | 263.463 | 139.0656 | 165.473 | 87.1349 | NR | 12.958 | 15449.8995 |
| **ST-IRDPSO** [203] | 447.5131 | 173.2975 | 263.4668 | 139.036 | 165.4843 | 87.1605 | NR | 12.958 | 15449.8945 |
| **DE[a]** [70] | 447.744 | 173.407 | 263.411 | 139.076 | 165.364 | 86.944 | NR | 12.957 | 15449.766 |
| **DE[b]** [204] | 448.27 | 172.96 | 263.44 | 139.3 | 165.28 | 86.68 | NR | 12.98 | 15449.5826 |
| **MCSA** [205] | 444.6373 | 174.641 | 265 | 139.2251 | 165.7121 | 86.6807 | NR | 12.9576 | 15449.1672 |
| **HHS** [206] | 447.496 | 173.314 | 263.445 | 139.055 | 165.475 | 87.125 | NR | 12.95 | 15,449.00 |
| **SOH-PSO** [207] | 438.21 | 172.58 | 257.42 | 141.09 | 179.37 | 86.88 | NR | 12.55 | 15,446.02 |
| **MTS** [208] | 448.1277 | 172.8082 | 262.5932 | 136.9605 | 168.2031 | 87.3304 | NR | 13.0205 | 15,450.06 |

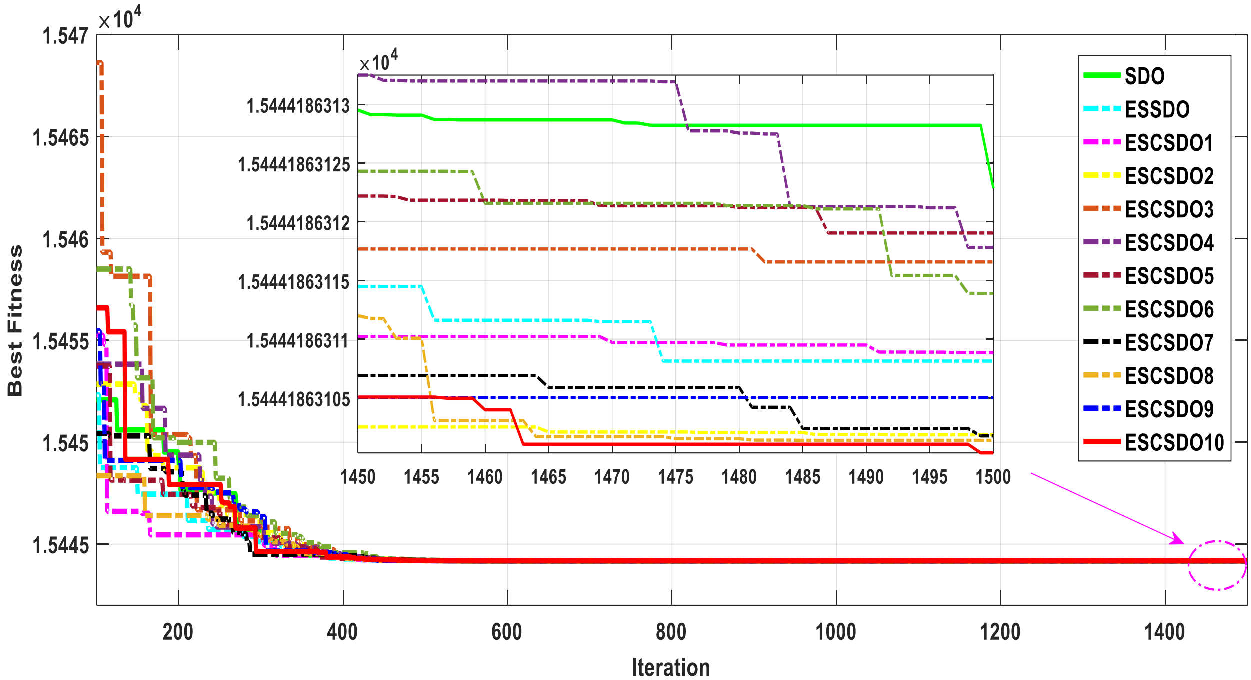


Figure 5.45: Fuel cost convergence curves of different techniques (Case study 1).

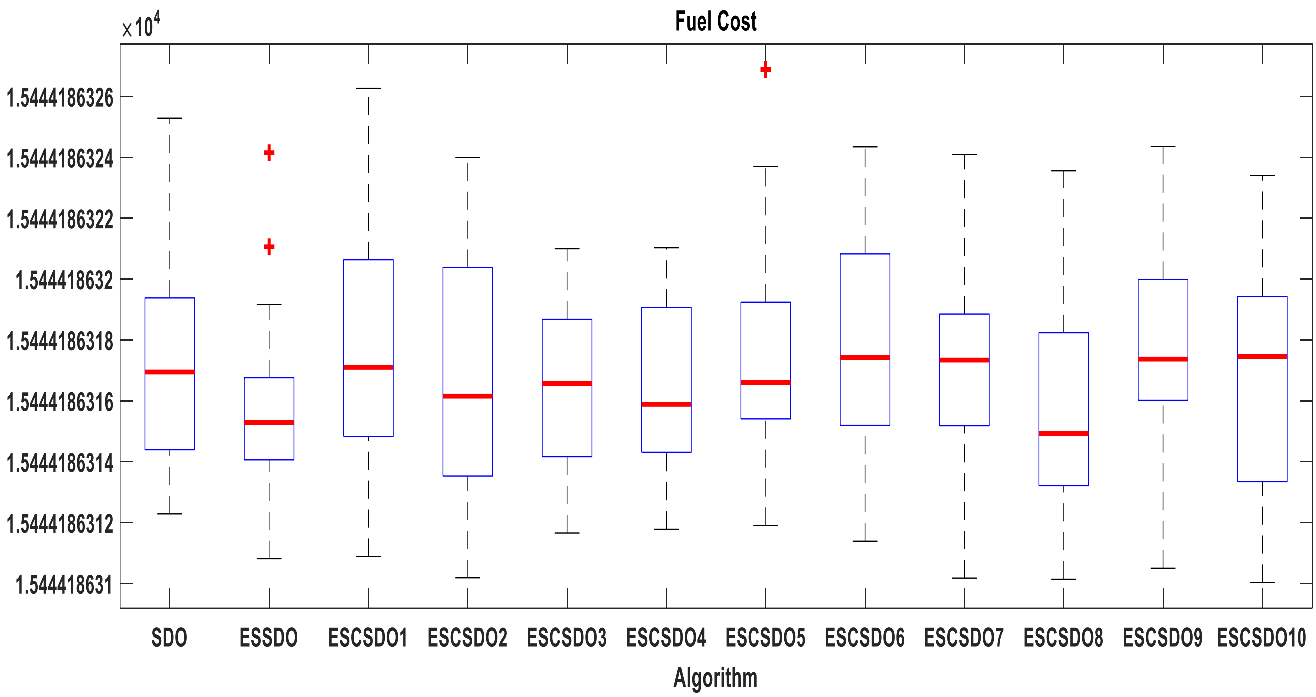


Figure 5.46: the best boxplot of different techniques (Case study 1).

Table 5.71: Fuel costs for Case 1 by various algorithms.

| Algorithm | Best | Worst | Median | Mean | STD |
|---|---|---|---|---|---|
| **SDO** | 15444.186312 | 15444.186325 | 15444.186317 | 15444.186317 | 3.42E-06 |
| **ESSDO** | 15444.186311 | 15444.186324 | **15444.186315** | **15444.186316** | 3.04E-06 |
| **ESCSDO1** | 15444.186311 | 15444.186326 | 15444.186317 | 15444.186318 | 4.51E-06 |
| **ESCSDO2** | **15444.186310** | 15444.186324 | 15444.186316 | **15444.186316** | 4.10E-06 |
| **ESCSDO3** | 15444.186312 | **15444.186321** | 15444.186317 | **15444.186316** | 2.93E-06 |
| **ESCSDO4** | 15444.186312 | **15444.186321** | 15444.186316 | **15444.186316** | **2.82E-06** |
| **ESCSDO5** | 15444.186312 | 15444.186327 | 15444.186317 | 15444.186318 | 3.55E-06 |
| **ESCSDO6** | 15444.186311 | 15444.186324 | 15444.186317 | 15444.186318 | 3.56E-06 |
| **ESCSDO7** | **15444.186310** | 15444.186324 | 15444.186317 | 15444.186317 | 3.71E-06 |
| **ESCSDO8** | **15444.186310** | 15444.186324 | **15444.186315** | **15444.186316** | 3.51E-06 |
| **ESCSDO9** | 15444.186311 | 15444.186324 | 15444.186317 | 15444.186318 | 3.31E-06 |
| **ESCSDO10** | **15444.186310** | 15444.186323 | 15444.186317 | 15444.186317 | 4.03E-06 |
| **GA** [71] | 15,459 | 15,524 | NR[a] | 15,469 | NR |
| **CBA** [199] | 15,450.24 | 15,518.66 | NR | 15,454.76 | 2.965 |
| **PSO** [71] | 15,450 | 15,492 | NR | 15,454 | NR |
| **NPSO-LRS** [200] | 15,450 | 15,454 | NR | 15,452 | NR |
| **MABC** [201] | 15,449.90 | 15,449.90 | NR | 15,449.90 | 6.04×10-8 |
| **MSSA** [202] | 15,449.90 | 15,453.55 | NR | 15,449.94 | 0.3647 |
| **ST-IRDPSO** [203] | 15,449.89 | NR | NR | 15,450.70 | 1.416 |
| **DE[a]** [70] | 15,449.77 | 15,449.87 | NR | 15,449.78 | NR |
| **DE[b]** [204] | 15,449.58 | 15,449.65 | NR | 15,449.62 | NR |
| **MCSA** [205] | 15,449.17 | 15,449.39 | NR | 15,449.24 | 0.2681 |
| **HHS** [206] | 15,449.00 | 15,453.00 | NR | 15,450.00 | NR |
| **SOH-PSO** [207] | 15,446.02 | 15,609.64 | NR | 15,497.35 | NR |

| | | | | | |
|---|---|---|---|---|---|
| **MTS** [208] | 15,450.06 | 15,453.64 | NR | 15,451.17 | NR |
| **GAAPI** [209] | 15449.78 | 15449.85 | NR | 15449.81 | NR |
| **DE** [70] | 15449.766 | 15449.777 | NR | 15449.874 | NR |
| **Jaya** [210] | 15446.5675 | 15573.5151 | NR | 15489.7034 | 13.3122 |
| **Jaya-M** [210] | 15446.0196 | 15498.5242 | NR | 15464.8797 | 10.9328 |
| **Jaya-SM** [210] | 15445.8001 | 15468.923 | NR | 15459.4744 | 8.4657 |
| **Jaya-SML** [210] | 15445.1682 | 15450.6497 | NR | 15447.291 | 6.2214 |
| **SA** [208] | 15461.1 | 15545.5 | NR | 15488.98 | 28.3678 |
| **TS** [208] | 15454.89 | 15498.05 | NR | 15472.56 | 13.7195 |
| **SSGA** [211] | 15447 | 15470 | NR | 15450 | 7.458 |
| **FA** [212] | 15450.509 | 15458.4427 | NR | 15452.531 | 2.048 |
| **CMFA** [212] | 15449.8994 | 15449.8994 | NR | 15449.8994 | 8.96E-06 |

#### 5.4.2.2 Case 2: 13 Units and the Load Demand 1800 MW.

In this case, the ESCSDO10 technique, conventional SDO, ESSDO, and HGS algorithms are implemented on a test system having thirteen thermal units to solve ELD problem with load demand is 1800 MW. The fuel cost with VPLE without considering power losses are taken into account. The system data are taken from Appendix H.

The best-scheduled powers obtained by the ESCSDO10 algorithm are given in Table 5.72. It is clear from Table 5.72 that the proposed ESCSDO10 achieves solution with the less cost (better quality) than the other techniques. The convergence characteristic curves and boxplots of the proposed ESCSDO10, conventional SDO, ESSDO, and HGS algorithms for this case is plotted in Fig. 5.47. In the convergence characteristic curves on Fig. 5.47, It is shown that the proposed algorithm converges in relatively fewer cycles, so it has good convergence properties and results in a low generation cost. In addition, the boxplot of the proposed ESCSDO algorithm is very narrow with the lowest values compared with those of the other algorithms. To obtain more insights on the quality of the solution, 20 individual runs were performed for these test cases and the statistical results obtained are tabulated in Table 5.73. From the statistical results, it is obvious that the generation costs obtained by different individual runs are closer to the optimal solution. Thus, validating that the proposed technique has excellent solution precision and a high-speed rate of convergence characteristics.

Table 5.72: The best solution values of fuel cost for the thirteen-unit system with VPLE without considering transmission losses (PD = 1800 MW).

| Algorithm | SDO | ESSDO | ESCSDO10 | HGS | TLBO [73] | NN-EPSO [213] |
|---|---|---|---|---|---|---|
| P1 | 448.799 | 448.799 | 538.5587 | 360.8537 | 448.7988 | 490 |
| P2 | 152.9354 | 152.9302 | 75.6427 | 360.00 | 224.6004 | 189 |
| P3 | 224.3995 | 224.4018 | 224.3995 | 224.4438 | 149.6106 | 214 |
| P4 | 159.7331 | 109.8673 | 109.8666 | 180.00 | 109.8659 | 160 |
| P5 | 60.00013 | 109.8665 | 109.8666 | 129.6487 | 109.8664 | 90 |
| P6 | 159.7331 | 109.8668 | 109.8666 | 60.00 | 109.8891 | 120 |
| P7 | 109.8665 | 159.7331 | 109.8666 | 112.2345 | 109.8607 | 103 |
| P8 | 109.8669 | 109.8665 | 109.8666 | 60.00 | 109.8962 | 88 |
| P9 | 109.8666 | 109.8688 | 109.8666 | 60.00 | 109.9019 | 104 |
| P10 | 40.00002 | 40.00002 | 40.00 | 40.00 | 77.3953 | 13 |
| P11 | 77.39991 | 40.00002 | 77.39996 | 40.00 | 77.4043 | 58 |
| P12 | 55.00 | 92.39986 | 92.39991 | 117.8193 | 92.4209 | 66 |
| P13 | 92.39992 | 92.40009 | 92.39991 | 55.00 | 70.4896 | 55 |
| C($/h) | 18041.48606 | 18028.56465 | 18028.18877 | 18552.18568 | 18115 | 18442.59 |

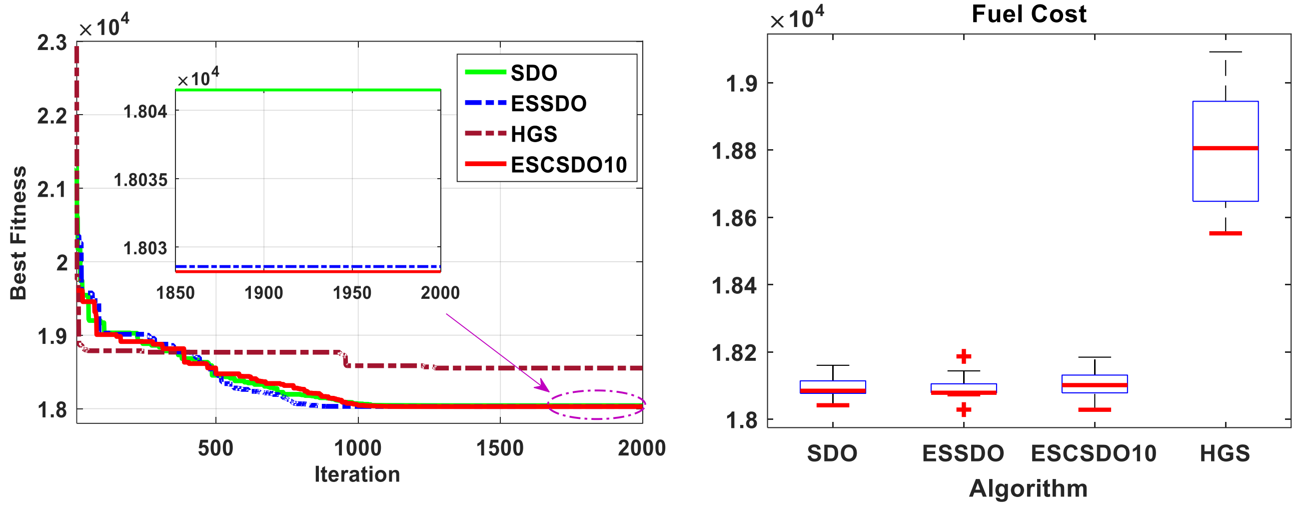


(a) Fuel cost convergence curves (b) best boxplot

Figure 5.47: The best boxplot of different techniques (Case study 2).

Table 5.73: The best solution values of fuel cost for the thirteen-unit system with valve point loading without considering transmission losses (PD = 1800 MW).

| Algorithm | SDO | ESSDO | ESCSDO10 | HGS |
|---|---|---|---|---|
| Best | 18041.49 | 18028.56 | 18028.19 | 18552.19 |
| Worst | 18160.18 | 18186.7 | 18184.35 | 19091.26 |
| Median | 18084.52 | 18078.67 | 18101.29 | 18805.21 |
| Mean | 18092.79 | 18090.5 | 18106.87 | 18816.5 |
| STD | 26.03665 | 32.17784 | 40.5607 | 179.723 |

#### 5.4.2.3 Case 3: 15 Units and the Load Demand 2630 MW.

This system consists of 15 units; System capacity and coefficient are given in Appendix I.1. The load demand is set to 2630 MW. In this system, some thermal units have no POZ, while one unit has two POZs and others have three ones. The coefficients B of the system to obtain network losses can be taken from Appendix I.2.

The best results obtained using the proposed ESCSDO10 algorithm for this case are detailed in Table 5.74. The obtained results are compared with those of SDO, ESSDO, HGS, APSO [214], CPSO2 [215], EO [216], and EO-SCA [217]. As is evident from Table 8, the ESCSDO10 achieves better results than the other methods. Furthermore, the obtained results satisfied all the constraints. Fig. 5.48 is presented the convergence curves and boxplots of the proposed ESCSDO10 and other competitive algorithms for the fuel cost of the 15 thermal units system. It is obvious from this figure that both ESSDO and ESCSDO10 provide the lower cost than other techniques. ESCSDO10 is actually an improvement of ESSDO and the original SDO technique. The best, worst, median, mean, and STD obtained using the proposed ESCSDO10 technique and many well-known algorithms are shown in Table 5.75.

Table 5.74: The best solution values of fuel cost for the fifteen-unit system for a demand of 2630 MW.

| Algorithm | SDO | ESSDO | ESCSDO10 | HGS | APSO [214] | CPSO2 [215] | EO [216] | EO-SCA [217] |
|---|---|---|---|---|---|---|---|---|
| P1 | 455 | 454.9999 | 455 | 455 | 455 | 450.02 | 455 | 455 |
| P2 | 379.9996 | 379.9992 | 379.9996 | 380 | 380.01004 | 454.06 | 380 | 380 |
| P3 | 129.9995 | 130 | 129.9999 | 130 | 130 | 124.81 | 130 | 129.99 |
| P4 | 130 | 129.9999 | 130 | 130 | 126.52284 | 124.81 | 130 | 130 |
| P5 | 169.9999 | 170 | 170 | 169.9999 | 170.01312 | 151.06 | 170 | 170 |
| P6 | 459.9999 | 460 | 460 | 460 | 460 | 460 | 460 | 460 |
| P7 | 429.9984 | 429.9998 | 430 | 430 | 428.28356 | 434.57 | 430 | 430 |
| P8 | 67.74251 | 70.71708 | 70.25793 | 60 | 60 | 148.46 | 60 | 67.91 |
| P9 | 61.83312 | 58.87155 | 59.33272 | 69.55549 | 25 | 63.59 | 69.871 | 62.38 |
| P10 | 159.9982 | 159.9986 | 159.9956 | 160 | 159.78932 | 101.12 | 160 | 160 |
| P11 | 79.99983 | 79.99998 | 80 | 80 | 80 | 28.655 | 80 | 80 |
| P12 | 79.99986 | 80 | 80 | 80 | 80 | 20.914 | 80 | 79.99 |
| P13 | 25.00081 | 25.00042 | 25.00012 | 25 | 33.70376 | 25.002 | 25 | 25 |
| P14 | 15.00454 | 15.00197 | 15.00058 | 15 | 55 | 54.414 | 15.206 | 15 |
| P15 | 15.00102 | 15.00174 | 15.00171 | 15 | 15 | 20.624 | 15.191 | 15 |
| Total power generation (MW) | 2659.57719 | 2659.59014 | 2659.58816 | 2659.55539 | 2658.3226 | 2662.1 | 2660.268 | 2660.27 |
| Ploss (MW) | 29.57719 | 29.59014 | 29.58816 | 29.55539 | 28.36552996 | 32.1303 | 30.2707 | 30.295 |
| C($/h) | 32692.413062 | 32692.40489 | 32692.40133 | 32692.64264 | 32742.7774 | 32834 | 32701.18 | 32700.51 |

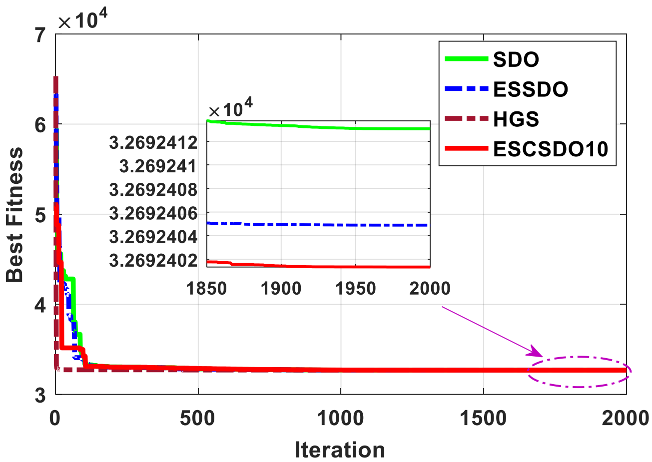


(a) Fuel cost convergence curves

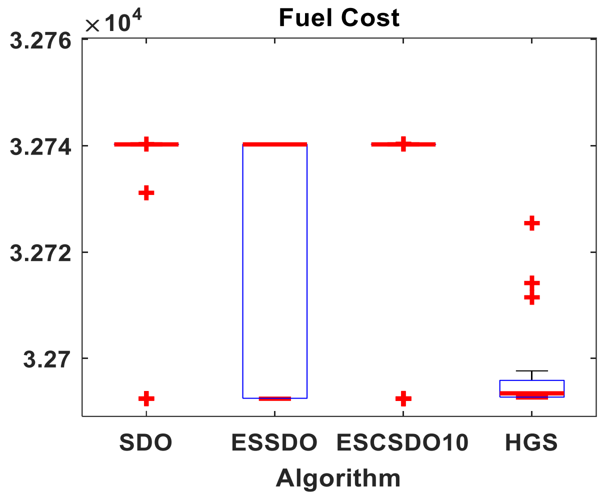


(b) best boxplot

Figure 5.48: the convergence curves and the best boxplot of different techniques (Case study 3).

Table 5.75: The best solution values of fuel cost for the fifteen-unit system for a demand of 2630 MW.

| Algorithm | Best | Worst | Median | Mean | STD |
|---|---|---|---|---|---|
| SDO | 32692.41 | 32740.32 | 32740.26 | 32732.64 | 17.4465 |
| ESSDO | 32692.4 | 32740.33 | 32740.26 | 32725.92 | 22.4866 |
| ESCSDO10 | 32692.4 | 32740.36 | 32740.26 | 32730.71 | 19.64 |
| HGS | 32692.64 | 32725.4 | 32693.4 | 32697.3 | 8.948 |
| EO [216] | 32701.18 | 32701.51 | NR[a] | 32701.31 | NR |
| ABC [218] | 32787.836 | NR | NR | 32791.5366 | NR |
| FA [219] | 32704.5 | 33175 | NR | 32856.1 | NR |
| MPSO-GA [220] | 32702 | 32755.19 | NR | 32701.31 | NR |
| EO-SCA [217] | 32700.51 | 32701.05 | NR | 32702.74 | NR |
| PSOSIF [221] | 32,706.88 | 32,709.92 | NR | 32,707.79 | 3.04 |
| GAAPI [209] | 32,732.95 | 32,756.01 | NR | 32,735.06 | NR |
| FA [219] | 32,704.45 | 33,175.00 | NR | 32,856.10 | NR |
| EPSO [222] | 32,704.83 | 32,762.01 | NR | 32,725.37 | NR |
| IAEDP [223] | 32,698.20 | 32,823.78 | NR | 32,750.22 | 29.2989 |
| EMA [224] | 32,704.45 | 32,704.45 | NR | 32,704.45 | NR |

| | | | | | |
|---|---|---|---|---|---|
| GABC [225] | 32,706.66 | 32706.81 | NR | 32,706.69 | 0.035838 |
| TLBO [226] | 32,697.22 | 32,697.22 | NR | 32,697.22 | 0 |
| Jaya [210] | 32712.6458 | 32822.9993 | NR | 32743.4613 | 47.0256 |
| Jaya-M [210] | 32707.0312 | 32743.6808 | NR | 32714.4386 | 12.0972 |
| Jaya-SM [210] | 32706.983 | 32728.2292 | NR | 32709.0463 | 8.7817 |
| Jaya-SML [210] | 32706.3578 | 32707.2925 | NR | 32706.6764 | 2.3244 |
| TS [227] | 32917.87 | 33245.54 | NR | 33066.76 | 66.82 |
| DSPSO-TS [227] | 32715.06 | 32730.39 | NR | 32724.63 | 8.4 |
| BF-NM [228] | 32784.5024 | NR | NR | 32976.81 | 85.77 |
| CSO [229] | 32709.36 | 32722.55 | NR | 32712.49 | 4.56 |
| CCSO [229] | 32706.64 | 32706.64 | NR | 32706.64 | 0.0007 |

#### 5.4.2.4 Case 4: 40 Units and the Load Demand 10,500 MW.

In this case, the solution to the ELD problem has been presented for a test system consisting of forty thermal units with VPLE and without considering the power loss. The total load demand is 10,500 MW and the system data is taken from Appendix E.1. With a larger scale power system, the number of local minima in the solution search space increases. This fact shows that optimization techniques must have a more powerful search capability to avoid early convergence.

The best scheduled powers provided using ESCSDO10, SDO, ESSDO, HGS, DE [230], TLBO [231], and HSSA [232] algorithm are given in Table 5.76. The results show that ESCSDO10 outperforms all other compared techniques in reaching optimal results. The convergence curve and the best boxplots of the ESCSDO10 and the other techniques are given in Fig. 5.49. The minimum, maximum, median, mean, STD values have been compared with ESCSDO10, SDO, ESSDO, HGS for the 20 trails for this case as presented in Table 5.77. In this case, the best, worst, mean value of generation costs and STD are 121,626.97 $/hr, 123,128.9 $/hr 122351.7 $/hr, and 412.2976 achieved by the proposed ESCSDO10 algorithm while only the best median value is achieved by the ESSDO algorithm.

Table 5.76: The best solution values of the total fuel cost for the forty-unit system.

| Algorithm | SDO | ESSDO | ESCSDO10 | HGS | DE [230] | TLBO [231] | HSSA [232] | QOPO [233] |
|---|---|---|---|---|---|---|---|---|
| P1 | 112.1391 | 111.3958 | 110.8002 | 114 | 110.952 | 110.868 | 113.9994 | 113.7611 |
| P2 | 113.106 | 111.7094 | 110.7814 | 114 | 113.300 | 111.068 | 113.9999 | 113.9886 |
| P3 | 97.40064 | 97.40771 | 97.3987 | 60.1394 | 98.616 | 97.633 | 119.9999 | 119.9993 |
| P4 | 179.7355 | 179.7576 | 179.7312 | 179.7998 | 184.149 | 179.774 | 189.9998 | 189.8949 |
| P5 | 87.80159 | 89.18163 | 87.79114 | 97 | 86.401 | 88.272 | 97 | 97 |
| P6 | 105.421 | 105.5467 | 139.9984 | 140 | 140.000 | 140.000 | 140 | 139.9986 |
| P7 | 259.6137 | 259.6439 | 259.5963 | 300 | 300.000 | 259.630 | 280.6695 | 300 |
| P8 | 284.6095 | 284.5999 | 284.5963 | 300 | 285.456 | 284.591 | 290.4195 | 299.9992 |
| P9 | 284.5989 | 284.6077 | 284.5915 | 300 | 297.511 | 284.671 | 292.5067 | 299.997 |
| P10 | 204.8536 | 130.0001 | 130.0107 | 130 | 130.000 | 130.096 | 130.0001 | 130 |
| P11 | 168.8005 | 94.00019 | 239.0063 | 94.00006 | 168.748 | 168.801 | 168.7998 | 94.0011 |
| P12 | 168.8032 | 168.801 | 166.3011 | 94 | 95.695 | 168.352 | 168.7998 | 94.35996 |
| P13 | 304.5121 | 394.275 | 214.7574 | 125 | 125.000 | 304.425 | 214.7598 | 125.1963 |
| P14 | 394.2813 | 394.2988 | 304.5057 | 394.2847 | 394.355 | 214.786 | 304.5196 | 304.5059 |
| P15 | 304.5089 | 304.5235 | 394.2829 | 394.2796 | 305.523 | 484.177 | 304.5196 | 394.4782 |
| P16 | 304.5268 | 394.2794 | 394.2769 | 394.2794 | 394.715 | 304.844 | 394.2793 | 394.2599 |
| P17 | 489.3018 | 489.2851 | 489.276 | 489.3126 | 489.797 | 489.198 | 489.2812 | 489.331 |
| P18 | 489.2864 | 489.3087 | 489.2794 | 489.2963 | 489.362 | 489.467 | 489.2795 | 489.4125 |
| P19 | 511.2827 | 511.3006 | 511.2789 | 511.2809 | 520.902 | 511.451 | 511.2795 | 511.2939 |
| P20 | 511.3339 | 511.28 | 511.2788 | 511.3354 | 510.641 | 511.289 | 511.2795 | 511.4796 |
| P21 | 523.3314 | 523.2836 | 523.2804 | 523.5524 | 524.534 | 523.244 | 523.2794 | 525.461 |
| P22 | 523.2799 | 523.2759 | 523.2774 | 523.366 | 526.698 | 523.275 | 523.7119 | 523.6933 |
| P23 | 523.2755 | 523.2844 | 523.2791 | 539.7297 | 530.747 | 523.400 | 523.2794 | 526.5896 |
| P24 | 523.4085 | 523.2795 | 523.2744 | 523.8539 | 526.327 | 523.329 | 523.2795 | 524.3047 |

| | | | | | | | | |
|---|---|---|---|---|---|---|---|---|
| P25 | 523.2736 | 523.3598 | 523.2783 | 523.3009 | 525.654 | 523.382 | 523.8181 | 524.7312 |
| P26 | 523.2832 | 523.3029 | 523.2836 | 523.3843 | 522.950 | 523.275 | 523.2794 | 523.5606 |
| P27 | 10.06301 | 10.01909 | 10.00249 | 10 | 10.000 | 10.068 | 13.8386 | 10 |
| P28 | 10.00807 | 10.01497 | 10.00074 | 10 | 11.552 | 10.018 | 11.7804 | 10.22341 |
| P29 | 10.00798 | 10.00053 | 10.00303 | 10 | 10.000 | 10.103 | 10.1857 | 10.08921 |
| P30 | 89.64376 | 90.34668 | 87.79601 | 97 | 89.908 | 90.550 | 94.8277 | 97 |
| P31 | 161.123 | 161.6513 | 189.9963 | 190 | 190.000 | 190.000 | 189.9999 | 190 |
| P32 | 189.9989 | 189.9978 | 189.9999 | 190 | 190.000 | 190.000 | 181.897 | 189.9998 |
| P33 | 189.9791 | 161.145 | 189.9845 | 190 | 190.000 | 190.000 | 187.162 | 190 |
| P34 | 164.7992 | 164.8925 | 164.8044 | 172.5026 | 198.840 | 164.902 | 164.8096 | 200 |
| P35 | 164.9028 | 164.919 | 164.8001 | 200 | 174.178 | 164.861 | 180.4562 | 200 |
| P36 | 164.8301 | 164.9784 | 164.7969 | 200 | 197.160 | 164.921 | 199.9853 | 199.9999 |
| P37 | 109.9967 | 95.76652 | 89.09699 | 110 | 110.000 | 110.000 | 108.2447 | 109.9804 |
| P38 | 97.59832 | 109.9943 | 89.11364 | 110 | 109.357 | 110.000 | 90.2908 | 110 |
| P39 | 109.9998 | 109.9976 | 89.11416 | 110 | 110.000 | 110.000 | 89.2026 | 110 |
| P40 | 511.2801 | 511.2872 | 511.2784 | 511.3023 | 510.975 | 511.279 | 511.2793 | 511.4108 |
| C($/h) | 121750.18 | 121873.64 | 121626.97 | 121869.54 | 121840 | 121685.00 | 121960.27 | 121789.6 |

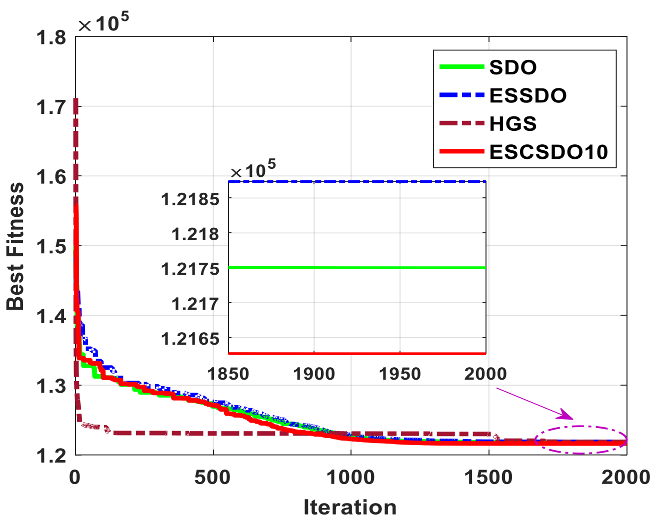


(a) Fuel cost convergence curves

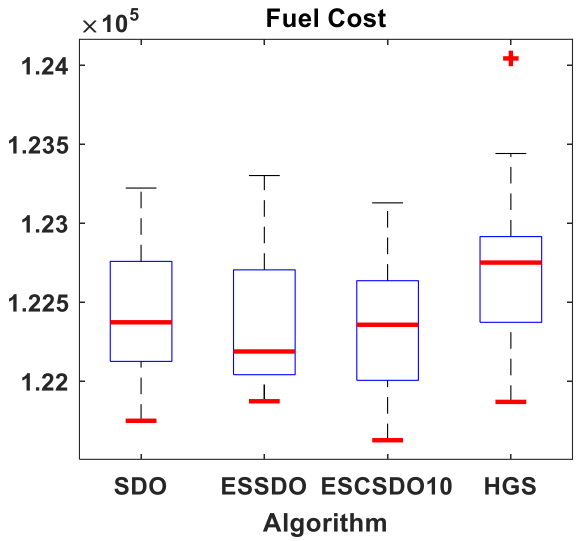


(b) best boxplot

Figure 5.49: the convergence curves and the best boxplot of different algorithms (Case study 4).

Table 5.77: The best solution values of the total fuel cost for the forty-unit system.

| Algorithm | SDO | ESSDO | ESCSDO10 | HGS |
|---|---|---|---|---|
| Best | 121750.2 | 121873.6 | 121626.97 | 121869.5 |
| Worst | 123222.7 | 123301.8 | 123128.9 | 124042.9 |
| Median | 122373.2 | 122188.6 | 122357.7 | 122751.1 |
| Mean | 122460.1 | 122380.5 | 122351.7 | 122751.2 |
| STD | 405.019 | 449.9904 | 412.2976 | 496.8103 |

### 5.4.3 Formulation of EED Problem as a Multi-objective Function

#### 5.4.3.1 Solving EED Problem using MOIMRFO Algorithm

*A. Scenario 1 : 6 thermal units with 225 MW load demand (fuel cost and SO2 emission).*

The PFs and BCS solutions obtained by MOMRFO and proposed MOMRFO–GBO algorithms are shown in Fig. 13. It can be seen that the PF of MOMRFO–GBO algorithm is much more densely-distributed than that of MOMRFO algorithm. The BCS found by MOMRFO–GBO algorithm which includes 4522.366 \$/h of fuel cost and 4760.87 kg/h of SO2 emission dominate the BCS found by MOMRFO method which includes 4541.581 \$/h of fuel cost and 4771.595 kg/h of SO2 emission as shown in Table 13.

*B. Scenario 2 : 6 thermal units with 225 MW load demand (fuel cost and NO$x$ emission).*

The PFs of scenario 2 found by MOMRFO and proposed MOMRFO–GBO algorithms are shown in Fig. 14. The BCS of each algorithm is also noted in Fig. 14. It is observed that the PF obtained by MOMRFO–GBO algorithm is better than these of MOMRFO method. In addition, Table 14 gives the control variables of BCS for Scenario 2 and it illustrates that the BCS of MOMRFO–GBO algorithm with 4421.113 \$/h of fuel cost and 3590.079 kg/h of NO$x$ emission dominates the BCS solutions of the MOMRFO algorithm.

*C. Scenario 3 : 6 thermal units with 225 MW load demand (fuel cost and CO2 emission).*

The performance of the MOMRFO–GBO algorithm in optimizing the fuel cost and the CO2 emission is studied in this scenario. Fig. 5.50 shows the PFs and BCS of scenario 3 and it can be clearly seen that MOMRFO–GBO algorithm achieves the preferable PF. Besides, the control variables of obtained BCS are listed in Table 5.78. It can be clearly observed that the BCS obtained by the MOMRFO–GBO algorithm which includes 4407.282 \$/h of fuel cost and 4120.251 kg/h of CO2 emission dominates the BCS obtained by the MOMRFO algorithm with 4409.72 \$/h of fuel cost and 4121.115 kg/h of CO2 emission.

### 5.4.3.2 Solving EED Problem using MOCAEO Algorithm

In this subsection, a MOCAEO4 algorithm is applied for obtaining the optimal point to minimize the first objective function (the fuel cost) with one of three emission types (SO2, NOx, and CO2) as the second objective function in the 6-unit power generation system for the fourth level of demand (250MW).

*1) CASE 1: the optimum values of the fuel cost and SO2 emission.*

In the 1st case, the MOCAEO4 algorithm is used for obtaining the best values of fuel cost (1st objective function) and SO2 emission (2nd objective function) simultaneously. Figure 5.50.a shows The Pareto optimal values of this case. The best solutions obtained by the MOCAEO4 algorithm are presented in Table 5.78. From this table, the best compromise fuel costs and emission of SO2 are 4348.79 \$/h and 5297.95 kg/h, respectively.

*2) CASE 2: the optimum values of the fuel cost and NOx emission.*

In the 2nd case, the MOCAEO4 algorithm is used for obtaining the best values of fuel cost (1st objective function) and NOx emission (2nd objective function) simultaneously. Figure 5.50.b shows The

Pareto optimal values of this case. The best solutions obtained by the MOCAEO4 algorithm are presented in Table 5.78. From this table, the best compromise fuel costs and emission of NOX are 4332.28 \$/h and 3789.72 kg/h, respectively.

*3) CASE 3: the optimum values of the fuel cost and CO2 emission.*

In the 3rd case, the MOCAEO4 algorithm is used for obtaining the best values of fuel cost (1st objective function) and emission of CO2 (2nd objective function) simultaneously. Figure 5.50.c shows The Pareto optimal values of this case. The best solutions obtained by the MOCAEO4 algorithm are presented in Table 5.78. From this table, the best compromise fuel costs and emission of CO2 are 4310.178 \$/h and 4323.98 kg/h, respectively.

Table 5.78: BCS for Multi-objective functions using MOCAEO4 (load=225MW).

| | Objective | Fuel Cost (\$/h) | Emission (kg/h) |
|---|---|---|---|
| **Case (1)** | Best Fuel Cost | 4343.48 | 5342.96 |
| | Best Emission of $SO_2$ | 4352.39 | 5285.28 |
| | Best Compromise | 4346.44 | 5310.487 |
| **Case (2)** | Best Fuel Cost | 4313.49 | 383979 |
| | Best Emission of $NO_x$ | 4332.28 | 3798.72 |
| | Best Compromise | 4321.18 | 3811.77 |
| **Case (3)** | Best Fuel Cost | 4309.51 | 4332.88 |
| | Best Emission of $CO_2$ | 4310.93 | 4319.83 |
| | Best Compromise | 4310.178 | 4323.98 |

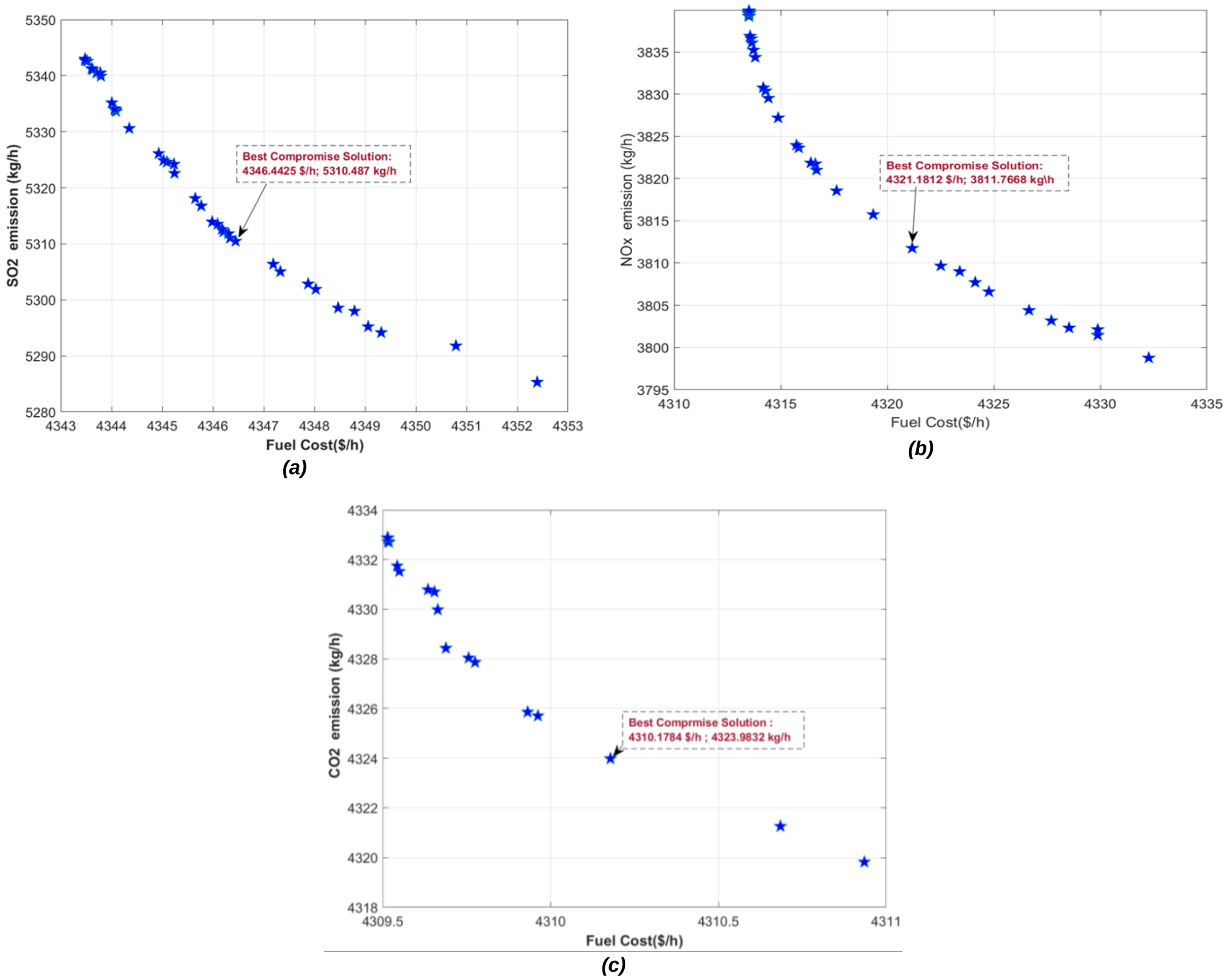


Figure 5.50: Pareto-optimal front for (a) Fuel cost and SO2 emission (b) Fuel cost and NOx emission (c) Fuel cost and CO2 emission.

### 5.4.3.3 Solving EED Problem using MOISMA Algorithm

The bi-objective case optimizes two objective functions at the same time. In this subsection, MOSMA and MOISMA are applied to minimize the total fuel costs and total emission with the valve point effect simultaneously. Different test systems (6-unit, 10-unit, 11-unit, and 40-unit) are used for validation of the proposed MOISMA.

*1) Case 1: 6 thermal units and the load demand 2.834 p.u.*

Table 5.79 presents the BCS obtained by the conventional and proposed algorithms for the 6-unit system. From this table, it can be observed that the MOISMA gives violation, fuel cost, and total emission lower than that obtained from MOSMA. The diagram of the PF for the 6-unit system is shown in Fig.

5.51. Fig. 5.51 shows the PFs and two BCS solutions obtained by MOSMA and MOISMA algorithms. It clearly indicates that the PF of MOISMA is significantly superior to that of MOSMA method.

Table 5.79: BCS obtained by the conventional and proposed algorithms for 6-unit system.

| Algorithm | MOSMA | MOISMA |
|---|---|---|
| **P1** | 0.292415 | 0.267784 |
| **P2** | 0.362209 | 0.372484 |
| **P3** | 0.544321 | 0.568783 |
| **P4** | 0.675412 | 0.662514 |
| **P5** | 0.548436 | 0.5435681 |
| **P6** | 0.438636 | 0.445258 |
| **V(MW)** | 1.24E-05 | **1.185E-05** |
| **PL** | 0.027441 | **0.026404** |
| **C($/h)** | 617.657 | **617.445** |
| **E(ton/h)** | 0.19979 | **0.19973** |

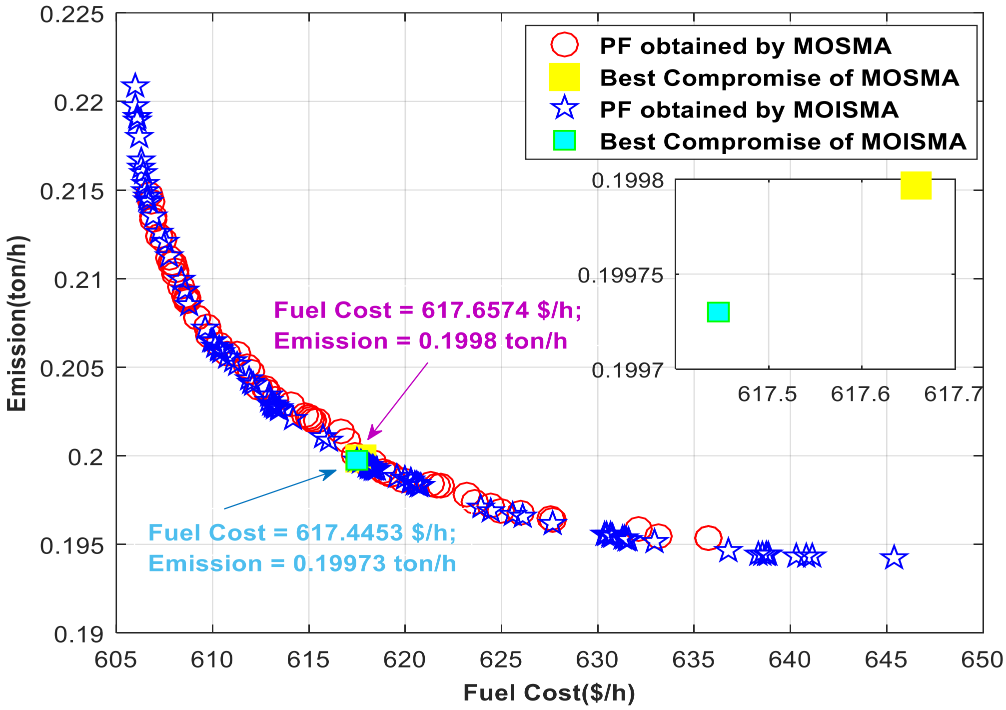


Figure 5.51: PFs of MOSMA and MOISMA for Case 1.

*2) Case 2: 10 thermal units and the load demand (2000 MW).*

Table 5.80 presents the control variables of BCS solutions for case 2. In great detail, the BCS obtained by MOISMA algorithm, including 113157.1 $/h of fuel cost and 4147.189 ton/h of total emission, dominates the one obtained by MOSMA method, which is composed by 113160.08 $/h of fuel cost and 4151.035 ton/h of the total emission. The PFs and BCS of MOSMA and MOISMA for case 2 is displayed in Fig. 5.52.

Table 5.80: BCS obtained by the conventional and proposed algorithms for the 10-unit system.

| Algorithm | MOSMA | MOISMA |
|---|---|---|
| **P1** | 54.99898 | 54.99892 |
| **P2** | 79.30741 | 79.99947 |
| **P3** | 75.7141 | 84.58053 |
| **P4** | 85.57688 | 85.61728 |
| **P5** | 134.7269 | 144.9902 |
| **P6** | 158.7503 | 146.2789 |
| **P7** | 299.9994 | 298.7859 |
| **P8** | 317.6831 | 323.046 |
| **P9** | 432.9296 | 429.4932 |
| **P10** | 444.8241 | 436.3989 |
| **V(MW)** | 0.049319 | **0.000184** |
| **PL** | 84.4615512 | **84.18962** |
| **C($/h)** | 113160.0834 | **113157.1** |
| **E(ton/h)** | 4151.0351 | **4147.189** |

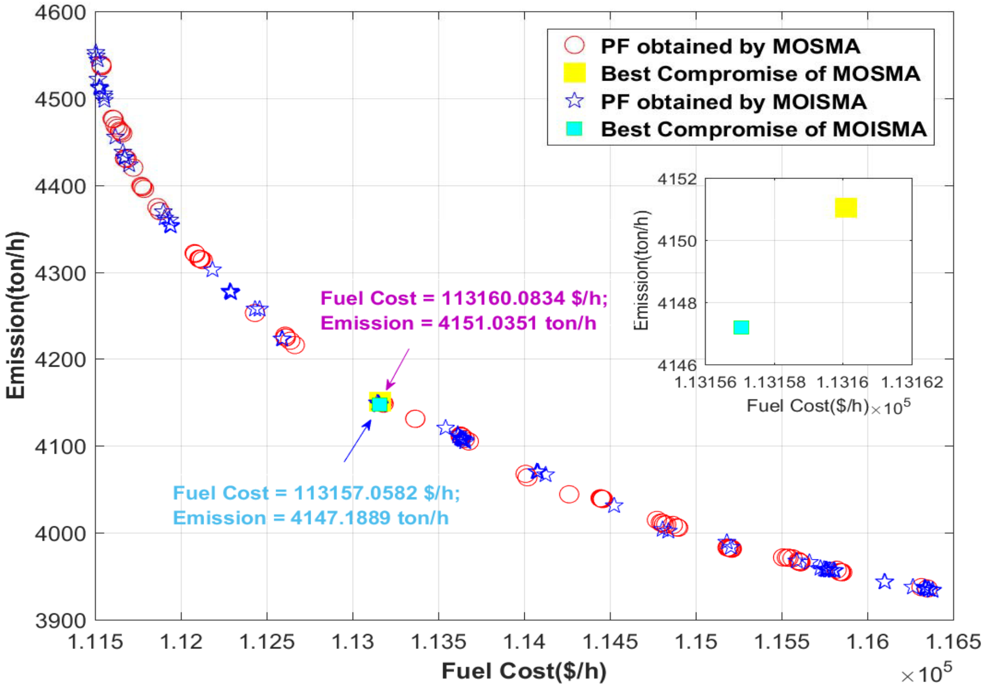


Figure 5.52: PFs of MOSMA and MOISMA for Case 2.

*3) Case 3: 11 thermal units and the load demand (2500 MW).*

The PFs and BCS solutions obtained by MOSMA and MOISMA algorithms are shown in Fig. 5.53. It can be intuitively seen that the PF of MOISMA algorithm is much more densely-distributed than that of MOSMA algorithm. The BCS found by MOISMA algorithm, which includes 12502.32 $/h of fuel cost and 1898.941 ton/h of total emission, dominate the BCS found by MOSMA method, which includes 12509.14 $/h of fuel cost and 1901.268 ton/h of total emission as shown in Table 5.81.

Table 5.81: BCS obtained by the conventional and proposed algorithms for the 11-unit system.

| **Algorithm** | **MOSMA** | **MOISMA** |
|---|---|---|
| **P1** | 160.5747 | 155.4639 |
| **P2** | 129.3908 | 127.7865 |
| **P3** | 166.5161 | 171.5115 |
| **P4** | 180.1807 | 185.0099 |
| **P5** | 136.7893 | 141.8601 |
| **P6** | 205.4702 | 202.7223 |
| **P7** | 144.686 | 178.2459 |
| **P8** | 353.3736 | 343.6647 |
| **P9** | 329.6248 | 329.4211 |
| **P10** | 372.0666 | 345.9288 |
| **P11** | 321.3729 | 318.3848 |
| **V(MW)** | 0.045627 | **0.00035743** |
| **C($/h)** | 12509.14 | **12502.32** |
| **E(ton/h)** | 1901.268 | **1898.941** |

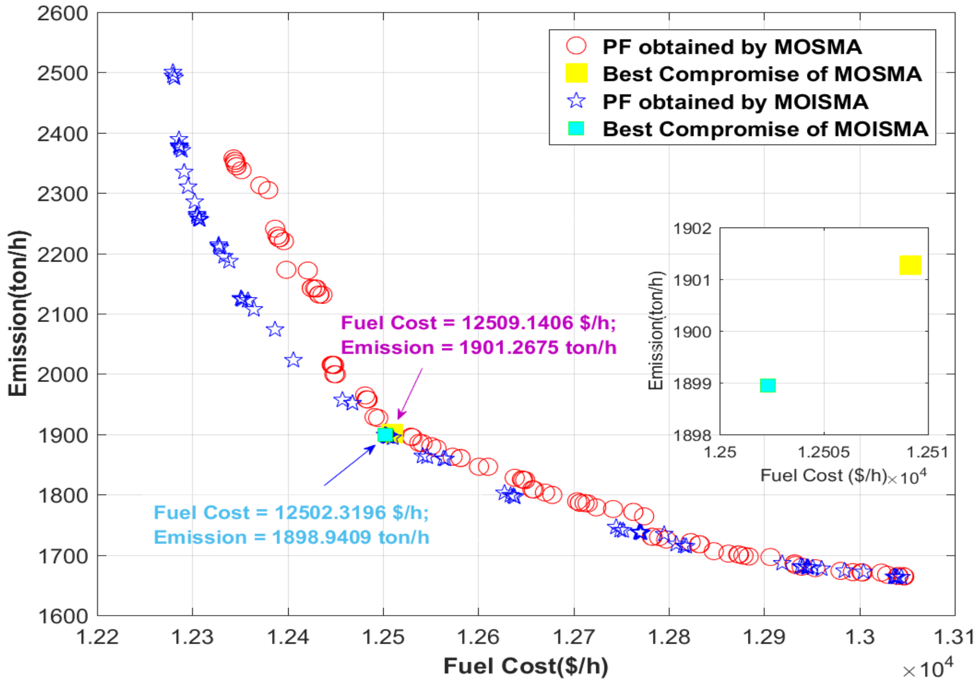


Figure 5.53: PFs of MOSMA and MOISMA for Case 3.

*4) Case 4: 40 thermal units and the load demand (10,500 MW)*

Table 5.82 provides the control variables of BCS solutions, and it illustrates that the BCS of MOISMA algorithm with 128854 $/h of fuel cost and 268123.9 ton/h of total emission dominates the BCS solutions of MOSMA approach. Furthermore, the comparison results of case 4 are summarized in Table 5.82. The BCS of each algorithm is also noted in Fig. 5.54. It intuitively shows the PF obtained by MOISMA algorithm is better than these of MOSMA method.

Table 5.82: BCS obtained by the conventional and proposed algorithms for the 40-unit system.

| **Algorithm** | **MOSMA** | **MOISMA** |
|---|---|---|
| **P1** | 36.6581 | 106.4596 |
| **P2** | 94.10899 | 98.4987 |
| **P3** | 78.36882 | 93.25813 |
| **P4** | 161.2073 | 183.5849 |
| **P5** | 65.95805 | 56.22773 |
| **P6** | 97.31122 | 115.5283 |
| **P7** | 269.5362 | 250.3779 |
| **P8** | 275.9292 | 299.9128 |
| **P9** | 289.2351 | 293.409 |
| **P10** | 130 | 217.884 |

| | | |
|---|---|---|
| **P11** | 257.475 | 274.0929 |
| **P12** | 359.1619 | 249.0477 |
| **P13** | 485.4511 | 498.405 |
| **P14** | 494.2098 | 302.4048 |
| **P15** | 388.773 | 478.4737 |
| **P16** | 468.3695 | 413.7042 |
| **P17** | 481.7396 | 490.3569 |
| **P18** | 499.4854 | 488.0915 |
| **P19** | 325.1944 | 464.5275 |
| **P20** | 435.1771 | 497.0222 |
| **P21** | 495.6378 | 461.6151 |
| **P22** | 500.4219 | 516.7007 |
| **P23** | 443.5696 | 418.4374 |
| **P24** | 485.1195 | 488.6662 |
| **P25** | 437.217 | 429.2396 |
| **P26** | 504.5181 | 484.0058 |
| **P27** | 46.10585 | 12.11016 |
| **P28** | 30.97538 | 10 |
| **P29** | 18.32196 | 10.93784 |
| **P30** | 97 | 53.35885 |
| **P31** | 168.9875 | 167.0447 |
| **P32** | 181.972 | 159.3065 |
| **P33** | 189.7907 | 178.6797 |
| **P34** | 179.3669 | 200 |
| **P35** | 198.1836 | 187.3998 |
| **P36** | 184.8197 | 173.103 |
| **P37** | 61.74886 | 42.44542 |
| **P38** | 43.17287 | 102.9936 |
| **P39** | 28.57111 | 25.16563 |
| **P40** | 511.943 | 507.4303 |
| **V(MW)** | 0.79321 | **0.092115** |
| **C($/h)** | 131572.8 | **128854** |
| **E(ton/h)** | 281521.6 | **268123.9** |

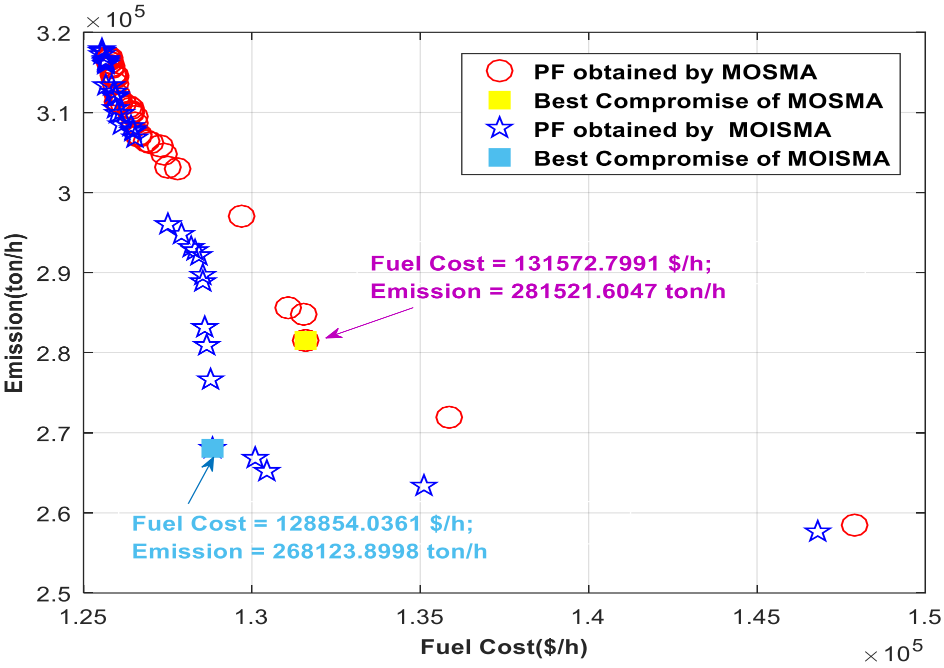


Figure 5.54: PFs of MOSMA and MOISMA for Case 4.

### 5.4.3.4 Solving EED Problem using MOMMPA Algorithm

Multi-objective Marine predators algorithm (MOMPA) and MOMMPA algorithms are applied in this subsection to minimize the fuel cost (first objective function) and one of three emission types (SO2, NOx, and CO2) as a second objective function in the 6-unit IEEE 30- bus system with 250 MW of demand.

*1) Case 1: Minimization of fuel cost and SO2 emission.*

In the 1st case, the MOMPA and MOMMPA algorithms are used for getting the most suitable values of fuel cost and SO2 emission simultaneously. In this case, the Pareto optimal values are shown in Figure 5.55. The BCSs obtained by the MOMPA and MOMMPA algorithms are presented in Table 5.83. From this table, it can be observed that MMPA provides the lowest values of fuel costs and emission of SO2 which are 4406.9727 $/h and 4966.1396 kg/h, respectively.

*2) Case 2: Minimization of fuel cost and NOx emission.*

The MOMPA and MOMMPA algorithms are used for achieving the optimal values of fuel cost and NOx emission simultaneously in the 2nd case. In this case, Figure 5.56 displays the Pareto optimal values. The BCSs obtained by the MOMPA and MOMMPA algorithms are presented in Table 5.83. We can see that the MMPA provides the BCSs between fuel and emission of NOX costs, which are 4381.1064 $/h and 3632.1305 kg/h, respectively.

*3) Case 3: Minimization of fuel cost and CO2 emission.*

In this case, the MOMPA and MOMMPA algorithms are used for reaching the optimum values of fuel cost and emission of CO2 simultaneously. Figure 5.57 presents the Pareto optimal values. The best solutions achieved by MOMPA and MOMMPA algorithms are presented in Table 5.83. From this table, the BCSs of MMPA for fuel costs and emission of CO2 are 4411.5296 $/h and 4113.0703 kg/h, respectively which are lower than the values obtained by the conventional MPA.

Table 5.83: BCS of obtained by the MOMPA and MOMMPA algorithms for 6-unit generation system (load=225MW).

| Case No. | Objective | MOMPA | MOMMPA |
|---|---|---|---|
| 1 | Fuel cost | 4422.5105 | 4406.9282 |
| | $So_2$ | 5004.7907 | 4966.3561 |
| 2 | Fuel cost | 4383.0501 | 4381.1064 |
| | $No_X$ | 3635.8501 | 3632.1305 |
| 3 | Fuel cost | 4414.9667 | 4411.5296 |
| | $Co_2$ | 4125.1976 | 4113.0561 |

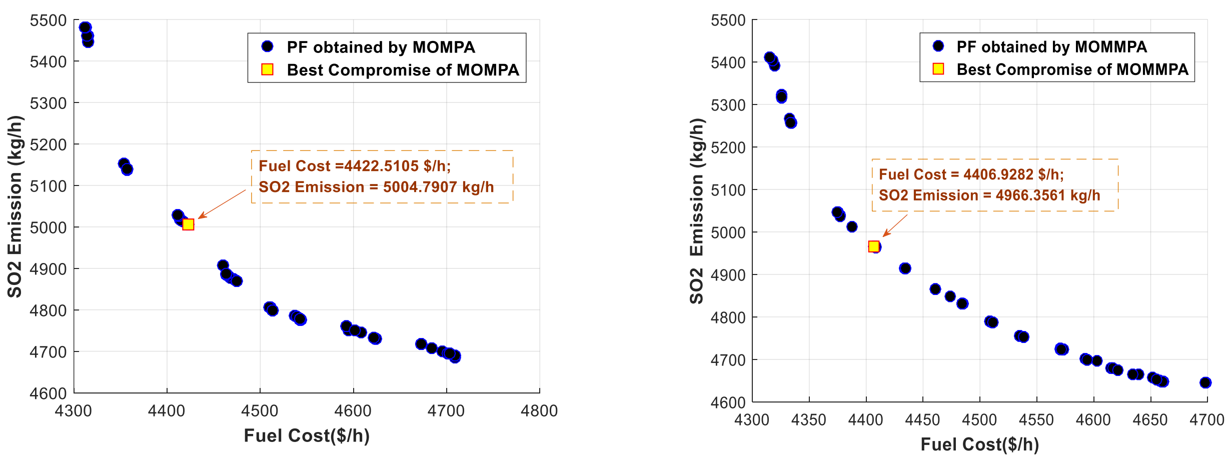


(a) (b)

Figure 5.55: Pareto front of Case 1 for load demand=225MW obtained by (a) MOMPA (b) MOMMPA.

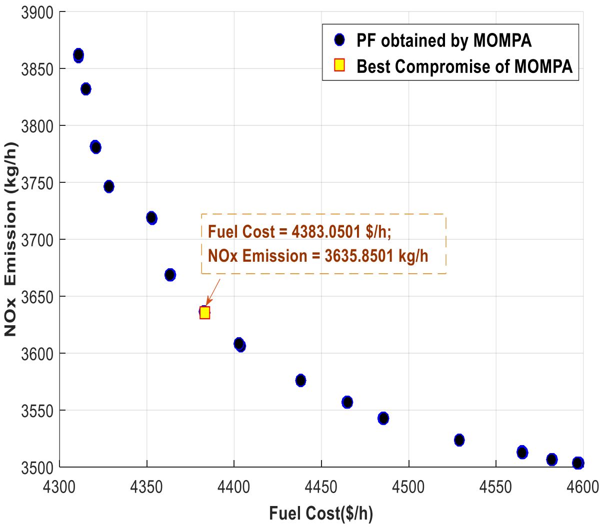


(a)

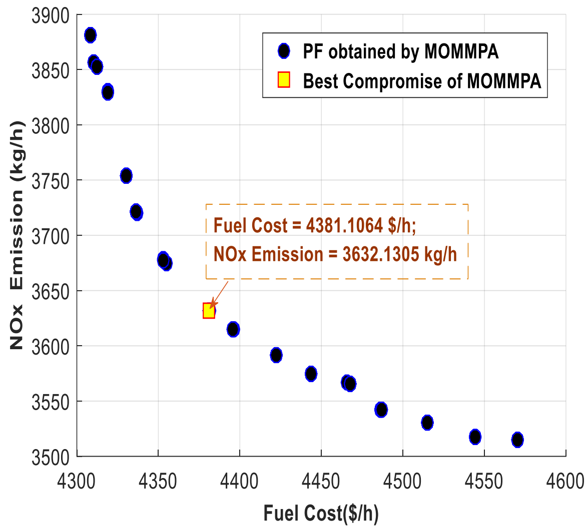


(b)

Figure 5.56: Pareto front of Case 2 for load demand=225MW obtained by (a) MOMPA (b) MOMMPA.

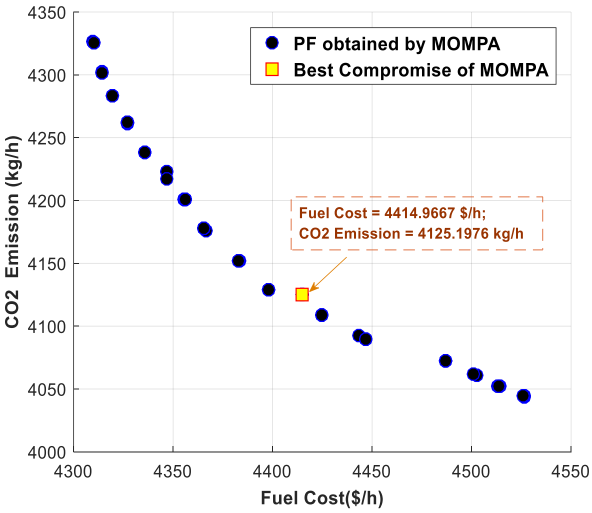


(a)

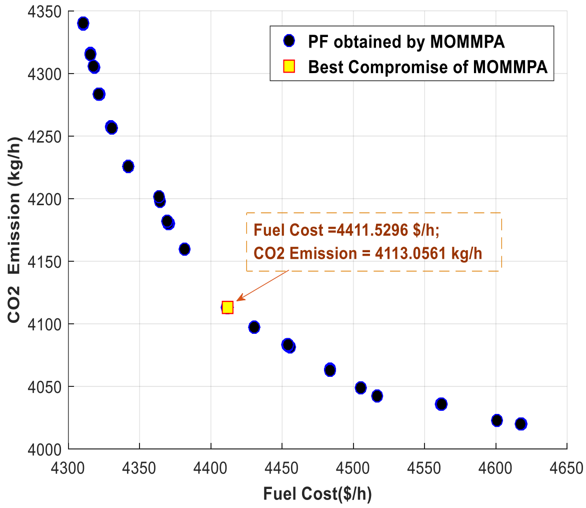


(b)

Figure 5.57: Pareto front of Case 3 for load demand=225MW obtained by (a) MOMPA (b) MOMMPA.

## 5.5 Solving DEED Problem using the MSSA Algorithm

In this section, the MSSA algorithm is applied to three-test systems (six-generator, ten-generator, and fourteen- generator). According to these three test systems, three cases studied are tabulated in Table 5.84. The entire scheduling period is 24 hours with 1-hour intervals, and the load per hour remains constant. In the simulation runs of the three cases, each algorithm is performed on a desktop computer with Core(TM) i5-4210U CPU (2.40 GHz), RAM 8 GB and Windows 8.1 64 bit operating system, using MATLAB R2016a software. The single line diagram of the IEEE 30-bus 6-generator (Case 1) test system is displayed in Figure 5.58. The load demands of the IEEE 30-bus 6-generator (Case 1) test system are provided in Table 5.85. The load forecast curve of test system 1 is displayed in Figure 5.59. The values of the fuel and emission coefficients of the IEEE 30-bus 6-generator test system is given in Table 5.86.

Table 5.84: List of three studied cases.

| Case no. | No. of Generators | No. of Buses | No. of decision variables | No. of equality constraints |
|---|---|---|---|---|
| Case 1 | 6 | 30 | 6×24=144 | 24 |
| Case 2 | 10 | NA | 10×24=240 | 24 |
| Case 3 | 14 | 118 | 14×24=336 | 24 |

Table 5.85: The load demands (MW) of the IEEE 30-bus 6-generator test system.

| Hour | $P_D$ | Hour | $P_D$ | Hour | $P_D$ |
|---|---|---|---|---|---|
| 1 | 3.25 | 9 | 5.45 | 17 | 5.15 |
| 2 | 3.90 | 10 | 5.20 | 18 | 5.75 |
| 3 | 3.50 | 11 | 5.50 | 19 | 5.25 |
| 4 | 3.00 | 12 | 5.75 | 20 | 5.25 |
| 5 | 3.35 | 13 | 5.25 | 21 | 4.55 |
| 6 | 4.00 | 14 | 5.15 | 22 | 4.25 |
| 7 | 4.75 | 15 | 4.75 | 23 | 4.25 |
| 8 | 5.05 | 16 | 5.30 | 24 | 4.00 |

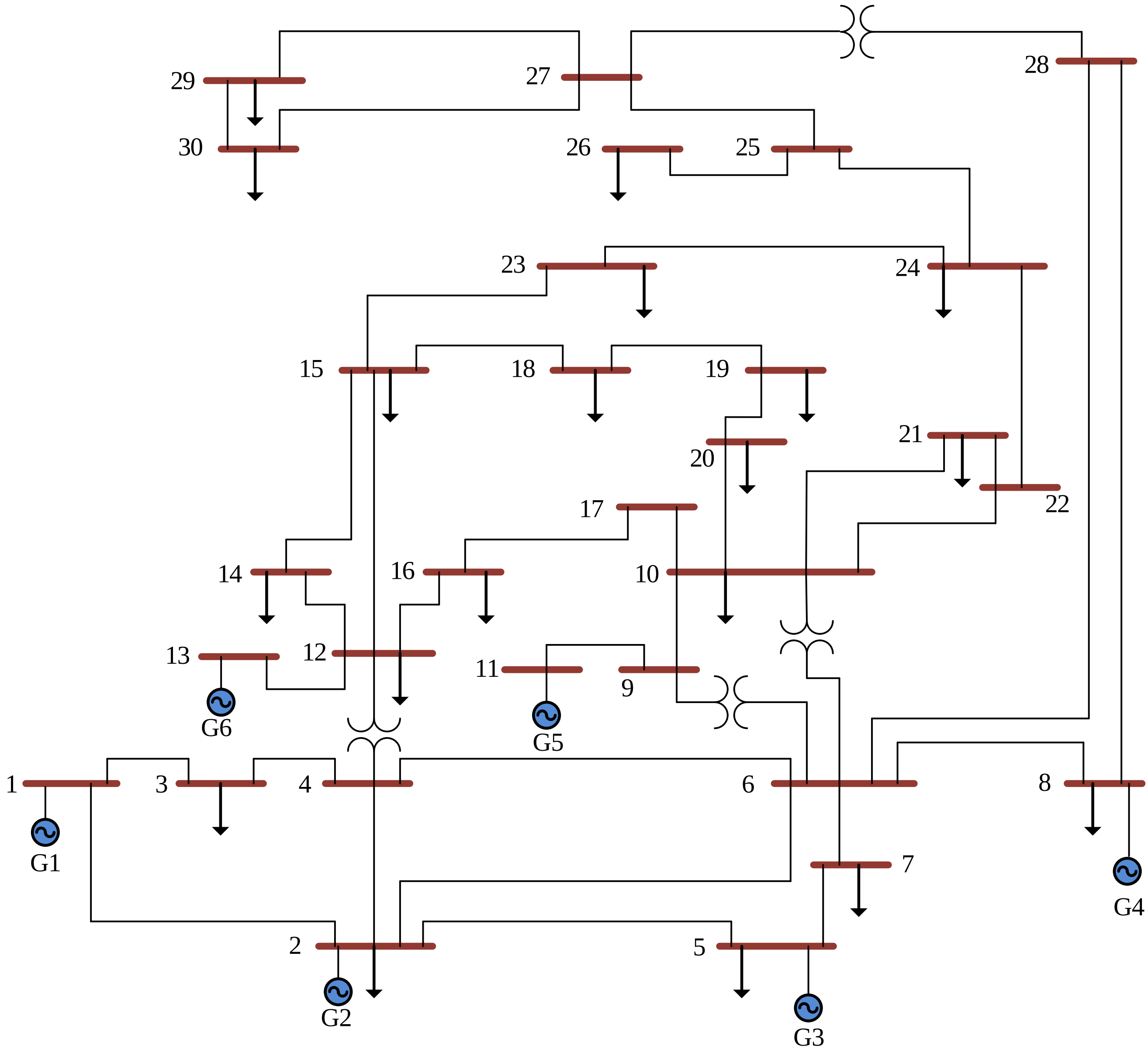


Figure 5.58: Single-line diagram of the IEEE 30-bus 6-generator test system.

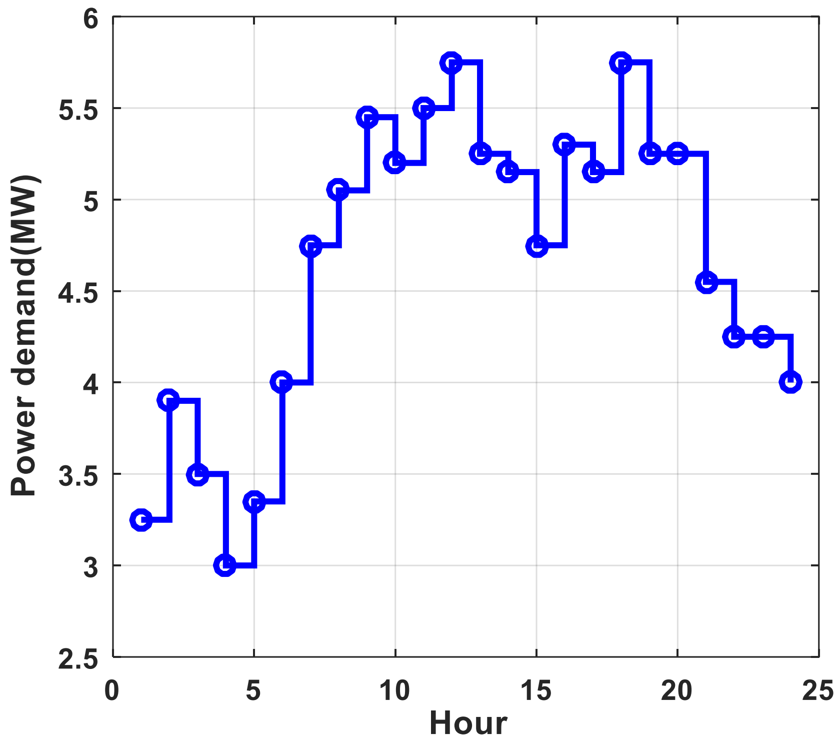


Figure 5.59: Load forecast curve for the IEEE 30-bus 6-generator test system.

Table 5.86: Generator and emission coefficients of the IEEE 30-bus 6-generator test system.

| unit | $a_i$($/h) | $b_i$($/MWh) | $c_i$($/(MW)$^2$) | $\alpha_i$ | $\beta_i$ | $\gamma_i$ | $\eta_i$ | $\delta_i$ | $P_{Gi}^{max}$ | $P_{Gi}^{min}$ |
|---|---|---|---|---|---|---|---|---|---|---|
| $P_{G1}$ | 10 | 200 | 100 | 4.091 | -5.543 | 6.49 | 2.00E-04 | 2.857 | 150 | 5 |
| $P_{G2}$ | 10 | 150 | 120 | 2.543 | -6.047 | 5.638 | 5.00E-04 | 3.333 | 150 | 5 |
| $P_{G3}$ | 20 | 180 | 40 | 4.258 | -5.094 | 4.586 | 1.00E-06 | 8 | 150 | 5 |
| $P_{G4}$ | 10 | 100 | 60 | 5.326 | -3.55 | 3.38 | 2.00E-03 | 2 | 150 | 5 |
| $P_{G5}$ | 20 | 180 | 40 | 4.258 | -5.094 | 4.586 | 1.00E-06 | 8 | 150 | 5 |
| $P_{G6}$ | 10 | 150 | 100 | 6.131 | -5.555 | 5.151 | 1.00E-05 | 6.667 | 150 | 5 |

The single line diagram of the 10-generator (Case 2) test system is shown in Figure 5.60. This test system has 39 buses, 46 lines, and10 thermal generation unit. The load demands of this system are tabulated in Table 5.87. The load forecast curve of case 2 is displayed in Figure 5.61 while the data pertaining to thermal power generating units such as fuel cost coefficients, pollution emission coefficients, the output power limits and ramp rate limits is shown in Tables 5.88 and 5.89. Table 5.90 presents The B-coefficients.

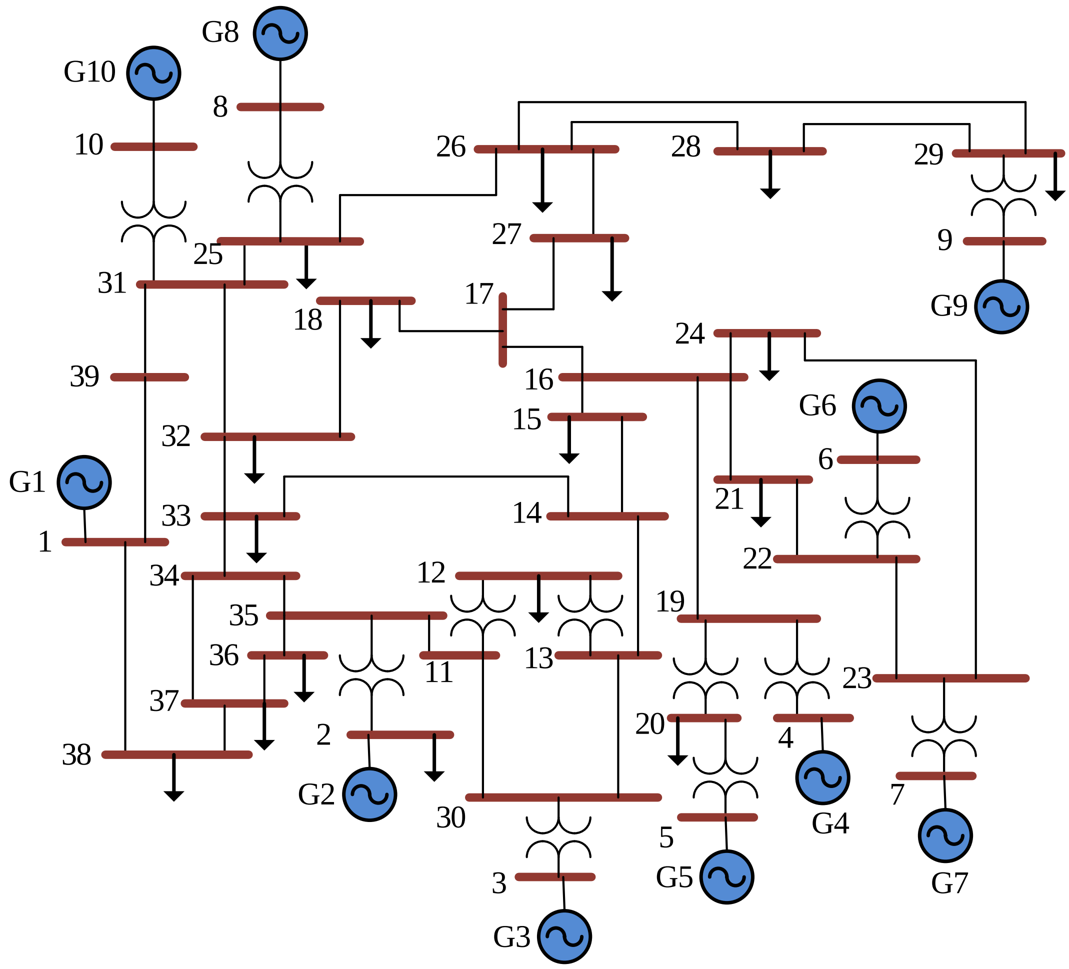


Figure 5.60: Single-line diagram of the 10-unit test system.

Table 5.87: The load demands (MW) of the 10-unit test system.

| Hour | $P_D$ | Hour | $P_D$ | Hour | $P_D$ |
|---|---|---|---|---|---|
| 1 | 1036 | 9 | 1924 | 17 | 1480 |
| 2 | 1110 | 10 | 2022 | 18 | 1628 |
| 3 | 1258 | 11 | 2106 | 19 | 1776 |
| 4 | 1406 | 12 | 2150 | 20 | 1972 |
| 5 | 1480 | 13 | 2072 | 21 | 1924 |
| 6 | 1628 | 14 | 1924 | 22 | 1628 |
| 7 | 1702 | 15 | 1776 | 23 | 1332 |
| 8 | 1776 | 16 | 1554 | 24 | 1184 |

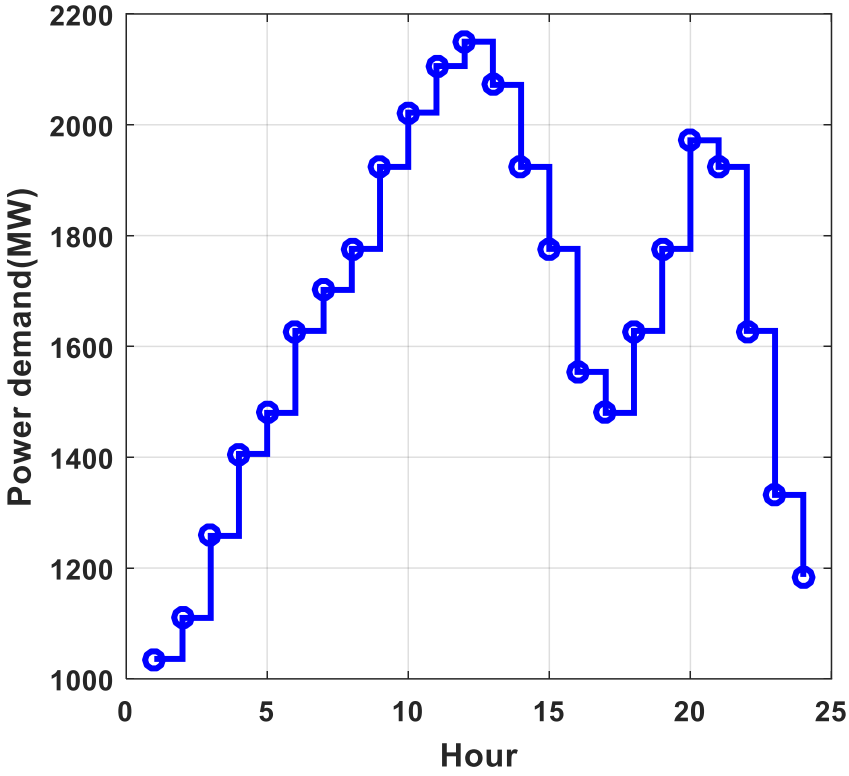


Figure 5.61: Load forecast curve for the 10-generator test system.

Table 5.88: Generator coefficients of the 10-unit test system.

| unit | $a_i$($/h) | $b_i$($/MWh) | $c_i$($/(MW)$^2$) | $d_i$($/h) | $e_i$(rad/MW) | $P_{Gi}^{min}$ | $P_{Gi}^{max}$ |
|---|---|---|---|---|---|---|---|
| $P_{G1}$ | 786.7988 | 38.5379 | 0.1524 | 450 | 0.041 | 150 | 470 |
| $P_{G2}$ | 451.3251 | 46.1591 | 0.1058 | 600 | 0.036 | 135 | 470 |
| $P_{G3}$ | 1049.998 | 40.3965 | 0.028 | 320 | 0.028 | 73 | 340 |
| $P_{G4}$ | 1243.531 | 38.3055 | 0.0354 | 260 | 0.052 | 60 | 300 |
| $P_{G5}$ | 1658.57 | 36.3278 | 0.0211 | 280 | 0.063 | 73 | 243 |
| $P_{G6}$ | 1356.659 | 38.2704 | 0.0179 | 310 | 0.048 | 57 | 160 |
| $P_{G7}$ | 1450.705 | 36.5104 | 0.0121 | 300 | 0.086 | 20 | 130 |
| $P_{G8}$ | 1450.705 | 36.5104 | 0.0121 | 340 | 0.082 | 47 | 120 |
| $P_{G9}$ | 1455.606 | 39.5804 | 0.109 | 270 | 0.098 | 20 | 80 |
| $P_{G10}$ | 1469.403 | 40.5407 | 0.1295 | 380 | 0.094 | 10 | 55 |

Table 5.89: Emission coefficients and ramp rate of the 10-unit test system.

| unit | $\alpha_i$ | $\beta_i$ | $\gamma_i$ | $\eta_i$ | $\delta_i$ | $UR_i$ | $DR_i$ |
|---|---|---|---|---|---|---|---|
| $P_1$ | 103.3908 | 2.4444 | 0.0312 | 0.5035 | 0.0207 | 80 | 80 |
| $P_2$ | 103.3908 | 2.4444 | 0.0312 | 0.5035 | 0.0207 | 80 | 80 |
| $P_3$ | 300.391 | 4.0695 | 0.0509 | 0.4968 | 0.0202 | 80 | 80 |
| $P_4$ | 300.391 | 4.0695 | 0.0509 | 0.4968 | 0.0202 | 50 | 50 |
| $P_5$ | 320.0006 | 3.8132 | 0.0344 | 0.4972 | 0.02 | 50 | 50 |
| $P_6$ | 320.0006 | 3.8132 | 0.0344 | 0.4972 | 0.02 | 50 | 50 |
| $P_7$ | 330.0056 | 3.9023 | 0.0465 | 0.5163 | 0.0214 | 50 | 30 |
| $P_8$ | 330.0056 | 3.9023 | 0.0465 | 0.5163 | 0.0214 | 30 | 30 |
| $P_9$ | 350.0056 | 3.9524 | 0.0465 | 0.5475 | 0.0234 | 30 | 30 |
| $P_{10}$ | 360.0012 | 3.9864 | 0.047 | 0.5475 | 0.0234 | 30 | 30 |

Table 5.90: The B-coefficients of the 10-unit test system.

| | | | | | | | | | | |
|---|---|---|---|---|---|---|---|---|---|---|
| $B_{ij}$ | 0.000049 | 0.000014 | 0.000015 | 0.000015 | 0.000016 | 0.000017 | 0.000017 | 0.000018 | 0.000019 | 0.00002 |
| | 0.000014 | 0.000045 | 0.000016 | 0.000016 | 0.000017 | 0.000015 | 0.000015 | 0.000016 | 0.000018 | 0.000018 |
| | 0.000015 | 0.000016 | 0.000039 | 0.00001 | 0.000012 | 0.000012 | 0.000014 | 0.000014 | 0.000016 | 0.000016 |
| | 0.000015 | 0.000016 | 0.00001 | 0.00004 | 0.000014 | 0.00001 | 0.000011 | 0.000012 | 0.000014 | 0.000015 |
| | 0.000016 | 0.000017 | 0.000012 | 0.000014 | 0.000035 | 0.000011 | 0.000013 | 0.000013 | 0.000015 | 0.000016 |
| | 0.000017 | 0.000015 | 0.000012 | 0.00001 | 0.000011 | 0.000036 | 0.000012 | 0.000012 | 0.000014 | 0.000015 |
| | 0.000017 | 0.000015 | 0.000014 | 0.000011 | 0.000013 | 0.000012 | 0.000038 | 0.000016 | 0.000016 | 0.000018 |
| | 0.000018 | 0.000016 | 0.000014 | 0.000012 | 0.000013 | 0.000012 | 0.000016 | 0.00004 | 0.000015 | 0.000016 |
| | 0.000019 | 0.000018 | 0.000016 | 0.000014 | 0.000015 | 0.000014 | 0.000016 | 0.000015 | 0.000042 | 0.000019 |
| | 0.00002 | 0.000018 | 0.000016 | 0.000015 | 0.00016 | 0.000015 | 0.000018 | 0.000016 | 0.000019 | 0.000044 |
| $B_{i0}$ | 0 | 0 | 0 | 0 | 0 | 0 | 0 | 0 | 0 | 0 |
| $B_{00}$ | 0 | | | | | | | | | |

Table 5.91 presents the load demands of the IEEE 118-bus 14-generator (Case 3) test system. The load forecast curve of case 3 is shown in Fig. 5.62. The values of the fuel and emission coefficients of these case is given in Table 5.92.

Table 5.91: The load demands (MW) of the IEEE 118-bus 14-generator test system.

| Hour | $P_D$ | Hour | $P_D$ | Hour | $P_D$ |
|---|---|---|---|---|---|
| 1 | 10.0 | 9 | 14.9 | 17 | 14.5 |
| 2 | 12.0 | 10 | 13.8 | 18 | 15.2 |

| | | | | | |
|---|---|---|---|---|---|
| 3 | 11.0 | 11 | 15.0 | 19 | 14.7 |
| 4 | 10.0 | 12 | 16.5 | 20 | 14.5 |
| 5 | 10.2 | 13 | 15.1 | 21 | 13.1 |
| 6 | 12.0 | 14 | 14.3 | 22 | 12.6 |
| 7 | 13.5 | 15 | 13.1 | 23 | 12.5 |
| 8 | 14.1 | 16 | 14.6 | 24 | 12.0 |

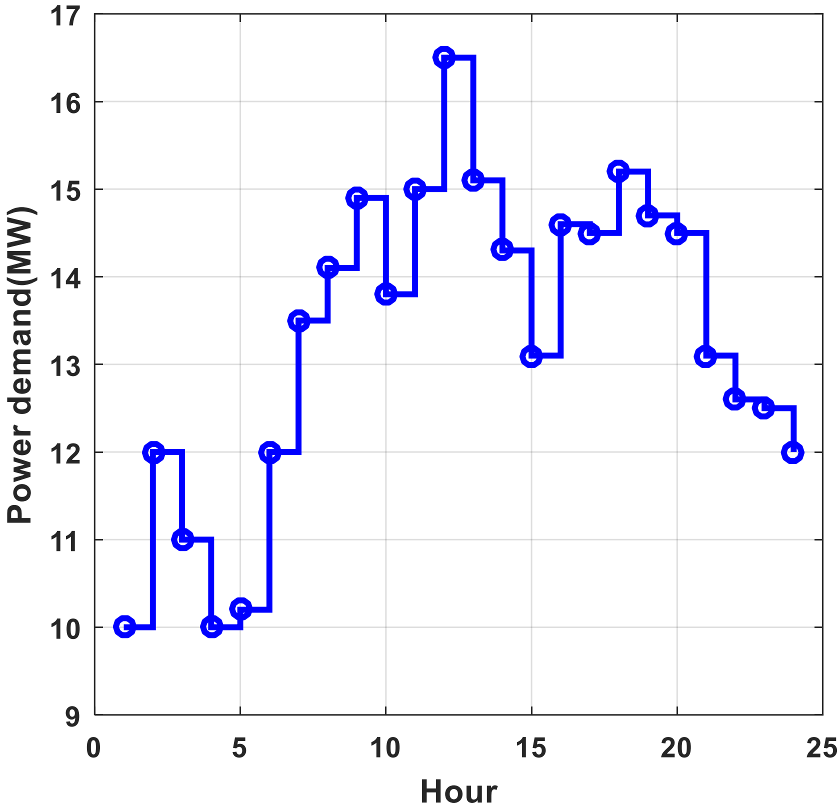


Figure 5.62: Load forecast curve for the IEEE 118-bus 14-generator test system.

Table 5.92: Generator and emission coefficients of the IEEE 118-bus 14-generator test system.

| unit | $a_i$($/h) | $b_i$($/MWh) | $c_i$($/(MW)$^2$) | $\alpha_i$ | $\beta_i$ | $\gamma_i$ | $P_{Gi}^{max}$ | $P_{Gi}^{min}$ |
|---|---|---|---|---|---|---|---|---|
| $P_{G1}$ | 150 | 189 | 0.5 | 0.016 | -1.5 | 23.333 | 300 | 50 |
| $P_{G2}$ | 115 | 200 | 0.55 | 0.031 | -1.82 | 21.022 | 300 | 50 |
| $P_{G3}$ | 40 | 350 | 0.6 | 0.013 | -1.249 | 22.05 | 300 | 50 |
| $P_{G4}$ | 122 | 315 | 0.5 | 0.012 | -1.355 | 22.983 | 300 | 50 |
| $P_{G5}$ | 125 | 305 | 0.5 | 0.02 | -1.9 | 21.313 | 300 | 50 |
| $P_{G6}$ | 70 | 275 | 0.7 | 0.007 | 0.805 | 21.9 | 300 | 50 |
| $P_{G7}$ | 70 | 345 | 0.7 | 0.015 | -1.401 | 23.001 | 300 | 50 |

| | | | | | | | | |
|---|---|---|---|---|---|---|---|---|
| $P_{G8}$ | 70 | 345 | 0.7 | 0.018 | -1.8 | 24.003 | 300 | 50 |
| $P_{G9}$ | 130 | 245 | 0.5 | 0.019 | -2 | 25.121 | 300 | 50 |
| $P_{G10}$ | 130 | 245 | 0.5 | 0.012 | -1.36 | 22.99 | 300 | 50 |
| $P_{G11}$ | 135 | 235 | 0.55 | 0.033 | -2.1 | 27.01 | 300 | 50 |
| $P_{G12}$ | 200 | 130 | 0.45 | 0.018 | -1.8 | 25.101 | 300 | 50 |
| $P_{G13}$ | 70 | 345 | 0.7 | 0.018 | -1.81 | 24.313 | 300 | 50 |
| $P_{G14}$ | 45 | 389 | 0.6 | 0.03 | -1.921 | 27.119 | 300 | 50 |

### A. Case 1: 6-Unit Test System

The 6-unit system is tested and the PF obtained by the proposed MSSA, MALO, and MOGOA algorithms is shown in Fig. 5.63. In addition, the best compromise solution of other algorithms such as MAMODE [112], and GSOMP [115] are displayed in Figure 5.63 to demonstrate the effectiveness of the proposed MSSA algorithm in achieving the optimal solution for the DEED problem.

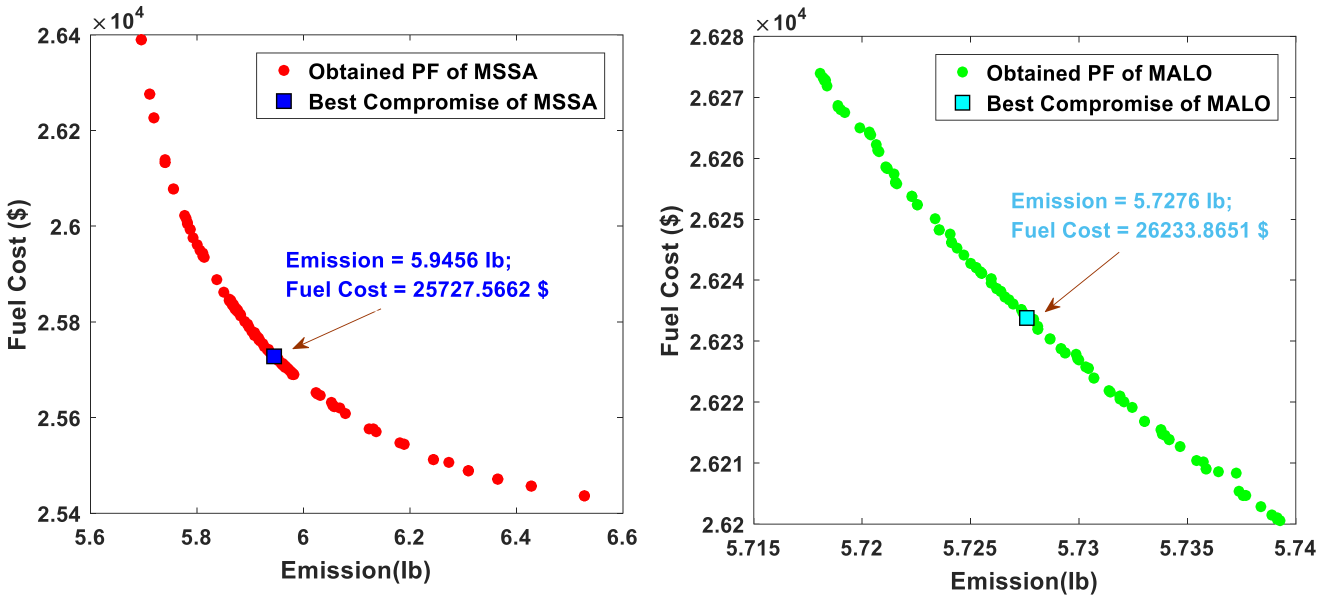


(a) MSSA (b) MALO

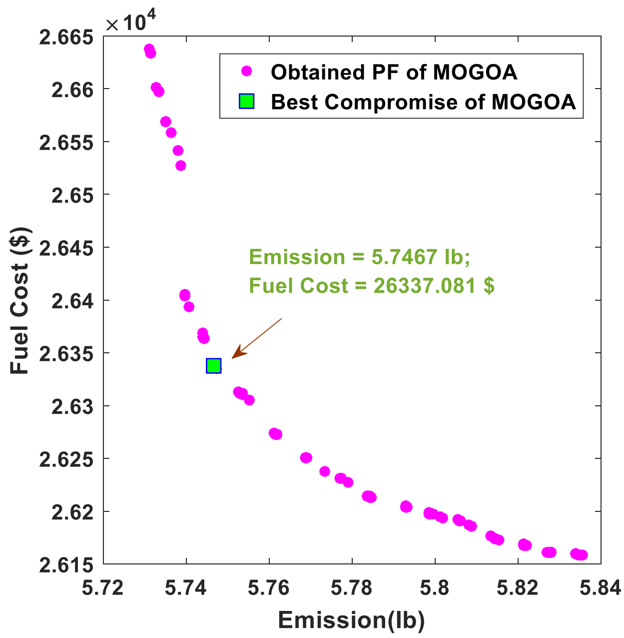


(c) MOGOA

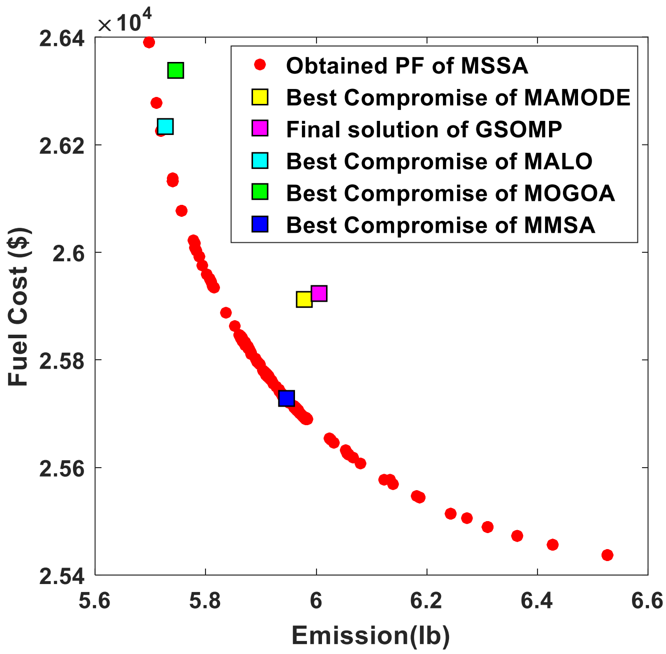


(d) MSSA and comparison of optimal solutions

Figure 5.63: PF of the first case with power loss obtained by (a) MSSA (b) MALO (c) MOGOA (d) MSSA and comparison of optimal solutions.

For comparison, the results of the BCS achieved by MSSA, MALO, MOGOA and MAMODE [112], GSOMP [115], MOPSO [115], and NSGA-II [115] are listed in Table 5.93. In comparison to different results, it can be found in Table 5.93 that the proposed MSSA algorithm has the optimal value of the BCS.

Table 5.93: Comparison of the optimum objective values of case 1.

| Method | Objectives | Fuel Cost ($) | Emission (Ib) |
|---|---|---|---|
| MSSA | Best Cost | 25437.59 | 6.52773 |
| | Best Emission | 26389.76 | 5.69654 |
| | Best Compromise | **25727.57** | **5.94564** |
| MALO | Best Cost | 26200.57 | 5.73927 |
| | Best Emission | 26273.83 | 5.71806 |
| | Best Compromise | 26233.87 | 5.72757 |
| MOGOA | Best Cost | 26158.07 | 5.83543 |
| | Best Emission | 26637.37 | 5.73097 |
| | Best Compromise | 26337.08 | 5.74666 |
| MAMODE | Best Cost | 25732 | NA |
| | Best Emission | NA | 5.7283 |
| | Best Compromise | 25912.89 | 5.97955 |

| | | | |
|---|---|---|---|
| GSOMP | Best Cost | 25493 | NA |
| | Best Emission | NA | 5.6847 |
| | Best Compromise | 25924.46 | 6.00415 |
| MOPSO | Best Cost | 25633.2 | NA |
| | Best Emission | NA | 5.6863 |
| NSGA-II | Best Cost | 25507.4 | NA |
| | Best Emission | NA | 5.6881 |

Bold values have the best performance

From the results presented in Table 5.94, the power balance constraints can be checked according to the detailed information of the compromise solution. It can be seen that the summation of the output of generating units equals to the power load plus transmission loss at each interval. The best PF achieved by MSSA is displayed in Figure 5.64.

Table 5.94: The BCS of the first case acquired using MSSA with power loss (p.u.).

| t | $P_1$ | $P_2$ | $P_3$ | $P_4$ | $P_5$ | $P_6$ | $P_T$ | $P_L$ | $P_D$ |
|---|---|---|---|---|---|---|---|---|---|
| 1 | 0.3068 | 0.3926 | 0.6113 | 0.8005 | 0.6690 | 0.4950 | 3.2752 | 0.0252 | 3.25 |
| 2 | 0.3760 | 0.4722 | 0.8176 | 0.9616 | 0.7564 | 0.5511 | 3.9348 | 0.0348 | 3.90 |
| 3 | 0.3109 | 0.4573 | 0.6931 | 0.8493 | 0.6620 | 0.5560 | 3.5287 | 0.0287 | 3.50 |
| 4 | 0.2697 | 0.3719 | 0.5970 | 0.6426 | 0.6305 | 0.5080 | 3.0196 | 0.0196 | 3.00 |
| 5 | 0.3240 | 0.4369 | 0.6214 | 0.8330 | 0.6568 | 0.5060 | 3.3782 | 0.0282 | 3.35 |
| 6 | 0.3700 | 0.5111 | 0.8599 | 0.9713 | 0.7568 | 0.5666 | 4.0358 | 0.0358 | 4.00 |
| 7 | 0.4673 | 0.6018 | 0.9944 | 1.1233 | 0.9327 | 0.6861 | 4.8056 | 0.0556 | 4.75 |
| 8 | 0.5225 | 0.6361 | 1.0820 | 1.1433 | 0.9867 | 0.7439 | 5.1145 | 0.0645 | 5.05 |
| 9 | 0.5634 | 0.7228 | 1.1207 | 1.2508 | 1.0785 | 0.7930 | 5.5292 | 0.0792 | 5.45 |
| 10 | 0.5478 | 0.6738 | 1.0600 | 1.1967 | 1.0742 | 0.7190 | 5.2716 | 0.0716 | 5.20 |
| 11 | 0.6053 | 0.6953 | 1.1598 | 1.2153 | 1.1160 | 0.7898 | 5.5815 | 0.0815 | 5.50 |
| 12 | 0.6297 | 0.7469 | 1.1529 | 1.3184 | 1.1386 | 0.8572 | 5.8437 | 0.0937 | 5.75 |
| 13 | 0.5358 | 0.6647 | 1.0635 | 1.2200 | 1.0455 | 0.7936 | 5.3230 | 0.0730 | 5.25 |
| 14 | 0.5614 | 0.6853 | 1.0480 | 1.1968 | 1.0295 | 0.7012 | 5.2220 | 0.0720 | 5.15 |
| 15 | 0.5151 | 0.6013 | 0.9823 | 1.0354 | 0.9633 | 0.7117 | 4.8091 | 0.0591 | 4.75 |
| 16 | 0.5863 | 0.6697 | 1.0924 | 1.1834 | 1.0571 | 0.7879 | 5.3769 | 0.0769 | 5.30 |
| 17 | 0.5480 | 0.6413 | 1.0702 | 1.1935 | 1.0275 | 0.7392 | 5.2197 | 0.0697 | 5.15 |
| 18 | 0.6483 | 0.7825 | 1.1536 | 1.3271 | 1.0989 | 0.8356 | 5.8460 | 0.0960 | 5.75 |
| 19 | 0.5509 | 0.6653 | 1.0803 | 1.2327 | 1.0223 | 0.7717 | 5.3233 | 0.0733 | 5.25 |
| 20 | 0.5788 | 0.6293 | 1.0482 | 1.2115 | 1.1082 | 0.7498 | 5.3258 | 0.0758 | 5.25 |
| 21 | 0.4362 | 0.5833 | 0.9479 | 1.0702 | 0.9487 | 0.6131 | 4.5995 | 0.0495 | 4.55 |
| 22 | 0.3931 | 0.5030 | 0.9248 | 0.9880 | 0.8860 | 0.5946 | 4.2896 | 0.0396 | 4.25 |
| 23 | 0.3901 | 0.5804 | 0.8155 | 0.9958 | 0.9065 | 0.6071 | 4.2954 | 0.0454 | 4.25 |
| 24 | 0.3915 | 0.4850 | 0.7786 | 0.9582 | 0.8404 | 0.5858 | 4.0395 | 0.0395 | 4.00 |

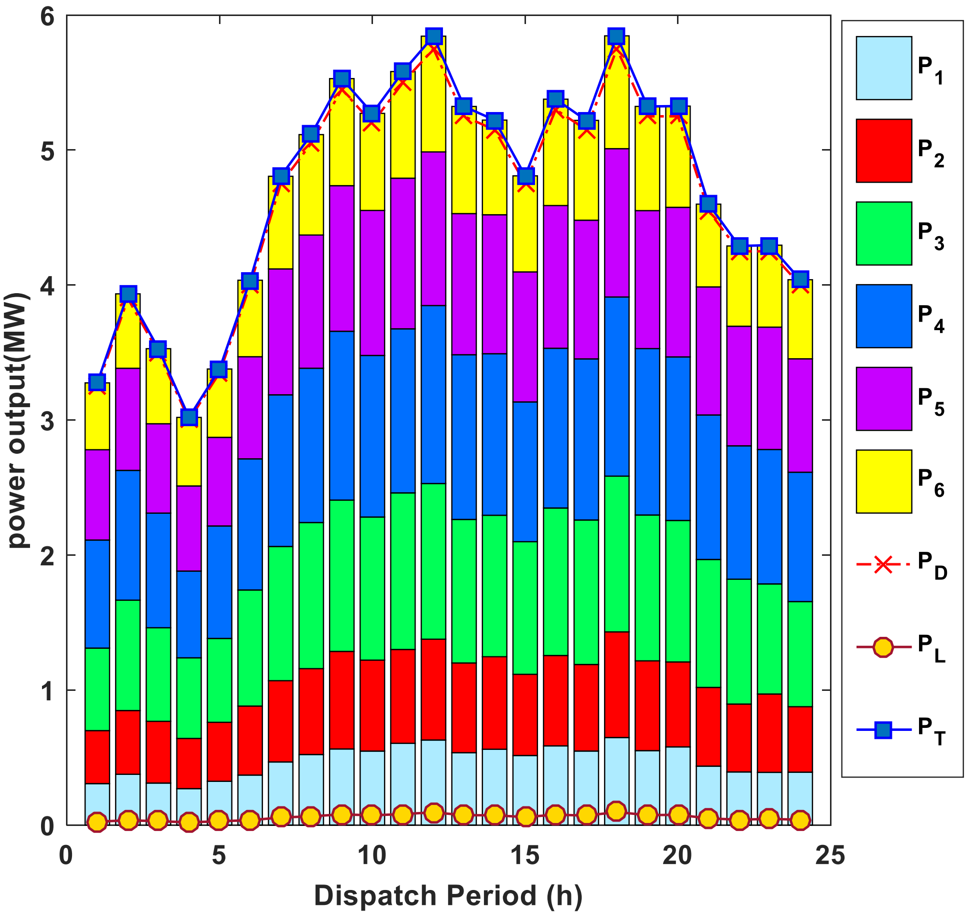


Figure 5.64: Constraints check for the BCS of the case 1 using MSSA.

### B. Case 2: 10-Unit Test System

Figure 5.65 presents the PF of the case two with transmission loss achieved using the proposed MSSA, MALO , MOGOA and the best compromise solution of other algorithms such as RCGA, NSGA-II, and MODE.

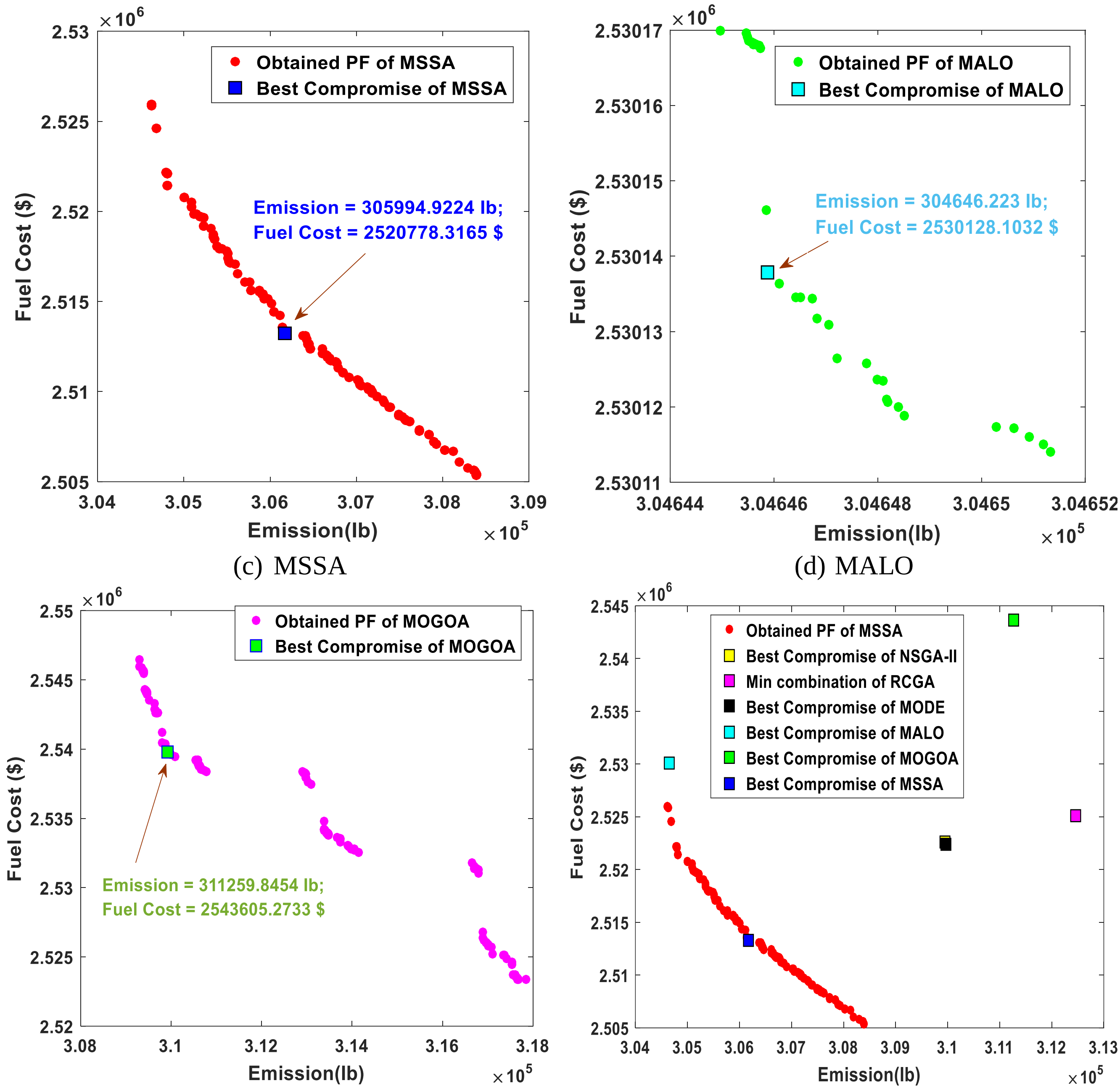


(c) MSSA (d) MALO

(c) MOGOA (d) MSSA and comparison of optimal solutions.

Figure 5.65: PF of the case 2 with power loss obtained by (a) MSSA (b) MALO (c) MOGOA (d) MSSA and comparison of optimum solutions.

The dispatching results of the case 2 that achieved using the proposed MSSA algorithm, are compared with other two well-known algorithms in detail, as displayed in Table 5.95. From this table, it is seen that the BCS of the proposed algorithm is $2.520778\times 10^6$ \$ and $3.05994\times 10^5$ lb, which is better than several compared techniques. In terms of economy and environment, the cost and emission of the BCS of the MSSA technique is superior to NSGA II [110], RCGA [110], MODE [111], MALO, and MOGOA. In general, the solution of the MSSA technique is superior to the comparison techniques.

Table 5.95: Comparison of the optimum objective values of case 2.

| Method | Objectives | Fuel Cost/$10^6$ (\$) | Emission/$10^5$ (Ib) |
|---|---|---|---|
| MSSA | Best Cost | 2.505334 | 3.083911 |
| | Best Emission | 2.525936 | 3.046193 |
| | BCS | **2.520778** | **3.05994** |
| MALO | Best Cost | 2.530114 | 3.0465133 |
| | Best Emission | 2.5301699 | 3.0464497 |
| | BCS | 2.530128 | 3.04646 |
| MOGOA | Best Cost | 2.5233373 | 3.178493 |
| | Best Emission | 2.546446 | 3.0928948 |
| | BCS | 2.5436 | 3.1126 |
| NSGA-II | Best Cost | 2.5168 | 3.1740 |
| | Best Emission | 2.6563 | 3.0412 |
| | BCS | 2.5226 | 3.0994 |
| RCGA | Min Cost | 2.5168 | 3.1740 |
| | Min Emission | 2.6563 | 3.0412 |
| | Min combination | 2.5251 | 3.1246 |
| MODE | Best Cost | 2.5123 | 3.0113 |
| | Best Emission | 2.5436 | 2.9607 |
| | BCS | 2.5224 | 3.0997 |

Bold values have the best performance

The details of the BCS attained using MSSA are shown in Table 5.96. At each interval, the summation of the output of generators matches the load demand plus the transmission loss mutually; the solution does not violate the equality restrictions at each time interval. From these simulation results, it can be concluded that, compared with other comparative techniques, the MSSA algorithm can provide best results, the efficiency of the MSSA algorithm for solving DEED problem is confirmed again. The power balance restrictions check of $P_T$, $P_D$ and $P_L$ at each interval is illustrated in Fig. 5.66.

Table 5.96: The BCS of the second case acquired using MSSA with transmission lossse (p.u.).

| t | $P_1$ | $P_2$ | $P_3$ | $P_4$ | $P_5$ | $P_6$ | $P_7$ | $P_8$ | $P_9$ | $P_{10}$ | $P_L$ | $P_D$ |
|---|---|---|---|---|---|---|---|---|---|---|---|---|
| 1 | 150.01 | 138.07 | 166.79 | 132.28 | 153.54 | 117.74 | 57.83 | 64.50 | 54.36 | 20.46 | 19.59 | 1036 |
| 2 | 150.09 | 142.01 | 135.31 | 167.76 | 148.41 | 134.97 | 70.44 | 74.86 | 65.90 | 42.62 | 22.38 | 1110 |
| 3 | 151.11 | 149.39 | 186.96 | 177.14 | 160.71 | 129.73 | 96.10 | 102.74 | 79.65 | 53.16 | 28.68 | 1258 |
| 4 | 180.36 | 173.72 | 188.94 | 189.97 | 170.87 | 159.04 | 125.90 | 118.29 | 79.96 | 55.00 | 36.05 | 1406 |
| 5 | 152.47 | 191.60 | 185.68 | 227.73 | 219.00 | 159.49 | 129.98 | 119.07 | 79.83 | 54.92 | 39.78 | 1480 |
| 6 | 216.24 | 195.52 | 216.39 | 264.98 | 241.20 | 157.90 | 129.89 | 119.96 | 79.93 | 54.92 | 48.92 | 1628 |
| 7 | 212.53 | 234.47 | 271.75 | 254.13 | 238.67 | 159.30 | 130.00 | 120.00 | 79.96 | 55.00 | 53.81 | 1702 |

| | | | | | | | | | | | | |
|---|---|---|---|---|---|---|---|---|---|---|---|---|
| 8 | 230.46 | 237.72 | 303.67 | 277.65 | 242.83 | 159.54 | 129.50 | 119.32 | 79.66 | 54.57 | 58.92 | 1776 |
| 9 | 283.42 | 303.83 | 325.48 | 295.22 | 242.08 | 160.00 | 129.92 | 119.88 | 79.99 | 54.99 | 70.80 | 1924 |
| 10 | 332.92 | 342.01 | 338.70 | 299.98 | 243.00 | 160.00 | 130.00 | 120.00 | 79.99 | 54.99 | 79.58 | 2022 |
| 11 | 376.74 | 389.20 | 339.96 | 300.00 | 243.00 | 160.00 | 129.99 | 120.00 | 80.00 | 55.00 | 87.88 | 2106 |
| 12 | 397.87 | 416.60 | 339.99 | 300.00 | 243.00 | 160.00 | 130.00 | 120.00 | 80.00 | 55.00 | 92.46 | 2150 |
| 13 | 356.03 | 372.61 | 339.88 | 299.98 | 242.96 | 159.99 | 130.00 | 119.99 | 79.99 | 55.00 | 84.44 | 2072 |
| 14 | 292.50 | 296.25 | 318.86 | 299.34 | 242.96 | 159.97 | 129.99 | 119.98 | 79.99 | 54.98 | 70.82 | 1924 |
| 15 | 230.56 | 229.74 | 292.52 | 294.79 | 242.63 | 160.00 | 129.58 | 120.00 | 80.00 | 55.00 | 58.82 | 1776 |
| 16 | 171.31 | 174.43 | 237.51 | 245.09 | 240.74 | 157.37 | 124.65 | 118.51 | 75.72 | 52.61 | 43.94 | 1554 |
| 17 | 157.28 | 150.24 | 203.43 | 235.55 | 238.54 | 155.80 | 127.08 | 119.30 | 77.52 | 54.81 | 39.54 | 1480 |
| 18 | 213.11 | 203.73 | 246.62 | 245.80 | 226.31 | 158.13 | 129.67 | 119.72 | 79.40 | 54.44 | 48.94 | 1628 |
| 19 | 232.58 | 239.14 | 295.31 | 280.12 | 242.93 | 159.98 | 129.98 | 119.92 | 79.96 | 55.00 | 58.93 | 1776 |
| 20 | 309.10 | 311.05 | 338.90 | 300.00 | 243.00 | 159.86 | 130.00 | 120.00 | 80.00 | 55.00 | 74.90 | 1972 |
| 21 | 286.57 | 288.13 | 334.04 | 297.93 | 243.00 | 160.00 | 130.00 | 120.00 | 80.00 | 55.00 | 70.67 | 1924 |
| 22 | 211.19 | 217.82 | 260.45 | 248.14 | 225.32 | 146.40 | 119.67 | 116.17 | 78.09 | 53.94 | 49.19 | 1628 |
| 23 | 151.66 | 139.84 | 197.33 | 208.20 | 202.88 | 104.38 | 129.89 | 117.26 | 71.11 | 41.56 | 32.11 | 1332 |
| 24 | 151.96 | 137.93 | 164.64 | 182.20 | 198.39 | 109.62 | 102.80 | 90.20 | 42.34 | 29.29 | 25.38 | 1184 |

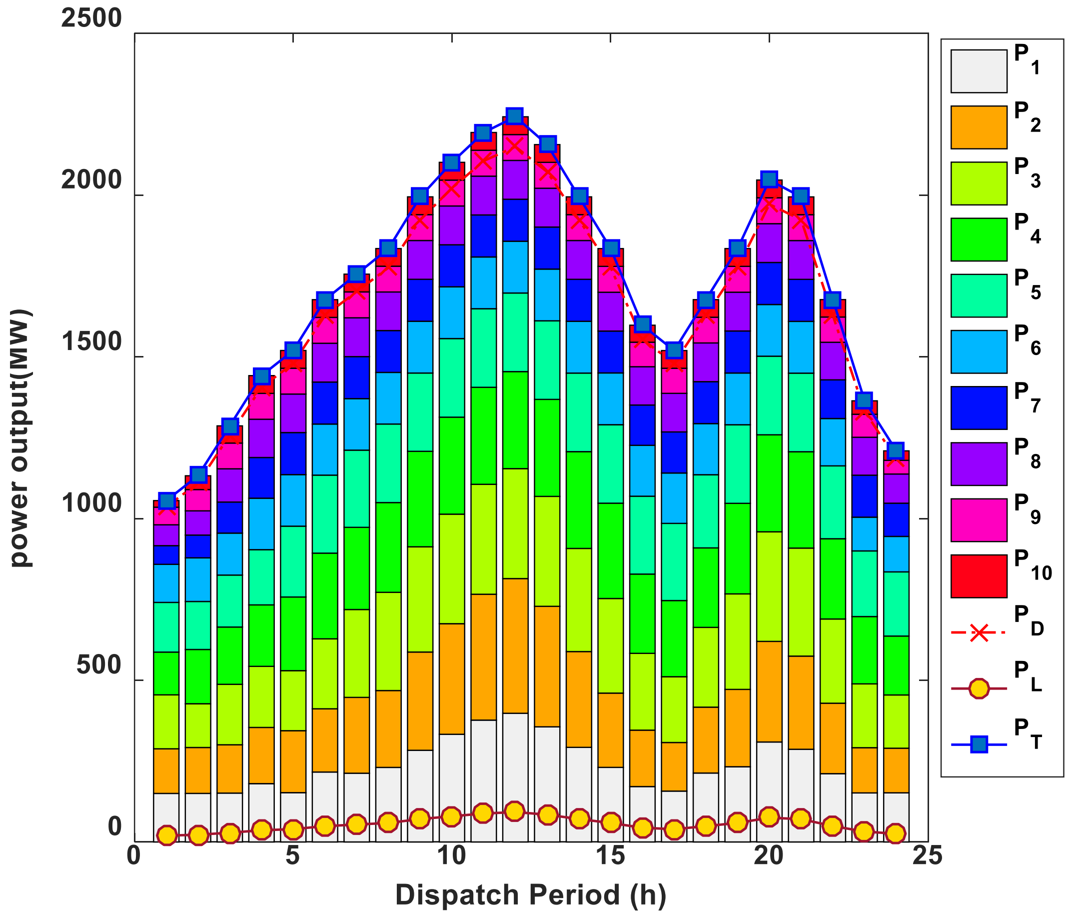


Figure 5.66: Constraints check for the BCS of the second case using MSSA.

### C. Case 3: 14-Unit Test System

The best PF of the case three with power loss attained using the proposed MSSA, MALO, and MOGOA algorithms is shown in Figure 5.67. It is seen that the BCS of the proposed MSSA technique is $1.292 \times 10^5$\$ and 98.1415 lb that is better than two compared techniques.

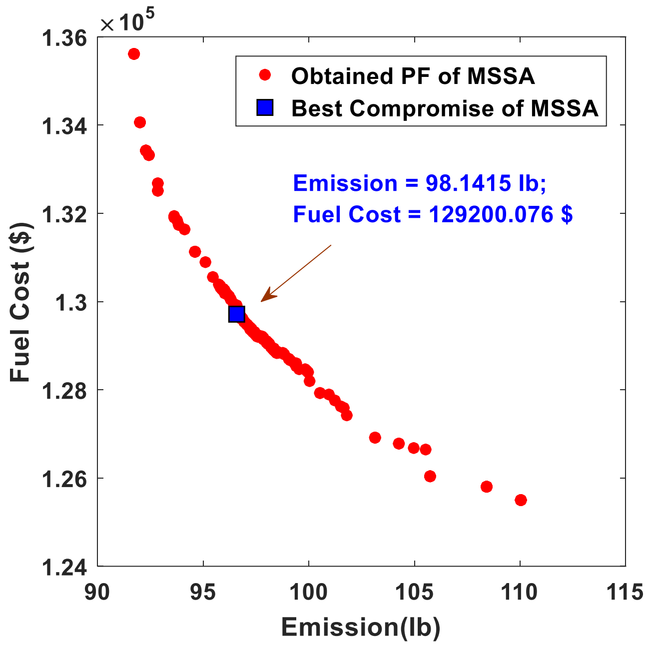


(e) MSSA

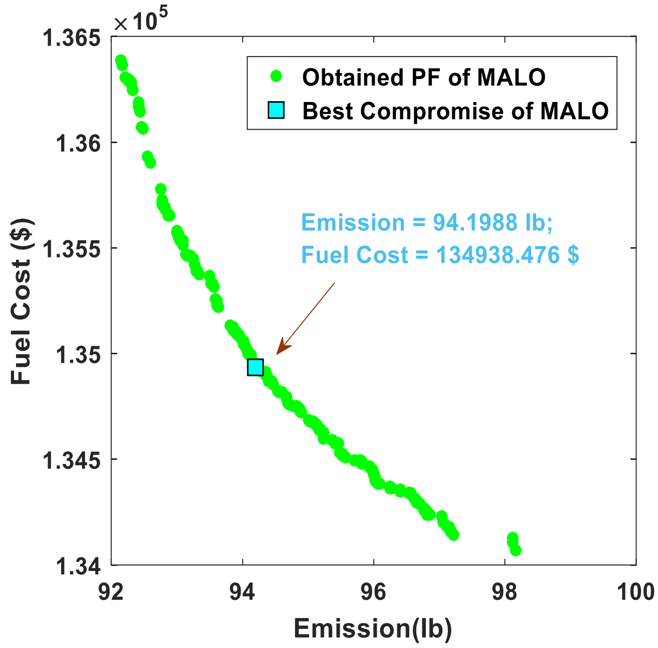


(f) MALO

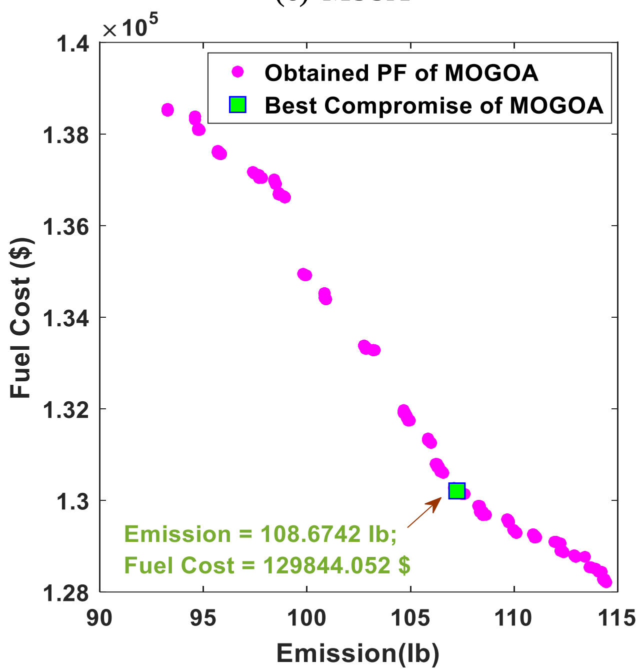


(c) MOGOA

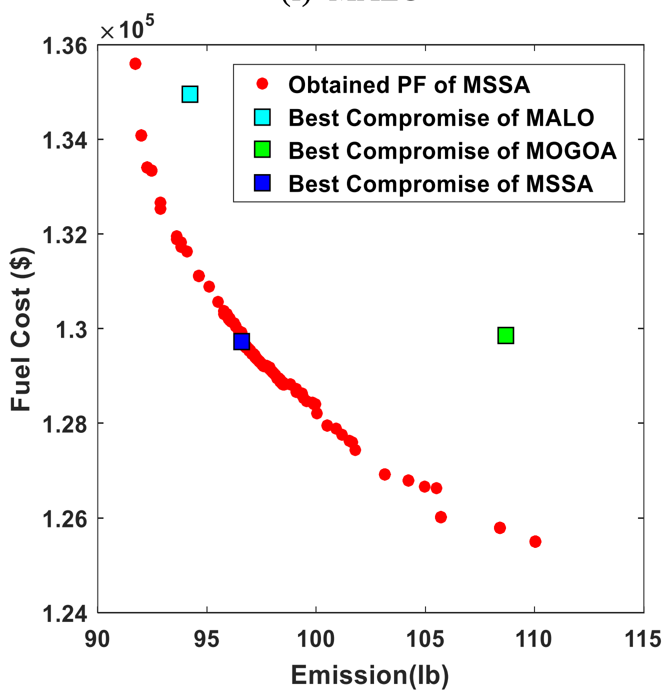


(d) MSSA and comparison of optimal solutions

Figure 5.67: PF of the third case with power loss obtained by (a) MSSA (b) MALO (c) MOGOA (d) MSSA and comparison of optimum solutions.

The simulation results of the proposed technique are compared with others that confirms the capability of the proposed technique to solve the DEED problem. The detailed compared results are displayed in Table 5.97.

Table 5.97: Comparison of the optimum objective values of case 2.

| Method | Objectives | Fuel Cost//$10^5$ ($) | Emission (Ib) |
|---|---|---|---|
| MSSA | Best Cost | 1.2548728 | 110.02359 |
| | Best Emission | 1.3560793 | 91.69988 |
| | Best Compromise | 1.29200 | 98.1415 |
| MALO | Best Cost | 1.3406945 | 98.15331 |
| | Best Emission | 1.3638826 | 92.150718 |
| | Best Compromise | 1.34938 | 94.1988 |
| MOGOA | Best Cost | 1.2822754 | 114.45838 |
| | Best Emission | 1.3853273 | 93.275504 |
| | Best Compromise | 1.29844 | 108.6742 |

Bold values have the best performance

The power outputs of the generating units are tabulated in Table 5.98 and the 24 h total fuel cost value and the value of the total emission are 129200.076 $ and 98.1415 Ib, respectively. It can be proved from Table 5.98 that the total generated power is equal to the summation of $P_L$ and $P_D$ and that all the inequality constraints are fulfilled that shows the efficacy of the MSSA algorithm. The output power of each generator, total power, load demand, and power loss are shown in Figure 5.68.

Table 5.98: The BCS of the third case attained using MSSA with transmission losses (p.u.).

| t | $P_1$ | $P_2$ | $P_3$ | $P_4$ | $P_5$ | $P_6$ | $P_7$ | $P_8$ | $P_9$ | $P_{10}$ | $P_{11}$ | $P_{12}$ | $P_{13}$ | $P_{14}$ | $P_L$ | $P_D$ |
|---|---|---|---|---|---|---|---|---|---|---|---|---|---|---|---|---|
| 1 | 1.8448 | 1.0056 | 0.7031 | 0.8494 | 0.6978 | 0.7539 | 0.6777 | 0.6474 | 0.7207 | 0.8242 | 0.7970 | 1.0141 | 0.6891 | 0.6274 | 1.8522 | 10.0 |
| 2 | 1.8686 | 1.5590 | 0.7619 | 0.8887 | 0.8204 | 0.7799 | 0.8150 | 0.6967 | 0.8426 | 1.0303 | 1.0040 | 1.3621 | 0.7007 | 0.6837 | 1.8136 | 12.0 |
| 3 | 1.9159 | 1.4781 | 0.7493 | 0.8146 | 0.8097 | 0.7498 | 0.7031 | 0.6984 | 0.9535 | 0.8321 | 0.8117 | 0.8954 | 0.6964 | 0.6315 | 1.7394 | 11.0 |
| 4 | 1.5969 | 1.2879 | 0.6443 | 0.7765 | 0.7695 | 0.7960 | 0.6510 | 0.6319 | 0.6807 | 0.7502 | 0.8043 | 1.1795 | 0.7743 | 0.6046 | 1.9476 | 10.0 |
| 5 | 1.5783 | 1.2570 | 0.8429 | 0.7314 | 0.7314 | 0.7883 | 0.7075 | 0.6977 | 0.7986 | 0.8820 | 0.8005 | 1.0211 | 0.6197 | 0.6664 | 1.9229 | 10.2 |
| 6 | 1.7012 | 1.3836 | 0.8931 | 1.0650 | 0.7281 | 0.8062 | 0.8671 | 0.8092 | 1.0783 | 0.9772 | 0.9998 | 1.1138 | 0.7438 | 0.6578 | 1.8242 | 12.0 |
| 7 | 1.8590 | 1.6225 | 1.0377 | 1.0833 | 1.0213 | 1.0505 | 0.8526 | 0.7107 | 1.0057 | 1.2990 | 1.0806 | 1.1119 | 0.8145 | 0.6702 | 1.7194 | 13.5 |
| 8 | 2.2770 | 1.7767 | 0.8949 | 0.9837 | 0.9789 | 1.0381 | 0.7910 | 0.8754 | 0.9454 | 1.3403 | 1.0184 | 1.2218 | 0.8397 | 0.7222 | 1.6034 | 14.1 |
| 9 | 1.9798 | 2.1283 | 0.8953 | 1.0316 | 0.8775 | 0.9845 | 0.9566 | 0.8269 | 1.2213 | 1.3621 | 1.1799 | 1.5283 | 0.8622 | 0.7757 | 1.7100 | 14.9 |
| 10 | 2.2102 | 1.7363 | 0.9107 | 0.9018 | 0.9547 | 0.8503 | 0.8137 | 1.0557 | 0.9148 | 1.2187 | 1.0422 | 1.3154 | 0.8075 | 0.7241 | 1.6560 | 13.8 |
| 11 | 2.2647 | 1.8614 | 0.8648 | 1.1936 | 1.0429 | 0.8684 | 1.0178 | 0.9309 | 1.0312 | 1.1771 | 1.0551 | 1.5499 | 1.0144 | 0.7607 | 1.6330 | 15.0 |
| 12 | 2.2892 | 1.9223 | 1.2679 | 1.5490 | 0.9783 | 1.1875 | 0.8261 | 0.9638 | 1.2831 | 1.2737 | 1.0947 | 1.6729 | 0.9701 | 0.7903 | 1.5689 | 16.5 |
| 13 | 2.1056 | 1.9158 | 1.0940 | 1.1415 | 0.9491 | 1.2375 | 0.8647 | 0.7604 | 1.0287 | 1.1263 | 1.3653 | 1.4299 | 0.9939 | 0.7363 | 1.6489 | 15.1 |
| 14 | 1.9923 | 1.7601 | 0.9725 | 1.0530 | 1.1690 | 0.9384 | 0.8627 | 0.8816 | 0.8881 | 1.3040 | 1.1878 | 1.4874 | 0.8726 | 0.6524 | 1.7218 | 14.3 |
| 15 | 2.0599 | 1.5643 | 0.8444 | 0.9778 | 0.9095 | 0.8642 | 0.7872 | 0.7977 | 0.9421 | 1.3365 | 1.1358 | 1.0737 | 0.8018 | 0.6860 | 1.6808 | 13.1 |
| 16 | 2.1009 | 1.7972 | 1.1459 | 1.0448 | 1.1458 | 0.9029 | 0.8425 | 0.8539 | 1.0513 | 1.2255 | 1.0421 | 1.3444 | 1.0195 | 0.7369 | 1.6536 | 14.6 |
| 17 | 2.1883 | 2.0192 | 0.9134 | 1.0916 | 1.1254 | 1.0463 | 0.9255 | 0.8499 | 0.9232 | 0.9825 | 1.0277 | 1.3759 | 0.9342 | 0.7155 | 1.6186 | 14.5 |
| 18 | 2.2892 | 2.1489 | 1.0146 | 1.1794 | 0.8802 | 1.1092 | 0.8609 | 0.7866 | 1.0821 | 1.1133 | 1.3164 | 1.4556 | 0.8095 | 0.7232 | 1.5690 | 15.2 |
| 19 | 2.1990 | 1.9796 | 0.8941 | 0.9135 | 1.0583 | 1.0535 | 0.8683 | 0.8093 | 1.0409 | 1.1729 | 1.2207 | 1.6510 | 0.8146 | 0.7100 | 1.6856 | 14.7 |
| 20 | 1.9954 | 1.6575 | 0.9303 | 1.0157 | 0.9446 | 1.1513 | 1.0201 | 0.8893 | 1.1961 | 1.1178 | 1.4577 | 1.3617 | 0.7764 | 0.7405 | 1.7543 | 14.5 |
| 21 | 2.2082 | 1.6239 | 0.8441 | 0.8003 | 0.9282 | 1.0949 | 0.7419 | 0.7442 | 0.9581 | 0.9384 | 1.0039 | 1.4912 | 0.7182 | 0.7269 | 1.7224 | 13.1 |
| 22 | 1.7212 | 1.9025 | 0.8127 | 0.8846 | 1.0127 | 0.8447 | 0.7468 | 0.7491 | 0.8413 | 1.1173 | 0.9040 | 1.2863 | 0.8112 | 0.7732 | 1.8075 | 12.6 |
| 23 | 1.9478 | 1.6296 | 0.8620 | 0.9937 | 0.8662 | 0.8004 | 0.7688 | 0.6997 | 0.9438 | 1.2162 | 0.9303 | 1.2251 | 0.6933 | 0.6424 | 1.7192 | 12.5 |
| 24 | 1.7457 | 1.8476 | 0.8600 | 0.8294 | 0.8312 | 0.9356 | 0.7420 | 0.7182 | 0.8128 | 1.1049 | 0.7625 | 1.1912 | 0.7391 | 0.6600 | 1.7803 | 12.0 |

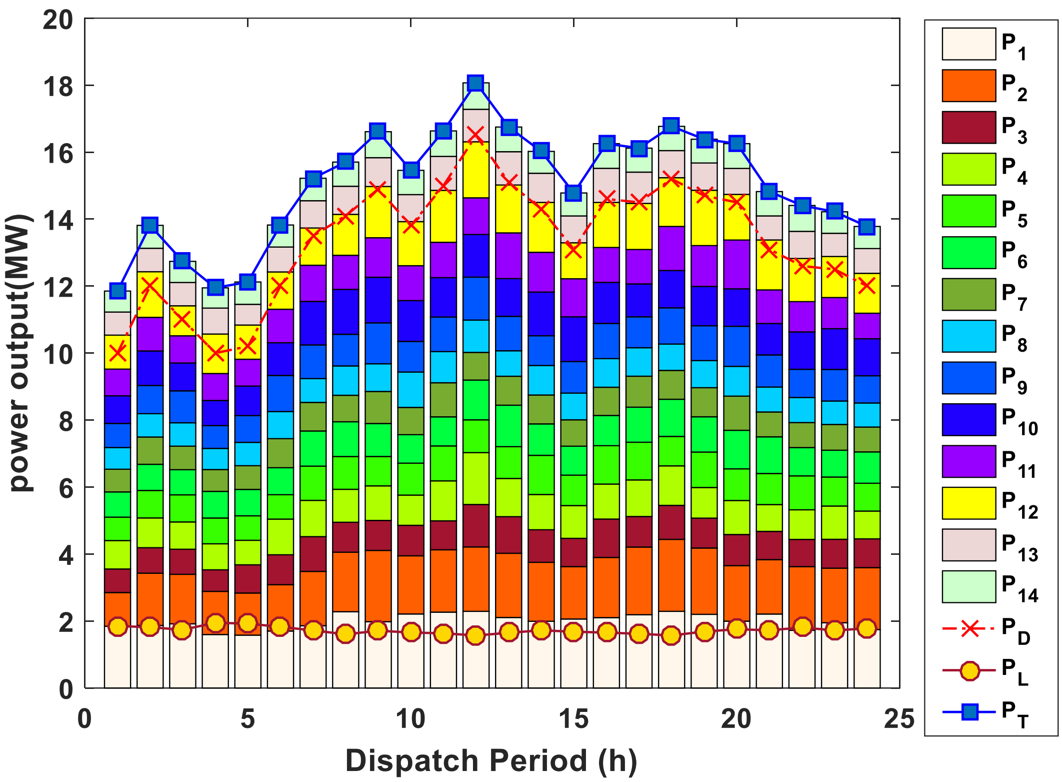


Figure 5.68: Constraints check for the BCS of the third case using MSSA.

The hypervolume (HV) indicator is a set measure used in multi-objective optimization technique to evaluate the performance of search algorithms. The hypervolume metric is the volume covered by the estimated PF $\boldsymbol{Y} = (y^{(1)}, y^{(2)}, \ldots\ldots, y^{(N)}$with respect to a given reference point $\boldsymbol{t} = (t_1, t_2, t_3)$.And the $HV(Y, t)$ is then defined as [234]:

$$HV(Y,t) = \left(t_1 - y_1^{(1)}\right)\left(t_2 - y_2^{(1)}\right)\left(t_3 - y_3^{(1)}\right) + \sum\nolimits_{i=2}^{N}\left(t_1 - y_1^{(i)}\right)\left(y_2^{(i-1)} - y_2^{(i)}\right)\left(y_3^{(i-1)} - y_3^{(1)}\right) \quad (5.1)$$

As depicted in Table 5.99, the HV of MSSA outperforms that of the other two techniques in terms of the best, worst, average and std dev. values that proves that the technique can achieve ND solutions with much better capability, uniformity and variety for the three cases compared to the other techniques.

Table 5.99: HV indicator values of results obtained for the three cases.

| Case no. | | MSSA | MALO | MOGOA |
|---|---|---|---|---|
| Case 1 | Best | **0.807653** | 0.636744 | 0.646386 |
| | Worst | **0.789138** | 0.171571 | 0.185795 |

| | | | | |
|---|---|---|---|---|
| | Mean | **0.800696** | 0.39641 | 0.438754 |
| | Std dev. | **0.006691** | 0.139975 | 0.14251 |
| Case 2 | Best | **0.665428** | 0.1914 | 0.617644 |
| | Worst | **0.08684** | 0 | 0.049874 |
| | Mean | 0.3104 | 0.07108 | **0.394762** |
| | Std dev. | 0.195818 | **0.080641** | 0.21163 |
| Case 3 | Best | 0.634702 | **0.704149** | 0.578087 |
| | Worst | **0.584107** | 0.427635 | 0.515367 |
| | Mean | **0.610866** | 0.554619 | 0.542181 |
| | Std dev. | **0.015048** | 0.095316 | 0.020538 |

Bold values have the best performance

## 5.6 Solving EED Problem Considering Stochastic RES using CBO Algorithm.

The effectiveness of the proposed CBO and the optimization framework are shown in this section by using both the standard and modified IEEE-30 and IEEE-57 bus test systems. The simulation results using ten different CBO variants, compared with that obtained by the standard BO, based on the standard IEEE-30 bus test systems. The potential for CBO is to minimize both the cumulative cost and optimization convergence rates. Twelve scenarios are evaluated, including different types of RES and CT.

### 5.6.1 Test System 1

The standard IEEE 30-bus system has 6 power generating units and 24 load buses. Also, 41 branches link the generators and load busses. The total connected loads of both active and reactive power are 2.834 p.u. 1.262 p.u., respectively. Bus 1 was selected as the slack bus. The voltage magnitude limits for both generating units and load busses are between 0.95 p.u. and 1.1 p.u. For the tap changing transformer, the tap setting is varied between 0.9 p.u. to 1.1 p.u. Furthermore, the VAR compensators are supposed to change between 0 and 0.05 p.u. In more details, all line and bus data can be found in [235]. The standard system was modified in this thesis as described in [235] to accommodate the conventional thermal generators units WT and SPV generators. The conventional thermal generators units are placed at buses 1, 2, and 8. However, one SPV generator is installed at bus 13. Two WT generators are placed at bus No. 5 and 11 with reactive power capability. Moreover, the modified test system network that comprises three different power generation sources is shown in Figure 5.69. It is worth mentioning that the WT and SPV outputs contain variations, which must be balanced by reserve and outputs of another generator collectively. Therefore, the total generation cost comprises the total operational cost of the conventional thermal generators, along with the penalty and reserve costs resulting from intermittency in the SPV and WT outputs.

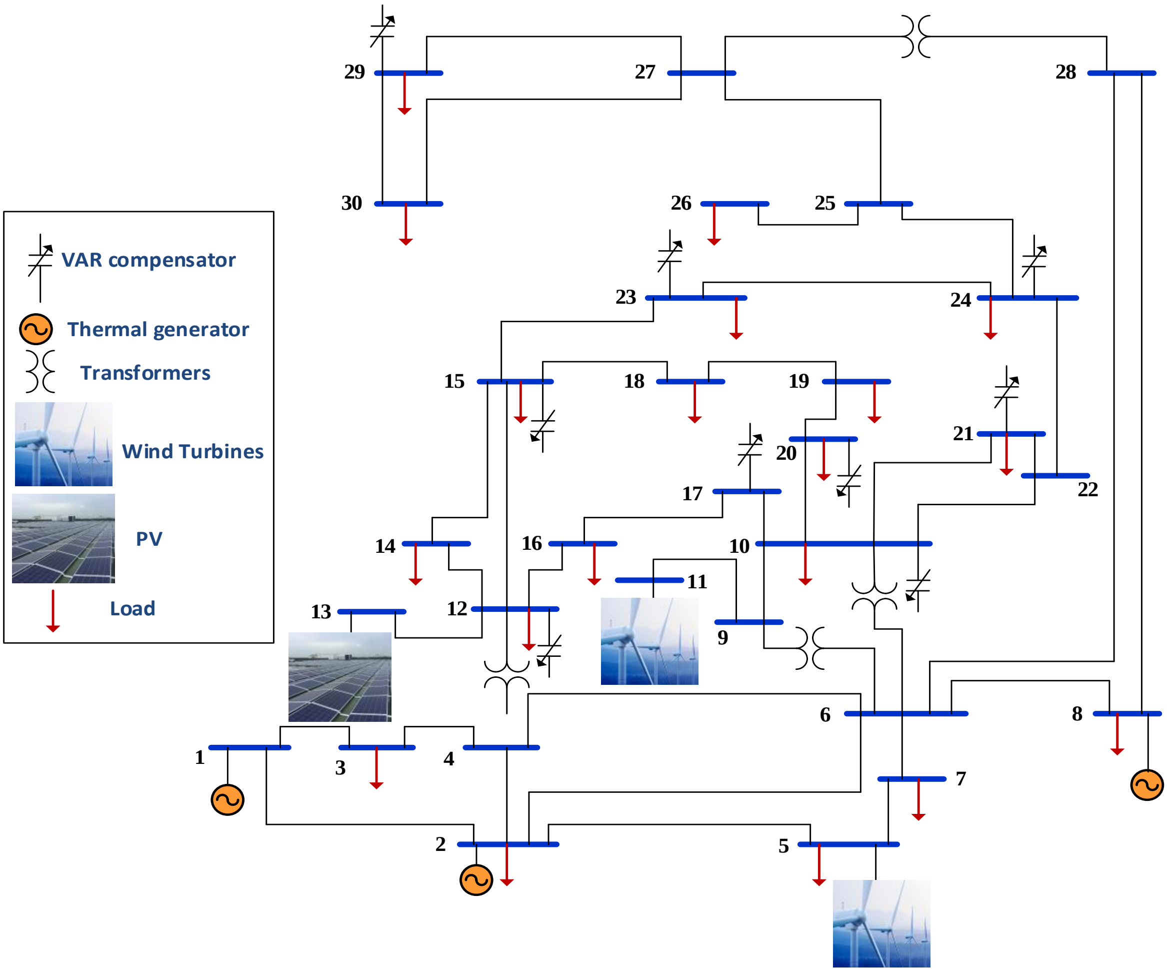


Figure 5.69: Modified IEEE 30-bus test system.

The mentioned PDF parameters in the previous section are used in the proposed case studies to compute wind speed. The wind frequency distribution by Weibull fitting [133] is shown in Fig. 5.70a and Fig. 5.70b at the bus No. 5 and 11, respectively. The requirements of Wind turbine design are introduced in [236]. The power curve is accomplished after running 8000 Monte-Carlo scenarios. The Weibull PDF parameters of WT generator at bus 5 are: c = 9, k = 2, whilst at bus 11 are: c = 10, k = 2 [237][238]. The Weibull mean is $M_{wt}$ = 7.976 and 8.862 m/s at bus 5 and 11, respectively. A 3 MW wind turbine was utilized at $v_{ci} = 3\ m/s$, $v_{co} = 25\ m/s$ and $v_{nom} = 16\ m/s$ based on the manufacture data sheet of Enercon E82-E4.

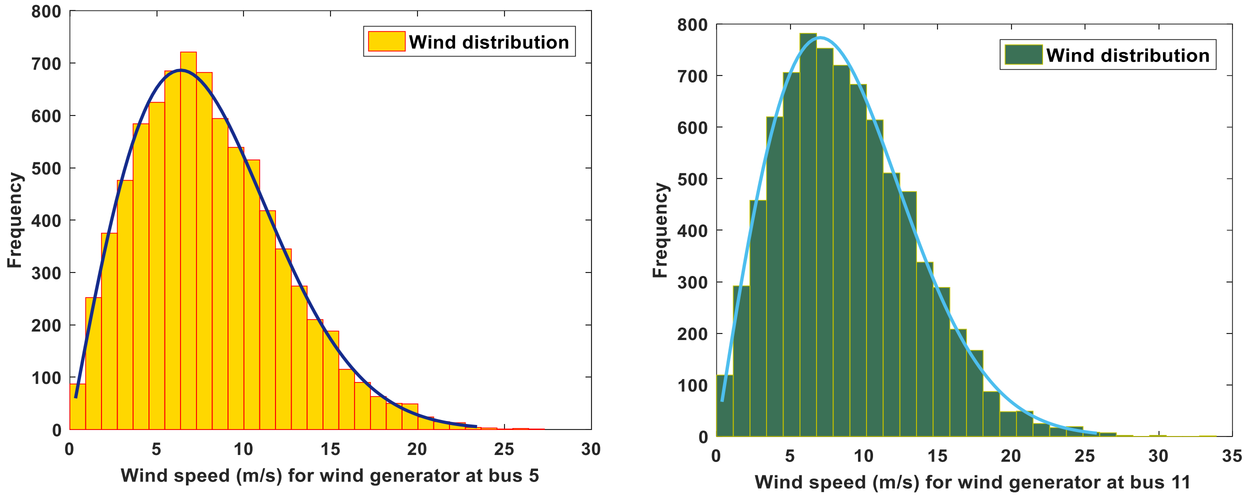


(a) (b)

Figure 5.70: Wind speed distribution for WT generators at bus 5 and 11.

In the same manner to describe the output of PV generators, the parameters of the lognormal PDF are chosen based on the mean and STD of the global irradiation, where $\sigma = 6, \mu = 0.6$ and lognormal mean equal *I=483 W/m.* After running the Monte-Carlo technique with a sample size of 8000, the frequency distribution and lognormal fitting of solar irradiance are shown in Fig.5.71. Fig.5.72 shows the histogram for the SPV generators output; it is seen that the SPV output has stochastic nature due to the variance in solar irradiance.

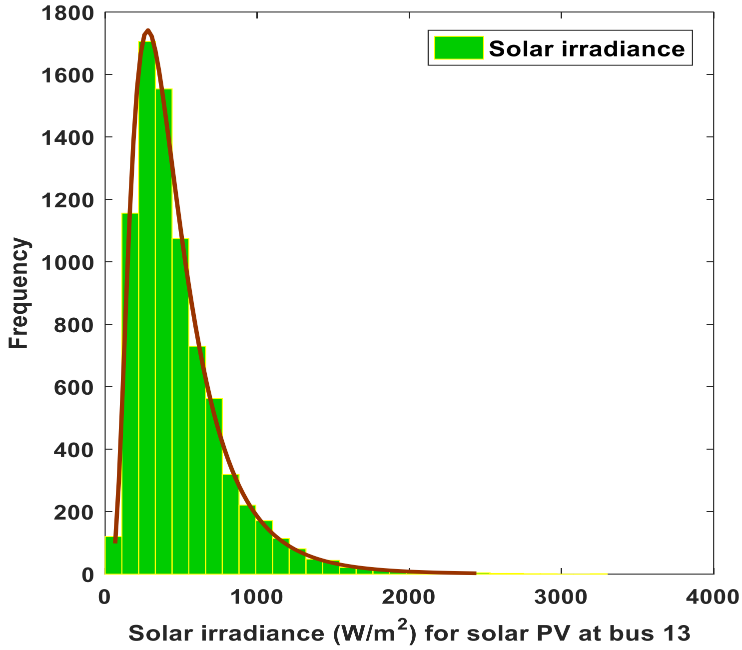


Figure 5.71: Solar irradiance distribution for SPV generators at bus13.

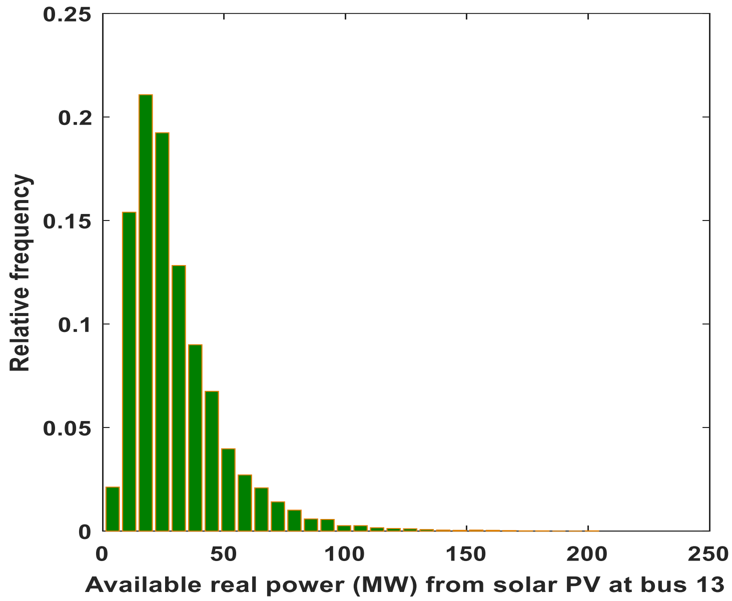


Figure 5.72: Active power distribution in (MW) from SPV generator at bus 13.

## 1) Case A

This case aims to investigate the effect of both scheduled power and PDF parameters of WT and SPV generators on the total generating cost.

### a. Effect of Scheduled Wind and Solar Power on the Total Cost

Using the Weibull PDF parameters besides a discussed wind turbine parameter selection in section 3, the impact of wind parameters on the cost by the proposed CBO5 is investigated in the present case. The direct cost coefficients of WT generators at buses 5 and 11 are 1.6 and 1.75, respectively. Further, the coefficient of penalty cost and reserve cost for utilizing wind power at these buses are assumed 1.5 at both buses, while the coefficient of reserve cost is assumed 3 at both buses. It is worth noting that the direct cost of RES is lower than the average cost of conventional thermal generators. Likewise, the penalty cost for not utilizing full the available wind power is lower than the direct cost of RES [239]. In this case, scheduled available wind power is varied from 0 to the rated power, where the direct, penalty, reserve, and total wind power costs are computed. Fig. 5.73 shows the variation of different cost components for wind power vs. the scheduled wind power. The results show a linear relationship between the scheduled wind power and the direct cost. In addition, a larger spinning reserve is required, which leads to an increase in the reserve cost then consequently, the generation costs move upwards. In addition, the penalty cost rightly decreases with a lower rate with increased scheduled power from wind. As a result, the total wind power cost is increased.

Similarly, cost variations appear due to related penalty and reserve costs coefficients when SPV output is underestimated /overestimated from scheduled power. To estimate the total cost of SPV generators, it is required to analyze the operation and maintenance cost. From [240], it is seen that selected the cost ranges for the present study are like to those of onshore wind power plants. So, the direct, reserve and penalty cost coefficients are assumed in [133] with 1.6, 3, and 1.5, respectively. Variation of solar power generation cost vs scheduled power is illustrated in Fig. 5.74. It is significant to observe that the total cost of SPV generators does not rise uniformly with PDF parameters of solar irradiance. In addition, the minimum cost is accomplished when scheduled power from SPV generators is set to 22 MW.

#### b. Effect of PDF Parameters on the Total Generating Cost of Wind and Solar Power

The cost of WT generator is directly affected by the Weibull distribution scale parameter *C*. This present case evaluates how Weibull distribution scale parameter variations affect WT generator cost while a fixed scheduled power. The shape parameter for both utilized WT generators at two specified buses is equal to $K = 2$. Also, the Rayleigh distribution is equal to a Weibull distribution with the same value of $K = 2$. Considering the same values of the cost coefficients used in the previous case and the output power of two WT generators are 25 MW and 20 MW, respectively. Fig.5.75 shows the relationships between WT generators cost and the Weibull distribution scale parameter. It is seen that; lowest value of costs is accomplished when the scale parameter's value is in the center of a certain range. Scale parameter with higher value denotes the propagation of higher wind speeds with a particular probability. This occurs since the scheduled power is still the same for a constant interval that increases penalty costs and raises the overall costs.

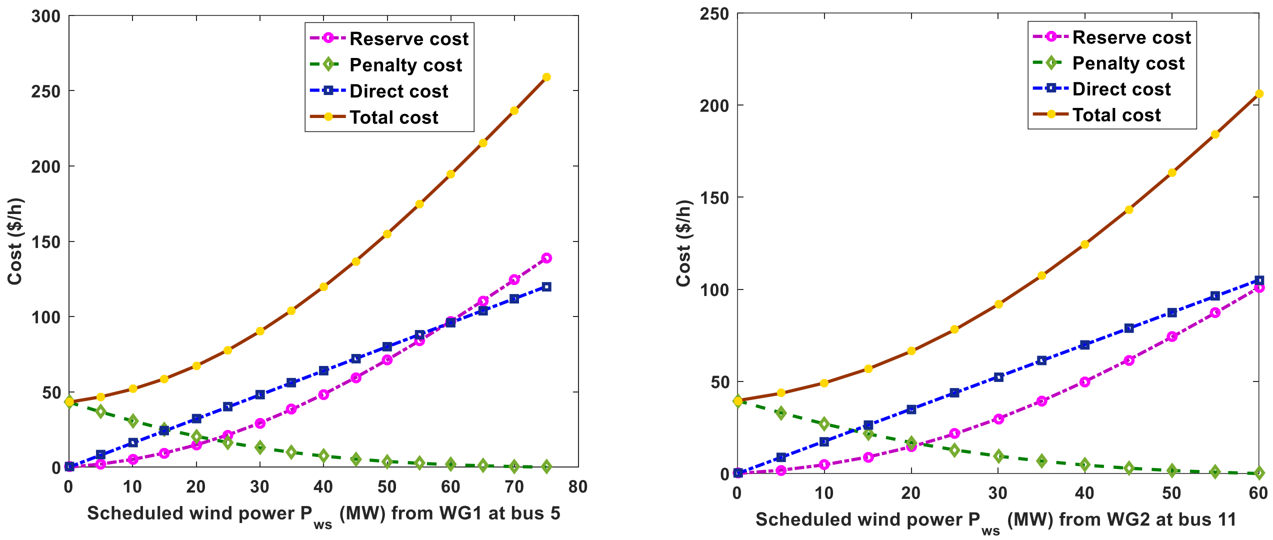


(a) (b)

Figure 5.73: Variation of wind power cost components vs scheduled wind power.

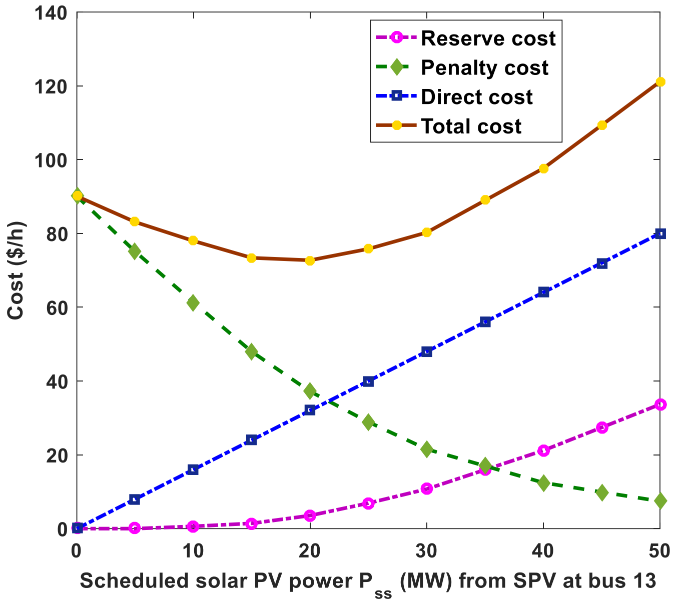


Figure 5.74: Variation of solar power cost components vs. scheduled solar power.

The relationship between the power cost of the SPV generator and the lognormal PDF mean (λ) is shown in Fig.5.76. In this study, λ is varied in the range of 2 to 7 with an increment of 0.5 [235]. The Scheduled power from the SPV generator is 20 MW with STD 0.6. Also, cost coefficients remain with the same values used in the previous case. The lowest cost of solar power is achieved when λ = 5.5. In addition, the penalty cost and reserve cost values are the same at λ = 5.8. It is observed that the penalty costs increase sharply for higher values of λ, which results in leading the overall cost to a higher level. However, a direct relationship between SPV generator output and solar irradiance is achieved with λ. When λ is low, then the SPV output is also low. High reserve powers are required to resist this status, which increases the reserve cost. When λ is high, the solar irradiance is also predicted high, so increasing SPV output power. In such a status, the penalty costs introduce an increase in the overall cost. Considering these two statuses, an appropriate value from the SPV output usually needs to be scheduled.

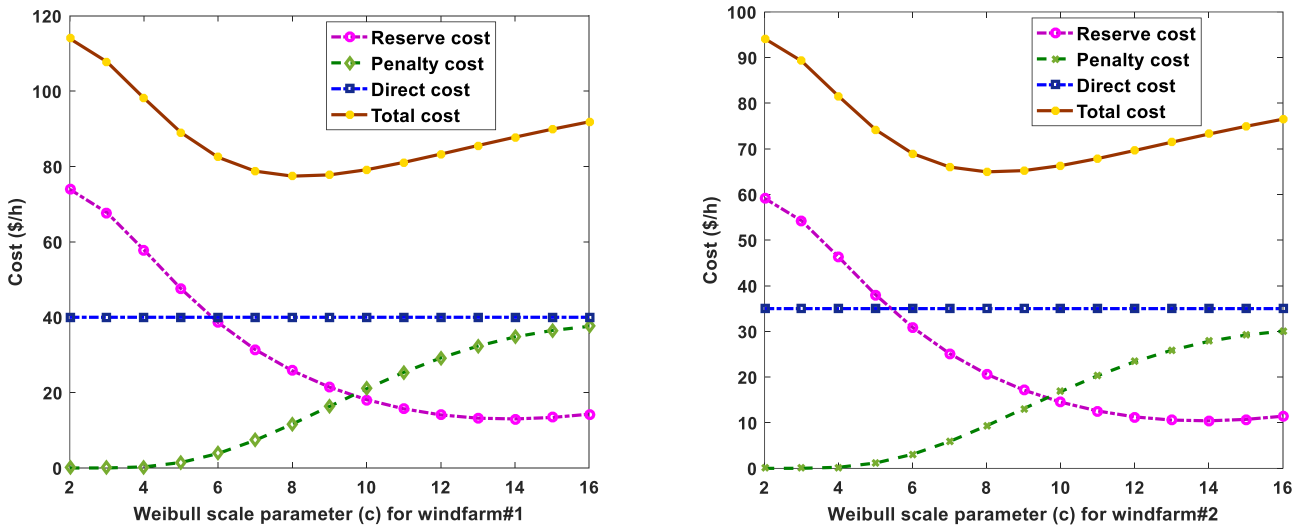


(a) (b)

Figure 5.75: Variation of wind power cost components vs Weibull scale parameter.

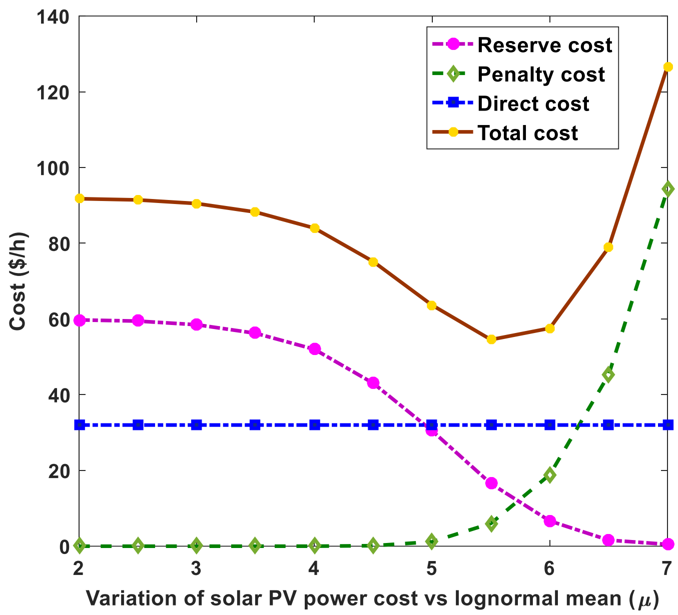


Figure 5.76: Variation of solar power cost components vs lognormal mean.

## 2) Case B

The proposed versions of CBO are utilized in this case to solve the EED problem with/without stochastic RES for different objective functions as follows:

### I. Case 1: Optimizing Total Generation Cost without Incorporating RES

In this section of the thesis, the performance of the CBO technique is investigated on the standard IEEE 30-bus test system without incorporating RES, where the fuel cost function is considered the objective function. For case 1, Eq. (3.28) calculates the fuel cost function. The optimal control settings obtained by suggested versions of CBO algorithms and the original BO are presented in Table 5.100, such as generator active power, generator voltage, transformer tap ratio, and reactive power from the capacitor bank. Also, the total generating cost as the main objective function, real power loss, emission, and voltage deviation are tabulated in Table 5.100. This comparison shows that the fuel cost obtained by the CBO5 method is better than that of the standard BO algorithm and other versions of CBO. However, the best fuel cost calculated by CBO5 for this case is 832.0752 $/h without any violation to the constraints, while the emission, real power loss, and voltage deviation became 0.319543 ton/h 10.68 MW, and 0.846898 p.u., respectively. The convergence characteristics of the compared optimization techniques of CBO versions and BO are shown in Fig. 5.77. Regarding the convergence graph, the CBO5 has a smooth convergence curve to the optimal solution without oscillations. Fig. 5.78 presents the voltage profile of all proposed versions of CBO and the original BO algorithms. This figure illustrates that all voltages magnitudes are within the specified limits (upper and lower bounds). The comparison of CBO5 with the original BO algorithm in terms of Best, Worst, Median, and STD of fuel cost is presented in Table 5.101.

### II. Case 2: Optimizing the Real Power Loss without Incorporating RES

This case aims to reduce the real power loss that is taken as the main objective function without Incorporating RES . The results of optimal control variables obtained by CBO5 and the original BO are tabulated in Table 5.102 From this table, the power loss is minimized to be 3.08819 MW while the fuel cost, the emission, and the voltage deviation became 1027.332 $/h 0.233633 ton/h, and 0.900771 p.u., respectively .The convergence characteristics for this case are illustrated in Fig. 5.79(a). This figure shows the best convergence by CBO5 .As in case 1, the voltages magnitude is within their limits for all buses, as shown in Fig. 5.80. The statistical results for the current case are tabulated in Table 5. This table shows that the CBO5 also achieves the smallest Best, Mean, Median, and STD values than the original BO.

Table 5.100: Simulation results of the proposed method and the BO method for case1.

| | Min | Max | BO | CBO1 | CBO2 | CBO3 | CBO4 | CBO5 | CBO6 | CBO7 | CBO8 | CBO9 | CBO10 |
|---|---|---|---|---|---|---|---|---|---|---|---|---|---|
| **Generator active power** | | | | | | | | | | | | | |
| **$P_{G1}$(MW)** | 50 | 200 | 198.6254 | 198.6991 | 198.6857 | 198.6739 | 198.7024 | 198.7367 | 198.5716 | 198.7221 | 198.9047 | 198.6208 | 198.7147 |
| **$P_{G2}$(MW)** | 20 | 80 | 45.21471 | 45.11906 | 44.77042 | 44.89704 | 44.56043 | 44.96156 | 44.60777 | 44.82217 | 45.24557 | 44.6228 | 44.66742 |
| **$P_{G5}$(MW)** | 15 | 50 | 18.2239 | 18.20115 | 18.57578 | 18.48418 | 18.77675 | 18.36983 | 18.84186 | 18.52777 | 17.98837 | 18.76609 | 18.67897 |
| **$P_{G8}$(MW)** | 10 | 35 | 10 | 10.04527 | 10 | 10 | 10.00599 | 10 | 10 | 10.00003 | 10 | 10.02919 | 10 |
| **$P_{G11}$(MW)** | 10 | 30 | 10.00101 | 10.00614 | 10.03021 | 10.00876 | 10.00022 | 10 | 10 | 10.0019 | 10.00003 | 10.00006 | 10 |
| **$P_{G13}$(MW)** | 12 | 40 | 12 | 12 | 12 | 12 | 12 | 12 | 12 | 12.0001 | 12.00029 | 12.00269 | 12.00001 |
| **Generator voltage** | | | | | | | | | | | | | |
| **$V_1$(p.u.)** | 0.95 | 1.1 | 1.0853 | 1.083108 | 1.082972 | 1.083702 | 1.082819 | 1.082705 | 1.085082 | 1.083031 | 1.080218 | 1.082642 | 1.082499 |
| **$V_2$(p.u.)** | 0.95 | 1.1 | 1.082611 | 1.1 | 1.090361 | 1.060996 | 1.1 | 1.1 | 1.072198 | 1.1 | 1.097758 | 1.059832 | 1.099925 |
| **$V_5$ (p.u.)** | 0.95 | 1.1 | 1.029013 | 1.027678 | 1.027467 | 1.027521 | 1.027396 | 1.026886 | 1.027424 | 1.026828 | 1.022684 | 1.081059 | 1.027605 |
| **$V_8$ (p.u.)** | 0.95 | 1.1 | 1.034571 | 1.023295 | 1.035512 | 1.034883 | 1.036265 | 1.035888 | 1.035348 | 1.009771 | 1.031406 | 1.034781 | 1.036244 |
| **$V_{11}$ (p.u.)** | 0.95 | 1.1 | 1.095888 | 1.070882 | 1.069605 | 1.057137 | 1.097282 | 1.075685 | 1.077993 | 1.1 | 1.055232 | 1.041216 | 1.099988 |
| **$V_{13}$ (p.u.)** | 0.95 | 1.1 | 1.037147 | 1.056721 | 1.053777 | 1.054794 | 1.025306 | 1.056338 | 1.053553 | 1.052925 | 1.0984 | 1.065886 | 1.026484 |
| **Transformer tap ratio** | | | | | | | | | | | | | |
| **$T_{11}$(6-9)** | 0.9 | 1.1 | 1.015298 | 1.034039 | 1.05907 | 1.009557 | 1.024553 | 1.007703 | 1.001557 | 1.099974 | 0.981481 | 0.961371 | 1.033192 |
| **$T_{12}$(6-10)** | 0.9 | 1.1 | 0.971798 | 0.920428 | 0.906353 | 0.957821 | 0.962566 | 0.959703 | 0.979863 | 0.9 | 0.981841 | 1.011796 | 0.962145 |
| **$T_{15}$(4-12)** | 0.9 | 1.1 | 0.969049 | 0.989422 | 0.981566 | 0.983852 | 0.97416 | 0.984684 | 0.972721 | 0.984992 | 1.015082 | 0.996291 | 0.973741 |
| **$T_{36}$(28-27)** | 0.9 | 1.1 | 0.974182 | 0.969703 | 0.973543 | 0.976203 | 0.984331 | 0.973367 | 0.97362 | 0.972554 | 0.979353 | 0.976633 | 0.970739 |
| **Capacitor bank** | | | | | | | | | | | | | |
| **$Q_{C10}$ (MVAR)** | 0 | 5 | 7.23E-09 | 0.004603 | 0.025006 | 0.03511 | 0 | 0.017517 | 0.05 | 0.005931 | 0.047326 | 0.05 | 0.044607 |
| **$Q_{C12}$ (MVAR)** | 0 | 5 | 0.049999 | 0.049983 | 0.035753 | 0.05 | 0.05 | 0.035957 | 0 | 0.049998 | 0 | 0.007414 | 0.05 |
| **$Q_{C15}$ (MVAR)** | 0 | 5 | 0.05 | 0.016845 | 0.038026 | 0.049601 | 0.045636 | 0.05 | 0.05 | 0.05 | 0.034575 | 0.04996 | 0.05 |
| **$Q_{C17}$ (MVAR)** | 0 | 5 | 0.023808 | 0.049535 | 0.049997 | 0.05 | 0.049975 | 0.032373 | 0.05 | 0.05 | 0.026928 | 0.047528 | 0.05 |
| **$Q_{C20}$ (MVAR)** | 0 | 5 | 0.042794 | 0.043324 | 0.039923 | 0.05 | 0.040803 | 0.032991 | 2.09E-06 | 0.048477 | 0.049651 | 0.05 | 0.0429 |

| | | | | | | | | | | | | | |
|---|---|---|---|---|---|---|---|---|---|---|---|---|---|
| **$Q_{C21}$ (MVAR)** | 0 | 5 | 0.049984 | 0.05 | 0.05 | 0.05 | 0.049904 | 0.05 | 0.05 | 0.05 | 0.049981 | 0.05 | 0.038009 |
| **$Q_{C23}$ (MVAR)** | 0 | 5 | 2.89E-19 | 0.05 | 0.05 | 0 | 0.034243 | 0.018485 | 0.033671 | 0.029605 | 0.03653 | 0.029278 | 0.00137 |
| **$Q_{C24}$ (MVAR)** | 0 | 5 | 0.049924 | 0.05 | 0.016185 | 0.05 | 0.05 | 0.05 | 0.048278 | 0.05 | 0.049987 | 0.05 | 0.049996 |
| **$Q_{C29}$ (MVAR)** | 0 | 5 | 0.021418 | 0.011182 | 0.022319 | 0.023411 | 0.037643 | 0.01673 | 0.019068 | 0.018267 | 0.027052 | 0.021731 | 0.017435 |
| **Objective function** | | | | | | | | | | | | | |
| **Fuel cost ($/h)** | | | 832.1145 | 832.0974 | 832.1366 | 832.1252 | 832.0994 | **832.0752** | 832.1081 | 832.1367 | 832.1684 | 832.1431 | 832.1241 |
| **Emission (ton/h)** | | | 0.31938 | 0.319503 | 0.319488 | 0.319459 | 0.319514 | 0.319543 | 0.319334 | 0.319524 | 0.319751 | 0.319407 | 0.319521 |
| **Power loss (MW)** | | | 10.67697 | 10.68265 | 10.67403 | 10.66395 | 10.65769 | 10.68 | 10.6331 | 10.68595 | 10.75089 | 10.64715 | 10.67302 |
| **Voltage deviation (p.u.)** | | | 0.83498 | 0.864783 | 0.840011 | 0.825256 | 0.886409 | 0.846898 | 0.854665 | 0.845794 | 0.834759 | 0.840725 | 0.890702 |

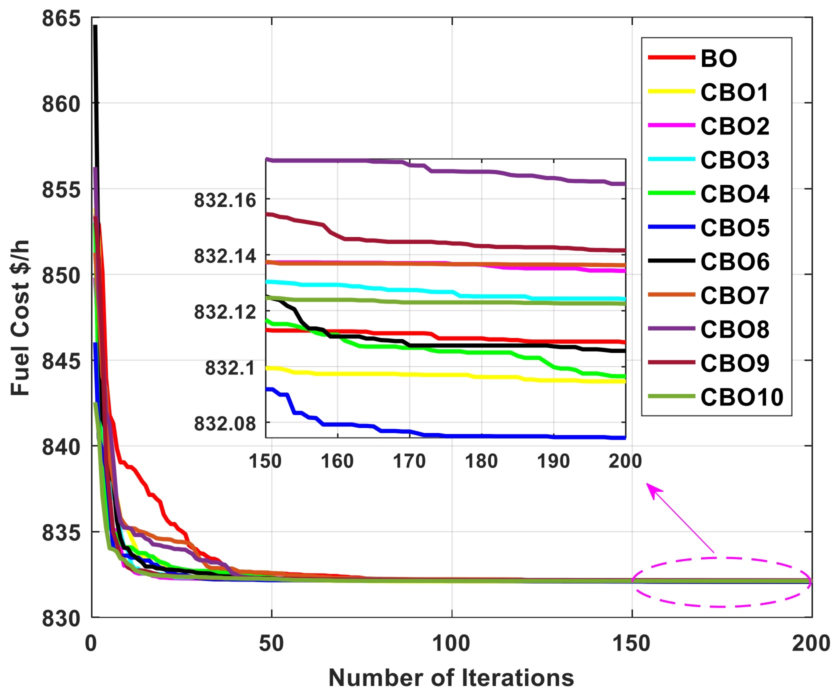


Figure 5.77: Convergence characteristic of all compared methods for case1.

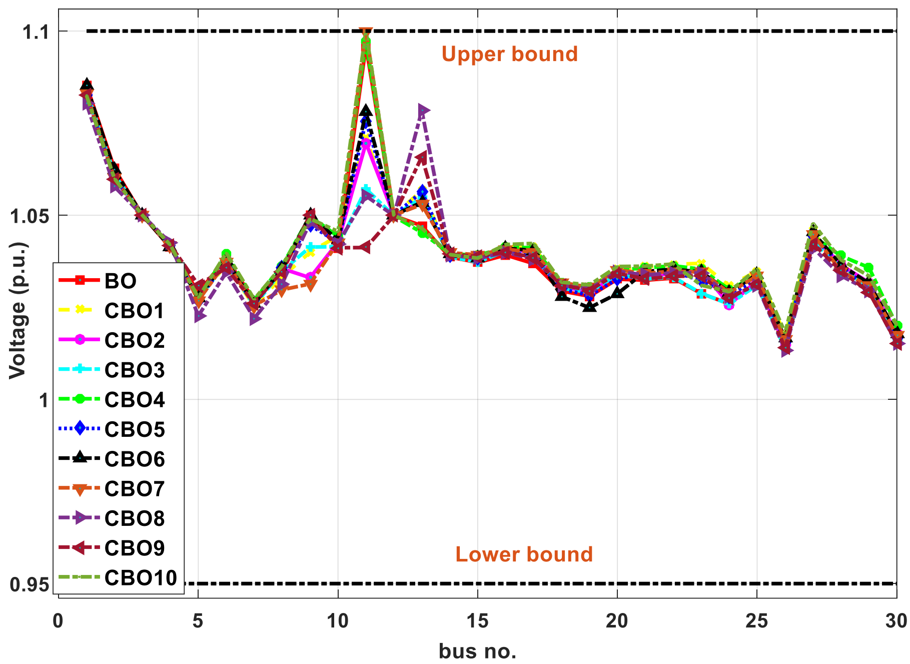


Figure 5.78: Voltage magnitude of all compared methods for case1.

Table 5.101: Statistical analysis of the total cost results obtained with different methods for Case1.

| Method | Best | Mean | Median | Worst | STD |
|---|---|---|---|---|---|
| BO | 832.11448096 | 832.3159239 | **832.217977** | 832.8043547 | 0.213989434 |
| CBO1 | 832.09738097 | 832.3483076 | 832.3223544 | 833.0282696 | 0.23393155 |
| CBO2 | 832.13660869 | 832.3138153 | 832.2985818 | 832.5276863 | 0.127775697 |
| CBO3 | 832.12515527 | 832.4124289 | 832.2463911 | 834.6937676 | 0.555892645 |
| CBO4 | 832.09944517 | 832.3744332 | 832.2782335 | 833.3874066 | 0.300424186 |
| CBO5 | **832.07517616** | **832.262603** | 832.2295532 | **832.4173286** | **0.106426901** |
| CBO6 | 832.10812904 | 832.4118822 | 832.2868731 | 833.5786145 | 0.364941685 |
| CBO7 | 832.13668677 | 832.2901096 | 832.2418044 | 832.7007641 | 0.140583761 |
| CBO8 | 832.16839578 | 832.284684 | 832.2281307 | 832.6251917 | 0.117317661 |
| CBO9 | 832.14305184 | 832.3872906 | 832.3449818 | 832.8088767 | 0.181949807 |
| CBO10 | 832.12410053 | 832.5580215 | 832.3585978 | 835.95637 | 0.842610868 |

### III. Case 3: Optimizing Total Generation Cost with Considering a Carbon Tax

In this case, the CBO5 algorithm is utilized to minimize the cumulative cost with the imposition of the CT without considering RES. In the present study, carbon tax $C_T$ is assumed with a rate of \$20/ton as in [239]. Then, its results are compared with the standard BO method. The results of this case are tabulated in Table 5.102. For the minimization of the cumulative cost, it can be noted that the CBO5 gives the best minimization of the cumulative cost, which is 837.7655 \$/h, while the real power loss, the emission, CT, and the voltage deviation became 10.66505 MW, 0.319507 ton/h, 17.83 \$/h, and 0.848031 p.u., respectively. The comparison of convergence characteristics of minimizing the cumulative cost with CT are depicted in Fig.5.79 (b). From this figure, the convergence curves from the CBO5 outperforms than that obtained from the BO. The voltages magnitudes of all buses of the CBO5 are within the specified limits, as shown in Fig. 5.80. Table 5.103 illustrates the comparison of statistical results yielded by CBO5 and the original BO algorithm.

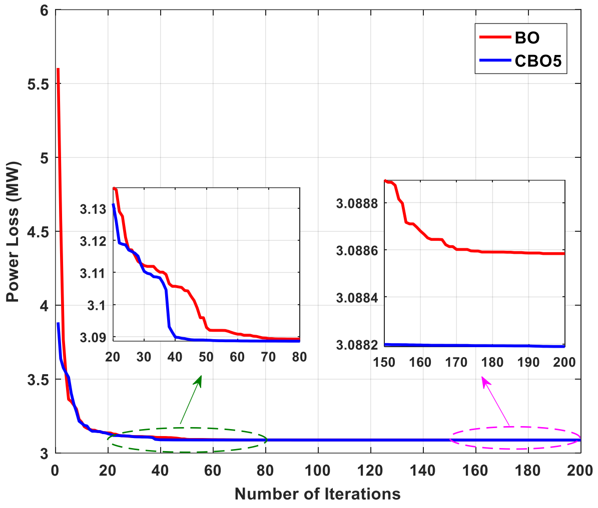


(a) Case 2

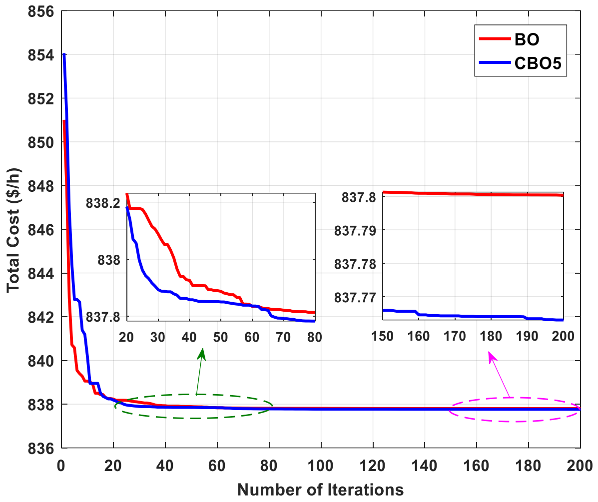


(b) Case 3

Figure 5.79: Convergence characteristic of CBO5 and BO for cases 2& 3.

Table 5.102: The Results of the proposed CBO5 method and BO method for cases 2 & 3.

| | | | Case 2 | | Case 3 | |
|---|---|---|---|---|---|---|
| | **Min** | **Max** | **BO** | **CBO5** | **BO** | **CBO5** |
| **Generator active power** | | | | | | |
| **$P_{G1}$(MW)** | 50 | 200 | 51.48872 | 51.48857 | 198.7282 | 198.7056 |
| **$P_{G2}$(MW)** | 20 | 80 | 80 | 80 | 44.85148 | 44.82563 |
| **$P_{G5}$(MW)** | 15 | 50 | 50 | 50 | 18.48704 | 18.52142 |
| **$P_{G8}$(MW)** | 10 | 35 | 35 | 34.99993 | 10 | 10 |
| **$P_{G11}$(MW)** | 10 | 30 | 30 | 29.99984 | 10.00151 | 10.00039 |
| **$P_{G13}$(MW)** | 12 | 40 | 39.99985 | 39.99984 | 12.00001 | 12.00006 |
| **Generator voltage** | | | | | | |
| **$V_1$(p.u.)** | 0.95 | 1.1 | 1.06111 | 1.061396 | 1.082316 | 1.082865 |
| **$V_2$(p.u.)** | 0.95 | 1.1 | 1.056967 | 1.057312 | 1.05966 | 1.1 |
| **$V_5$ (p.u.)** | 0.95 | 1.1 | 1.037555 | 1.037837 | 1.02634 | 1.027826 |
| **$V_8$ (p.u.)** | 0.95 | 1.1 | 1.044163 | 1.043956 | 1.033842 | 1.034909 |
| **$V_{11}$ (p.u.)** | 0.95 | 1.1 | 1.051582 | 1.041716 | 1.063828 | 1.061986 |
| **$V_{13}$ (p.u.)** | 0.95 | 1.1 | 1.054497 | 1.05654 | 1.057566 | 1.055204 |
| **Transformer tap ratio** | | | | | | |
| **$T_{11}$(6-9)** | 0.9 | 1.1 | 1.019284 | 1.047293 | 1.013279 | 0.983736 |
| **$T_{12}$(6-10)** | 0.9 | 1.1 | 0.932402 | 0.900001 | 0.938206 | 1.003173 |
| **$T_{15}$(4-12)** | 0.9 | 1.1 | 0.991923 | 0.991199 | 0.993955 | 0.9872 |
| **$T_{36}$(28-27)** | 0.9 | 1.1 | 0.974778 | 0.974566 | 0.97541 | 0.978693 |
| **Capacitor bank** | | | | | | |
| **$Q_{C10}$ (MVAR)** | 0 | 5 | 0.028518 | 0.045774 | 0.009227 | 0.049775 |
| **$Q_{C12}$ (MVAR)** | 0 | 5 | 0.020393 | 0.001478 | 0.049977 | 0.043561 |

| | | | | | | |
|---|---|---|---|---|---|---|
| **$Q_{C15}$ (MVAR)** | 0 | 5 | 0.046537 | 0.046257 | 0.049785 | 0.042716 |
| **$Q_{C17}$ (MVAR)** | 0 | 5 | 0.05 | 0.05 | 0.05 | 0.049929 |
| **$Q_{C20}$ (MVAR)** | 0 | 5 | 0.042133 | 0.042052 | 0.04109 | 0.038074 |
| **$Q_{C21}$ (MVAR)** | 0 | 5 | 0.05 | 0.05 | 0.05 | 0.05 |
| **$Q_{C23}$ (MVAR)** | 0 | 5 | 0.031086 | 0.031389 | 0.032529 | 0.04989 |
| **$Q_{C24}$ (MVAR)** | 0 | 5 | 0.05 | 0.05 | 0.05 | 0.05 |
| **$Q_{C29}$ (MVAR)** | 0 | 5 | 0.018052 | 0.019602 | 0.022632 | 0.01851 |
| Objective function | | | | | | |
| Fuel cost ($/h) | | | 1027.334 | 1027.332 | 832.1032 | 832.0687 |
| Emission (ton/h) | | | 0.233633 | 0.233633 | 0.319534 | 0.319507 |
| Total cost ($/h) | | | - | - | 837.8005 | **837.7655** |
| Carbon tax ($/h) | | | - | - | 17.83 | 17.83 |
| Power loss (MW) | | | 3.088588 | **3.088195** | 10.66829 | 10.66505 |
| Voltage deviation (p.u.) | | | 0.905851 | 0.900771 | 0.864543 | 0.848031 |

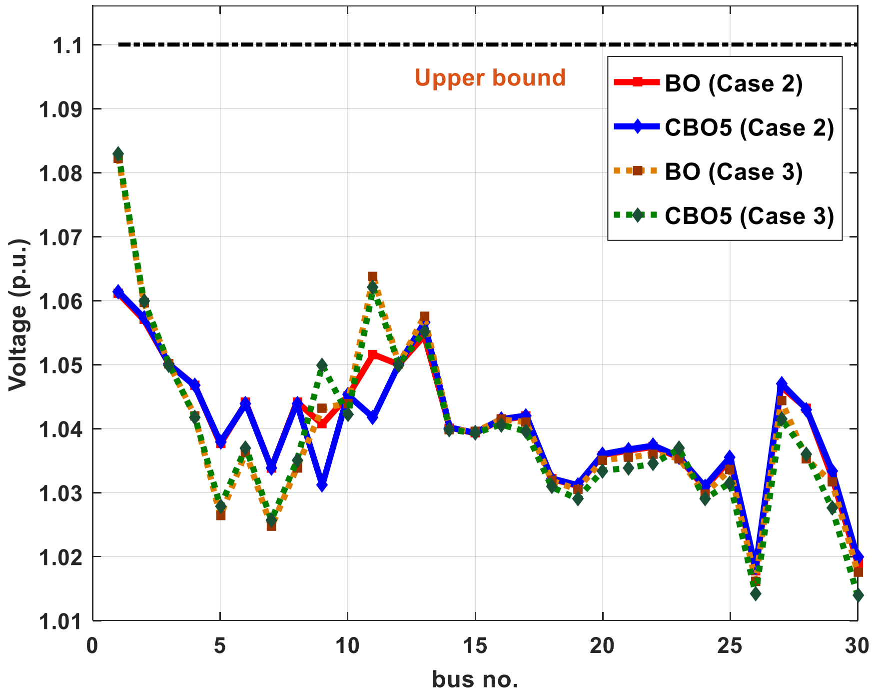


Figure 5.80: Voltage profiles of compared methods for cases 2 & 3.

Table 5.103: Statistical analysis for cases 2 & 3.

| Case no. | Method | Best | Mean | Median | Worst | STD |
|---|---|---|---|---|---|---|
| Case 2 | BO | 3.08858773 | 3.142113765 | 3.113191618 | 3.420240129 | 0.077467375 |
| | CBO5 | **3.08819485** | **3.098197495** | **3.09751512** | **3.116976241** | **0.008002977** |
| Case 3 | BO | 837.8004995 | 838.1715663 | **837.9152852** | 840.1457422 | 0.583449443 |
| | CBO5 | **837.7655243** | **837.9594622** | 837.9311724 | **838.1693743** | **0.114139838** |

Furthermore, the proposed CBO algorithm’s results are compared with more than 10 well-known algorithms' results for cases 1 and 2. This comparison for the two cases is presented in Table 5.104. It is seen from this table that the CBO achieved lower function values, which confirms the robustness and efficacy of the proposed technique and other recent optimization techniques such as Ensemble of constraint handling techniques with DE (ECHT-DE), feasibly solutions with DE (SF-DE), the self-adaptive penalty with DE (SP-DE), etc.

Table 5.104: Comparison of CBO5 algorithm with the original BO algorithm and previous studies for single objective cases of IEEE 30-bus system.

| Case # | Algorithm | Fuel cost ($/h) | Emission (t/h) | Ploss (MW) | VD (p.u.) |
|---|---|---|---|---|---|
| Case 1 | CBO5 | **832.0752** | 0.319543 | 10.68 | 0.846898 |
| | BO | 832.1145 | 0.31938 | 10.67697 | 0.83498 |
| | ECHT-DE [241] | 832.1356 | 0.43765 | 10.6772 | 0.80326 |
| | SF-DE [241] | 832.0882 | 0.43730 | 10.6387 | 0.84935 |
| | SP-DE [241] | 832.4813 | 0.43651 | 10.6762 | 0.75042 |
| | PSO [242] | 832.6871 | – | – | – |
| | ICBO [242] | 830.4531[a] | – | 10.2370 | 1.7450[a] |
| | BSA [243] | 830.7779[a] | 0.4377 | 10.2908 | 1.2050[a] |
| | APFPA [244] | 830.4065[a] | – | 10.2178 | 1.8909[a] |
| Case 2 | CBO5 | 1027.332 | 0.233633 | **3.088195** | 0.900771 |
| | BO | 1027.334 | 0.233633 | 3.088588 | 0.905851 |
| | MSA [245] | – | 0.20727 | 3.1005 | 0.88868 |
| | DSA [246] | – | 0.20826 | 3.0945 | – |
| | GPU-PSO [247] | – | – | 3.2601 | – |
| | ARCBBO [248] | – | 0.2073 | 3.1009 | 0.8913 |
| | EM [249] | – | – | 3.1775 | – |
| | IEM [249] | – | – | 2.8699[a] | – |
| | APFPA [244] | – | – | 2.8463[a] | 2.0720[a] |
| | ABC [250] | – | – | 3.1078 | – |
| | EGA-DQLF [251] | – | – | 3.2008 | – |
| | GEM [243] | – | 0.2072 | 2.8863[a] | 1.9755[a] |

[a] Infeasible solution, constraint on load bus voltage is violated.

### IV. Case 4: Optimizing Total Generation Cost With RES

According to Eq.(3.37), optimization scheduling of conventional thermal generators and RES for minimizing the total generation cost is performed. The cost coefficients of WT generators at buses 5 and 11 are like case A. The PDF parameters of WT and SPV generators as given in section 4 are utilized. Table 5.105 summarizes the obtained optimal control variables for this case in the same manner as case 1 but considering RES. The simulation results show that the CBO5 is more efficient because it gives better results than the BO algorithm. Hence, for this case, the CBO5 outperforms the BO algorithm in terms of the total generation cost with a value of 781.3524 \$/h. The convergence characteristics of the compared optimization algorithms are presented in Fig.5.81 (a). As shown, the CBO5 has a smooth with fast convergence curve. Fig. 5.82 shows the voltage profiles of the CBO5 and other proposed methods for all buses. It is shown that all voltage magnitudes are within the specified boundaries. However, the voltage profile for CBO5 has the better profile at all buses when compared to the BO algorithm. The statistical analysis is performed and tabulated in Table 5.106. The results prove that the CBO5 has better minimum STD over other original BO methods.

### V. Case 5: Optimizing Real Power Losses With RES

Optimization scheduling of both conventional thermal generators and RES to minimize the real power loss is presented in this case. With the same cost coefficients and the PDF parameters of WT and PV generators utilized in case 4, the best results yielded by the proposed CBO5 technique are presented in Table 5.104 and the results of the original BO algorithm. From Table 5.101, it can be seen that the CBO5 yielded a real power loss value of 1.832164 MW compared with the result of 1.833118 MW by the BO algorithm. Fig.5.81 (b) compares the convergence curves of real power loss for this case. This figure shows that the convergence characteristics of real power loss for the CBO5 technique outperform those from the compared BO algorithm. As in case 4, the voltage profiles of all buses obtained using the CBO5 and the BO are illustrated in Fig.5.82. It is seen that the voltage profile for CBO5 has a better voltage profile when compared to BO technique. The statistical results for the current case are summarized in Table 5.105. According to Table 5.106, it is established that the CBO5 also achieves the lowest Best, Mean, Median, and STD values than the BO algorithm.

### VI. Case 6: Optimizing the Total Generation Cost by Considering a Carbon Tax and RES.

As in case 3, by employing Eq.(3.38) with incorporating RES, the CBO5 algorithm is applied to minimize the cumulative cost with the imposition of the CT. Further, the penetration of RES is forecasted to increase, and the simulation results prove this. The last two columns of Table 5.105 show the best results obtained using the CBO5 alongside the BO algorithm for optimizing the power generation schedule of all relevant parameters considering the CT. From this table, it is seen that higher penetration of RES is accomplished compared to Case 4. In the optimal generation schedule, the range of RES penetration depends on both CT imposed and the emission volume. Moreover, the comparison of convergence characteristics for case 3 is yielded by CBO5 with the BO is illustrated in Fig.5.81(c). It is confirmed that CBO5 has the best performance to minimize the cumulative cost. In the same manner, Fig. 5.82 illustrates the voltage profiles for the current case. For all buses, the operating voltages are within the specified range.

Table 5.105: Results of the proposed CBO5 method and BO method for cases 4, 5 and 6.

| | | | **Case 4** | | **Case 5** | | **Case 6** | |
|---|---|---|---|---|---|---|---|---|
| | **Min** | **Max** | **BO** | **CBO5** | **BO** | **CBO5** | **BO** | **CBO5** |
| Generator active power | | | | | | | | |
| $P_{G1}$(MW) | 50 | 200 | 134.908 | 134.9078 | 7.645585 | 7.634951 | 125.4761 | 124.7555 |
| $P_{G2}$(MW) | 20 | 80 | 27.83719 | 28.14207 | 61.50441 | 61.47893 | 33.34418 | 31.51679 |
| $P_{W1}$(MW) | 0 | 75 | 43.43267 | 43.54993 | 75 | 75 | 46.22567 | 45.26177 |
| $P_{G8}$(MW) | 10 | 35 | 10 | 10 | 35 | 35 | 10 | 10 |
| $P_{W2}$(MW) | 0 | 60 | 36.68972 | 36.77103 | 60 | 60 | 38.95007 | 38.1232 |
| $P_{S1}$(MW) | 0 | 50 | 36.31506 | 35.8098 | 46.08312 | 46.11828 | 34.75265 | 39.0851 |
| Generator voltage | | | | | | | | |
| $V_1$(p.u.) | 0.95 | 1.1 | 1.071532 | 1.071571 | 1.0538 | 1.054095 | 1.070459 | 1.069179 |
| $V_2$(p.u.) | 0.95 | 1.1 | 1.056449 | 1.056559 | 1.054491 | 1.054778 | 1.056739 | 1.056593 |
| $V_5$ (p.u.) | 0.95 | 1.1 | 1.034488 | 1.034492 | 1.045138 | 1.045352 | 1.035747 | 1.03585 |
| $V_8$ (p.u.) | 0.95 | 1.1 | 1.090926 | 1.059025 | 1.094693 | 1.051321 | 1.068384 | 1.041066 |
| $V_{11}$ (p.u.) | 0.95 | 1.1 | 1.1 | 1.09827 | 1.098714 | 1.1 | 1.1 | 1.099998 |
| $V_{13}$ (p.u.) | 0.95 | 1.1 | 1.049476 | 1.049468 | 1.059987 | 1.062491 | 1.0497 | 1.060039 |
| Objective function | | | | | | | | |
| Fuel cost ($/h) | | | 781.7198 | **781.3524** | 958.5272 | 957.8938 | 790.6987 | 790.9503 |
| Fuel thermal unit cost | | | 438.3715 | 439.3802 | 358.1352 | 358.014 | 435.0614 | 427.1315 |
| Wind generation cost | | | 244.2747 | 244.9571 | 464.6296 | 464.6296 | 261.9756 | 255.6239 |
| Solar generation cost | | | 99.07357 | 97.0151 | 135.7624 | 135.2502 | 93.66172 | 108.1948 |
| Emission (ton/h) | | | 1.762253 | 1.76216 | 0.099828 | 0.099827 | 0.99819 | 0.957464 |
| Total cost ($/h) | | | - | - | - | - | 808.4964 | **808.0219** |
| Carbon tax ($/h) | | | - | - | - | - | 17.83 | 17.83 |
| Power loss (MW) | | | 5.782634 | 5.780656 | 1.833118 | **1.832164** | 5.348664 | 5.342363 |
| Voltage deviation (p.u.) | | | 0.454874 | 0.454963 | 0.531491 | 0.538215 | 0.458006 | 0.486436 |
| Generator reactive power | | | | | | | | |
| $Q_{G1}$(MVAR) | -20 | 150 | -2.1961 | -2.29821 | -6.04861 | -5.84803 | -2.84362 | -5.65912 |
| $Q_{G2}$(MVAR) | -20 | 60 | 11.47038 | 11.67913 | 5.905437 | 6.579832 | 10.97277 | 13.33378 |
| $Q_{W1}$(MVAR) | -30 | 35 | 22.44562 | 22.33918 | 20.50373 | 20.80685 | 22.37656 | 23.1282 |
| $Q_{G8}$(MVAR) | -15 | 40 | 40 | 40 | 40 | 37.81501 | 40 | 35.89478 |
| $Q_{W2}$(MVAR) | -25 | 30 | 30 | 30 | 30 | 30 | 30 | 30 |
| $Q_{S1}$(MVAR) | -20 | 25 | 15.31231 | 15.30408 | 18.61107 | 19.61333 | 15.36297 | 19.13591 |

Finally, Table 5.106 sums up the statistical analysis performed by various algorithms besides the proposed algorithm, such as grasshopper optimization algorithm (GOA), black widow optimization algorithm (BWOA), GWO, ant lion Optimizer (ALO), PSO, GSA, moth-flame optimization (MFO), barnacles mating optimizer (BMO), and the conventional BO algorithm for the three cases. Obviously, the CBO5 technique outperforms these algorithms from the previous literature and the original BO for cases 4, 5, and 6. It is shown from this table that the proposed CBO5 algorithm presents a superior performance in terms of accuracy and robustness. Furthermore, the results of some recent techniques, including jellyfish search optimizer (JS), artificial bee colony (ABC), Chaos Game Optimization (CGO), Giza pyramids construction (GPC), Flower pollination algorithm (FPA), genetic algorithms (GA), crow search algorithms (CSA), success history-based adaptive differential evolution-feasible solutions (SHADE-SF), GWO, PSO, MFO, multi-operator differential evolution algorithm (MODE), and hybridization of PSO with GWO (HPSO-GWO) for these cases are presented in Table 5.107. This table confirms the efficacy of the proposed CBO5 technique and proves its supremacy on more than 19 techniques in different cases of the EED problem.

Table 5.106: Statistical analysis for cases 4, 5 and 6.

| Case no. | Method | Best | Mean | Median | Worst | STD |
|---|---|---|---|---|---|---|
| Case 4 | BO | 781.7197605 | 782.3550213 | 782.3092122 | 783.2470357 | 3.47E-01 |
| | CBO5 | **781.3524007** | **782.2580216** | **782.2807345** | **782.732256** | 3.65E-01 |
| | GOA [252] | 785.7109 | 804.0168 | - | 823.4731 | 9.52E+00 |
| | BWOA [252] | 784.8148 | 788.2471 | - | 795.4683 | 5.83E+00 |
| | GWO [252] | 781.6645 | 783.0412 | - | 783.3359 | 2.75E-01 |
| | ALO [252] | 781.6562 | 784.3253 | - | 791.9234 | 2.49E+00 |
| | PSO [252] | 781.9047 | 784.9048 | - | 794.4221 | 2.52E+00 |
| | GSA [252] | 782.2237 | 785.8603 | - | 794.8996 | 2.43E+00 |
| | MFO [252] | 781.6928 | 782.492 | - | 783.9305 | 4.77E-01 |
| | BMO [252] | 781.6519 | 781.8187 | - | 783.5284 | **3.44E-01** |
| Case 5 | BO | 1.833116197 | 1.87402079 | 1.859883433 | 1.923364852 | 3.13E-02 |
| | CBO5 | **1.832163805** | **1.856660468** | **1.85210747** | **1.897404142** | **2.40E-02** |
| | GOA [252] | 2.2043 | 3.619731 | - | 11.92648 | 2.25E+00 |
| | BWOA [252] | 2.1403 | 2.364899 | - | 2.734243 | 1.23E-01 |
| | GWO [252] | 2.0616 | 2.168241 | - | 2.680391 | 3.66E-01 |
| | ALO [252] | 2.0845 | 2.323007 | - | 2.762308 | 1.74E-01 |
| | PSO [252] | 2.1572 | 2.253856 | - | 3.053334 | 2.50E-01 |
| | GSA [252] | 2.5464 | 3.258794 | - | 5.410662 | 5.11E-01 |
| | MFO [252] | 2.0694 | 2.108907 | - | 2.19696 | 3.34E-02 |
| | BMO [252] | 2.0646 | 2.095184 | - | 2.142221 | 2.54E-02 |
| Case 6 | BO | 808.4946721 | 809.1820118 | 809.0531943 | 810.5598586 | 5.23E-01 |
| | CBO5 | **808.0220664** | **808.8406762** | **808.8640024** | **809.2685809** | 3.09E-01 |
| | GOA [252] | 822.3074 | 839.1499 | - | 857.8005 | 9.32E+00 |
| | BWOA [252] | 821.4095 | 824.358 | - | 830.89 | 2.66E+00 |
| | GWO [252] | 811.2516 | 811.4707 | - | 811.6266 | 1.26E-01 |
| | ALO [252] | 811.4334 | 811.7083 | - | 814.2972 | 5.36E-01 |
| | PSO [252] | 811.5916 | 812.7758 | - | 818.8017 | 1.43E+00 |
| | GSA [252] | 811.5264 | 811.7708 | - | 813.3572 | 4.97E-01 |
| | MFO [252] | 811.4229 | 811.7398 | - | 812.4613 | 3.42E-01 |
| | BMO [252] | 810.7982 | 810.7739 | - | 811.1199 | **1.45E-01** |

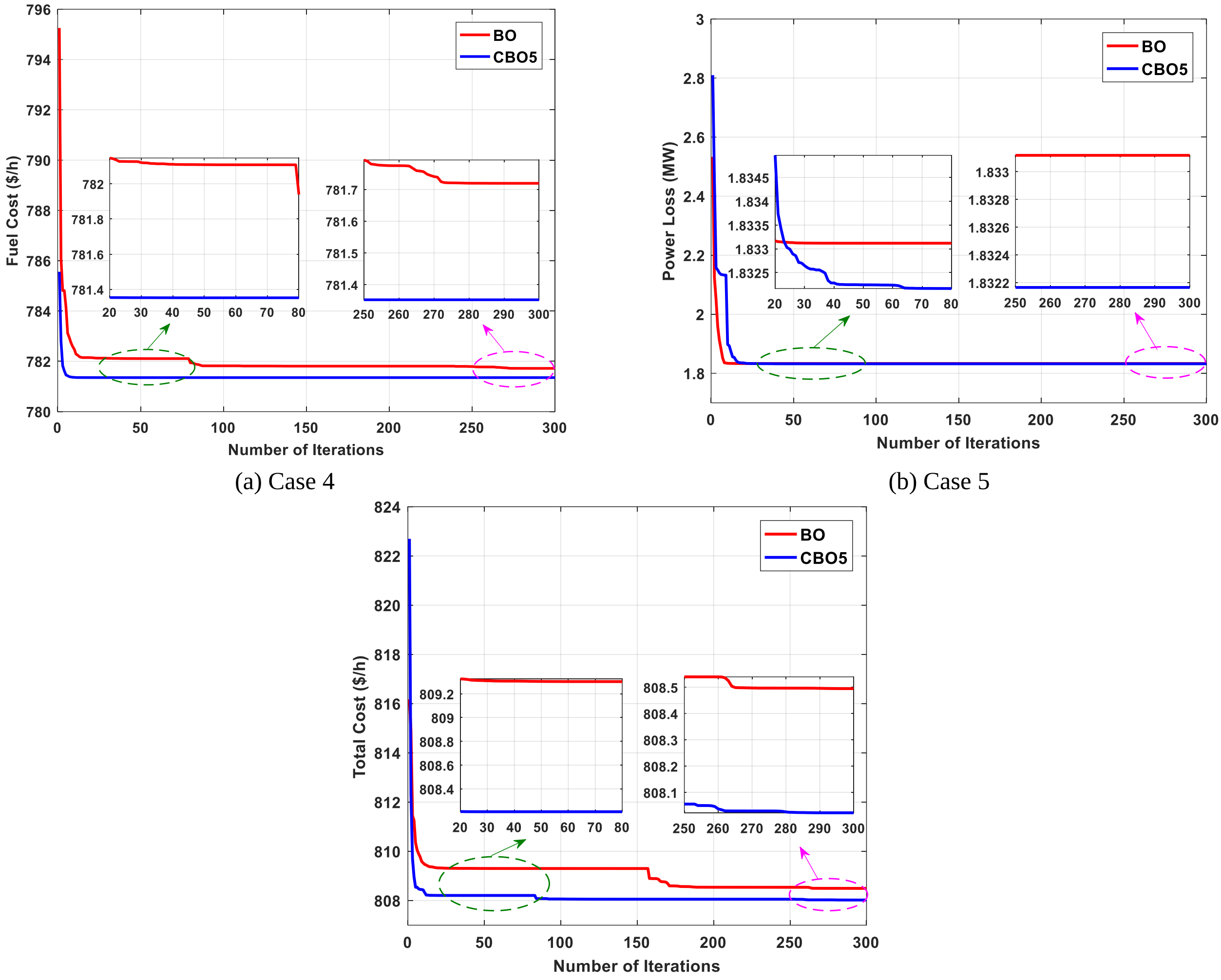


(a) Case 4

(b) Case 5

(c) Case 6

Figure 5.81: Convergence characteristic of CBO5 and BO for cases 4, 5 and 6.

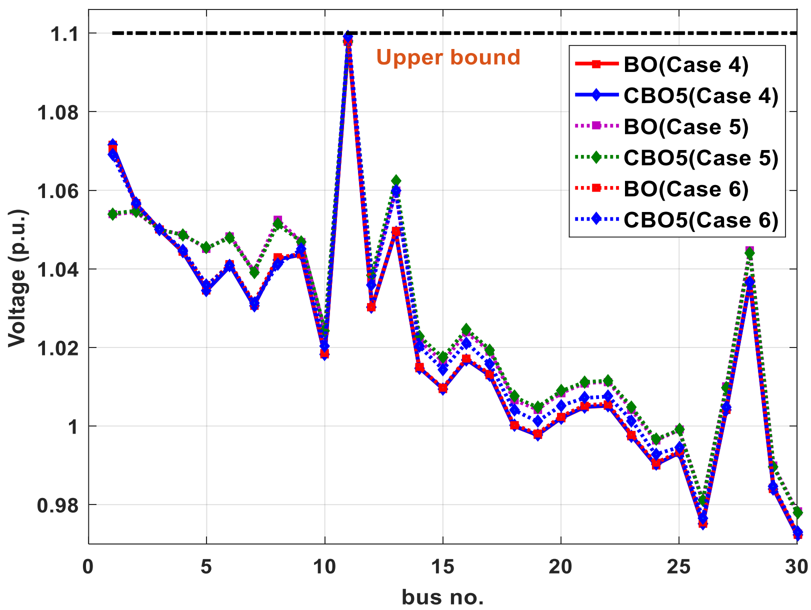

Figure 5.82: Voltage profiles of compared methods for cases 4, 5 and 6.

Table 5.107: Comparison of CBO5 algorithm with the original BO algorithm and previous studies for single objective cases (4, 5, and 6) of IEEE 30-bus system.

| Case # | Algorithm | Fuel cost ($/h) | Emission (t/h) | Ploss (MW) | VD (p.u.) |
|---|---|---|---|---|---|
| Case 4 | CBO5 | **781.3524** | 1.76216 | 5.780656 | 0.454874 |
| | BO | 781.7198 | 1.762253 | 5.782634 | 0.454963 |
| | JS [253] | 781.6387 | 1.761998 | 5.773893 | 0.448284 |
| | CGO [253] | 782.1950203 | 1.761969 | 5.685199 | 0.453825 |
| | FPA [253] | 782.8596 | 1.762312 | 5.863689 | 0.455137 |
| | GPC [253] | 782.4229 | 1.764097 | 5.843226 | 0.537061 |
| | GA [235] | 787.84 | 2.76 | 6.43 | 0.87 |
| | PSO [235] | 785.82 | 2.36 | 6.79 | 1.08 |
| | CSA [235] | 784.77 | 1.96 | 6.47 | 0.85 |
| | ABC [235] | 783.81 | 1.75 | 6.06 | 0.56 |
| | GWO [235] | 781.40 | 1.75 | 5.44 | 1.05 |
| | MODE-OPF [254] | 782.3592764 | - | - | - |
| | SHADE-SF [133] | 782.503 | 1.762 | 5.77 | 0.463 |
| Case 5 | CBO5 | 957.8938 | 0.099827 | **1.832163805** | 0.538215 |
| | BO | 958.5272 | 0.099828 | 1.833116197 | 0.531491 |
| Case 6 | CBO5 | **808.0219** | 0.957464 | 5.342363 | 0.486436 |
| | BO | 808.4964 | 0.99819 | 5.348664 | 0.458006 |
| | JS [253] | 810.12101 | 0.89377 | 5.276 | 0.46884 |
| | CGO [253] | 811.4568 | 0.902467 | 5.377988 | 0.499635 |
| | FPA [253] | 811.6664 | 0.923031 | 5.307636 | 0.465664 |
| | GPC [253] | 810.324 | 0.916127 | 5.327113 | 0.507454 |
| | GA [235] | 814.72 | 1.36 | 5.63 | 0.64 |
| | PSO [235] | 811.49 | 0.98 | 5.46 | 0.48 |
| | CSA [235] | 811.53 | 0.92 | 5.44 | 0.49 |
| | ABC [235] | 811.26 | 0.89 | 5.31 | 0.47 |
| | GWO [235] | 809.93 | 0.86 | 4.99 | 1.07 |
| | SHADE-SF [133] | 810.346 | 0.891 | 5.276 | 0.469 |
| | MFO [255] | 809.969 | 0.898 | 5.010 | 1.067 |
| | HPSO-GWO [256] | 809.277 | 0.914 | 5.132 | 0.462 |

[a] Infeasible solution, constraint on load bus voltage is violated.

## 5.6.2 Test System 2

In this subsection, a medium-scale test system of the modified IEEE-57 bus test system is implemented to prove the suitability and scalability of the CBO for medium-scale systems. The system consists of seven generators including four conventional thermal generators, two WT generators and one SPV generator; fifty load buses; eighty branches. The voltage magnitude limits for all buses are between 0.95 -1.1 p.u.

The total connected loads for active and reactive power are 12.508 p.u. 3.364 p.u. at 100 MVA base, respectively. More details of the data, emission, and cost coefficients of the IEEE-57 bus system are given [257]. In the following case studies for solving the EED in the IEEE-57 bus test system, the best results are obtained under equality and inequality constraints given in Eqs. (3.43)–(3.51).

Cases 7–9 are considered to solve the EED problem without RES to establish the efficacy of the proposed CBO5. The optimal control variables with the corresponding results for three considered objective functions for minimizing the total generating cost without imposing CT, minimizing the real power loss, and minimizing the total generating cost with imposing CT are presented in Table 5.108. The convergence characteristics for these cases are given in Fig.5.83. In addition, Fig.5.84 shows that all voltage magnitudes by CBO5 are within their limits, and CBO5 has a better voltage profile than the compared BO algorithm for all cases. However, these cases can be presented as follows:

**Case 7:** The main objective function of this case study is to decrease the total operating fuel cost. The fuel cost achieved by the proposed CBO5 algorithm is 41666.24 $/hr, and this value is the best result compared with that obtained using the BO algorithm. At the same time, the emission level, real power loss, voltage deviation, and the voltage stability index became 1.352409 ton/h, 14.85959 MW, 1.697282 p.u., and 0.278571 p.u., respectively. From Table 5.108, it can be noted that the proposed CBO5 gives the best results for minimizing fuel costs compared with the BO algorithm.

**Case 8:** In this case, the real power loss minimization is considered the main objective function. The real power loss is minimized to be 9.955717 MW while the fuel costs, emission, voltage deviation, and voltage stability index became 44567.04 $/h, 1.105042 ton/h, 1.679816 p.u. and 0.279129 p.u., respectively. From Table 5.108, it is observed that the best result for minimizing real power loss is achieved by CBO5 when compared with the BO algorithm.

Table 5.108: Results of the proposed CBO5 method and BO method for cases 7, 8 and 9.

| | | | Case 7 | | Case 8 | | Case 9 | |
|---|---|---|---|---|---|---|---|---|
| | **Min** | **Max** | **BO** | **CBO5** | **BO** | **CBO5** | **BO** | **CBO5** |
| Generator active power | | | | | | | | |
| $P_{G1}$(MW) | 0 | 576 | 142.7743 | 142.7915 | 174.9728 | 178.6854 | 143.0531 | 142.7197 |
| $P_{G2}$(MW) | 30 | 100 | 90.19244 | 90.38392 | 30 | 30 | 92.20437 | 90.6409 |
| $P_{G3}$(MW) | 40 | 140 | 44.9847 | 45.25163 | 140 | 134.846 | 45.10395 | 45.04671 |
| $P_{G6}$(MW) | 30 | 100 | 70.45563 | 70.39143 | 99.99762 | 99.99974 | 72.94854 | 71.59962 |
| $P_{G8}$(MW) | 100 | 550 | 460.1464 | 460.3926 | 305.9038 | 307.2246 | 457.5174 | 459.7178 |
| $P_{G9}$(MW) | 30 | 100 | 96.63655 | 96.74015 | 99.96983 | 100 | 96.90143 | 96.39607 |
| $P_{G12}$(MW) | 100 | 410 | 360.4599 | 359.7084 | 409.9307 | 410 | 357.9451 | 359.5547 |
| Generator voltage | | | | | | | | |
| $V_1$(p.u.) | 0.95 | 1.1 | 1.068701 | 1.066665 | 1.066729 | 1.065168 | 1.064178 | 1.062095 |

| | | | | | | | | |
|---|---|---|---|---|---|---|---|---|
| $V_2$(p.u.) | 0.95 | 1.1 | 1.066424 | 1.064343 | 1.062514 | 1.061365 | 1.062116 | 1.059981 |
| $V_3$ (p.u.) | 0.95 | 1.1 | 1.058204 | 1.056268 | 1.063823 | 1.06388 | 1.054645 | 1.052765 |
| $V_6$(p.u.) | 0.95 | 1.1 | 1.061668 | 1.059556 | 1.061691 | 1.061822 | 1.059528 | 1.061764 |
| $V_8$ (p.u.) | 0.95 | 1.1 | 1.074487 | 1.07622 | 1.068629 | 1.067475 | 1.075274 | 1.074041 |
| $V_9$ (p.u.) | 0.95 | 1.1 | 1.049872 | 1.050607 | 1.047356 | 1.047262 | 1.048379 | 1.047081 |
| $V_{12}$ (p.u.) | 0.95 | 1.1 | 1.05086 | 1.051465 | 1.050802 | 1.052756 | 1.047157 | 1.045979 |
| Capacitor bank | | | | | | | | |
| $Q_{C18}$ (MVAR) | 0 | 20 | 10.198 | 5.084277 | 8.755611 | 7.764916 | 12.21105 | 8.16114 |
| $Q_{C25}$ (MVAR) | 0 | 20 | 13.84537 | 12.81139 | 15.60203 | 13.53967 | 13.12904 | 13.81369 |
| $Q_{C53}$ (MVAR) | 0 | 20 | 11.70113 | 11.01722 | 12.75123 | 13.15801 | 12.64346 | 11.9624 |
| Transformer tap ratio | | | | | | | | |
| $T_{19}$(4-18) | 0.9 | 1.1 | 1.069633 | 1.034583 | 1.0928 | 1.05031 | 0.900012 | 0.937933 |
| $T_{20}$(4-18) | 0.9 | 1.1 | 0.999451 | 0.939249 | 0.930333 | 1.031141 | 1.099982 | 1.025207 |
| $T_{31}$(21-20) | 0.9 | 1.1 | 1.045801 | 1.011281 | 1.001453 | 1.071854 | 1.00902 | 1.008322 |
| $T_{35}$(24-25) | 0.9 | 1.1 | 1.00294 | 0.974787 | 1.1 | 0.908503 | 1.043702 | 1.1 |
| $T_{36}$(24-25) | 0.9 | 1.1 | 1.031886 | 1.046757 | 0.946079 | 1.1 | 0.980871 | 0.932915 |
| $T_{37}$(24-26) | 0.9 | 1.1 | 1.03434 | 1.032326 | 1.00506 | 0.98854 | 1.036381 | 1.029856 |
| $T_{41}$(7-29) | 0.9 | 1.1 | 0.995134 | 0.994727 | 0.996236 | 0.996313 | 0.998887 | 0.995242 |
| $T_{46}$(34-32) | 0.9 | 1.1 | 0.96096 | 0.961015 | 0.950025 | 0.951205 | 0.960265 | 0.969007 |
| $T_{54}$(11-41) | 0.9 | 1.1 | 0.9162 | 0.913632 | 1.037943 | 0.90606 | 0.9 | 0.907877 |
| $T_{58}$(15-45) | 0.9 | 1.1 | 0.981886 | 0.981072 | 0.982663 | 0.982779 | 0.978985 | 0.976813 |
| $T_{59}$(14-46) | 0.9 | 1.1 | 0.968734 | 0.966545 | 0.973583 | 0.970881 | 0.963378 | 0.962864 |
| $T_{65}$(10-51) | 0.9 | 1.1 | 0.97479 | 0.976017 | 0.977511 | 0.977373 | 0.972604 | 0.971138 |
| $T_{66}$(13-49) | 0.9 | 1.1 | 0.940854 | 0.93782 | 0.943897 | 0.940648 | 0.936124 | 0.935383 |
| $T_{71}$(11-43) | 0.9 | 1.1 | 0.975222 | 0.974105 | 0.95584 | 0.97761 | 0.978299 | 0.972614 |
| $T_{73}$(40-56) | 0.9 | 1.1 | 0.97591 | 0.991325 | 1.047203 | 0.989166 | 0.997103 | 0.984115 |
| $T_{76}$(39-57) | 0.9 | 1.1 | 0.970954 | 0.964976 | 1.007276 | 0.956589 | 0.970735 | 0.971606 |
| $T_{80}$(9-55) | 0.9 | 1.1 | 1.002546 | 1.001638 | 0.98587 | 0.987936 | 1.001733 | 0.996861 |
| Objective function | | | | | | | | |
| Fuel cost ($/h) | | | 41667.03 | **41666.24** | 44799.15 | 44567.04 | 41667.54 | 41666.86 |
| Emission (ton/h) | | | 1.352963 | 1.352409 | 1.099789 | 1.105042 | 1.340179 | 1.349873 |
| Total cost ($/h) | | | - | - | - | - | 41691.45 | **41690.94** |
| Carbon tax ($/h) | | | - | - | - | - | 17.83 | 17.83 |
| Power loss (MW) | | | 14.84992 | 14.85959 | 9.974691 | **9.955717** | 14.87384 | 14.87548 |
| Voltage deviation (p.u.) | | | 1.636026 | 1.697282 | 1.72999 | 1.679816 | 1.639563 | 1.648446 |
| *L*-index (max) | | | 0.279554 | 0.278571 | 0.28068 | 0.279129 | 0.279054 | 0.279868 |
| Generator reactive power | | | | | | | | |
| $Q_{G1}$(MVAR) | -140 | 200 | 48.68674 | 46.05551 | 41.43618 | 35.07896 | 46.55154 | 45.66637 |
| $Q_{G2}$(MVAR) | -17 | 50 | 50.62978 | 50.27508 | 49.97858 | 49.99539 | 50.02996 | 50.02675 |
| $Q_{G3}$(MVAR) | -10 | 60 | 33.49309 | 36.50477 | 29.98118 | 33.99622 | 34.20023 | 31.53403 |
| $Q_{G6}$(MVAR) | -8 | 25 | -4.87987 | -7.82605 | -6.99093 | -5.90412 | -8.00321 | 0.617702 |
| $Q_{G8}$(MVAR) | -140 | 200 | 47.15352 | 54.26851 | 50.90107 | 46.27143 | 55.32088 | 51.13646 |
| $Q_{G9}$(MVAR) | -3 | 9 | 8.999538 | 8.997678 | 8.952382 | 8.996319 | 8.984235 | 9.001633 |
| $Q_{G12}$(MVAR) | -150 | 155 | 52.92708 | 56.67265 | 43.06637 | 50.5751 | 52.19551 | 53.0369 |

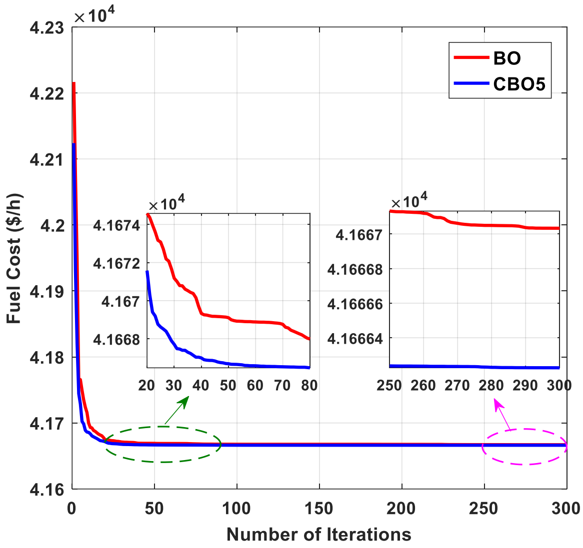


(a) Case 7

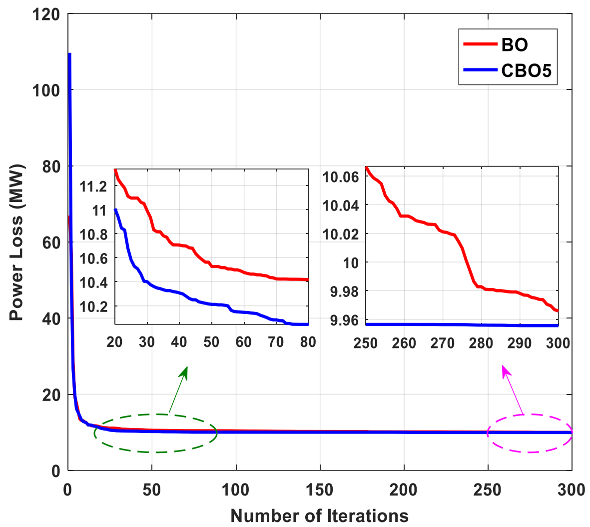


(b) Case 8

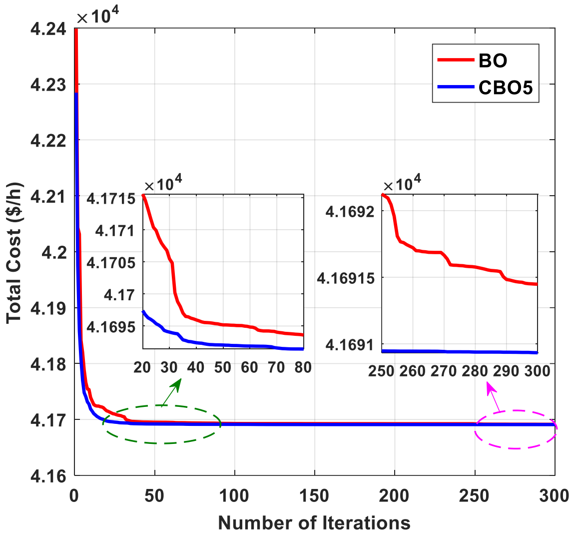


(c) Case 9

Figure 5.83: Convergence characteristic of CBO5 and BO for cases 7, 8 and 9.

**Case 9:** In this case, the objective function aims to minimize fuel costs by considering imposing a carbon tax. Using the proposed CBO5, the total cost is minimized to be 41690.94 $/h, where the fuel costs, emission, CT, real power loss, voltage deviation, and voltage stability index became 41666.86 $/h, 1.349873 ton/h, 17.83 $/h, 14.87548 MW, 1.648446 p.u. , and 0.279868 p.u., respectively. From Table 5.108, it can be confirmed that the proposed CBO5 obtains the best results compared with the BO algorithm.

Also, to estimate the robustness of the CBO5, a statistical analysis is conducted. However, the best, the mean, the Median, the worst, and STD are computed for these cases and shown in Table 5.109. One can observe that the best, the mean, and the worst values of the considered objective functions obtained by the

CBO5 are very close, which reveals the capability of the CBO5 to achieve the best solution or very near to it in each run.

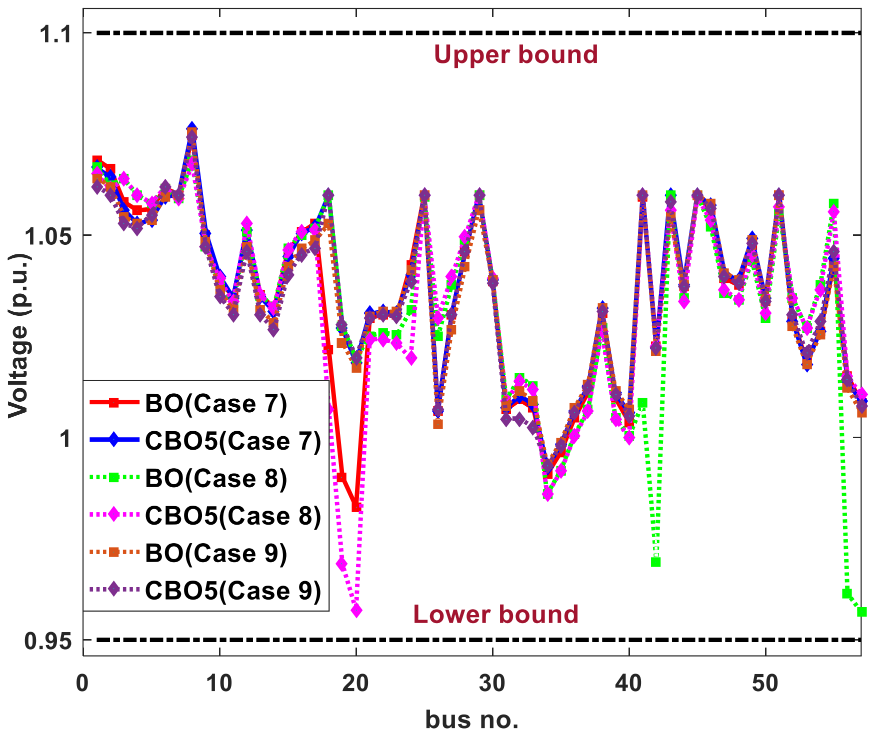


Figure 5.84: Voltage profiles of compared methods for cases 7,8 and 9.

Table 5.109: The Statistical analysis for cases 7,8 and 9.

| Case no. | Method | Best | Mean | Median | Worst | STD |
|---|---|---|---|---|---|---|
| Case 7 | BO | 41667.03409 | 41675.22151 | 41671.70027 | 41693.16048 | 8.527563174 |
| | CBO5 | **41666.23663** | **41668.57336** | **41667.13323** | **41684.00307** | **4.187697142** |
| Case 8 | BO | 9.974691103 | 10.21021949 | **10.13157982** | 10.72890627 | 0.222606525 |
| | CBO5 | **9.95571668** | **10.1684184** | 10.16496739 | **10.55189755** | **0.163241655** |
| Case 9 | BO | 41691.44782 | 41701.52668 | 41697.38732 | 41723.78741 | 9.331295153 |
| | CBO5 | **41690.94253** | **41696.52955** | **41695.39938** | **41707.59411** | **4.54549932** |

Finally, According to the results in Table 5.110, the proposed CBO5 algorithm provided a slightly better result than the original BO algorithm in solving the problem of case7. Compared with the other techniques, the difference in fuel cost was further increased in the IEEE 57-bus system, which is a larger power system than the IEEE 30-bus system. The result from the CBO5 algorithm, the original BO algorithm, MSA, DSA, improved colliding bodies optimization (ICBO), enhanced colliding bodies optimization (ECBO), differential evolution (DE), PSO, ABC, biogeography based optimization (BBO), adaptive real coded biogeography-based optimization (ARCBBO), modified imperialist competitive algorithm and teaching-learning algorithm (MICA-TLA), TLBO, lévy mutation TLBO (LTLBO), and evolving ant direction differential evolution (EADDE) were 41,666.24 $/h, 41,667.03 $/h, 41,673.72 $/h, 41,686.82 $/h, 41,697.33 $/h, 41,702.66 $/h, 41,689.73 $/h, 42,386.37 $/h, 41,715.76 $/h, 41,841.85 $/h, 41,698.93 $/h, 41,686 $/h,, 41,675.05 $/h,, 41,695.66 $/h, 41,679.55 $/h, 41,713.62 $/h, respectively. It is shown that the result of the proposed CBO5 algorithm was the best result for Case 7 compared to those of the other algorithms.

Table 5.110: Comparison of CBO5 algorithm with the original BO algorithm and previous studies for single objective cases of IEEE 57-bus system.

| Case # | Algorithm | Fuel cost ($/h) | Emission (t/h) | Ploss (MW) | VD (p.u.) |
|---|---|---|---|---|---|
| Case 7 | CBO5 | **41,666.23663** | 1.352409 | 14.85959 | 1.697282 |
| | BO | 41,667.03409 | 1.352963 | 14.84992 | 1.636026 |
| | MSA [245] | 41,673.72 | 1.9526 | 15.0526 | 1.5508 |
| | DSA [246] | 41,686.82 | - | - | 1.0833 |
| | ICBO [242] | 41,697.33 | - | 15.5470 | 1.3173 |
| | ECBO [242] | 41,702.66 | - | - | - |
| | DE [242] | 41,689.73 | - | - | - |
| | PSO [242] | 42,386.37 | - | - | - |
| | ABC [242] | 41,715.76 | - | - | - |
| | GA [242] | 41,841.85 | - | - | - |
| | BBO [242] | 41,698.93 | - | - | - |
| | ARCBBO [248] | 41,686 | - | 15.3769 | - |
| | MICA-TLA [258] | 41,675.05 | - | 15.0149 | 1.6161 |
| | TLBO [259] | 41695.6626 | - | 15.7469 | - |
| | LTLBO [259] | 41679.5451 | - | 15.1589 | - |
| | EADDE [260] | 41,713.62 | - | 16.09 | 1.0977 |

[a] Infeasible solution, constraint on load bus voltage is violated.

In the same manner, as studied in the modified IEEE-30 bus system, the following cases are presented with incorporating WT generators to minimize the fuel cost with and without carbon gas emission and real power loss. Utilizing the same cost coefficients of WT generators presented in case A. Further, The PDF parameters of WT generators have the same values as given in section 4. The optimal variables of results for all cases are summarized in Table 5.111. Fig. 5.85 compares the convergence characteristics of CBO5 and the BO algorithm. The CBO5 algorithm converges faster for most cases, but the compared BO technique demonstrates stable and fast convergence characteristics. Fig.5.86 shows that all voltages values are within specified limits for all considered cases.

**Case 10:** This case is like Case-4 in the IEEE-30 bus system to reduce total fuel cost by incorporating WT generators without considering the emission. The results in Table 5.111 show that the proposed CBO5 algorithm is more efficient in finding the optimal global solution when compared to the BO algorithm.

This table shows that the fuel cost is 31602.45 \$/h, while the emission , real power loss ,voltage deviation ,and the voltage stability index are 1.174147 ton/hr 16.19773 MW, 1.545702 p.u. and 0.280737 p.u. , respectively.

**Case 11:** This case considers real power loss minimization as the main objective function. Using the proposed CBO5 with WT generators, the real power loss is reduced to 9.573578 MW, which is more than case 8 (without RES) by 3.8383%. Furthermore, the fuel cost, emissions, voltage deviation and voltage stability index become 35561.46/\$ h, 0.989715 ton/h, 1.685101 p.u. and 0.280487 p.u., respectively.

**Case 12:** In this case, the aim of the objective functions in case 9 but to incorporate WT generators. However, the total cost is decreased to be 31625.54173 \$/h, while the fuel costs, emission, carbon tax, real power loss , voltage deviation and voltage stability index became 31603.21 \$/h, 1.172094 ton/h, 17.83 \$/h, 16.19843 MW ,1.509428 p.u. , and 0.280526 p.u. , respectively. With higher penetration of RES, the value of fuel cost and emission in CBO5 are reduced by 24.1526% and 9.7565% compared to case 9 (without RES).

The statistical results are conducted and tabulated for cases 10, 11, and 12, as seen in Table 5.112. Again, the CBO5 is more robust than the standard BO algorithm from the table.

Table 5.111: Results of the proposed CBO5 method and BO method for cases 10, 11 and 12.

| | | | **Case 10** | | **Case 11** | | **Case 12** | |
|---|---|---|---|---|---|---|---|---|
| | **Min** | **Max** | **BO** | **CBO5** | **BO** | **CBO5** | **BO** | **CBO5** |
| Generator active power | | | | | | | | |
| $P_{G1}$(MW) | 0 | 576 | 136.9883 | 136.7953 | 180.0127 | 177.1987 | 137.2891 | 136.7083 |
| $P_{G2}$(MW) | 30 | 100 | 49.76187 | 50.82713 | 30 | 30.00082 | 52.76404 | 51.52651 |
| $P_{G3}$(MW) | 40 | 140 | 42.49689 | 42.54706 | 118.4475 | 126.0842 | 42.32723 | 42.45348 |
| $P_{W1}$(MW) | 0 | 150 | 150 | 150 | 126.3598 | 112.7824 | 150 | 150 |
| $P_{G8}$(MW) | 100 | 550 | 424.192 | 424.0137 | 275.5855 | 284.309 | 419.5832 | 423.5313 |
| $P_{W2}$(MW) | 0 | 120 | 119.9995 | 120 | 120 | 120 | 120 | 120 |
| $P_{G12}$(MW) | 100 | 410 | 343.5703 | 342.8145 | 410 | 409.9983 | 344.8822 | 342.7789 |
| Generator voltage | | | | | | | | |
| $V_1$(p.u.) | 0.95 | 1.1 | 1.051309 | 1.0561 | 1.061479 | 1.066815 | 1.038682 | 1.051575 |
| $V_2$(p.u.) | 0.95 | 1.1 | 1.047748 | 1.052773 | 1.05661 | 1.063062 | 1.035356 | 1.048515 |
| $V_3$ (p.u.) | 0.95 | 1.1 | 1.046776 | 1.050719 | 1.055962 | 1.065742 | 1.034619 | 1.048564 |
| $V_6$(p.u.) | 0.95 | 1.1 | 1.06492 | 1.065558 | 1.058594 | 1.06387 | 1.061643 | 1.067197 |
| $V_8$ (p.u.) | 0.95 | 1.1 | 1.071408 | 1.071301 | 1.063574 | 1.070212 | 1.073628 | 1.07255 |
| $V_9$ (p.u.) | 0.95 | 1.1 | 1.043148 | 1.044862 | 1.044477 | 1.052424 | 1.039691 | 1.044847 |
| $V_{12}$ (p.u.) | 0.95 | 1.1 | 1.037199 | 1.042317 | 1.047987 | 1.058003 | 1.028484 | 1.041361 |
| Capacitor bank | | | | | | | | |
| $Q_{C18}$ (MVAR) | 0 | 20 | 6.49E-07 | 13.81544 | 13.90482 | 0.001871 | 20 | 20 |
| $Q_{C25}$ (MVAR) | 0 | 20 | 13.93044 | 14.53243 | 10.51095 | 15.25083 | 10.73774 | 11.46375 |
| $Q_{C53}$ (MVAR) | 0 | 20 | 13.69509 | 10.92787 | 12.98852 | 10.89218 | 13.19914 | 13.27246 |

| | | | | | | | | |
|---|---|---|---|---|---|---|---|---|
| Transformer tap ratio | | | | | | | | |
| $T_{19}$(4-18) | 0.9 | 1.1 | 0.911746 | 1.091384 | 1.018504 | 0.98321 | 0.983096 | 0.96747 |
| $T_{20}$(4-18) | 0.9 | 1.1 | 1.003614 | 0.980493 | 0.990904 | 0.974761 | 1.069372 | 1.055328 |
| $T_{31}$(21-20) | 0.9 | 1.1 | 1.012165 | 1.039816 | 1.009528 | 1.023598 | 1.031582 | 1.00373 |
| $T_{35}$(24-25) | 0.9 | 1.1 | 0.945103 | 0.95227 | 0.989373 | 1.075884 | 0.962985 | 0.900001 |
| $T_{36}$(24-25) | 0.9 | 1.1 | 1.0998 | 1.1 | 0.977979 | 0.962627 | 1.026048 | 1.1 |
| $T_{37}$(24-26) | 0.9 | 1.1 | 1.037795 | 1.034689 | 1.016129 | 1.009844 | 1.035478 | 1.032377 |
| $T_{41}$(7-29) | 0.9 | 1.1 | 0.995671 | 0.99536 | 0.988057 | 0.996203 | 0.995254 | 1.002594 |
| $T_{46}$(34-32) | 0.9 | 1.1 | 0.969285 | 0.967943 | 0.959248 | 0.957015 | 0.962784 | 0.9643 |
| $T_{54}$(11-41) | 0.9 | 1.1 | 0.9 | 0.909532 | 0.903629 | 1.032369 | 0.9 | 0.90598 |
| $T_{58}$(15-45) | 0.9 | 1.1 | 0.968821 | 0.972759 | 0.978494 | 0.985957 | 0.958744 | 0.968416 |
| $T_{59}$(14-46) | 0.9 | 1.1 | 0.956681 | 0.960838 | 0.963655 | 0.971972 | 0.946251 | 0.962975 |
| $T_{65}$(10-51) | 0.9 | 1.1 | 0.96382 | 0.967708 | 0.971413 | 0.983411 | 0.958182 | 0.96633 |
| $T_{66}$(13-49) | 0.9 | 1.1 | 0.932834 | 0.933202 | 0.932271 | 0.948075 | 0.921064 | 0.933461 |
| $T_{71}$(11-43) | 0.9 | 1.1 | 0.96785 | 0.96739 | 0.973522 | 0.963961 | 0.957102 | 0.966489 |
| $T_{73}$(40-56) | 0.9 | 1.1 | 0.978994 | 0.989572 | 0.99139 | 1.01385 | 0.992495 | 0.989265 |
| $T_{76}$(39-57) | 0.9 | 1.1 | 0.986788 | 0.96151 | 0.962282 | 0.995067 | 0.997444 | 0.96186 |
| $T_{80}$(9-55) | 0.9 | 1.1 | 1.003125 | 0.997629 | 0.996618 | 0.997187 | 0.993963 | 1.001047 |
| Objective function | | | | | | | | |
| Fuel cost ($/h) | | | 31603.21 | 31602.45 | 34848.87 | 35561.46 | 31608.56 | 31603.21 |
| Fuel thermal unit cost ($/h) | | | 30673.95 | 30673.19 | 34021.6 | 34789.9 | 30679.3 | 30673.95 |
| Wind generation cost ($/h) | | | 929.2571 | 929.2592 | 827.2723 | 771.561 | 929.2592 | 929.2592 |
| Emission (ton/h) | | | 1.176602 | 1.174147 | 0.96663 | 0.989715 | 1.161806 | 1.172094 |
| Total cost ($/h) | | | - | - | - | - | 31629.28 | 31625.54 |
| Carbon tax ($/h) | | | - | - | - | - | 17.83 | 17.83 |
| Power loss (MW) | | | 16.20888 | 16.19773 | 9.605545 | 9.573578 | 16.04583 | 16.19843 |
| Voltage deviation (p.u.) | | | 1.540082 | 1.545702 | 1.65516 | 1.685101 | 1.417123 | 1.509428 |
| *L*-index (max) | | | 0.280615 | 0.280737 | 0.278044 | 0.280487 | 0.27986 | 0.280526 |
| Generator reactive power | | | | | | | | |
| $Q_{G1}$(MVAR) | -140 | 200 | 44.76024 | 44.55739 | 41.22398 | 30.32486 | 137.2891 | 39.07301 |
| $Q_{G2}$(MVAR) | -17 | 50 | 49.92548 | 51.64599 | 49.9736 | 49.86503 | 39.48904 | 49.99684 |
| $Q_{G3}$(MVAR) | -10 | 60 | 44.47831 | 35.18091 | 20.12369 | 39.47751 | 50.00524 | 30.12627 |
| $Q_{G6}$(MVAR) | -8 | 25 | -0.98574 | -7.2014 | -7.53608 | -5.88456 | 19.49379 | -6.23201 |
| $Q_{G8}$(MVAR) | -140 | 200 | 51.56645 | 47.1454 | 51.44385 | 47.87953 | -6.61966 | 48.99044 |
| $Q_{G9}$(MVAR) | -3 | 9 | 8.991763 | 8.999695 | 9.181663 | 8.571043 | 71.1253 | 9.000454 |
| $Q_{G12}$(MVAR) | -150 | 155 | 53.58612 | 58.66146 | 47.96259 | 53.42812 | 8.972786 | 62.25965 |

Table 5.112: The Statistical analysis for cases 10, 11 and 12.

| Case no. | Method | Best | Mean | Median | Worst | STD |
|---|---|---|---|---|---|---|
| Case 10 | BO | 31603.21195 | 31616.46108 | 31608.68458 | 31642.28651 | 13.85787214 |
| | CBO5 | **31602.44771** | **31612.03763** | **31608.44284** | **31632.41326** | **9.11786124** |
| Case 11 | BO | 9.605545418 | 9.86487765 | 9.794855414 | 11.03740007 | 0.313604968 |
| | CBO5 | **9.573578081** | **9.761324494** | **9.702683982** | **10.07715062** | **0.176327123** |
| Case 12 | BO | 31629.2796 | 31651.46155 | 31637.08036 | 31727.50628 | 29.22940237 |
| | CBO5 | **31625.54173** | **31642.24821** | **31636.50259** | **31686.23477** | **17.32578888** |

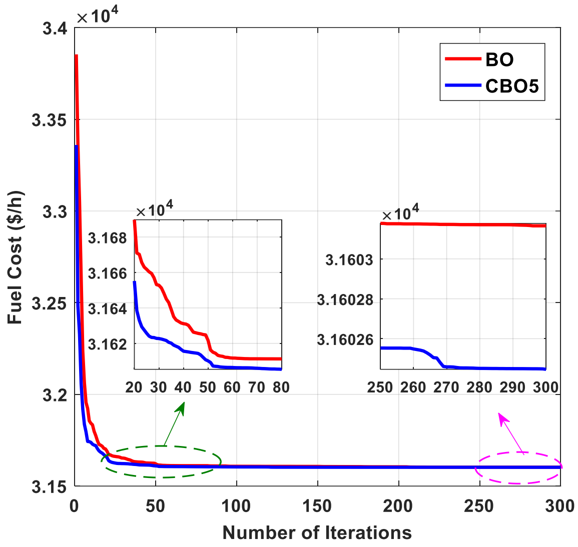


(a)Case 10

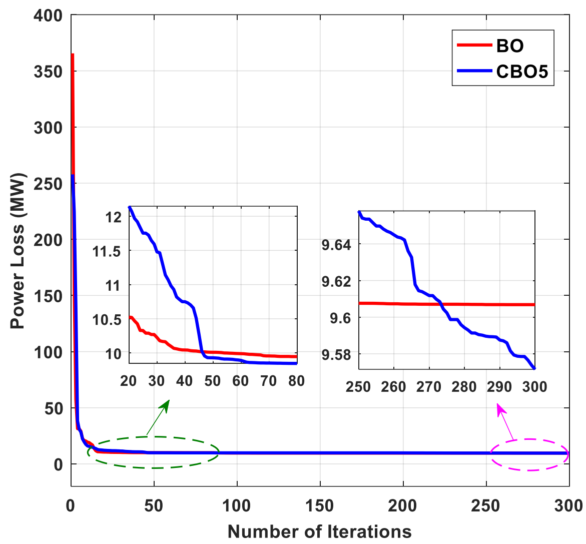


(b) Case 11

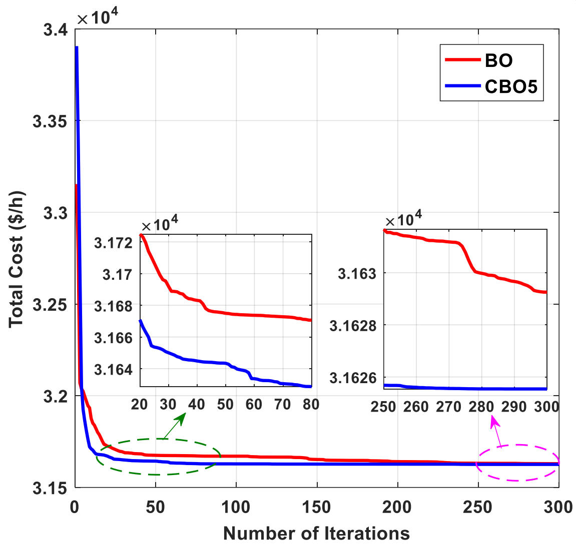


(c) Case 12

Figure 5.85: Convergence characteristic of CBO5 and BO for cases 10,11and 12.

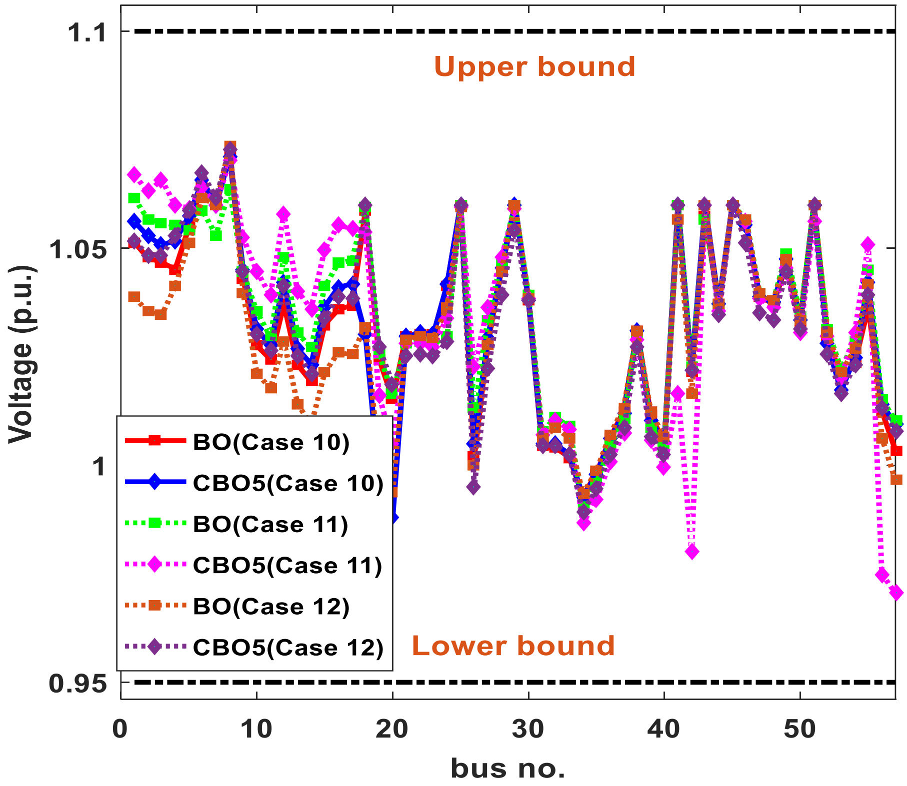


Figure 5.86: Voltage profiles of compared methods for cases 10, 11 and 12.

# Chapter 6

## Conclusions and Future Works

- *Conclusions of Thesis.*
- *Future Works*

# Chapter 6

# Conclusions and Future Works

## 6.1 Conclusions of the Thesis

This thesis has proposed different techniques to solve the economic emission dispatch (EED), dynamic economic emission dispatch (DEED), and . The proposed techniques have been compared with recent and other well-known optimization techniques. However, the main contributions of the thesis are summarized as follows:

- The performance of these proposed algorithms have been evaluated using well-known CEC'17 test functions, and different scales electrical systems including small scale systems (3-generators, 5-generators), medium scale systems (6-generators, 10-generators, 11-generators, 13-generators, 14-generators, 15-generators), and large scale systems (26-generators, 40-generators, and 110-generators) at different levels of demand and considering various operating constraints such as power losses, power boundaries, ramp rate limits, POZ, and VPLE.
- In addition, these proposed algorithms have been exploited to solve multi-objective EED and DEED problems; hence multi-objective algorithms have been developed.
- The developed techniques have been successfully applied to get the feasible optimal solutions to the single EED, multi-objective EED and DEED problems with the aim of achieving economic and environmental profits.
- The proposed algorithms could avoid the local optima and has a strong convergence rate compared with the other algorithms.
- The obtained results prove the effectiveness and superiority of the proposed techniques compared with the conventional algorithms as well as other well-known optimization techniques in the literature.
- In DEED problem, the fuel cost and total pollutant emission are optimized as incompatible objectives through a definite dispatch time. The nonlinear aspects of the generating units' ramp rate limits, valve point effect, variation of the load

demand and transmission losses are considered. A multi-objective Salp swarm algorithm (MSSA) is suggested to solve the DEED problem.

- The PFs obtained for the assessed algorithms demonstrate the supremacy of the solutions achieved using the proposed MSSA algorithm, which indicates the efficacy and applicability of the model in solving complicated MOPs specific to power systems operation.
- Finally, The proposed CBO5 algorithm has been modified to achieve the best solution for the stochastic EED solution in case of considering time-varying load, the uncertainty of wind and solar PV units and the obtained results of several recent algorithms such as MSA, DSA, ICBO, ECBO, DE, PSO, ABC, BBO, ARCBBO, MICA-TLA, TLBO, LTLBO, EADDE and other recent algorithms for solving the EED problem. This comparison with other recently published algorithms is executed to confirm the effectiveness and accuracy of the proposed CBO5.

## 6.2 Future Works

This research work leads to various promising topics for future investigations. Despite all efforts made in this research work to improve modern power system operation, some short-comes still exist to be addressed. From my point of view for future work, number of issues that can be handled are summarized in the following points:

- Applying the proposed optimization algorithms for solving other complex optimization problems in electrical field or other areas such as optimal coordination of directional overcurrent relays and optimal power flow (OPF) study considering the integration of storage devices such as batteries (electric vehicles), pumped hydro and FACTs devices..

- Solving the problem of dynamic economic emission dispatch with various of renewable energy resources including the wind and solar energy.

- Addressing the coordination of dispatch of Electric Vehicles (EVs) and uncertainties of Renewable energy using the recent optimization algorithms.

- Determining the optimal relay settings using the proposed techniques with predictive methods to improve the performance of adaptive protection.

# List of Publications

Some contents of this thesis have been published to international conferences and journals indexed in Journal Citation Reports (JCR)/Science Edition (Thomson Reuters) as follows:

## Journal papers (JCR):

[1] Hassan, Mohamed H., et al. "An improved manta ray foraging optimizer for cost-effective emission dispatch problems." *Engineering Applications of Artificial Intelligence* 100 (2021): 104155.

[2] Hassan, Mohamed H., et al. "Developing chaotic artificial ecosystem-based optimization algorithm for combined economic emission dispatch." *IEEE Access* 9 (2021): 51146-51165.

[3] Hassan, Mohamed H., et al. "Development and application of slime mould algorithm for optimal economic emission dispatch." *Expert Systems with Applications* 182 (2021): 115205.

[4] Hassan, Mohamed H., et al. "A modified Marine predators algorithm for solving single- and multi-objective combined economic emission dispatch problems." *Computers & Industrial Engineering* 164 (2022): 107906.

[5] Hassan, Mohamed H., et al. "Developing chaotic Bonobo optimizer for optimal power flow analysis considering stochastic renewable energy resources." *Int J Energy Res*. 2022; 1- 35.

[6] Hassan, Mohamed H., et al. "ESMA-OPF: Enhanced Slime Mould Algorithm for Solving Optimal Power Flow Problem." *Sustainability*, *14*(4), 2305.

[7] Hassan, Mohamed H., et al. "Optimal Power Flow Analysis Based on Hybrid Gradient-Based Optimizer with Moth–Flame Optimization Algorithm Considering Optimal Placement and Sizing of FACTS/Wind Power". *Mathematics*, *10*(3), 361.

[8] Hassan, Mohamed H., et al. "A modified Rao-2 algorithm for optimal power flow incorporating renewable energy sources. " *Mathematics*, *9*(13), 1532.

# References


[1] B. Shaw, S. P. Ghoshal, and V. Mukherjee, “Solution of combined economic and emission dispatch problems using hybrid craziness-based PSO with differential evolution,” in *2011 IEEE Symposium on Differential Evolution (SDE)*, Apr. 2011, pp. 1–8, doi: 10.1109/SDE.2011.5952061.

[2] R. Bharathi, M. J. Kumar, D. Sunitha, and S. Premalatha, “Optimization of combined Economic and Emission dispatch problem - A comparative study,” in *8th International Power Engineering Conference, IPEC 2007*, 2007, pp. 134–139.

[3] X. Chen, B. Xu, and W. Du, “An Improved Particle Swarm Optimization with Biogeography-Based Learning Strategy for Economic Dispatch Problems,” *Complexity*, vol. 2018, pp. 1–15, Jul. 2018, doi: 10.1155/2018/7289674.

[4] B. Y. Qu, Y. S. Zhu, Y. C. Jiao, M. Y. Wu, P. N. Suganthan, and J. J. Liang, “A survey on multi-objective evolutionary algorithms for the solution of the environmental/economic dispatch problems,” *Swarm Evol. Comput.*, vol. 38, pp. 1–11, Feb. 2018, doi: 10.1016/j.swevo.2017.06.002.

[5] M. E. Munawer, “Human health and environmental impacts of coal combustion and post-combustion wastes,” *J. Sustain. Min.*, vol. 17, no. 2, pp. 87–96, 2018, doi: 10.1016/j.jsm.2017.12.007.

[6] X. Xia and A. M. Elaiw, “Optimal dynamic economic dispatch of generation: A review,” *Electr. Power Syst. Res.*, vol. 80, no. 8, pp. 975–986, Aug. 2010, doi: 10.1016/j.epsr.2009.12.012.

[7] C. K. Chanda, D. Maity, and S. Banerjee, “Solution of economic load dispatch problem using biogeography based optimization technique considering valve point loading effect,” *Int. J. Electr. Energy*, vol. 5, no. 1, pp. 58–64, 2017, doi: 10.18178/ijoee.5.1.58-64.

[8] G. Abbas, J. Gu, U. Farooq, M. U. Asad, and M. El-Hawary, “Solution of an economic dispatch problem through particle swarm optimization: A detailed survey - part i,” *IEEE Access*, vol. 5, pp. 15105–15141, 2017, doi: 10.1109/ACCESS.2017.2723862.

[9] R. Al-Nahhal, A. F. Naiem, and Y. G. Hegazy, “Economic load dispatch problem using particle swarm optimization technique considering wind power penetration,” *SEST 2019 - 2nd Int. Conf. Smart Energy Syst. Technol.*, pp. 1–6, 2019, doi: 10.1109/SEST.2019.8849005.

[10] S. Prathiba, R and Moses, M Balasingh and Sakthivel, “Flower pollination algorithm applied for different economic load dispatch problems,” *Int. J. Eng. Technol.*, vol. 6, no. 2, pp. 1009--1016, 2014.

[11] L. Yang, E. S. Fraga, and L. G. Papageorgiou, “Mathematical programming formulations for non-smooth and non-convex electricity dispatch problems,” *Electr. Power Syst. Res.*, vol. 95, pp. 302–308, Feb. 2013, doi: 10.1016/j.epsr.2012.09.015.

[12] J. X. V. Neto, G. Reynoso-Meza, T. H. Ruppel, V. C. Mariani, and L. dos S. Coelho, “Solving non-smooth economic dispatch by a new combination of continuous GRASP algorithm and differential evolution,” *Int. J. Electr. Power Energy Syst.*, vol. 84, pp. 13–24, Jan. 2017, doi: 10.1016/j.ijepes.2016.04.012.

[13] W. R. Graham, C. A. Hall, and M. Vera Morales, “The potential of future aircraft technology for noise and pollutant emissions reduction,” *Transp. Policy*, vol. 34, pp. 36–51, 2014, doi: 10.1016/j.tranpol.2014.02.017.

[14] P. Mannion, K. Mason, S. Devlin, and J. Duggan, “Dynamic economic emissions dispatch optimisation using multi-agent reinforcement learning,” *Adapt. Learn. Agents Work. (at AAMAS 2016)*, 2016.

[15] N. I. Nwulu and X. Xia, “Multi-objective dynamic economic emission dispatch of electric power generation integrated with game theory based demand response programs,” *Energy Convers. Manag.*, vol. 89, pp. 963–974, 2015, doi: 10.1016/j.enconman.2014.11.001.

[16] X. Wei and H. Bai, “Semi-definite programming-based method for security-constrained unit commitment with operational and optimal power flow constraints,” *Gener. Transm. Distrib. IET*, vol. 1, no. 2, pp. 182–197, 2007, doi: 10.1049/iet-gtd.

[17] M. T. Hagh, S. M. S. Kalajahi, and N. Ghorbani, “Solution to economic emission dispatch problem including wind farms using Exchange Market Algorithm Method,” *Appl. Soft Comput.*, vol. 88, p. 106044, Mar. 2020, doi: 10.1016/j.asoc.2019.106044.

[18] H. Rezaie, M. H. Kazemi-rahbar, B. Vahidi, and H. Rastegar, “Journal of computational design and engineering solution of combined economic and emission dispatch problem using a novel chaotic improved harmony search algorithm,” *J. Comput. Des. Eng.*, vol. 6, no. 3, pp. 447–467, 2019, doi: 10.1016/j.jcde.2018.08.001.

[19] K. T. Chaturvedi, M. Pandit, and L. Srivastava, “Modified neo-fuzzy neuron-based approach for economic and environmental optimal power dispatch,” *Appl. Soft Comput. J.*, vol. 8, no. 4, pp. 1428–1438, 2008, doi: 10.1016/j.asoc.2007.10.010.

[20] F. P. Mahdi, P. Vasant, M. Abdullah-Al-Wadud, J. Watada, and V. Kallimani, “A quantum-inspired particle swarm optimization approach for environmental/economic power dispatch problem using cubic criterion function,” *Int. Trans. Electr. Energy Syst.*, vol. 28, no. 3, p. e2497, Mar. 2018, doi: 10.1002/etep.2497.

[21] S. Krishnamurthy and R. Tzoneva, “Impact of price penalty factors on the solution of the combined economic emission dispatch problem using cubic criterion functions,” in *2012 IEEE Power and Energy Society General Meeting*, Jul. 2012, pp. 1–9, doi: 10.1109/PESGM.2012.6345312.

[22] Z. Ullah, S. Wang, J. Radosavljevic, and J. Lai, “A Solution to the Optimal Power Flow Problem Considering WT and PV Generation,” *IEEE Access*, vol. 7, pp. 46763–46772, 2019, doi: 10.1109/ACCESS.2019.2909561.

[23] “IRENA, R. E. S. (2018). The International Renewable Energy Agency, Abu Dhabi, 2018..”

[24] X. Fang, B.-M. Hodge, H. Jiang, and Y. Zhang, "Decentralized wind uncertainty management: Alternating direction method of multipliers based distributionally-robust chance constrained optimal power flow," *Appl. Energy*, vol. 239, pp. 938–947, Apr. 2019, doi: 10.1016/j.apenergy.2019.01.259.

[25] S. S. Reddy, "Optimal scheduling of thermal-wind-solar power system with storage," *Renew. Energy*, vol. 101, pp. 1357–1368, Feb. 2017, doi: 10.1016/j.renene.2016.10.022.

[26] H. M. Dubey, M. Pandit, and B. K. Panigrahi, "Hybrid flower pollination algorithm with time-varying fuzzy selection mechanism for wind integrated multi-objective dynamic economic dispatch," *Renew. Energy*, vol. 83, pp. 188–202, Nov. 2015, doi: 10.1016/j.renene.2015.04.034.

[27] P. Kayal and C. K. Chanda, "Optimal mix of solar and wind distributed generations considering performance improvement of electrical distribution network," *Renew. Energy*, vol. 75, pp. 173–186, Mar. 2015, doi: 10.1016/j.renene.2014.10.003.

[28] P. P. Biswas, P. N. Suganthan, R. Mallipeddi, and G. A. J. Amaratunga, "Optimal reactive power dispatch with uncertainties in load demand and renewable energy sources adopting scenario-based approach," *Appl. Soft Comput.*, vol. 75, pp. 616–632, Feb. 2019, doi: 10.1016/j.asoc.2018.11.042.

[29] M. Güçyetmez and E. Çam, "A new hybrid algorithm with genetic-teaching learning optimization (G-TLBO) technique for optimizing of power flow in wind-thermal power systems," *Electr. Eng.*, vol. 98, no. 2, pp. 145–157, Jun. 2016, doi: 10.1007/s00202-015-0357-y.

[30] S. P. Shalini and K. Lakshmi, "Solution to Economic Emission Dispatch problem using Lagrangian relaxation method," in *2014 International Conference on Green Computing Communication and Electrical Engineering (ICGCCEE)*, Mar. 2014, pp. 1–6, doi: 10.1109/ICGCCEE.2014.6922314.

[31] S.-D. Chen and J.-F. Chen, "A direct Newton–Raphson economic emission dispatch," *Int. J. Electr. Power Energy Syst.*, vol. 25, no. 5, pp. 411–417, Jun. 2003, doi: 10.1016/S0142-0615(02)00075-3.

[32] L. G. Papageorgiou and E. S. Fraga, "A mixed integer quadratic programming formulation for the economic dispatch of generators with prohibited operating zones," *Electr. Power Syst. Res.*, vol. 77, no. 10, pp. 1292–1296, Aug. 2007, doi: 10.1016/j.epsr.2006.09.020.

[33] F. P. Mahdi, P. Vasant, V. Kallimani, J. Watada, P. Y. S. Fai, and M. Abdullah-Al-Wadud, "A holistic review on optimization strategies for combined economic emission dispatch problem," *Renew. Sustain. Energy Rev.*, vol. 81, pp. 3006–3020, Jan. 2018, doi: 10.1016/j.rser.2017.06.111.

[34] L. A. Koridak and M. Rahli, "Optimization of the emission and economic dispatch by the genetic algorithm," *Prz. Elektrotechniczny*, vol. 86, no. 11 A, pp. 363–366, 2010.

[35] M. Basu, "A simulated annealing-based goal-attainment method for economic

emission load dispatch of fixed head hydrothermal power systems," *Int. J. Electr. Power Energy Syst.*, vol. 27, no. 2, pp. 147–153, Feb. 2005, doi: 10.1016/j.ijepes.2004.09.004.

[36] P. Pao-La-Or, A. Oonsivilai, and T. Kulworawanichpong, "Combined economic and emission dispatch using particle swarm optimization," *WSEAS Trans. Environ. Dev.*, vol. 6, no. 4, pp. 308–317, Apr. 2010.

[37] A. Y. Abdelaziz, E. S. Ali, and S. M. Abd Elazim, "Combined economic and emission dispatch solution using Flower Pollination Algorithm," *Int. J. Electr. Power Energy Syst.*, vol. 80, pp. 264–274, Sep. 2016, doi: 10.1016/j.ijepes.2015.11.093.

[38] A. S. Tomar, H. M. Dubey, and M. Pandit, "Combined Economic Emission Dispatch Using Spider Monkey Optimization," 2020, pp. 809–818.

[39] R. Dong and S. Wang, "New Optimization Algorithm Inspired by Kernel Tricks for the Economic Emission Dispatch Problem With Valve Point," *IEEE Access*, vol. 8, pp. 16584–16594, 2020, doi: 10.1109/ACCESS.2020.2965725.

[40] A. A. Abou El Ela, M. A. Abido, and S. R. Spea, "Differential evolution algorithm for emission constrained economic power dispatch problem," *Electr. Power Syst. Res.*, vol. 80, no. 10, pp. 1286–1292, Oct. 2010, doi: 10.1016/j.epsr.2010.04.011.

[41] H. Hardiansyah, "Dynamic economic emission dispatch using ant lion optimization," *Bull. Electr. Eng. Informatics*, vol. 9, no. 1, pp. 12–20, Feb. 2020, doi: 10.11591/eei.v9i1.1664.

[42] T. Dutta, S. Bhattacharyya, S. Dey, and J. Platos, "Border Collie Optimization," *IEEE Access*, vol. 8, pp. 109177–109197, 2020, doi: 10.1109/ACCESS.2020.2999540.

[43] C. L. Chiang, "Improved genetic algorithm for power economic dispatch of units with valve-point effects and multiple fuels," *IEEE Trans. Power Syst.*, vol. 20, no. 4, pp. 1690–1699, 2005, doi: 10.1109/TPWRS.2005.857924.

[44] M. A. Abido, "Multiobjective evolutionary algorithms for electric power dispatch problem," *IEEE Trans. Evol. Comput.*, vol. 10, no. 3, pp. 315–329, 2006, doi: 10.1109/TEVC.2005.857073.

[45] M. Basu, "Economic environmental dispatch using multi-objective differential evolution," *Appl. Soft Comput. J.*, vol. 11, no. 2, pp. 2845–2853, 2011, doi: 10.1016/j.asoc.2010.11.014.

[46] C. C. Kuo, "A novel coding scheme for practical economic dispatch by modified particle swarm approach," *IEEE Trans. Power Syst.*, vol. 23, no. 4, pp. 1825–1835, 2008, doi: 10.1109/TPWRS.2008.2002297.

[47] Z. L. Gaing, "Particle swarm optimization to solving the economic dispatch considering the generator constraints," *IEEE Trans. Power Syst.*, vol. 18, no. 3, pp. 1187–1195, 2003, doi: 10.1109/TPWRS.2003.814889.

[48] S. Pothiya, I. Ngamroo, and W. Kongprawechnon, "Ant colony optimisation for

economic dispatch problem with non-smooth cost functions," *Int. J. Electr. Power Energy Syst.*, vol. 32, no. 5, pp. 478–487, 2010, doi: 10.1016/j.ijepes.2009.09.016.

[49] P. K. Roy and S. Bhui, "Multi-objective quasi-oppositional teaching learning based optimization for economic emission load dispatch problem," *Int. J. Electr. Power Energy Syst.*, vol. 53, pp. 937–948, 2013, doi: 10.1016/j.ijepes.2013.06.015.

[50] U. Güvenç, Y. Sönmez, S. Duman, and N. Yörükeren, "Combined economic and emission dispatch solution using gravitational search algorithm," *Sci. Iran.*, vol. 19, no. 6, pp. 1754–1762, 2012, doi: 10.1016/j.scient.2012.02.030.

[51] M. Jevtic, N. Jovanovic, J. Radosavljevic, and D. Klimenta, "Moth swarm algorithm for solving combined economic and emission dispatch problem," *Elektron. ir Elektrotechnika*, vol. 23, no. 5, pp. 21–28, 2017, doi: 10.5755/j01.eie.23.5.19267.

[52] F. Paquin, J. Rivnay, A. Salleo, N. Stingelin, and C. Silva, "Multi-phase semicrystalline microstructures drive exciton dissociation in neat plastic semiconductors," *J. Mater. Chem. C*, vol. 3, no. 1, pp. 10715–10722, 2015, doi: 10.1039/b000000x.

[53] S. H. A. Kaboli and A. K. Alqallaf, "Solving non-convex economic load dispatch problem via artificial cooperative search algorithm," *Expert Syst. Appl.*, vol. 128, pp. 14–27, Aug. 2019, doi: 10.1016/j.eswa.2019.02.002.

[54] G.-G. Wang, A. H. Gandomi, A. H. Alavi, and D. Gong, "A comprehensive review of krill herd algorithm: variants, hybrids and applications," *Artif. Intell. Rev.*, vol. 51, no. 1, pp. 119–148, Jan. 2019, doi: 10.1007/s10462-017-9559-1.

[55] T. A. A. Victoire and A. E. Jeyakumar, "Hybrid PSO-SQP for economic dispatch with valve-point effect," *Electr. Power Syst. Res.*, vol. 71, no. 1, pp. 51–59, 2004, doi: 10.1016/j.epsr.2003.12.017.

[56] L. dos Santos Coelho and V. C. Mariani, "Combining of chaotic differential evolution and quadratic programming for economic dispatch optimization with valve-point effect," *IEEE Trans. Power Syst.*, vol. 21, no. 2, pp. 989–996, 2006, doi: 10.1109/TPWRS.2006.873410.

[57] A. Goudarzi, Y. Li, and J. Xiang, "A hybrid non-linear time-varying double-weighted particle swarm optimization for solving non-convex combined environmental economic dispatch problem," *Appl. Soft Comput. J.*, vol. 86, no. xxxx, p. 105894, 2020, doi: 10.1016/j.asoc.2019.105894.

[58] Z. Xin-gang, L. Ji, M. Jin, and Z. Ying, "An improved quantum particle swarm optimization algorithm for environmental economic dispatch," *Expert Syst. Appl.*, vol. 152, p. 113370, Aug. 2020, doi: 10.1016/j.eswa.2020.113370.

[59] J. Li, H. Lei, A. H. Alavi, and G.-G. Wang, "Elephant Herding Optimization: Variants, Hybrids, and Applications," *Mathematics*, vol. 8, no. 9, p. 1415, Aug. 2020, doi: 10.3390/math8091415.

[60] Y. Feng, S. Deb, G.-G. Wang, and A. H. Alavi, "Monarch butterfly optimization: A comprehensive review," *Expert Syst. Appl.*, vol. 168, p. 114418, Apr. 2021, doi:

10.1016/j.eswa.2020.114418.

[61] J. N. Kuk, R. A. Gonçalves, L. M. Pavelski, S. M. Guse Scós Venske, C. P. de Almeida, and A. T. Ramirez Pozo, "An empirical analysis of constraint handling on evolutionary multi-objective algorithms for the Environmental/Economic Load Dispatch problem," *Expert Syst. Appl.*, vol. 165, p. 113774, Mar. 2021, doi: 10.1016/j.eswa.2020.113774.

[62] J. C. Dodu, P. Martin, A. Merlin, and J. Pouget, "An optimal formulation and solution of short-range operating problems for a power system with flow constraints," *Proc. IEEE*, vol. 60, no. 1, pp. 54–63, 1972, doi: 10.1109/PROC.1972.8557.

[63] C. L. Chen and S. C. Wang, "Branch-and-bound scheduling for thermal generating units," *IEEE Trans. Energy Convers.*, vol. 8, no. 2, pp. 184–189, Jun. 1993, doi: 10.1109/60.222703.

[64] J. Parikh and D. Chattopadhyay, "A multi-area linear programming approach for analysis of economic operation of the Indian power system," *IEEE Trans. Power Syst.*, vol. 11, no. 1, pp. 52–58, 1996, doi: 10.1109/59.485985.

[65] Ji-Yuan Fan and Lan Zhang, "Real-time economic dispatch with line flow and emission constraints using quadratic programming," *IEEE Trans. Power Syst.*, vol. 13, no. 2, pp. 320–325, May 1998, doi: 10.1109/59.667345.

[66] J. Nanda, "Economic emission load dispatch with line flow constraints using a classical technique," *IEE Proc. - Gener. Transm. Distrib.*, vol. 141, no. 1, p. 1, 1994, doi: 10.1049/ip-gtd:19949770.

[67] J. F. Bard, "Short-Term Scheduling of Thermal-Electric Generators Using Lagrangian Relaxation," *Oper. Res.*, vol. 36, no. 5, pp. 756–766, Oct. 1988, doi: 10.1287/opre.36.5.756.

[68] P. Lowery, "Generating Unit Commitment by Dynamic Programming," *IEEE Trans. Power Appar. Syst.*, vol. PAS-85, no. 5, pp. 422–426, May 1966, doi: 10.1109/TPAS.1966.291679.

[69] D. C. Walters and G. B. Sheble, "Genetic algorithm solution of economic dispatch with valve point loading," *IEEE Trans. Power Syst.*, vol. 8, no. 3, pp. 1325–1332, 1993, doi: 10.1109/59.260861.

[70] N. Noman and H. Iba, "Differential evolution for economic load dispatch problems," *Electr. Power Syst. Res.*, vol. 78, no. 8, pp. 1322–1331, Aug. 2008, doi: 10.1016/j.epsr.2007.11.007.

[71] Z.-L. Gaing, "Particle swarm optimization to solving the economic dispatch considering the generator constraints," *IEEE Trans. Power Syst.*, vol. 18, no. 3, pp. 1187–1195, Aug. 2003, doi: 10.1109/TPWRS.2003.814889.

[72] K. Bhattacharjee, A. Bhattacharya, and S. H. nee Dey, "Oppositional Real Coded Chemical Reaction Optimization for different economic dispatch problems," *Int. J. Electr. Power Energy Syst.*, vol. 55, pp. 378–391, Feb. 2014, doi: 10.1016/j.ijepes.2013.09.033.

[73] S. Banerjee, D. Maity, and C. K. Chanda, “Teaching learning based optimization for economic load dispatch problem considering valve point loading effect,” *Int. J. Electr. Power Energy Syst.*, vol. 73, pp. 456–464, Dec. 2015, doi: 10.1016/j.ijepes.2015.05.036.

[74] A. Bhattacharya and P. K. Chattopadhyay, “Biogeography-Based Optimization for Different Economic Load Dispatch Problems,” *IEEE Trans. Power Syst.*, vol. 25, no. 2, pp. 1064–1077, May 2010, doi: 10.1109/TPWRS.2009.2034525.

[75] V. K. Kamboj, S. K. Bath, and J. S. Dhillon, “Solution of non-convex economic load dispatch problem using Grey Wolf Optimizer,” *Neural Comput. Appl.*, vol. 27, no. 5, pp. 1301–1316, Jul. 2016, doi: 10.1007/s00521-015-1934-8.

[76] V. K. Kamboj, A. Bhadoria, and S. K. Bath, “Solution of non-convex economic load dispatch problem for small-scale power systems using ant lion optimizer,” *Neural Comput. Appl.*, vol. 28, no. 8, pp. 2181–2192, Aug. 2017, doi: 10.1007/s00521-015-2148-9.

[77] W.-K. Hao, J.-S. Wang, X.-D. Li, M. Wang, and M. Zhang, “Arithmetic optimization algorithm based on elementary function disturbance for solving economic load dispatch problem in power system,” *Appl. Intell.*, Jan. 2022, doi: 10.1007/s10489-021-03125-4.

[78] H.-P. Lee, T.-T. Nguyen, T.-K. Dao, V.-D. Vu, and T.-G. Ngo, “An Enhanced Flower Pollination Algorithm for Power System Economic Load Dispatch,” 2022, pp. 77–86.

[79] R. E. Perez-Guerrero and J. R. Cedefio-Maldonado, “Differential evolution based economic environmental power dispatch,” in *Proceedings of the 37th Annual North American Power Symposium, 2005.*, pp. 191–197, doi: 10.1109/NAPS.2005.1560523.

[80] B. K. Panigrahi, V. Ravikumar Pandi, S. Das, and S. Das, “Multiobjective fuzzy dominance based bacterial foraging algorithm to solve economic emission dispatch problem,” *Energy*, vol. 35, no. 12, pp. 4761–4770, Dec. 2010, doi: 10.1016/j.energy.2010.09.014.

[81] Y. A. Gherbi, H. Bouzeboudja, and F. Z. Gherbi, “The combined economic environmental dispatch using new hybrid metaheuristic,” *Energy*, vol. 115, pp. 468–477, Nov. 2016, doi: 10.1016/j.energy.2016.08.079.

[82] V. K. Jadoun, N. Gupta, K. R. Niazi, and A. Swarnkar, “Modulated particle swarm optimization for economic emission dispatch,” *Int. J. Electr. Power Energy Syst.*, vol. 73, pp. 80–88, Dec. 2015, doi: 10.1016/j.ijepes.2015.04.004.

[83] H. Narimani *et al.*, “A multi-objective framework for multi-area economic emission dispatch,” *Energy*, vol. 154, pp. 126–142, Jul. 2018, doi: 10.1016/j.energy.2018.04.080.

[84] M. Amiri, S. Khanmohammadi, and M. A. Badamchizadeh, “Floating search space: A new idea for efficient solving the Economic and emission dispatch problem,” *Energy*, vol. 158, pp. 564–579, Sep. 2018, doi: 10.1016/j.energy.2018.05.062.

[85] A. Chatterjee, S. P. Ghoshal, and V. Mukherjee, “Solution of combined economic and emission dispatch problems of power systems by an opposition-based harmony search algorithm,” *Int. J. Electr. Power Energy Syst.*, vol. 39, no. 1, pp. 9–20, Jul. 2012, doi: 10.1016/j.ijepes.2011.12.004.

[86] Y.-C. Liang and J. R. Cuevas Juarez, “A normalization method for solving the combined economic and emission dispatch problem with meta-heuristic algorithms,” *Int. J. Electr. Power Energy Syst.*, vol. 54, pp. 163–186, Jan. 2014, doi: 10.1016/j.ijepes.2013.06.022.

[87] V. R. Pandi, B. K. Panigrahi, W.-C. Hong, and R. Sharma, “A Multiobjective Bacterial Foraging Algorithm to Solve the Environmental Economic Dispatch Problem,” *Energy Sources, Part B Econ. Planning, Policy*, vol. 9, no. 3, pp. 236–247, Jul. 2014, doi: 10.1080/15567249.2010.485167.

[88] N. Khan, G. Sidhu, and F. Gao, “Optimizing Combined Emission Economic Dispatch for Solar Integrated Power Systems,” *IEEE Access*, pp. 1–1, 2016, doi: 10.1109/ACCESS.2016.2587665.

[89] R. M. Rizk-Allah, R. A. El-Sehiemy, and G.-G. Wang, “A novel parallel hurricane optimization algorithm for secure emission/economic load dispatch solution,” *Appl. Soft Comput.*, vol. 63, pp. 206–222, Feb. 2018, doi: 10.1016/j.asoc.2017.12.002.

[90] J. Pitono, “Optimization of economic-emission dispatch by particle swarm optimization (PSO) using cubic criterion functions and various price penalty factors,” *Astra Salvensis*, vol. 6, no. 3, pp. 749–762, 2018.

[91] F. P. Mahdi, P. Vasant, M. Abdullah-Al-Wadud, J. Watada, and V. Kallimani, “A quantum-inspired particle swarm optimization approach for environmental/economic power dispatch problem using cubic criterion function,” *Int. Trans. Electr. Energy Syst.*, vol. 28, no. 3, pp. 1–19, 2018, doi: 10.1002/etep.2497.

[92] N. A. Amoli, S. Jadid, H. A. Shayanfar, and F. Barzinpour, “Solving economic dispatch problem with cubic fuel cost,” pp. 1–5, 2012.

[93] R. Ramachandaran and P. Avirajamanjula, “Modified biogeography based optimization algorithm for power dispatch using max / max price penalty factor,” vol. 118, no. 18, pp. 3813–3818, 2018.

[94] R. Karthikeyan, S. Subramanian, and E. B. Elanchezhian, “Combined economic and multiple emissions optimization considering third order polynomials using grasshopper optimization algorithm,” *Int. J. Innov. Technol. Explor. Eng.*, vol. 8, no. 8, pp. 274–284, 2019.

[95] D. Gonidakis and A. Vlachos, “A new sine cosine algorithm for economic and emission dispatch problems with price penalty factors,” *J. Inf. Optim. Sci.*, vol. 40, no. 3, pp. 679–697, 2019, doi: 10.1080/02522667.2018.1453667.

[96] F. P. Mahdi, P. Vasant, M. Abdullah-Al-Wadud, V. Kallimani, and J. Watada, “Quantum-behaved bat algorithm for many-objective combined economic emission dispatch problem using cubic criterion function,” *Neural Comput. Appl.*, vol. 31, no.

10, pp. 5857–5869, 2019, doi: 10.1007/s00521-018-3399-z.

[97] K. D. Bodha, V. K. Yadav, and V. Mukherjee, “Formulation and application of quantum-inspired tidal firefly technique for multiple-objective mixed cost-effective emission dispatch,” *Neural Comput. Appl.*, vol. 0, 2019, doi: 10.1007/s00521-019-04433-0.

[98] S. Kamel, E. H. Houssein, M. H. Hassan, M. Shouran, and F. A. Hashim, “An Efficient Electric Charged Particles Optimization Algorithm for Numerical Optimization and Optimal Estimation of Photovoltaic Models,” *Mathematics*, vol. 10, no. 6, p. 913, Mar. 2022, doi: 10.3390/math10060913.

[99] M. H. Hassan, S. Kamel, A. Selim, T. Khurshaid, and J. L. Domínguez-García, “A Modified Rao-2 Algorithm for Optimal Power Flow Incorporating Renewable Energy Sources,” *Mathematics*, vol. 9, no. 13, p. 1532, Jun. 2021, doi: 10.3390/math9131532.

[100] M. H. Hassan, S. Kamel, M. A. El-Dabah, T. Khurshaid, and J. L. Dominguez-Garcia, “Optimal Reactive Power Dispatch With Time-Varying Demand and Renewable Energy Uncertainty Using Rao-3 Algorithm,” *IEEE Access*, vol. 9, pp. 23264–23283, 2021, doi: 10.1109/ACCESS.2021.3056423.

[101] S. Mirjalili, A. H. Gandomi, S. Z. Mirjalili, S. Saremi, H. Faris, and S. M. Mirjalili, “Salp Swarm Algorithm: A bio-inspired optimizer for engineering design problems,” *Adv. Eng. Softw.*, vol. 114, pp. 163–191, Dec. 2017, doi: 10.1016/j.advengsoft.2017.07.002.

[102] G. P. Granelli, M. Montagna, G. L. Pasini, and P. Marannino, “Emission constrained dynamic dispatch,” *Electr. Power Syst. Res.*, vol. 24, no. 1, pp. 55–64, Jul. 1992, doi: 10.1016/0378-7796(92)90045-3.

[103] M. Basu, “Dynamic Economic Emission Dispatch Using Evolutionary Programming and Fuzzy Satisfying Method,” *Int. J. Emerg. Electr. Power Syst.*, vol. 8, no. 4, Oct. 2007, doi: 10.2202/1553-779X.1146.

[104] F. Benhamida and R. Belhachem, “Dynamic Constrained Economic/Emission Dispatch Scheduling Using Neural Network,” *Adv. Electr. Electron. Eng.*, vol. 11, no. 1, Mar. 2013, doi: 10.15598/aeee.v11i1.745.

[105] N. Pandit, A. Tripathi, S. Tapaswi, and M. Pandit, “An improved bacterial foraging algorithm for combined static/dynamic environmental economic dispatch,” *Appl. Soft Comput.*, vol. 12, no. 11, pp. 3500–3513, Nov. 2012, doi: 10.1016/j.asoc.2012.06.011.

[106] K. Thenmalar, S. Ramesh, and S. Thiruvenkadam, “Opposition Based Differential Evolution Algorithm for Dynamic Economic Emission Load Dispatch (EELD) with Emission Constraints and Valve Point Effects,” *J. Electr. Eng. Technol.*, vol. 10, no. 4, pp. 1508–1517, Jul. 2015, doi: 10.5370/JEET.2015.10.4.1508.

[107] M. Basu, “Particle Swarm Optimization Based Goal-Attainment Method for Dynamic Economic Emission Dispatch,” *Electr. Power Components Syst.*, vol. 34, no. 9, pp. 1015–1025, Sep. 2006, doi: 10.1080/15325000600596759.

[108] B. Bahmanifirouzi, E. Farjah, and T. Niknam, “Multi-objective stochastic dynamic economic emission dispatch enhancement by fuzzy adaptive modified theta particle swarm optimization,” *J. Renew. Sustain. Energy*, vol. 4, no. 2, p. 023105, Mar. 2012, doi: 10.1063/1.3690959.

[109] A. M. Elaiw, X. Xia, and A. M. Shehata, “Hybrid DE-SQP and hybrid PSO-SQP methods for solving dynamic economic emission dispatch problem with valve-point effects,” *Electr. Power Syst. Res.*, vol. 103, pp. 192–200, Oct. 2013, doi: 10.1016/j.epsr.2013.05.015.

[110] M. Basu, “Dynamic economic emission dispatch using nondominated sorting genetic algorithm-II,” *Int. J. Electr. Power Energy Syst.*, vol. 30, no. 2, pp. 140–149, Feb. 2008, doi: 10.1016/j.ijepes.2007.06.009.

[111] M. Basu, “Multi-objective Differential Evolution for Dynamic Economic Emission Dispatch,” *Int. J. Emerg. Electr. Power Syst.*, vol. 15, no. 2, pp. 141–150, Apr. 2014, doi: 10.1515/ijeeps-2013-0060.

[112] X. Jiang, J. Zhou, H. Wang, and Y. Zhang, “Dynamic environmental economic dispatch using multiobjective differential evolution algorithm with expanded double selection and adaptive random restart,” *Int. J. Electr. Power Energy Syst.*, vol. 49, pp. 399–407, Jul. 2013, doi: 10.1016/j.ijepes.2013.01.009.

[113] Z. Zhu, J. Wang, and M. H. Baloch, “Dynamic economic emission dispatch using modified NSGA-II,” *Int. Trans. Electr. Energy Syst.*, vol. 26, no. 12, pp. 2684–2698, Dec. 2016, doi: 10.1002/etep.2228.

[114] P. K. Roy and S. Bhui, “A multi-objective hybrid evolutionary algorithm for dynamic economic emission load dispatch,” *Int. Trans. Electr. Energy Syst.*, vol. 26, no. 1, pp. 49–78, Jan. 2016, doi: 10.1002/etep.2066.

[115] C. X. Guo, J. P. Zhan, and Q. H. Wu, “Dynamic economic emission dispatch based on group search optimizer with multiple producers,” *Electr. Power Syst. Res.*, vol. 86, pp. 8–16, May 2012, doi: 10.1016/j.epsr.2011.11.015.

[116] L.-L. Li, Z.-F. Liu, M.-L. Tseng, S.-J. Zheng, and M. K. Lim, “Improved tunicate swarm algorithm: Solving the dynamic economic emission dispatch problems,” *Appl. Soft Comput.*, vol. 108, p. 107504, Sep. 2021, doi: 10.1016/j.asoc.2021.107504.

[117] S. Qian, H. Wu, and G. Xu, “An improved particle swarm optimization with clone selection principle for dynamic economic emission dispatch,” *Soft Comput.*, vol. 24, no. 20, pp. 15249–15271, Oct. 2020, doi: 10.1007/s00500-020-04861-4.

[118] D. C. Walters and G. B. Sheble, “Genetic algorithm solution of economic dispatch with valve point loading,” *IEEE Trans. Power Syst.*, vol. 8, no. 3, pp. 1325–1332, 1993, doi: 10.1109/59.260861.

[119] D. Zou, S. Li, Z. Li, and X. Kong, “A new global particle swarm optimization for the economic emission dispatch with or without transmission losses,” *Energy Convers. Manag.*, vol. 139, pp. 45–70, 2017, doi: 10.1016/j.enconman.2017.02.035.

[120] M. Suman, “Coulomb ’ s and Franklin ’ s laws based optimization for nonconvex economic and emission dispatch problems,” vol. 20, pp. 225–238, 2020.

[121] J. M. Calvin and A. Žilinskas, “On efficiency of a single variable bi-objective optimization algorithm,” *Optim. Lett.*, vol. 14, no. 1, pp. 259–267, 2020, doi: 10.1007/s11590-019-01471-4.

[122] S. A. El-Sattar, S. Kamel, R. A. El Sehiemy, F. Jurado, and J. Yu, “Single- and multi-objective optimal power flow frameworks using Jaya optimization technique,” *Neural Comput. Appl.*, vol. 31, no. 12, pp. 8787–8806, 2019, doi: 10.1007/s00521-019-04194-w.

[123] S. Sivasubramani and K. S. Swarup, “Multi-objective harmony search algorithm for optimal power flow problem,” *Int. J. Electr. Power Energy Syst.*, vol. 33, no. 3, pp. 745–752, 2011, doi: 10.1016/j.ijepes.2010.12.031.

[124] A. M. Shaheen, R. A. El-Sehiemy, and S. M. Farrag, “Solving multi-objective optimal power flow problem via forced initialised differential evolution algorithm,” *IET Gener. Transm. Distrib.*, vol. 10, no. 7, pp. 1634–1647, 2016, doi: 10.1049/iet-gtd.2015.0892.

[125] A. Dolatnezhadsomarin and E. Khorram, “Two efficient algorithms for constructing almost even approximations of the Pareto front in multi-objective optimization problems,” *Eng. Optim.*, vol. 51, no. 4, pp. 567–589, 2019, doi: 10.1080/0305215X.2018.1479405.

[126] S. Duman, S. Rivera, J. Li, and L. Wu, “Optimal power flow of power systems with controllable wind-photovoltaic energy systems via differential evolutionary particle swarm optimization,” *Int. Trans. Electr. Energy Syst.*, vol. 30, no. 4, Apr. 2020, doi: 10.1002/2050-7038.12270.

[127] X. Shen, D. Zou, N. Duan, and Q. Zhang, “An efficient fitness-based differential evolution algorithm and a constraint handling technique for dynamic economic emission dispatch,” *Energy*, vol. 186, p. 115801, Nov. 2019, doi: 10.1016/j.energy.2019.07.131.

[128] Z. Li, D. Zou, and Z. Kong, “A harmony search variant and a useful constraint handling method for the dynamic economic emission dispatch problems considering transmission loss,” *Eng. Appl. Artif. Intell.*, vol. 84, pp. 18–40, Sep. 2019, doi: 10.1016/j.engappai.2019.05.005.

[129] M. K. Sattar, A. Ahmad, S. Fayyaz, S. S. Ul Haq, and M. S. Saddique, “Ramp rate handling strategies in Dynamic Economic Load Dispatch (DELD) problem using Grey Wolf Optimizer (GWO),” *J. Chinese Inst. Eng.*, vol. 43, no. 2, pp. 200–213, Feb. 2020, doi: 10.1080/02533839.2019.1694446.

[130] E. E. Elattar and S. K. ElSayed, “Modified JAYA algorithm for optimal power flow incorporating renewable energy sources considering the cost, emission, power loss and voltage profile improvement,” *Energy*, vol. 178, pp. 598–609, Jul. 2019, doi: 10.1016/j.energy.2019.04.159.

[131] P. K. Adhvaryyu, P. K. Chattopadhyay, and A. Bhattacharya, “Dynamic optimal power

flow of combined heat and power system with Valve-point effect using Krill Herd algorithm," *Energy*, vol. 127, pp. 756–767, May 2017, doi: 10.1016/j.energy.2017.03.046.

[132] A. Qazi *et al.*, "Towards Sustainable Energy: A Systematic Review of Renewable Energy Sources, Technologies, and Public Opinions," *IEEE Access*, vol. 7, pp. 63837–63851, 2019, doi: 10.1109/ACCESS.2019.2906402.

[133] P. P. Biswas, P. N. Suganthan, and G. A. J. Amaratunga, "Optimal power flow solutions incorporating stochastic wind and solar power," *Energy Convers. Manag.*, vol. 148, pp. 1194–1207, Sep. 2017, doi: 10.1016/j.enconman.2017.06.071.

[134] A. Panda and M. Tripathy, "Security constrained optimal power flow solution of wind-thermal generation system using modified bacteria foraging algorithm," *Energy*, vol. 93, pp. 816–827, Dec. 2015, doi: 10.1016/j.energy.2015.09.083.

[135] L. Shi, C. Wang, L. Yao, Y. Ni, and M. Bazargan, "Optimal Power Flow Solution Incorporating Wind Power," *IEEE Syst. J.*, vol. 6, no. 2, pp. 233–241, Jun. 2012, doi: 10.1109/JSYST.2011.2162896.

[136] A. E. Chaib, H. R. E. H. Bouchekara, R. Mehasni, and M. A. Abido, "Optimal power flow with emission and non-smooth cost functions using backtracking search optimization algorithm," *Int. J. Electr. Power Energy Syst.*, vol. 81, pp. 64–77, Oct. 2016, doi: 10.1016/j.ijepes.2016.02.004.

[137] A. Jahid, M. S. Islam, M. S. Hossain, M. E. Hossain, M. K. H. Monju, and M. F. Hossain, "Toward Energy Efficiency Aware Renewable Energy Management in Green Cellular Networks With Joint Coordination," *IEEE Access*, vol. 7, pp. 75782–75797, 2019, doi: 10.1109/ACCESS.2019.2920924.

[138] R. Roy and H. T. Jadhav, "Optimal power flow solution of power system incorporating stochastic wind power using Gbest guided artificial bee colony algorithm," *Int. J. Electr. Power Energy Syst.*, vol. 64, pp. 562–578, Jan. 2015, doi: 10.1016/j.ijepes.2014.07.010.

[139] S. Surender Reddy, P. R. Bijwe, and A. R. Abhyankar, "Real-Time Economic Dispatch Considering Renewable Power Generation Variability and Uncertainty Over Scheduling Period," *IEEE Syst. J.*, vol. 9, no. 4, pp. 1440–1451, Dec. 2015, doi: 10.1109/JSYST.2014.2325967.

[140] W. Zhao, Z. Zhang, and L. Wang, "Manta ray foraging optimization: An effective bio-inspired optimizer for engineering applications," *Eng. Appl. Artif. Intell.*, vol. 87, p. 103300, Jan. 2020, doi: 10.1016/j.engappai.2019.103300.

[141] N. Lynn and P. N. Suganthan, "Heterogeneous comprehensive learning particle swarm optimization with enhanced exploration and exploitation," *Swarm Evol. Comput.*, vol. 24, pp. 11–24, Oct. 2015, doi: 10.1016/j.swevo.2015.05.002.

[142] I. Ahmadianfar, O. Bozorg-Haddad, and X. Chu, "Gradient-based optimizer: A new metaheuristic optimization algorithm," *Inf. Sci. (Ny).*, vol. 540, pp. 131–159, Nov. 2020, doi: 10.1016/j.ins.2020.06.037.

[143] E. Cuevas, A. Echavarría, and M. A. Ramírez-Ortegón, “An optimization algorithm inspired by the States of Matter that improves the balance between exploration and exploitation,” *Appl. Intell.*, vol. 40, no. 2, pp. 256–272, Mar. 2014, doi: 10.1007/s10489-013-0458-0.

[144] W. Zhao, L. Wang, and Z. Zhang, “Artificial ecosystem-based optimization: a novel nature-inspired meta-heuristic algorithm,” *Neural Comput. Appl.*, vol. 32, no. 13, pp. 9383–9425, Jul. 2020, doi: 10.1007/s00521-019-04452-x.

[145] A. S. Menesy, H. M. Sultan, A. Selim, M. G. Ashmawy, and S. Kamel, “Developing and Applying Chaotic Harris Hawks Optimization Technique for Extracting Parameters of Several Proton Exchange Membrane Fuel Cell Stacks,” *IEEE Access*, vol. 8, pp. 1146–1159, 2020, doi: 10.1109/ACCESS.2019.2961811.

[146] G. I. Sayed, A. E. Hassanien, and A. T. Azar, “Feature selection via a novel chaotic crow search algorithm,” *Neural Comput. Appl.*, vol. 31, no. 1, pp. 171–188, Jan. 2019, doi: 10.1007/s00521-017-2988-6.

[147] W. Ahmed, A. Selim, S. Kamel, J. Yu, and F. Jurado, “Probabilistic Load Flow Solution Considering Optimal Allocation of SVC in Radial Distribution System,” *Int. J. Interact. Multimed. Artif. Intell.*, vol. 5, no. 3, p. 152, 2018, doi: 10.9781/ijimai.2018.11.001.

[148] B. Society and A. Journal, “The life history of physarum polycephalum Author ( s ): Frank L . Howard,” vol. 18, no. 2, pp. 116–133, 2014.

[149] S. Li, H. Chen, M. Wang, A. A. Heidari, and S. Mirjalili, “Slime mould algorithm: A new method for stochastic optimization,” *Futur. Gener. Comput. Syst.*, vol. 111, pp. 300–323, 2020, doi: 10.1016/j.future.2020.03.055.

[150] S. Mirjalili, “SCA: A Sine Cosine Algorithm for solving optimization problems,” *Knowledge-Based Syst.*, vol. 96, pp. 120–133, Mar. 2016, doi: 10.1016/j.knosys.2015.12.022.

[151] A. Faramarzi, M. Heidarinejad, S. Mirjalili, and A. H. Gandomi, “Marine Predators Algorithm: A nature-inspired metaheuristic,” *Expert Syst. Appl.*, vol. 152, p. 113377, 2020, doi: 10.1016/j.eswa.2020.113377.

[152] S. Liang, Jing J and Qin, A Kai and Suganthan, Ponnuthurai N and Baskar, “Comprehensive learning particle swarm optimizer for global optimization of multimodal functions,” *IEEE Trans. Evol. Comput.*, vol. 10, pp. 281–295, 2006.

[153] P. N. Lynn, Nandar and Suganthan, “Heterogeneous comprehensive learning particle swarm optimization with enhanced exploration and exploitation,” *Swarm Evol. Comput.*, vol. 24, pp. 11–24, 2015.

[154] A. Baadji, Bousaadia and Bentarzi, Hamid and Bakdi, “Comprehensive learning bat algorithm for optimal coordinated tuning of power system stabilizers and static VAR compensator in power systems,” *Eng. Optim. Taylor \& Fr.*, pp. 1–19, 2019.

[155] W. Zhao, L. Wang, and Z. Zhang, “Supply-Demand-Based Optimization: A Novel

Economics-Inspired Algorithm for Global Optimization," *IEEE Access*, vol. 7, pp. 73182–73206, 2019, doi: 10.1109/ACCESS.2019.2918753.

[156] F. A. Alturki, A. A. Al-Shamma'a, H. M. H. Farh, and K. AlSharabi, "Optimal sizing of autonomous hybrid energy system using supply-demand-based optimization algorithm," *Int. J. Energy Res.*, vol. 45, no. 1, pp. 605–625, Jan. 2021, doi: 10.1002/er.5766.

[157] Xin-She Yang, S. Deb, and Xingshi He, "Eagle strategy with flower algorithm," in *2013 International Conference on Advances in Computing, Communications and Informatics (ICACCI)*, Aug. 2013, pp. 1213–1217, doi: 10.1109/ICACCI.2013.6637350.

[158] H. Yapıcı and N. Çetinkaya, "An Improved Particle Swarm Optimization Algorithm Using Eagle Strategy for Power Loss Minimization," *Math. Probl. Eng.*, vol. 2017, pp. 1–11, 2017, doi: 10.1155/2017/1063045.

[159] E. Emary and H. M. Zawbaa, "Impact of Chaos Functions on Modern Swarm Optimizers," *PLoS One*, vol. 11, no. 7, p. e0158738, Jul. 2016, doi: 10.1371/journal.pone.0158738.

[160] M. H. Hassan, S. Kamel, S. Q. Salih, T. Khurshaid, and M. Ebeed, "Developing Chaotic Artificial Ecosystem-Based Optimization Algorithm for Combined Economic Emission Dispatch," *IEEE Access*, vol. 9, pp. 51146–51165, 2021, doi: 10.1109/ACCESS.2021.3066914.

[161] S. Saremi, S. Mirjalili, and A. Lewis, "Biogeography-based optimisation with chaos," *Neural Comput. Appl.*, vol. 25, no. 5, pp. 1077–1097, Oct. 2014, doi: 10.1007/s00521-014-1597-x.

[162] J. Wang, Y. Gao, and X. Chen, "A Novel Hybrid Interval Prediction Approach Based on Modified Lower Upper Bound Estimation in Combination with Multi-Objective Salp Swarm Algorithm for Short-Term Load Forecasting," *Energies*, vol. 11, no. 6, p. 1561, Jun. 2018, doi: 10.3390/en11061561.

[163] A. K. Das and D. K. Pratihar, "A New Bonobo optimizer (BO) for Real-Parameter optimization," in *2019 IEEE Region 10 Symposium (TENSYMP)*, Jun. 2019, pp. 108–113, doi: 10.1109/TENSYMP46218.2019.8971108.

[164] R. Y. Abdelghany, S. Kamel, H. M. Sultan, A. Khorasy, S. K. Elsayed, and M. Ahmed, "Development of an Improved Bonobo Optimizer and Its Application for Solar Cell Parameter Estimation," *Sustainability*, vol. 13, no. 7, p. 3863, Mar. 2021, doi: 10.3390/su13073863.

[165] T. Adhinarayanan, "Particle swarm optimisation for economic dispatch with cubic fuel cost function," vol. 00, pp. 6–9, 2006, doi: 10.1109/TENCON.2006.344059.

[166] R. T. F. A. King and H. C. S. Rughooputh, "Elitist multiobjective evolutionary algorithm for environmental/economic dispatch," *2003 Congr. Evol. Comput. CEC 2003 - Proc.*, vol. 2, pp. 1108–1114, 2003, doi: 10.1109/CEC.2003.1299792.

[167] I. Ziane, F. Benhamida, A. Graa, and Y. Salhi, "Combined economic emission dispatch with new price penalty factors," *2015 4th Int. Conf. Electr. Eng. ICEE 2015*, no. Icee, 2016, doi: 10.1109/INTEE.2015.7416864.

[168] I. Ziane, F. Benhamida, and A. Graa, "Simulated annealing algorithm for combined economic and emission power dispatch using max/max price penalty factor," *Neural Comput. Appl.*, vol. 28, no. s1, pp. 197–205, 2017, doi: 10.1007/s00521-016-2335-3.

[169] M. H. Pitono, Joko and Soepriyanto, Adi and Purnomo, "Advance optimization of economic emission dispatch by particle swarm optimization (pso) using cubic criterion functions and various price penalty factors," *J. Ilm. KURSOR*, vol. 7, no. 3, 2014.

[170] I. Ziane, F. Benhamida, and A. Graa, "Simulated annealing algorithm for combined economic and emission power dispatch using max/max price penalty factor," *Neural Comput. Appl.*, vol. 28, no. S1, pp. 197–205, Dec. 2017, doi: 10.1007/s00521-016-2335-3.

[171] P. Ramachandaran, Ramesh and Avirajamanjula, "Modified biogeography based optimization algorithm for power dispatch using max/max price penalty factor," *Int. J. Pure Appl. Math.*, vol. 118, no. 18, pp. 3813--3818, 2018.

[172] D. Gonidakis and A. Vlachos, "A new sine cosine algorithm for economic and emission dispatch problems with price penalty factors," *J. Inf. Optim. Sci.*, vol. 40, no. 3, pp. 679–697, Apr. 2019, doi: 10.1080/02522667.2018.1453667.

[173] A. Rajagopalan, P. Kasinathan, K. Nagarajan, V. K. Ramachandaramurthy, V. Sengoden, and S. Alavandar, "Chaotic self-adaptive interior search algorithm to solve combined economic emission dispatch problems with security constraints," *Int. Trans. Electr. Energy Syst.*, vol. 29, no. 8, Aug. 2019, doi: 10.1002/2050-7038.12026.

[174] U. Güvenç, "Combined economic emission dispatch solution using genetic algorithm based on similarity crossover," *Sci. Res. Essays*, vol. 5, no. 17, pp. 2451–2456, Sep. 2010.

[175] U. Güvenç, Y. Sönmez, S. Duman, and N. Yörükeren, "Combined economic and emission dispatch solution using gravitational search algorithm," *Sci. Iran.*, vol. 19, no. 6, pp. 1754–1762, Dec. 2012, doi: 10.1016/j.scient.2012.02.030.

[176] R. Eberhart and J. Kennedy, "A new optimizer using particle swarm theory," in *MHS'95. Proceedings of the Sixth International Symposium on Micro Machine and Human Science*, pp. 39–43, doi: 10.1109/MHS.1995.494215.

[177] G.-G. Wang, S. Deb, and L. dos S. Coelho, "Elephant Herding Optimization," in *2015 3rd International Symposium on Computational and Business Intelligence (ISCBI)*, Dec. 2015, pp. 1–5, doi: 10.1109/ISCBI.2015.8.

[178] L. Guo, G.-G. Wang, A. H. Gandomi, A. H. Alavi, and H. Duan, "A new improved krill herd algorithm for global numerical optimization," *Neurocomputing*, vol. 138, pp. 392–402, Aug. 2014, doi: 10.1016/j.neucom.2014.01.023.

[179] A. Faramarzi, M. Heidarinejad, S. Mirjalili, and A. H. Gandomi, "Marine Predators

Algorithm: A nature-inspired metaheuristic," *Expert Syst. Appl.*, vol. 152, p. 113377, Aug. 2020, doi: 10.1016/j.eswa.2020.113377.

[180] L. Abualigah, A. Diabat, S. Mirjalili, M. Abd Elaziz, and A. H. Gandomi, "The Arithmetic Optimization Algorithm," *Comput. Methods Appl. Mech. Eng.*, vol. 376, p. 113609, Apr. 2021, doi: 10.1016/j.cma.2020.113609.

[181] M. Singh and J. S. Dhillon, "Multiobjective thermal power dispatch using opposition-based greedy heuristic search," *Int. J. Electr. Power Energy Syst.*, vol. 82, pp. 339–353, 2016, doi: 10.1016/j.ijepes.2016.03.016.

[182] M. Orero, SO and Irving, "Large scale unit commitment using a hybrid genetic algorithm," *Int. J. Electr. Power \& Energy Syst.*

[183] T. Adhinarayanan and M. Sydulu, "Particle Swarm Optimisation for Economic Dispatch with Cubic Fuel Cost Function," in *TENCON 2006 - 2006 IEEE Region 10 Conference*, 2006, pp. 1–4, doi: 10.1109/TENCON.2006.344059.

[184] N. A. Amoli, S. Jadid, and H. A. Shayanfar, "Solving economic dispatch problem with cubic fuel cost function by firefly algorithm," 2012.

[185] R. T. F. Ah King and H. C. S. Rughooputh, "Elitist multiobjective evolutionary algorithm for environmental/economic dispatch," in *The 2003 Congress on Evolutionary Computation, 2003. CEC '03.*, vol. 2, pp. 1108–1114, doi: 10.1109/CEC.2003.1299792.

[186] J. and others Pitono, "Optimization of economic-emission dispatch by particle swarm optimization (PSO) using cubic criterion functions and various price penalty factors," *Astra Salvensis-revista de istorie si cultura*, vol. 6. Transilvanian Association for the Literarure and Culture of Romanian People (ASTRA), pp. 749–762, 2018.

[187] R. Karthikeyan, S. Subramanian, and E. B. Elanchezhian, "Combined economic and multiple emissions optimization considering third order polynomials using grasshopper optimization algorithm," *Int. J. Innov. Technol. Explor. Eng.*, vol. 8, no. 8, pp. 274–284, Jun. 2019.

[188] M. H. Hassan, S. Kamel, S. Q. Salih, T. Khurshaid, and M. Ebeed, "Developing Chaotic Artificial Ecosystem-based Optimization Algorithm for Combined Economic Emission Dispatch," *IEEE Access*, pp. 1–1, 2021, doi: 10.1109/ACCESS.2021.3066914.

[189] L. Zhao, Weiguo and Zhang, Zhenxing and Wang, "Manta ray foraging optimization: An effective bio-inspired optimizer for engineering applications," *Eng. Appl. Artif. Intell. Elsevier*, vol. 87, p. 103300, 2020.

[190] S. Li, Shimin and Chen, Huiling and Wang, Mingjing and Heidari, Ali Asghar and Mirjalili, "Slime mould algorithm: A new method for stochastic optimization," *Futur. Gener. Comput. Syst. Elsevier*, 2020.

[191] S. Mirjalili, "SCA: a sine cosine algorithm for solving optimization problems," *Knowledge-based Syst. Elsevier*, vol. 96, pp. 120–133, 2016.

[192] S. Liang, Jing J and Qin, A Kai and Suganthan, Ponnuthurai N and Baskar, “Comprehensive learning particle swarm optimizer for global optimization of multimodal functions,” *IEEE Trans. Evol. Comput. IEEE*, vol. 10, pp. 281–295, 2006.

[193] M. H. Hassan, E. H. Houssein, M. A. Mahdy, and S. Kamel, “An improved Manta ray foraging optimizer for cost-effective emission dispatch problems,” *Eng. Appl. Artif. Intell.*, vol. 100, p. 104155, Apr. 2021, doi: 10.1016/j.engappai.2021.104155.

[194] S. Krishnamurthy, “Comparative analyses of min-max and max-max price penalty factor approaches for multi criteria power system dispatch problem with valve point effect loading using Lagrange ’ s method,” pp. 1–7, 2011.

[195] A. Theerthamalai and S. Maheswarapu, “An effective non-iterative ‘λ-logic based’ algorithm for economic dispatch of generators with cubic fuel cost function,” *Int. J. Electr. Power Energy Syst.*, vol. 32, no. 5, pp. 539–542, 2010, doi: 10.1016/j.ijepes.2009.11.002.

[196] S. Ganesan and S. Subramanian, “Non-convex economic thermal power management with transmission loss and environmental factors: Exploration from direct search method,” *Int. J. Energy Sect. Manag.*, vol. 6, no. 2, pp. 228–238, 2012, doi: 10.1108/17506221211242086.

[197] S. Mirjalili, S. M. Mirjalili, and A. Lewis, “Grey Wolf Optimizer,” *Adv. Eng. Softw.*, vol. 69, pp. 46–61, Mar. 2014, doi: 10.1016/j.advengsoft.2013.12.007.

[198] S. Kaur, L. K. Awasthi, A. L. Sangal, and G. Dhiman, “Tunicate Swarm Algorithm: A new bio-inspired based metaheuristic paradigm for global optimization,” *Eng. Appl. Artif. Intell.*, vol. 90, p. 103541, Apr. 2020, doi: 10.1016/j.engappai.2020.103541.

[199] B. R. Adarsh, T. Raghunathan, T. Jayabarathi, and X.-S. Yang, “Economic dispatch using chaotic bat algorithm,” *Energy*, vol. 96, pp. 666–675, Feb. 2016, doi: 10.1016/j.energy.2015.12.096.

[200] A. I. Selvakumar and K. Thanushkodi, “A New Particle Swarm Optimization Solution to Nonconvex Economic Dispatch Problems,” *IEEE Trans. Power Syst.*, vol. 22, no. 1, pp. 42–51, Feb. 2007, doi: 10.1109/TPWRS.2006.889132.

[201] D. C. Secui, “A new modified artificial bee colony algorithm for the economic dispatch problem,” *Energy Convers. Manag.*, vol. 89, pp. 43–62, Jan. 2015, doi: 10.1016/j.enconman.2014.09.034.

[202] W. T. Elsayed, Y. G. Hegazy, F. M. Bendary, and M. S. El-bages, “Modified social spider algorithm for solving the economic dispatch problem,” *Eng. Sci. Technol. an Int. J.*, vol. 19, no. 4, pp. 1672–1681, Dec. 2016, doi: 10.1016/j.jestch.2016.09.002.

[203] W. T. Elsayed, Y. G. Hegazy, M. S. El-bages, and F. M. Bendary, “Improved Random Drift Particle Swarm Optimization With Self-Adaptive Mechanism for Solving the Power Economic Dispatch Problem,” *IEEE Trans. Ind. Informatics*, vol. 13, no. 3, pp. 1017–1026, Jun. 2017, doi: 10.1109/TII.2017.2695122.

[204] W. T. Elsayed and E. F. El-Saadany, “A Fully Decentralized Approach for Solving the

Economic Dispatch Problem," *IEEE Trans. Power Syst.*, vol. 30, no. 4, pp. 2179–2189, Jul. 2015, doi: 10.1109/TPWRS.2014.2360369.

[205] F. Mohammadi and H. Abdi, "A modified crow search algorithm (MCSA) for solving economic load dispatch problem," *Appl. Soft Comput.*, vol. 71, pp. 51–65, Oct. 2018, doi: 10.1016/j.asoc.2018.06.040.

[206] M. Fesanghary and M. M. Ardehali, "A novel meta-heuristic optimization methodology for solving various types of economic dispatch problem," *Energy*, vol. 34, no. 6, pp. 757–766, Jun. 2009, doi: 10.1016/j.energy.2009.02.007.

[207] K. T. Chaturvedi, M. Pandit, and L. Srivastava, "Self-Organizing Hierarchical Particle Swarm Optimization for Nonconvex Economic Dispatch," *IEEE Trans. Power Syst.*, vol. 23, no. 3, pp. 1079–1087, Aug. 2008, doi: 10.1109/TPWRS.2008.926455.

[208] S. Pothiya, I. Ngamroo, and W. Kongprawechnon, "Application of multiple tabu search algorithm to solve dynamic economic dispatch considering generator constraints," *Energy Convers. Manag.*, vol. 49, no. 4, pp. 506–516, Apr. 2008, doi: 10.1016/j.enconman.2007.08.012.

[209] I. Ciornei and E. Kyriakides, "A GA-API Solution for the Economic Dispatch of Generation in Power System Operation," *IEEE Trans. Power Syst.*, vol. 27, no. 1, pp. 233–242, Feb. 2012, doi: 10.1109/TPWRS.2011.2168833.

[210] J. Yu, C.-H. Kim, A. Wadood, T. Khurshaid, and S.-B. Rhee, "Jaya Algorithm With Self-Adaptive Multi-Population and Lévy Flights for Solving Economic Load Dispatch Problems," *IEEE Access*, vol. 7, pp. 21372–21384, 2019, doi: 10.1109/ACCESS.2019.2899043.

[211] C.-C. Kuo, "A novel string structure for economic dispatch problems with practical constraints," *Energy Convers. Manag.*, vol. 49, no. 12, pp. 3571–3577, Dec. 2008, doi: 10.1016/j.enconman.2008.07.007.

[212] Y. Yang, B. Wei, H. Liu, Y. Zhang, J. Zhao, and E. Manla, "Chaos Firefly Algorithm With Self-Adaptation Mutation Mechanism for Solving Large-Scale Economic Dispatch With Valve-Point Effects and Multiple Fuel Options," *IEEE Access*, vol. 6, pp. 45907–45922, 2018, doi: 10.1109/ACCESS.2018.2865960.

[213] S. M. V. Pandian and K. Thanushkodi, "An evolutionary programming based efficient particle swarm optimization for economic dispatch problem with valve-Point loading," *Eur. J. Sci. Res.*, vol. 52, no. 3, pp. 385–397, 2011.

[214] B. K. Panigrahi, V. Ravikumar Pandi, and S. Das, "Adaptive particle swarm optimization approach for static and dynamic economic load dispatch," *Energy Convers. Manag.*, vol. 49, no. 6, pp. 1407–1415, Jun. 2008, doi: 10.1016/j.enconman.2007.12.023.

[215] J. Cai, X. Ma, L. Li, and P. Haipeng, "Chaotic particle swarm optimization for economic dispatch considering the generator constraints," *Energy Convers. Manag.*, vol. 48, no. 2, pp. 645–653, Feb. 2007, doi: 10.1016/j.enconman.2006.05.020.

[216] S. Agnihotri, A. Atre, and H. K. Verma, "Equilibrium Optimizer for Solving Economic Dispatch Problem," in *2020 IEEE 9th Power India International Conference (PIICON)*, Feb. 2020, pp. 1–5, doi: 10.1109/PIICON49524.2020.9113048.

[217] A. Atre, S. Agnihotri, and H. K. Verma, "Hybrid EO-SCA Based Economic Load Dispatch," in *2020 IEEE First International Conference on Smart Technologies for Power, Energy and Control (STPEC)*, Sep. 2020, pp. 1–6, doi: 10.1109/STPEC49749.2020.9297737.

[218] S. K. Nayak, K. R. Krishnanand, B. K. Panigrahi, and P. K. Rout, "Application of Artificial Bee Colony to economic load dispatch problem with ramp rate limits and prohibited operating zones," in *2009 World Congress on Nature & Biologically Inspired Computing (NaBIC)*, 2009, pp. 1237–1242, doi: 10.1109/NABIC.2009.5393751.

[219] X.-S. Yang, S. S. Sadat Hosseini, and A. H. Gandomi, "Firefly Algorithm for solving non-convex economic dispatch problems with valve loading effect," *Appl. Soft Comput.*, vol. 12, no. 3, pp. 1180–1186, Mar. 2012, doi: 10.1016/j.asoc.2011.09.017.

[220] H. Barati and M. Sadeghi, "An efficient hybrid MPSO-GA algorithm for solving non-smooth/non-convex economic dispatch problem with practical constraints," *Ain Shams Eng. J.*, vol. 9, no. 4, pp. 1279–1287, Dec. 2018, doi: 10.1016/j.asej.2016.08.008.

[221] N. Ghorbani, S. Vakili, E. Babaei, and A. Sakhavati, "Particle swarm optimization with smart inertia factor for solving non-convex economic load dispatch problems," *Int. Trans. Electr. Energy Syst.*, vol. 24, no. 8, pp. 1120–1133, Aug. 2014, doi: 10.1002/etep.1766.

[222] M. N. Abdullah, A. H. Abu Bakar, N. A. Rahim, and H. Moklis, "Economic load dispatch with nonsmooth cost functions using evolutionary particle swarm optimization," *IEEJ Trans. Electr. Electron. Eng.*, vol. 8, no. S1, pp. S30–S37, 2013, doi: 10.1002/tee.21915.

[223] V. S. Aragón, S. C. Esquivel, and C. A. Coello Coello, "An immune algorithm with power redistribution for solving economic dispatch problems," *Inf. Sci. (Ny).*, vol. 295, pp. 609–632, Feb. 2015, doi: 10.1016/j.ins.2014.10.026.

[224] N. Ghorbani and E. Babaei, "Exchange market algorithm for economic load dispatch," *Int. J. Electr. Power Energy Syst.*, vol. 75, pp. 19–27, Feb. 2016, doi: 10.1016/j.ijepes.2015.08.013.

[225] H. T. Jadhav and R. Roy, "Gbest guided artificial bee colony algorithm for environmental/economic dispatch considering wind power," *Expert Syst. Appl.*, vol. 40, no. 16, pp. 6385–6399, Nov. 2013, doi: 10.1016/j.eswa.2013.05.048.

[226] S. H. Nee Dey, "Teaching Learning Based Optimization for Different Economic Dispatch Problems," *Sci. Iran. 21(3),* pp. 870-884., 2014.

[227] S. Khamsawang and S. Jiriwibhakorn, "DSPSO–TSA for economic dispatch problem with nonsmooth and noncontinuous cost functions," *Energy Convers. Manag.*, vol. 51, no. 2, pp. 365–375, Feb. 2010, doi: 10.1016/j.enconman.2009.09.034.

[228] B. K. Panigrahi and V. Ravikumar Pandi, “Bacterial foraging optimisation: Nelder–Mead hybrid algorithm for economic load dispatch,” *IET Gener. Transm. Distrib.*, vol. 2, no. 4, p. 556, 2008, doi: 10.1049/iet-gtd:20070422.

[229] J. Yu, C.-H. Kim, and S.-B. Rhee, “Clustering cuckoo search optimization for economic load dispatch problem,” *Neural Comput. Appl.*, vol. 32, no. 22, pp. 16951–16969, Nov. 2020, doi: 10.1007/s00521-020-05036-w.

[230] M. Basu, “Economic environmental dispatch using multi-objective differential evolution,” *Appl. Soft Comput.*, vol. 11, no. 2, pp. 2845–2853, Mar. 2011, doi: 10.1016/j.asoc.2010.11.014.

[231] P. K. Roy and S. Bhui, “Multi-objective quasi-oppositional teaching learning based optimization for economic emission load dispatch problem,” *Int. J. Electr. Power Energy Syst.*, vol. 53, pp. 937–948, Dec. 2013, doi: 10.1016/j.ijepes.2013.06.015.

[232] M. S. Alkoffash, M. A. Awadallah, M. Alweshah, R. A. Zitar, K. Assaleh, and M. A. Al-Betar, “A Non-convex Economic Load Dispatch Using Hybrid Salp Swarm Algorithm,” *Arab. J. Sci. Eng.*, vol. 46, no. 9, pp. 8721–8740, Sep. 2021, doi: 10.1007/s13369-021-05646-z.

[233] V. Basetti *et al.*, “Economic Emission Load Dispatch Problem with Valve-Point Loading Using a Novel Quasi-Oppositional-Based Political Optimizer,” *Electronics*, vol. 10, no. 21, p. 2596, Oct. 2021, doi: 10.3390/electronics10212596.

[234] G. Wang, Y. Zha, T. Wu, J. Qiu, J. Peng, and G. Xu, “Cross entropy optimization based on decomposition for multi-objective economic emission dispatch considering renewable energy generation uncertainties,” *Energy*, vol. 193, p. 116790, Feb. 2020, doi: 10.1016/j.energy.2019.116790.

[235] I. U. Khan, N. Javaid, K. A. A. Gamage, C. J. Taylor, S. Baig, and X. Ma, “Heuristic Algorithm Based Optimal Power Flow Model Incorporating Stochastic Renewable Energy Sources,” *IEEE Access*, vol. 8, pp. 148622–148643, 2020, doi: 10.1109/ACCESS.2020.3015473.

[236] W. T. Part, “Design Requirements; IEC 61400-1. ,” *Int. Electrotech. Comm. Geneva, Switzerland.*, 2005.

[237] J. M. Morales, A. J. Conejo, K. Liu, and J. Zhong, “Pricing Electricity in Pools With Wind Producers,” *IEEE Trans. Power Syst.*, vol. 27, no. 3, pp. 1366–1376, Aug. 2012, doi: 10.1109/TPWRS.2011.2182622.

[238] “The UK Renewable Energy. Accessed: Jul. 18, 2020. [Online]. Available: http://www.reuk.co.uk/wordpress/wind/wind-speed-distribution-weibull/.” www.reuk.co.uk/wordpress/wind/wind-speed-distribution-weibull/.

[239] F. Yao, Z. Y. Dong, K. Meng, Z. Xu, H. H.-C. Iu, and K. P. Wong, “Quantum-Inspired Particle Swarm Optimization for Power System Operations Considering Wind Power Uncertainty and Carbon Tax in Australia,” *IEEE Trans. Ind. Informatics*, vol. 8, no. 4, pp. 880–888, Nov. 2012, doi: 10.1109/TII.2012.2210431.

[240] V. Black, “Cost and performance data for power generation technologies,” *Nat. Renew. Energy Lab., Golden, CO, USA, Tech. Rep.*, 2012.

[241] P. P. Biswas, P. N. Suganthan, R. Mallipeddi, and G. A. J. Amaratunga, “Optimal power flow solutions using differential evolution algorithm integrated with effective constraint handling techniques,” *Eng. Appl. Artif. Intell.*, vol. 68, pp. 81–100, Feb. 2018, doi: 10.1016/j.engappai.2017.10.019.

[242] H. R. E. H. Bouchekara, A. E. Chaib, M. A. Abido, and R. A. El-Sehiemy, “Optimal power flow using an Improved Colliding Bodies Optimization algorithm,” *Appl. Soft Comput.*, vol. 42, pp. 119–131, May 2016, doi: 10.1016/j.asoc.2016.01.041.

[243] H. R. E. H. Bouchekara, A. E. Chaib, and M. A. Abido, “Multiobjective optimal power flow using a fuzzy based grenade explosion method,” *Energy Syst.*, vol. 7, no. 4, pp. 699–721, Nov. 2016, doi: 10.1007/s12667-016-0206-8.

[244] B. Mahdad and K. Srairi, “Security constrained optimal power flow solution using new adaptive partitioning flower pollination algorithm,” *Appl. Soft Comput.*, vol. 46, pp. 501–522, Sep. 2016, doi: 10.1016/j.asoc.2016.05.027.

[245] A.-A. A. Mohamed, Y. S. Mohamed, A. A. M. El-Gaafary, and A. M. Hemeida, “Optimal power flow using moth swarm algorithm,” *Electr. Power Syst. Res.*, vol. 142, pp. 190–206, Jan. 2017, doi: 10.1016/j.epsr.2016.09.025.

[246] K. Abaci and V. Yamacli, “Differential search algorithm for solving multi-objective optimal power flow problem,” *Int. J. Electr. Power Energy Syst.*, vol. 79, pp. 1–10, Jul. 2016, doi: 10.1016/j.ijepes.2015.12.021.

[247] V. Roberge, M. Tarbouchi, and F. Okou, “Optimal power flow based on parallel metaheuristics for graphics processing units,” *Electr. Power Syst. Res.*, vol. 140, pp. 344–353, Nov. 2016, doi: 10.1016/j.epsr.2016.06.006.

[248] A. Ramesh Kumar and L. Premalatha, “Optimal power flow for a deregulated power system using adaptive real coded biogeography-based optimization,” *Int. J. Electr. Power Energy Syst.*, vol. 73, pp. 393–399, Dec. 2015, doi: 10.1016/j.ijepes.2015.05.011.

[249] H. R. El-Hana Bouchekara, M. A. Abido, and A. E. Chaib, “Optimal Power Flow Using an Improved Electromagnetism-like Mechanism Method,” *Electr. Power Components Syst.*, vol. 44, no. 4, pp. 434–449, Feb. 2016, doi: 10.1080/15325008.2015.1115919.

[250] M. Rezaei Adaryani and A. Karami, “Artificial bee colony algorithm for solving multi-objective optimal power flow problem,” *Int. J. Electr. Power Energy Syst.*, vol. 53, pp. 219–230, Dec. 2013, doi: 10.1016/j.ijepes.2013.04.021.

[251] M. S. Kumari and S. Maheswarapu, “Enhanced Genetic Algorithm based computation technique for multi-objective Optimal Power Flow solution,” *Int. J. Electr. Power Energy Syst.*, vol. 32, no. 6, pp. 736–742, Jul. 2010, doi: 10.1016/j.ijepes.2010.01.010.

[252] M. H. Sulaiman and Z. Mustaffa, “Optimal power flow incorporating stochastic wind and solar generation by metaheuristic optimizers,” *Microsyst. Technol.*, vol. 27, no. 9,

pp. 3263–3277, Sep. 2021, doi: 10.1007/s00542-020-05046-7.

[253] M. Farhat, S. Kamel, A. M. Atallah, and B. Khan, "Optimal Power Flow Solution Based on Jellyfish Search Optimization Considering Uncertainty of Renewable Energy Sources," *IEEE Access*, vol. 9, pp. 100911–100933, 2021, doi: 10.1109/ACCESS.2021.3097006.

[254] R. M. Hossain MA, Sallam KM, Elsayed SS, Chakrabortty RK, "Optimal Power Flow Considering Intermittent Solar and Wind Generation using Multi-Operator Differential Evolution Algorithm.," *Preprints.org*, 2021.

[255] S. Pandya and H. R. Jariwala, "Single- and Multiobjective Optimal Power Flow with Stochastic Wind and Solar Power Plants Using Moth Flame Optimization Algorithm," *Smart Sci.*, pp. 1–41, Sep. 2021, doi: 10.1080/23080477.2021.1964692.

[256] M. Riaz, A. Hanif, S. J. Hussain, M. I. Memon, M. U. Ali, and A. Zafar, "An Optimization-Based Strategy for Solving Optimal Power Flow Problems in a Power System Integrated with Stochastic Solar and Wind Power Energy," *Appl. Sci.*, vol. 11, no. 15, p. 6883, Jul. 2021, doi: 10.3390/app11156883.

[257] M. A. Taher, S. Kamel, F. Jurado, and M. Ebeed, "Modified grasshopper optimization framework for optimal power flow solution," *Electr. Eng.*, vol. 101, no. 1, pp. 121–148, Apr. 2019, doi: 10.1007/s00202-019-00762-4.

[258] M. Ghasemi, S. Ghavidel, S. Rahmani, A. Roosta, and H. Falah, "A novel hybrid algorithm of imperialist competitive algorithm and teaching learning algorithm for optimal power flow problem with non-smooth cost functions," *Eng. Appl. Artif. Intell.*, vol. 29, pp. 54–69, Mar. 2014, doi: 10.1016/j.engappai.2013.11.003.

[259] M. Ghasemi, S. Ghavidel, M. Gitizadeh, and E. Akbari, "An improved teaching–learning-based optimization algorithm using Lévy mutation strategy for non-smooth optimal power flow," *Int. J. Electr. Power Energy Syst.*, vol. 65, pp. 375–384, Feb. 2015, doi: 10.1016/j.ijepes.2014.10.027.

[260] K. Vaisakh and L. R. Srinivas, "Evolving ant direction differential evolution for OPF with non-smooth cost functions," *Eng. Appl. Artif. Intell.*, vol. 24, no. 3, pp. 426–436, Apr. 2011, doi: 10.1016/j.engappai.2010.10.019.

# Appendices

## Appendix A

For 6-units (30- bus test system), The coefficients of fuel cost and operational limits can be found in Table A.1. In addition, The coefficients of $SO_2$ Emission, $NO_x$ Emission, and $CO_2$ Emission and their max/max PPF can be found in Table A.2, A.3, and A.4, respectively.

TABLE A.1. The coefficients of fuel cost and operational limits

| Unit | Ai ($10^{-3}$) | Bi | ci ($10^2$) | di ($10^3$) | $P_{i,min}$ (MW) | $P_{i,max}$ (MW) |
|---|---|---|---|---|---|---|
| P1 | 0.1000 | 0.092 | 0.145 | - 0.1360 | 50 | 200 |
| P2 | 0.4000 | 0.025 | 0.220 | - 0.0035 | 20 | 80 |
| P3 | 0.6000 | 0.075 | 0.230 | - 0.0810 | 15 | 50 |
| P4 | 0.2000 | 0.100 | 0.135 | - 0.0145 | 10 | 50 |
| P5 | 0.1300 | 0.120 | 0.115 | - 0.0098 | 10 | 50 |
| P6 | 0.4000 | 0.084 | 0.125 | 0.0756 | 12 | 40 |

TABLE A.2. The coefficients of SO2 Emission and its max/max PPF

| Unit | The coefficients of $SO_2$ emission | | | | max/max PPF of $SO_2$ |
|---|---|---|---|---|---|
| | $e_{SO2i}$ | $f_{SO2i}$ | $g_{SO2i}$ | $h_{SO2i}$ | $h_s$ |
| 1 | 0.0005 | 0.150 | 17.00 | -90 | 1.09 |
| 2 | 0.0014 | 0.055 | 12.00 | -30.5 | 1.06 |
| 3 | 0.0010 | 0.035 | 10.00 | -80 | 2.11 |
| 4 | 0.0020 | 0.070 | 23.50 | -34.5 | 0.60 |
| 5 | 0.0013 | 0.120 | 21.50 | 19.75 | 0.68 |
| 6 | 0.0021 | 0.080 | 22.50 | 25.60 | 0.62 |

TABLE A.3. the coefficients of $NO_X$ Emission and its max/max PPF

| Unit | The coefficients of $NO_x$ emission | | | | max/max PPF of $No_x$ |
|---|---|---|---|---|---|
| | $e_{NOxi}$ | $f_{NOxi}$ | $g_{NOxi}$ | $h_{NOxi}$ | $h_n$ |
| 1 | 0.0012 | 0.052 | 18.5 | -26 | 0.94 |
| 2 | 0.0004 | 0.045 | 12.0 | -35 | 1.50 |
| 3 | 0.0016 | 0.050 | 13.0 | -15 | 1.39 |
| 4 | 0.0012 | 0.070 | 17.5 | 74 | 0.83 |
| 5 | 0.0003 | 0.040 | 8.5 | 89 | 2.17 |
| 6 | 0.0014 | 0.024 | 15.5 | 75 | 1.09 |

TABLE A.4. the coefficients of $CO_2$ Emission and its max/max PPF

| Unit | The coefficients of $CO_2$ emission | max/max PPF of $CO_2$ |
|---|---|---|

| | $e_{CO2i}$ | $f_{CO2i}$ | $g_{CO2i}$ | $h_{CO2i}$ | $h_c$ |
|---|---|---|---|---|---|
| 1 | 0.0015 | 0.092 | 14.0 | - 16.0 | 0.78 |
| 2 | 0.0014 | 0.025 | 12.5 | - 93.5 | 1.19 |
| 3 | 0.0016 | 0.055 | 13.5 | - 85.0 | 1.44 |
| 4 | 0.0012 | 0.010 | 13.5 | - 24.5 | 1.13 |
| 5 | 0.0023 | 0.040 | 21.0 | - 59.0 | 0.75 |
| 6 | 0.0014 | 0.080 | 22.0 | - 70.0 | 0.7158 |

# Appendix B

For 11-unit test system, the Generation limits, Fuel cost coefficients and Emission coefficients can be found in Table B.1.

Table B.1. Data of the 11-unit system: Generation limits, Fuel cost coefficients and Emission coefficients

| Unit | $P_{i,min}$(MW) | $P_{i,max}$(MW) | $a_i$(\$) | $b_i$(\$/MW) | $c_i$(\$/MW$^2$) | $\alpha_i$ | $\beta_i$ | $\gamma_i$ |
|---|---|---|---|---|---|---|---|---|
| 1 | 20 | 250 | 387.85 | 1.92699 | 0.00762 | 33.93 | -0.67767 | 0.00419 |
| 2 | 20 | 210 | 441.62 | 2.11969 | 0.00838 | 24.62 | -0.69044 | 0.00461 |
| 3 | 20 | 250 | 422.57 | 2.19196 | 0.00523 | 33.93 | -0.67767 | 0.00419 |
| 4 | 60 | 300 | 552.5 | 2.01983 | 0.0014 | 27.14 | -0.54551 | 0.00683 |
| 5 | 20 | 210 | 557.75 | 2.22181 | 0.00154 | 24.15 | -0.40006 | 0.00751 |
| 6 | 60 | 300 | 562.18 | 1.91528 | 0.00177 | 27.14 | -0.54551 | 0.00683 |
| 7 | 20 | 215 | 568.39 | 2.10681 | 0.00195 | 24.15 | -0.40006 | 0.00751 |
| 8 | 100 | 455 | 682.93 | 1.99138 | 0.00106 | 30.45 | -0.51116 | 0.00355 |
| 9 | 100 | 455 | 741.22 | 1.99802 | 0.00117 | 25.59 | -0.56228 | 0.00417 |
| 10 | 110 | 460 | 617.83 | 2.12352 | 0.00089 | 30.45 | -0.41116 | 0.00355 |
| 11 | 110 | 465 | 674.61 | 2.10487 | 0.00098 | 25.59 | -0.56228 | 0.00417 |

# Appendix C

For 6-unit test system, the Generation limits, Fuel cost coefficients and Emission coefficients can be found in Table C.1.

Table C.1. Data of the 6-unit system: Generation limits, Fuel cost coefficients and Emission coefficients

| Unit | $P_{i,min}$(MW) | $P_{i,max}$(MW) | $a_i$($) | $b_i$($/MW) | $c_i$($/MW2) | $\alpha_i$ | $\beta_i$ | $\gamma_i$ | $\eta_i$ | $\delta_i$ |
|---|---|---|---|---|---|---|---|---|---|---|
| 1 | 0.05 | 0.5 | 10 | 200 | 100 | 4.091 | -5.554 | 6.49 | 2.00E-04 | 2.857 |
| 2 | 0.05 | 0.6 | 10 | 150 | 120 | 2.543 | -6.047 | 5.638 | 5.00E-04 | 3.333 |
| 3 | 0.05 | 1 | 20 | 180 | 40 | 4.258 | -5.094 | 4.586 | 1.00E-06 | 8 |
| 4 | 0.05 | 1.2 | 10 | 100 | 60 | 5.326 | -3.55 | 3.38 | 2.00E-03 | 2 |
| 5 | 0.05 | 1 | 20 | 180 | 40 | 4.258 | -5.094 | 4.586 | 1.00E-06 | 8 |
| 6 | 0.05 | 0.6 | 10 | 150 | 100 | 6.131 | -5.555 | 5.151 | 1.00E-05 | 6.667 |

# Appendix D

For 10-unit test system, the Generation limits and Fuel cost coefficients can be found in Table D.1. In addition, Emission coefficients can be found in Table D.2.

Table D.1. Data of the 10-unit system with valve-point effect: Generation limits and Fuel cost coefficients

| Unit | $P_{i,min}$(MW) | $P_{i,max}$(MW) | $a_i$($) | $b_i$($/MW) | $c_i$($/MW$^2$) | $d_i$($) | $e_i$(1/MW) |
|---|---|---|---|---|---|---|---|
| 1 | 10 | 55 | 1000.403 | 40.5407 | 0.12951 | 33 | 0.0174 |
| 2 | 20 | 80 | 950.606 | 39.5804 | 0.10908 | 25 | 0.0178 |
| 3 | 47 | 120 | 900.705 | 36.5104 | 0.12511 | 32 | 0.0162 |
| 4 | 20 | 130 | 800.705 | 39.5104 | 0.12111 | 30 | 0.0168 |
| 5 | 50 | 160 | 756.799 | 38.539 | 0.15247 | 30 | 0.0148 |
| 6 | 70 | 240 | 451.325 | 46.1592 | 0.10587 | 20 | 0.0163 |
| 7 | 60 | 300 | 1243.531 | 38.3055 | 0.03546 | 20 | 0.0152 |
| 8 | 70 | 340 | 1049.998 | 40.3965 | 0.02803 | 30 | 0.0128 |
| 9 | 135 | 470 | 1658.569 | 36.3278 | 0.02111 | 60 | 0.0136 |
| 10 | 150 | 470 | 1356.659 | 38.2704 | 0.01799 | 40 | 0.0141 |

Table D.2. Data of the 10-unit system: Emission coefficients

| Unit | $\alpha_i$ | $\beta_i$ | $\gamma_i$ | $\eta_i$ | $\delta_i$ |
|---|---|---|---|---|---|
| 1 | 360.0012 | -3.9864 | 0.04702 | 0.25475 | 0.01234 |
| 2 | 350.0056 | -3.9524 | 0.04652 | 0.25475 | 0.01234 |
| 3 | 330.0056 | -3.9023 | 0.04652 | 0.25163 | 0.01215 |
| 4 | 330.0056 | -3.9023 | 0.04652 | 0.25163 | 0.01215 |
| 5 | 13.8593 | 0.3277 | 0.0042 | 0.2497 | 0.012 |
| 6 | 13.8593 | 0.3277 | 0.0042 | 0.2497 | 0.012 |
| 7 | 40.2669 | -0.5455 | 0.0068 | 0.248 | 0.0129 |
| 8 | 40.2669 | -0.5455 | 0.0068 | 0.2499 | 0.01203 |
| 9 | 42.8955 | -0.5112 | 0.0046 | 0.2547 | 0.01234 |
| 10 | 42.8955 | -0.5112 | 0.0046 | 0.2547 | 0.01234 |

# Appendix E

For 40-unit test system, the Generation limits and Fuel cost coefficients can be found in Table E.1. In addition, Emission coefficients can be found in Table E.2.

Table E.1. Data of the 40-unit system with valve-point effect: Generation limits and Fuel cost coefficients

| Unit | $P_{i,min}$(MW) | $P_{i,max}$(MW) | $a_i$($) | $b_i$($/MW) | $c_i$($/MW$^2$) | $d_i$($) | $e_i$(1/MW) |
|---|---|---|---|---|---|---|---|
| 1 | 36 | 114 | 0.0069 | 6.73 | 94.705 | 100 | 0.084 |
| 2 | 36 | 114 | 0.0069 | 6.73 | 94.705 | 100 | 0.084 |
| 3 | 60 | 120 | 0.02028 | 7.07 | 309.54 | 100 | 0.084 |
| 4 | 80 | 190 | 0.00942 | 8.18 | 369.03 | 150 | 0.063 |
| 5 | 47 | 97 | 0.0114 | 5.35 | 148.89 | 120 | 0.077 |
| 6 | 68 | 140 | 0.01142 | 8.05 | 222.33 | 100 | 0.084 |
| 7 | 110 | 300 | 0.00357 | 8.03 | 287.71 | 200 | 0.042 |
| 8 | 135 | 300 | 0.00492 | 6.99 | 391.98 | 200 | 0.042 |
| 9 | 135 | 300 | 0.00573 | 6.6 | 455.76 | 200 | 0.042 |
| 10 | 130 | 300 | 0.00605 | 12.9 | 722.82 | 200 | 0.042 |
| 11 | 94 | 375 | 0.00515 | 12.9 | 635.2 | 200 | 0.042 |
| 12 | 94 | 375 | 0.00569 | 12.8 | 654.69 | 200 | 0.042 |
| 13 | 125 | 500 | 0.00421 | 12.5 | 913.4 | 300 | 0.035 |
| 14 | 125 | 500 | 0.00752 | 8.84 | 1760.4 | 300 | 0.035 |
| 15 | 125 | 500 | 0.00708 | 9.15 | 1728.3 | 300 | 0.035 |
| 16 | 125 | 500 | 0.00708 | 9.15 | 1728.3 | 300 | 0.035 |
| 17 | 220 | 500 | 0.00313 | 7.97 | 647.85 | 300 | 0.035 |
| 18 | 220 | 500 | 0.00313 | 7.95 | 649.69 | 300 | 0.035 |
| 19 | 242 | 550 | 0.00313 | 7.97 | 647.83 | 300 | 0.035 |
| 20 | 242 | 550 | 0.00313 | 7.97 | 647.81 | 300 | 0.035 |
| 21 | 254 | 550 | 0.00298 | 6.63 | 785.96 | 300 | 0.035 |
| 22 | 254 | 550 | 0.00298 | 6.63 | 785.96 | 300 | 0.035 |
| 23 | 254 | 550 | 0.00284 | 6.66 | 794.53 | 300 | 0.035 |
| 24 | 254 | 550 | 0.00284 | 6.66 | 794.53 | 300 | 0.035 |
| 25 | 254 | 550 | 0.00277 | 7.1 | 801.32 | 300 | 0.035 |
| 26 | 254 | 550 | 0.00277 | 7.1 | 801.32 | 300 | 0.035 |
| 27 | 10 | 150 | 0.52124 | 3.33 | 1055.1 | 120 | 0.077 |
| 28 | 10 | 150 | 0.52124 | 3.33 | 1055.1 | 120 | 0.077 |
| 29 | 10 | 150 | 0.52124 | 3.33 | 1055.1 | 120 | 0.077 |
| 30 | 47 | 97 | 0.0114 | 5.35 | 148.89 | 120 | 0.077 |
| 31 | 60 | 190 | 0.0016 | 6.43 | 222.92 | 150 | 0.063 |
| 32 | 60 | 190 | 0.0016 | 6.43 | 222.92 | 150 | 0.063 |
| 33 | 60 | 190 | 0.0016 | 6.43 | 222.92 | 150 | 0.063 |
| 34 | 90 | 200 | 0.0001 | 8.95 | 107.87 | 200 | 0.042 |
| 35 | 90 | 200 | 0.0001 | 8.62 | 116.58 | 200 | 0.042 |
| 36 | 90 | 200 | 0.0001 | 8.62 | 116.58 | 200 | 0.042 |
| 37 | 25 | 110 | 0.0161 | 5.88 | 307.45 | 80 | 0.098 |
| 38 | 25 | 110 | 0.0161 | 5.88 | 307.45 | 80 | 0.098 |
| 39 | 25 | 110 | 0.0161 | 5.88 | 307.45 | 80 | 0.098 |
| 40 | 242 | 550 | 0.00313 | 7.97 | 647.83 | 300 | 0.035 |

Table E.2. Data of the 40-unit system: Emission coefficients

| Unit | $\alpha_i$ | $\beta_i$ | $\gamma_i$ | $\eta_i$ | $\delta_i$ |
|---|---|---|---|---|---|
| 1 | 0.048 | -2.22 | 60 | 1.31 | 0.0569 |
| 2 | 0.048 | -2.22 | 60 | 1.31 | 0.0569 |
| 3 | 0.0762 | -2.36 | 100 | 1.31 | 0.0569 |
| 4 | 0.054 | -3.14 | 120 | 0.9142 | 0.0454 |
| 5 | 0.085 | -1.89 | 50 | 0.9936 | 0.0406 |
| 6 | 0.0854 | -3.08 | 80 | 1.31 | 0.0569 |
| 7 | 0.0242 | -3.06 | 100 | 0.655 | 0.02846 |
| 8 | 0.031 | -2.32 | 130 | 0.655 | 0.02846 |
| 9 | 0.0335 | -2.11 | 150 | 0.655 | 0.02846 |
| 10 | 0.425 | -4.34 | 280 | 0.655 | 0.02846 |
| 11 | 0.0322 | -4.34 | 220 | 0.655 | 0.02846 |
| 12 | 0.0338 | -4.28 | 225 | 0.655 | 0.02846 |
| 13 | 0.0296 | -4.18 | 300 | 0.5035 | 0.02075 |
| 14 | 0.0512 | -3.34 | 520 | 0.5035 | 0.02075 |
| 15 | 0.0496 | -3.55 | 510 | 0.5035 | 0.02075 |
| 16 | 0.0496 | -3.55 | 510 | 0.5035 | 0.02075 |
| 17 | 0.0151 | -2.68 | 220 | 0.5035 | 0.02075 |
| 18 | 0.0151 | -2.66 | 222 | 0.5035 | 0.02075 |
| 19 | 0.0151 | -2.68 | 220 | 0.5035 | 0.02075 |
| 20 | 0.0151 | -2.68 | 220 | 0.5035 | 0.02075 |
| 21 | 0.0145 | -2.22 | 290 | 0.5035 | 0.02075 |
| 22 | 0.0145 | -2.22 | 285 | 0.5035 | 0.02075 |
| 23 | 0.0138 | -2.26 | 295 | 0.5035 | 0.02075 |
| 24 | 0.0138 | -2.26 | 295 | 0.5035 | 0.02075 |
| 25 | 0.0132 | -2.42 | 310 | 0.5035 | 0.02075 |
| 26 | 0.0132 | -2.42 | 310 | 0.5035 | 0.02075 |
| 27 | 1.842 | -1.11 | 360 | 0.9936 | 0.0406 |
| 28 | 1.842 | -1.11 | 360 | 0.9936 | 0.0406 |
| 29 | 1.842 | -1.11 | 360 | 0.9936 | 0.0406 |
| 30 | 0.085 | -1.89 | 50 | 0.9936 | 0.0406 |
| 31 | 0.0121 | -2.08 | 80 | 0.9142 | 0.0454 |
| 32 | 0.0121 | -2.08 | 80 | 0.9142 | 0.0454 |
| 33 | 0.0121 | -2.08 | 80 | 0.9142 | 0.0454 |
| 34 | 0.0012 | -3.48 | 65 | 0.655 | 0.02846 |
| 35 | 0.0012 | -3.24 | 70 | 0.655 | 0.02846 |
| 36 | 0.0012 | -3.24 | 70 | 0.655 | 0.02846 |
| 37 | 0.095 | -1.98 | 100 | 1.42 | 0.0677 |
| 38 | 0.095 | -1.98 | 100 | 1.42 | 0.0677 |
| 39 | 0.095 | -1.98 | 100 | 1.42 | 0.0677 |
| 40 | 0.0151 | -2.68 | 220 | 0.5035 | 0.02075 |

# Appendix F

For 110-unit test system, the Generation limits and Fuel cost coefficients can be found in Table F.1.

Table F.1. Data of the 110-unit system: Generation limits and Fuel cost coefficients

| Unit | $P_{i,min}$(MW) | $P_{i,max}$(MW) | $a_i$($) | $b_i$($/MW) | $c_i$($/MW$^2$) | Unit | $P_{i,min}$(MW) | $P_{i,max}$(MW) | $a_i$($) | $b_i$($/MW) | $c_i$($/MW$^2$) |
|---|---|---|---|---|---|---|---|---|---|---|---|
| 1 | 2.4 | 12 | 0.0253 | 25.547 | 24.389 | 56 | 25.2 | 96 | 0.0098 | 14.327 | 82.136 |
| 2 | 2.4 | 12 | 0.0265 | 25.675 | 24.411 | 57 | 25.2 | 96 | 0.0099 | 14.354 | 82.298 |
| 3 | 2.4 | 12 | 0.028 | 25.803 | 24.638 | 58 | 35 | 100 | 0.0092 | 14.38 | 82.464 |
| 4 | 2.4 | 12 | 0.0284 | 25.932 | 24.76 | 59 | 35 | 100 | 0.0094 | 14.407 | 82.626 |

| | | | | | | | | | | | |
|---|---|---|---|---|---|---|---|---|---|---|---|
| 5 | 2.4 | 12 | 0.0286 | 26.061 | 24.888 | 60 | 45 | 120 | 0.0072 | 19 | 218.895 |
| 6 | 4 | 20 | 0.012 | 37.551 | 117.755 | 61 | 45 | 120 | 0.0071 | 19.1 | 219.335 |
| 7 | 4 | 20 | 0.0126 | 37.664 | 118.108 | 62 | 45 | 120 | 0.007 | 19.2 | 219.775 |
| 8 | 4 | 20 | 0.0136 | 37.777 | 118.458 | 63 | 54.3 | 185 | 0.0066 | 11.694 | 143.735 |
| 9 | 4 | 20 | 0.0143 | 37.89 | 118.821 | 64 | 54.3 | 185 | 0.0057 | 11.715 | 144.029 |
| 10 | 15.2 | 76 | 0.0088 | 13.327 | 81.136 | 65 | 54.3 | 185 | 0.0058 | 11.737 | 144.318 |
| 11 | 15.2 | 76 | 0.0089 | 13.354 | 81.298 | 66 | 54.3 | 185 | 0.0059 | 11.758 | 144.597 |
| 12 | 15.2 | 76 | 0.0091 | 13.8 | 81.464 | 67 | 70 | 197 | 0.0036 | 24 | 269.131 |
| 13 | 15.2 | 76 | 0.0093 | 13.407 | 81.626 | 68 | 70 | 197 | 0.0036 | 24.1 | 269.649 |
| 14 | 25 | 100 | 0.0062 | 18 | 217.895 | 69 | 70 | 197 | 0.0036 | 24.2 | 270.176 |
| 15 | 25 | 100 | 0.0061 | 18.1 | 218.335 | 70 | 150 | 360 | 0.0025 | 11.862 | 187.057 |
| 16 | 25 | 100 | 0.006 | 18.2 | 218.775 | 71 | 160 | 400 | 0.0029 | 8.492 | 320.002 |
| 17 | 54.3 | 155 | 0.0046 | 10.694 | 142.735 | 72 | 160 | 400 | 0.003 | 8.503 | 321.91 |
| 18 | 54.3 | 155 | 0.0047 | 10.715 | 143.029 | 73 | 60 | 300 | 0.0054 | 13.327 | 52.136 |
| 19 | 54.3 | 155 | 0.0048 | 10.737 | 143.318 | 74 | 50 | 250 | 0.0055 | 12.354 | 42.298 |
| 20 | 54.3 | 155 | 0.0049 | 10.758 | 143.597 | 75 | 30 | 90 | 0.0099 | 11.38 | 32.464 |
| 21 | 68.9 | 197 | 0.0026 | 23 | 259.131 | 76 | 12 | 50 | 0.0031 | 9.407 | 23.626 |
| 22 | 68.9 | 197 | 0.0026 | 23.1 | 259.649 | 77 | 160 | 450 | 0.0024 | 14 | 220 |
| 23 | 68.9 | 197 | 0.0026 | 23.2 | 260.176 | 78 | 150 | 600 | 0.0023 | 13.1 | 190 |
| 24 | 140 | 350 | 0.0015 | 10.862 | 177.057 | 79 | 50 | 200 | 0.0036 | 13.2 | 250 |
| 25 | 100 | 400 | 0.0019 | 7.492 | 210.002 | 80 | 20 | 120 | 0.0049 | 13.5 | 230 |
| 26 | 100 | 400 | 0.0019 | 7.503 | 211.91 | 81 | 10 | 55 | 0.0061 | 24 | 70 |
| 27 | 140 | 500 | 0.0014 | 12 | 210 | 82 | 12 | 40 | 0.007 | 14.5 | 60 |
| 28 | 140 | 500 | 0.0013 | 12.1 | 180 | 83 | 20 | 80 | 0.0088 | 14.2 | 210 |
| 29 | 50 | 200 | 0.0026 | 12.2 | 240 | 84 | 50 | 200 | 0.0022 | 13.4 | 150 |
| 30 | 25 | 100 | 0.0039 | 12.5 | 220 | 85 | 80 | 325 | 0.0048 | 11.3 | 130 |
| 31 | 10 | 50 | 0.0051 | 23 | 60 | 86 | 120 | 440 | 0.0053 | 8.9 | 80 |
| 32 | 5 | 20 | 0.005 | 13.5 | 50 | 87 | 10 | 35 | 0.0021 | 14.4 | 90 |
| 33 | 20 | 80 | 0.0078 | 13.2 | 200 | 88 | 20 | 55 | 0.0033 | 14.3 | 80 |
| 34 | 75 | 250 | 0.0012 | 12.4 | 140 | 89 | 20 | 100 | 0.0034 | 13.9 | 125 |
| 35 | 110 | 360 | 0.0038 | 10.3 | 120 | 90 | 40 | 220 | 0.0037 | 13.8 | 160 |
| 36 | 130 | 400 | 0.0043 | 9.9 | 90 | 91 | 30 | 140 | 0.0066 | 13.7 | 50 |
| 37 | 10 | 40 | 0.0011 | 13.4 | 80 | 92 | 40 | 100 | 0.0043 | 13.6 | 400 |
| 38 | 20 | 70 | 0.0023 | 13.3 | 70 | 93 | 100 | 440 | 0.0022 | 8.4 | 260 |
| 39 | 25 | 100 | 0.0034 | 12.9 | 115 | 94 | 100 | 500 | 0.0055 | 7.6 | 110 |
| 40 | 20 | 120 | 0.0067 | 12.8 | 150 | 95 | 100 | 600 | 0.0032 | 7.5 | 170 |
| 41 | 40 | 180 | 0.0056 | 12.7 | 40 | 96 | 200 | 700 | 0.0077 | 7.2 | 140 |
| 42 | 50 | 220 | 0.0023 | 12.6 | 300 | 97 | 3.6 | 15 | 0.0353 | 26.547 | 26.389 |
| 43 | 120 | 440 | 0.0012 | 7.4 | 250 | 98 | 3.6 | 15 | 0.0365 | 26.675 | 25.411 |
| 44 | 160 | 560 | 0.0045 | 6.6 | 100 | 99 | 4.4 | 22 | 0.038 | 26.803 | 25.638 |
| 45 | 150 | 660 | 0.0022 | 6.5 | 160 | 100 | 4.4 | 22 | 0.0384 | 26.932 | 25.76 |
| 46 | 200 | 700 | 0.0067 | 6.2 | 130 | 101 | 10 | 60 | 0.021 | 15.3 | 65 |
| 47 | 5.4 | 32 | 0.0353 | 26.547 | 34.389 | 102 | 10 | 80 | 0.023 | 16 | 82 |
| 48 | 5.4 | 32 | 0.0365 | 26.675 | 34.411 | 103 | 20 | 100 | 0.024 | 20.2 | 86 |

| | | | | | | | | | | | |
|---|---|---|---|---|---|---|---|---|---|---|---|
| 49 | 8.4 | 52 | 0.038 | 26.803 | 34.638 | 104 | 20 | 120 | 0.035 | 20.2 | 84 |
| 50 | 8.4 | 52 | 0.0384 | 26.932 | 34.761 | 105 | 40 | 150 | 0.034 | 25.6 | 75 |
| 51 | 8.4 | 52 | 0.0386 | 17.061 | 34.888 | 106 | 40 | 280 | 0.037 | 30.5 | 56 |
| 52 | 12 | 60 | 0.032 | 38.551 | 127.755 | 107 | 50 | 520 | 0.039 | 32.5 | 67 |
| 53 | 12 | 60 | 0.0326 | 36.664 | 128.108 | 108 | 30 | 150 | 0.035 | 26 | 68 |
| 54 | 12 | 60 | 0.0236 | 38.777 | 128.458 | 109 | 40 | 320 | 0.028 | 25.8 | 69 |
| 55 | 12 | 60 | 0.0243 | 38.89 | 128.821 | 110 | 20 | 200 | 0.026 | 27 | 72 |

# Appendix G

For 6-unit test system, the generating unit capacity, coefficients, ramp rate limits and prohibited zones of generating units can be found in Table G.1. In addition, The real loss B - coefficients for 6 - unit test system can be found in Table G.2.

Table G.1. Data of the 6-unit system: generating unit capacity, coefficients, ramp rate limits and prohibited zones of generating units

| Unit | $P_{i,min}$(MW) | $P_{i,max}$(MW) | $a_i$($) | $b_i$($/MW) | $c_i$($/MW$^2$) | $P_i^0$ | $UR_i$ | $DR_i$ | Prohibited Operating Zones |
|---|---|---|---|---|---|---|---|---|---|
| 1 | 100 | 500 | 240 | 0.7 | 0.007 | 440 | 80 | 120 | [210,240] [350,380] |
| 2 | 50 | 200 | 200 | 10 | 0.0095 | 170 | 50 | 90 | [90,110] [140,160] |
| 3 | 80 | 300 | 220 | 8.5 | 0.009 | 200 | 65 | 100 | [150,170] [210,240] |
| 4 | 50 | 150 | 200 | 11 | 0.009 | 150 | 50 | 90 | [80,90] [110,120] |
| 5 | 50 | 200 | 220 | 10.5 | 0.008 | 190 | 50 | 90 | [90,110] [140,150] |
| 6 | 50 | 120 | 190 | 12 | 0.0075 | 110 | 50 | 90 | [75,85] [100,105] |

Table G.2. The real loss B-coefficients for 6-unit test system

| $B_{ij}$ | 1 | 2 | 3 | 4 | 5 | 6 |
|---|---|---|---|---|---|---|
| 1 | 0.0017 | 0.0012 | 0.0007 | -0.0001 | -0.0005 | -0.0002 |
| 2 | 0.0012 | 0.0011 | 0.0009 | 0.0001 | -0.0006 | -0.0001 |
| 3 | 0.0007 | 0.0009 | 0.0031 | 0.0000 | -0.0010 | -0.0006 |
| 4 | -0.0001 | 0.0001 | 0.0000 | 0.0024 | -0.0006 | -0.0008 |
| 5 | -0.0005 | -0.0006 | -0.0010 | -0.0006 | 0.0129 | -0.0002 |
| 6 | -0.0002 | -0.0001 | -0.0006 | -0.0008 | -0.0002 | 0.0150 |
| $B_{0i}$=1.0e-3* | -0.3908 | -0.1297 | 0.7047 | 0.0591 | 0.2161 | -0.6635 |
| $B_{00}$ | 0.056 | | | | | |

# Appendix H

For 13-unit test system, the Generation limits and Fuel cost coefficients can be found in Table H.1.

Table H.1. Data of the 13-unit system with valve-point effect: Generation limits and Fuel cost coefficients

| Unit | Pi,min(MW) | Pi,max(MW) | ai($) | bi($/MW) | ci($/MW2) | di($) | ei(1/MW) |
|---|---|---|---|---|---|---|---|

| | | | | | | | |
|---|---|---|---|---|---|---|---|
| 1 | 0 | 680 | 0.00028 | 8.1 | 550 | 300 | 0.035 |
| 2 | 0 | 360 | 0.00056 | 8.1 | 309 | 200 | 0.042 |
| 3 | 0 | 360 | 0.00056 | 8.1 | 307 | 200 | 0.042 |
| 4 | 60 | 180 | 0.00324 | 7.74 | 240 | 150 | 0.063 |
| 5 | 60 | 180 | 0.00324 | 7.74 | 240 | 150 | 0.063 |
| 6 | 60 | 180 | 0.00324 | 7.74 | 240 | 150 | 0.063 |
| 7 | 60 | 180 | 0.00324 | 7.74 | 240 | 150 | 0.063 |
| 8 | 60 | 180 | 0.00324 | 7.74 | 240 | 150 | 0.063 |
| 9 | 60 | 180 | 0.00324 | 7.74 | 240 | 150 | 0.063 |
| 10 | 40 | 120 | 0.00284 | 8.6 | 126 | 100 | 0.084 |
| 11 | 40 | 120 | 0.00284 | 8.6 | 126 | 100 | 0.084 |
| 12 | 55 | 120 | 0.00284 | 8.6 | 126 | 100 | 0.084 |
| 13 | 55 | 120 | 0.00284 | 8.6 | 126 | 100 | 0.084 |

# Appendix I

For 15-unit test system, the generating unit capacity, coefficients, ramp rate limits and prohibited zones of generating units can be found in Table I.1. In addition, The real loss B - coefficients for 15 - unit test system can be found in Table I.2.

Table I.1. Data of the 15-unit system: generating unit capacity, coefficients, ramp rate limits and prohibited zones of generating units

| Unit | Pi,min(MW) | Pi,max(MW) | $a_i$($) | $b_i$($/MW) | $c_i$($/MW2) | $P_i^0$ | $UR_i$ | $DR_i$ | Prohibited Operating Zones |
|---|---|---|---|---|---|---|---|---|---|
| 1 | 671 | 10.1 | 0.000299 | 150 | 455 | 400 | 80 | 120 | |
| 2 | 574 | 10.2 | 0.000183 | 150 | 455 | 300 | 80 | 120 | [185 255] [305 335] [420 450] |
| 3 | 374 | 8.8 | 0.001126 | 20 | 130 | 105 | 130 | 130 | |
| 4 | 374 | 8.8 | 0.001126 | 20 | 130 | 100 | 130 | 130 | |
| 5 | 461 | 10.4 | 0.000205 | 150 | 470 | 90 | 80 | 120 | [180 200] [305 335] [390 420] |
| 6 | 630 | 10.1 | 0.000301 | 135 | 460 | 400 | 80 | 120 | [230 255] [365 395] [430 455] |
| 7 | 548 | 9.8 | 0.000364 | 135 | 465 | 350 | 80 | 120 | |
| 8 | 227 | 11.2 | 0.000338 | 60 | 300 | 95 | 65 | 100 | |
| 9 | 173 | 11.2 | 0.000807 | 25 | 162 | 105 | 60 | 100 | |
| 10 | 175 | 10.7 | 0.001203 | 25 | 160 | 110 | 60 | 100 | |
| 11 | 186 | 10.2 | 0.003586 | 20 | 80 | 60 | 80 | 80 | |
| 12 | 230 | 9.9 | 0.005513 | 20 | 80 | 40 | 80 | 80 | [30 40] [55 65] |
| 13 | 225 | 13.1 | 0.000371 | 25 | 85 | 30 | 80 | 80 | |
| 14 | 309 | 12.1 | 0.001929 | 15 | 55 | 20 | 55 | 55 | |
| 15 | 323 | 12.4 | 0.004447 | 15 | 55 | 20 | 55 | 55 | |

Table I.2. The real loss B-coefficients for 15-unit test system

| $B_{ij}$=1.0e-3* | 1 | 2 | 3 | 4 | 5 | 6 | 7 | 8 | 9 | 10 | 11 | 12 | 13 | 14 | 15 |
|---|---|---|---|---|---|---|---|---|---|---|---|---|---|---|---|
| 1 | 1.4 | 1.2 | 0.7 | -0.1 | -0.3 | -0.1 | -0.1 | -0.1 | -0.3 | -0.5 | -0.3 | -0.2 | 0.4 | 0.3 | -0.1 |
| 2 | 1.2 | 1.5 | 1.3 | 0 | -0.5 | -0.2 | 0 | 0.1 | -0.2 | -0.4 | -0.4 | 0 | 0.4 | 1 | -0.2 |

| | | | | | | | | | | | | | | | |
|---|---|---|---|---|---|---|---|---|---|---|---|---|---|---|---|
| 3 | 0.7 | 1.3 | 7.6 | -0.1 | -1.3 | -0.9 | -0.1 | 0 | -0.8 | -1.2 | -1.7 | 0 | -2.6 | 11.1 | -2.8 |
| 4 | -0.1 | 0 | -0.1 | 3.4 | -0.7 | -0.4 | 1.1 | 5 | 2.9 | 3.2 | -1.1 | 0 | 0.1 | 0.1 | -2.6 |
| 5 | -0.3 | -0.5 | -1.3 | -0.7 | 9 | 1.4 | -0.3 | -1.2 | -1 | -1.3 | 0.7 | -0.2 | -0.2 | -2.4 | -0.3 |
| 6 | -0.1 | -0.23 | -0.9 | -0.4 | 1.4 | 1.6 | 0 | -0.6 | -0.5 | -0.8 | 1.1 | -0.1 | -0.2 | -1.7 | 0.3 |
| 7 | -0.1 | 0 | -0.1 | 1.1 | -0.3 | 0 | 1.5 | 1.7 | 1.5 | 0.9 | -0.5 | 0.7 | 0 | -0.2 | -0.8 |
| 8 | -0.1 | 0.1 | 0 | 5 | -1.2 | -0.6 | 1.7 | 16.8 | 8.2 | 7.9 | -2.3 | -3.6 | 0.1 | 0.5 | -7.8 |
| 9 | -0.3 | -0.2 | -0.8 | 2.9 | -1 | -0.5 | 1.5 | 8.2 | 12.9 | 11.6 | -2.1 | -2.5 | 0.7 | -1.2 | -7.2 |
| 10 | -0.5 | -0.4 | -1.2 | 3.2 | -1.3 | -0.8 | 0.9 | 7.9 | 11.6 | 20 | -2.7 | -3.4 | 0.9 | -1.1 | -8.8 |
| 11 | -0.3 | -0.4 | -1.7 | -1.1 | 0.7 | 1.1 | -0.5 | -2.3 | -2.1 | -2.7 | 14 | 0.1 | 0.4 | -3.8 | 16.8 |
| 12 | -0.2 | 0 | 0 | 0 | -0.2 | -0.1 | 0.7 | -3.6 | -2.5 | -3.4 | 0.1 | 5.4 | -0.1 | -0.4 | 2.8 |
| 13 | 0.4 | 0.4 | -2.6 | 0.1 | -0.2 | -0.2 | 0 | 0.1 | 0.7 | 0.9 | 0.4 | -0.1 | 10.3 | -10.1 | 2.8 |
| 14 | 0.3 | 1 | 11.1 | 0.1 | -2.4 | -1.7 | -0.2 | 0.5 | -1.2 | -1.1 | -3.8 | -0.4 | -10.1 | 57.8 | -9.4 |
| 15 | -0.1 | -0.2 | -2.8 | -2.6 | -0.3 | 0.3 | -0.8 | -7.8 | -7.2 | -8.8 | 16.8 | 2.8 | 2.8 | -9.4 | 128.3 |
| $B_{0i}$=1.0e-3* | -0.1 | -0.2 | 2.8 | -0.1 | 0.1 | -0.3 | -0.2 | -0.2 | 0.6 | 3.9 | -1.7 | 0 | -3.2 | 6.7 | -6.4 |
| $B_{00}$ | 0.0055 | | | | | | | | | | | | | | |

# الملخص العربي

يعد الإرسال الاقتصادي (ED) أحد المفاهيم الأساسية في إدارة أنظمة الطاقة الكهربائية وأنظمة التشغيل. من ناحية أخرى ، مع تزايد الاهتمام باعتبارات انبعاثات الملوثات ، أصبح إيجاد حل للانبعاثات قضية أساسية لنظام توليد الطاقة إلى جانب التكلفة الإجمالية للوقود في جميع أنحاء العالم. يعد تقليل انبعاثات غازات الاحتباس الحراري وتكلفة الوقود المبادئ الرئيسية لمشكلة تحسين إرسال الانبعاثات الاقتصادية (EED). تحسين إرسال الانبعاثات الاقتصادية هي طريقة تستخدم لتقييم مخرجات المولدات في نظام الطاقة من أجل تقليل تكاليف الوقود والانبعاثات في نفس الوقت مع تلبية قيود المساواة وعدم المساواة ، بما في ذلك قيود توازن الطاقة وقيود حد الطاقة.

في هذه الأطروحة ، يتم حل مشكلة إرسال الانبعاثات الاقتصادية بناءً على وظائف فردية / متعددة الأهداف باستخدام خوارزميات تحسين معروفة ومتطورة. تُستخدم خوارزميات التحسين التالية لتحقيق الحل الأمثل لمشكلة EED استنادًا إلى وظيفة هدف واحدة ؛ خوارزمية التحسين المستندة إلى النظام البيئي الاصطناعي (AEO) ، خوارزمية التحسين المستندة إلى النظام البيئي الفوضوي الاصطناعي (CAEO) ، تحسين البحث عن شعاع مانتا راي (MRFO) ، مُحسِّن قائم على التدرج (GBO) ، هجين (MRFO – GBO) ، تحسين العرض والطلب (SDO) ، خوارزمية تحسين إستراتيجية النسر القائمة على العرض والطلب مع الفوضى (ESCSDO). أيضًا ، تم اقتراح خوارزمية البحرية المفترسة (MPA) خوارزمية المفترسات البحرية المحسنة (MMPA) لحل مشكلة CEED المدمجة باستخدام عامل غرامة السعر الأقصى / الأقصى (PPF) لتقييد النظام اللاخطي. يعتبر PPF لتحويل مشكلة ذات أربعة أهداف إلى مشكلة تحسين ذات هدف واحد. بينما تم اقتراح خوارزمية قوالب الوحل (SMA) ، وخوارزمية قوالب الوحل (ISMA) المحسّنة وتطبيقها لحل مشاكل EED مع الأخذ في الاعتبار تأثير نقطة الصمام. فيما يتعلق بالمشكلة ثنائية الهدف ، يتم دمج نهج باريتو مع تقنيات MMPA و MPA و SMA و ISMA و AEO و CAEO للوصول إلى مجموعة من الحلول غير الخاضعة للسيطرة (ND) ، ثم يتم استخدام الطريقة الضبابية (fuzzy method) لاختيار أفضل حل وسط (BCS).

أظهرت النتائج أن الخوارزميات المقترحة أقوى من الخوارزميات الأخرى المعروفة. يتم أيضًا تحقيق الحلول المجدية باستخدام الخوارزميات المقترحة ، والتي تعدل جدول التوليد دون التأثير علي حدود التوليد التشغيلي. تقدم نتائج المحاكاة دليلاً على الأداء الفعال للتقنيات المقترحة في حل مجموعة متنوعة من مشاكل EED في جميع حالات الدراسة.

وتحتوى الرسالة علي ستة أبواب :-

- الباب الأول وعنوانه: Introduction

يحتوى هذا الباب علي مقدمة عامة عن أهمية تحسين إرسال الانبعاثات الاقتصادية. كما يعرض الأهداف الرئيسية للرسالة وتقسيماتها.

- الباب الثاني وعنوانه: Literature Review

يستعرض هذا الباب الطرق التقليدية والحديثة المثلى المستخدمة لحل مشكلة تحسين إرسال الانبعاثات الاقتصادية. بالإضافة إلى ذلك ، يناقش هذا الفصل الأساليب التي تم اقتراحها لإيجاد أفضل حل لمشكلة تحسين إرسال الانبعاثات الاقتصادية.

- الباب الثالث وعنوانه: Formulation of economic emission dispatch (EED) problem

هذا الباب يقدم الصياغة الرياضية لمشكلة تحسين إرسال الانبعاثات الاقتصادية كمشكلة ذات هدف واحد و كذلك تتم صياغة مشكلة التنسيق كمشكلة متعددة الأهداف. يتم وصف القيود الأساسية لهذه المشكلة.

- الباب الرابع وعنوانه: Recent and Developed Optimization Techniques for Solving EED Problem

في هذا الباب، يتم إقتراح تعديلات علي خوارزميات مختلفة وذلك بهدف تحسين أداءها وإستخدامها لحل مشكلة إرسال الانبعاثات الاقتصادية. كما تم اقتراح تحسينات مختلفة لتحسين أداء خوارزميات التحسين التقليدية ، والتي يمكن تلخيصها على النحو التالي ؛ CAEO و ISMA و MMPA و ESCSDO و SDO لمشكلة EED الفردية و MOCAEO و MOISMA و MMMPA لمشكلة EED متعددة الأهداف.

- الباب الخامس وعنوانه: Results and Discussion

فى هذا الباب يتم إختبار الطرق المقترحة على شبكات مختلفة للتحقق من قدرة التقنيات. و يتم عرض نتائج الإختبارات و مناقشتها و كذلك مقارنة النتائج التي تم الحصول عليها مع طرق أخرى.

- الباب السادس وعنوانه: Conclusions and Future Works

في هذا الباب تم عرض خلاصة النتائج التى تم التوصل إليها خلال الدراسة كما تم عرض إقتراحات لدراسات مستقبلية مكملة لهذه الدراسة

# التوليد الاقتصادي للكهرباء في الزمن الحقيقي مع مراعاة عدم اليقين لموارد الطاقة المتجددة باستخدام تقنيات تحسين فعالة

مـقدمـة من

**المهندس / محمد حسني حسن سلامة**

**للحصول علي درجة الدكتوراه**

**فى**

**الهندسة الكهربية**

## لجنة الاشراف على الرسالة

1. أ.د. لؤى سعد الدين نصرت - جامعة أسوان- مصر
2. أ.د. فرانسسكو خورادو- جامعة خاين- أسبانيا
3. أ.م.د. صلاح محمد كامل - جامعة أسوان – مصر

## لجنة المناقشة والحكم على الرسالة

| | | |
|---|---|---|
| 1. | أ.د/ عبد العظيم عبد الله عبد السلام عبد الله | أستاذ بقسم الهندسة الكهربية - كلية الهندسة - جامعة قناة السويس |
| 2. | أ.د/ محمد محمود علي | أستاذ بقسم الهندسة الكهربية - كلية الهندسة - جامعة أسوان |
| 3. | أ.د/ لؤى سعد الدين نصرت | أستاذ بقسم الهندسة الكهربية - كلية الهندسة - جامعة أسوان |
| 4. | أ.م.د/ صلاح محمد كامل | أستاذ مساعد بقسم الهندسة الكهربية - كلية الهندسة - جامعة أسوان |

كليـة الهندسـة

جامـعة اسـوان

# التوليد الاقتصادي للكهرباء في الزمن الحقيقي مع مراعاة عدم اليقين لموارد الطاقة المتجددة باستخدام تقنيات تحسين فعالة

**رسالة علمية مقدمة الى الدراسات العليا بكلية الهندسة**

**جامعة أسوان**

**كاستيفاء جزئي لمتطلبات الحصول على درجة الدكتوراه**

**في**

**الهندسة الكهربية**

مـقدمـة من


## المهندس/ محمد حسني حسن سلامة

ماجستير الهنـدسـة الكهربيـة – كلية الهندسة – جامعة القاهرة


**إبريل 2022**